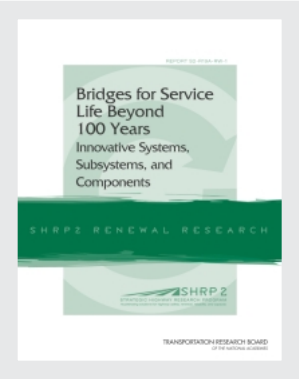

Bridges for Service Life Beyond 100 Years: Innovative Systems, Subsystems, and Components

DETAILS

0 pages | 8.5 x 11 | PAPERBACK
ISBN 978-0-309-43388-4 | DOI 10.17226/22479

AUTHORS

Azizinamini, Atorod; Power, Edward H.; Myers, Glenn F.; and Ozyildirim, H. Celik

The Second
STRATEGIC HIGHWAY RESEARCH PROGRAM

SHRP 2 REPORT S2-R19A-RW-1

Bridges for Service Life Beyond 100 Years:

Innovative Systems, Subsystems, and Components

Atorod Azizinamini
Florida International University

Edward H. Power
HDR Engineering, Inc.

Glenn F. Myers
Atkins North America Inc.

H. Celik Ozyildirim
Virginia Center for Transportation Innovation and Research

TRANSPORTATION RESEARCH BOARD

WASHINGTON, D.C.
2014
www.TRB.org

Subject Areas

Bridges and Other Structures
Highways
Maintenance and Preservation
Materials

The Second Strategic Highway Research Program

America's highway system is critical to meeting the mobility and economic needs of local communities, regions, and the nation. Developments in research and technology—such as advanced materials, communications technology, new data collection technologies, and human factors science—offer a new opportunity to improve the safety and reliability of this important national resource. Breakthrough resolution of significant transportation problems, however, requires concentrated resources over a short time frame. Reflecting this need, the second Strategic Highway Research Program (SHRP 2) has an intense, large-scale focus, integrates multiple fields of research and technology, and is fundamentally different from the broad, mission-oriented, discipline-based research programs that have been the mainstay of the highway research industry for half a century.

The need for SHRP 2 was identified in *TRB Special Report 260: Strategic Highway Research: Saving Lives, Reducing Congestion, Improving Quality of Life,* published in 2001 and based on a study sponsored by Congress through the Transportation Equity Act for the 21st Century (TEA-21). SHRP 2, modeled after the first Strategic Highway Research Program, is a focused, time-constrained, management-driven program designed to complement existing highway research programs. SHRP 2 focuses on applied research in four areas: Safety, to prevent or reduce the severity of highway crashes by understanding driver behavior; Renewal, to address the aging infrastructure through rapid design and construction methods that cause minimal disruptions and produce lasting facilities; Reliability, to reduce congestion through incident reduction, management, response, and mitigation; and Capacity, to integrate mobility, economic, environmental, and community needs in the planning and designing of new transportation capacity.

SHRP 2 was authorized in August 2005 as part of the Safe, Accountable, Flexible, Efficient Transportation Equity Act: A Legacy for Users (SAFETEA-LU). The program is managed by the Transportation Research Board (TRB) on behalf of the National Research Council (NRC). SHRP 2 is conducted under a memorandum of understanding among the American Association of State Highway and Transportation Officials (AASHTO), the Federal Highway Administration (FHWA), and the National Academy of Sciences, parent organization of TRB and NRC. The program provides for competitive, merit-based selection of research contractors; independent research project oversight; and dissemination of research results.

SHRP 2 Report S2-R19A-RW-1

ISBN: 978-0-309-27363-3

Copyright Information

Note: SHRP 2 report numbers convey the program, focus area, project number, and publication format. Report numbers ending in "w" are published as web documents only.

Notice

The project that is the subject of this report was a part of the second Strategic Highway Research Program, conducted by the Transportation Research Board with the approval of the Governing Board of the National Research Council.

The members of the technical committee selected to monitor this project and to review this report were chosen for their special competencies and with regard for appropriate balance. The report was reviewed by the technical committee and accepted for publication according to procedures established and overseen by the Transportation Research Board and approved by the Governing Board of the National Research Council.

The opinions and conclusions expressed or implied in this report are those of the researchers who performed the research and are not necessarily those of the Transportation Research Board, the National Research Council, or the program sponsors.

The Transportation Research Board of the National Academies, the National Research Council, and the sponsors of the second Strategic Highway Research Program do not endorse products or manufacturers. Trade or manufacturers' names appear herein solely because they are considered essential to the object of the report.

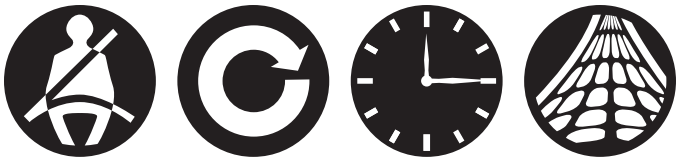

SHRP 2 Reports

Available by subscription and through the TRB online bookstore:
www.TRB.org/bookstore

Contact the TRB Business Office:
202-334-3213

More information about SHRP 2:
www.TRB.org/SHRP2

THE NATIONAL ACADEMIES

Advisers to the Nation on Science, Engineering, and Medicine

The **National Academy of Sciences** is a private, nonprofit, self-perpetuating society of distinguished scholars engaged in scientific and engineering research, dedicated to the furtherance of science and technology and to their use for the general welfare. On the authority of the charter granted to it by Congress in 1863, the Academy has a mandate that requires it to advise the federal government on scientific and technical matters. Dr. Ralph J. Cicerone is president of the National Academy of Sciences.

The **National Academy of Engineering** was established in 1964, under the charter of the National Academy of Sciences, as a parallel organization of outstanding engineers. It is autonomous in its administration and in the selection of its members, sharing with the National Academy of Sciences the responsibility for advising the federal government. The National Academy of Engineering also sponsors engineering programs aimed at meeting national needs, encourages education and research, and recognizes the superior achievements of engineers. Dr. C. D. (Dan) Mote, Jr., is president of the National Academy of Engineering.

The **Institute of Medicine** was established in 1970 by the National Academy of Sciences to secure the services of eminent members of appropriate professions in the examination of policy matters pertaining to the health of the public. The Institute acts under the responsibility given to the National Academy of Sciences by its congressional charter to be an adviser to the federal government and, on its own initiative, to identify issues of medical care, research, and education. Dr. Harvey V. Fineberg is president of the Institute of Medicine.

The **National Research Council** was organized by the National Academy of Sciences in 1916 to associate the broad community of science and technology with the Academy's purposes of furthering knowledge and advising the federal government. Functioning in accordance with general policies determined by the Academy, the Council has become the principal operating agency of both the National Academy of Sciences and the National Academy of Engineering in providing services to the government, the public, and the scientific and engineering communities. The Council is administered jointly by both Academies and the Institute of Medicine. Dr. Ralph J. Cicerone and Dr. C. D. (Dan) Mote, Jr., are chair and vice chair, respectively, of the National Research Council.

The **Transportation Research Board** is one of six major divisions of the National Research Council. The mission of the Transportation Research Board is to provide leadership in transportation innovation and progress through research and information exchange, conducted within a setting that is objective, interdisciplinary, and multimodal. The Board's varied activities annually engage about 7,000 engineers, scientists, and other transportation researchers and practitioners from the public and private sectors and academia, all of whom contribute their expertise in the public interest. The program is supported by state transportation departments, federal agencies including the component administrations of the U.S. Department of Transportation, and other organizations and individuals interested in the development of transportation. **www.TRB.org**

www.national-academies.org

SHRP 2 STAFF

Ann M. Brach, *Director*
Stephen J. Andrle, *Deputy Director*
Neil J. Pedersen, *Deputy Director, Implementation and Communications*
Cynthia Allen, *Editor*
Kenneth Campbell, *Chief Program Officer, Safety*
JoAnn Coleman, *Senior Program Assistant, Capacity and Reliability*
Eduardo Cusicanqui, *Financial Officer*
Richard Deering, *Special Consultant, Safety Data Phase 1 Planning*
Walter Diewald, *Senior Program Officer, Safety*
Shantia Douglas, *Senior Financial Assistant*
Charles Fay, *Senior Program Officer, Safety*
Carol Ford, *Senior Program Assistant, Renewal and Safety*
Jo Allen Gause, *Senior Program Officer, Capacity*
Rosalind Gomes, *Accounting/Financial Assistant*
James Hedlund, *Special Consultant, Safety Coordination*
Alyssa Hernandez, *Reports Coordinator*
Ralph Hessian, *Special Consultant, Capacity and Reliability*
Andy Horosko, *Special Consultant, Safety Field Data Collection*
William Hyman, *Senior Program Officer, Reliability*
Linda Mason, *Communications Officer*
Reena Mathews, *Senior Program Officer, Capacity and Reliability*
Matthew Miller, *Program Officer, Capacity and Reliability*
Michael Miller, *Senior Program Assistant, Capacity and Reliability*
David Plazak, *Senior Program Officer, Capacity and Reliability*
Rachel Taylor, *Senior Editorial Assistant*
Dean Trackman, *Managing Editor*
Connie Woldu, *Administrative Coordinator*

ACKNOWLEDGMENTS

This work was sponsored by the Federal Highway Administration in cooperation with the American Association of State Highway and Transportation Officials. The project was managed by SHRP 2 Renewal senior program officers Monica Starnes (December 2007 through January 2011), Mark Bush (January 2011 through November 2011), and Jerry DiMaggio (December 2011 onward).

The principal investigator was Atorod Azizinamini, Chairperson of the Civil and Environmental Engineering Department at Florida International University. Contributions from the following research team members to this final report are greatly appreciated: Eric S. Kline of KTA, Inc.; David W. Whitmore of Vector Corrosion; Dennis R. Mertz of the University of Delaware; and Don White of the Georgia Institute of Technology.

Graduate students Nima Ala, Saeed Doust, Marcelo Da Silva, and Ardalan Sherafati obtained their PhD degrees and Luke Glaser and Kyle Burnet obtained their MS degrees by carrying out various research tasks within Project R19A. The contributions of Aaron Yakel, research associate at Florida International University, and Kromel Hanna, research associate at the University of Nebraska–Lincoln (Omaha campus), are also greatly acknowledged.

Special thanks to Aaron Yakel for his assistance with putting the report in its final format, and to Christine Boyer of Boyer Associates for editing the final report.

The authors also thank Martin Burke, private consultant; Reid W. Castrodale of Carolina Stalite Company; David Darwin of the University of Kansas; Simon Greensted of Sterling Lloyd; Mark Kaczinski of D. S. Brown Company; Ralph Oesterle of CTL Group; Duncan Paterson of HDR Engineering, Inc.; Charles Roeder of the University of Washington; and Ronald J. Watson of R. J. Watson, Inc.

Various bridge committees within the AASHTO Subcommittee on Bridges and Structures provided valuable input and review comments. Special thanks are due to AASHTO Technical Committee T-9 and its chair, Bruce Johnson, for his leadership and help. Members of Project R19A TETG are appreciated for their valuable technical comments and guidance throughout the project. The University of Nebraska–Lincoln (UNL) provided the testing facility to perform the experimental work while the principal investigator was at UNL.

FOREWORD

Jerry A. DiMaggio, D.GE, PE, *SHRP 2 Senior Program Officer*

The design of bridges for service life is gaining importance. This report, *Bridges for Service Life Beyond 100 Years: Innovative Systems, Subsystems, and Components,* discusses the main product of SHRP 2 Project R19A within the Renewal area: the *Design Guide for Bridges for Service Life* (the *Guide*). Both are available at the Transportation Research Board website (http://www.trb.org/Design/Blurbs/168760.aspx).

The main objective of the *Guide* is to provide information and guidance and to define procedures to systematically approach service life and durability for both new and existing bridges. The *Guide* equips users with knowledge to develop specific solutions for a bridge under consideration in a systematic manner by using a standard framework with specifics being different. In some respects, the R19A *Guide* may be considered a foundational reference that will be built on, expanded, modified, and progressively embraced differently at project and program levels by the bridge and structures community. The future path of development and mainstream acceptance and implementation may be similar to that of load resistance factor design (LRFD) specifications. Results from the knowledge gained through the project are communicated throughout the report in ways that bridge professionals can implement in practice.

Providing safety for the public by having adequate strength is the cornerstone of the framework used by engineers for bridge design. This approach has not been restricted to bridges; for example, it has also been the framework used in various building codes. Significant changes to our contemporary bridge design practice have also been mainly related to strength issues. The transition to LRFD is a well-known recent example. A review of bridges that have lasted more than 100 years provides valuable lessons related to achieving long service lives.

The R19A Report details the steps undertaken in the development of the *Guide.* The report also provides results from extensive individual research efforts that have led to new concepts that can mitigate factors historically limiting the service life of bridges. The report highlights the research approach, topics, and challenges in developing the *Guide,* as well as the literature searches that were conducted and identifies Phase 1 and Phase 2 tasks within the project. The report also provides information on a related project, R19B. Practical approaches to using the *Guide,* along with future development of the *Guide,* are also presented in the report.

CONTENTS

Executive Summary

The design of bridges for service life is gaining importance as limited resources demand enhancing the service life of existing and new bridges. The cost of addressing service life issues at the design stage is significantly lower than the cost of taking maintenance and preservation actions while a bridge is in service. Currently, design for service life is approached by using individual strategies aimed at enhancing the service life of a particular problematic bridge element that has historically limited a bridge's service life. However, design for service life must be approached in a systematic manner using a general framework that is applicable for all bridges, while also allowing for specifics that are unique from one bridge to another. These unique differences are necessary because design for service life is a context-sensitive problem requiring consideration of local experiences, practice, and owner preferences.

The main objective of the Second Strategic Highway Research Program (SHRP 2) Project R19A, Bridges for Service Life Beyond 100 Years: Innovative Systems, Subsystems, and Components, is to develop approaches to service life design for existing and new bridges. The main product of this project is the *Design Guide for Bridges for Service Life* (the *Guide*), which is now available through TRB (http://www.trb.org/Design/Blurbs/168760.aspx).

The objective of the *Guide* is to provide information about and define procedures for systematically designing for service life and durability for both new and existing bridges. The *Guide* includes new concepts and approaches that offer improvements to current practice and have the potential to enhance the service life of bridges. Its approach to design for service life is to provide a body of knowledge relating to bridge durability under different exposure conditions and constraints and to establish an array of options capable of enhancing service life. A solution for a particular service life issue is highly dependent on many factors that vary from location to location and state to state, because a solution depends on local practices and preferences. Consequently, use of the *Guide* is not intended to dictate a unique solution for any specific service life problem or to identify the best and only solution. Rather, it equips the reader with a body of knowledge for developing specific solutions best suited to stated conditions and constraints.

This final report details the steps used in the development of the *Guide.* It also provides results from extensive individual research efforts that have led to the development of new details and concepts that can mitigate factors that have historically limited the service life of bridges.

In the course of developing the *Guide,* the research team explored various approaches for design for service life and identified the elements of a systematic approach, as well as ways to present the information in a transparent form that could be used by bridge owners and lead to development of bridges with enhanced service life. An important aspect of developing a systematic approach for design for service life was identifying the problems that have historically limited the service life of bridges. Several surveys and literature searches were conducted to identify current service life challenges. For select and high-priority service life challenges, potential

solutions were identified and proof of concept tests were carried out. The entire body of knowledge developed during the project was summarized in the *Guide.*

Tasks within the project were divided into Phase 1 and Phase 2. During Phase 1 of the project, steps were undertaken to identify problems, the state of the practice, and technological gaps. The outcome of Phase 1 was a scope of work intended to address a select number of the identified technological gaps and to develop an outline of a methodology that could lead to the design of bridges for service life. Phase 2 consisted of conducting the scope of work identified in Phase 1 and developing a methodology to design bridges for service life. Chapter 2 of the *Guide* describes the efforts undertaken to identity the service life challenges.

The results of efforts to identify the research needs and challenges with respect to service life are provided in Chapter 3. These are nine main categories: concrete durability; bridge decks; substructure; bearings; expansion joints, joints, and jointless bridges; fatigue and fracture; structural steel corrosion protection; steel bridge systems; and concrete bridge systems.

A literature search and other related tasks were conducted to identify topics needing research with respect to design of bridges for service life. Those service life issues requiring further research were divided into three categories. Research topics in Category 1 and 2 were selected for proof of concept testing within the R19A project. Category 1 topics were the highest priority and received the greatest efforts. A list of Category 1 and 2 research topics is summarized in Chapter 3 (Table 3.12). A list of Category 3 research topics recommended to be carried out by others is provided in Appendix A.

Category 1 and 2 research topics are further divided into four major categories: joints, bearings, enhancing corrosion resistance of concrete bridges, and bridge decks.

Category 1 and 2 research topics required conducting 14 research studies. Chapter 3 provides a brief look at the objectives, scope, results, and recommendations resulting from these 14 individual studies. Providing the full details of all these topics would make this final report unwieldy; therefore, references to theses, dissertations, and published papers are provided for those interested in obtaining additional information. These individual research topics resulted in the development of new details and concepts, some with associated design provisions. Some of these details and design provisions are listed in the appendices of this report, and some of the developed information is listed in the *Guide.* For example, the results of the efforts leading to the development of complete design provisions for jointless bridges are provided in Chapter 8 of the *Guide.*

Select information from the 14 research studies plus the results of other efforts undertaken within the project form the body of knowledge incorporated in the *Guide* for design of existing and new bridges for service life.

CHAPTER 1

Background

Second Strategic Highway Research Program Background

The Second Strategic Highway Research Program (SHRP 2) was authorized by Congress to address some of the most pressing needs related to the nation's highway system: the high toll taken by highway deaths and injuries, aging infrastructure that must be rehabilitated with minimum disruption to users, and congestion stemming both from inadequate physical capacity and from events that reduce the effective capacity of a highway facility. SHRP 2 is divided into four areas:

- Safety: to study the interaction between human and highway safety and comprehend the interaction among various factors involved in highway crashes, such as driver, vehicle, and infrastructure, and to develop effective solutions;
- Renewal: to develop technologies and solutions to support the systematic rehabilitation of highway infrastructure in a way that is rapid, presents minimal disruption to users, and results in long-lasting facilities;
- Reliability: to develop basic analytical techniques, design procedures, and institutional approaches to comprehending and addressing such areas as crashes, work zones, special events, inclement weather, and improving travel time reliability; and
- Capacity: to develop transportation planning that more accurately integrates economic, community, and environmental considerations into highway capacity.

The overall objective of SHRP 2 highway renewal is to achieve renewal that is performed rapidly, causes minimum disruption, and produces long-lived facilities. A related objective is to achieve such renewal not just on isolated, high-profile projects, but consistently throughout the nation's highway system.

Problem Statement

Bridge service life has been at the forefront of bridge owners' concerns for several years, particularly in the form of growing fiscal needs for bridge maintenance. As bridge maintenance costs increase, available funds for new facilities and for upgrading existing facilities become more difficult to budget. Bridge maintenance and repair affect mobility and contribute to traffic interruption. Bridge owners are spending significant portions of their annual budgets on maintenance and repair. Enhancing the service life of existing and new bridges will enhance mobility and reduce the maintenance and repair costs of bridges.

Providing safety for the public by having adequate strength for constructed facilities has been the cornerstone of the framework used by engineers during bridge design. This philosophy has served the building industry well, where most structural elements are protected from weather elements. Over the years, the design for strength has been polished, streamlined, and perfected. In the case of bridges, however, the structural elements are subject to various environmental and traffic loads. The majority of maintenance and repair actions for bridges are created by service life–related factors.

The design for service life is currently approached in a haphazard manner. Various specifications provide design and detailing provisions to address historically observed bridge service life challenges. However, there is a need to develop a service life design approach for bridges that is systematic, formal, and coherent. The design for service life of bridges should be approached in the same manner as that used for strength.

Research Objectives

The overall objective of the SHRP 2 renewal program is to achieve renewal that is performed rapidly, causes minimum traffic disruption, and produces long-lived facilities. As part of this objective, the R19A project calls for strategies to develop

high-performing bridges by identifying the problematic areas and providing solutions at the bridge system, subsystem, and component levels. The knowledge gained through this effort must be communicated with bridge professionals in ways that can be implemented in practice.

Specific objectives of the project included

- Identifying the problems that have historically limited the service life of bridges and, while learning from bridges of all span lengths, concentrating on bridges with maximum span lengths of 300 ft;
- Developing promising concepts that can enhance the service life of bridges, performing proof of concept tests, and making specific recommendation for future research by others; and
- Communicating the results with the bridge community.

Scope of Study

The research focused on developing a systematic, comprehensive, and coherent approach for design of bridges for service life. The research team explored various approaches for design for service life and identified the elements of a systematic approach, as well as ways of presenting the information in a transparent form that could be used by bridge owners and lead to development of bridges with enhanced service life. An important aspect of developing a systematic approach for design for service life was identifying the problems that have historically limited the service life of bridges. Several surveys and literature searches were conducted to identify current service life challenges. For select and high-priority service life challenges, potential solutions were identified and proof of concept tests were carried out.

Project Outcome

The body of knowledge developed during the project was summarized in the main project deliverable, the *Design Guide for Bridges for Service Life* (the *Guide*), which provides a systematic and comprehensive approach for designing bridges for service life.

The main objective of the *Guide* is to provide information about, and define procedures for, systematically designing both new and existing bridges for service life and durability. The initial approach to designing for service life is to provide a body of knowledge relating to bridge durability under different exposure conditions and constraints and to establish an array of options capable of enhancing service life relative to those conditions. However, the philosophy used in the *Guide* could also be used to establish a plan for designing a specific bridge for service life by customizing certain steps within the framework.

Included in the *Guide* are 11 chapters, each devoted to particular bridge elements, components, subsystems, or systems. Collectively, these chapters provide a basis for approaching service life design in a logical, systematic manner.

CHAPTER 2

Research Approach

This chapter outlines the efforts, steps, and approaches used to fulfill the project objectives.

To accomplish the final goals of Project R19A, tasks were divided into Phase 1 and Phase 2. During Phase 1, steps were taken to identify specific problems, comprehend the current state of the practice, and locate technological gaps. The outcome of Phase 1 was a scope of work intended to address a select number of the identified technological gaps and develop an outline of a methodology that could lead to the design of bridges for service life. Phase 2 consisted of conducting the scope of work that had been identified in Phase 1 and developing a methodology for designing bridges for service life.

The following sections briefly describe the efforts leading to identifying the bridge service life issues.

Department of Transportation Surveys

The R19A project conducted a comprehensive survey in early 2008; results are provided in Chapter 3. About a year later, a related SHRP 2 project, R19B (Bridges for Service Life Beyond 100 Years: Service Limit State Design), conducted a shorter survey. Figure 2.1 shows the 20 states that responded to the R19A survey and 15 states that responded to the R19B project. Combined, the two surveys covered a large portion of the United States, as well as the province of Ontario, Canada.

The objective of the Federal Highway Administration (FHWA) Long-Term Bridge Performance Program (LTBP) is to compile quantitative information from bridges nationwide. The R19A research team initiated communication with the LTBP as early as 2008. Within the LTBP, a number of states were interviewed to identify problematic issues that prevent bridges from achieving long service life. Figure 2.2 shows the states that were interviewed by the LTBP and states that responded to the R19A survey. The LTBP interviewed several states that did not respond to the R19A survey.

Aspects of R19B Survey Results Related to R19A Scope of Work

The following excerpt from the R19B survey indicates the service life problematic areas:

> The survey responses indicate that there are many serviceability issues relating to expansion joints and deck cracking. The other responses include: deterioration/section loss of beam ends, painting of steel members, problems with bearings, corrosion of reinforcement, and deck overlays.

Figure 2.3 illustrates the responses to the first question in the R19B survey.

Summary of Consultant Survey Results

After submission of the Phase 1 report and while the research team was waiting to receive review comments, one additional survey was carried out by the R19A research team that sought input from design consulting firms HDR, Inc. and Atkins (previously PBS&J), which subcontracted to the R19A project. Figure 2.4 shows the locations where these two firms have local offices. The survey focused on gathering the experience of HDR, Inc. and Atkins bridge professionals with respect to bridge durability in the states where they provide services.

A series of questions was asked of multiple HDR, Inc. and Atkins offices representing states across the country regarding their experience with local bridge durability and service life issues. Questions were asked regarding service life and maintenance requirements for bridge systems, subsystems, and components. Combined responses were received from bridge personnel representing Arizona, California, Colorado, Florida, Illinois, Missouri, Massachusetts, Nevada, North Carolina, Nebraska, Ohio, and Pennsylvania.

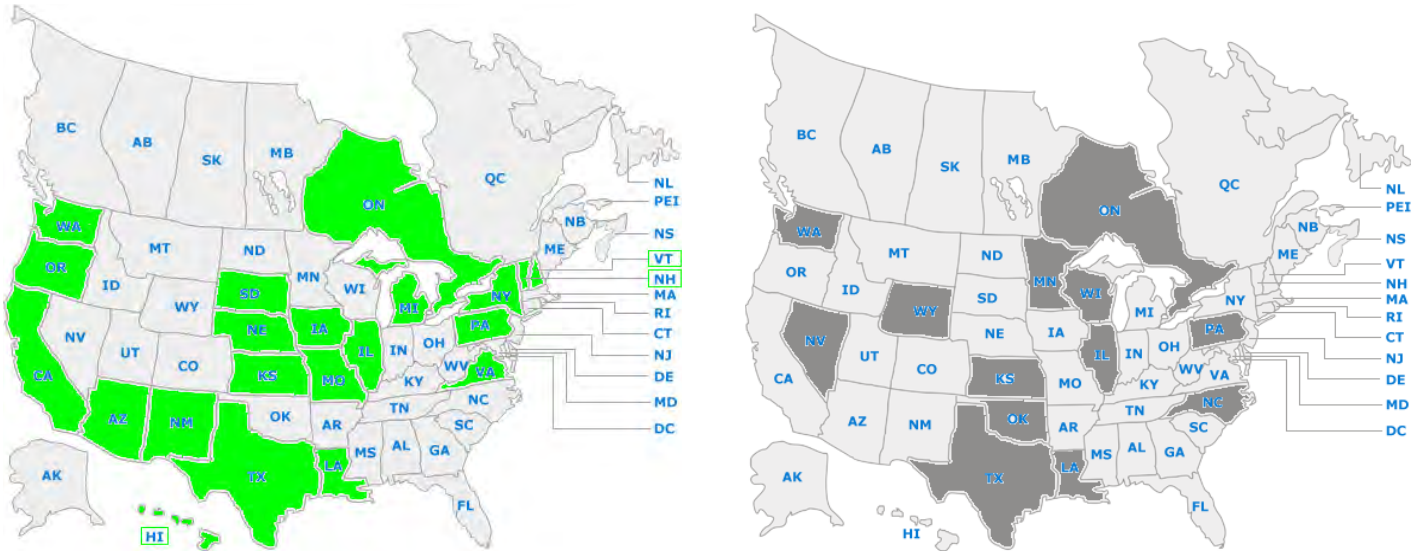

(a) (b)

Figure 2.1. States that responded to the (a) R19A and (b) R19B surveys.

Bridge System Service Life and Durability

The first series of questions dealt with what common steel or concrete bridge system (such as steel girder, steel truss, prestressed concrete girder) is the most problematic regarding service life and typically requires the highest level of maintenance. The predominant answers were painted steel trusses and steel girders. Other responses included concrete or steel bridges with deck joints, posttensioned segmental girders in aggressive environments, and concrete spalling. Some respondents noted that all systems require some form of maintenance.

- *Reasons for these situations*—Major reasons for system service life reduction and maintenance were steel corrosion due to deicing chemicals or saltwater environment, paint system failures and need for cleaning, corrosion of reinforcing steel, leaking deck joints, and fatigue.
- *Potential needed research*—Responses included improved coating systems and noncorrosive deicing materials.

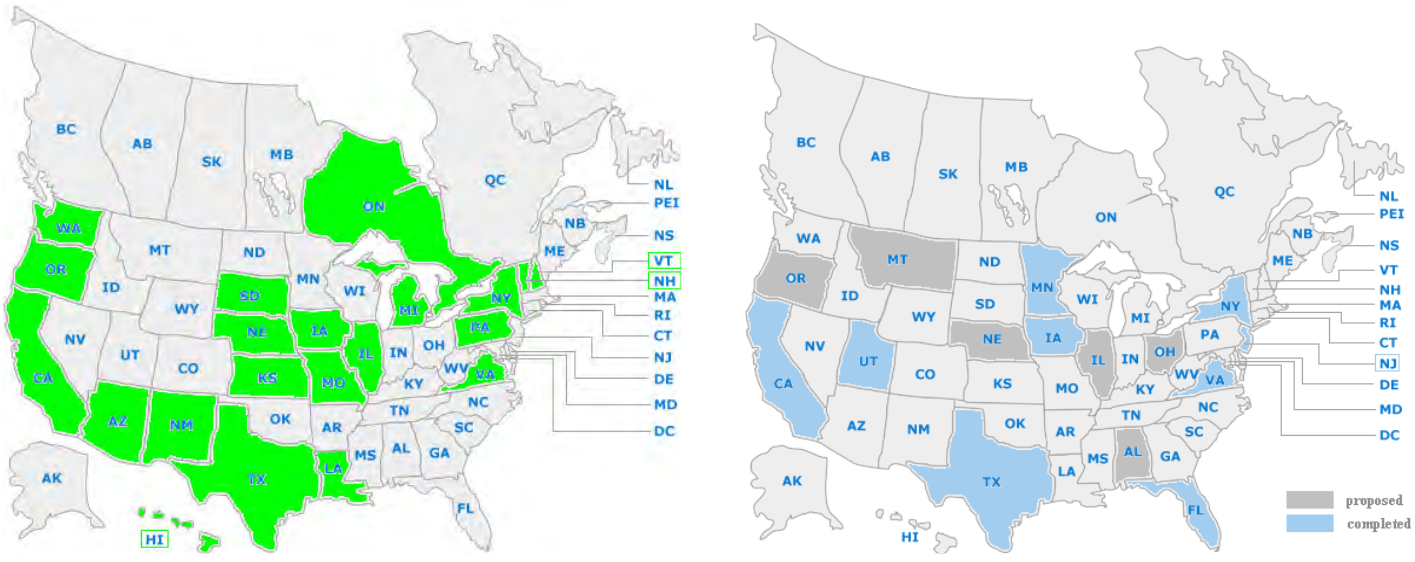

(a) (b)

Figure 2.2. States that responded to the (a) R19A and (b) LTBP surveys.

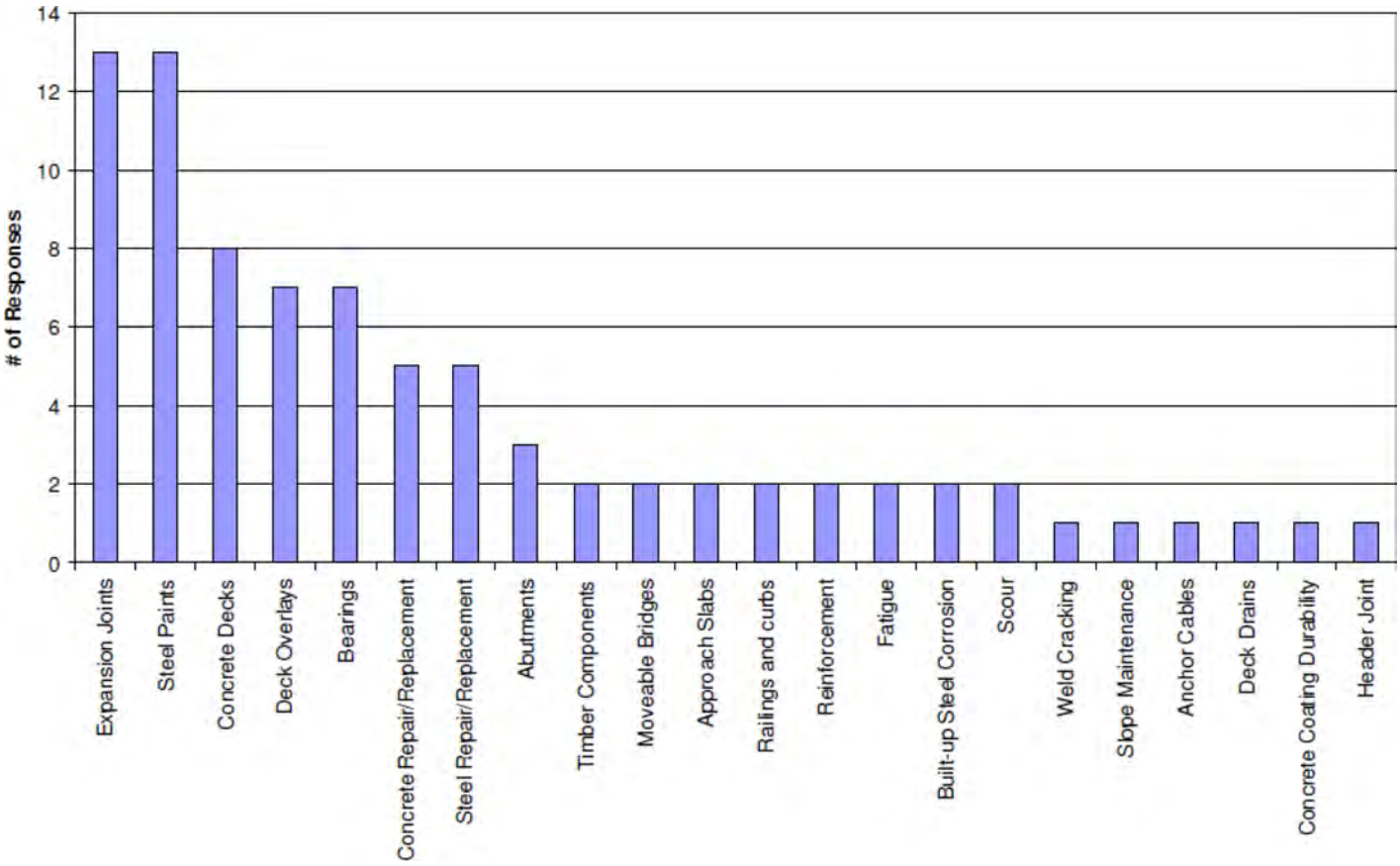

Figure 2.3. Responses to SHRP 2 R19B Survey Question 1.

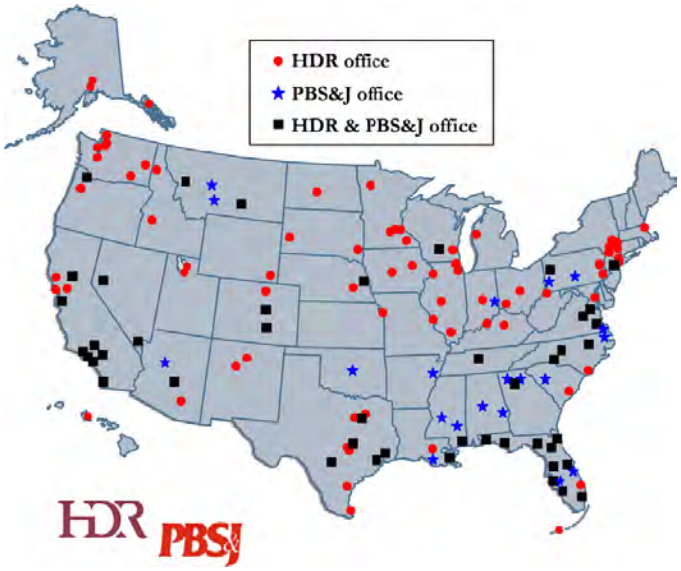

Figure 2.4. U.S. map with locations of branch offices for HDR, Inc., and Atkins.

- *Systems that have performed the best*—Most respondents listed prestressed concrete girder systems, particularly prestressed I-girders and nonskewed prestressed girders. Others mentioned continuous systems without joints and weathering steel girder systems.

Bridge Subsystem Service Life and Durability

The second series of questions dealt with what subsystem (such as decks, piers, abutments) is the most problematic regarding service life and typically requires the highest level of maintenance.

Concrete decks were by far the most predominant answer. Other answers included areas below open joints, substructure, and hinges in continuous box girder bridges.

- *Reasons for these situations*—Reasons for deck service life issues were environmental effects, moisture, chlorides, corrosion of reinforcing steel, material quality and construction issues, higher traffic and loads, and cracking.
- *Potential needed research*—Many areas of potential research were noted, including improved materials (high-performance concrete) and details, improved reinforcing

steel protection, improved deck preservation systems, improved joint details, and effective concrete curing.
- *Subsystems that have performed the best*—For decks, the respondents identified the best performers as cast-in-place decks with adequate reinforcing bar cover, cast-in-place decks with burlap curing and strict enforcement of temperature gradient during pouring, high-quality concrete and quality control methods, and properly constructed latex-modified concrete– or microsilica-modified concrete–overlaid decks. Other responses included integral bridges and piers and abutments when joints are eliminated.

Bridge Component Service Life and Durability

The third series of questions asked what common bridge components (such as a bearing type, sliding surface in bearings, expansion joint type, joints in approach slab, and so forth) are the most problematic regarding service life and typically require the highest level of maintenance.

Deck expansion joints, including strip seals, compression seals, modular joints, and joints of all types were the predominant response. Problems with bearings, especially older steel rocker types, were also listed frequently. Additional responses included joint seals and bearings in skewed bridges and problems with hinges.

- *Reasons for these situations*—Reasons for joint failure were environmental and traffic distresses, plow damage, material failure, adhesive failure, improper installation, lack of maintenance, and distortion due to skew. Freezing of steel rocker bearings was the greatest reason for bearing problems.
- *Potential needed research*—Areas listed for potential research included improved joint systems and materials, longer jointless systems and methods for eliminating joints, analytical studies on effects of skew on joint and bearing movement, and joint systems that work with skews. Research areas for bearings included improved bearing details and further studies of reinforced elastomeric bearings, sliding surfaces, and disk bearings.
- *Components that have performed the best*—Eliminating joints and the use of integral and semi-integral abutments were the greatest responses. Nonskewed bridges were also mentioned. Of the joint types, strip seal joints were identified as performing the best for shorter movements. Steel-reinforced elastomeric bearings were identified as the best bearing performer. Disk bearings also were mentioned.

Input from Long-Term Bridge Performance Program

Starting in 2008, R19A team members established communication with the LTBP project, led by Rutgers University, and held a number of meetings at FHWA headquarters, during which a summary of R19A activities, research direction, and survey results were presented and the importance of collaboration was emphasized.

Input from AASHTO Bridge Committees

Throughout the project, the research team received feedback from various American Association of State Highway and Transportation Officials (AASHTO) bridge committees through presentations at the committee meetings and phone conferences. Table 2.1 summarizes some of the major activities related to communication with AASHTO bridge technical committees during Phase 1 of the project. Throughout

Table 2.1. Summary of Communications with AASHTO Bridge Subcommittees

Date	Activity	Participants
February 2008	Presentations to AASHTO T-14 Committee on Steel Bridges	R19A research team
April 2008	Presentation to AASHTO T-10 Committee on Concrete Bridges	R19A research team
January 2009	Presentation to AASHTO T-5 on R19A's activities during 2009 TRB annual meeting	R19A research team
February 2009	Joint meeting in Orlando, Fla., with AASHTO T-14 and AISI Steel Bridge Task Force	R19A research team
July 2009	Presentation to AASHTO T-2 Committee on Bearings and Expansion Devices	Atorod Azizinamini and Ed Power
July 2009	Presentation to AASHTO T-9 Committee on Bridge Preservation	Atorod Azizinamini
July 2009	Presentation to AASHTO T-10 Committee on Concrete Design	Glenn Myers
July 2009	Presentation to AASHTO T-14 Committee on Steel Bridges	Ed Power and Dennis Mertz
July 2009	Presentation to AASHTO SCOBS general session	Atorod Azizinamini
Throughout Phase 1	Several phone seminars with various state bridge engineers	R19A research team

Note: SCOBS = Subcommittee on Bridges and Structures.

the project, various presentations were made during every AASHTO bridge subcommittee meeting.

Input from Experts Outside the R19A Research Team

Several individuals with expertise related to the R19A research theme were identified, and meetings and phone conferences were held to acquire their input. Table 2.2 briefly summarizes some of the major activities related to these communications during Phase 1 meetings. Additional meetings beyond those listed in Table 2.2 were also held during Phases 1 and 2.

Input from Industry

Several companies were contacted to acquire their input and viewpoints, including companies involved with expansion joints and bearing manufacturing, various reinforcing bar manufacturers, and a representative from the coating industry.

Literature Search

A comprehensive literature search identified available information worldwide. Published, unpublished, and ongoing research projects were examined to better comprehend the state of knowledge.

Phase 1 Major Findings

The results of Phase 1 activities, which revealed the need for the development of a systematic approach for design for service life, were used to develop a scope of work for Phase 2 of the investigation.

The major conclusion from the Phase 1 study was that there was a need to develop a stand-alone document that was comprehensive, coherent, transparent, and devoted to design of bridges for service life—a document that could be used by the bridge community to design new and existing bridges for service life in a systematic manner. Therefore, it was decided to develop such a stand-alone document. This document became the *Design Guide for Bridges for Service Life* (the *Guide*).

Figure 2.5 summarizes the various activities leading to development of the *Guide.* Identifying the problematic issues causing service life problems was the first undertaking. Several tasks, including department of transportation (DOT) surveys and input from the industry, were performed to gather this information. The results of many activities, listed in the Problematic Issues box shown in Figure 2.5, led to the establishment of problems needing considerations during design for service life of bridges.

As noted in Figure 2.5, the problematic issues identified through the various listed tasks fell into several major categories. Within each category, various problems needing research to fill the knowledge gap were identified. The project resources were limited, preventing research into all the identified problems, and priority had to be established. Technology, strategy, and ranking tables were developed as part of the decision-making process for streamlining and identifying the research topics and ranking their priority.

Technology, strategy, and ranking tables were used to divide the selected research topics into three categories, as shown in the Suggested Topics block of Figure 2.5. Within the scope of this project, research studies were carried out on higher-priority topics (Categories 1 and 2). Category 3 research topics were left for others to complete. Because of the limited resources and as part of the project requirements, the scope of work for research studies carried out for Category 1 and 2 topics was limited to proof of concept tests, signifying that additional work would be needed before the concepts are used in practice. The level of investigation conducted on Category 1 was generally greater than that conducted for Category 2. Chapter 3 lists the Category 1 and 2 research topics investigated within the R19A project, and Category 3 research topics are described in Appendix A.

Results of research studies conducted on Category 1 and 2 topics are included in the *Guide.* However, the new concepts, details, and design provisions were placed in appendices of the *Guide,* signifying that they should be used with caution until such time as more research has been conducted.

Table 2.2. Summary of Communications with Experts Outside the Research Team: Phase 1

Date	Activity	Participants
April 2008	Phone seminars on bridge deck and concrete durability with David Darwin (University of Kansas)	R19A research team, SHRP 2 program officer, ad hoc committee, and David Darwin
May 2008	Phone seminars on bearing design with Charles Roeder (University of Washington)	R19A research team, ad hoc committee, and Charles Roeder
May 2008	Phone seminars on durability of steel bridges with John Fisher (Lehigh University)	R19A research team and John Fisher
May 2008	Phone seminars on joint durability with Cathy French (University of Minnesota)	R19A research team and Cathy French

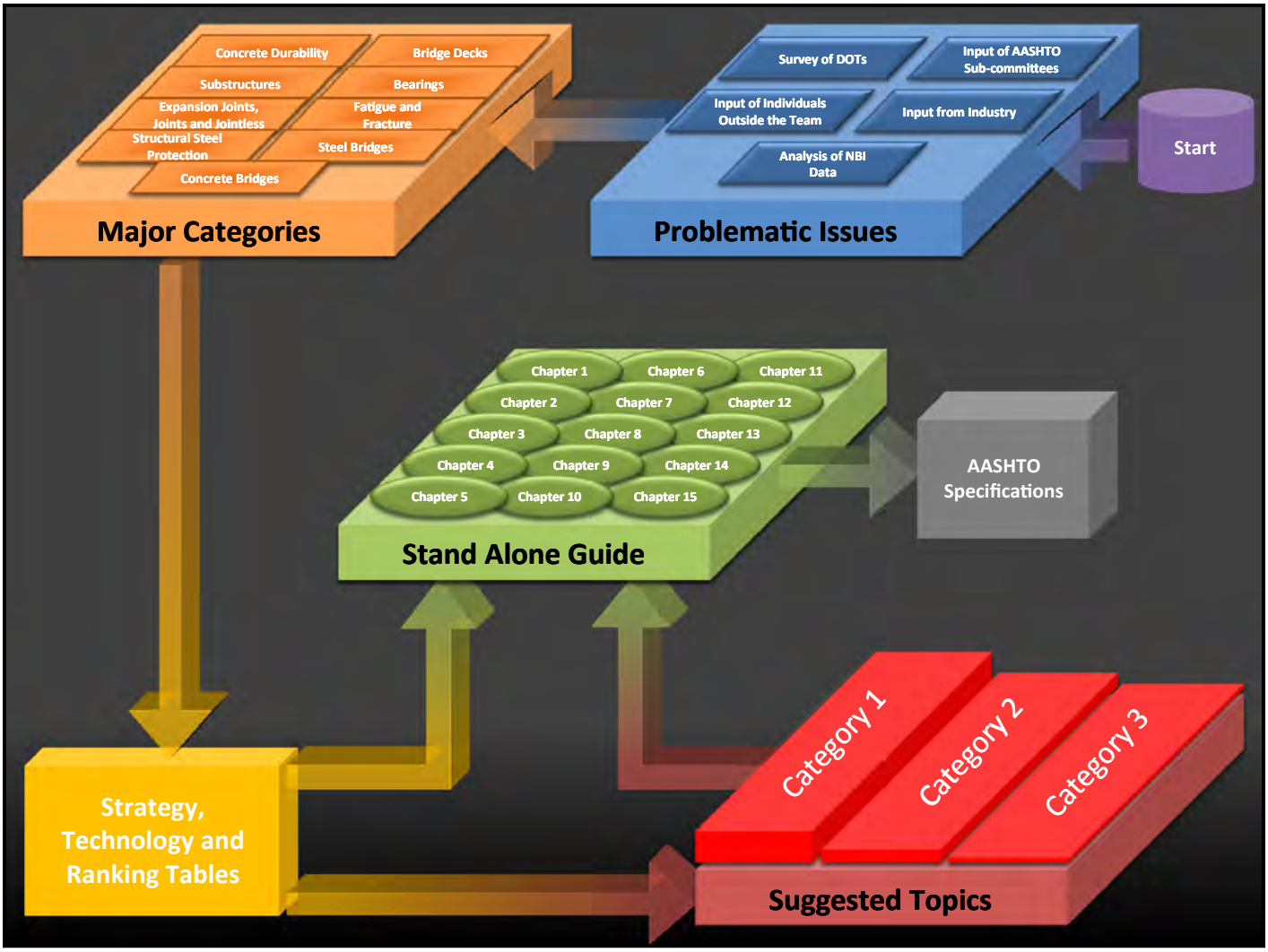

Figure 2.5. Overall project activities.

Guide: Project Main Product

Information summarized in the *Guide* was obtained through many activities and resources, including

- Results of research studies conducted on Category 1 and 2 research topics;
- Available information from the *AASHTO LRFD Bridge Design Specifications* (AASHTO 2004, 2010b) and *AASHTO LRFD Bridge Construction Specifications* (AASHTO 2010a);
- Research results developed by other investigations;
- Synthesis of state-of-the-art information related to various topics covered by the *Guide;* and
- Input from AASHTO bridge subcommittees, DOTs, industry, and nonprofit organizations representing various industries.

The *Guide* is a stand-alone document and contains the summary findings of the entire project related to service life design.

The use of the *Guide* was originally intended for bridges with maximum span lengths of 300 ft or less. However, the general framework developed for design for service life and described in Chapter 1 of the *Guide* is applicable to any span length and bridge type.

With permission of the SHRP 2 program officer, the first use of the *Guide* was in the form of a brief summary of Chapter 1 that was provided to short-listed consultants on the new Tappan Zee Bridge in New York in 2012. Through a series of meetings and presentations, the New York Thruway Authority and New York DOT decided to make the brief summary of the *Guide* available to the consultants as a reference for service life design of bridges.

CHAPTER 3

Findings and Applications

This chapter summarizes the project findings that ultimately led to the development of the main product of the project, the *Design Guide for Bridges for Service Life* (the *Guide*).

Categories of Bridge Service Life Issues

The results of the literature search and other activities (see Chapter 2 for details) that were performed in Phase 1 to identify and comprehend a broad range of service life issues and develop a general framework for service life design were grouped into the following nine categories:

- Concrete durability;
- Bridge decks;
- Substructure;
- Bearings;
- Expansion joints, joints, and jointless bridges;
- Fatigue and fracture;
- Structural steel corrosion protection;
- Steel bridge systems; and
- Concrete bridge systems.

The main reason for dividing the research findings into these nine categories was to develop an organized approach that would assist in identifying and prioritizing the knowledge gaps related to service life design and to establish the scope of further research to be conducted in Phase 2 of the study.

The following sections briefly summarize the information gathered under each of these general categories.

Concrete Durability

Concrete bridge structures are subjected to severe conditions, yet to be cost-effective they must provide satisfactory performance for long periods of time. The greatest durability challenge identified for these types of structures was corrosion of reinforcing steel, which is due mainly to cracking or poor concrete cover (or both) that allows moisture and chloride intrusion. In addition to the key factor of chloride solutions, hydroxyl ions and the concentration and movement of oxygen are important factors in the corrosion of reinforcing steel. Cracking can be caused by loads or environmental effects. In a new bridge structure, cracking is mainly attributed to moisture loss and temperature change. As a structure ages, corrosion, physical effects, and chemical reactions can also contribute to cracking. Concretes that have low permeability and minimal cracks have reduced infiltration of water and aggressive solutions, enabling extended service life. Design, material selection, and construction practices should be properly executed to ensure minimal cracking and reduced infiltration of aggressive solutions and to further resist damage due to freeze–thaw cycles, abrasion, and chemical attack.

In design, proper drainage details can minimize ponding and prolonged exposure of bridge components to aggressive solutions, thus minimizing corrosion and other environmental distress. Similarly, proper cover depth is essential to slow the intrusion of chlorides to the reinforcing steel.

In material selection, a very efficient way of resisting the intrusion of chlorides is using supplementary cementitious material (SCM) (pozzolans and slag) to reduce concrete permeability, along with a proper water–cementitious materials ratio (w/cm). When concrete is exposed to cycles of freezing and thawing, it must be properly air entrained, have sound aggregates, and have the maturity to develop sufficient strength for long-lasting service. In general, the total air content of the mixture is determined. However, the air void parameters that indicate the distribution and size of the voids are needed for proper protection against freezing and thawing. A minimum compressive strength of 4,000 psi is commonly specified in bridge decks to resist freezing and thawing and salt scaling. Concrete with hard siliceous aggregates and satisfactory compressive strength is needed to ensure a safe road surface with proper wear and skid resistance.

Good construction practices, mainly ensuring the proper location of reinforcing steel for proper cover depth, consolidation, and curing, are essential for longevity. Curing is generally achieved by external treatment of concrete, such as covering by wet burlap and plastic or by misting. However, the provision of moisture for the inside of the concrete through internal curing is also very beneficial, especially for concretes with low w/cm. Proper consolidation will minimize entrapped air voids that can reduce strength and durability. For areas that are hard to reach and areas that are congested with reinforcement, self-consolidating concrete may be the solution.

The use of performance specifications, rather than prescriptive specifications, should be adopted to ensure the quality needed. In performance-type specifications, the characteristics of the mixture are specified rather than the mixture itself, allowing the material supplier and contractor to be innovative in the selection of materials and in the proportioning of the mixture. The material supplier, contractor, and the user share responsibility, as the material supplier and contractor are responsible for the development of the product and the user for its acceptance.

To extend concrete bridge service life in existing structures, preventive maintenance should be emphasized and proper repairs should be performed before extensive damage occurs and costly rehabilitation is required. It is very important to keep concrete dry for improved durability when it is exposed outdoors. Ponding of the surfaces that keeps concrete saturated should be avoided by proper design and preventive maintenance. The scope of repair or rehabilitation work can vary significantly, from sealing of cracks to application of overlays to replacement of large components such as bridge decks. Preventive maintenance may also include tasks as simple as washing the structure to eliminate chloride buildup.

Selection of concrete materials and mixture proportions is usually based on empirical relationships between concrete mixtures and laboratory and field performance. This approach assumes that the concrete selected supports the desired service life for the structure. The use of deterioration models involves predicting service life by using calculations in which degradation mechanisms and reaction rates for those mechanisms are considered. However, many service life prediction methods focus on the effect of one degradation process. Experience has shown that degradation results either when one or more degradation processes are operative or from the interaction of environment and loads. These combined effects complicate the prediction of service life for both new and existing structures; in addition, the environmental factors and loads may not be well defined.

Corrosion of reinforcing steel can cause serious and costly damage to reinforced concrete structures. Concrete is a brittle material that is prone to cracking and as such may not be able to adequately protect the steel. For additional steel protection, corrosion-resistant steel reinforcement, cathodic protection, and electrochemical chloride extraction (ECE) should be seriously considered to increase the service life of bridges.

Synopsis of Literature Search and Other Available Information on Concrete Durability

In general, the study identified factors affecting concrete durability that included environment, design practice, material properties and their proportioning, and construction practices and workmanship. Other factors such as specifications, cracking, and selection of protective systems were also found to affect durability. The study summarized various protective systems that included corrosion-resistant reinforcement, certain admixtures, cathodic protection, and ECE. Corrective measures for service life extension, predicting service life of new structures and existing structures, and life-cycle cost analysis were also investigated. The literature search also identified various types of concrete distress and deterioration and the possible solutions.

Factors Affecting Concrete Durability

- *Environmental influences*—Exposure to harmful environmental factors such as chemicals, cycles of freezing and thawing, temperature and moisture changes, vibration, and impact can significantly reduce the service life of concrete.
- *Design practice*—Design and specification issues such as reinforcement types and detailing, joints, long slender components, inadequate creep provisions, and poor drainage can affect reinforced concrete deterioration. Service life is greatly increased by selecting appropriate design features that provide satisfactory drainage, sufficient cross section and reinforcement, proper cover, adequate stability, and small deformations.
- *Materials and proportioning*—Selection of proper ingredients and using them in proper proportions also affects durability. Cementitious materials should be of the sufficient amount and of the right type; for example, portland cements are selected with low tricalcium aluminate (C_3A) if concrete is exposed to sulfates, and low alkali contents when alkali–silica reaction (ASR) is a concern. Aggregates with poor particle shape and poor gradation would have higher water demand, paste content, and increased w/cm adversely affecting the durability. The w/cm should not be too low; a range between 0.40 and 0.45 is commonly used for bridge decks. This, in combination with the use of SCM (pozzolans or slag) provides for low permeability (Ozyildirim 1998, 1999).
- *Construction practices and workmanship*—Attention to good construction practices is crucial for achieving long-term durability of reinforced concrete. Proper cover depth is essential to slow the intrusion of chlorides to the level of reinforcing steel. Proper consolidation is needed to eliminate

entrapped air voids that would reduce strength and facilitate the penetration of aggressive solutions. Proper curing enables the hydration reactions to continue and reduces volumetric changes that can cause cracking. Adding extra water at the job site adversely affects the strength and durability. A well-qualified and trained workforce and well-executed workmanship increases productivity, reduces material waste, and provides expected service life. Proper use of test methods are needed to ensure that quality concrete is achieved.

Specifications

Current specifications generally are of a prescriptive type requiring a recipe of ingredients. They restrict innovation by limiting the use of many possible combinations of materials. In performance-type specifications, the characteristics of the mixture are specified rather than the mixture itself, allowing the producer to be innovative in the selection of materials and in the proportioning of the mixture. The contractor and the user share responsibility: the contractor is responsible for development of the product, and the user for its acceptance. Compensation can be adjusted by inclusion of bonus and penalty depending on the quality of the product. Bonuses would encourage the production of quality material and adherence to proper construction practices that would lead to longevity and minimal distress, such as reduced cracking in the structure. Penalties or rejections would get the attention of the contractor and encourage the contractor to take corrective actions.

Cracking

Cracking can be due to loads or environmental effects (ACI 224R 2001; TRB 2006). In new bridge structures, cracking is primarily attributed to moisture loss and temperature change. With age, corrosion, physical and chemical reactions, and loads can also contribute to cracking. To reduce cracking, shrinkage should be reduced; however, cracking also depends on other factors such as restraint, elastic modulus, creep, and tensile strength. Proper selection of materials and proportioning can reduce moisture- and temperature-related factors. For example, reductions in water content and paste content reduce shrinkage; large aggregate sizes also help to reduce shrinkage; and reduced cement contents and replacement of cements with supplementary cementitious materials contribute to reduction in heat generation. For reduced thermal gradients and reduced contraction, aggregates with a low coefficient of thermal expansion can be used. In addition, aggregates with low modulus of elasticity are desirable to ensure lower stresses for a given deformation. Proper proportioning and curing are essential to reducing cracking. Internal curing through the use of reservoirs, such as prewetted lightweight aggregates, supplies water throughout a freshly placed cementitious mixture. This water maximizes hydration and minimizes self-desiccation and its accompanying stresses, which may produce early-age cracking (Bentz and Weiss 2011). Fibers are also used to control cracking.

Protective Systems in Reinforced Concrete

Several types of protective systems such as corrosion-resistant reinforcement, cathodic protection, ECE, sealers, membranes, and overlays are available to improve the durability of reinforced concrete. However, it is very important to use the proper materials and procedures to achieve the longevity sought.

- *Corrosion-resistant reinforcement*—Corrosion-resistant reinforcement provides more resistance to corrosion through a higher corrosion threshold value. Thus, high amounts of chlorides can penetrate to the level of reinforcement without causing significant damage to the reinforcing steel. These systems include epoxy-coated reinforcement, galvanized reinforcement, titanium reinforcement, stainless steel reinforcement, stainless steel–clad reinforcement, nickel-clad reinforcement, and copper-clad reinforcement.
- *Admixtures for corrosion protection*—Chemical admixtures can be added to concrete during batching to protect against corrosion of embedded steel reinforcement due to chlorides. There are two main types: corrosion-inhibiting (protection for steel) and physical-barrier (reducing the ingress of harmful solutions) admixtures. Some corrosion-inhibiting admixtures also act as physical-barrier admixtures.
- *Cathodic protection*—When it was first introduced, cathodic protection was used mainly to prevent further corrosion after repair of damaged structures. Later, however, according to Polder (1998), cathodic protection was incorporated into new construction in an effort to prevent corrosion from starting. For cathodic protection, both impressed current and sacrificial anode, or galvanic systems, have been used successfully on bridges in the United States. Impressed current systems are used most often on bridge decks. According to Kepler et al. (2000), sacrificial anode systems are generally used in substructures.
- *Electrochemical chloride extraction*—ECE is applied to concrete structures containing reinforcement to extract chlorides from the concrete. Studies indicate that ECE can successfully remove substantial amounts of chloride from contaminated concrete and leads to an increase in the pH of the concrete and repassivation of corroding reinforcing steel (Kepler et al. 2000). A list of projects published (Sharp et al. 2002) demonstrates that ECE is a promising bridge restoration alternative. The systems worked best on bridge decks, but most agencies cannot afford to close a bridge deck or limit traffic flow for 4 to 8 weeks at a time, which is required for treatment. With ECE, the possibility exists of initiating the ASR as a side effect, as alkali metal ions are rearranged and hydroxyl ions are generated at the reinforcement. Studies have indicated that the ASR can be mitigated by lithium (Velivasakis et al. 1997).

Correction Measures for Service Life Extension

Various repair techniques are available to extend the service life of a concrete structure. In repair, the deteriorated materials, components, or elements are replaced or corrected (ACI 546 2006). The selection of a proper repair material is one of many interrelated steps; equally important are surface preparation, the method of application, construction practices, and inspection. Initially, a condition evaluation is needed that includes design and construction documents, visual observation, and destructive and nondestructive testing. For repair materials, durability rather than high strength is the desired property. Due to high early strengths and high early modulus of elasticity, conventional repair materials are prone to cracking. Conventional portland cement concrete is widely used to repair structures. It is readily available and economical. However, in aggressive environments, portland cement concrete modified with silica fume, acrylics, styrene–butadiene latex, or epoxy may be needed for longevity. The specified repair material must be dimensionally compatible with the existing concrete substrate to minimize the potential for failure. In repairs, due to traffic flow and time constraints, rapid-setting materials are sought that provide short setting time and high early compressive strength. Durability should be carefully checked.

Predicting Service Life of Reinforced Concrete

Many service life prediction methods focus on the effect of one degradation process (ACI 365 2000). Experience has shown, however, that degradation results when one or more degradation processes are operative or from the interaction of the environment and loads (Hookham 1990). Service life can be limited by many factors, such as the presence of chlorides, cycles of freezing and thawing, critical saturation, volume changes due to moisture and temperature, and to a lesser degree, by carbonation or aggressive chemicals, such as acids and sulfates. For large elements and for those kept wet by contact with the ground or water, alkali aggregate reaction and delayed ettringite formation (high early temperatures) can be a problem. Temperatures should be kept down during early curing, and supplementary cementitious materials should be used. Service life is also influenced by mechanical loads, such as fatigue, vibration, and local overloads.

Methods that have been used for predicting the service lives of construction materials include estimates based on experience, deductions from performance of similar materials, accelerated testing results, mathematical modeling based on the chemistry and physics of expected degradation processes, and applications of reliability and stochastic concepts (Clifton and Knab 1989). Several mathematical models have been developed to predict the service life of concrete subjected to degradation processes such as corrosion, sulfate attack, leaching, and freeze–thaw damage (Clifton 1991; Williamson et al. 2007).

Prediction of Remaining Service Life

The methods for predicting the remaining service life of existing concrete structures are basically the same as those for new structures (ACI 365 2000).

Most of the reported work on predicting remaining service lives of reinforced concrete structures has dealt with corrosion of the concrete reinforcement. Two major prediction approaches that have been pursued are the modeling approach and corrosion measurements (ACI 365 2000).

Extrapolation techniques can be used to predict the remaining service life of a concrete structure. Based on a set of known points obtained by inspection or tests, new points can be predicted, but this technique will often lead to a less meaningful result with greater uncertainty.

Commercial Software to Predict Service Life

Commercial software programs are available for predicting service life. LIFECON is the Integrated and Predictive Life-Cycle Maintenance and Management Planning System, which includes life-cycle cost, life-cycle performance, life-cycle ecology, and health and comfort (Soderqvist and Vesikari 2003). STADIUM can be used to follow the transport of ions and liquids in reactive porous media. The successor model to STADIUM, SUMMA, is under development and will include a number of enhancements, including an improved user interface (Heffron 2007). SUMMA will also be able to handle cracks in concrete, representing an important refinement because concrete cracking is very common and facilitates penetration of chlorides. Life-365 is a standard model developed for predicting the service life and life-cycle cost of reinforced concrete exposed to chlorides. The DURACON software that can predict chloride profiles for future ages is available for use at both the design and construction phase.

DIFFUZON combines diffusion transport and local chemical equilibrium for all species of a cementitious material. Multilayer-systems commercial software named FEMMASSE MLS incorporates pertinent physical and mechanical models governing the behavior of the structural elements under consideration.

Life-Cycle Cost Analysis

The National Institute of Standards and Technology (Fuller and Petersen 1995) defines life-cycle cost as "the total discounted dollar cost of owning, operating, maintaining and disposing of a building or a building system" over a period of time. Life-cycle cost analysis is an economic evaluation technique that determines the total cost of owning and operating a facility over a period of time.

Types of Distress and Deterioration

Distresses in concrete structures lead to deterioration that can cause premature failure and require costly repairs or reconstruction. There are three basic visual symptoms of

distress in a concrete structure: cracking, spalling, and disintegration. The effects of deterioration may not be manifested visually. For example, internal cracking may not be visually observed for a long time even though the structural integrity may be reduced to an unacceptable level. Deterioration of material properties mostly sets in under the combined action of internal and external factors. Internal factors are those that determine a material's quality (i.e., the way it is made, placed, and cured). The quality is governed by characteristics such as shrinkage, creep, and thermal behavior, which are inherent in its nature. External causes of deterioration are broadly grouped as physical, chemical, or mechanical. There are also the biological factors; however, they are not considered to be major concerns. The main physical factors are fluctuations of moisture content, temperature, carbonation, freezing and thawing, salt crystallization, wear, and fire; the main chemical factors are aggressive gases and liquids causing corrosion, alkali aggregate reactions, sulfate attack, and acid attack; the main mechanical factors are load, friction, and vibration.

Analysis of DOT Survey

Eighteen states and one Canadian province responded to the department of transportation (DOT) survey submitted by the R19A research team. A summary of the survey results for the various numbered requests and questions related to concrete durability follows.

1. **Prioritize the following durability-related distresses that are most commonly found in existing bridge structures.**
   Table 3.1 shows the range of rating values that corresponded to various levels of distress frequency for the different structural elements. The rating scale considered was from 1 to 5.

Table 3.1. Rating Scale Considered in Study

Rating Range	Frequency
1.00–1.67	Routinely found
1.67–3.00	Occasionally found
3.00–4.33	Rarely found
4.33–5.00	Considered not found

The most common deck-related stress was the corrosion of reinforcement, rated as 1.6. Freezing and thawing (2.6) and abrasion and wear (2.9) were found to be a problem occasionally. ASR (3.9) was considered rare in occurrence, and sulfate attack (4.7) was considered not to be a problem (see Figure 3.1).

For beams, the corrosion of reinforcement (2.2) was occasionally considered to be a problem. Freezing and thawing (3.1) and ASR (3.7) were rarely a problem. Sulfate attack (4.8) and abrasion and wear (4.9) were considered not to be a problem (see Figure 3.2).

The corrosion of reinforcement (2.1) in piers was considered to be a problem occasionally. Freezing and thawing (3.2), ASR (3.6), and abrasion and wear (4.3) were rarely a problem, and sulfate attack (4.7) was considered not to be a problem (see Figure 3.3).

Finally, at the foundations, the corrosion of reinforcement (3.2), freezing and thawing (4.1), and ASR (4.1) were rarely found to cause any problem. Sulfate attack (4.5) and abrasion and wear (4.9) were considered not to be a problem (see Figure 3.4).

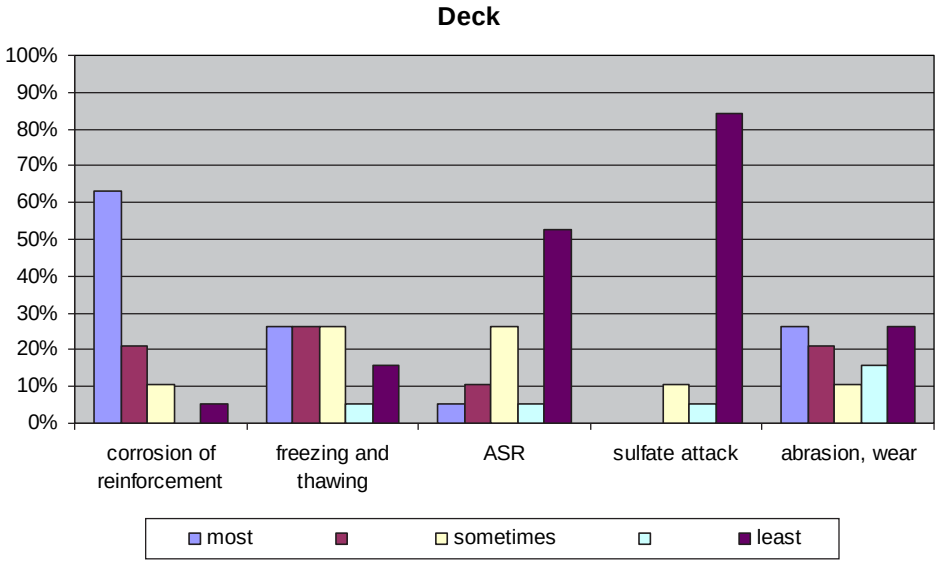

Figure 3.1. Survey results for deck-related distresses.

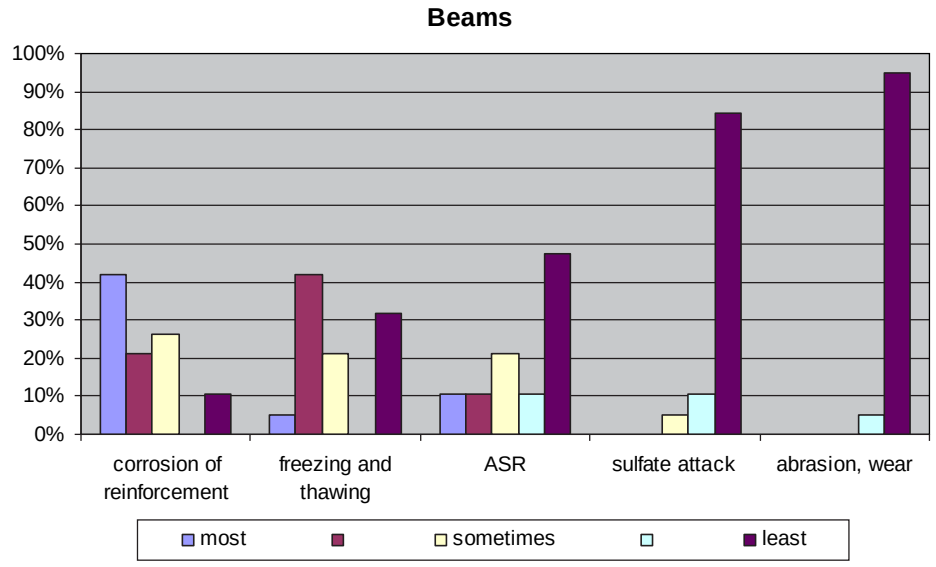

Figure 3.2. Survey results for beam-related distresses.

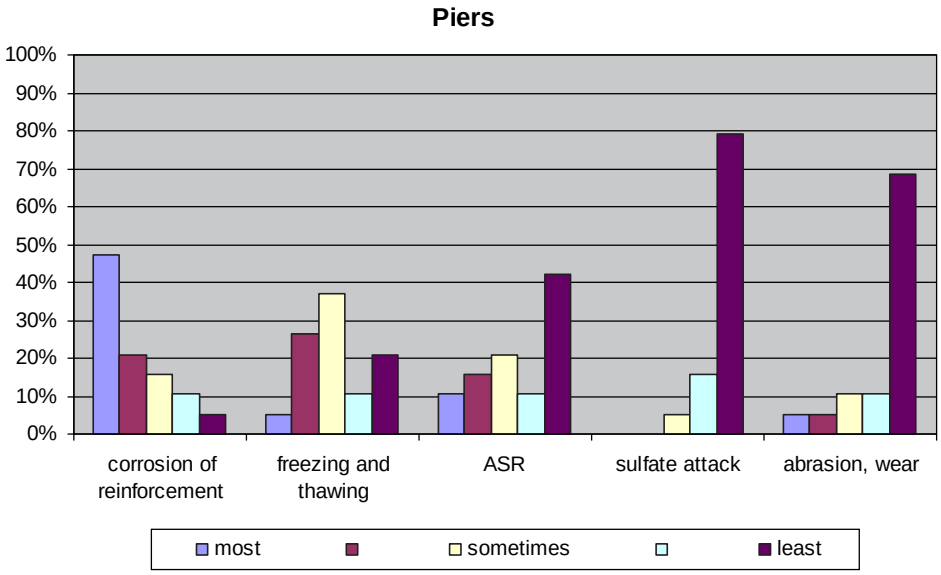

Figure 3.3. Survey results for pier-related distresses.

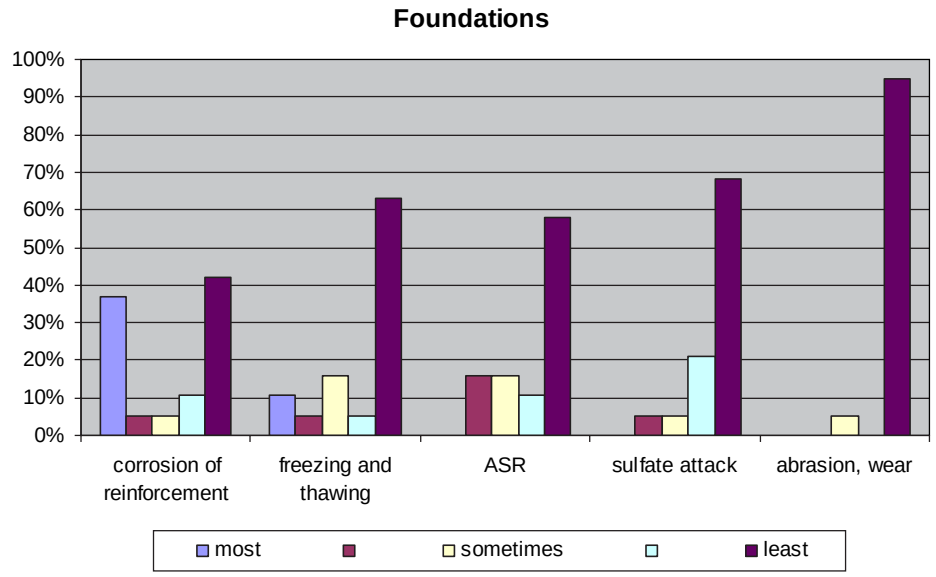

Figure 3.4. Survey results for foundation-related distresses.

2. **How do you detect corrosion?**
Eighty-nine percent of the states surveyed answered this question, with the exceptions of Pennsylvania and Virginia. Fifty-eight percent of those states, which included California, Iowa, Michigan, Missouri, Nebraska, New Mexico, New York, Texas, and Washington, indicated that they perform visual inspections during which they usually look for signs of concrete deterioration such as spalling, delamination, and cracking. In addition to visual inspection, 6% perform chloride content tests, another 6% do half-cell tests, 6% take cores to determine the loss of section, and 18% do both chloride and half-cell testing (see Figure 3.5).

The survey results show that 40% did not mention explicitly that they perform visual inspection; 28% perform both chloride and half-cell tests, and only 12% perform half-cell testing alone.

In addition to chloride and half-cell testing, Ontario mentioned linear polarization and Galvapulse as additional tests.

The threshold for chloride content was provided by only 26% of the states. The values varied from 1 lb/yd^3 in Kansas and 1.4 lb/yd^3 in Illinois to 2 lb/yd^3 in California, Missouri, and Texas. Also, 26% provided information about the threshold for half-cell potential, with values varying from –200 mV in New York, –290 mV in Missouri, and –350 mV in California, Hawaii, and Kansas.

3. **Classify as routinely, occasionally, rarely, not accepted, the type of reinforcement used in your past bridge projects.**
Table 3.2 shows the rating value for different types of reinforcement. The considered rating scale was 1 = routinely, 2 = occasionally, 3 = rarely, and 4 = not used. Figure 3.6 shows the survey results for types of reinforcement used.

4. **Indicate the frequency of encountering corrosion that requires corrective action of prestressing strands in precast concrete products.**
In spite of the different nomenclature adopted from each state, it was possible to distinguish seven types of structures. Prestressed I-girders were the most common; these were either occasionally (in Hawaii, Illinois, Iowa, New Mexico, New York, Ontario, and Pennsylvania) or rarely (in Arizona, Michigan, Missouri, Oregon, Texas, and Washington) found to need some corrective action. The second structures most mentioned were prestressed box beams, which were found to have some corrosion issues frequently (Illinois and New York), occasionally (New Mexico), and rarely (Missouri and Washington). This was followed by precast void slabs, which were either rarely (Arizona, Oregon, and Washington) or never (New Hampshire) found to have corrosion problems. The fourth was prestressed T-girders, for which there was occasionally (Hawaii and New York), rarely (Illinois), and never (New Hampshire) any need for corrective action due to corrosion. Posttensioned (Arizona, Oregon, and Texas) and prestressed double T (Missouri and Nebraska) structures were occasionally to rarely found to have problems. The last structures mentioned (New Hampshire and Texas) were deck panels, without any problem reported to date.

Figure 3.7 shows the survey results for corrosion encountered in prestressing strands. A high number of N/A answers were provided by the states.

5. **What measures are taken to extend the life of girders with corroded pretensioned, prestressing strands?**
The answers varied from doing nothing to total replacement of the girder. Cleaning and patching were usually mentioned. Epoxy injection, flexible topical treatment, and waterborne sealer were some alternatives mentioned.

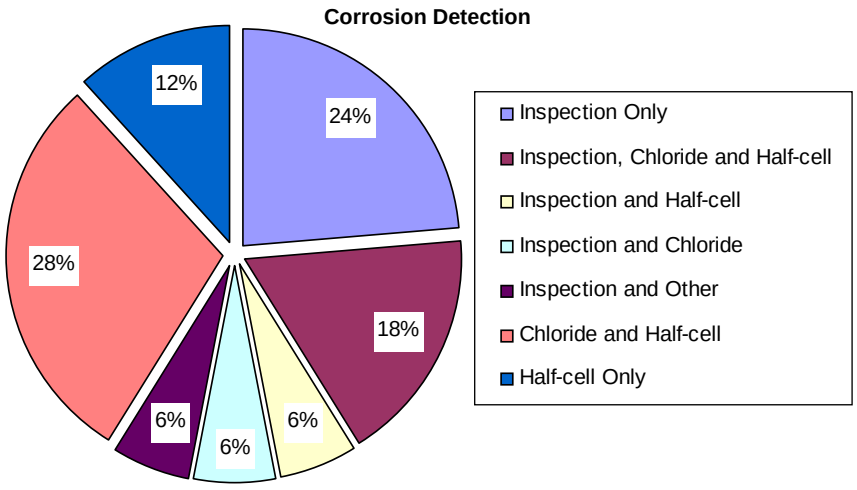

Figure 3.5. Survey results for corrosion detection.

Table 3.2. Rating Value for Different Types of Reinforcement

Type	Rating	Routinely (%)	Occasionally (%)	Rarely (%)	Not Used (%)
Considered Routinely Used					
Epoxy-coated reinforcement	1.2	89	5	0	5
Prestressing strands (longitudinal)	1.3	89	0	0	11
Carbon steel (black)	1.4	84	5	0	11
Considered Occasionally Used					
Posttension tendons (longitudinal)	2.1	37	32	21	11
Prestressing strands (transverse)	2.2	37	26	16	21
Posttension tendons (transverse)	2.2	21	47	21	11
Considered Rarely Used					
Stainless steel	2.7	11	16	63	11
Galvanized steel	3.1	5	16	42	37
Black with sacrificial anode	3.1	5	11	53	32
Carbon-fiber reinforcement	3.3	0	16	42	42
Black with impressed current	3.3	5	5	42	47
Glass-fiber reinforcement	3.5	5	5	26	63
Considered Not Used					
Chromium alloy (A-1035)	3.5	5	5	21	68
Galvanized and epoxy coated	3.6	5	0	21	74
Stainless steel clad	3.6	5	0	21	74
Epoxy-coated prestressing strands	3.7	0	5	21	74
Chromium alloy (A-1035)	3.7	0	5	21	74
Carbon-fiber reinforcement prestressing	3.7	0	0	26	74
Galvanized prestressing strands	3.8	0	0	16	84
Other: MMFX	3.9	0	0	5	95

After rehabilitation, some states monitor the structure until it is replaced. Some states affirmed that they usually find cracks at the ends of girders, allowing water to penetrate and corrode the strands.

Preventive measures such as increasing the overlay cover, keeping water off by adding deck grooves, using drains, and either sealing or eliminating joints were also mentioned. Cathodic protection with a low current was mentioned, as well.

6. **Indicate the frequency of encountering corrosion that requires corrective action of posttensioning tendons structures.**
   Corrosion is rarely found at most posttensioned structures (see Figure 3.8). The survey showed no difference in the answers for different structures. Only Oregon had a different answer for the substructure, which had a slight effect on average results. N/A answers might be explained by the fact that some states affirmed that they do not have many posttensioned structures to experience distress.
7. **What measures are taken to extend the life of girders with corroded posttensioning tendons?**
   Some states affirmed that they do not have very many structures in this category. Therefore, they have not experienced corrosion yet. Measures are similar to prestressed structures (see Question 5). In regard to the question "Where corroded tendons have been found, indicate the percent repaired or replaced," none of the surveyed states responded. The exceptions were New York, which stated that 100% were replaced, and Washington, which stated that 50% were repaired and 50% were replaced.
8. **How are the following durability related issues addressed in structural design and detailing for new construction?**
   Corrosion of reinforcement—Eighty-four percent of the states (excepting New Mexico, Texas, and Washington) mentioned additional cover, and 74% of the DOTs surveyed (including Arizona, California, Hawaii, Illinois,

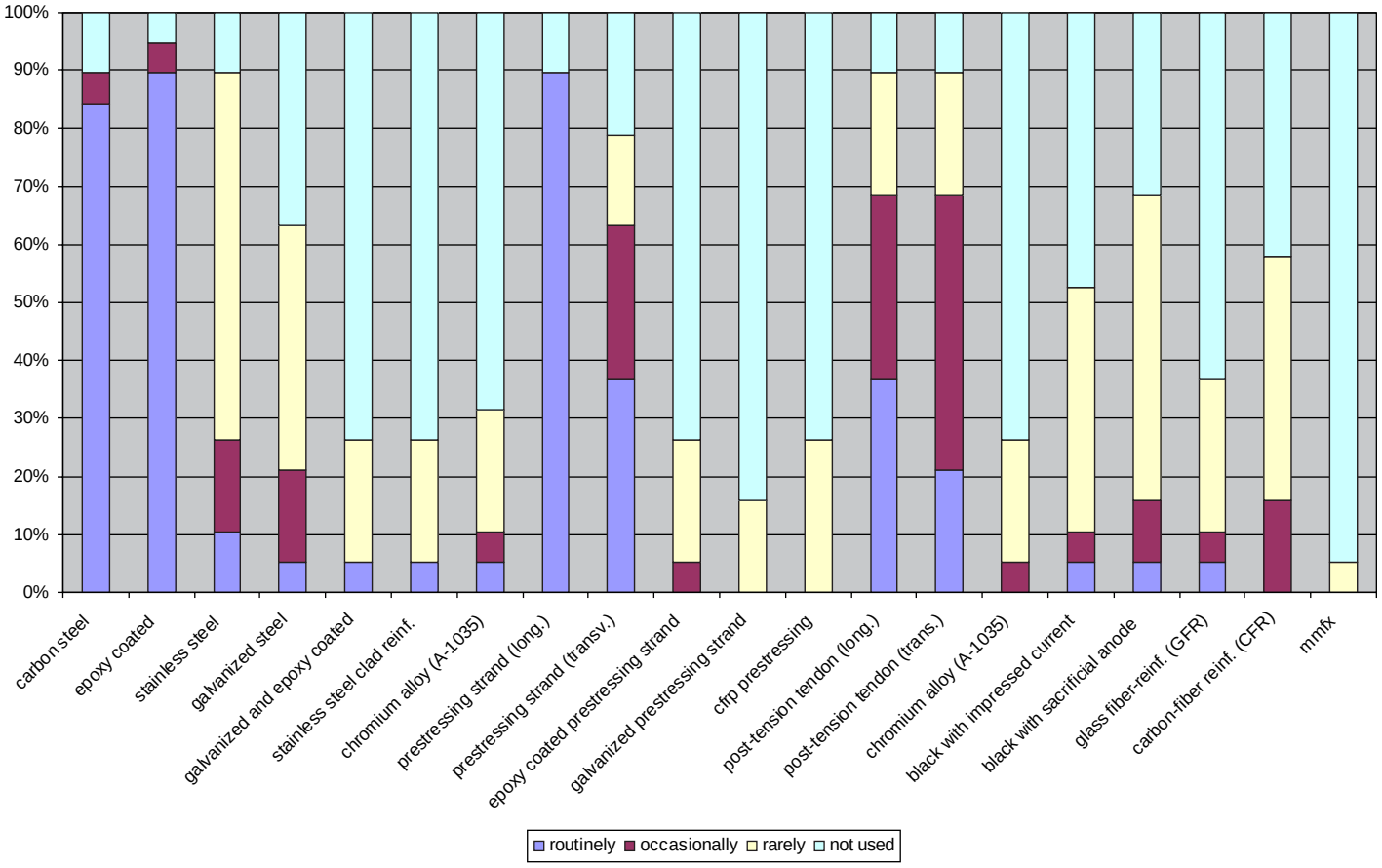

Figure 3.6. Survey results for type of reinforcement used.

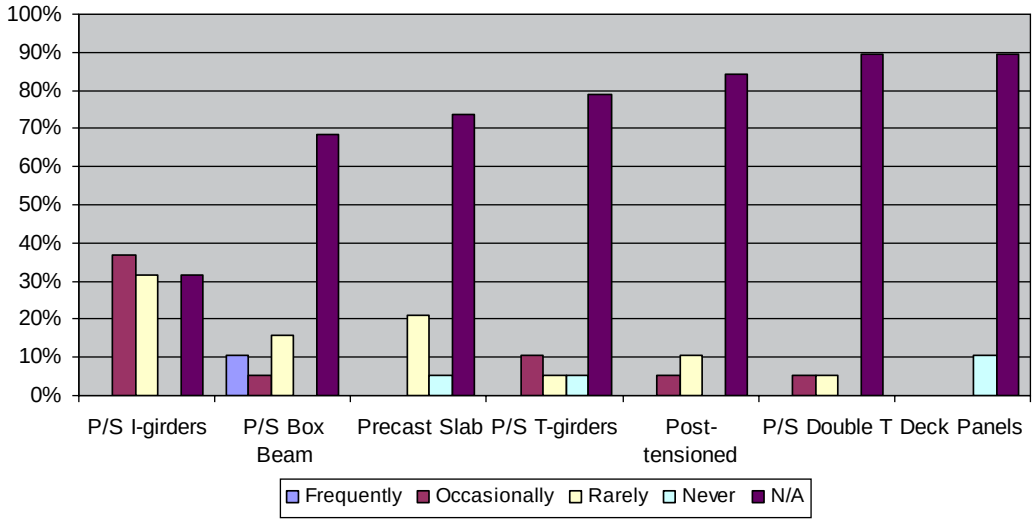

Figure 3.7. Survey results for corrosion encountered in prestressing strands. N/A = not applicable.

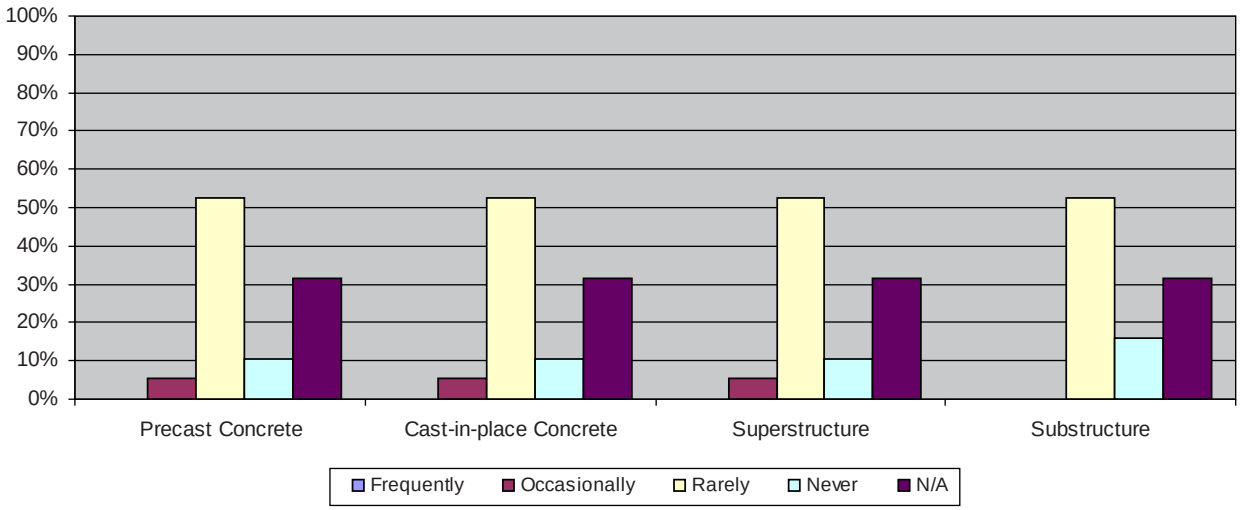

Figure 3.8. Survey results for corrosion encountered in posttensioning tendons.

Iowa, Kansas, Michigan, Missouri, Nebraska, New Mexico, New York, Ontario, Oregon, and Washington) mentioned epoxy-coated reinforcement as the protective measure taken to prevent corrosion of reinforcement. Corrosion inhibitors, silica fume, and fly ash are some of the supplementary cementitious materials mentioned by 26%. Drainage (mentioned by 21%) includes measures such as proper design, grooving, removing joints, and placing catch basins high to keep water off. Only 16% mentioned high-performance concrete (HPC) and 11% w/cm ratio. In Figure 3.9, "Others" represents 21% and includes measures such as cathodic protection, stainless steel, or galvanized rebar and glass fiber–reinforced polymer (GFRP) reinforcement.

Freezing and thawing—Thirty-seven percent addressed freezing and thawing issues with air-entrainment specification. Twenty-six percent mentioned drainage and twenty-one percent mentioned sealer. "Others" included epoxy-coated reinforcement, cover, HPC, SCM, shallow foundation, and membranes; these were mentioned by 34%. Eleven percent did not consider freezing and thawing to be a problem. Figure 3.10 shows the survey results for freezing and thawing.

Alkali–silica reaction—ASR is addressed by 42% of the states by using selected source of aggregate. SCM, such as pozzolan and fly ash, is used by 26%. "Others" included drainage, sealer, and air entrainment (11%). ASR is not considered to be an issue by 42% of the states. Figure 3.11 shows the survey results for addressing ASR.

Sulfate attack—Sulfate attack is addressed by 16% of the states either by using Type V cement (low C_3A), aggregate selection, or other measures such as HPC, drainage, and sealers. Fifty-eight percent consider sulfate attack an issue that should be addressed (see Figure 3.12).

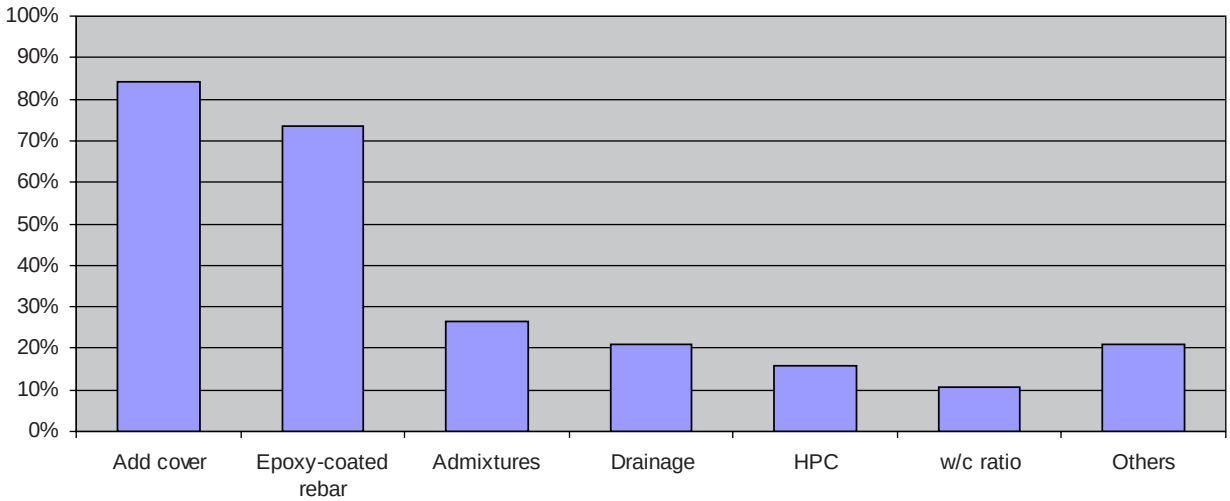

Figure 3.9. Survey results for addressing corrosion of reinforcement.

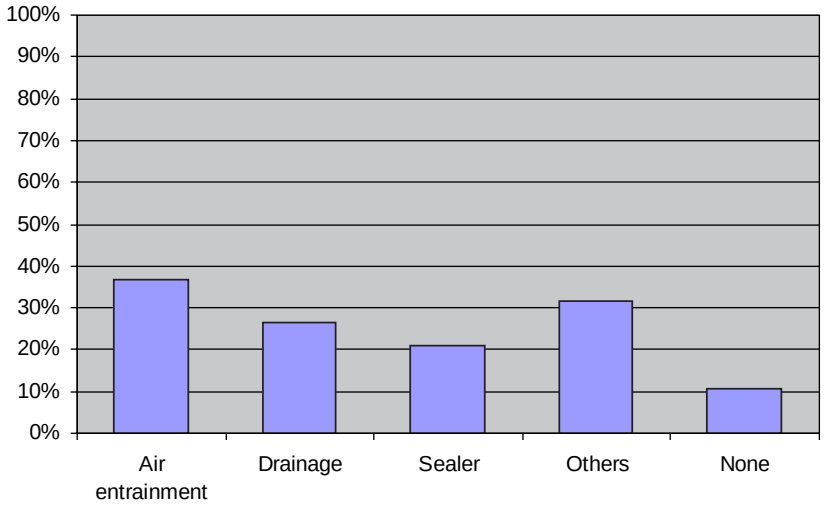

Figure 3.10. Survey results for addressing freezing and thawing.

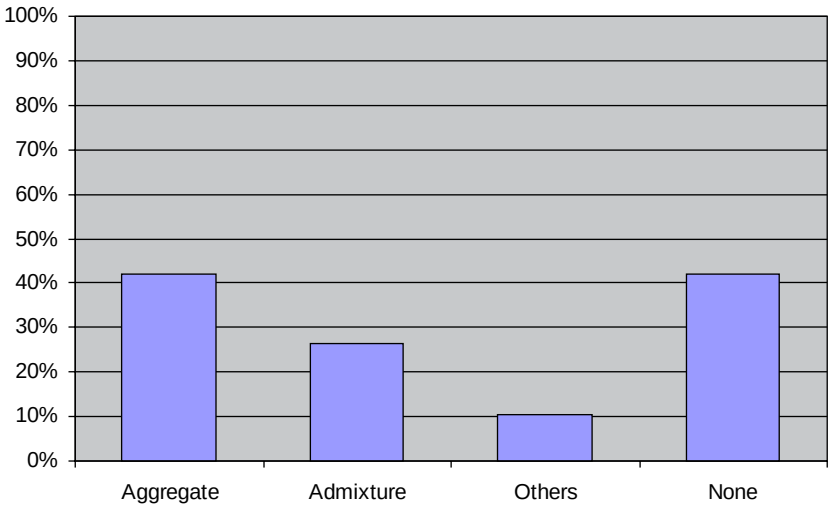

Figure 3.11. Survey results for addressing ASR.

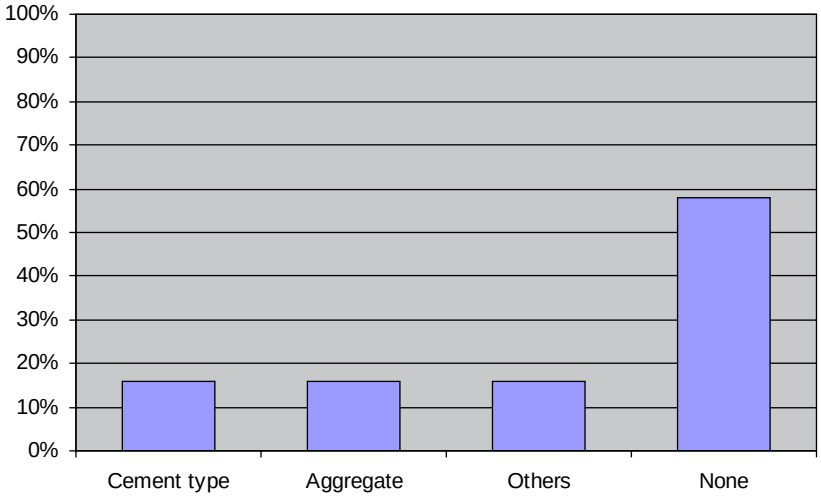

Figure 3.12. Survey results for addressing sulfate attack.

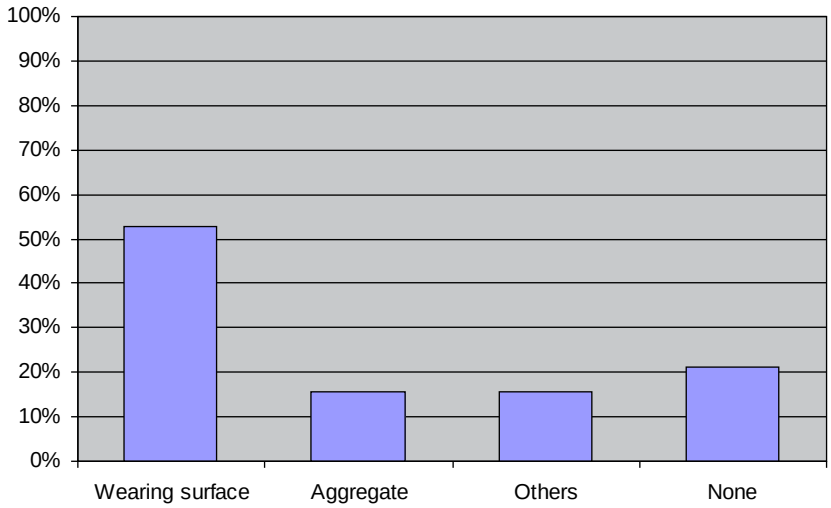

Figure 3.13. Survey results for addressing abrasion and wear.

Abrasion and wear—Fifty-three percent of the respondents considered measures such as extra cover, overlay, and wearing surface to address abrasion and wear. Sixteen percent mentioned either hard aggregate selection or other measures such as membranes, SCM, and material selection. Twenty-one percent do not consider abrasion and wear to be a problem (see Figure 3.13).

9. How are material selection and proportioning addressed in new construction for the following durability-related distresses?

Corrosion of reinforcement—Fifty-eight percent of the states mentioned epoxy-coated reinforcement and 53% mentioned SCM (fly ash and slag) and chemical admixture (i.e., shrinkage-reducing admixture) as measures they have taken. HPC was mentioned by 37%. Corrosion inhibitor was mentioned by 32%. The category "Others" included measures such as w/cm, stainless steel, cathodic protection, GFRP, carbon fiber–reinforced polymer, and water repellent; these measures were mentioned by 37% (see Figure 3.14).

Freezing and thawing—Eighty-nine percent of states mentioned they address freeze–thaw distresses with air entrainment. Twenty-six percent mentioned w/cm ratio, and only 11% mentioned HPC with low permeability. "Others" (mentioned by 16%) included measures such as uniform aggregate to minimize paste content, low-absorption aggregate and silane water repellents. Eleven percent did not address freezing and thawing as it is not a problem (see Figure 3.15).

Alkali–silica reaction—SCM (fly ash, pozzolan, silica fume, and slag) was mentioned by 53%. Prequalified sources of aggregate were mentioned by 32% of the states. Twenty-one percent mentioned others such as state specification, HPC with low permeability, and drainage.

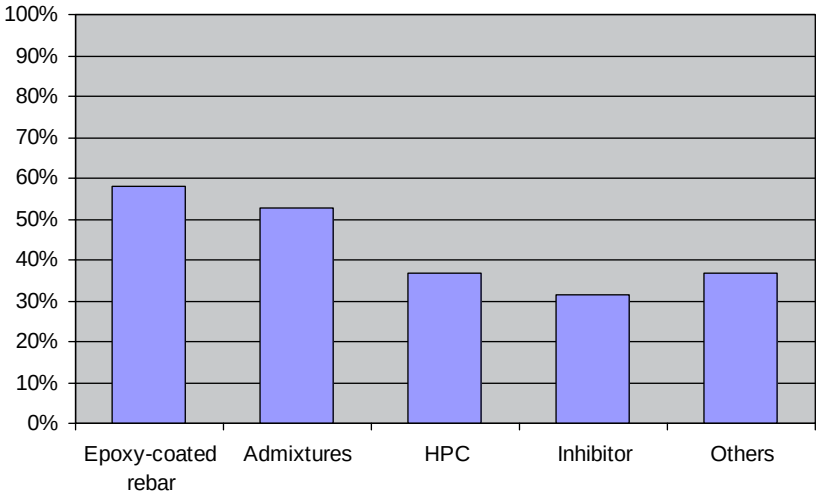

Figure 3.14. Survey results for addressing corrosion of reinforcement.

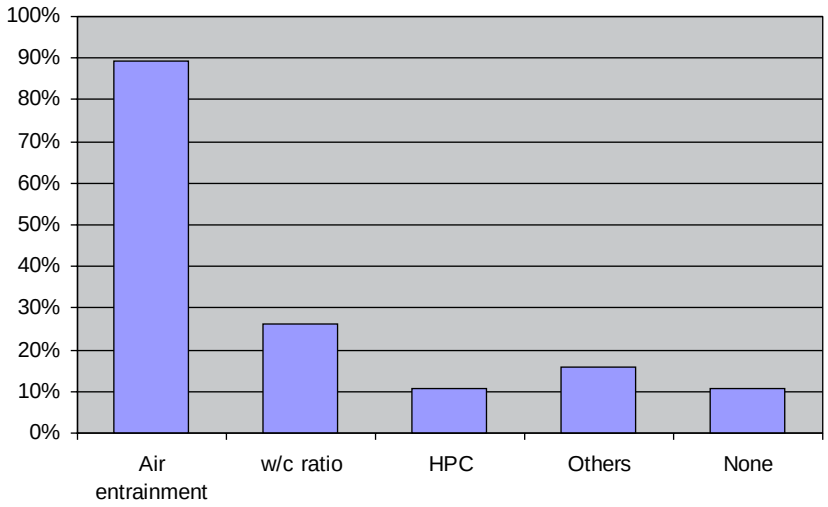

Figure 3.15. Survey results for addressing freezing and thawing.

Twenty-one percent did not take any measures and do not consider it to be an issue (see Figure 3.16).

Sulfate attack—Sulfate attack is addressed by 16% of the states by using Type V cement (low C_3A). Eleven percent mentioned either pozzolan or "Others," which included low-permeability concrete or state specification. The great majority, 63%, do not consider sulfate attack to be an issue (see Figure 3.17).

Abrasion and wear—Hard aggregate is considered by 37% of the states. HPC is considered by 16%. "Others" (mentioned by only 11%) included measures such as either early curing or SCM (silica fume). Twenty-six percent of the states had no measures to address abrasion and wear (see Figure 3.18).

10. How are the following construction practices addressed in new construction for durability of concrete?

Delivery and pumping—As shown in Figure 3.19, field testing, such as slump and air content determination, is performed by 47% of the states. Some states sample from the end of the pump hose. Inspection, including good practices, close monitoring, limiting free fall, and having a short interval between delivery and use (ensure continuous supply), was mentioned by 37%. "Others" (mentioned by only 11%) included self-consolidating concrete or adding superplasticizer, state specification, and the amount of air entrainment. The method of conveyance was not considered by 16% of the states.

Consolidation—Inspection to ensure good practices was mentioned by 32%. Proper vibration by using an automatic, timed vibrator and vibration applied at vertical point was mentioned by 26%. "Others" included self-consolidating concrete, state specification, and ACI standard; these were mentioned by 42%. Consolidation was not considered by 21% (see Figure 3.20).

Curing—Wet cure and application (burlap or plastic cover) were mentioned by 74% of the states. The curing time

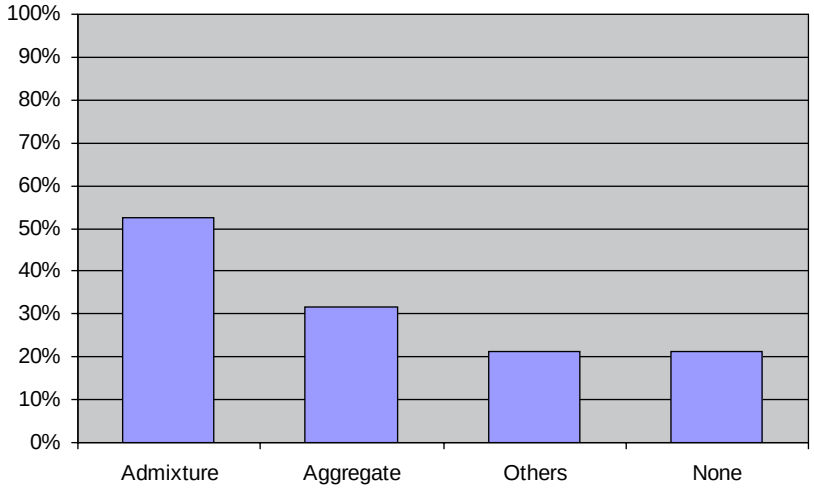

Figure 3.16. Survey results for addressing ASR.

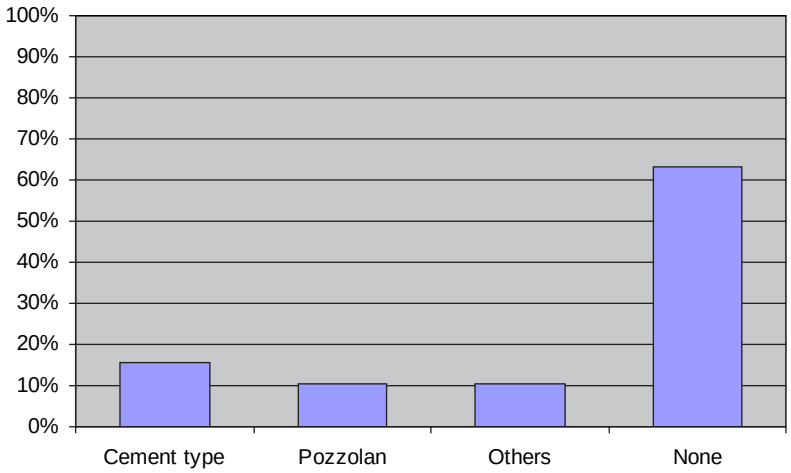

Figure 3.17. Survey results for addressing sulfate attack.

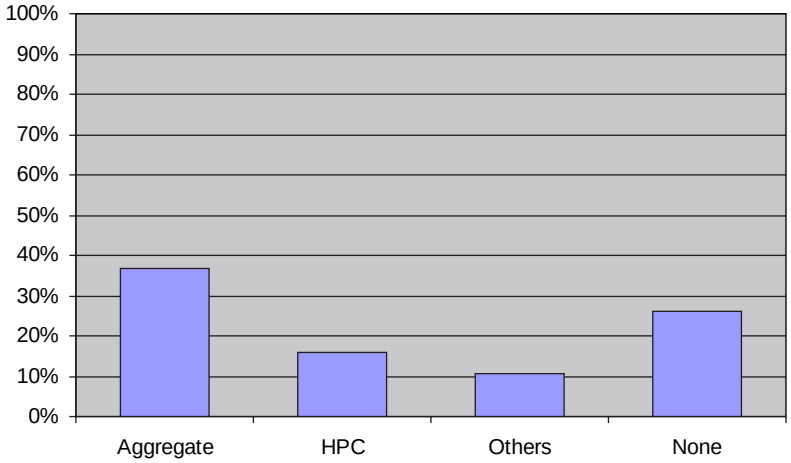

Figure 3.18. Survey results for addressing abrasion and wear.

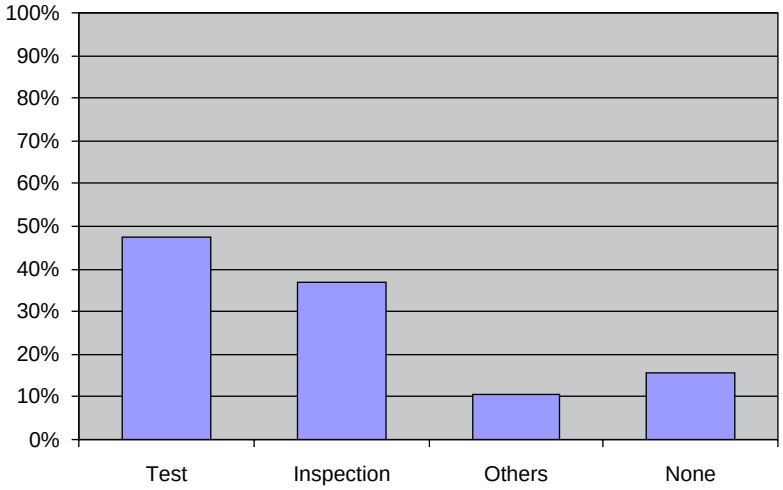

Figure 3.19. Survey results for practicing related to delivery and pumping.

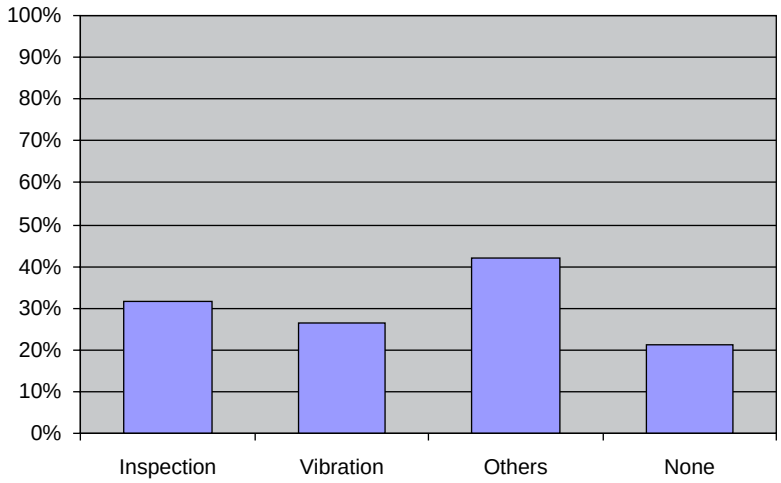

Figure 3.20. Survey results for practices related to consolidation.

varied from 4 to 14 days, but 7 to 10 days was the most common duration. Inspection to ensure proper curing procedures was mentioned by 16%. "Others" (mentioned by 42%) included shorter time between finishing operation and cure application, uses of membrane, and state specification (see Figure 3.21).

11. **Which form of specification (either prescriptive or performance) do you use for durability?**
    Twenty-six percent of the states (Arizona, California, Hawaii, Illinois, and Virginia) mentioned either state specification or a contact. Hawaii will move to performance in the future. Iowa uses prescriptives for standard decks and performance for HPC. Kansas uses only performance. Michigan, New York, Texas, and Vermont use both, with limited performance specifications. Missouri uses more prescriptive but is moving to performance. New Mexico uses only performance and requires a detailed demonstration from the concrete supplier. New Hampshire uses prescriptive except for decks, for which the state specifies air entrainment, permeability, strength, and quality control–quality assurance. Ontario looks mostly for end result with some prescribed limits. Oregon uses only prescriptive, and Pennsylvania uses only performance specifications.

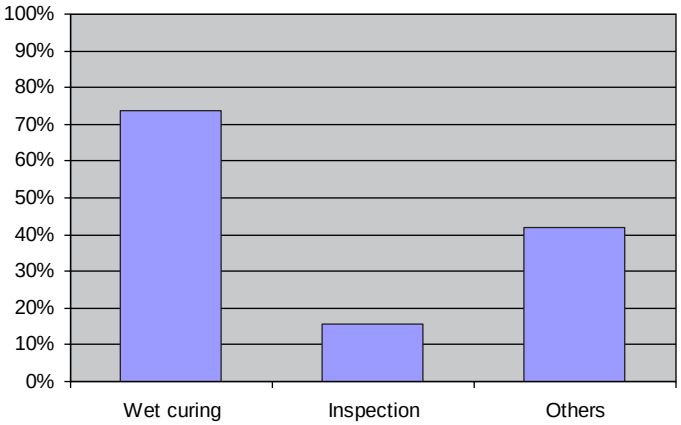

Figure 3.21. Survey results for practices related to curing.

12. **How are the following durability-related distresses corrected in existing structures?**
    Corrosion of reinforcement—Repair procedures (removing unsound concrete, cleaning, and removing and replacing the reinforcement) and patching were mentioned by 89% of the states. New Mexico said corrosion is not a problem, and Virginia did not answer, representing 11%. Beyond repairing, cathodic protection was mentioned by 21% of the states. Other measures ("Others"), such as corrosion inhibitor, zinc anode, and breathable sealers, were mentioned by 21% (see Figure 3.22).
    Freezing and thawing—As shown in Figure 3.23, repair procedures and water-repellent sealer were mentioned by 26% of the states. Overlay was mentioned by 21%, and 37% either reported that freezing and thawing is not a problem or did not answer.
    Alkali–silica reaction—As shown in Figure 3.24, repair and sealer application were mentioned by 37% of the states. Overlay was mentioned by 11%. "Others" (mentioned by 38%) included either exclusion of water moisture (drainage), confinement of the structure, or SCM. Thirty-two percent either did not answer or do not consider ASR to be a problem.
    Sulfate attack—Eighty-four percent of the states affirmed that either sulfate attack is not an issue or did not answer. Illinois mentioned overlay, scarification, and deck sealer; Michigan mentioned replacement; and Pennsylvania mentioned concrete removal and patching using vitrified clay liner plates.

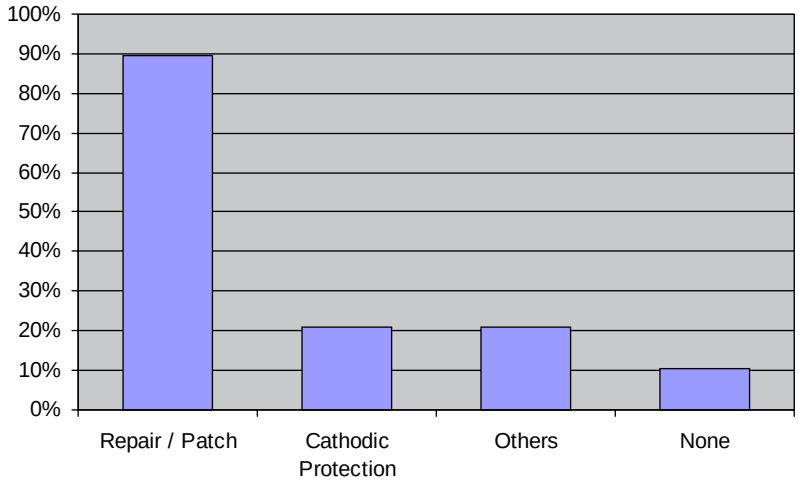

Figure 3.22. Survey results for correcting corrosion of reinforcement.

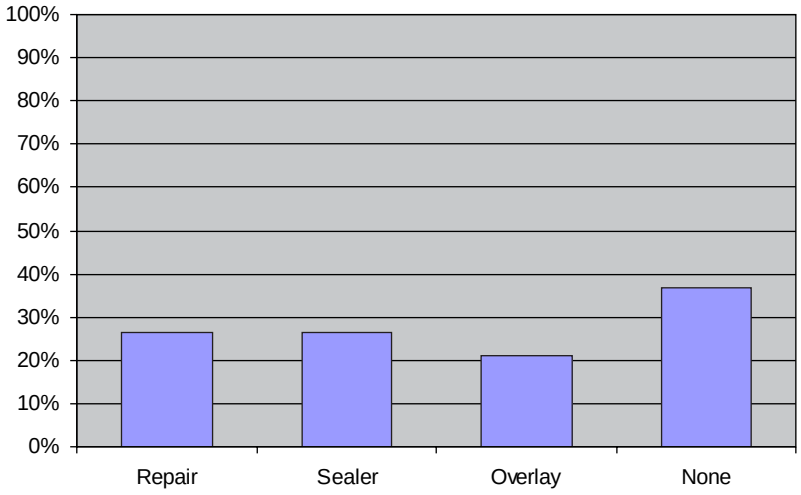

Figure 3.23. Survey results for correcting freezing and thawing.

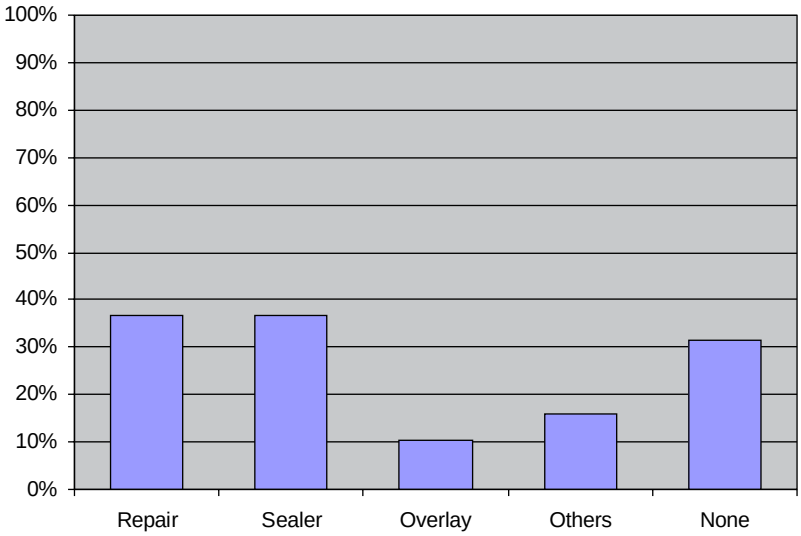

Figure 3.24. Survey results for correcting ASR.

Abrasion and wear—Fifty-eight percent of the states addressed the abrasion and wear issue by using overlay, and 42% do not have abrasion and wear as an issue or did not answer.

13. **If you have damage due to reinforcing steel corrosion, what is your method of repair?**
    Ninety-five percent of the states surveyed affirmed that cleaning and patching are their method of repair for decks, except Pennsylvania, which indicated that decks are programmed for replacement. The barrier is replaced by 89%. Oregon and Vermont did not mention any method. Beams are repaired by cleaning and patching by 89% of the respondents. Some states mentioned either replacing the reinforcement or the whole beam. New Hampshire and Vermont did not mention any method of repair. Substructure-related problems are addressed by 95%, with cleaning and patching considered as their method of repair. Table 3.3 shows the life of these component repairs.
14. **Does your state use any models to predict the service life of structures in new construction?**
    Ninety-five percent of the surveyed states do not use any models; Iowa was the sole exception. They affirm that epoxy-coated reinforcement is projected to reach 50 years before deck repair and overlay are needed. Hawaii has a model, but it is not used frequently.
15. **Does your state or province use any models to predict the service life of existing structures (remaining life) based on condition surveys and concrete testing?**
    Seventy-nine percent of the surveyed DOTs do not use any models. Michigan, Nebraska, Ontario, and Oregon, which represent 21%, indicated such use. Hawaii indicated interest for use in the future.
16. **Please list any completed or ongoing research regarding concrete durability or service life of bridges.**
    New Hampshire and Virginia did not answer. Eighty-nine percent provided contact information, such as the name of the researcher, contact number, link, and some detail about the project.

Bridge Decks

The primary function of a bridge deck is to provide a safe riding surface for traffic and direct structural support of wheel loads. In most regions of the United States, deterioration of bridge decks has been a major cause of reported bridge deficiencies. To provide longer service life, the integrity of the bridge deck must be maintained. Degradation can result in loss of capacity or unsafe driving conditions, or both. With sufficient degradation, the reduction in carrying capacity can lead to failure, and unsafe driving conditions can lead to deadly traffic accidents.

Most of the bridge decks in current use are made of cast-in-place (CIP) reinforced concrete. Other systems include full-depth CIP concrete slab superstructure, precast concrete deck panels, exodermic decks, steel orthotropic decks, fiber-reinforced polymer decks, and adjacent member superstructure systems. The types of deterioration experienced in bridge decks are mainly scaling, mortar flaking, freeze–thaw damage, abrasion damage, alkali–aggregate reactivity, excessive cracking and spalling, and delaminations due to corrosion of the reinforcement.

A literature search was performed to establish the principal issues relating to bridge deck durability. This information was supplemented by highway department survey results, which identified additional research and procedures for current practice in the construction of bridge decks under their authority.

Degradation of service life due to corrosion caused by cracking of bridge deck elements is identified as a significant issue to be addressed. The intrusion and concentration of chlorides allowed by deck cracking is identified as a concern nationwide, particularly in areas where deicing salts are used, and in marine environments. A dual strategy of corrosion protection incorporating improved concrete quality and reinforcement protection systems has been adopted by most highway agencies for their bridges. This strategy often consists of a low-shrinkage, low heat of hydration concrete with epoxy-coated reinforcement.

Several systems present opportunities to have long service life. These include CIP concrete bridge decks using stainless steel reinforcing, orthotropic steel bridge decks with proper fatigue detailing and plate thickness, full-depth precast concrete deck panels with appropriate joint details and closure of gaps over shear connectors, and adjacent member bridges with appropriate shear key joint design.

Table 3.3. Component Repair Due to Corroded Steel

Component	Minimum (years)	Maximum (years)	Average (years)	SD (years)	Provided answer (%)
Deck	1	40	17.2	9.20	84
Barrier	1	40	16.8	11.6	53
Beam	5	50	17.4	11.2	63
Substructure	5	30	16.3	6.20	74

Note: SD = standard deviation.

Description and Discussion of Bridge Deck Types

The predominant bridge deck system in the United States consists of CIP reinforced concrete. Conventional concrete decks, either CIP or precast, were the major focus of this study; however, the service life of other bridge deck systems was also investigated. The service life of the following bridge deck types was studied:

- CIP concrete bridge decks;
- Full-depth CIP concrete slab superstructures;
- Segmental concrete superstructure systems;
- Precast concrete deck panels;
- Steel orthotropic bridge decks;
- Fiber-reinforced polymer (FRP) bridge decks and superstructures; and
- Adjacent member superstructure systems.

A summary of the information on the listed bridge deck systems is reported in the *Guide*.

Causes of Bridge Deck Deterioration

In most regions of the United States, deterioration of bridge decks has been a major cause of bridge deficiency. This deterioration has been shown to substantially increase with the use of deicing salts on bridges. Although deterioration occurs to concrete, the principal cause for the deficiencies is a direct result of bridge deck cracking, which significantly reduces the chloride intrusion protection of the reinforcement provided by concrete cover. Early detection and subsequent sealing of cracks, such as by epoxy injection, have been shown to increase durability of bridge decks; however, this procedure is not considered a primary defense strategy for addressing the cracking issue. Elimination of cracking is the primary goal.

For CIP bridge decks on longitudinal stringers, one of the primary causes of cracking is the restraint developed when the composite deck is locked in with the supporting girders, occurring as the deck concrete reaches initial set.

Precast Concrete Deck Panels

Precast deck systems provide many benefits over traditional CIP deck systems in bridge construction. The quality of precast deck systems is generally superior to field-cast concrete decks. The variability of construction due to environmental conditions is eliminated in the plant through the use of consistent casting operations and curing techniques.

Orthotropic Steel Bridge Deck

Historically, orthotropic steel bridges have not been problem free. Their design and construction is more complex than conventional bridge construction, and they demand special measures for routine inspection and maintenance. Fatigue cracking has been observed more frequently in such bridges throughout the world due to the numerous complicated welded details subject to complex stresses. Early analytical tools were limited in their ability to quantify the stress states at these details, limiting the experimental fatigue database. In addition, the fatigue performance of many of these details is highly sensitive to the construction techniques. Detailing practices have relied heavily, and continue to rely, on experience gained through trial and error. One clear advantage to the orthotropic steel deck is that it is a highly redundant system, and cracking is typically considered a mere nuisance to be observed rather than a serious threat to the strength or integrity of the structure. Wearing surfaces have also exhibited performance problems with cracking, rutting, shoving, delamination, or some combination of these stresses, which have often resulted in excessive maintenance and resurfacing. The delamination of the wearing surfaces is generally attributed to the small thickness of the top plates used in orthotropic decks.

The corrosion resistance of orthotropic steel decks has been very good overall. The top side is protected by the wearing surface, and the bottom side can be protected with a conventional paint system. Like any steel bridge structure, it may require regular maintenance in terms of repainting. However, the coating on the underside of the deck can last a very long time if it is not subjected to direct saltwater spray. Orthotropic decks are typically made continuous, without joints, for extended lengths, which minimizes potential locations for water penetration. The individual ribs are typically sealed with end plates that prevent moisture from entering the interior of the rib. Outside the United States, a common approach has been to use a fully closed box girder cross section and employ an in-service dehumidification system on the interior to essentially eliminate the possibility of corrosion; thus, there is no need for an interior paint system. However, this system is expensive from an operational standpoint. One of the primary advancements for orthotropic bridges is in the technique for engineering analysis and design. For orthotropic bridges to become cost-effective in the United States, standardization is the goal.

Fiber-Reinforced Polymer Bridge Deck

Because FRP application is an emerging technology, the performance history for FRP bridge decks and superstructure systems is very limited and does not lend itself to credible projections of extended service life. Deterioration of these structures has included delamination of the FRP material (Alampalli et al. 2004) and cracking and delamination of the wearing surface. Causes for wearing surface cracking and delamination from FRP material may be related to material property differences (e.g., coefficient of thermal expansion) and response of the flexible structural system. The cause for the delamination of the FRP material was not reported.

Adjacent Member Superstructure Systems

Most of the deterioration of bridges with adjacent member superstructure systems occurs due to a breakdown of grout or concrete in the keyway between the girders, allowing water and chloride intrusion into the joints. It is possible that water may also leak into the voids inside the adjacent box members. In addition to creating a potential for deterioration due to corrosion and freeze–thaw damage, accumulation of water could create additional weight unaccounted for in the design.

Similar experiences with the breakdown of these joints throughout the country give credence to the idea that the transverse design and detailing of these systems requires additional thought to ensure that the system transfers the required loads across the joint and remains watertight. Failure to transfer loads across the joint could potentially overstress the individual member, resulting in a lower-rated capacity. Little guidance is provided in the *AASHTO LRFD Bridge Design Specifications* (2004, 2010b) (*LRFD Specifications*) relating to the moments and the shears that are transferred across this joint.

Protection of Existing Bridges

Bridge protection systems to extend the life of existing structures include epoxy injection into cracks; the use of coatings, such as sealers, membranes and overlays; cathodic protection; and chloride extraction systems. Although some of these systems perform satisfactorily, their life is limited, and they are certainly not maintenance free. Additionally, their effectiveness in delaying damage is dependent on whether the conditions around the elements being protected have already begun to deteriorate. Detection is critical to providing adequate advance warning of deterioration to program and execute repair strategies.

The following subsections describe approaches for protecting bridge decks for extending service life.

Sealers

Sealers are expected to minimize the intrusion of aggressive solutions into concrete. Today, silanes are popular sealers, followed by siloxanes, silicates, epoxies, gums, acrylics, urethanes, chlorinated rubber, silicones, and vinyls (NCHRP Synthesis 209). Sealers have been difficult to assess and have been reported to have a wide range of performance (NCHRP Synthesis 333 2004).

Membranes

Membranes are perhaps the most effective way to protect bridge decks and obtain long service life. Agencies in Europe do not have the service life issues with bridge deck that U.S. agencies do. The main reason is the use of membranes. The quality and extent of service life that could be achieved by use of membranes depends on the quality of the material used and installation methods. Early experiences with membrane in the United States in the 1980s were unsuccessful, mainly because of lower-quality material and poor installation techniques.

Overlays

Concrete overlays create a low-permeability protective layer over the conventional concrete on bridge decks (NCHRP Synthesis 333 2004). An overlay serves as a barrier to chloride ions, therefore increasing the time required for the concentration of chloride ions, at the level of the reinforcement, to reach the threshold for corrosion. Low-permeability overlays also decrease water penetration into a structure, allowing it to dry out, which reduces chloride ion mobility. Overlays can be applied to new decks or as a rehabilitation method on existing decks (Kepler et al. 2000); however, overlays have limited effectiveness when applied to existing decks. If chloride ions are already present in the deck when the overlay is placed, then the only protection that the overlay can offer is a decrease in moisture infiltration (Sherman et al. 1993).

The most common types of overlay include

- Latex-modified concrete overlays;
- Low-slump dense concrete overlays;
- Silica fume concrete overlays;
- Polymer concrete overlays; and
- Very-high-early-strength concrete overlays.

Cathodic Protection

Cathodic protection systems are designed to protect the reinforcement. The potential of the reinforcement is shifted in the negative direction either by impressed current or sacrificial anodes. If steel is made cathodic, corrosion will stop (Virmani and Clemeña 1998). Impressed current is most common and uses a titanium mesh anode in a concrete overlay (Kepler et al. 2000).

Some states have reported successful use of the cathodic protection system, but others have cited difficulties with reliability and maintenance of the system. Cathodic protection systems have not been proven to be maintenance free or cost-effective (NCHRP Synthesis 333 2004).

Electrochemical Chloride Extraction

ECE can be employed when high levels of chlorides are present at the level of reinforcing steel (Virmani and Clemeña 1998). This procedure enables the extraction of chlorides from concrete and leads to an increase in the pH of concrete that repassivates the steel. The life expectancy of a treated reinforced concrete is not known. The system is described in detail below under "Research Categories."

Analysis of DOT Survey

The results of the survey conducted by the R19A research team indicate that the predominant type of bridge deck used

by the respondents is the CIP normal-weight concrete deck on stringers, followed by full-depth CIP concrete slab superstructures and then precast concrete slab–box beam superstructures (see Figure 3.25). Other systems, such as lightweight concrete, full-depth precast concrete on stringers, steel grid (exodermic), and steel orthotropic decks are rarely used. Three states indicated occasional to routine use of timber decks. Several states indicated use of precast concrete deck panels in composite and noncomposite configurations.

Several respondents provided estimates of expected service life in years for the various bridge deck types identified, as shown in Figure 3.26. The service life varied significantly from state to state for many of the categories (e.g., 30 to 75 years for CIP normal-weight concrete decks on stringers without overlay). On average, most of the bridge deck systems averaged between a 40- to 50-year service life, except for steel grid and timber deck systems, which averaged around a 20-year service life. There was no indication that decks built under current standards exhibited substantially different service life with or without overlays.

The predominant type of reinforcement used by the respondents is epoxy-coated reinforcement, with only one respondent indicating that this type of reinforcement is not acceptable (see Figure 3.27). This single state is not in an environment where deicing salts are used. The other reinforcing types are rarely used, but are being studied for use in several states.

The predominant types of maintenance issues reported by the respondents for CIP concrete bridge decks that are rated poor or worse are illustrated in Figure 3.28. Four of the six dominant maintenance issues appear related, as deck cracking leads to chloride intrusion that results in deck delamination and spalling.

The ranking of the routinely recurring maintenance issues encountered for CIP concrete bridge decks that are rated poor or worse indicates that chloride intrusion is the most important issue faced by the respondents, closely followed by deck cracking, deck delamination, and spalling (see Figure 3.29). Although the survey results for maintenance issues identified by the respondents ranked chloride intrusion slightly less than deck cracking, deck delamination, and spalling, two-thirds of the states providing a response to this answer ranked chloride intrusion as the number one concern for the subject bridge decks.

Thicker concrete cover, use of epoxy-coated reinforcement and higher-quality concrete with air entrainment, lower heat of hydration, and proper curing were identified as means

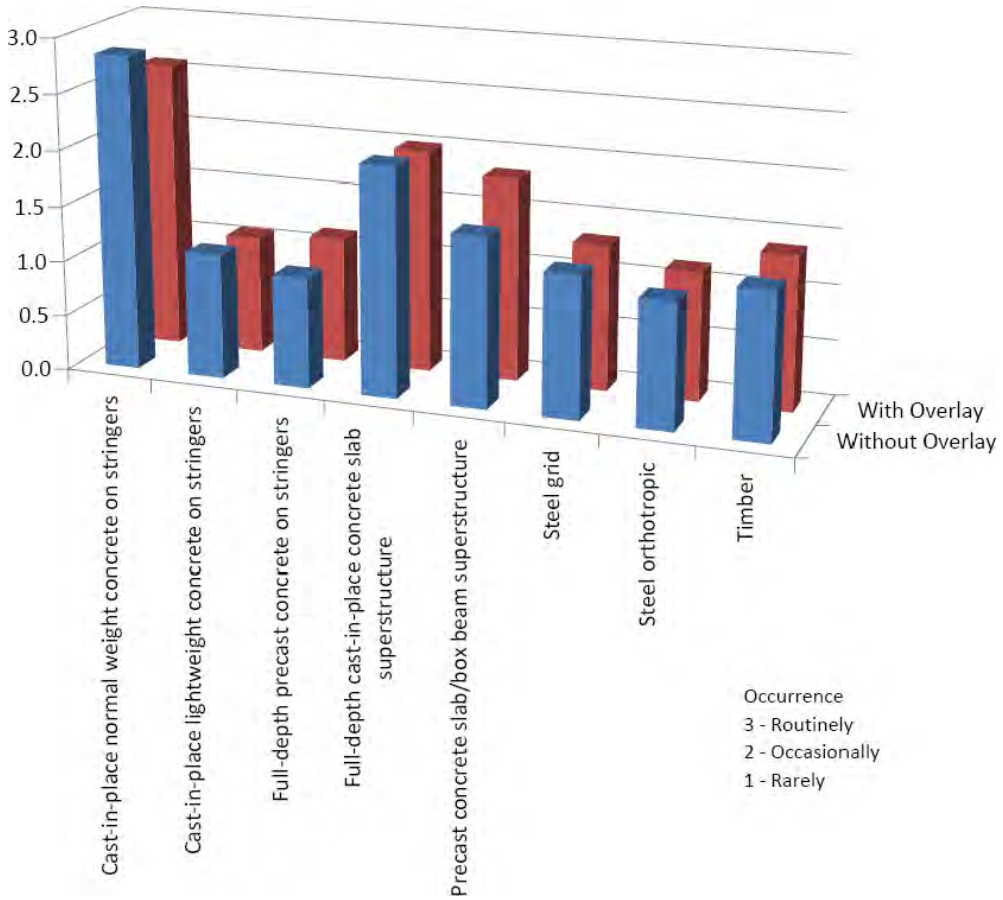

Figure 3.25. Survey results for bridge deck types used by the respondents.

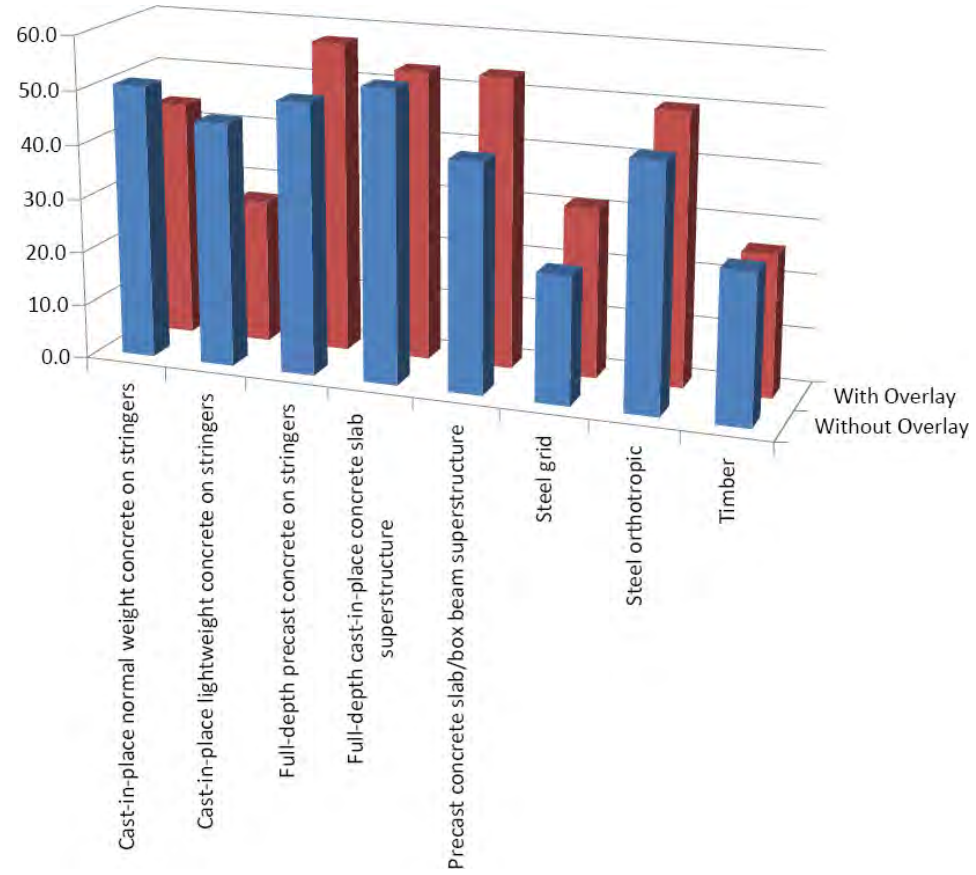

Figure 3.26. Survey results for bridge deck life expectancy.

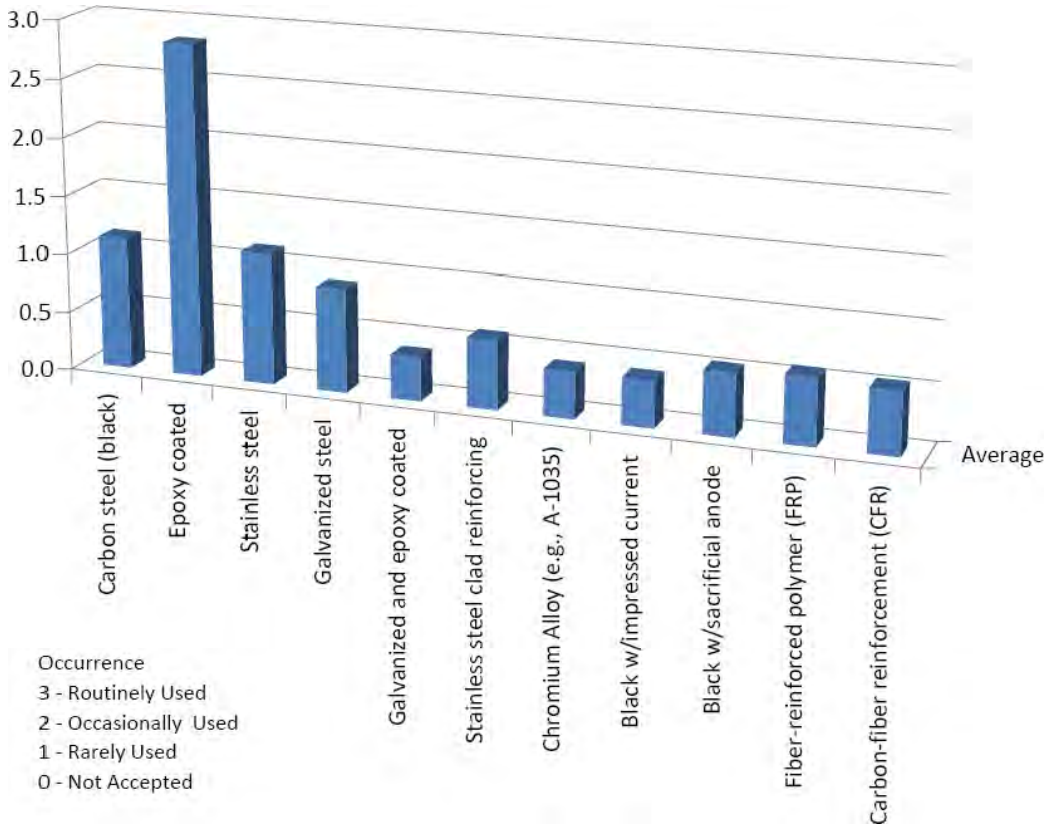

Figure 3.27. Survey results for reinforcement types used by the respondents.

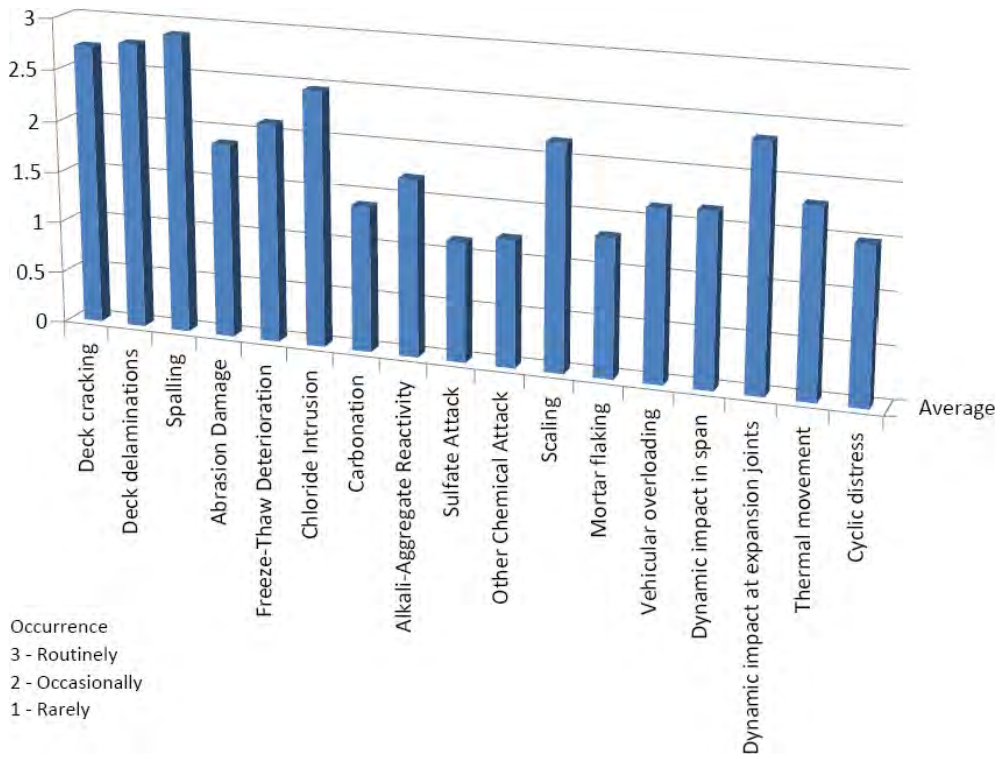

Figure 3.28. Survey results for bridge deck maintenance issues reported by the respondents.

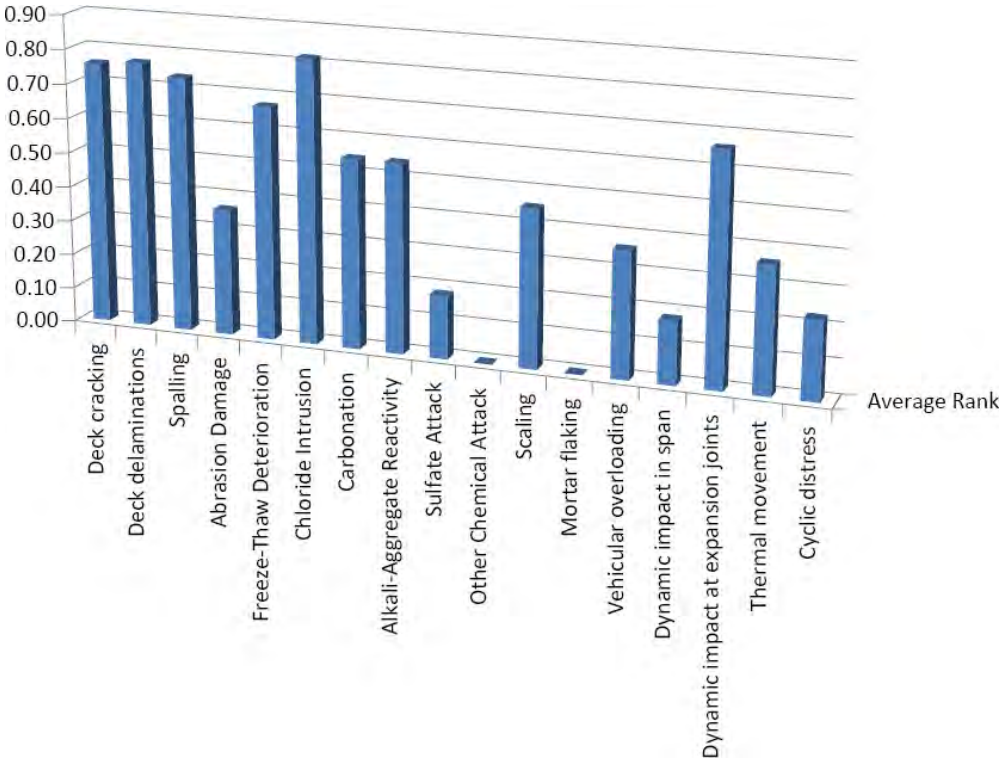

Figure 3.29. Survey results for bridge deck maintenance issues reported by the respondents.

used for increasing the durability of bridge decks in new construction.

The issues associated with increased durability identified by those who responded are ranked in order of importance in Figure 3.30. Most of these issues are related to the quality of concrete and the reduction of deck cracking. Use of corrosion-resistant reinforcement is also identified as one of the most important durability strategies for bridge decks.

The survey requested specific information regarding experience with practices and specifications that may affect bridge longevity. These questions dealt with deck-forming practices, different environmental conditions, concrete mix design, curing methods, and special maintenance procedures. A summary of the responses follows.

The majority of respondents indicated they did not experience differences in bridge deck longevity as a result of different forming systems (e.g., removable, composite or noncomposite steel stay-in-place, composite or noncomposite concrete stay-in-place). Some respondents had issues with reflective cracking over concrete stay-in-place forms, but three states indicated good performance of these systems. Other states do not allow steel stay-in-place forms due to the inability to inspect the bottom of the concrete slab. These states indicated that leakage can occur through cracking, which is hidden by the forms, delaying the response to the deterioration, thereby reducing the bridge deck service life.

Respondents in states that experience differences in environmental conditions within their state indicated there are performance differences based on these conditions. California respondents indicated they experience twice the deck life for bridges in benign environments compared with those located in a more aggressive chloride environment (e.g., road salts). Abrasions from chain wear and truck traffic volumes were also identified as contributing factors to decreased bridge deck life.

Respondents indicated that concrete mix design and curing methods are very important to increasing the service life of concrete bridge decks. Numerous states have implemented high-performance concrete mix design aiming for low permeability, low heat of hydration, and reduced cracking. Kansas has also developed a low-cracking HPC mix design for use in that state. Most respondents employ 7- to 14-day wet curing of decks with special requirements to quickly control evaporation from the deck surface.

Most respondents indicated that they do not use overlays for new construction, although there are exceptions. The responses indicated that overlays are used primarily for

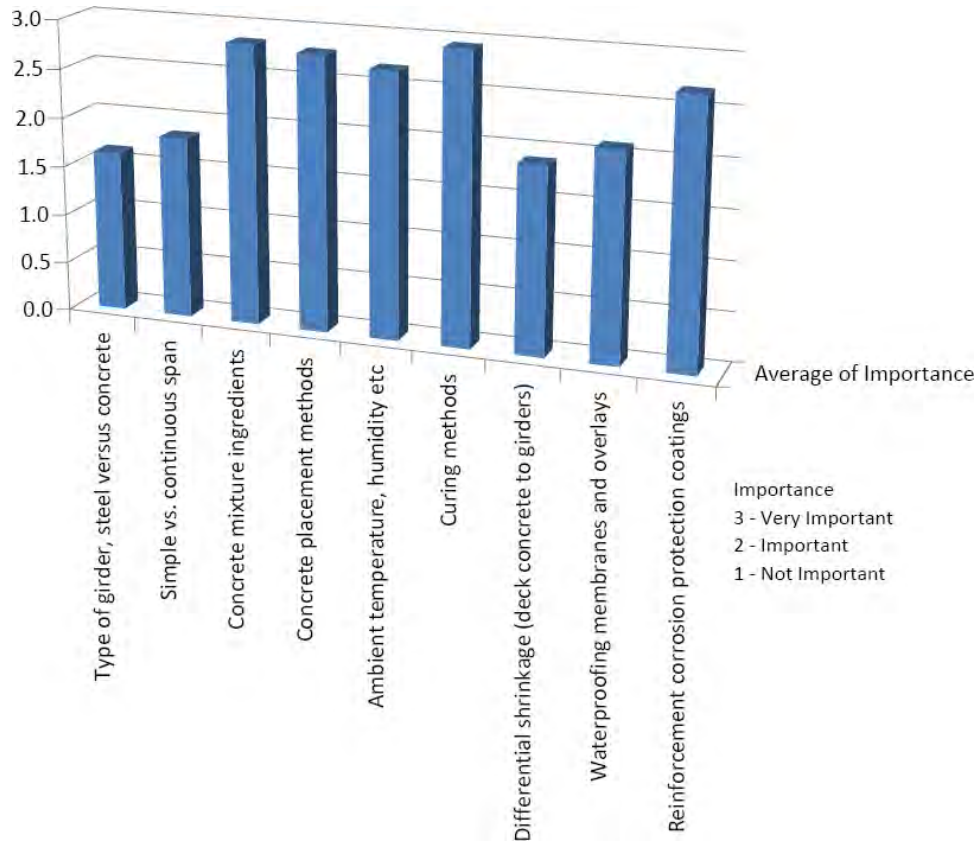

Figure 3.30. Survey results for important durability issues to be considered in new construction.

extending the life of existing structures, with seven of the 17 respondents indicating that overlays are not used at all. Sealing of cracks with epoxy injection or sealers was identified as a special maintenance procedure to increase the service life of bridge decks. The elimination of joints and drains was also indicated as beneficial.

A majority of the respondents indicated that they have undertaken research and testing in the past or are currently undertaking research and testing of materials or construction procedures (or both) for bridge deck longevity. This research and testing addresses such issues as quality of concrete, use of GFRP reinforcement and other noncorroding reinforcement, and GFRP-reinforced decks and reports on problems associated with their use.

Respondents did not indicate that they considered the use of noncomposite or partially composite bridge decks to control transverse cracking or to facilitate deck replacement.

Respondents indicated a willingness to exchange a higher initial bridge deck cost for increased durability, although there was a caution that this investment had to be cost-effective and reasonable considering budget constraints.

Few respondents provided information relative to the present value of CIP decks when built as part of new structures and of CIP decks when built as replacement decks on existing structures. The information provided indicates that the cost to reconstruct a concrete bridge deck is about 160% to 225% of the cost for new construction of a similar deck.

Substructure

Substructure is defined as the structural elements required to support the superstructure; these elements typically include those from the top of support bearings down through the foundation. The function of these elements is to transfer all vertical and horizontal loads from the superstructure to the foundation supporting strata. To provide longer service life, the integrity of the substructure must be maintained. With sufficient degradation, the reduction in carrying capacity can lead to collapse.

The principal issues relating to reduced durability of substructure elements were researched. This deterioration is due to environmental factors, such as seismic events and hydraulic conditions leading to bridge scour, and corrosion in extremely aggressive environments.

As the designs of bridges begin to anticipate longer service life, the mean recurrence of forces due to conditions in the bridge environment, such as stream flow, vessel aberrance, seismic activity, and vehicle collision, needs to be reassessed to determine if the applied factors of safety are adequate for the increased probability of exceedance associated with a longer life.

Degradation of service life due to corrosion on substructure elements is also identified as a significant issue. The intrusion and concentration of chlorides caused by joint and bridge drainage leakage is identified as a concern nationwide, particularly in areas where deicing salts are used. Corrosion due to chloride intrusion is also identified as an issue in splash zones of extremely aggressive environments, whether in marine areas or adjacent to underpass roadways where deicing salts are used.

Degradation of the substructure and bearings can also result in changes in stiffness that can adversely affect the distribution of forces within the superstructure and to the individual components of the substructure.

The extension of the service life of new and existing substructure components includes risk mitigation for mean recurrence–level events, improved materials and protection systems for substructure components, and proper maintenance and replacement (as needed) for proper bearing function.

Description and Discussion of Substructure Types

The substructure component includes all elements that support the superstructure and transfer vertical and horizontal loads from the superstructure to foundation materials through spread foundations, piles, or drilled shafts. The following substructure types and components were studied with respect to service life:

- Substructure types
  - Abutments;
  - Piers; and
  - Bents.
- Substructure components
  - Piles;
  - Drilled shafts;
  - Spread foundations;
  - Modular precast construction; and
  - Integral pier and abutment details.

A summary of the information on the listed substructure systems is reported in the *Guide.*

Causes of Substructure Deterioration

The numerous causes of substructure deterioration, which are documented in the research for this project, can be categorized in three areas:

- Improper consideration of design and service life in establishing appropriate measure to address mean recurrence–level event forces;
- Deterioration caused by corrosion and section loss, primarily from chloride intrusion; and
- Seized bearings and unintended movement restraint.

Mean Recurrence–Level Event Forces

As bridge service life increases, bridges are subjected to environmental conditions for a longer period of time. Many of these conditions are accounted for in design by the use of traditional recurrence values of extreme environmental conditions such as for hydraulic stages, wind loads, and seismic events. Design for vessel impact is treated similarly. The increased design life from 50-year (pre-load and resistance factor design or LRFD) to 75-year (LRFD) to 100-plus-year service life increases the statistical probability of exceeding the design recurrence–level event. These mean recurrence–level events include

- Hydraulic flood events resulting in bridge scour;
- Seismic events;
- Vessel collision events;
- Vehicle impact events; and
- Fire events.

Substructure Deterioration Due to Corrosion and Section Loss

Corrosion deterioration in substructure elements is due to numerous causes, including chloride intrusion due to leakage of expansion joints and bridge drainage where deicing salts are used to remove snow and ice from bridge decks; chloride intrusion due to direct salt splash from traffic traveling on roadways below the bridge where deicing salts are used to remove snow and ice from the pavement; chloride intrusion found in marine and brackish water environments affecting exposed elements; and corrosion due to concrete cracking induced by ASR and other concrete quality issues. Many of the issues affecting durability of the substructure are similar to the issues affecting the bridge in general.

Seized Bearings and Unintended Movement Restraint

The structural design of the substructure is based on a distribution of longitudinal and transverse forces associated with the allowable movement of the superstructure. Fixed bearings provide an anchor that is intended to restrict "walking" of the superstructure that results from shrinkage and cycling of expansion and contraction; they are usually located longitudinally near the point of zero movement of a supported multispan superstructure unit. The remaining bearings are designed to allow the superstructure to either move or slide over the top of the substructure, thereby reducing restraining forces that would otherwise be required to resist the movement. Improper function, or seizing, of the bearings results in unintended movement restraint that can raise the force resisted by the substructure well above the intended design. This unintended restraint can cause unanticipated cracking with greater potential for corrosion.

Protection of Substructure

The extension of the service life of new and existing substructures includes risk mitigation for mean recurrence–level events, improved materials and protection systems for substructure components, and proper maintenance and replacement (as needed) for proper bearing function.

The following subsections discuss approaches for protecting the substructure for the purpose of extending service life.

Risk Mitigation

Proper risk categorization of a structure should be performed based on longer life to establish proper force effects for new structures and retrofit requirements for existing structures.

Material Protection

Improvements to service life of new substructures can be achieved through the following material improvements and protection schemes:

- Develop substructure components using specifications for construction materials that have strong resistance to saltwater environments.
- Use HPC specifications to reduce concrete permeability in splash zones and its chemical resistance to salt water, including increased concrete quality and density, use of noncorroding reinforcement, and other methodologies.
- Incorporate cathodic protection strategies.
- Consider jacketing systems for piles and shafts in critical parts of the elements to protect these parts before damage and chloride intrusion can occur.
- Eliminate bridge joints, and channel bridge drainage away from the substructure.

Improvements to the service life of existing substructures can be achieved through retrofit and rehabilitation by using the following techniques:

- Add corrosion protection with embedded sacrificial anodes.
- Encapsulate piles with jacketing.
- Improve the passivation around reinforcing steel through the removal of chloride ions.

Analysis of DOT Survey

The results of the survey performed by the R19A research team indicated that the predominant maintenance issues faced by state DOTs relate to substructures. These issues and their severity are shown in Figure 3.31.

The primary issues faced routinely by the states are chloride intrusion issues relating to leakage of expansion joints and bridge drainage systems. This issue is addressed further in the

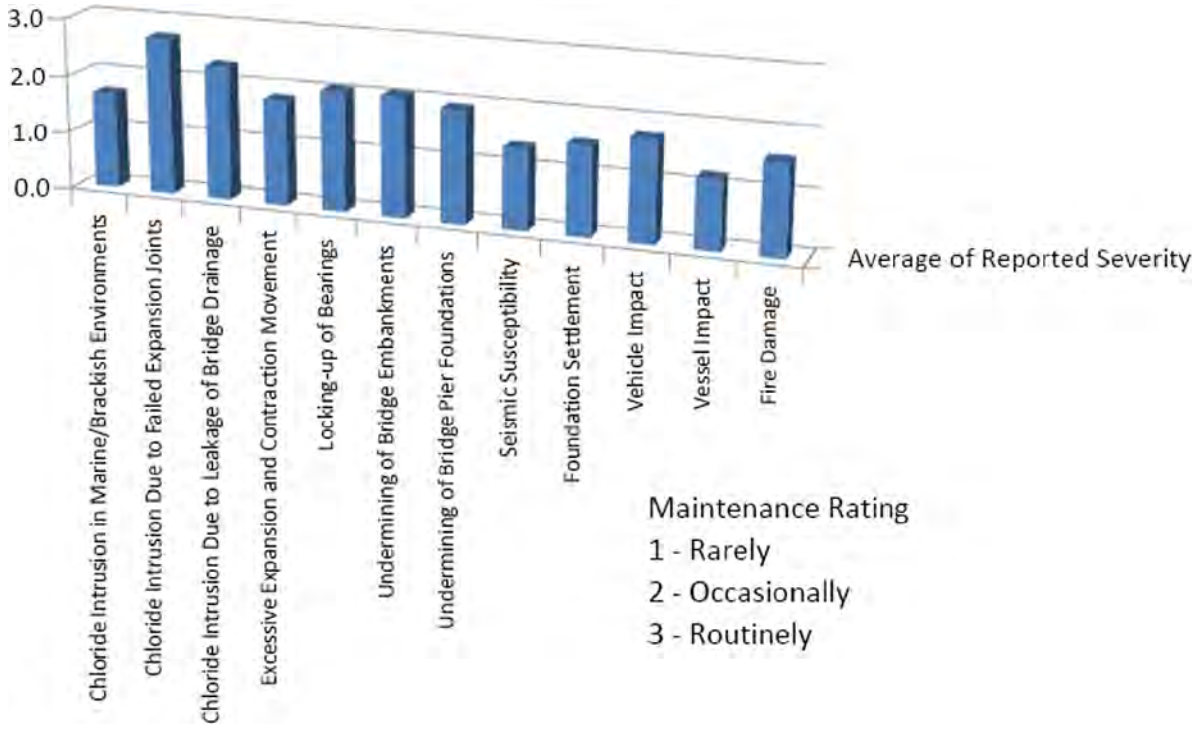

Figure 3.31. Survey results for reported severity of issues relating to substructure durability.

section titled "Expansion Joints, Joints, and Jointless Bridges." Many states appear to be addressing these issues by moving toward jointless bridges, on which storm water is collected at bridge approaches.

Chloride-intrusion issues relating to marine environments ranked equally high in states with marine environments. Little information was provided as to the methodology for addressing these concerns.

Other areas of concern in which individual states indicated routine maintenance issues related to excessive expansion and contraction, including complete closure of joints, lock-up of bearings, scour at embankments and bridge pier foundations, and vehicle impact. All other items were ranked as occasional or rare. These issues are addressed further in the report sections "Expansion Joints, Joints, and Jointless Bridges" and "Bearings."

In general, the adequacy of current inspection methods to identify maintenance issues in a timely manner for substructures was ranked as excellent or acceptable. Areas in which individual states indicated unacceptable procedures included assessment of chloride intrusion, seismic susceptibility, scour detection, and foundation settlement.

Bearings

Bearings are an important bridge element that must be considered when evaluating ways to extend overall bridge service life. Bridge superstructures experience translational movements and rotations caused by traffic loading, thermal effects, creep and shrinkage, wind and seismic forces, initial construction tolerances, and other sources. Bridge bearings are designed and built to accommodate these movements and rotations while supporting required gravity loads, transmitting those loads to the substructure, and providing the necessary restraint to the structure. Proper functioning of bridge bearings is assumed in the analysis and design of overall bridge systems. Bearing failure, or improper behavior, can lead to significant changes in load distribution and overall structural behavior that are not accounted for in the design and can significantly affect the superstructure–substructure interaction. Recent instances of rocker bearing rollover have nearly led to catastrophic span collapses. Clearly, bridge bearings play a critical role in overall bridge behavior and service life. Further, they represent a small cost in proportion to the overall structure cost, but can potentially cause big problems if they are not maintained or do not function properly.

This part of the study focused on the various bearing types currently used, identifying related problems and determining which options have the best potential for achieving 100-plus years of service life. It also looked at bridge systems that eliminate bearings by using integral girder–pier construction. The information compiled in this study was used to develop a detailed chapter in the *Guide* related to bridge bearings.

Current Bearing Types and Usage

The study identified the following main categories of bearings in use today:

- Elastomeric bearings, which include steel-reinforced pads and plain elastomeric pads;
- Cotton duck pads (CDPs);
- Sliding bearings, using polytetrafluorethylene (PTFE) pads;
- Manufactured high-load multirotational (HLMR) bearings, which include pot bearings, disc bearings, and spherical bearings; and
- Mechanical, fabricated steel bearings, for fixed application and for expansion application using rollers or rockers.

A literature review was conducted to compile existing research and relevant data regarding the performance of these bearing types and identify promising concepts. Design, materials, manufacturing, construction practices, maintenance, and imposed loads were considered. The results of research and testing were evaluated to understand the mechanics and behavior of various bearings and evaluate future research needs.

Phone seminars were conducted with Charles Roeder, bearing researcher at the University of Washington, and with representatives from D. S. Brown and R. J. Watson, both major bearing manufacturers, to gain further insight and ask specific questions related to bearing life. Research team members and various state DOT bridge engineers were invited to participate in these seminars.

The DOT survey responses related to bearings were analyzed to determine trends in the industry. DOT data regarding use of various bearings, types of related problems, service life, extent of maintenance, and frequency of bearing replacement were compiled and compared.

The following subsections summarize the compiled information related to service life for the various identified bearing types.

Elastomeric Bearings

From the DOT survey and other references, steel-reinforced elastomeric (SRE) bearings are the most widely used bearing type among nearly all states and have a good history of service. SRE bearings have become the most common type in recent years because of their desirable performance characteristics, durability, low maintenance requirements, and relative economy. Elastomeric bearings have no movable parts and accommodate movement and rotation by deformation of an elastomeric pad, which can be neoprene or natural rubber. Lateral and longitudinal movement is accommodated by the pad's ability to deform in shear. These bearings can accommodate combined movements in both longitudinal and transverse directions; circular elastomeric bearings have been used to efficiently accommodate multirotation and direction requirements.

Plain, unreinforced elastomeric pads are used for short spans on which loads and movements can be accommodated by a single layer of elastomer. As vertical load and movement requirements increase, thin reinforcing plates are combined with multiple layers of elastomer to form a laminated, reinforced elastomeric assembly. Steel and fiberglass reinforcement layers have been used; however, fiberglass is weaker, more flexible, and does not bond as well to the elastomer as does steel reinforcement. Therefore, the use of thin steel plate reinforcement has become the norm.

Elastomeric bearings have been used in the United States since the 1950s. A report published by DuPont in 1959, *Design of Neoprene Bridge Bearing Pads,* served as a design reference for many years, and included standard procedures to accommodate compressive stress and shear deformation for various neoprene hardness levels. Soon after, the 1961 American Association of State Highway and Transportation Officials (AASHTO) specification included the first formal bearing design procedure in the United States (Roeder and Stanton 1991). Although these early design provisions generally resulted in satisfactory designs, certain limitations became increasingly apparent; NCHRP Project 10-20 was established in 1981 to develop improved design procedures. In the 1980s, Stanton and Roeder conducted studies as part of this program to examine the complex nature of elastomeric bearing pads. A good summary of general research and practice up to 1980 is provided in NCHRP Report 248 by Stanton and Roeder (1982). NCHRP Project 10-20 also conducted tests to assess bearing compression, rotation, shear, stability, fatigue, and low-temperature behavior. Results of this work were reported in NCHRP Reports 298 and 325 (Roeder et al. 1987, 1989).

Later, additional studies under NCHRP Project 10-51 were conducted on low-temperature behavior and on the requirements for various materials tests; the results were reported in NCHRP Report 449 (Yura et al. 2001). This report recommended specifications and new test methods for evaluating essential properties of elastomeric bearings.

NCHRP Report 596: Rotation Limits for Elastomeric Bearings (Stanton et al. 2008) provides a good overall review of the mechanics of SRE bearing behavior and potential failure modes.

SRE bearings typically are a very robust system and problems have been rare, but errors in design have led to pad failure. Previous research and testing have identified various potential failure modes and developed design requirements that address them (Stanton et al. 2008). Shear delamination between layers of elastomer and steel reinforcing plates is the most significant potential mode of failure. This problem can be caused by excessive shear strains due to combined axial load, rotation, and shear, and it is exacerbated by cyclic shear

strain due to traffic load. The *LRFD Specifications* now provide updated requirements for considering combined shear strain, along with other design requirements that address shear deformation, pad instability, plate fracture, and compressive deflection. Two design methods have been established in the *LRFD Specifications:* a simplified and conservative Method A and a more detailed Method B. Method A is the most widely used method.

Another reported field problem associated with elastomeric bearings, albeit in only few instances, has been "walking out," or bearings slipping from their original position under the girder. Chen and Yura (1995) investigated slippage of elastomeric pads experienced on Texas bridges. McDonald et al. (2000) reported on the slippage of elastomeric pads and the results of a survey of state DOTs, bearing manufacturers, and other researchers to gain knowledge on the subject. Heymsfield et al. (2001) reported on the pad slippage experienced on Louisiana bridges and discussed the causes and recommended practical guidelines to remedy the problem. Slippage was occurring primarily in elastomeric pads made of natural rubber because of paraffin that was added during the manufacturing process to meet required ozone degradation requirements established by AASHTO. Neoprene pads have inherently greater ozone resistance and do not need wax additives. When used, these waxes over time will bleed to the bearing surfaces and drastically reduce the coefficient of friction between the bearing and its contact surface, which leads to slipping (Chen and Yura 1995). McDonald et al. (2000) reported on various remedial measures from a survey of state DOTs; these measures included

- Only using neoprene pads;
- Banning the use of antiozonant wax additives;
- Vulcanizing bearing to sole plate for steel bridges, or having anchoring details;
- Having positive attachment when low bearing stresses exist;
- Inspecting bridges annually; and
- Cleaning contact surfaces when replacing natural rubber bearings with neoprene bearings.

In summary, when SRE bearings are adequately designed, manufactured, and installed it is believed that they have the best potential for achieving 100-plus years of service life with practically no long-term maintenance requirements. They have broad application to most bridges, both concrete and steel superstructures, that fall within the 300-ft span range for this study, and they are applicable for multidirectional movement (as with curved and skewed bridges). There is broad use of this type of bearing among the states, and there are over 50 years of service experience in the United States, and even more abroad, to verify these conclusions. Manufacturing quality has been very good and has improved significantly in the last 20 years. However, to achieve 100-plus-year service life, even greater emphasis must be placed on manufacturing quality assurance.

Because of some past problems related to improper design, it is recommended that an updated design guide for SRE bearings be developed that would supplement the current *LRFD Specifications*. The guide would provide detailed guidance and understanding of the mechanics and behavior of these bearings and would help avoid design problems.

Additional cyclic compression testing is still recommended, however, to supplement newer combined compression–rotation design recommendations. This additional fatigue testing, particularly for shear strain due to compressive loading, could also help develop a life prediction model.

Cotton Duck Pads

CDPs are another type of elastomeric bearing that is occasionally used in some states. They have typically been used more for precast concrete I-girder bridges and have been used with span lengths up to the 150- to 180-ft range.

CDPs are preformed, elastomeric pads consisting of very thin layers of elastomer (less than 1/60 in.) interlaid with fabric. The fabric can be cotton or polyester. The fabric layers are many, and closely spaced, which gives CDPs high compressive strength and stiffness. These closely spaced layers, however, provide high shear stiffness and much smaller shear deformation capacity than other elastomeric bearing types provide. As a consequence, CDPs tolerate large compressive stresses but limited shear deformation because interlayer splitting occurs at relatively small shear strains. Thus, larger movement requirements with CDPs must be accommodated by the addition of a PTFE sliding surface. Recent design recommendations have been developed and incorporated into the *LRFD Specifications* (Lehman et al. 2003).

The overall performance of CDPs depends on their stiffness and deformation capacity, which can vary among manufacturers. To ensure adequate performance from CDPs, quality control testing measures have also been developed.

CDPs have not been widely used and their service history is limited, but there is a potential for this bearing type within a defined operational range (i.e., bridge systems that have short movement and rotation requirements). CDP applications using PTFE sliding surfaces for accommodating larger movements are subject to the limitations for PTFE wear, which are discussed in the next subsection.

Because of their limited use and service history, and the need for PTFE sliding surfaces for movement, CDPs are less recommended than SRE bearings for long service life.

Polytetrafluorethylene Sliding Bearings

With certain combinations of high load, movement, and rotation, the capacity of elastomeric bearings to accommodate

the required translation through shear deformation can be exceeded. In these cases, additional movement capacity must be provided by the use of sliding surfaces. Further, all other types of bearings—including CDP and HLMR pot, disc, and spherical bearings—use sliding surfaces to accommodate expansion requirements.

Currently, PTFE is the material used for sliding surfaces in the United States. Its low frictional characteristics, chemical inertness, and resistance to weathering and water absorption make it an attractive material for bridge bearing applications.

The sliding movement is typically provided by a very smooth stainless steel plate sliding on a PTFE surface. The stainless steel surface is larger than the PTFE surface so that the full movement can be achieved without exposing the PTFE. The stainless steel is typically placed on top of the PTFE to prevent contamination with dirt or debris. PTFE sliding bearings may be guided, allowing movement in only one direction, or non-guided, allowing multidirectional movement. When PTFE sliding surfaces are combined with elastomeric pads, the elastomeric pad must be designed to accommodate the shear force that is needed to overcome the PTFE friction resistance.

Sliding surfaces develop a frictional force that acts on the superstructure, substructure, and bearing. As a result, friction is an important design consideration; the low frictional resistance of PTFE makes it useful for this application. The coefficient of friction of PTFE increases with decreasing temperature and with decreasing contact pressure. It also increases if the mating surface is rough or contaminated with dust or dirt. Proper design, fabrication, and field installation are all essential for proper performance.

Plain, unfilled PTFE is the most common material used for sliding bearings. However, plain PTFE wears under certain service conditions, particularly when subjected to combinations of high contact pressure, high rates of movement, and low temperatures, and may require replacement after a period of time. Fast sliding speeds, especially those associated with traffic movements, have been shown to be much more critical for PTFE wear than slow movements due to temperature (Stanton et al. 1999). Therefore, wear of the PTFE sliding surface is one of the critical factors affecting service life for these types of bearings, and it is not recommended to use plain PTFE as a sliding surface for bearings subject to relatively high sliding speeds and low temperatures. Further, there are minimal data to develop a life prediction model for sliding surfaces. Designers need to have the capability of predicting the expected service life of sliding surfaces for maintenance and replacement purposes.

Woven or glass-filled PTFE surfaces provide much higher overall wear resistance, especially at higher sliding speeds (Stanton et al. 1999). However, these surfaces have higher friction coefficients that must be taken into account in the bridge system design.

Dimpled and lubricated PTFE also provides exceptional wear resistance and low friction, but the long-term reliability and effectiveness of lubrication is questionable (Stanton et al. 1999). Dimples are spherical indentations machined into the PTFE surface to act as reservoirs for storage of lubrication. Silicone greases are specified because they are effective at low temperatures and do not attack the sliding material. Dimpled and lubricated PTFE has been used in Europe, but in the United States it has been used only in special cases on large spherical bearings where very low coefficient of friction requirements are needed to reduce friction loads on substructures.

PTFE may creep (or cold flow) laterally when subjected to high compressive stress and shorten the life of the bearing. The reduction in PTFE thickness may also allow hard contact between metal components. Thus, although the compressive stress should be high to reduce friction, it must also be limited to control creep. PTFE is frequently recessed for one-half its thickness and bonded to control creep and permit larger compressive stress.

Filled PTFE, which is reinforced with fiberglass or carbon fibers, has significantly greater resistance to creep and is sometimes used to resist creep or cold flow.

Maurer sliding material (MSM) is an alternative sliding material developed in Germany as a higher-performing substitute for current PTFE-based sliding material. The new material is an ultrahigh-molecular-weight polyethylene that has performed well in recent field applications and experimental testing in Europe. It has been shown to provide exceptional wear resistance, but when used in a dry condition (without lubrication) it has a much higher friction coefficient than plain PTFE. The friction coefficient reduces, however, with higher contact pressures. When used in a dimpled and lubricated condition, its friction coefficient reduces considerably and is more comparable to lubricated PTFE.

Testing was performed as part of this study on high-performance sliding materials to compare friction coefficients, wear rates, and accumulated wear by considering a number of parameters, including contact pressure, speed of movement, and total accumulated movement. The goal was to evaluate these materials for improved wear resistance and to determine if it was feasible to develop a deterioration model. Materials tested included

- Plain PTFE as a base;
- Fluorogold, which is a fiberglass-reinforced PTFE; and
- MSM, which is an ultrahigh-molecular-weight polyethylene.

The results of this study are included in Appendix D. The testing showed significantly improved wear resistance of these high-performance sliding materials over plain PTFE. It also

showed that a wear rate model could be established for PTFE-based materials considering a pressure–velocity factor.

High-Load Multirotational Bearings

When design loads and rotations exceed the reasonable limits for elastomeric bearings, HLMR bearings have typically been considered. HLMR situations often occur with longer spans; with curved or highly skewed bridges; or with complex framing, such as with straddle bents. In these cases the axis of rotation or the direction of movement, or both, are either not fixed or may be difficult to determine. The current *LRFD Specifications* now incorporate research findings on HLMR bearings reported in *NCHRP Report 432: High-Load Multi-Rotational Bridge Bearings* (Stanton et al. 1999).

HLMR bearings include pot, disc, and spherical bearings. Each HLMR bearing type is unique in how it accommodates large loads and rotations. All are fabricated in fixed and expansion versions. The expansion versions accommodate translational movement by means of PTFE sliding elements. Expansion versions may be guided, allowing movement in only one direction, or nonguided, allowing multidirectional movement. The following paragraphs describe and compare the three types of HLMR bearings.

Pot bearings have been the most-used HLMR bearing. The main elements of these bearings include a shallow steel cylinder, or pot, which contains a tight-fitting elastomeric disc that is thinner than the depth of the cylinder. A machined steel piston fits inside the cylinder and bears directly on the elastomeric disc. Brass rings are used to seal the elastomer between the piston and pot components. Vertical load is carried through the piston of the bearing and is resisted by compressive stress in the elastomeric pad. The pad is deformable, but almost incompressible in its confined condition; it is often idealized as behaving hydrostatically. Rotation can occur about any axis and is accommodated by deformation of the elastomeric pad. Horizontal loads on a pot bearing are resisted by direct contact between the pot wall and the piston.

Early on, pot bearings developed a bad reputation for sealing ring failure and leakage of elastomer, but improvements through testing, improved design requirements, and improved manufacturing tolerances have solved many of the early problems. There have not been recent reported failures. However, they are still susceptible to internal wear and are less likely to reach long service life. The *AASHTO LRFD Bridge Construction Specifications* (AASHTO 2010a) require cyclic testing to confirm long-term performance.

Pot bearings require a high degree of quality control in the fabrication and field installation process and an accurate determination of design loads and displacements to achieve satisfactory performance. Adequate clearances must be provided to allow proper displacement without binding. Through the years, they have been the most economical and common HLMR bearing and have been implemented on bridges throughout the United States.

Disc bearings were proprietary until recently and are now becoming more popular. They consist of a hard polyether urethane circular disc sandwiched between upper and lower steel plates with a center shear pin device to resist horizontal load. The discs are stiff enough to support the compressive load, yet can deform to permit rotation. However, rotational stiffness for a disc bearing is several times that of a pot bearing.

Disc bearings are reasonably economical, but widespread use has been limited because of their originally patented and proprietary status, which made them available only from a single source. Now, there are several reputable bearing manufacturers that can supply disc bearings, and usage has increased.

Since their first use in the early 1970s, these bearings have had good performance, and there have been few reported field problems. Potential service life problems would likely be associated with production or operation defects related to design and manufacturing. Current specifications are minimal regarding design, and are generally performance related. Therefore, performance testing and manufacturing quality control measures are necessary to verify compliance.

Previous research and testing of disc bearings for combined load and rotation (Stanton et al. 1999) showed that rotation of disc bearings is partly accommodated by uplift of the steel plates from the urethane disc, especially if the compressive load is light. This uplift should not result in any problems with fixed bearings, but it could be a concern with sliding bearings, since uplift of the disc produces edge loading on the PTFE sliding surface. To mitigate this potential problem, the *LRFD Specifications* limit the edge contact stress on PTFE surfaces. High edge pressure can accelerate PTFE wear as described previously.

Tests also showed the urethane disc to be somewhat deformed and abraded by cyclic rotations, but the damage was not severe enough to affect performance. The *AASHTO LRFD Bridge Construction Specifications* (AASHTO 2010a) require cyclic testing to confirm long-term performance.

Spherical bearings are the most robust of all HLMR types and are used primarily for accommodating large rotations about one or more axes. Rotation is developed by sliding a convex stainless steel surface against a concave spherical PTFE surface. The rotation occurs about the center of the radius of the curved surface, and the maximum rotation is limited only by the geometry and clearances of the bearing. Translational movement is accomplished by incorporating a flat PTFE sliding surface. Horizontal loads may be partially resisted by the curved geometry, but large horizontal loads may require additional external restraint.

Spherical bearings require a high level of accurate machining for proper mating of the convex and concave spherical surfaces. As a result, they are generally the most expensive

HLMR type. The advantage, however, is their ability to accommodate higher gravity loads and rotations. They are also considered to be the most reliable.

Spherical bearings are subject to PTFE wear, which can limit their service life. Variations in friction with different types of PTFE and under different temperature and load conditions cause variations in behavior that can lead to performance issues. Woven PTFE has often been used with spherical bearings in the United States, and dimpled and lubricated PTFE is often used in Canada and Europe.

Mechanical Steel Bearings

Mechanical steel bearings were used extensively up through the 1970s for steel bridges and some concrete bridges for both fixed and expansion conditions. Many existing bridges still have these types of bearings, and some states still use them for new construction. Steel bearings transmit loads through direct metal-to-metal contact. Most fixed bearings rely on a pin or knuckle to allow rotation while restricting translational movement. Rockers, rollers, and sliding bearings are common expansion types historically used. Typically, steel bearings are expensive to fabricate, install, and maintain, which is why elastomeric bearings have become popular. Moreover, steel bearings typically provide unidirectional movement. These types of bearings are fully designed by the engineer to accommodate loads, movements, and rotations and can accommodate large requirements.

Bronze-lubricated plate bearings have been used in conjunction with steel bearings to accommodate smaller levels of movement at expansion ends, but they are not used very often today. PTFE sliding surfaces have replaced bronze sliding plates because of a much lower coefficient of friction and lower cost.

When functioning properly, mechanical steel bearings generally provide the closest representation of assumed structural end conditions. Mechanical steel bearings have been used extensively over the years, but corrosion and freezing have been problems, particularly when the bearings are located below leaking deck joints. Steel rocker bearings have also performed poorly in seismic events and have been replaced as part of seismic retrofit in many instances. Mechanical steel bearings require a high level of maintenance, but if properly protected and maintained their service life can match the superstructure they support. Elastomeric and HLMR bearings, however, have typically replaced these older steel mechanical types in new construction in most states.

The literature regarding fabricated steel bearings typically relates to discovered field problems. Rockers that are overrotated or corroded and frozen bearings causing other forms of distress in pier caps or at the ends of concrete beams are occasionally observed during maintenance inspections. On rare occasions, these problems have been encountered by the traveling public.

Fyfe et al. (2006) reported that steel rocker and roller bearings, along with older-type metal sliding plates, are the most susceptible to freezing in position. When bearings are frozen, bridges have developed their own provisions for contraction and expansion such as pier cap cracking or rocking of piers or abutments.

Modjeski and Masters (2008) reported on a rocker bearing failure on a 32-year-old bridge in Pittsburgh, Pennsylvania, on which the rocker bearings at one pier tipped over due to continual buildup of debris and corrosion below a leaking deck expansion joint. Many bridges have performed satisfactorily with steel bearings; however, this failure illustrates the importance of continual maintenance, particularly in areas affected by leaking joints.

A corrosion protection plan is also critical for these types of bearings, especially when they are located below deck joints. Galvanizing, metalizing, and use of zinc-rich primers provide the best forms of protection, in descending order.

System Approaches to Improved Bearing Service Life

From a bridge system point of view, use of integral construction that eliminates or minimizes the number of bearings is desirable. Eliminating or minimizing the number of deck joints whenever possible is also desirable. Eliminating deck joints prevents deck drainage and debris from spilling on bearings and causing deterioration, particularly with steel bearings, or steel surfaces on components of other types.

Integral girder–pier construction has been used in some cases for resolving clearance issues and avoiding sharp skews, but it can also be considered for eliminating bearings and resulting maintenance issues. Most integral girder–pier construction to date has been with steel girders and CIP posttensioned concrete caps. However, many integral caps have also been constructed within prestressed concrete girder and concrete box girder systems using conventional reinforcement without posttensioning. These various integral pier cap subsystems have performed well to date. The next subsection, "Integral Construction," discusses these systems in greater detail.

Skewed, curved, and wide bridges subject bearings to multidirectional movements or rotations, or both. Improper bearing orientation or inadequate multidirectional movement capacity can lead to higher stresses, wear, and reduced service life. The National Steel Bridge Alliance (NSBA 2005) provides guidance for proper orientation of expansion bearings in curved and skewed bridges.

Bridges wider than three lanes can experience significant transverse thermal movement. Guides and keeper assemblies should be limited to the interior portions of the bridge that do not experience large transverse movements. Bearing details

for outer portions on wide bridges should be designed to accommodate transverse movement.

Proper inspection of bearings during their service life is critical to evaluate proper performance, wear, and deterioration. Early detection of problems can allow maintenance or repair before more serious conditions can develop. Shallower bearing types can be difficult to properly inspect, particularly when limited headroom prevents close access. Consideration should be made in overall bridge system design to allow access for proper inspection and maintenance of bearings, including

- Considerations to improve bearing service life;
- Regular inspection of bearings to detect problems early;
- Regular maintenance performance and general cleaning when bearings are exposed to dirt and debris, washing surfaces, and cleaning troughs below open-finger dams;
- Cleaning and painting of steel surfaces on mechanical steel bearings to prevent corrosion; and
- Repairing or replacing bearings that are not functioning before other problems occur due to higher stress on girders or piers.

Converting existing jointed construction systems to continuous systems to eliminate joints and thus protect bearings below (and other elements) can be very beneficial. States vary regarding how this is done. Standard recommended details should be developed to facilitate design, construction, and performance.

Regardless of expected service life, bearings are subjected to severe service conditions and have a high potential for unintended consequences related to improper design, manufacturing, installation, and maintenance that can lead to shorter service lives than other bridge elements. Consideration should be given in overall bridge system design to allow for easy replacement of bearings with minimal traffic disruption. AASHTO (2004) and NSBA (2005) provide recommended bearing details that facilitate replacement. The following items should be considered during design to allow for bearing replacement:

- Jacking locations should be provided at every girder. An alternative is to provide for jacking under a diaphragm that lifts adjacent girders simultaneously.
- An unattached bearing can easily be pulled from its position when the load is removed. Anchor bolts should be placed so that they do not impede the removal of the bearing.
- Bearings should be detailed in a way that they can be replaced with only 0.25 in. of jacking so as not to cause a bump at the top of the deck that would affect traffic.

Bridge inspections and inspection data collection for bearings should be expanded to identify the bridge system for bearings, bearing types, conditions, and other relevant data. These recommendations for more detailed bearing data collection can be used within the Federal Highway Administration (FHWA) Long-Term Bridge Performance program, which is intended to study the deterioration and durability of bridges and the impacts of maintenance and repair. These recommendations can also be used to supplement the types of data collected for use within bridge management systems such as PONTIS. Improved data collection for bearings can be useful in determining and scheduling required maintenance and for developing more accurate deterioration models.

Integral Construction

General Concept

Integral, CIP posttensioned bent caps have been in service in Tennessee since 1978 (Wasserman 1987) and were part of an interchange in Knoxville. This technique allows girders to pass directly through the pier's cap, rather than over the top in the traditional manner, thus overcoming vertical clearance restrictions and avoiding extreme skews (Wasserman 1987). The reported bridge system used longitudinal steel girders with single-column reinforced concrete piers. The construction methods and overall performance were described. To date, the structure has exhibited good performance. Other benefits sited were reduction in fill height, seismic resistance, and aesthetics.

Within interchanges, directional ramps often cross other roadways on a skew. In these cases, the ramp piers are often placed to match the skew, which minimizes the crossing span. An alternative is to keep the ramp piers normal to the upper roadway and to either lengthen the span or raise the profile to provide the necessary vertical and horizontal clearance. Use of integral pier caps with single-column piers allows the pier caps to be placed normal to the roadway, thereby avoiding the sharp skew, while still maintaining the minimum span length and minimum ramp profile. This arrangement has a distinct advantage when the abutments are also placed normal to the ramp. Having both the abutments and piers in a consistent orientation normal to the roadway eliminates complexity in design and construction.

Integral pier cap construction also has the advantage of eliminating bearings.

NCHRP Project 12-54

NCHRP Project 12-54 and the subsequent *NCHRP Report 527: Integral Steel Box-Beam Pier Caps* (Wassef et al. 2004) reported on research conducted by Modjeski and Masters, Inc. and Iowa State University to develop recommended design methodologies and details for integral connections between steel superstructures and concrete substructures. The study first evaluated data on the state of the art for integral connections. A questionnaire was sent to state DOTs, industry associations, and select domestic and foreign bridge designers to determine

the extent and type of use. The main reason reported for using integral pier caps was to increase underclearance and to avoid sharp skews (94% of cases). Enhancing seismic performance was cited in 33% of cases. Steel plate girders were used in most of the bridge superstructures using integral pier caps. Most integral pier caps (76%) were supported on single-column piers. The majority of integral pier caps (90%) were made from concrete, and the remaining caps were made from steel. No cost data were available, but the respondents estimated a reduction in weight of steel and an increase in cost of fabrication and erection. They also estimated a savings on approach roadway costs due to the reduced height of fill. Performance history was reported as good, but long-term service data on many of the reported bridges were not available because they were new.

Fourteen pier cap systems were initially examined, with variations in steel and concrete superstructures and variations in reinforced concrete, posttensioned concrete, and steel caps. Criteria were developed to assist in scoring the various cap systems and selecting a system for further studies. Systems with the highest scores were as follows:

- Steel I-girders on single-column piers and posttensioned concrete pier caps;
- Steel I-girders on multicolumn piers with columns located under each girder; and
- Steel I-girders on single-column piers and steel box beam pier caps.

Previous research on integral cap connections by Caltrans at the University of California at San Diego (UCSD) evaluated several integral connection systems and selected a steel girder with a posttensioned concrete cap for study and testing that was similar to the first system identified by NCHRP 12-54. To avoid duplicating the UCSD studies, NCHRP 12-54 chose the steel I-girders with steel box beam cap for further study.

The study team concluded it was feasible to integrally connect reinforced concrete columns to steel box beam caps by extending the column longitudinal reinforcement through holes in the pier cap flange and filling the pier cap compartment directly above the column with concrete.

UCSD Studies

Performance of integral pier details for steel bridges in seismic regions was researched by Patty et al. (2002) at UCSD. They concluded that posttensioned concrete diaphragms provided the best behavior in seismic regions.

According to the same study, posttensioning the concrete diaphragm is an effective way of controlling the torsional-type cracks that could form in the diaphragm when the bridge is subjected to ground motion parallel to the span length (longitudinal).

DOT Survey for Bearings

The following analysis summarizes the 19 state DOT responses to the R19A project survey for bridge bearings. The survey questions for bearings focused on several key issues, including

- Bearing types used and frequency of use;
- Problems experienced with the various types used;
- Service life experienced and expected;
- Types of bearing improvements that have been developed or used;
- Frequency and types of maintenance performed;
- Frequency and reasons for bearing replacement;
- Provisions incorporated into new designs to facilitate bearing replacement;
- Use of integral piers and abutment caps to eliminate bearings;
- Orientation of bearings on curved or skewed bridges;
- Accommodations for transverse movements on wide bridges; and
- State DOT research activities related to bearings.

These issues are discussed in the following sections.

Bearing Types Used by DOTs

Figure 3.32 summarizes the reported use of the various bearing types by the responding number of state DOTs. The chart identifies use in three categories: used frequently, occasionally, or rarely. The following list identifies the abbreviations shown in Figure 3.32:

- SRE: steel-reinforced elastomeric bearings;
- Plain E: plain elastomeric pads;
- PTFE: sliding bearings using PTFE pads;
- CD: cotton duck pads;
- HLMR P: pot bearings;
- HLMR D: disc bearings;
- HLMR S: spherical bearings; and
- Steel: fabricated mechanical steel bearings.

SRE bearings were reported as the most frequently used bearing type by all survey respondents. They were reported as routinely used by nearly all states for both steel and concrete bridges. Plain elastomeric pads were used routinely by a few and occasionally by several DOT respondents, but were mostly used for concrete bridges.

PTFE sliding bearings were reported routinely used by several respondents for both steel and concrete bridges; a few DOTs reported using them occasionally.

CDPs are not widely used and were reported routinely used only by Nebraska; only a few other states reported occasionally; most reported rarely or did not respond.

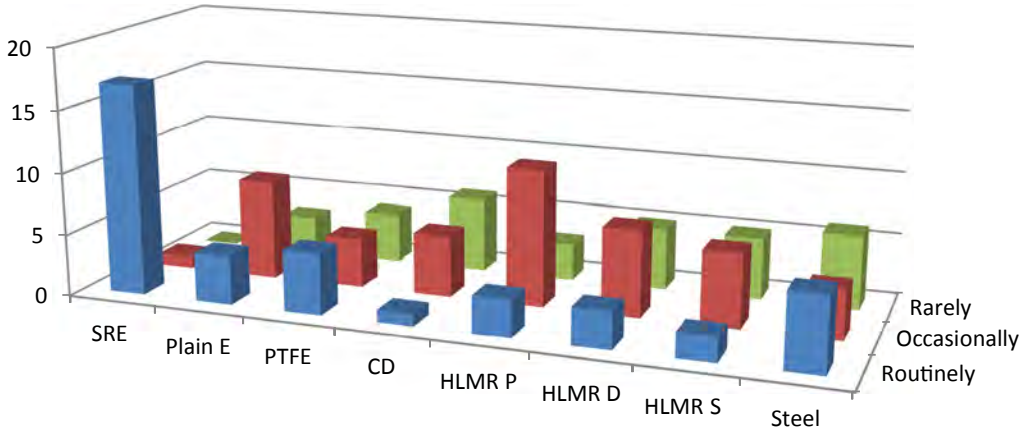

Figure 3.32. Bearing type use by respondents.

HLMR bearings are used when required by higher loads and rotations, typically for longer spans or for curved and skewed bridges. Pot, disc, and spherical bearings were all reported used. Pots were the most reported of this type, followed closely by discs and to a lesser extent by spherical bearings. HLMR bearings were reported used for both steel and concrete bridges, but many respondents indicated their use for steel bridges only.

Fabricated steel bearings (fixed, rocker, or roller) are still used by many DOT respondents in varying degrees, primarily for steel bridges, but a few indicated use also for concrete bridges. One respondent who reported occasional use indicated that they are no longer used on new bridges. One indicated that these types used to be their standard. Five DOTs reported using them rarely now.

A few respondents reported using seismic isolation bearings (not shown in the Figure 3.32) occasionally for both steel and concrete bridges.

Bearing Problems Experienced

Bearing deterioration caused by deck drainage through open or leaking deck joints was reported by nearly all the responding DOTs. Steel bearings were predominantly affected.

Bearing freezing (restricted lateral or rotational movement) and steel element corrosion, both associated with steel bearings, were the predominant bearing problems and were reported routinely or occasionally by nearly all respondents. However, corrosion on exposed steel elements on all other bearing types was also reported as occasionally by a few respondents.

The following list describes the types of problems experienced with the various bearing types. Aside from freezing and corrosion, there were no routinely found bearing problems; all other problems noted were reported as occasionally or rarely.

- Elastomeric bearings had elastomeric material failure due to excessive loading or deformation as the most commonly reported problem, but the frequency was reported as occasional by eight respondents, and rarely or never by 10 respondents. Material degradation from environmental effects occurred, but to a much lesser degree. Walking out from under girders and slipping was reported by three respondents, but this problem type was not specifically asked in the survey, so it may be possible that other respondents have experienced this but did not add it to their response.
- CDPs had no routinely or occasionally reported problems.
- PTFE material failure was reported as occasional by three respondents, but rarely or never by the rest.
- HLMR component failure was also reported to be occasional by a few respondents, but it was mostly reported as rarely or never.
  - Pot bearing failure due to elastomer leakage through sealing rings was reported occasionally by three states, but four others reported rarely or never.
  - Disc bearings were reported to have had component problems occasionally by two states, but six states reported rarely or never.
  - Spherical bearings were reported by two states to have component problems rarely or never.

Service Life of Bearings

There was some variation among the responding DOTs concerning expected and experienced service life for the various types of bearings that were reported used. Overall, expected service life typically ranged between 50 and 75 years, but some types, such as PTFE sliding bearings or HLMR bearings, were more typically expected to last at the lower end of the range (30 to 50 years). It should be mentioned, however, that experiments carried out within this research project (reported in Appendix D) indicated that PTFE has a much shorter service life. Elastomeric bearings were expected to last at the higher end of the range, closer to 75 years.

Experienced service life varied more. In some cases, low experienced service life was reported, but the report was

Table 3.4. Ranges of Service Life Reported for Different Bearing Types

Bearing Types	Expected Service Life (years)	Experienced Service Life (years)	Comments
Elastomeric	50–75, closer to 75	15–50	Experienced service life limited by current years in service
Cotton duck	75	35–50	Only two DOTs reported
PTFE	30–75	30–50	
HLMR	30–75, mostly 50	10+ pots 15–40 others	Early pots had problems. Lower service life often limited by current years in service
Fabricated steel	50–75	15–100	Oldest type of bearing in service

actually the current number of years that the bearing type has been in service, which did not represent its actual full service life. This was also the case with some HLMR bearing types. Typically, sliding PTFE bearings experience wear on the PTFE surfaces that can shorten service life. Manufactured HLMR bearings are typically more complicated, with more wearing components that can also affect service life. Early pot bearings experienced service problems. Fabricated steel bearings have experienced long service life when protected and maintained. When subjected to a buildup of debris and corrosion, they have exhibited very short service lives. Table 3.4 summarizes the ranges of service life reported.

Bearing Improvements to Improve Service Life

The DOTs were asked if they had developed or used any bearing improvements that had the potential for extending bearing service life. Table 3.5 summarizes their responses. Some respondents identified various improvements, which included

- Use of integral construction and jointless bridges, which eliminate bearings and prevent deterioration due to leaking joints;
- Use of elastomeric bearings, which have had improved performance results;
- Improved PTFE bearings with improved PTFE hybrids or thicker PTFE surfaces, and keepers or recesses to prevent PTFE material from creeping out (PTFE surfaces wear over time, and improved PTFE hybrids or thicker PTFE surfaces can provide longer life); and
- Use of galvanized anchor bolts.

Special Protection for Steel Elements in Bearings to Prevent Corrosion

The DOTs were asked if they used any special coatings, paint systems, or types of steel for steel elements in bearings to prevent corrosion and extend service life. Some respondents identified various methods of protection. These included

- Hot-dip galvanizing;
- Metalizing;
- Inorganic zinc-rich primer applied in shop;
- Use of the same paint system as steel girders; and
- Some use of weathering steel.

Table 3.5. Bearing Improvement Methods

Bearing Improvement	No. of DOTs Reporting	Comments
Use of integral construction and jointless bridges	3	Eliminates bearings and bearing problems and prevents deterioration from deck drainage
Use of elastomeric bearings	4	Illinois reported use of SRE bearings since the 1970s with excellent results. Iowa reported using simplified bearings with noncorrosive elements and preferred bearings with neoprene.
Use of thicker or improved PTFE plates	2	For longer wear
Use of keepers with PTFE sliding bearings	1	Prevents creeping out
Use of etched, bonded, and recessed PTFE surfaces	1	Prevents creeping out
Use of galvanized anchor bolts	1	Prevents component corrosion
Limit bearing types specified	1	Only uses steel-reinforced elastomeric, spherical, or seismic isolation bearings

Table 3.6. Special Protection for Steel Elements in Bearings

Steel Element Protection	No. of DOTs Reporting	Comments
Hot-dip galvanizing	3	Hawaii galvanizes bearing plates with elastomeric bearings. Iowa reports most steel components are galvanized.
Metalizing	2	
Inorganic zinc shop coat	5	Ontario also reported using epoxy–polyurethane field paint system.
Painting system same as steel girders	6	New York uses a paint system for bearings even with weathering steel bridges. Texas reports that steel bearings have always been painted.
Use of weathering steel	5	Iowa reports only a few parts use weathering steel. Nebraska uses weathering steel for sole plates. New Hampshire and Texas use weathering steel in some cases. Virginia uses weathering steel when joints are eliminated.

Ontario reported having no data to evaluate concerning how any special protection has extended service life. New Hampshire assumed a 10-year increase in service life with their painting program, but had no supporting data. Table 3.6 summarizes the responses concerning protection for steel elements in bearings.

Requirements for Specifying New HLMR Bearings

The DOTs were asked whether they specified certain manufacturers or performance requirements when specifying new bearings, particularly HLMR types. Most respondents reported specifying performance requirements such as loads, movements, and rotations, and they have standard supporting special provisions. Some respondents detail a specific type on the contract plans, but allow substitutions based on provided loads, movements, and rotations.

Frequency and Types of Bearing Maintenance

Some respondents reported routine bearing maintenance, but most reported maintenance as occasionally or rarely performed. Cleaning and washing, cleaning and painting, lubricating, resetting, unfreezing, and replacing were the types of maintenance reported. For some bearing types, the reported maintenance correlated with the types of problems associated with that bearing type. For example, maintenance for fabricated steel bearings included cleaning and painting, resetting and unfreezing (all associated with steel corrosion and tipping). Maintenance for elastomeric bearings included resetting (associated with walking out and slipping), and for PTFE bearings included unfreezing (associated with PTFE wear or binding).

Reasons for Bearing Replacement

The reasons reported for bearing replacement also correlated well with the problems experienced and reported by the responding DOTs. Table 3.7 summarizes the responses.

The most common reasons reported for bearing replacement were corrosion and freezing of older fabricated steel bearings, typically pertaining to steel bridges. Frequency was reported occasionally to rarely. It was not uncommon for these types of bearings to be replaced when older bridges were rehabilitated. When replaced, SRE bearings or other types were used. In some cases, excess rotation or tipping was reported, and resulted in either replacement or resetting. Replacing high-profile steel bearings due to seismic retrofit was also reported by some respondents.

Elastomeric bearings have been replaced or reset, but frequencies are typically reported as rare. Walking out from under girders was the most reported reason, but still only in a few instances. Other reported reasons were excess vertical or horizontal deformation, being undersized for loads (which also results in excess deformations), and material failure or degradation (which was reported to occur rarely). California

Table 3.7. Reasons for Bearing Replacement

Bearing Types	Reasons for Replacing	No. of DOTs Reporting
Elastomeric	Excess vertical or horizontal deformation	3
	Undersized for load capacity	1
	Material failure	1
	Walking out	3
PTFE	Stainless or PTFE plates debonding	1
HLMR (pots)	Leaking elastomer	1 (rarely)
Fabricated steel bearings	Corrosion	13
	Freezing or nonfunctioning	5
	Tipping or excess rotation	2
	Seismic retrofit	5

Table 3.8. Provisions to Facilitate Bearing Replacement and Minimize Traffic Disruption

Provisions to	No. of DOTs Reporting	Comments
Facilitate Bearing Replacement		
Provide jacking points and adequate clearance	9	California supports bridge for dead load and live load to replace bearings.
Provide recesses in steel plates versus welding to allow easier removal of parts	1	
Use reinforced elastomeric bearings	1	They have had good performance with this bearing type and do not anticipate replacement.
Do not incorporate any provisions	6	
Minimize Traffic Disruption		
Use jacking and blocking with some traffic disruption	4	Traffic resumed after blocking structure.
Use hydraulic jacks to lift deck	1	No report on traffic impact
Allow jacking with traffic	1	In some instances
Support bridge for dead load and live load	1	California allows 0.5-in. bump across deck joints.
Replace bearings at night with temporary road closure	2	
Remove live load	1	
Normally close bridge for rehabilitation	1	
Do not incorporate any provisions	5	Virginia said done on case-by-case basis.

reported having to replace elastomeric bearings on rare occasions due to curling or delamination due to prestress shortening (i.e., excessive shear deformation).

For sliding PTFE bearings, stainless or PTFE plate debonding was reported by a few states.

Provisions in New Designs to Facilitate Bearing Replacement

The DOTs were asked whether they incorporate any provisions in new bridge designs that would facilitate future bearing replacement. They were also asked whether their provisions for bearing replacement would allow the work to be done with minimal traffic disruption. Many respondents reported that new designs allow for bearing replacement by providing jacking points with sufficient capacity to raise the girders. Providing adequate clearance below to install jacks was also mentioned. Most DOTs reported that traffic would have to be moved away from the jacking location while jacking, but traffic could still be maintained on the bridge. Blocking the structure immediately after jacking would allow all traffic to resume while actually replacing the bearings with minimal disruption. Table 3.8 summarizes the various responses.

Use of Integral Pier Caps to Eliminate Bearings

The DOTs were asked if they used integral pier–bent caps as a way to eliminate bearings and to indicate the frequency and purpose of their use of integral construction. Most of the respondents reported that they have rarely or never used integral pier caps as a way to eliminate bearings. The few that did indicate this technique as used routinely were primarily referring to use at integral abutments.

Several respondents reported using integral piers occasionally for resolving vertical clearance issues. Other respondents reported use of integral piers for accommodating sharp skews, for eliminating deck joints, and for frame behavior in seismic events. Table 3.9 summarizes the responses.

Types of Integral Pier–Bent Caps

The DOTs were asked what types of integral pier–bent caps they have used. CIP reinforced concrete construction was the most commonly reported type, but most respondents were referring to construction at integral abutments. CIP posttensioned caps, steel boxes, and twin steel-plate I-girders were also reported as types for integral pier construction. Table 3.10 summarizes the various responses.

Table 3.9. Purpose for Using Integral Construction

Purpose	Used Routinely	Used Occasionally	Used Rarely or Never
To eliminate bearings	4	1	12
For vertical clearance issues	1	7	11
Other	4	1	

Table 3.10. Types of Integral Pier Caps

Types of Construction	No. of DOTs Reporting
CIP reinforced concrete caps	12
CIP posttensioned concrete caps	4
Steel box girders	5
Twin steel-plate I-girders	1
Steel integral caps	1
Inverted T caps with continuous deck	1

Bearing Orientation for Curved Girder and Skewed Bridges to Accommodate Thermal Expansion

The DOTs were asked how they orient bearings on curved and highly skewed bridges to accommodate thermal expansion. Most DOTs responded to the curved girder bridge question, citing two methods of orientation. The first method was to orient the bearings to match the orientation of the girders at the particular expansion bearing location. The other method was to orient the bearings along a chord from the fixed location to the particular expansion bearing. Nearly equal numbers of respondents reported using each method.

For sharply skewed bridges, those that responded typically oriented the bearings in line with the girders. California, however, reported orienting bearings perpendicular to the skew.

Table 3.11 summarizes the various responses for curved girder bearing orientation.

Accommodating Transverse Thermal Movements on Wide Bridges

The DOTs were also asked how they accommodate transverse thermal movements on wide bridges. The most common response was to use elastomeric or multidirectional bearings that can accommodate the transverse movement and can also provide additional lateral clearance to guide bars or other lateral restraints. Some states reported using longitudinal deck joints that limit the amount of potential transverse movement. Some also reported that they do not have wide bridges and have not experienced a problem.

Table 3.11. Bearing Orientation for Curved Girder Bridges

Bearing Orientation for Curved Girder Bridges	No. of DOTs Reporting
In line with girder	8
On chords	7
Use HLMR bearings to accommodate movements	1
No criteria: leave to design engineer	2

DOT Research Programs Dealing with Performance and Durability of Bridge Bearings

The DOTs were asked if they have been involved in any research programs dealing with performance and durability of bridge bearings. A few indicated they have supported research, but most had not. The state of Washington has been very active with NCHRP projects at the University of Washington.

Expansion Joints, Joints, and Jointless Bridges

Bridge elements are subjected to various loads, including traffic and environmental loads. The applied loads result in movement of bridge elements. The most important factor affecting the service life of bridges is how thermal expansion and contraction of the bridge elements is addressed.

Review of the available literature and discussions and meetings with other researchers and organizations were used to identify the status of the practice and identify the challenges. The following sources of information were used to achieve this objective:

- Results of a literature search;
- Analysis of the DOT survey responses;
- Review of unpublished research data conducted by the Construction Technology Laboratories and sponsored by FHWA in the late 1990s;
- Review of the details listed in the final draft of "Connection Details for Prefabricated Bridge Elements and Systems," which was developed by a FHWA sponsored project. The research team had obtained the 2011 draft of this publication from FHWA. This report has since been published (2012) and is now available through the FHWA website;
- Input from AASHTO bridge subcommittees;
- Input from researchers outside the team;
- Input from industry; and
- Input from SHRP 2 review panel and staff.

Available information indicated that within current practice, the thermal movement of the bridge is handled in two distinct ways. One option is to provide expansion joints at designated locations within the superstructure. By doing so, the designer forces the entire thermal deformation to take place at these discrete locations. The other option is to make the superstructure and deck continuous and assume that the thermal movement will be accommodated by flexibility of the substructure elements, such as piles. In such cases, the movable joints (commonly referred to as expansion joints) are usually moved away from the bridge abutment and placed near the end of the approach slab.

The most common practice to accommodate thermal expansion and contraction has been to provide expansion

joints over the abutments and piers. Numerous expansion joint types have been developed, mainly by private companies. The fact that transportation agencies have not been able to agree on one or even a few expansion joint types is indicative of the challenges related to the effectiveness and service life of expansion joints. Almost all expansion joints leak, and most, even with proper maintenance, have a service life of less than 10 years. It is often said that the best joint is no joint. Expansion joints are perhaps the most important factor affecting the deterioration of bridge elements. Results of the survey conducted clearly indicate that elimination of expansion joints can greatly enhance the service life of bridges. A leaky joint allows salt and other chemicals to penetrate below the deck and causes many maintenance and deterioration problems. A FHWA study (Fincher 1983) reports that over a 5-year period, more than 60% of joints evaluated were leaking water, and that the other 40% had problems that were actually decreasing their service lives. Another study conducted by Wallbank (1989) evaluated 200 concrete bridges and found leaking expansion joints to be the major cause of bridge element deterioration.

The trend in recent years has been to eliminate expansion joints or to reduce their numbers. Developments in jointless bridges and ideas such as link slab reflect this trend. Surprisingly, investigations carried out in the joints area of research have been relatively small compared with topics related to other bridge elements. Unfortunately, quantitative data on long-term performance of various expansion joints are, for the most part, not available.

The service life of bridges could be enhanced significantly if expansion joints were eliminated altogether or moved away from the bridge superstructure and into the roadway (the end of the approach slab). The common assumption made in jointless bridges is that the flexibility of the substructure is the mechanism that allows thermal expansion and contraction, allowing the joint to be placed off the bridge at the end of the approach slab. Recent work in Australia by Bridge et al. (2005) and Griffiths et al. (2005) has resulted in the development of a completely jointless bridge, with no expansion joint anywhere in the system, even outside the bridge or at end of approach slab. In Australia, several such bridges have been constructed; to date, their performance has been excellent.

A very important observation with respect to jointless bridges is the variation in design requirements among those states that use jointless bridges. Results of a survey and other related activities indicate that there is a wide range of variation in design approach used for jointless bridges. Most important variations deal with maximum bridge length as a function of the material type, effect of skew, design of piles, and details over abutment and pier. Most states using jointless bridges report observed cracking at the abutment location, especially for bridges with skew. These states report that they have not found an effective way to eliminate the observed cracking.

Review of DOT practices and available design provisions for jointless bridges indicated a need for the development of uniform design provisions and accompanying details for jointless bridges. Further, there is a need to develop methodologies and details using a scientific approach that could allow extending maximum bridge lengths for jointless bridges. The need for having a scientific approach for the design and construction of jointless bridges along with appropriate details is magnified by the fact that the most effective way to enhance the service life of existing or new bridges is to eliminate joints as much as possible. Contrary to common belief, jointless integral abutment bridges have lower initial cost, in addition to many other advantages. Therefore, there is no major disadvantage in using jointless bridges.

In the immediate future, bridges in many parts of the country will continue to incorporate joints, despite the many long-term advantages of jointless bridges. Thus, it was concluded that it was important to address the service life design of expansion joints as well as to address the design, construction, and maintenance of jointless bridges.

The current trend in bridge engineering is to have modular bridge systems. One of the most important characteristics of modular bridge systems is the inclusion of many different joint types. FHWA has recently published a manual containing different possible joints that could be used in conjunction with prefabricated bridge elements. The integrity of the modular bridge system depends, to a large extent, on the durability and service life of the various joints used in these systems.

Following are brief descriptions of some of the major findings during the initial phase of the R19A project with respect to jointless bridges, expansion devices, and completely jointless or seamless bridge systems; a summary of DOT surveys related to expansion joints and jointless systems is also provided. These findings influenced the scope of research carried out in the area of jointless systems and expansion devices.

Jointless Bridge Systems

Henry Derthick, former engineer of structures at the Tennessee DOT, once stated, "The only good joint is no joint." Most states have adopted design procedures that reduce or eliminate the use of joints for short to moderate span lengths. However, design methods and construction details vary significantly from state to state.

In jointless bridges, joints are eliminated over the abutment or pier, or both. For long-span bridges, the flexibility of piers is sometimes used to accommodate bridge expansion and contraction within the bridge length. In these situations, the piers have to be flexible enough to accommodate expansion and contraction movements within the span lengths. When pier flexibility is relied on to accommodate bridge movement between piers, the formation of cracks in concrete piers needs

to be a design consideration. Current practice in jointless bridge design demands placing a joint outside the bridge, that is, either just outside the abutment or at the end of the approach slab. Various details could be used to accomplish this objective. Details connecting the superstructure to the piers in jointless bridges can also vary. Three main options are identified:

- The superstructure could be made integral with the substructure, which has the advantage of eliminating the need for bearings altogether. However, movement of the superstructure can result in the development of cracking in the piers, which could result in service life problems, especially if piers are located within splash zones.
- Connections between the pier and the superstructure could be made to act as a pin (commonly referred to as "fixed" in design drawings). This option will demand bearings and will require designing the pier for bridge movement. The bearing design for this option will require accommodating rotation only.
- Connections between the pier and the superstructure could be made to act as a roller (commonly referred to as "expansion" in design drawings). This option will require having bearings and designing them to accommodate horizontal movement as well as slight rotation. The pier design does not, however, require accommodating deflection in the traffic direction.

The design of piers and piles at the abutment is one area in which there are differences of opinion on details and design provisions and for which a need for further research was identified. Some states orient steel piles so that bending is about a minor axis; others orient them so that bending takes place about a strong axis. The effect of soil surrounding the piles at the abutments is accounted for by determining the point of fixity, where piles could be assumed to act as a fixed cantilever and behave as a flagpole. Pile designs are generally dictated by capacity, ductility, and stability. Piles at the abutment for integral systems behave as a flagpole carrying a vertical load. Therefore, capacity and stability should be a design consideration. Extreme thermal movement could also create a low cycle fatigue concern. As a result, ductility should also be a design item.

The important factor that limits the maximum length of jointless bridges is the capacity, stability, and ductility of piles at the abutments. As much as possible, attempts should be made to use integral abutments. In current practice, DOTs resort to semi-integral abutment details when they think that piles are not capable of providing adequate capacity, stability, and ductility.

The most desirable detail over the pier would be to make the superstructure and substructure integral. This will require the pier to accommodate thermal movements without causing any adverse consequence, such as the formation of cracks and resultant durability problems.

The following is a discussion of current practice related to jointless systems and details.

Details Used Over Abutments

Experimental studies of integral abutment bridges began in the 1930s (McCullough 1930). Early bridges of this type were relatively short, ranging in length from 50 to 100 ft. Subsequent increases in allowable length were based empirically on reports of successful performance of prototype bridges. Over time, various highway agencies have developed their own design criteria along with concomitant limits on length, skew, and horizontal curvature. In January 1980, FHWA released Technical Advisory T 5140.13, *Integral, No-Joint Structures and Required Provisions for Movement.* This advisory was aimed at providing state and local highway agencies with data and state-of-the-art information pertaining to integral abutments, continuous bridge lengths, and specification-oriented movement requirements. Since this time, further progress has occurred in the development of various jointless bridge concepts, including

- Full integral abutments, in which bridge girders are cast into a concrete end diaphragm that is connected to a concrete pile cap typically supported by a single row of piles;
- Semi-integral abutments, in which the concrete end diaphragm is not rigidly connected to the substructure;
- Deck extensions, in which the end of the deck slab is simply extended over a traditional backwall and into the adjoining approach pavement; and
- Shifted joint details, in which the joint is shifted between a semi-integral diaphragm and a fixed backwall. This detail is not currently used in practice.

Full integral abutments are used commonly in many states for bridges having maximum total lengths from 250 to 400 ft. Thermal movements are accommodated within the foundation and are typically assumed to be unrestrained in the design of the superstructure. Within current practice, measures to accommodate thermal movements vary significantly (Burke, Jr. 1990). These measures include

- Limiting the bridge length, skew, horizontal curvature, or some combination of these factors;
- Use of select backfill materials or uncompacted backfill, or both;
- Spanning the area disturbed by the foundation movements immediately behind the abutments with the approach slab, thus avoiding settlement of the slab and associated surcharge loads;
- Limiting the foundations to a single row of vertical piles;
- Limiting the pile type and requiring a minimum pile length;

- Orienting vertical H-piles such that they are subjected to weak-axis bending due to longitudinal movements;
- Providing a hinge detail within the abutment to limit the moment developed at the tops of the piles;
- Anchoring the approach slab to the superstructure with a detail that allows rotation of the approach slab at the abutment to accommodate settlement of the approach fill; and
- Providing an expansion joint at the roadway end of the approach pavement.

Some of the items listed are, in fact, the opposite of what should be done. For instance, turning the piles about a weak axis of bending has a net effect of reducing the maximum bridge length that could be used as a result of reduction in pile capacity, ductility limit, and stability limit.

Details for Jointless Bridges at Interior Supports of Multispan Bridges

Various details were found to be used over the interior supports of multispan bridges to eliminate joints, including simple spans for dead load made continuous for live load, link spans, and engineered cementitious composites.

Dead Load Made Continuous for Live Load

One of the concepts implemented by owner agencies for concrete bridges has been the use of simple spans for dead load made continuous for live load (Freyermuth 1969; Oesterle et al. 1989). A common implementation of this type of construction involves the use of precast, prestressed girders connected with a continuous CIP deck slab. Girders are simply supported for dead load, but continuity is achieved with deck steel as negative moment reinforcement over the piers. In addition, the girders are made integral with the interior pier diaphragms. The concept of a simple span made continuous has also been applied to eliminate interior joints and improve the construction speed and design economy for short- and medium-span steel girder bridges (Azizinamini et al. 2008; Azizinamini 2013). The concept of a simple span for dead load and continuous for live load for steel bridges has many advantages, among them completely eliminating joints and accelerating construction.

Unfortunately, some simple made continuous prestressed concrete girder bridges have experienced severe cracking in the girders near the interior diaphragms. One example that has been studied extensively was on the Francis Case Memorial Bridge spanning the Washington Channel of the Potomac River in the District of Columbia (Telang and Mehrabi 2003). The prime cause of this distress was the restraint of upward creep of the prestressed girders under the influence of prestressing. According to Telang and Mehrabi, "By providing a large amount of positive moment reinforcement at the diaphragms, designers inadvertently make the diaphragm area stronger than the adjacent girder sections, thereby forcing the cracking to occur in far more critical but weaker areas of the girder span." The article states, "In closing, it is important to note that this seemingly simple transformation of simple-span prestressed girders to continuous spans should be attempted with caution, and significant attention must be paid during analysis and design to include loading conditions that can cause counterintuitive behavior such as secondary positive moments at the piers. Most importantly, positive moment reinforcement should be designed and detailed such that any cracking, if it occurs, should be limited to the relatively less critical diaphragm region of this type of structural system." Further discussion of this problem and solutions to avoid it have been published by Oesterle et al. (2004) and Arockiasamy and Sivakumar (2005).

Link Slab

Link slab is a type of detail that is used in conjunction with existing or new bridges having girders that act as simple beams for both dead load and live load. In this type of deck detail, the slab spans continuously over the length between the adjacent girders while the adjacent girders are kept as simple spans (see Figure 3.33). The length of the deck connecting the two adjacent simple-span girders is called the link slab (Caner and Zia 1998). Link slabs generally require less deck reinforcement, but they have more girder positive moment

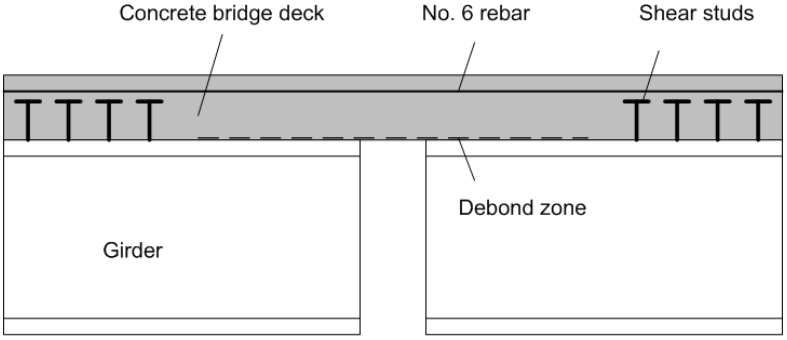

Figure 3.33. Conceptual detail for link slab.

demands than simple-made-continuous designs. It is believed that Caner and Zia (1998) were the first to develop the link slab idea. Limited analysis and laboratory experiments were carried out, and design recommendations were provided (Caner and Zia 1998). The use of this promising detail has been very limited due to field-observed cracking. Link slabs are not common in the snow belt states. A crack is invariably formed due to deck slab rotation as the bridge is loaded with live load.

Recently, Wing and Kowalsky (2005) described the monitoring and assessment of a pilot study link slab bridge in North Carolina. To eliminate the observed cracking problem, Kim et al. (2004) have researched the application of engineered cementitious composites (ECC) to enhance crack-width control, deformation capacity, fatigue performance, and construction and placement of link slabs.

From 1995 through 1998, Caner and Zia published several reports and papers that synthesized results from research conducted over a number of years focusing on the behavior of jointless bridge decks supported by simple-span girders. They addressed instantaneous effects due to live load plus impact, thermal effects due to temperature variations, and time-dependent effects due to creep and shrinkage of the concrete. Both experimental and analytical studies were conducted, and a method of design for the deck region between simply supported girders, referred to as the link slab, was developed based on the research results. The majority of the studies and the development of the design recommendations are documented in Caner (1996) and Zia et al. (1995). Caner and Zia (1998) provide a summary of the developments.

The experimental program involved two composite specimens, including a continuous reinforced concrete deck slab cast on two simple-span steel beams, and a similar slab cast on two simple-span precast concrete beams. The steel bridge was tested with four support configurations: HRRH, RHRH, RRRR, and RHHR, where H stands for hinge and R stands for roller. The first and last letters indicate the conditions at two exterior supports, and the other letters indicate the conditions at two interior supports. The concrete bridge was tested with the same support conditions, except for the RRRR configuration, which is an unlikely condition in the field. The goal in testing different support conditions was to observe if there were any differences in the behavior of the jointless deck under different support conditions. In all cases, the beams were loaded to no more than 40% of the estimated ultimate load capacity to observe behavior in the elastic range. The final ultimate load test was performed using the RHHR support configuration. For each specimen, test results showed that the load–deflection behavior at the midspans of the girders, the link slab rebar stresses, and the crack widths in the link slab were essentially the same for all support conditions.

The researchers concluded that the link slab offered negligible rotational end restraint to the bridge girders and that the link slab can be analyzed as a beam subjected to the same end rotations as the adjacent girders. It was also found that the actions within the link slabs were predominantly flexural, which was contrary to a number of previous analytical solutions that assumed that the link slabs acted primarily as an axially loaded element. The researchers found that under service-load conditions, the link slab would crack, primarily due to bending. In addition, the authors found that earlier programs developed by Gastal (1986) and El-Safty (1994) were capable of predicting the forces, stresses, and crack widths in the link slab due to thermal and creep and shrinkage effects. Caner (1996) modified the programs developed by Gastal and El-Safty to properly capture the link slab actions. All the solutions were based on beam theory. The reinforcing bar stresses compared reasonably well with the data measured from the experimental tests. The predicted crack widths were somewhat larger than the measured crack widths. The researchers concluded that bending and cracking under live load plus impact were the governing factors that must be considered in the design of the link slab. Although the program as modified by Caner (1996) was believed to be capable of predicting the forces, stresses, and crack widths in the link slab due to thermal and creep and shrinkage effects, the authors recommended that these predictions would need to be validated by future tests, preferably under field conditions.

Caner and Zia proposed a procedure for link slab design that focused on estimating the moment in the link slabs based on the rotations imposed by the simply supported girders and assuming cross-section properties for the link slab. Given this moment, the longitudinal reinforcement for the link slab is designed using a conservative working stress such as 40% of the yield strength of the rebar. Debonding of 5% of each girder span adjacent to the link slabs was recommended, although the impact of not debonding over this length does not appear to have been addressed. The crack-control criteria of the *AASHTO Standard Specifications for Highway Bridges* was used to limit the crack width at the surface of the deck to 0.013 in., considered appropriate for exterior exposure (AASHTO 1996).

Five hypothetical jointless bridges were considered by Caner (1996) to illustrate the recommended design procedure. In all cases, loading a single span with a single HS20-44 truck load did not cause the link slabs to crack. However, loading two adjacent spans caused cracking in the link slabs. Caner observed that longer spans produced larger link slab stresses due to larger end rotations.

When thermal and creep and shrinkage effects were included in the analysis, the crack widths and rebar stresses in the link slab depended on the number and location of the horizontal restraints on the bridge. When the bridge was horizontally restrained at only one of its supports, the link slab stresses due to thermal or time-dependent effects were very small because the bridge was assumed free to move horizontally

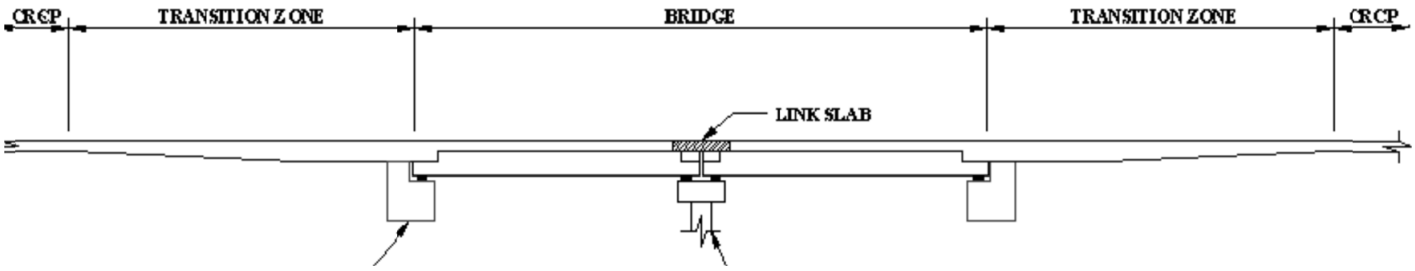

Figure 3.34. The CRCP jointless bridge system constructed in Australia.

on unrestrained supports. If horizontally restrained bridges were subjected to thermal or creep and shrinkage effects, it was found that the link slab rebar stresses could exceed the yield strength of Grade 60 bars. In such cases, it was recommended that the size of the rebars could be increased or the spacing of the bars could be decreased to better control the rebar stresses and crack widths.

Caner and Zia suggested a design of the link slab using only one layer of rebar placed near the top of the deck, but suggested that two layers could be used to improve performance in bridges having horizontal restraints. Caner (1996) also suggested consideration of the use of fiber-reinforced concrete in the link slab region to improve the tensile capacity of the concrete, as well as to improve crack control. He also suggested the use of galvanized or epoxy-coated rebar in the link slabs when corrosion protection is warranted. Tests under repeated loading were also suggested to evaluate the link slab response.

In more recent work, the North Carolina DOT has implemented the recommendations by Caner and Zia in a single field study. The results of this research are documented in Wing and Kowalsky (2005). Kim et al. (2004) have considered the use of fiber-reinforced concrete in link slab construction. In summary, within this project it was concluded that behavior of link slab was not well understood and there was a need for additional work.

Engineered Cementitious Composites

ECC is a fiber-reinforced, cement-based composite material that achieves high ductility under tensile and shear loading. Maximum ductility in excess of 3% under uniaxial loading can be attained with 2% fiber content by volume. One obvious use of ECC in bridges is in negative moment regions over interior supports where the concrete slab is in tension, such as the link slab method. Crack size greatly affects the permeability of the concrete, which is responsible for allowing deleterious agents to reach the reinforcement, resulting in corrosion. This corrosion, in turn, causes expansive forces resulting in spalling of the concrete cover. The self-limiting crack-size property of ECC prevents this process from occurring. Permeability tests show that ECC loaded to the strain hardening stage (1.5%) tends to behave like sound concrete (Li 2003).

Completely Jointless Bridge Systems

Having a structure with no joints is feasible. Rail bridges with continuous welded rails, in which the rails contain absolutely no joints, are a case in point. They are designed to take some movement and resist some force without any adverse performance consequence.

Very recently, a few bridges in Australia have been constructed with absolutely no joints. The system has been in operation for more than 7 years and has demonstrated excellent performance. Thus far, the concept has been used with continuously reinforced concrete pavements (CRCP), which is used in a few states, such as Oregon.

Figure 3.34 shows a representation of the bridge system constructed in Australia.

This system replaces the conventional system shown in Figure 3.35.

In a jointless bridge system, the approach slab and the joints over the abutment and approach slab are eliminated.

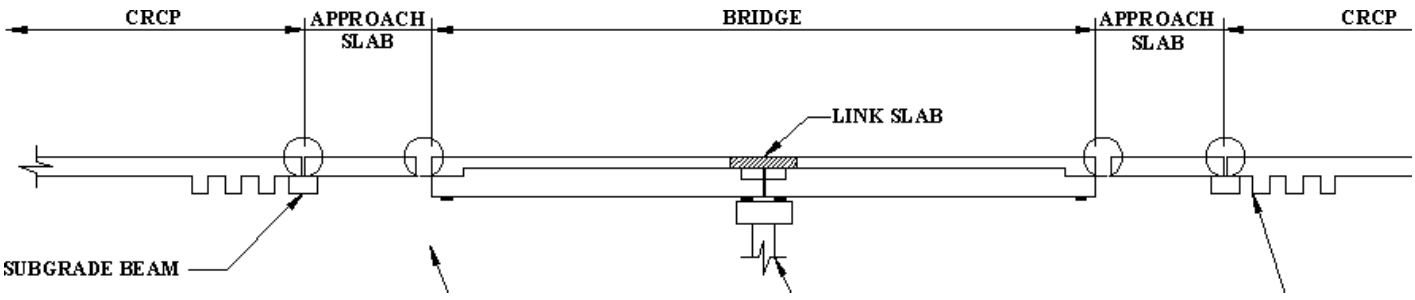

Figure 3.35. The conventional joint system in bridges consists of two joints on both ends of the approach slab.

The concrete deck is made continuous over the abutment and is connected to the pavement. The system is designed to accommodate the resulting tension and compression forces generated by making the deck and pavement seamless and continuous.

The transition zone in the system, which has a length equal to approximately the bridge length, is used to accommodate movements associated with the bridge superstructure when it contracts. The transition zone is also designed to take the resulting compression loads without buckling. A detailed description of the system is provided by Griffiths et al. (2005).

Synopsis of Literature Search and Other Available Information on Expansion Joint Systems

The amount of research on the durability, behavior, and performance of expansion joints is surprisingly limited. In recent years, however, more attention has been paid to expansion joints than previously. This is evidenced by a 1994 British colloquium (Pritchard 1994), a 1996 FHWA workshop (Burke, Jr. 1996), and a 2005 FHWA conference on the topic (Arockiasamy and Sivakumar 2005), in addition to various research studies being funded by different states (Arockiasamy et al. 2004; Fennema et al. 2004; Brena et al. 2007; Civjan et al. 2007).

A review of the available literature demonstrated that an ideal expansion joint should be able to (Lee 1994):

- Accommodate thermal expansion and contraction;
- Accommodate movement due to traffic-induced loads;
- Provide a smooth ride;
- Prevent the creation of hazards and safety issues;
- Accommodate needs during snow removal;
- Prevent leaking of moisture and other chemicals to elements below the superstructure;
- Have a long service life;
- Be maintenance free or require minimal maintenance; and
- Be cost-effective.

Summaries of the major findings for various expansion devices are provided in the *Guide*.

Analysis of DOT Survey

The observed or estimated service lives of various expansion joints are fairly short and range between 1 and 30 years. The answers provided by responding agencies varied significantly. Part of this variation is attributed to the different climate and traffic conditions to which bridges are subjected. Nevertheless, the maximum service life is well below 100 years. Figure 3.36 summarizes the observed or estimated service life for the compression seal joint type along with maximum permitted longitudinal movements.

One of the questions asked of the states in the general section of the survey regarded which freeze–thaw zones best described their climate. The three options provided were high freeze–thaw, medium freeze–thaw, and low freeze–thaw regions. The information provided in Figure 3.36 is organized based on the freeze–thaw regions the states are located in.

Figures 3.37, 3.38, and 3.39 show the same information for strip seal expansion joints, modular expansion joints, and finger-plate joints, respectively.

A review of the information provided in Figures 3.36 through 3.39 indicates

- The variation in observed or estimated service life is the greatest for compression seal joints.
- The maximum longitudinal movement permitted is the smallest for compression seal joints.
- The maximum observed or estimated service life is more consistent for strip seal, modular, and finger-plate expansion joints.
- The maximum observed or estimated service life is the highest for finger-plate joint types, with some states reporting it to be about 50 years.
- There are no obvious trends between the freeze–thaw region that the state is located in and the observed or estimated service life or the maximum longitudinal movement allowed for certain joint types.

One of the consequences of having joints is damage to the ends of steel and concrete girders in existing bridges. Of particular interest was the identification of effective retrofitting alternatives for existing bridges. Survey results indicated that states that do not use salt experience little or no damage to girder ends due to expansion joint presence. Hawaii and Arizona are among these states. This may suggest that in regions where bridges are not salted, the use of expansion joints along with proper maintenance and painting or metalizing girder ends may be allowed while achieving long service life.

The previous scenario aside, many states have bridges with damaged girder ends due to the presence of expansion joints. A question was asked inquiring what techniques are used to repair these damaged ends. All respondents gave similar answers. These techniques included painting the ends of steel bridges, removing the damaged portion of the concrete and patching it with cementitious material, and sealing the expansion joints. Ontario was the only agency that also uses cathodic protection in addition to other techniques for repairing the damaged ends. This is a good practice, as simply patching the damaged concrete may amount to nothing more than hiding the internal corrosion problems that might, with greater consequences, resurface.

Typical damages reported due to the presence of expansion joints included damage to girder ends; various types of damage

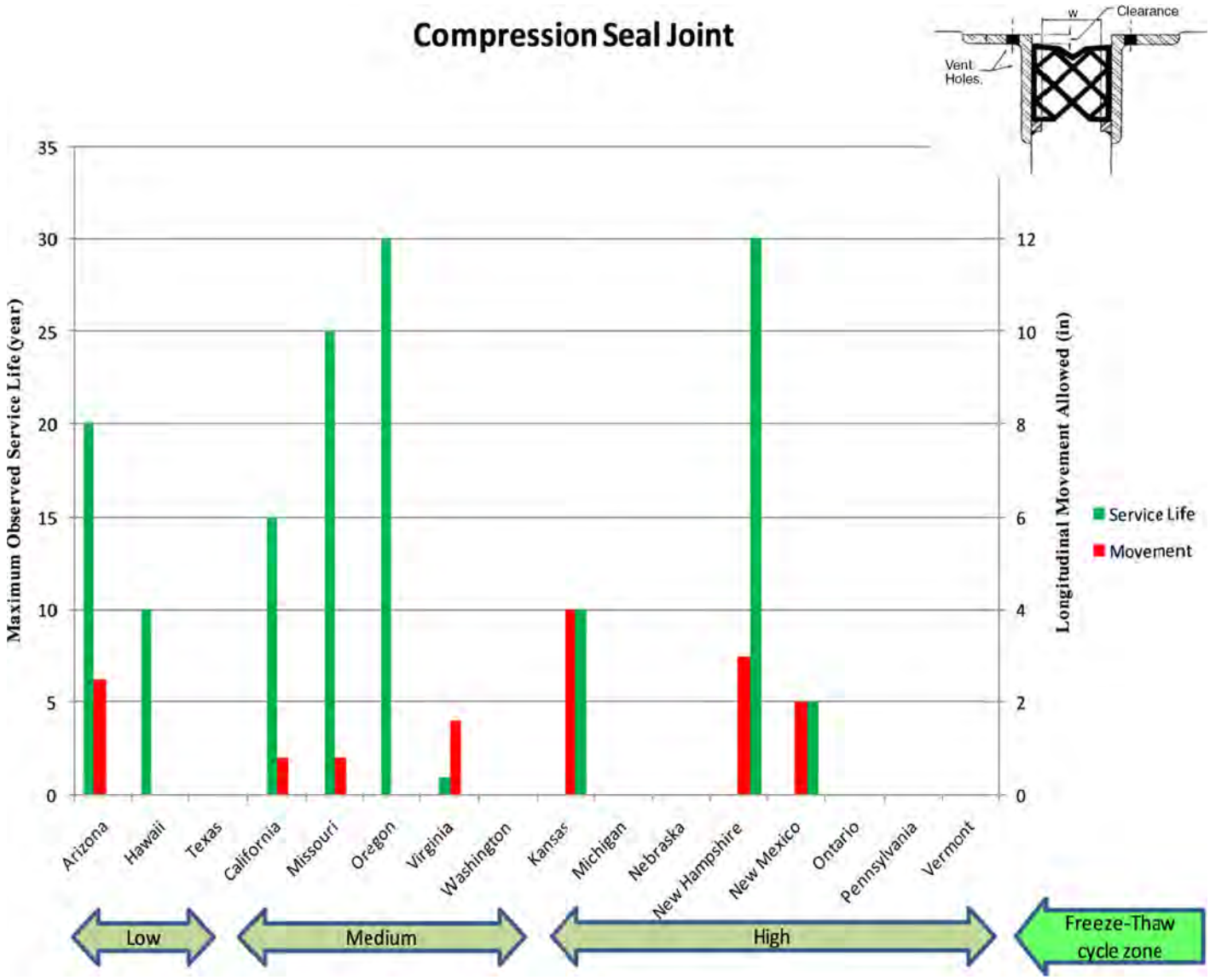

Figure 3.36. Summary of service life and maximum permitted movement for compression seal joint type.

to bearings, including failure of the bearings to accommodate anticipated movements; deterioration of the substructure; deterioration of the abutment backwall and wingwall; and shifting of the bridges with skews. Figure 3.40 summarizes typical damages to various bridge systems as a direct result of expansion joint presence. This figure summarizes the frequency of typical damage as a function of freeze–thaw region. The vertical dimension is the number of states observing certain failure modes, and the two horizontal axes are the freeze–thaw region and the type of damage typical to various bridge elements.

As expected, the frequency of occurrence of any given damage type is the highest in high freeze–thaw regions. This further confirmed that leakage of moisture and other chemicals through expansion joints, especially where roads are salted, is a major source of bridge deterioration.

A large number of states (about 50%) eliminate expansion joints by making simple-span bridges continuous over piers. However, the design procedure and details used vary considerably among these states.

States using jointless bridges agree on one issue: the types of damage seen in jointless bridges are minor, and the expected or observed service life ranges between 50 and 75 years. However, states using jointless bridges have significantly different design provisions. The maximum bridge length that could be used in conjunction with jointless bridges varies significantly for both steel and concrete bridges. The maximum skew allowed also varies. There is, however, a trend in design provisions for jointless bridges. Every state using jointless bridges specifies a smaller maximum bridge length for steel bridges than for concrete bridges. Some states tie the maximum

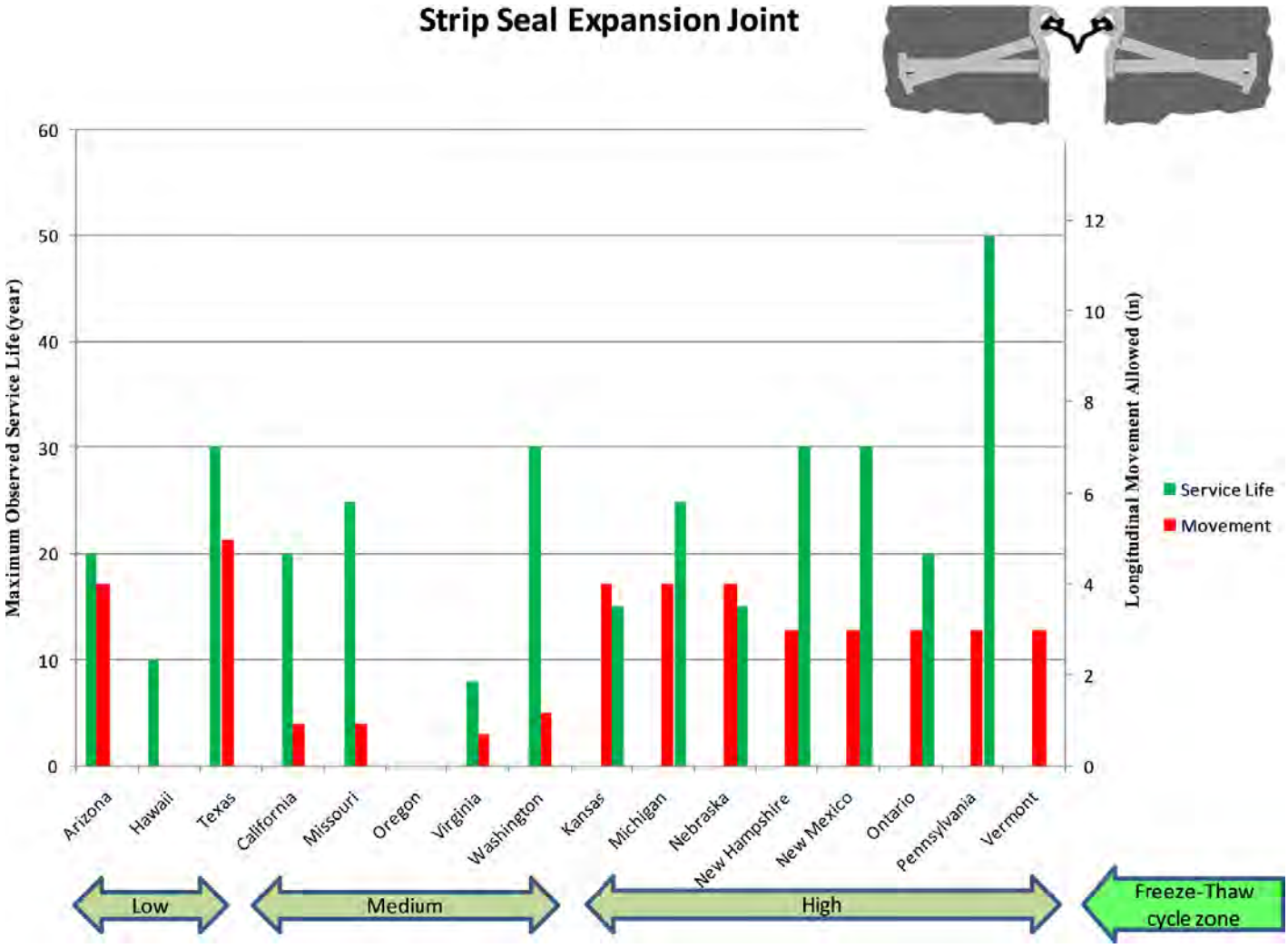

Figure 3.37. Summary of service life and maximum permitted movement for strip seal expansion joint type.

bridge length to the skew angle. As skew angle increases, the maximum allowed bridge length is reduced. Some states, especially in the West Coast area, allow jointless bridges for concrete structures and do not have specific design provisions for steel bridges. In summary, the lack of a national standard for jointless bridges has resulted in limited use, with significantly different design provisions among states using them.

One approach to eliminate joints is to make the concrete deck continuous over piers and still have the girders act as simply supported spans by using a link slab. This idea was originally developed in North Carolina and was further researched in Michigan by incorporating the use of fiber-reinforced concrete. The number of states using a link slab as a means for eliminating joints in simple-span bridges is very small. Part of this trend could be related to the short history of link slab use, field-observed cracking problems, and a lack of AASHTO-approved design provisions. None of the states responding reported use of a link slab with fiber-reinforced concrete in continuous girder bridges. Ideas similar to link slab have the potential to replace the reinforcing requirement in Section 6.10.1.7 of the *LRFD Specifications,* which is meant for crack control over predominately negative flexural regions. In addition, link slab appears to be the only method for converting existing simple-span bridges into simple-span bridges with a continuous deck over pier.

Analysis of the published data, discussion with other researchers, and survey analysis indicates that almost all expansion joints have a relatively short service life and will eventually leak.

Finger-plate joints are reported to have the best performance; however, it is important to remember that finger-plate joints are used on relatively longer-span bridges and are typically subjected to better maintenance programs. However, jointless bridges are reported to have satisfactory service life, with an observed or expected service life from 50 to 75 years. Indications are that observed damage at abutments is small in jointless

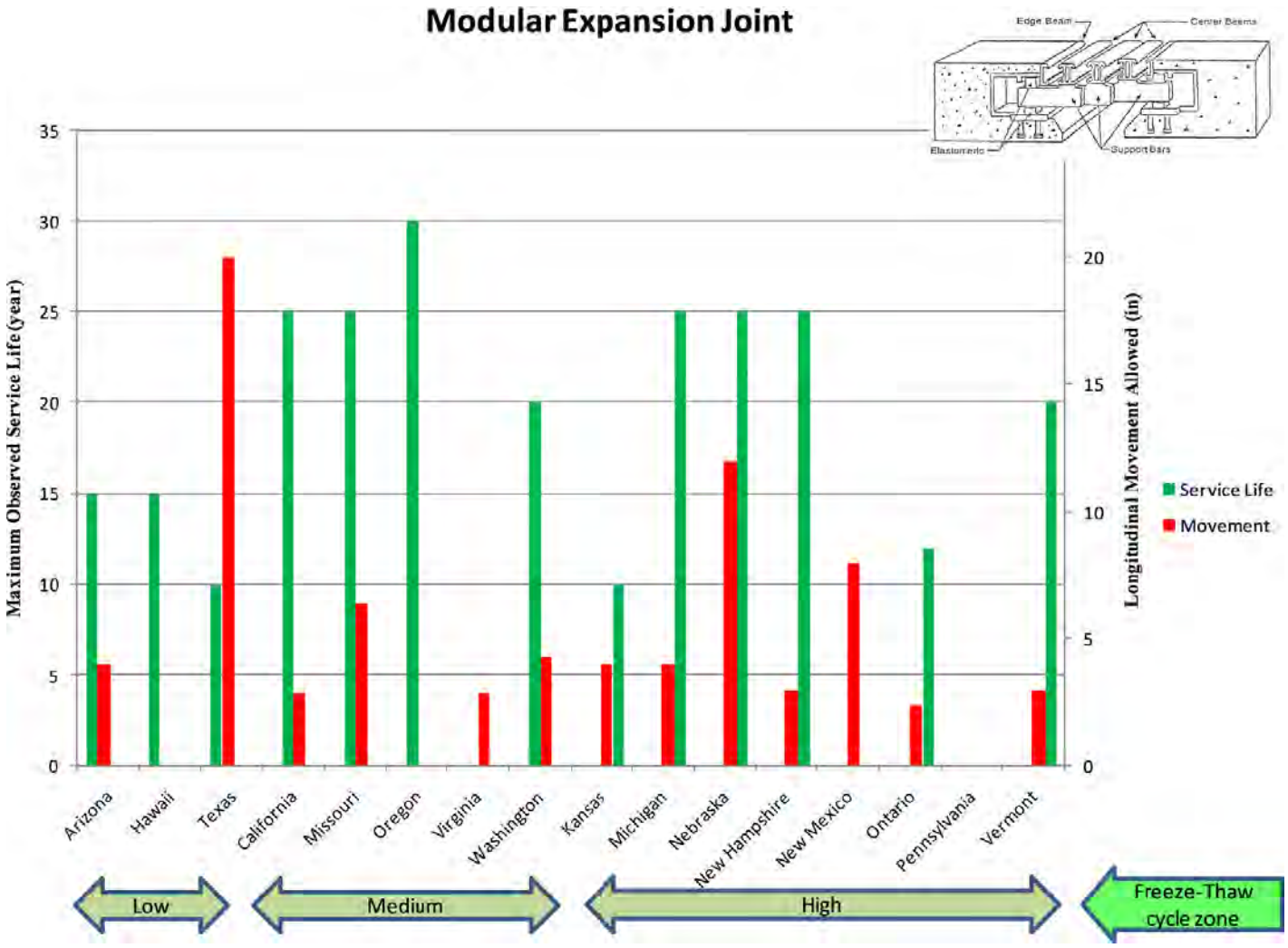

Figure 3.38. Summary of service life and maximum permitted movement for modular expansion joint type.

bridges and can be attributed to lack of available, scientifically based procedures to accommodate movement.

Fatigue and Fracture

Fatigue and fracture can result when tensile stresses are applied to members and connections containing inherent flaws at weld toes or bolt holes due to fabrication. These flaws could be mitigated during design through selection of more fatigue-resistant details or during construction by eliminating or carefully selecting locations for field welding. Cracks can grow from welded details, as well as bolted details. Base metal does not typically govern designs, as the flaws in welded and bolted details are more critical and propagate before base-metal flaws. The governing stress parameter for fatigue is stress range; fracture is controlled by total tensile stress. Details exhibit varying degrees of stress concentration with inherent flaws of varying size. Stress concentration is more predominate in details with lower fatigue resistance, and flaw size is more predominate in details with higher fatigue resistance.

Fatigue of metal structures is the steady state propagation of preexisting flaws due to repetitive loads below the critical loads for strength. Steel bridges do not fail in fatigue, but in fracture, which is the unstable propagation of a larger flaw (most likely the result of fatigue).

Fatigue of steel structures is categorized in the *LRFD Specifications* as either load-induced fatigue (6.6.1.2) or distortion-induced fatigue (6.6.1.3). According to the *LRFD Specifications,*

> When proper detailing practices are not followed, fatigue cracking has been found to occur due to strains not normally computed in the design process. This type of fatigue cracking is called distortion-induced fatigue. Distortion-induced fatigue often occurs in the web near a flange at a welded connection plate for a cross-frame where a rigid load path has not been

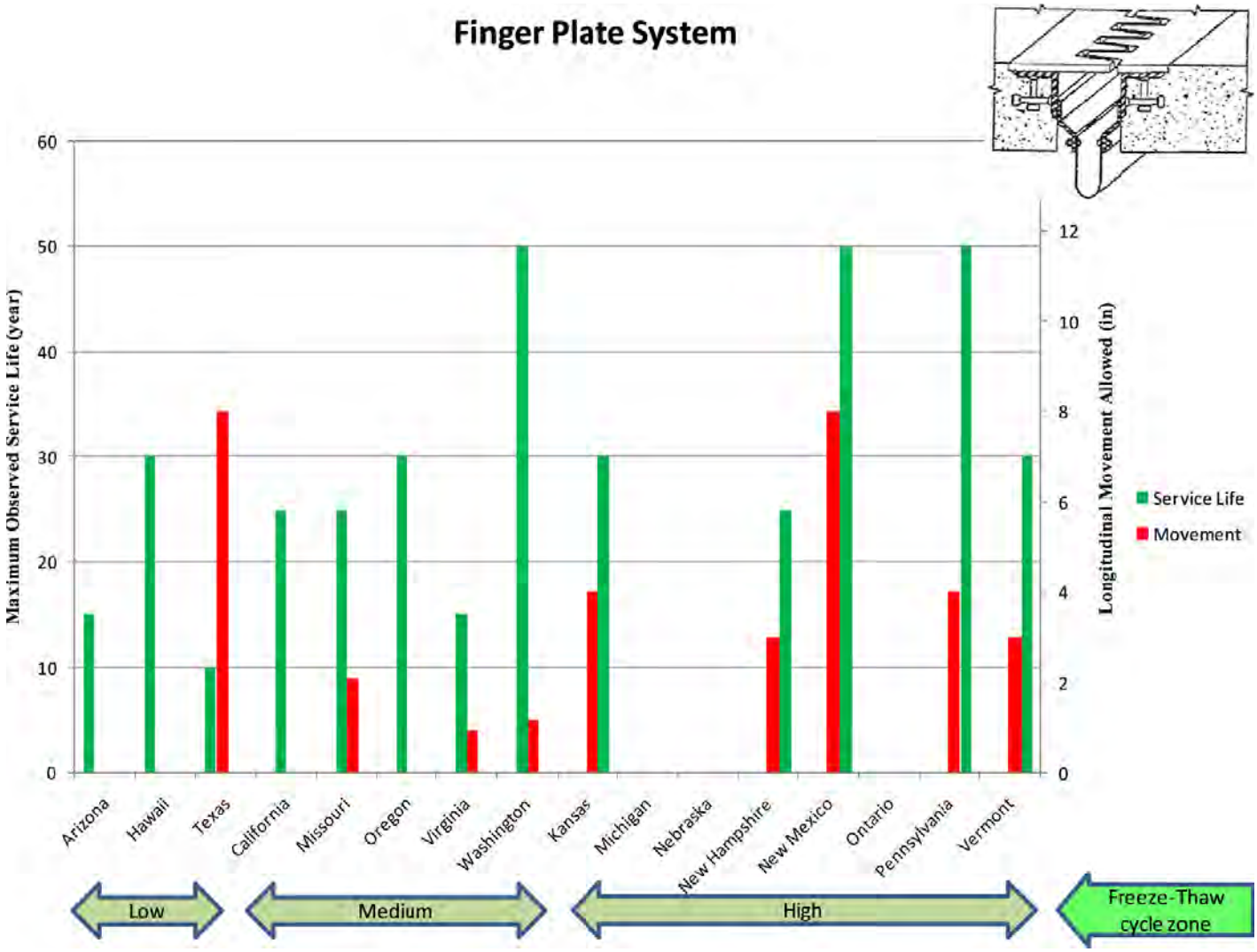

Figure 3.39. Summary of service life and maximum permitted movement for finger-plate joint type.

provided to adequately transmit the force in the transverse member from the web to the flange.

Fatigue due to the stresses computed during the design process (typically in-plane stresses) is called load-induced fatigue.

Synopsis of Published Literature and Other Search Activities

Research studies beginning in the 1970s have resulted in the development of better details and design approaches that have greatly reduced, if not eliminated, the potential for fatigue and fracture of new steel bridges. Typical modern steel bridges, designed in accordance with the *LRFD Specifications,* rigorously address fatigue and fracture issues. Bridges designed before 1974 may still experience load-induced fatigue cracking; those designed before 1984 may still experience distortion-induced fatigue cracking.

Fracture resistance is addressed in the current *LRFD Specifications* by material toughness requirements that vary with certain climatic temperature zones.

Description and Discussion of Details Reported to Cause Fatigue Cracking

Details consisting of connections between, and attachments to, steel bridge components can be susceptible to fatigue cracking. In-service fatigue cracking is the propagation of preexisting inherent flaws due to fabrication. Table 6.6.1.2.3-1 of the of the *LRFD Specifications* describes typical steel bridge details, both welded and bolted, which are susceptible to load-induced fatigue cracking if not properly designed. These details are grouped in eight detail categories (A, B, B′, C, C′, D, E, and E′)

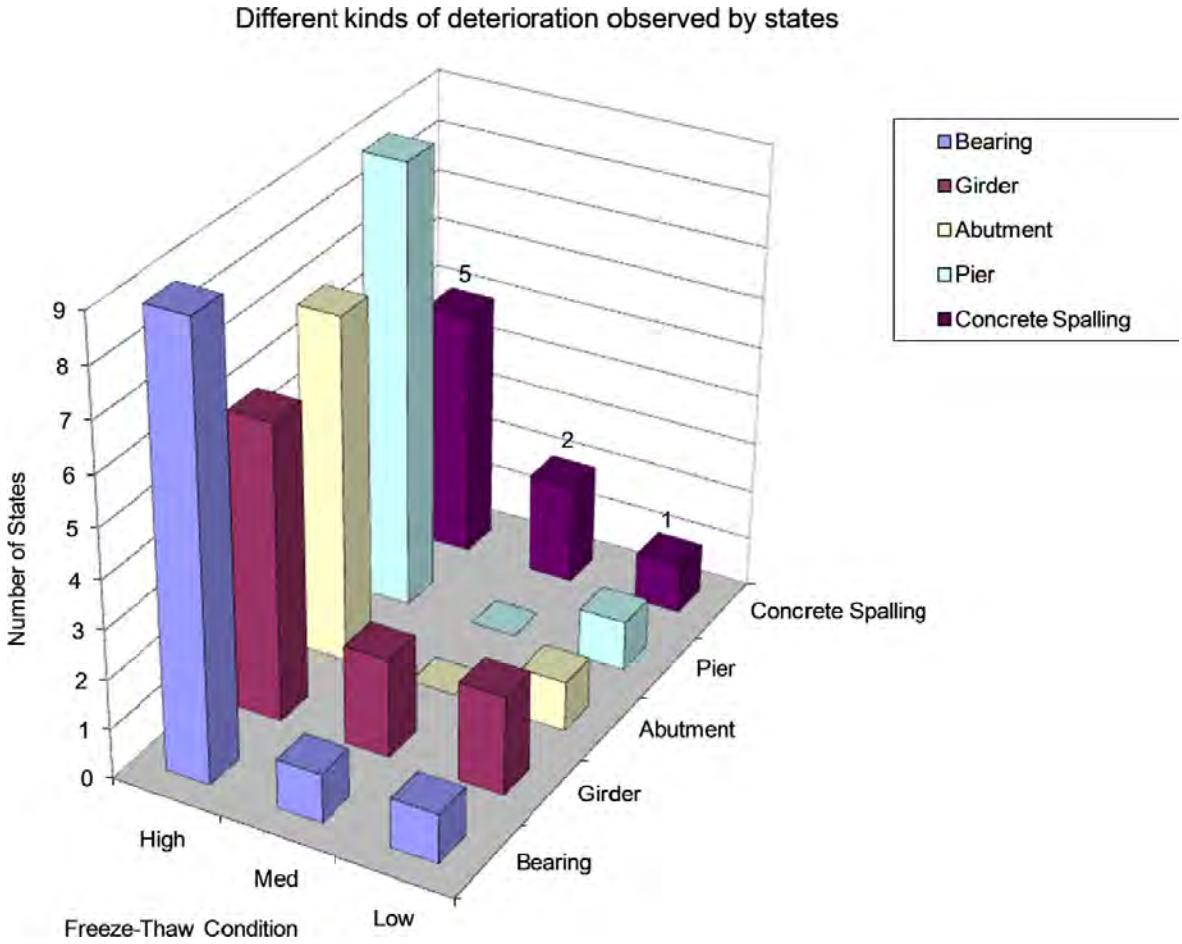

Figure 3.40. Deterioration types as a direct consequence of having bridge joints.

according to fatigue resistance, with letters higher in the alphabet denoting details with lower fatigue resistance. For example, fillet welded connections of girder flanges to their webs is defined as detail Category B. Transverse connections plates welded to girder webs and flanges are detail Category C′.

Causes of Observed Fatigue Cracking

Modern steel bridges should not exhibit fatigue cracking or fractures if designed and detailed in accordance with the *LRFD Specifications*. Bridges designed before 1974 for load-induced fatigue and before 1984 for distortion-induced fatigue may exhibit cracking, as these types of fatigue were not considered in their design and detailing as they are today.

Load-induced fatigue cracking in older bridges (designed before the mid 1970s) is a result of the lack of design criteria when they were originally designed. These cracks result when the fatigue stress range exceeds the fatigue resistance.

Distortion-induced fatigue cracking in older bridges (designed before the mid 1980s) is a result of the lack of properly codified detailing practices. These cracks typically occur when girders are not detailed to act as a complete system. For example, transverse connection plates not rigidly connected to girder flanges can result in fatigue cracks in the unreinforced web gaps.

Ranking of Details with Respect to Reported Performances

The detail categories of Article 6.6.1.2.3 of the *LRFD Specifications* rank the fatigue resistance of typical steel bridge details. They are ranked according to fatigue resistance (or limiting stress range to achieve a 75-year life), although no detail is ultimately better than the next as the applied stress range defines their acceptability. For example, an overstressed Category B detail is worse than an understressed Category E detail.

Analysis of DOT Survey

DOTs report fatigue cracking of older bridges designed before the adoption of the current load-induced or distortion-induced fatigue design provisions.

Methods for Improving Service Life of New Structures

Bridge systems, subsystems, or components alone do not exhibit fatigue cracking. It is the welded and bolted details of these components that can be susceptible to fatigue. Bridge details designed in accordance with *LRFD Specifications* should not experience fatigue crack propagation during the specified 75-year design life. Bridges with detail Categories A through C′ typically are designed for infinite life. There is no improvement necessary for these bridge details. In some cases, bridges cannot be designed with only detail Categories A through C′; finite-life design may be necessary for detail Categories D, E, or E′. To extend the 75-year design life to 100 years, the number 100 should be substituted into *LRFD* Equation 6.6.1.2.5-2 in place of the number 75, as suggested in the commentary to Article 6.6.1.2.5. Thus, new bridge systems, subsystems, and components should only use these details with well-defined fatigue resistance that can be accommodated through proper design and detailing.

Methods for Improving the Service Life of Existing Structures

When a refined remaining life calculation suggests low remaining fatigue life, which may occur for bridges that were designed before the establishment of modern fatigue provisions, ultrasonic impact treatment (UIT) can be applied to details to enhance their remaining load-induced fatigue life through the introduction of beneficial compressive residual stresses. Note, however, that in many cases, remaining fatigue-life calculations yield low or negative lives due to crude estimates of stress along with the high degree of uncertainty associated with fatigue resistance. Research has demonstrated that UIT can improve the load-fatigue resistance of an end-welded cover-plated beam (detail Category E) up to detail Category C or better, and the fatigue resistance of transverse stiffeners (detail Category C) up to detail Category B or better. AASHTO is currently considering codifying a one-category fatigue-resistance improvement for welded details properly treated with UIT.

For bridges with details susceptible to distortion-induced fatigue cracking (details currently prohibited by AASHTO), two retrofit solutions exist: eliminating the driving force of the distortion or providing a positive attachment (welded or bolted) across the short flexible gaps. A catalogue of distortion-induced fatigue cracking retrofits could be compiled.

Methods for Improving the Efficiencies of Safety Inspection Procedures

Normal safety inspection procedures have been efficient in locating early-stage fatigue cracks in existing bridges during routine biennial inspections. However, newer enhanced monitoring systems using real-time methodologies can be very effective in monitoring critical locations.

Methods for Improving the Efficiencies of Maintenance Procedures

Maintenance or lack of maintenance has little or no effect on fatigue resistance. Active corrosion does not allow the development of propagating flaws as the corrosion in effect blunts the crack tips by "eating away" the stress concentrations of the sharp crack tips. Only arrested corrosion could cause accelerated crack propagation through increased stress concentrations. In such cases, any severe stress concentrations due to corrosion should be ground smooth before painting.

Conclusions

Steel highway bridges designed since the adoption of the current fatigue provisions should not exhibit cracking during their 75-year design lives. Extending this design life can easily be accomplished by modifying the finite-life equation. For most common bridge details (detail Categories A through C′), infinite life is often already provided. Bridges consisting of new systems, subsystems, and components should continue to use these welded and bolted details with well-defined fatigue resistances. If the details of any new systems, subsystems, or components cannot be categorized according to the detail categories of the *LRFD Specifications,* fatigue-resistance experimentation would be necessary to quantify the resistance required to achieve 100 years or more of service life.

Protection of Steel Bridges for Corrosion

Corrosion is a fundamental limitation of steel as a material of construction, and it is one of the primary causes of reduced service life for steel bridges. In its simplest form, corrosion of steel is the result of its exposure to oxygen and moisture and is accelerated in the presence of chloride ions from roadway deicing salt or from other sources, like seawater. The use of deicing agents composed chiefly from materials with readily soluble chloride ions creates an atmosphere in which unprotected steel corrodes quickly. The precursors of steel for metal bridges, cast and wrought iron, were largely immune to corrosion because the very high or alternately very low carbon content caused them to corrode much more slowly than steel. To achieve long-term service life, the corrosion potential of steel for a given environment must be addressed as part of an overall corrosion protection plan.

The R19A research program conducted a literature and industry survey along with a survey of state DOTs to identify current approaches to structural steel corrosion protection.

Results of these surveys combined with research team experience were further used in developing Chapter 6 of the *Guide,* which relates to corrosion protection of steel bridges.

The following subsections summarize the literature and industry surveys, and a summary of the DOT survey is given at the end. Current strategies used to prevent corrosion of steel in bridges are discussed, and further recommendations for improving service life are presented.

Synopsis of Published Literature

Briefly, the literature search conducted as part of this research revealed that

- FHWA has an active research, development, and testing program for coatings. Recent confirmatory research has been reported on two-coat systems and their ability to perform as well as the traditional three-coat system in use since approximately 1965. Recent promising work on the testing of one-coat system candidate materials for steel bridges has also been reported. Future research on the use of nanotechnology in coatings is under consideration.
- For new construction, the coating systems and procedures, although improved, are basically unchanged since the late 1960s. New steel receives a coating system consisting of a zinc-rich primer, an epoxy midcoat, and a urethane topcoat, all applied over steel cleaned in accordance with SSPC-SP 10 Near-White Metal Blast Cleaning.
- Maintenance overcoating is a process in which a new coating is applied over an existing coating. Based on industry knowledge and the DOT survey information obtained in this study, the coating systems include acrylic, calcium sulfonate, epoxy sealer–epoxy–urethane, epoxy sealer–urethane, polyester, and polyaspartic.
- Maintenance recoating is a process in which a new coating system is applied over a surface from which all old coating material has been removed. Based on the literature search, industry knowledge, and the DOT survey information obtained during this study for maintenance recoating, the most commonly used system consists of an organic or inorganic zinc-rich primer with an epoxy midcoat and a urethane topcoat.
- A recent special grade of weathering steel has been used in a small bridge in California. The bridge, discussed in more detail in the subsection on using corrosion-resistant steels, is fabricated from steel meeting the requirements of ASTM A1010-01 (2001). Among other requirements, this special grade of weathering steel contains between 10.5% to 12.5% chromium. A study conducted by experts from a major steel producer indicates that uncoated steel coupons were free of corrosion when exposed at the 25-m line (from high tide) at Kure Beach, North Carolina.

Synopsis of Other Search Activities

Interviews with coating suppliers, resin producers, consultants, and other engineering professionals from various foreign countries were also performed and are briefly summarized as follows.

It is apparent that for coating systems, the best practice abroad is similar to the best practice in the United States, which was substantiated through conversations with representatives from China, Korea, Japan, and Western Europe. Although the actual coating systems are similar, one thing notably lacking in the United States is a codification of a comprehensive set of best practices for coating steel bridges. At least one country, the United Kingdom, appears to have a good start in the codification of some of the necessary practices needed to specifically target achieving improvements in bridge durability via protective coatings (Volume 1, *Highway Structures Approved Procedures,* Section 3 General Design, Part 8 Ba57/01 Design for Durability, Parts 5 and 6).

One major coating supplier interviewed did not believe that it would be possible with current technology to have a coating system not containing zinc that could last for 100 years. That same supplier did believe that a coating system containing a zinc primer could last 100 years. There are evolutionary changes under way in zinc coating. One supplier uses zinc flakes in coatings to obtain both barrier effects and galvanic effects in a combined effort to fight corrosion. Another vendor cited the reported success of flake glass–reinforced polyester coating material applied in multiple layers to drilling platforms in the North Sea. Some vendors are supplying advanced fluoropolymer-based coatings. These materials are said by these suppliers to provide a quantum improvement in color, gloss, and resistance to ultraviolet light. The march forward in the art and science of advancing the type and durability of various coating types continues.

Strategies Used to Prevent Steel Corrosion

Two main strategies are used to prevent corrosion of steel in bridges: the use of coatings and the use of corrosion-resistant materials.

Use of Coatings

Engineers have historically used coatings as one way to mitigate the negative impact of the environment on steel.

Fundamentally, a sure way to protect steel from corrosion is to keep it from getting wet. A major way that coatings protect steel from moisture is by providing a barrier to the elements. The key to corrosion protection by the use of coatings lies in the ability of the primer to inhibit corrosion when (or if) water penetrates the barrier layer(s) and the steel surface is subjected to repeated wet–dry cycles.

It is generally recognized that in an effective, multicoat coating system, the primary purpose of the coating layer closest to the steel surface is corrosion protection to the steel surface beneath. Any special aesthetic considerations can be accommodated in the subsequent coating layers. In some dry climates of the country where corrosion is not an issue, aesthetic considerations can play a more compelling role. The DOT survey confirms that states such as Arizona expect 50-plus years of service life for the same system expected to last 20 to 30 years elsewhere.

From the very earliest years in the steel bridge era, beginning in ~1874 in the United States with the construction of the Eads Bridge in St. Louis, Missouri, lead and chromium rust-inhibitive pigments were added to paint to supplement the barrier protection offered by a coating film. For almost 100 years, until ~1965, the use of lead- or chromium-pigmented, multilayer coatings was the norm during new bridge construction and maintenance overcoating and in maintenance repainting.

After 1965, bridge coating engineers turned away from coatings containing these toxic heavy metal pigments and settled on coatings containing metallic zinc as the corrosion-resistant pigment. The DOT survey indicated that all respondents use a system that includes a zinc-rich primer. As long as the zinc pigment in the coating is in close metal-to-metal contact with the steel substrate, the coating can provide galvanic protection to the steel. Galvanic protection is provided when zinc and steel (iron) are connected in the presence of air (oxygen) and moisture. In this coupling of materials, zinc (the more noble metal) will oxidize (corrode) in preference to the iron (steel). The preferential oxidation of zinc provides protection for the steel as long as there is nearby zinc left to consume. When the zinc is consumed, the steel beneath will be subject to corrosion. The method of attack taken since the mid 1960s has been to use a so-called "belt and suspenders" approach. When these coating systems are applied, the zinc-containing primers provide corrosion protection to the steel and, to protect the zinc-containing coating layer from oxidation due to oxygen, moisture, and air pollutants, additional coating layers are applied over the zinc-rich primer.

When a steel surface protected by a coating system using a zinc-rich primer is bathed in saltwater and subjected to many wet–dry cycles, inevitably discontinuities in the coating provide a pathway through the coating for moisture to reach the steel surface beneath. As a result, the zinc begins to react to protect the steel from corroding. Eventually, the zinc in the zinc-rich primer is consumed, and corrosion in the form of red rust is evident. It may take many decades for the corrosion protection offered by zinc to be consumed before corrosion of the steel is evident. Thereafter, the rate of corrosion is dictated by the local factors surrounding the steel (e.g., wet–dry cycles, chloride contamination, humidity).

In a landmark literature survey compiled by Albias, von Loden, Onderzock, and Advies, which was published in the *Journal of Protective Coatings and Linings* in February 1997, the researchers opined that "[i]t has been clearly established that soluble salts on the surface of steel will increase the rate of corrosion and paint breakdown for many [coating] systems now in use." This conclusion is as true today as it was then. The authors offered several conclusions:

- From available data, it is not possible to establish a definitive allowable level of chloride contaminants.
- In relation to the durability of the paint system, a maximum chloride level of 10 to 50 mg/m^2 is allowed, depending on the use and exposure conditions. This is only a rough guideline.
- Under specific conditions, higher maximum levels of chloride (up to hundreds of milligrams per square meter) are allowed for special, durable paint systems (e.g., zinc silicate).
- Exposure to marine conditions or industrial environments considerably increases the chloride contamination of steel.
- Abrasive blast cleaning does not remove all the chloride.
- Results of detection methods for soluble chlorides are affected by temperature, mechanical forces, and the chemicals and type of analytical method used.
- The effect on steel of the hydrochloric acid generated as a consequence of the corrosion reaction is devastating.

Therefore, the removal of as much chloride as possible during blast cleaning and other surface preparation efforts is crucial. Although there is still not complete agreement as to the precise level of chloride residue that is acceptable, Appendix A, Table A-2 of the current version of the Society for Protective Coatings (formerly Steel Structures Painting Council or SSPC) surface preparation standard SSPC SP-12 (Surface Preparation and Cleaning of Metals by Waterjetting Prior to Recoating) identifies three levels of chloride removal:

- NV-1: 0 μg/cm^2;
- NV-2: 7 μg/cm^2; and
- NV-3: up to 50 μg/cm^2.

The level most commonly specified by the respondents to the DOT survey conducted as part of this research was 7 μg/cm^2.

It is believed that complete removal of all chlorides via only dry blast cleaning is at best unlikely, and at worst, provides a false sense of security, even if white metal blast cleaning (SSPC SP-5, White Metal Blast Cleaning) is specified. Cleaning efforts beyond abrasive blast cleaning are usually needed.

Various types of coatings including painting, galvanizing, and metalizing, are discussed in Chapter 6 of the *Guide.* This chapter was developed as a best practices guide for preventing corrosion of exposed structural steel for bridges.

Use of Corrosion-Resistant Steels

Weathering steel (coated or uncoated) has been the subject of much research since its initial use on bridges in about 1970. When small amounts of copper, chromium, nickel, phosphorous, silicon, manganese or combinations of these metals are added to carbon steel, a low-alloy carbon steel results that has improved corrosion resistance. These weathering steels enjoy vastly enhanced corrosion resistance that can render them impervious to corrosion in many exposure environments. The degree of corrosion resistance afforded is dependent on a number of variables including climatic conditions, pollution levels, and the degree of sheltering from the atmosphere, as well as the composition of the steel itself. These variables influence the locations where its use is recommended.

When weathering steel is properly exposed, a rusty red-orange to brown or purple-tinted patina forms. When the steel is exposed to the atmosphere, the corrosion rate becomes stabilized within about 3 to 5 years. In rural areas with little pollution, a somewhat longer period may be required to form this well-adhered protective patina.

The formation of the protective patina requires a series of wet and dry periods. In areas where the steel is sheltered from the rain, the dark patina is also not able to form. Rather, a layer of light rust forms and provides protection for the steel beneath. However, when weathering steel is used in locations where regular wet–dry cycles occur, the steel is corrosion resistant to the point that no coating is necessary.

There are some limitations to the advantage and recommended use of weathering steel in certain environments. For example, in areas with high concentrations of corrosive industrial or chemical fumes, the weathering steels exhibit a much higher corrosion rate and, instead of forming the tight corrosion-resistant patina, loose rust particles are formed on the steel surface. Under these conditions, the film formed will likely provide little protection. In a saltwater marine environment or in a salt-rich area exposed to chloride-containing deicing materials, the protective patina will never form, and weathering steel offers little advantage, as the corrosion rate will equal that of regular carbon steel.

With continuous wetness, such as in immersion applications or underground, weathering steel also offers no advantage. There were concerns about the effect of acid rain and diesel exhaust on the formation of the protective patina. Investigations by steel producers and the steel industry have indicated that neither has an effect on the corrosion rate of weathering steel.

Guidance regarding the use of weathering steel has been offered by FHWA in *Technical Advisory T5140.22: Uncoated Weathering Steel in Structures* (1989). This document provides general information about the history, limitations, and recommendations for the use of weathering steel.

In the DOT survey conducted for this research, about half the respondents using weathering steel also paint all or parts of their weathering steel bridges. The use of painted weathering steel appears to offer significant "belt and suspenders" protection to steel in locations where corrosion issues are not present and provides paint protection in areas with conditions that would otherwise limit the use of weathering steel.

A weathering-type steel that could withstand wet conditions including water containing chlorides and still resist corrosion would present a desirable solution to the limitations cited above. Such a material would constitute a true noncoating corrosion-resistant option. One potential steel that meets these requirements, which is ASTM A1010 steel, has recently been developed. The corrosion resistance has been accomplished by chemically augmenting the steel production formula to produce a material said to be a "corrosion-proof" weathering steel. ASTM A1010 contains 10.5% to 12.5% chromium and is said by its vendors to be immune to corrosion based on tests performed in Kure Beach, North Carolina, in the 25-m test site.

This "corrosion-proof" weathering steel has been used on one structure in 2004 in Colusa County, California, and was reported in a presentation given at the 2004 Prefabricated Bridge Elements and Systems Conference. The bridge design was a prefabricated lightweight technology called a multicell box girder. Reportedly, less than 23 tons of A1010 were needed to form the structure of this short-span bridge with overall dimensions of 72 ft long by 32 ft wide. Other bridge structures have been reported in Illinois, Texas, and Oregon.

Chapter 6 of the *Guide* discusses the recommended uses of corrosion-resistant steels.

Recommendations for Improved Service Life

In addition to the use of coatings and corrosion-resistant steel described above, the R19A research team identified a number of areas that hold great promise in the battle to resist corrosion of steel.

First, they include a recommendation to immediately require that corrosion resistance, as a crucial element of bridge durability, be a "hold-point design requirement" in every new and rehabilitated steel structure. "Hold point" in this context means that further progress on the design would depend on having a corrosion review performed and a corrosion-resistance plan established.

In addition to the first recommendation to design corrosion resistance into every steel bridge, other considerations include

- Building in quality through the use of best practices in painting;
- Researching and developing methods to remove chloride ions from steel surfaces that have already been contaminated with chloride ions;
- Developing new superdurable coating materials by both basic and applied research efforts, including industry-to-industry technology transfer;

- Using a corrosion-resistance maintenance plan for every steel bridge, including painting priority, cost estimate, and timetable;
- Using coatings to seal precast and cast-in-place (CIP) concrete bridge elements against the intrusion of water containing chlorides from deicing materials and from sea salt spray in seacoast locations;
- Researching whether the very costly removal of mill scale is a necessity for corrosion protection of hot-rolled steel (the necessity of completely removing mill scale is questioned);
- Evaluating the possible development and expansion of the use of cathodic protection methods on structural steel on bridges;
- Continuing funding for corrosion protection and resistance during all phases of the life of the structure including design, construction, and remedial maintenance over the 100-year life of a structure, as it is simply not possible to build it and leave it alone with no maintenance for 100 years;
- Evaluating the widespread use of alternative corrosion-resistance approaches, such as thermal spray metallizing, hot-dip galvanizing, and weathering steel alone or in combination, both with and without additional coating; and
- Performing research leading to the development and use of alternative noncorrosive deicing materials.

In addition to the considerations listed above, one truly novel concept was put forth during this research. That suggestion is to apply some form of zinc coating to the steel during the hot-rolling process. One obvious benefit is that at hot-rolling temperatures, there is already a great deal of thermal energy in the steel. Application of a coating of zinc at that point will eliminate the need for reheating the steel or the wire in the case of thermal spraying or the application of a molten zinc bath during hot-dip galvanizing. If a metal more active than iron in the corrosion series, like zinc, were employed, then long-term corrosion protection could be built in rather than added on. If this method were to prove possible, it could obviate the need for any subsequent treatment for corrosion resistance. The savings could prove to be very substantial. No mention of this approach to corrosion protection was noted in the literature survey part of this research project.

It is recommended that these areas be further investigated through additional research. There is little doubt that the least cost and biggest payback is found in the first recommendation: building in quality through the use of best practices in painting. Designing corrosion protection into every project from the very beginning of the project design stages will cause a dramatic lengthening of the maintain–repair–replace cycle. Despite the conservative DOT expectation of only 30 years, there are many steel bridges coated with zinc coating–based systems that are up to about 45 years old. If corrosion resistance were intentionally designed into a structure by managing the configuration and details of bridge design and detailing, such structures may well last 100 years before major recoating is needed. Of course, some maintenance painting, including incidental or spot or zone repairs to mitigate nicks from traffic-propelled or storm-driven debris or vehicular or other impact, will likely be required at least once or twice.

The identification and uniform adoption of painting best practices is doubtless another major area of inquiry. If there were an actual "AASHTO Bridge Corrosion Protection Guide Specification" that cited best practices in bridge painting, repainting, and overcoating, a tremendous savings and lengthening of the bridge painting maintenance service life would result.

Analysis of DOT Survey

The following issues were apparent from analysis of the DOT survey:

- Painting is widely used among most respondents.
- Weathering steel is used somewhat, with five of 16 respondents reporting use on over 50% of their bridge structures.
- Most states are following the still current, but dated, FHWA guidance document *T5140.22: Uncoated Weathering Steel in Structures* (FHWA 1989).
- Only one state (Michigan) uses no weathering steel.
- On weathering steel bridges that are painted, virtually all respondents say that they paint the ends of the steel beneath joint areas.
- All states surveyed that responded use zinc-rich paint systems. Most expect to get 20 to 30 years of service life. A few states use water-based versions of the protective system including an acrylic topcoat. They indicate that they expect 20 to 30 years performance before removal or reworking.
- AASHTO's National Transportation Product Evaluation Program is a set of test data on coatings that is free and could be beneficial in placing coatings on a qualified products list. The testing is funded by coating suppliers. Seven respondents indicated that they do not use the data, one state has its own testing standard, and the remaining states can access a wealth of free test data. There are opportunities for state DOTs to mix the means of protection so that more resistive means of protection are explored to protect steel in the most aggressively exposed areas. Most states do not allow the submission of alternative coatings on projects.
- Some form of training is supplied or required for coating inspectors in most of the states surveyed (11 of 19). Painting contractor certification is required by about one-third of the DOT respondents. There may be an opportunity for others to consider specifying the existing SSPC painting contractor certification program.
- All states responding (17 of 19) require the complete removal of mill scale, and only one specifies a coating to apply

over mill scale. A two-coat system is approved on the North East Protective Coating Committee (NEPCOAT) qualified products list. Most states do not allow the use of a two-coat system.
- The coatings on all NEPCOAT qualified products lists have been extensively tested both in the NEPCOAT program and the National Transportation Product Evaluation Program. These materials, although promising, do not have a long proven field history. Cost savings by using two coats instead of three are estimated at 3% of the steel cost (free on board shop) of a new steel bridge.
- Striping, although optional, is considered an excellent practice and is required by most DOTs responding. However, they do not mandate its use.
- Maintenance repainting strategies and materials used vary widely among the DOTs. Most use a zinc-rich primer.
- Overcoating material selection varies widely among the states. There are at least nine systems used by the 17 states responding.
- Chloride removal practices vary widely, as do acceptance criteria. Most states responding require the criteria described in SSPC SP-12, Waterjetting NV-2 (<7 μg/cm^2). There is room for improvement in chloride removal techniques before a feasible method will emerge.
- The decision to overcoat versus recoat is generally made at the district level. There is an opportunity for successful research in the evaluation of maintenance planning.
- Wash water is retained or contained by about half the states. It is assumed that these practices are in response to urging by the department of natural resources or department of environmental protection in those states. The retention process, as dictated by others, can control the maintenance painting cost of both bridge maintenance repainting and overcoating.
- Most states contain solid waste even when lead paint is not involved on the project.
- Finally, it appears that painting funds and lead-based paint continue to be big problems in most states. There are still thousands of bridges coated with lead-based paint, which means that the lead-based paint problem will extend well into the future.

Steel Bridge Systems

Steel bridge systems have the potential for achieving a service life well over 100 years, but they must be designed, constructed, and maintained properly to achieve this goal. The primary component of a steel bridge system is the steel superstructure. However, the overall system also includes other important components and elements such as the deck, joints, bearings, and substructure, all of which are discussed in more detail in separate sections of this report. All the subsystems and components that make up the overall bridge system are affected differently by external factors, such as heavy loading or harsh environment, and require varying levels of maintenance to achieve 100-plus years of service life. In areas of severe impact, some elements may have to be replaced before the service life of the overall system is reached. All the various elements that make up a steel bridge system are addressed in this report, and recommendations are made to improve service life. The design must first consider the durability of all system components and address the individual maintenance and replacement needs as part of an overall approach to service life design.

This study identified the most common steel bridge systems used in practice along with newer promising systems that have incorporated accelerated bridge construction concepts and details. Service life issues were identified, and recommendations for improving service life were proposed.

The findings and results of this study were incorporated into the *Guide* in Chapter 2, Bridge System Selection.

Typical Steel Bridge Systems

The most common steel bridge systems used today are composite multigirder deck systems using rolled beams, plate girders, or tub girders. These systems can be single- or multispan and are either straight or curved. Simple-span systems were often used in the past, but most multispan systems today are continuous. Rolled-beam bridges using W-shapes are used in shorter spans, up to about 100 ft for simple spans and up to about 120 ft for continuous spans. Welded plate girders are mostly used for spans over 120 ft (NSBA 2005).

Until the 1970s, many bridges were designed with systems using two deck girders, transverse floor beams, and longitudinal stringers. Poor fatigue details in these earlier welded bridges, however, led to cracking, and the issue of fracture criticality became a major concern. Multigirder bridges with inherent redundancy became the desired configuration (NSBA 2005).

Steel bridge systems have typically used composite CIP concrete decks, but other deck types, including precast concrete panels with or without posttensioning are also common, particularly when used with accelerated construction techniques. Substructures generally consist of reinforced concrete piers and abutments.

A variation to the typical multigirder system is the girder–substringer system, which has been used as an economical concept for longer spans (beyond about 275 ft). This system uses several heavy girders with wide girder spacing and rolled-beam stringers supported midway between the main girders by truss K-type cross frames.

For many years, bridges were designed as a series of simple spans with expansion joints at each pier because they were easy to design and construct. Leaking joints, however, became a leading cause of structural deterioration, and the desire to

eliminate joints became prevalent. Multispan steel girder systems were also shown to be much more efficient when designed as continuous systems, so continuous design became commonplace.

Multispan systems have typically been fully continuous for both dead load and live load, but new systems, typically with spans up to 150 ft, have been introduced with a simple for dead load and continuous for live load concept. These systems combine the advantage of simple-span construction with the efficiency of live load continuity and the durability that comes from not having joints.

Continuous steel bridge systems using integral abutments were developed as a way to eliminate joints altogether. Integral pier cap construction was also developed as a way to avoid sharp skews or longer spans in interchange ramp bridges. Integral pier caps also have the advantage of eliminating bearings, which can minimize future maintenance requirements.

Steel plate girder systems have been used for spans up to about 500 ft. Spans up to 400 ft have been designed economically with parallel flanges. Variable-depth haunched girders have been used in the 350- to 500-ft range. Use of high-performance steel (HPS 70W) has shown economy for plate girder and tub girder systems in most span ranges over 150 ft. For plate girders, a hybrid combination using HPS 70W in negative moment top and bottom flanges and positive moment bottom flanges has been shown to be the most economical system. Trusses, arches, cable-stayed, and suspension systems have also been used for longer span applications, typically over 500 ft. For spans up to 300 ft, which is the limit for this research, deck girder systems are the most applicable.

Causes of Deterioration in Steel Bridge Systems

The National Bridge Inventory (NBI 2013) database shows clearly that steel bridge systems have the potential for achieving service life well over 100 years. However, if they are not designed, constructed, and maintained properly, they can be affected by certain environmental and loading conditions that can lead to serviceability problems and reduced service life. Most major steel bridges that are in the 100-plus-year category have undergone deck replacements and other types of major rehabilitation during their service lives that have kept them alive.

The major causes of deterioration for steel elements within a steel bridge system are fatigue and fracture, as well as corrosion.

Fatigue and Fracture

Early welded steel structures have a history of cracking at certain types of weld details due to load- and distortion-induced fatigue. Cracking at I-beam cover plate terminations or at other longitudinal weld terminations in tension zones was particularly evident. Cracking in girder webs due to out-of-plane bending within stiffener web gap regions next to cross-frame attachments also became a common problem. Subsequently, extensive research and laboratory testing have provided an understanding of fatigue behavior, and different weld detail types were found to have varying levels of fatigue susceptibility. Newer design provisions and recommended details were developed that provide solutions for both load- and distortion-induced fatigue to achieve desired service life.

Steel bridges do not fail in fatigue, but in fracture, which is the rapid, unstable propagation of a larger flaw (most likely the result of fatigue). Fatigue crack initiation is independent of steel type and strength, but possible brittle fracture is influenced by steel toughness, among other variables. Early steels were more susceptible to brittle fracture, but in recent years, new high-performance steels—HPS 50W, 70W and 100W—have been developed with very high toughness characteristics. Although somewhat more costly than conventional-grade steels, high-performance steels are now encouraged where applicable, particularly in nonredundant or fracture-critical applications. Use of high-performance steel allows time for fatigue cracks, if developed, to be found during regular bridge safety inspections before fracture can occur.

Fatigue and fracture should not be an issue in new steel bridges designed in accordance with the latest guidelines of the *LRFD Specifications.* Extensive research has been done in recent years to identify causes and solutions for fatigue- and fracture-related problems. When using proper details and fabrication methods, both load- and distortion-induced fatigue problems should not be an issue in achieving desired service life.

Corrosion

Corrosion, the result of exposure to oxygen and moisture, is one of the fundamental limitations of steel as a main construction material. Corrosion is greatly accelerated in the presence of chloride ions from roadway deicing salt or salt spray in a marine environment. Deck drainage with deicing salt leaking through open deck joints is a leading cause of steel element corrosion in bridges.

To achieve long-term bridge durability, a corrosion-resistance plan must be a design requirement for every new or rehabilitated steel structure. This plan should include the use of painting best practices and a maintenance plan that addresses painting priorities and timetables. Details that serve to protect and keep the steel dry must be included in the design. Among these are bridge system solutions that eliminate deck joints, preventing salt-contaminated drainage from reaching steel elements below.

Painting best practices now include paint systems that contain metallic zinc as the corrosion-resistant pigment. Zinc coatings provide galvanic protection to the steel, in which zinc (the more noble metal) will oxidize (corrode) in preference

to the steel. To protect the zinc coating layer from oxidation, additional coating layers are applied over the zinc-rich primer.

Many studies demonstrate the value of zinc coatings as a steel protection system. In addition to zinc-rich paint, these zinc coatings also include galvanizing and metalizing. Their use should be considered carefully as part of the best plan for achieving a 100-plus-year service life.

Weathering steel has also found widespread use in steel bridges, and has been used in both unpainted and painted applications. Although no formal research exists to support the practice, painted weathering steel following a "belt and suspenders" approach is commonly used in locations where corrosion issues would otherwise limit the use of weathering steel, such as directly below deck joints. In addition to weathering steel, a new stainless steel for bridges, ASTM A1010, has been developed for use in severely corrosive environments.

Other Issues

Other deterioration types are related to damage caused by external sources such as truck impact or fire, which are hazard related. These issues are further addressed in the *Guide*.

Strategies for Improving the Service Life of Steel Bridge Systems

New Bridges

In addition to the previous discussion regarding fatigue and corrosion protection, additional solutions for addressing steel system service life for new bridges include

- Integral abutments to eliminate deck joints.
- New steel systems that eliminate deck joints at piers; these systems include a concept for simple for dead load, continuous for live load.
- New steel systems that provide for accelerated construction, including modular construction with predecked panels. These modular systems require special attention to both transverse and longitudinal connection details for achieving long-term durability.
- Modular orthotropic deck systems are also a consideration. These systems also require special attention to both transverse and longitudinal connection details.

Existing Bridges

In addition to regularly scheduled maintenance, additional solutions for addressing steel system service life for existing bridges include (1) retrofitting existing simple-span steel bridges to continuous systems and (2) retrofitting existing fatigue-sensitive details or using special techniques that improve fatigue resistance, such as UIT.

The first solution, retrofitting existing simple-span steel bridges to continuous systems, has been implemented by many state DOTs, who have developed guidelines for converting existing simple-span steel bridges to continuous by splicing the girders over piers when they were being rehabilitated, particularly when decks were being replaced. Benefits of converting to continuous spans include reducing the potential of continued deterioration due to leaking joints, increasing resistance to seismic displacements, and slightly improving the load-carrying capacity of the superstructure.

However, according to NYSDOT (2008), the design for continuity retrofit needs to consider the system behavior of continuous girders as opposed to original simple-span behavior. For multispan continuous systems, larger movements may be realized at abutments or at interior piers if original fixed conditions are converted to full expansion conditions. In addition, increased vulnerability to fatigue may result due to portions of the retrofitted beams being subject to stress reversals and higher stress ranges than the original simple-span construction. The end regions of retrofitted girders originally designed for small, simple-span positive moments are subjected to larger-magnitude negative moments. Although the deck joints over the piers are eliminated, the retrofitted deck in this area is subjected to tension under service loads, and crack control measures must be considered. Continuity can also increase seismic loads on individual piers depending on retrofitted bearing fixity configurations. Deck replacement projects provide excellent opportunities to include girder retrofit because girders will be readily accessible, and future costs of maintaining the joints will be eliminated.

States use several methods to convert existing simple-span bridges to continuous, including full continuity, continuous for live load only, and continuous deck only (link slab concept).

The second solution for addressing steel system service life for existing bridges involves retrofitting fatigue-sensitive details or using special techniques to improve fatigue resistance, such as UIT. Load-induced fatigue cracking has been one of the biggest problems with older welded steel bridges, particularly those with Category E and Category E′ details. UIT, which is designed to improve the fatigue resistance of an existing welded detail (Fisher et al. 2002), imparts impact energy to the surface of the material in areas in which fatigue cracking is likely to occur. It is performed with a tool that contains an ultrasonic transducer and a set of small steel transfer pins that are free to move relative to the transducer. The ultrasonic transducer generates resonant high-frequency pulses that impart energy to the material surface through the steel transfer pins. The imparted energy results in a zone of plastic deformation near the surface of the material, the introduction of compressive stresses up to 2 mm (0.08 in.) deep, and the relaxation of residual tensile stresses due to the original welding operation. All these material changes combine to prevent the formation of a surface crack under cyclic loading.

Testing performed by Fisher et al. (2002) at Lehigh University has demonstrated that UIT is effective in improving the fatigue resistance of many of the details found on structural steel bridges in the United States. For example, testing has shown that UIT can greatly increase the fatigue resistance of a cover plate termination, a Category E detail, and achieve a Category C or better fatigue strength. UIT is applicable to new construction and as a retrofit for maintenance and repair procedures.

Chapter 2 of the *Guide* provides more detailed information about the performance of steel bridges.

Concrete Bridge Systems

The performance of unreinforced concrete as a durable material has been demonstrated in many historic structures, including the Pantheon in Rome, which was constructed around AD 126. Although unreinforced concrete provides excellent strength and durability in compression, its tension capacity is extremely limited and has a reduced ductility due to cracking. The introduction of steel bar reinforcement to enhance the tension capacity of unreinforced concrete allowed it to be used in more conventional beam applications other than elements in compression.

The use of reinforced concrete in bridge systems has a relatively short history. Its first recorded application in the United States was in the Alvord Lake Bridge in Golden Gate Park (San Francisco, California), which was constructed in 1889 and is still in service today. As advancements in concrete and steel reinforcement technology have occurred over the years, so has the use of this material in bridge systems throughout the United States. The introduction of prestressing into concrete bridges in the 1950s has resulted in a startling increase in its ability to meet the needs of a growing transportation network.

The longevity of concrete bridge systems is affected by many environmental factors. Corrosion of steel reinforcement remains one of the principal causes of deterioration of these structures. Advancements in reinforcement-protection systems have enhanced the durability of concrete bridges tremendously, particularly when exposed to harsh environments. Concrete bridge systems have the potential for achieving long service life if properly designed, constructed, inspected, and maintained.

As with steel bridge systems, the overall concrete bridge system also includes other important components and elements such as deck, joints, bearings, and substructure, which are all discussed in more detail in the *Guide.* The design must first consider the durability of all system components and address the individual maintenance and replacement needs as part of an overall approach to service life design.

Chapter 2 of the *Guide* provides a more detailed discussion of concrete bridges.

Common Concrete Bridge Systems

Several common reinforced concrete bridge systems are used in the United States. The type of system implemented at a particular site is generally dictated by economy and the system's ability to provide the required span or geometric requirements, such as curvature. The most commonly used concrete bridge superstructures are discussed in the following subsections.

Cast-in-Place Slab Systems

CIP slab superstructures commonly span less than 50 ft and are typically used over minor water crossings. They were traditionally constructed as a series of simple spans, but in recent years, the use of continuous spans has gained favor, eliminating the joints over substructure units.

Precast Concrete Adjacent Members

Precast concrete adjacent member superstructure systems consist of multiple precast beam elements set side by side and connected either with a CIP closure joint, posttensioning, composite concrete topping, or a combination of these connection methodologies. The precast elements commonly consist of either conventionally reinforced or prestressed solid rectangular sections, rectangular boxes, or double Ts. Precast solid and voided slabs also fall into this category. Precast adjacent box beams are the most prevalent adjacent box girder superstructure for short- and medium-span bridges (typically 20 to 127 ft), especially on secondary roadways.

Precast Concrete I-Girders

Precast I-girders are the most commonly used concrete bridge superstructure. These girders are made of high-performance plant-produced materials and are generally very durable. I-girders with a composite deck slab behave distinctly differently from adjacent box girders, which are described above. Adjacent box girders are not typically covered with a CIP composite slab, and the sections are torsionally stiffer. In a bridge system consisting of I-girders with composite CIP slabs, commonly referred to as beam–slab bridges, the longitudinal stringers are typically prestressed concrete girders. The use of precast prestressed concrete girders traditionally has been limited to simple spans up to approximately 150 ft; however, with recent optimization of girder sections, precast girders with spans greater than 200 ft can be achieved. The girders can also be made continuous for live load.

Cast-in-Place Posttensioned Box Girders

A superstructure of CIP posttensioned box girders is cast continuously on falsework. This type of superstructure has become very popular in several states, particularly California, Arizona, and Nevada, and has been used in spans up to 350 ft. This type of construction lends itself to local construction

industry practices in areas where contractors can economically provide the required falsework. Similar to segmental construction, CIP on falsework offers the advantage of longer spans than conventional girders and can easily accommodate curved alignments. CIP construction also allows clean lines and architectural finishes that improve the aesthetics. The use of posttensioning further enhances concrete durability.

Designing the structures as a frame and using monolithic connections between the superstructure and piers also eliminates bearings, which eliminates associated future maintenance. A potential disadvantage of this type of construction is difficulty in replacing the deck or widening the bridge.

Segmental Posttensioned Concrete Box Girders

Specialty systems using segmental posttensioned concrete box girders have been used for spans greater than those that can be achieved with stringer-type girders and for bridge geometries with horizontal curvature. They are further divided into cantilever construction and span-by-span construction, and can be either precast or CIP. One of the advantages of segmental concrete bridges is the type of construction technique used, which minimizes the interruption to traffic during construction. Recently, however, there have been major concerns about corrosion of steel strands in grouted duct (Azizinamini and Gull 2012a, 2012b). This concern is especially important as there is no reliable technique to detect corrosion in steel strands embedded in concrete. Inspections of external ducts are relatively easier. However, development of a reliable methodology to detect corrosion in duct embedded in concrete remains an active research topic.

Segmental Spans

Segmental spans can be cast to match the shape of the alignment, making them particularly suited to curvature. Spliced girders are typically used on relatively straight alignments; however, they have also been used for curved alignments in recent years in Nebraska and Colorado. Segmental and spliced posttensioned girder bridges have been observed to have improved deck performance due to the precompression of the deck.

Modular Pretopped Concrete Girder Units

These superstructures using modular pretopped concrete girder units are primarily developed for accelerated bridge construction. They consist of precast beams or girders constructed monolithically with sections of the deck, which are then connected with CIP joints in the field.

Causes of Deterioration

The literature search supplemented by the results of the DOT surveys performed during this study revealed numerous causes of deterioration in concrete systems, subsystems, and components. The various causes for concrete deterioration are discussed in detail in the sections of this report dealing with concrete durability and bridge decks. The degree and severity of concrete deterioration depends on the environmental influences to which the bridge is subjected. The principal influences include

- Environmental volumetric influences, including physical influences, such as the effects from moisture and temperature change; wear; and freezing and thawing;
- Chemical influences, including exposure to chlorides, sulfates, carbon dioxide, alkalis, and various acids; and
- Loading influences, including vibration and impact.

The durability of concrete exposed to these influences is highly dependent on design practice, materials, and their proportioning and workmanship during construction. Although all these influences are important, the principal deterioration of concrete systems, subsystems, and components is the corrosion of the steel reinforcement, which results in severe cracking, spalling, and delamination of the surrounding concrete. The protection provided by the depassivated zone around the steel reinforcement is often compromised by cracking of the concrete.

Concrete bridge decks are particularly affected by environmental influences. Bridge deck cracks are typically parallel to the steel reinforcement in the top layer. This cracking orientation can cause the concrete surrounding the steel reinforcement to reach the corrosion threshold limit within 6 months to a year in environments where the top of the bridge deck is exposed to chlorides, such as deicing salts.

Concrete superstructures and substructures in marine environments are not exposed to the same concentration of chlorides as the top of a bridge deck directly in contact with deicing salts. They are, however, susceptible to the same type of corrosion, only at a slower rate through the same mechanism of failure.

Strategies to Enhance Service Life of Concrete Bridges

Several strategies have been developed to address the durability of concrete systems, subsystems, and components. These strategies, which are fully described in the concrete durability section of this report, include

- Proportioning of concrete to provide low permeability and low cracking potential;
- Use of noncorrosive materials (e.g., stainless steel) and protective coatings (e.g., epoxy);
- Prestressing or posttensioning of elements to eliminate cracking;

- Use of more sophisticated strategies, such as cathodic protection and electrochemical chloride extraction;
- Use of overlays and membranes on bridge decks; and
- Various combinations of the above strategies.

The use and application of these strategies is highly dependent on the environment in which the concrete systems are exposed. A single strategy that fits all conditions within the United States does not exist. These strategies must be reviewed by each governing agency for applicability.

Research Categories

Following the literature search and other related tasks previously described, a number of research topics were identified to fill the knowledge gap with respect to design of bridges for service life. Service life issues needing further research were divided into three categories, with Category 1 research topics having the highest priority. Category 1 and 2 research topics were selected to conduct proof of concept tests within the R19A project. As required by the original scope of work, and recognizing the limited resources within the project, proof of concept tests were intended to examine the feasibility of the ideas and leave detailed research to others. Greater effort was spent on Category 1 research topics.

Category 3 research topics (see Appendix A) were identified and are recommended to be carried out by others.

Table 3.12 lists Category 1 and 2 research projects as approved by SHRP 2 to carry out proof of concept tests.

The following sections briefly describe the scope of work carried out and the results and findings for the Category 1 and 2 topics listed in Table 3.12. Based on priority, project resources, and other limitations, the level of efforts on each topic varied. When possible, the following information is provided for each topic:

- Problem statement;
- Objectives;
- Scope of work;
- Results; and
- Recommendations for future research.

The final major section of this chapter describes the development and provides an outline of the *Guide*.

Link Slab

Problem Statement

A link slab is a type of detail used in conjunction with existing or new bridges in which the girders act as simple beams for both dead and live loads. In this type of deck detail, the slab spans continuously over the length between the adjacent simple-span girders (see Figure 3.41). The use of link slabs, however, has been limited primarily to short-span bridges in warm climates. The Phase 1 report provides a detailed description of past work and current status with respect to link slabs.

Objectives

The limited use of link slabs in cold climate areas are due to two factors: (1) lack of understanding of the force transfer

Table 3.12. List of Category 1 and 2 Research Topics

Research Topic		Category
Joints	Link slab	2
	Converting simple spans to continuous	2
	Jointless bridges	1
	Seamless bridge systems	2
	Expansion joints	2
	Joints in modular systems - Adjacent box - Closure pour	1
Bearings	High-performing sliding surface	2
Enhancing corrosion resistance of concrete bridges	Corrosion-resistant reinforced concrete structures	2
	New galvanic systems to achieve long-term corrosion protection	2
Bridge deck	Self-stressing deck systems: CIP	2
	Self-stressing deck systems: precast	1
	Delayed composite systems	2
	Membranes for bridge deck	1

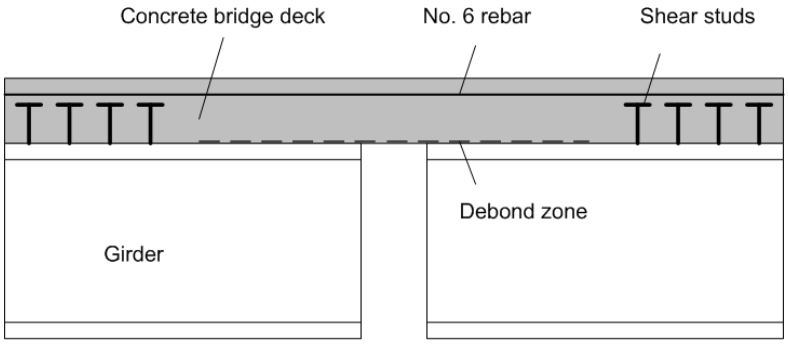

Figure 3.41. Conceptual detail for link slab.

mechanism and load demand for which the link slab should be designed and (2) lack of thorough information about feasible details that can prevent formation of extensive cracking and leakage of moisture onto the bridge elements below the deck. The main objective of the link slab study was to comprehend the behavior of link slabs and recommend the scope of work that could lead to the development of appropriate details.

Scope of Work

In this research, several multispan bridges containing link slabs were instrumented to determine the motion at their expansion joints, located at the bridge abutments, and at the link slab details between the girders at the bridge piers. Finite element analyses were performed to analytically investigate the link slab behavior, and mechanistic models were developed to represent the overall link slab response. The primary focus of the field instrumentation was to determine the bridge displacements and the deformations within the vicinity of the link slab under thermal loads. The researchers instrumented the bridges with dial gauges to measure longitudinal movements and with DEMEC (DEmountable MEChanical strain gauge) points to measure expansion and contraction across the construction joint or control joint at the link slab. The finite element analyses were conducted to evaluate the potential magnitude and distribution of strains in the link slab region. Emphasis was placed on a particular link slab detail currently used in the state of Georgia; however, variations on the Georgia detail, including different details used by other states, were also considered. The detailed studies are documented in Davidson et al. (2012) and Snedeker et al. (2011).

Results

The field results showed that girder ends resting on fixed bearings, which for prestressed concrete girders have round holes for dowel bars at the bearings, have essentially the same ability to displace longitudinally due to daily thermal loads as those that sit on expansion bearings, which have slotted holes for the dowel bars. Furthermore, because of the annulus around the dowel bars at the bearings, little to no force is generated in the bearings due to the girder rotations. Even if the dowel bars are in contact with the holes within the girders, the force that can be induced in these bars is not sufficient to develop any significant stress or strain within the link slabs. In addition, the longitudinal forces induced by the deformation of typical elastomeric bearings are not sufficient to develop any significant stress or strain within the link slabs. Thus, little to no force occurs in the link slab reinforcement crossing the construction joint.

Estimates of shrinkage strains in the link slab showed that a crack of sufficient width could easily exist in the link slab at the top of the deck so that the concrete on one side of the crack would not contact concrete on the other side of the crack. A finite element analysis showed that the deformations due to thermal and live loadings are not sufficient to close such a shrinkage crack that may exist in the deck. Therefore, essentially no moment is created in the link slab due to girder rotations. Debonding of the concrete slab on top of the girders adjacent to the link slab is not needed to achieve good performance of the link slab. Good performance of the link slab detail is contingent on the proper forming of a controlled joint near the midlength of the link slab and the proper sealing and maintenance of this joint. Damage was observed in a small number of instances from evaluation of a large set of bridges in Georgia. In all cases where damage was observed within the link slab, the damage involved either (1) an unraveling of the edge of the slab due to inadequate chamfering or rounding of the edge of the slab at the construction or controlled joint or (2) spalling of concrete from a patch located adjacent to the controlled joint.

The reinforcing bars crossing the link slab provide bridge deck continuity for longitudinal and transverse loads due to vehicle braking, wind, and earthquake, and they act as dowel bars transferring shear between one side of the deck crack to the other. However, there is little shear transfer when transverse edge beams supporting the deck are placed between the girders at the ends of the girders. The research observed that in bridges with minor skew angles up to approximately 20°

from the nonskewed orientation, extension of the top mat of reinforcing bars across the link slab is sufficient.

Conclusions and Recommendations

Based on the research study carried out, the following conclusions and recommendations are made with respect to design and construction of link slabs.

Debonding versus No Debonding

Many bridge organizations require debonding of the link slab from the girders and any edge beams or diaphragms over a length of up to 5% of the girder span length on each side of the link. Common practice is then to assume that the girders impose a rotation of $\theta_1 + \theta_2$ at the ends of the link slab, where θ_1 and θ_2 are the end rotations of each of the girders, and that the link slab is subjected to pure bending between the ends of the debonded zone. Basic kinematics does not allow a uniform curvature of $(\theta_1 + \theta_2)/L_d$ in the link slab, where L_d is the length of the debonded zone. The link slab can only reach the curvature of the girders at the ends of the girders, since it is in contact with the top of the girders. Furthermore, the girders have essentially zero curvature at their simply supported ends. Obviously, the true three-dimensional response of the link slab is more complex than the simple $(\theta_1 + \theta_2)/L_d$ curvature assumption. However, if there is a relatively wide top flange of the girder, such as in various precast sections, the restraint from the girders would appear to force a concentration in curvature across a short length of the link slab, located between the ends of the girders.

Based on the above findings, debonding of the slab from the girder should not degrade the performance; however, based on the research conducted in this study, the impact of debonding is expected to be minimal. Good performance of link slabs has been observed without the use of debonding.

Note that for precast concrete construction, the shear stirrups generally are placed close to the ends of the girders, and the slab concrete is used in the calculation of the composite girder shear strengths. Therefore, for precast concrete construction, it is not practical to debond the slab from the girders.

It can be surmised that in many cases, the behavior of the link slab under live load and negative temperature gradients may involve the development of compression toward its bottom surface due to bending about a neutral axis near the top mat of the rebar. This compressive force can be reacted by the girder shear connectors at the ends of the link. In addition, these forces can be relieved by restrained shrinkage strains that occur due to early curing of the concrete. Hence, the link slab strains due to the girder end rotations may contribute mostly to the closing of small, unavoidable shrinkage cracks that occur due to early restrained deformations. The behavior under positive temperature gradients is similar, but the top of the slab is in compression due to the upward movement of the simply supported girders.

Influence of Skew

Due to the differential vertical displacements between the girders at a given bridge cross section, as one moves away from a skewed bearing line, and when end diaphragms are used, due to the relatively large in-plane stiffness of the diaphragms, the tendency is for the girders to move (twist) in opposite directions on each side of the skewed bearing line. This movement generates a tendency for displacements normal to the skewed bearing line either at the slab level or at the bearing level. The neutral axis of the composite girders is generally located in the slab or close to the top of the girders. As noted above, the measured rotations also tend to be about an axis within the depth of the link slab at the ends of the girders. Therefore, the greatest tendency for displacements is normal to the skewed bearing line and at the bottom of the girders. The typical bearing details are flexible enough to allow these movements.

Selection of Link Slab Reinforcing

A wide variety of reinforcing layouts are used by different bridge organizations. In many cases, concerns are expressed about terminating any of the reinforcing steel within the link slab region. Some organizations terminate all the slab-reinforcing steel at the link slab, place a construction joint at the center of the link slab, and continue one top mat of reinforcing steel across the joint. The most important attributes of the rebar continued across the joint are that (1) there is sufficient steel area such that the rebar is not yielded due to any deformations experienced by the link slab, and (2) the bar spacing is sufficiently small such that any cracks within the link slab other than at a formed or saw-cut joint remain small and well distributed. Lepech and Li (2009a) point out that "[t]he large majority of concrete link slabs within Michigan that have shown distress or required maintenance were found to have too little reinforcement included in the design, or the reinforcement was not installed properly by the contractor."

For link slabs at bearing lines having sharp skew angles, it is recommended that at least one mat of rebar be continued through the joint in both the longitudinal and transverse directions.

For link slabs at bearing lines having a minor skew, some organizations orient the transverse reinforcing steel parallel to the bearing line. This technique avoids the need to terminate transverse reinforcing steel at a construction joint or the need to continue these bars through a construction joint.

Use of a Saw-Cut or Formed Joint

One common practice is to place a saw-cut or a formed (troweled) joint at the midlength of the link slab. The intent is to force a larger crack to occur at this specific location, where

the crack can be sealed and maintained. A number of cases have been observed by the investigators in which, due to inadequate preparation of this joint, spalling or unraveling of the concrete occurred at the edge of the joint. In addition, it is important that if a saw cut is placed in the link slab, this cut must be made shortly after the concrete placement to ensure that the intended crack control occurs. By specifying a formed joint rather than a saw cut, the engineer can have some additional confidence that the joint will be placed early enough for it to be effective.

At highly skewed bearing lines, it is recommended that the saw cut or formed joint be placed over the pier, parallel to the skew. However, over a short distance at the edges of the slab, the joint should be turned at 90° to the edge of the deck.

Because it is expected that saw cut or formed joints can be easily damaged by snow plows, their use is not recommended in cold regions.

Waterproofing

One option that alleviates the need for a saw cut or formed joint is to provide a waterproofing membrane for the deck. When a membrane is employed, there is no longer any need for a saw cut or formed joint. The reinforcing steel can be designed to control the crack size within the link slab, and the membrane guards against penetration of moisture into the deck.

Separation of Edge Beams or Diaphragms

In cases in which edge beams or diaphragms are placed at the ends of the girders, it is important that sufficient spacing be provided between these components on each side of the joint to accommodate the anticipated sum of the maximum girder rotations on each side of the joint, assuming that the center of rotation is about the top mat of reinforcing steel in the link slab.

Application of Fiber-Reinforced Concrete

Recent research by Lepech and Li (2009a, 2009b) and Qian et al. (2009) has developed and demonstrated the use of fiber-reinforced concrete (or engineered cementitious composite [ECC] material) to attain excellent durability of link slabs while accommodating the deformations imposed on them by simply supported girder end rotations due to live and thermal loading conditions. Figure 3.42 shows a schematic of the link slab detail proposed by these investigators. Lepech and Li (2009a) provide a complete design procedure based on their findings. The design involves the use of a debond zone in which the shear connectors between the girder and the deck are removed to prevent composite action. Outside the debond zone on either end of the link slab are transition zones in which the shear connection and composite action between the girder and the deck are reestablished. The ECC is placed using a separate closure pour after the decks have been placed on each side of the link slab. Lepech and Li calculate a maximum girder end rotation demand based on the maximum girder service vertical deflections for use in their design procedure. If a deflection limit of $L/800$ is used, the design rotations are 0.00375 radians. The link slab is assumed to be subjected to uniform bending via these end rotations, and steel reinforcement is provided in the link to develop the corresponding induced moment. The ECC material is used to address the crack width serviceability requirements.

The investigators recognize that in warm climates, link slab details using conventional reinforced concrete perform well, such that the cost of the advanced material, the extra construction step, and the joint between the concrete slab and the ECC are not required.

Converting Simple Spans to Continuous

Problem Statement

In the past, a large number of steel bridges were constructed as a series of simple spans with deck expansion joints at each pier. This was a popular system concept because it was easy to design and construct. Leaking deck joints, however, have become a leading cause of deterioration and subsequent reduced service life for all types of bridges. Converting existing simple-span systems to continuous and eliminating deck joints has been used as a way to extend service life of existing bridges.

Some state DOTs have developed specific guidelines for splicing girders over piers; others have addressed this on a

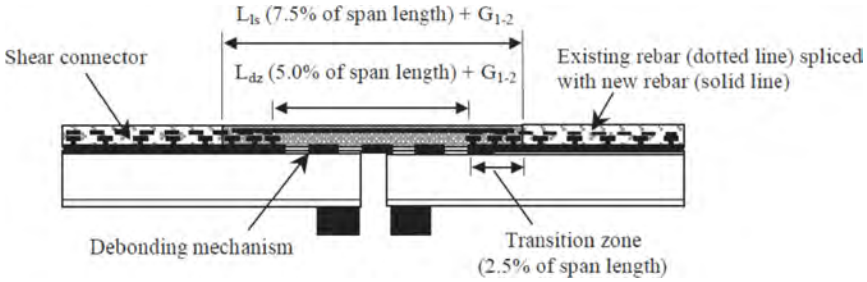

Source: Lepech and Li 2009a.

Figure 3.42. Schematic of ECC link slab detail.

case-by-case design basis. As a result, many variations exist in the industry. There is a need to provide more uniform and consistent guidelines regarding design criteria, details, and performance that will result in cost-effective service life extension.

Objectives

The objectives of this study were to review current criteria and details in the industry for converting existing simple-span steel bridges to continuous and to develop recommendations for consistent cost-effective approaches.

Scope of Work

The scope of work for this study included

- Collecting, reviewing, and summarizing information from various states and from the current literature;
- Developing recommended criteria for continuity retrofit, including guidelines for analysis considering system behavior; and
- Recommending appropriate details.

Results

Additional detail on this study is given in Appendix B.

A literature survey and a brief survey of national HDR, Inc. offices were conducted to identify current industry and state DOT practices for converting existing simple-span steel bridges to continuous.

It was found that a number of states have performed such conversions, primarily during deck replacement rehabilitations, but few have specific design procedures or standard details. New York State DOT has detailed guidance in their design manual. Tennessee and New Mexico have reported on specific project applications. Some states have guidelines for new design, but not for retrofit of existing design. These details for new design, however, could also be adapted for continuity retrofit.

There are two primary reasons for continuity retrofit: eliminating deck joints and increasing live load–carrying capacity. Details used for achieving continuity over piers can vary depending on the desired outcome.

Three methods have typically been used for continuity retrofit:

- Converting girders to fully continuous for dead load and live load (dead load in this case refers to concrete slab and composite dead load);
- Converting to continuous for live load only (partially continuous); and
- Converting by using a continuous slab over the joint and not connecting the girders (link slab).

In the fully continuous retrofit, the girder flanges and web are spliced, and a single bearing is used under the converted girder. Except for steel dead load, the converted girder is fully continuous for all subsequent dead and live loads, and it behaves like a conventional continuous girder. Because of the significant additional negative moment at piers, splice plates have to be extended to accommodate the negative moment region. Top flange splice plates are typically bolted. Bottom flange cover plates can be field welded, and a butt connection splice made in compression with wedges. Although the greater amount of field work required for this type of conversion makes it the most expensive, it permits greater carrying capacity.

In the continuous for live load retrofit, only the flanges are spliced, and separate bearings are used under the existing girder ends at the piers, similar to the existing configuration. Top and bottom flange splice plates are typically used, but the extension is less than required for the fully continuous retrofit. Splice plate connections are made similar to that described above. In these instances, the girder continuity connection at the piers is made after the deck is poured. In reality, composite dead load is then carried in the continuous system.

An economical and functional modification to this concept is to eliminate the top flange splice plate and use a CIP concrete diaphragm along with the reinforced concrete deck to carry the negative live load moment. The bottom flange connection is still made as described above. This concept has shown to be a reliable solution.

The link slab concept has been used by several states as part of retrofits to eliminate deck joints; it is discussed at length in the previous section on link slabs. With the link slab, girders are assumed to carry the same dead and live load as in the simple-span configuration. This is the most economical solution, but it may result in deck cracking over the piers, which may be objectionable in northern climates with heavy use of deicing chemicals. It also provides the least ability to increase load-carrying capacity.

In all cases when converting to full or partial continuity, the resulting system behavior must be considered. Effects of negative moment over piers with respect to strength and fatigue must be considered and accounted for. Revised bridge end movement resulting from continuity retrofit and converting existing bearings from fixed to expansion at some locations must also be considered and accounted for.

Conclusions and Recommendations

Continuity retrofit is typically performed to eliminate deck joints or to increase girder carrying capacity. Three general methods of converting existing simple-span steel bridges to continuous have been used: fully continuous, partially continuous, and link slab. Fully continuous retrofits tend to be costly but provide the greatest potential for increasing load-carrying capacity. Partially continuous retrofits are generally more

economical and recommended. Newer tested details that eliminate the top flange splice are also recommended.

System behavior of the retrofitted continuous system in regard to girder strength and fatigue and revised bridge movement must be considered and accounted for.

Jointless Bridges

Problem Statement

Leaking deck joints have been a major cause of bridge deterioration and reduced service life, especially where roadway drainage carrying deicing chemicals can spill onto bridge elements below. Elimination of bridge deck expansion joints is therefore an important consideration in bridge system selection to provide long-term service life. A jointless bridge, also commonly referred to as an integral bridge, has a continuous deck with no expansion joints over the superstructure, abutments, and piers. In this type of bridge structure, all movement due to thermal effects, creep, and shrinkage strain is accommodated either within the system itself or at the ends of the approach slabs where the slabs meet the roadway pavement. Unfortunately, at present there are no complete and scientific guidelines for designing jointless bridges. Under the SHRP 2 R19A project, a study was carried out to develop comprehensive guidelines for the design, construction, and maintenance of jointless bridges. This section provides a brief overview of the results obtained for this task. Chapter 8 of the *Guide* provides a detailed discussion of the design, construction, and maintenance issues related to jointless bridges, as well as various details associated with jointless bridges.

Types of Jointless Bridges

Three main types of jointless bridges are described in this subsection: integral and semi-integral jointless bridges, which are commonly used in practice, and a new class of jointless bridges referred to as seamless jointless bridges. The main characteristic of the seamless system is that expansion joints are eliminated altogether, and the bridge deck is connected to the approach road pavement with no expansion joint.

Integral bridges have a superstructure constructed monolithically with the abutments, encasing the ends of the superstructure within the backwall. The main characteristics of integral bridges are their jointless construction and flexible abutment foundations. The system is structurally continuous, and the abutment foundation is flexible longitudinally. The movement of the superstructure is accommodated by the foundation.

The main elements of an integral bridge system consist of bridge deck, girders, integral cast abutments, and approach slabs. The bridge movement is accommodated at the ends of the approach slabs. In addition, sleeper slabs are commonly used to provide vertical support for the ends of the approach slab where the slabs abut the roadway pavement.

Semi-integral bridges are defined as having an end diaphragm serving as the abutment backwall; the end diaphragm is cast encasing the superstructure ends. In this system, the superstructure rests on expansion bearings, and the end diaphragm is not restrained longitudinally with respect to the pile cap or abutment stem. The deck may be sliding or cast monolithically with the backwall, but it does not have a joint above the abutment. The foundation is rigid longitudinally, where superstructure movement is accommodated through bearings.

The main elements of a semi-integral bridge system consist of bridge deck, girders, abutment stem and bearing seat, integral cast diaphragm backwall, approach slab, and sleeper slab. The bridge movement is accommodated at the ends of the approach slabs.

Jointless Bridges in Use

A detailed history of jointless bridges is provided by Burke, Jr. (2009) and summarized here. On the basis of a nationwide mail survey of state and provincial transportation departments, it appears that the Ohio highway department was one of the first agencies to initiate the routine use of continuous construction for multispan bridges. However, these bridges had expansion joints at abutments; Ohio began this practice in 1930.

The Tennessee DOT is now leading the way in construction of continuous bridges. For example, the Long Island Bridge of Kingsport was constructed in 1980 using 29 continuous spans without a single intermediate deck expansion joint.

Continuous integral bridges with steel main members in the 300-ft range have performed successfully for years in North Dakota, South Dakota, and Tennessee. Continuous integral bridges with concrete main members 500 to 800 ft long have been constructed in Kansas, California, Colorado, and Tennessee.

As of 1987, 11 states reported building continuous integral bridges in the 300-ft range. Missouri and Tennessee reported even longer lengths. Missouri reported steel and concrete bridges of 500 and 600 ft, respectively. Tennessee reported lengths of 400 and 800 ft for similar bridges. Sixty percent of those departments responding to the 1987 survey were using integral construction for continuous bridges.

More recently, the Tennessee DOT completed the Happy Hollow Creek Bridge, a seven-span prestressed concrete curved integral bridge with a total length of over 1,175 ft.

Advantages of Jointless Bridges

Henry Derthick, former engineer of structures at the Tennessee DOT, once stated, "The only good joint is no joint." In keeping with this statement, the known advantages of the jointless bridge systems include

- Lower initial cost;
- Lower maintenance cost;

- Prevention of leakage of moisture to bridge elements below deck, resulting in longer service life;
- Improved ride quality;
- Easier and faster construction;
- Easier inspection;
- Simplified bridge details;
- Elimination of bearings (except for semi-integral);
- Ideal suitability for bridges with skew and curvature or located in high seismic areas; and
- Enhanced buoyancy resistance of the bridge.

Because of these advantages, many DOTs have started using jointless bridges; however, the design provisions vary significantly from one state to another.

Cost-Effectiveness of Jointless Bridges

Jointless bridges have a significant cost savings advantage compared with traditional bridges with expansion joints. Cost savings are realized both during initial construction and throughout the life of the bridge because of reduced maintenance. This is particularly true for bridges with integral abutments.

The *Guide* provides detailed estimates of cost savings that could be achieved by using jointless bridges as compared with including expansion devices in the superstructure.

Factors Affecting Performance of Jointless Bridges

Results of the study indicated that DOTs are very satisfied with performance of jointless bridges. The only service life issue reported was the existence of cracking in the case of skewed bridges. The *Guide* provides extensive coverage of this issue and provides design recommendations. Factors affecting the performance of jointless bridges include

- Curvature;
- Skew;
- Bearings;
- Connection of superstructure and substructure; and
- Other conditions, including
  - Site conditions,
  - Deterioration of piling, and
  - Abutment wall type (i.e., reinforced concrete versus mechanically stabilized earth walls).

The *Guide* provides detailed discussion and recommendations to address each of the above factors.

New Concepts to Extend Applicability of Jointless Bridges

Flexible foundations are typically used for jointless bridges to reduce the induced forces and increase the length of jointless bridges (Burke, Jr. 2009). Deep foundations are widely used to support jointless bridges as they are relatively flexible and not prone to scour. The main criterion limiting the application of jointless bridges is the lateral displacement capacity of their supporting piles.

Flexible Pile Cap Connection

Research conducted revealed that providing a pin-type connection at the pile head can effectively reduce the stiffness and thereby lower the moments developed in the pile as a result of lateral movement, because the pile will deform in a single rather than a double curvature shape. Some researchers have studied different details to provide rotational capacity over the pile head. However, the reported details can only handle relatively small movements and in some cases require additional investigation. Within the SHRP 2 R19A project, a study was carried out and a new pin head detail was developed that provides significantly larger lateral displacement capabilities (Sherafati 2011; Sherafati and Azizinamini 2013). This new pin head pile detail consists of encasing the ends of the pile embedded in the pile cap beam with an elastomeric material, which, in turn, allows the pile head to act as a pin. The consequence is to have the pile bend in a single curvature, reduce the maximum moment in the pile, and move the location of maximum moment from the pile head end to within the length of the pile. The end result is allowing the pile to have larger lateral movement capabilities and consequently allowing use of larger bridge lengths in conjunction with jointless bridges. Details of this new pile head detail and corresponding design provisions are provided in Chapter 8 of the *Guide*.

A flexible pile cap connection can be used to reduce the stiffness of the piles to lateral displacement. In this case, the developed moments as a result of the pile head deflection are reduced, and eventually lateral displacement capacity can be increased.

To achieve a flexible pile cap connection, the embedded portion of the pile head in the stub cap beam can be encased in a soft material casing. This material will eventually be embedded in the concrete cap. This condition allows for relative rotation of the pile head with respect to the cap. A proposed detail is shown in Figure 3.43. An elastomer casing is used to allow for rotation. The end plate is welded to the end of the pile to reduce the stress concentration at the pile head, and another plate is embedded in the concrete cap, using shear studs, to spread the applied end load and prevent crushing of the concrete in the vicinity of the pile head. These two plates can slide freely against each other.

The main advantage of this detail is that it can increase the pile head lateral displacement capacity by reducing the stiffness of the system, which allows for construction of longer bridges using jointless bridge systems. Further, because of reduced lateral stiffness, smaller forces are developed in the cap, as well as in the superstructure. A prefabricated cap with circular holes can be constructed for accelerated construction, as shown in Figure 3.44. This will eliminate the need for forming and casting concrete for the cap, which results in considerable savings in construction time and cost.

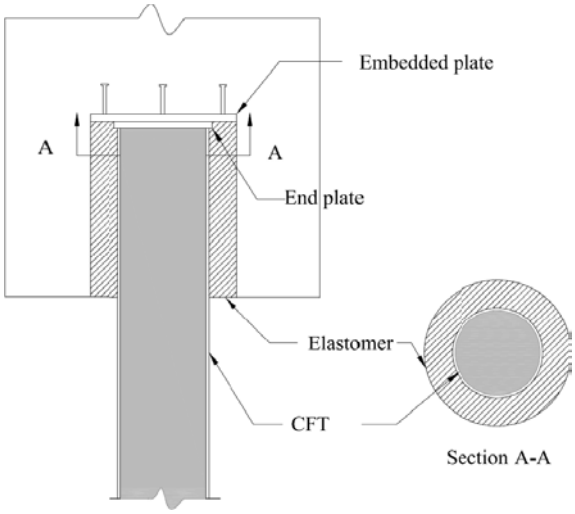

Figure 3.43. Proposed detail of flexible pile cap connection. CFT = concrete-filled tube.

Extension to Curved Girder Bridges

Another new concept is related to extending the application of the jointless bridge systems to the case of curved girder bridges. Detailed parametric studies were carried out to identify the factors that affect the performance of jointless curved girder bridges (Doust 2011; Doust and Azizinamini 2011a, 2011b). The study was confined to steel girder bridges. The *Guide* provides the design steps that should be considered when using jointless bridges for curved girder bridges.

Objectives

Results of the survey indicated that the design of jointless bridges is mainly based on trial and error and that there is a lack of scientifically based design provisions for jointless bridges. The objective of this study was to develop a comprehensive guideline for the design of jointless bridges in a format usable in design office.

Scope of Work

The scope of the work included a review of the available published and unpublished studies. Further tasks were carried out to extend the application of jointless bridges to longer bridges, as well as curved bridges.

An experimental study was carried out to comprehend the performance of the proposed detail. Using the results of experimental data and by conducting numerical and analytical studies, a design provision was then developed, which is reported elsewhere (Sherafati and Azizinamini 2013).

Experimental Program

Experimental studies were conducted on two pile cap connections. The objective of these tests was to comprehend the merits of the concept and develop suggestions for further investigation. The first specimen involved a relatively rigid connection and represented the current practice. The second specimen, however, consisted of the proposed connection detail and represented the flexible connection. The first test specimen (with rigid pile head) was used as a reference point to assess the merits of the proposed pile head detail.

The specimens were oriented horizontally during testing, such that the load representing the lateral movements of the bridge was applied using the two vertical actuators, as shown in Figure 3.45. The test specimens were positioned perpendicular to the loading frame and elevated using concrete blocks, posttensioned to the floor (see Figure 3.45). Axial load, simulating the gravity loads, was applied using Dywidag rods passed through a small-diameter plastic duct placed in the middle of the concrete-filled tube (CFT) specimens.

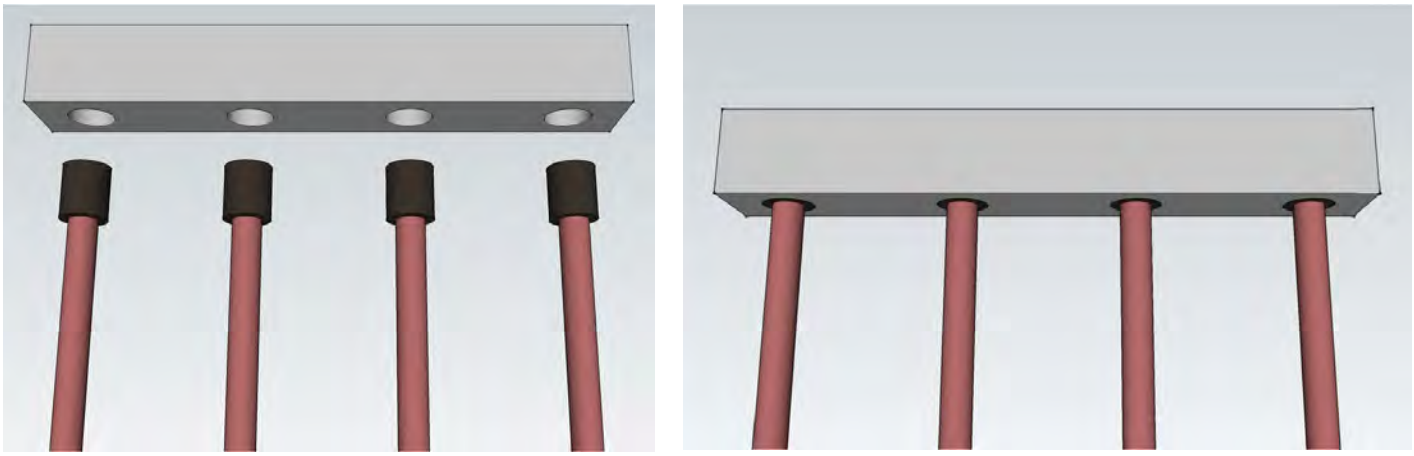

Figure 3.44. Prefabricated pile cap.

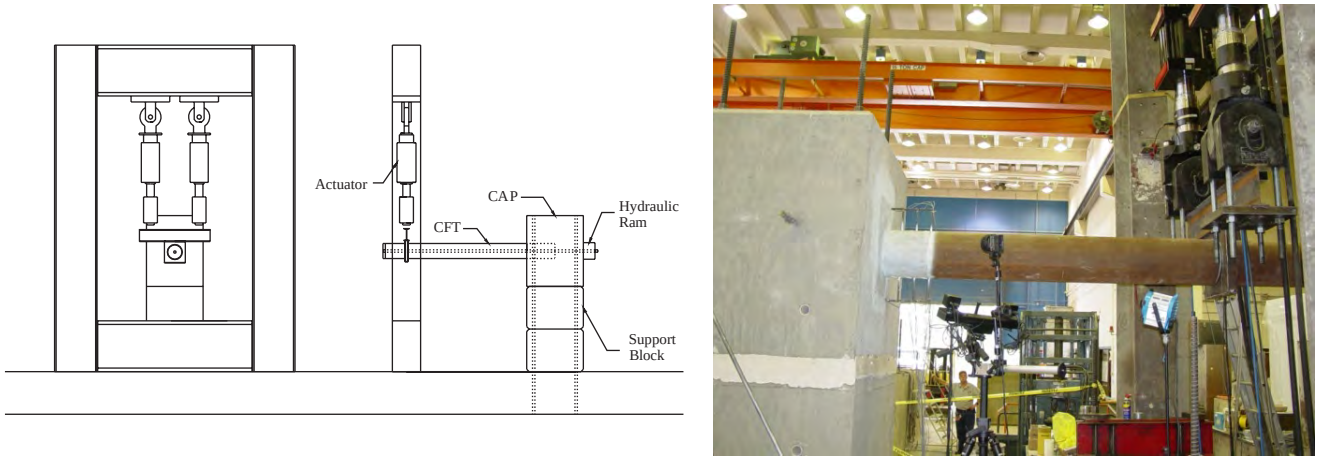

Figure 3.45. Test setup.

Results

Figure 3.46 shows the load–deflection curves for cycling of both specimens at increasing displacement levels obtained from the ultimate loading of Specimen 1 and the initial loading of Specimen 2. The displacement in these curves corresponds to the lateral displacement under the actuators. The apparent boldness of the line in Figure 3.46 is due to the fact that five individual cycles were performed, and the results overlie each other. This is true for all but the last set of cycles of Specimen 1, as noted in the figure, when fracture had occurred and was progressively growing with each cycle. Note that the nonlinearity in Specimen 1 started around a ±1.00-in. deflection, which corresponds to the point at which strain gauges indicated plastic straining close to the connection.

Specimen 2 displayed lower initial stiffness, which was the intent of the design. In this specimen the stiffness then dropped at a displacement of approximately ±2.0 in. of deflection. This change in stiffness was related to slippage of elastomeric casing with respect to the pipe surface. Although the curves appear somewhat similar, there are different underlying mechanisms that account for the behavior.

Envelopes of moment–rotation curves are presented in Figure 3.47a for both specimens. The moment is evaluated by multiplying the lateral load by its arm plus the second-order moments developed by the axial load due to the deflection of the pile. The rotation is calculated using the deflections recorded by the first row of potentiometers on the top and the bottom. These curves are then fit by bilinear curves for further analyses. The initial stiffness in Specimen 1 is almost four times the corresponding value in Specimen 2.

Using the results of moment–rotation analysis, the pile is modeled in SAP2000 by using beam elements. A nonlinear link element representing the rotational stiffness of the connection is assigned to one end. A 120-kip axial load is applied to the free end of the beam. The lateral load is then applied, and the corresponding displacement is extracted from the analysis.

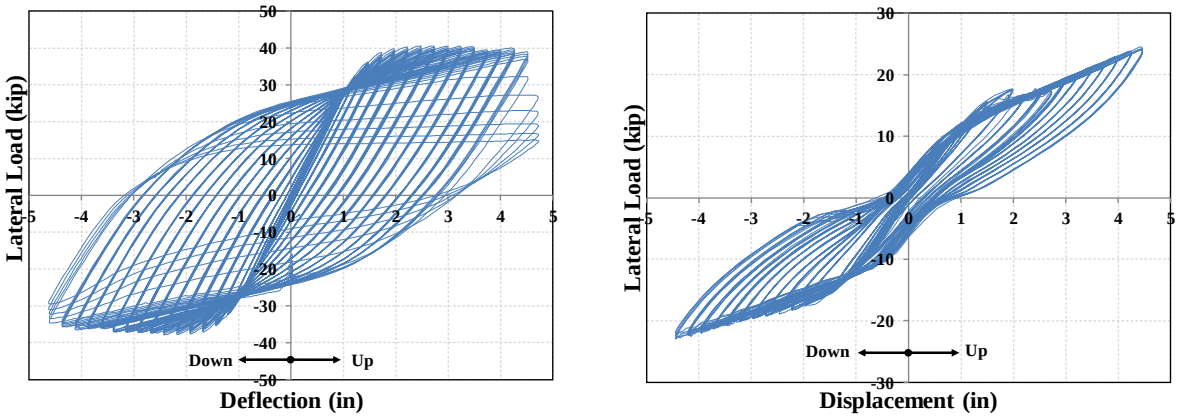

Figure 3.46. Load–deflection curves for (a) Specimen 1 and (b) Specimen 2.

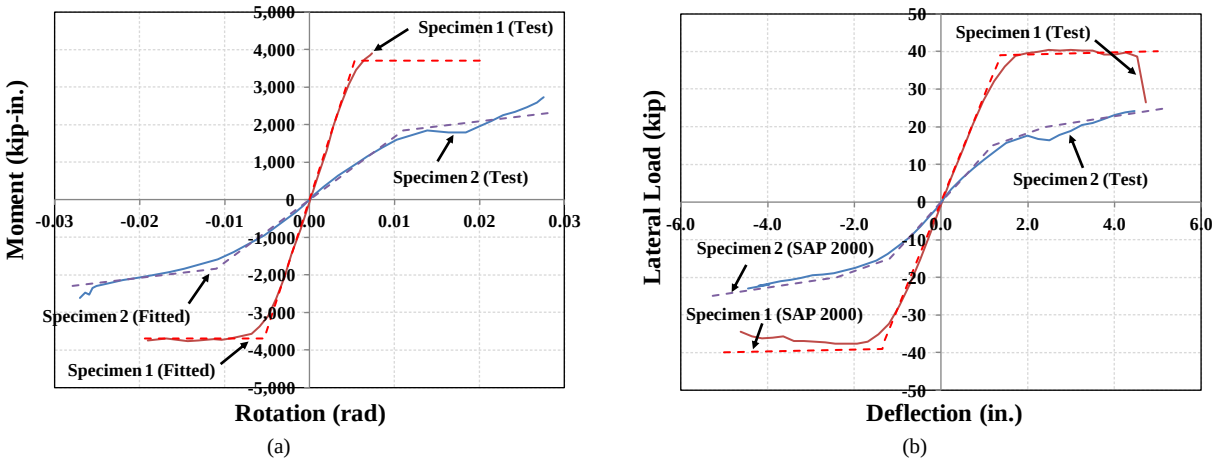

Figure 3.47. (a) Moment–rotation curves for specimens from the test and fitted bilinear curves, and (b) load–deflection curves from the test compared with the results of SAP2000 analysis.

Note that the $P - \Delta$ effect is also considered in the analysis. Figure 3.47b shows the load deflection results from the testing compared with the analysis results from SAP2000 using rotational springs representing the pile cap connection. As shown, the analysis results match well with the test results, validating the moment–rotation stiffness calculations.

The steel casing of the pile in the rigid connection began to yield at a displacement level of ±1.00 in. In the flexible connection, however, yielding was not present up to a displacement level of ±4.25 in., which is the displacement level at which lifetime cyclic testing was performed.

Both specimens were then subjected to a number of cycles that would be expected from a lifetime of service equal to 100 years. Unfortunately, the displacement level applied to the flexible connection was overly optimistic, and although the exposed elements showed no distress, failure occurred after 13,000 cycles. The failure appeared to be caused by localized issues at the embedded end of the column that can be easily mitigated through improved detailing.

Analytical investigations using the experimental results indicate that the flexible pile cap connection can increase the lateral displacement capacity of the piles by a factor of up to 3.8 in. for medium clay.

Conclusions and Recommendations

SHRP 2 R19A has developed detailed design, construction, and maintenance provisions for using jointless bridges. The complete summary of these provisions is provided in Chapter 8 of the *Guide.* The provisions allow, for the first time, design and use of jointless bridges without resorting to the trial-and-error approach currently practiced. The application of jointless bridges is extended to longer-length bridges by introducing a detail capable of making pile ends act like a pin compared with a fixed head. Further, design provisions are provided to extend the application of jointless bridges to the case of curved girder bridges. However, there is a need to carry out additional work, as outlined in the *Guide,* before applying the jointless bridge details to the case of curved girder bridges in practice.

Seamless Bridge Systems

Problem Statement

For current U.S. practice, integral abutment bridges represent the best approach to eliminate joints, which are a major contributor to the reduced service life of bridges. In the current system, shown in Figure 3.48, expansion devices are placed at the end of approach slab.

The level of maintenance required when expansion devices are placed at the end of the approach slab is significantly less than when expansion devices are placed over the abutment. Nevertheless, these expansion devices placed at the end of approach slab still need to be maintained.

Introduction

A seamless bridge system is presented that provides for bridges with long service lives by eliminating the joints over the bridge length, approach slab, and a segment of the roadway.

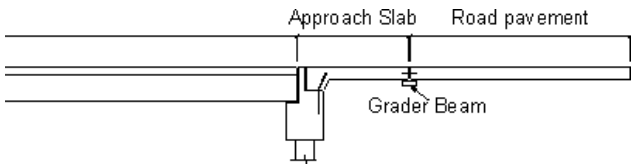

Figure 3.48. Schematic of the current U.S. practice for bridge–roadway interface.

The original idea of the seamless system was developed in Australia for use with continuously reinforced concrete pavements (CRCP) (Bridge et al. 2005). The proposed modifications have been made to the Australian system to adapt it to accommodate typical U.S. practice, in which most pavements are either jointed plain concrete or flexible pavement.

Description of Proposed System

In a seamless bridge expansion devices are eliminated entirely, even at the end of the approach slab, such that the bridge deck and pavement become continuous (seamless). The concept was first developed by Bridge et al. (2005) in Australia, has no joints at all, and was intended to be used with CRCP (Figure 3.49). In the case of CRCP, the transition region and CRCP are seamlessly connected. There is no movement where the transition region ends and the CRCP starts. However, there will be compressive forces (during bridge expansion) or tensile forces (during bridge contraction). In the case of CRCP, because the pavement is reinforced and continuous, the level of tensile and compressive forces that are generated can be tolerated. In the case of flexible or jointed pavement, at the end of transition region (see Figure 3.50), the level of forces generated must be near zero. Further, the movement must be small to eliminate any need for expansion devices (i.e., less than 0.25 in.). Therefore, all that is needed are dowel bars to achieve a smooth transition-zone roadway. In both the Australian and proposed systems, the transition zone is defined as the region between the bridge approach slab and the end joint (or a segment of the CRCP roadway in the Australian system). In the case of the Australian version of the system, all bridge movements are dissipated throughout the transition zone (via friction between the paving and base soil in the Australian system with CRCP). Both in the Australian and proposed versions, during bridge contraction, the opening and closing of microcracks in the transition zone contribute to a reduction in the end joint movements.

The advantages of the seamless bridge systems include low maintenance costs, longer service life, elimination of leakage of moisture to bridge elements below deck, improved ride quality, reduced noise, and elimination of grade beams at the end of approach slab. The seamless bridge system also provides a good mechanism for resisting the lateral loads in the pavement associated with skewed or curved girder bridges.

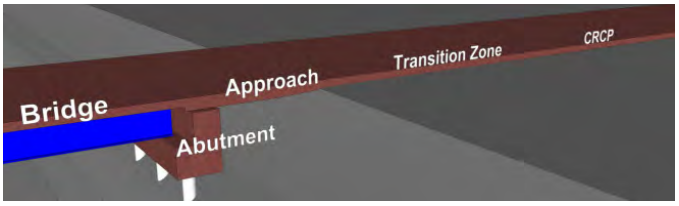

Figure 3.49. CRCP–bridge interface as developed in Australia.

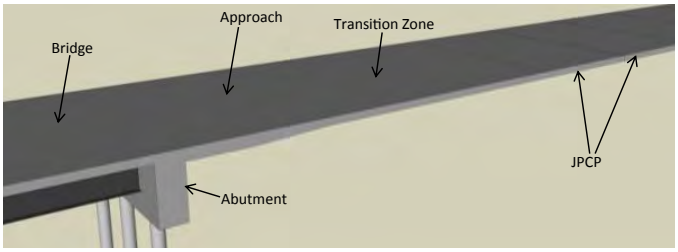

Figure 3.50. The seamless bridge concept for U.S. practice to be used with jointed plain concrete pavement (JPCP).

One of the best uses of seamless bridges could be in seismic applications because of the continuity between bridge deck and pavement. This continuity provides a good mechanism to resist the longitudinal forces generated during major seismic events.

Objectives

The objective of this research topic was to adapt the seamless bridge system, originally developed in Australia, for use in the United States. The original idea of the seamless system was developed in Australia for use with CRCP (Bridge et al. 2005). The specific objective therefore, was to modify the Australian system to accommodate jointed plain concrete or flexible pavement, which are the dominant pavement types used in the United States.

Scope of Work

The key factor in adapting the seamless bridge system to U.S. practice was to develop an appropriate transition system and associated design provisions. At the end of the transition region, the goal was to achieve minimal end movements. Further, within the transition region the goal was to achieve a predictable and controlled crack pattern and controlled axial forces.

The system that was developed to meet these needs is shown in Figure 3.51. The transition slab is connected to a secondary slab, which is embedded below grade. The two slabs are connected by a series of small piles. The secondary slab increases the stiffness of the transition region, resulting in the desired short transition length. A similar system, without the secondary slab, may lose its effectiveness after multiple cycles due to compaction of the soil surrounding the small piles. A combination of experimental, numerical, and analytical studies was carried out to develop the design provisions for the seamless system shown in Figure 3.51.

A special reinforcement reduction detail is used over the length of the transition zone to achieve a controlled crack

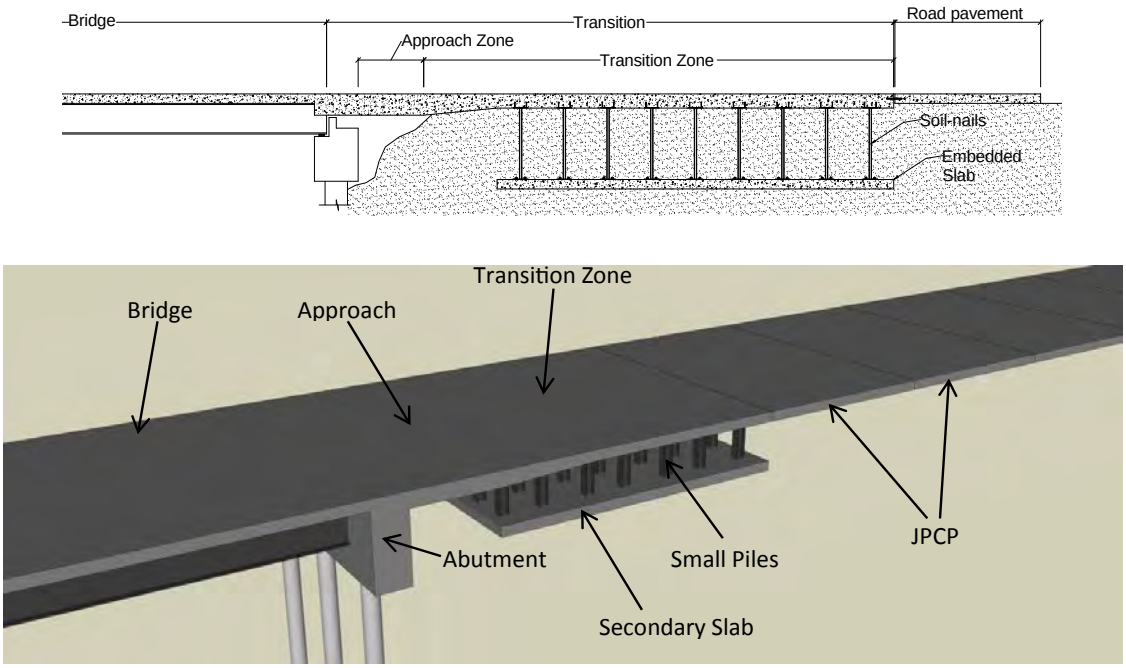

Figure 3.51. Schematic and rendering of the recommended practice for bridge–roadway interface.

pattern when the bridge system is in tension. The system behavior in tension (temperature reduction with bridge contraction) is an important factor because the crack pattern plays a major role in design life and maintenance costs. Figure 3.52 shows a transition in which the reinforcement detail helps to maintain the desirable crack pattern (Jung et al. 2007). The amount of reinforcement is reduced over the length of the transition region as the force is reduced.

Experimental Program

The experimental phase of the investigation consisted of constructing a segment of the newly developed transition system in the laboratory and subjecting it to cyclic horizontal loads, simulating the axial loads that would be developed in the transition region due to thermal loads. The experiment revealed the general behavior of the proposed system under cyclic loading and its effectiveness in reducing the bridge end-joint movements, the stiffness of the transition region, and its capability in effectively reducing the bridge movements at the end joint. In addition, the development of cracks, the behavior of the proposed small pile–concrete slab connection detail, and the effect of controlled density fill (CDF) on the transition behavior were investigated.

The test specimen represented a segment of the transition system for the prototype bridge. Based on the results of the parametric study (Ala and Azizinamini 2013a), short W10 × 49 piles spaced 4 ft longitudinally were used to connect the

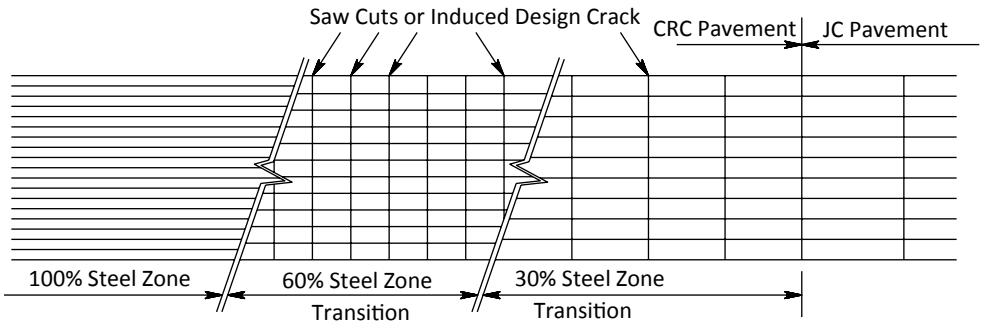

Figure 3.52. Gradual transition from continuously reinforced to jointed pavement.

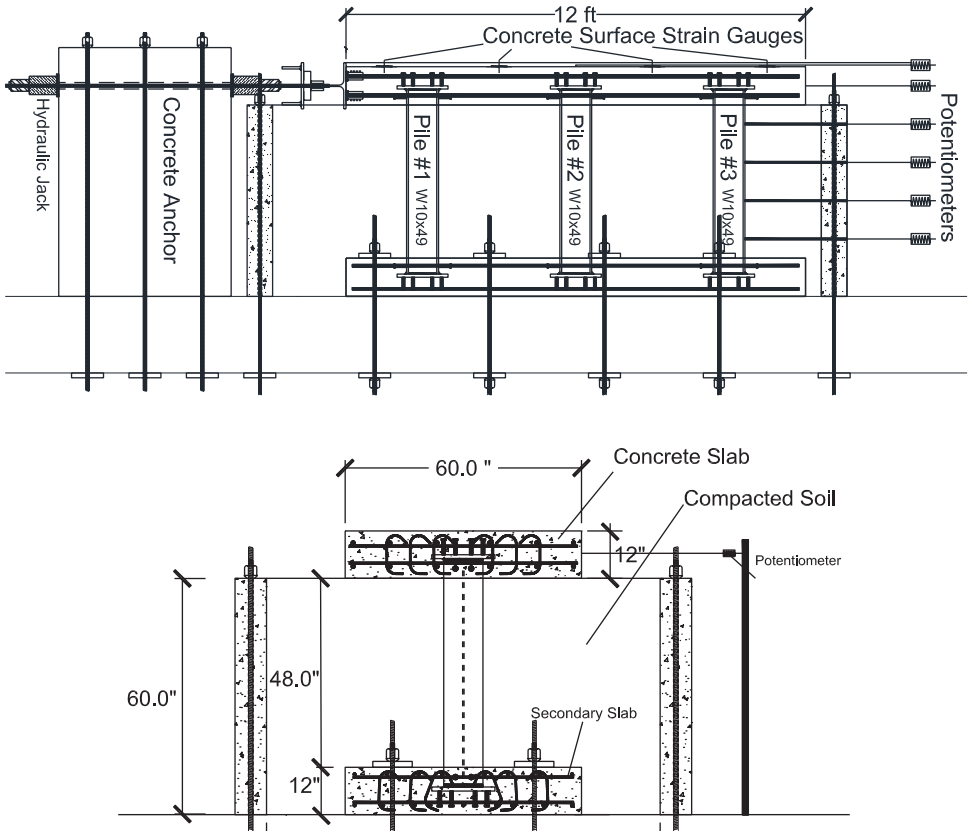

Figure 3.53. Schematic of the experiment.

top slab (transition region) to the bottom secondary slab. The secondary slab was installed at a depth of 4 ft below grade. The top and bottom slabs were each 12 ft long, 5 ft wide, and 12 in. thick. To simulate the effect of soil surrounding the piles, this system was constructed in a 15-ft-long, 9-ft-wide, and 5-ft-deep concrete container filled with CDF (compacted sand and gravel mix). A large concrete anchor block was built next to the concrete box that provided a reaction for the hydraulic actuators. Figure 3.53 shows schematically the different elements of the test setup. The lower, or secondary, slab was fixed against any movement by using posttensioning rods. The upper slab, representing the transition region, rested on the CDF. Loading consisted of moving this slab back and forth, horizontally, using the hydraulic ram, as shown in Figure 3.53.

One important design aspect of the proposed seamless system is the pile-to-slab connection design. Failure of the connection between the piles and slabs must be prevented. Further, the entire assembly should be user friendly during construction. The connection detail between the piles and slabs is shown in Figure 3.54. The connection consisted of a plate welded to the pile ends with shear studs.

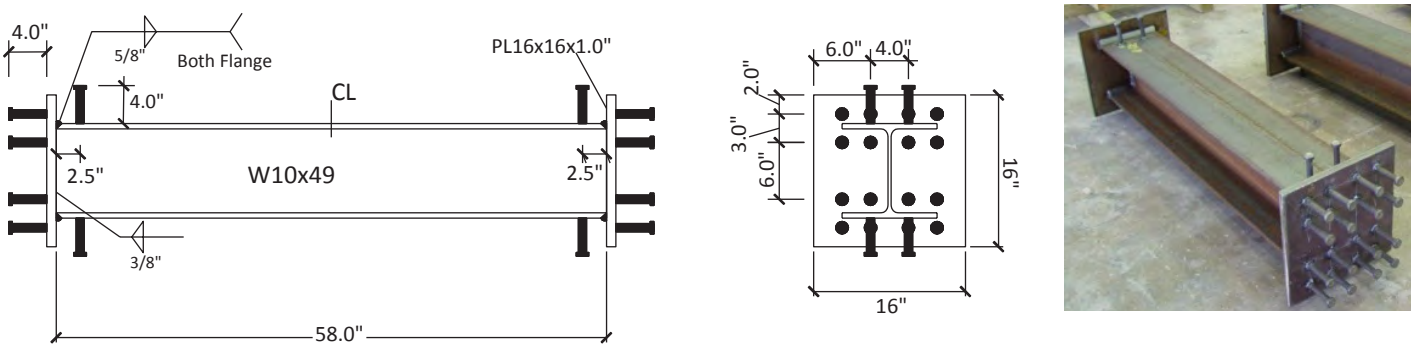

Figure 3.54. Small piles used in the test to connect the upper and lower slabs.

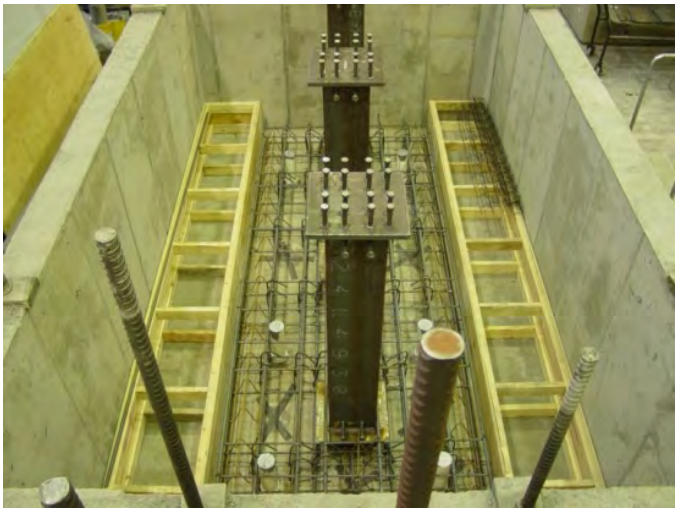

Figure 3.55. Concrete box, three small piles, concrete forms for the bottom slab, and the bottom slab reinforcement.

Figure 3.55 shows a photograph of the concrete box, reinforcement and forming of the bottom slab, and the three small piles.

The soil compaction procedure consisted of pouring and spreading the soil in the concrete box (in 4-in.-thick increments before the compaction), and then watering while compacting the soil using a vibratory plate or hand tamper (or both). Figure 3.56 shows the test specimen after the completion of placing compacted soil inside the concrete box. The length of piles extending beyond the compacted soil and to be embedded in the top slab was about 5 in.

The final step in construction of the test specimen consisted of placing the reinforcement for the top slab, as shown in Figure 3.57, and casting the top slab.

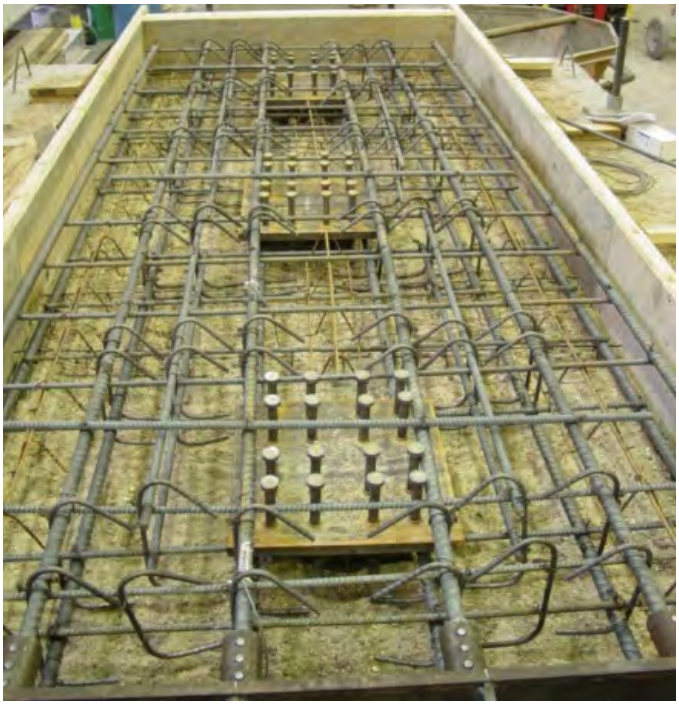

Figure 3.57. Reinforcement of the top slab.

Figure 3.58 shows the final test setup.

Displacement-controlled loading was used to move the top slab in a horizontal direction to simulate the thermal movements that are applied to a bridge transition slab from the bridge.

Results

After the test was concluded, the soil beneath the top slab was removed to observe the condition of the piles and their connections to the top and bottom slabs. Figure 3.59 through

Figure 3.56. The relative density of the compacted soil is measured using a nuclear density device.

(a)

(b)

Figure 3.58. Views of the final test setup: (a) west and (b) east.

Figure 3.61 show photographs of the piles and slabs after the conclusion of the test and following the removal of the soil in the concrete box. As shown in Figure 3.59, voids had developed on both sides of the piles in the vicinity of the connections. The widths of the voids were equal to the width of the piles and were about 5 in. deep. Development of such voids may necessitate designing the top slab for punching shear. This aspect of the problem needs additional research before the concept is used in practice.

The ideal connection between the piles and the top and bottom slabs is one that would perform elastically without

Figure 3.59. Compaction of CDF around a small pile.

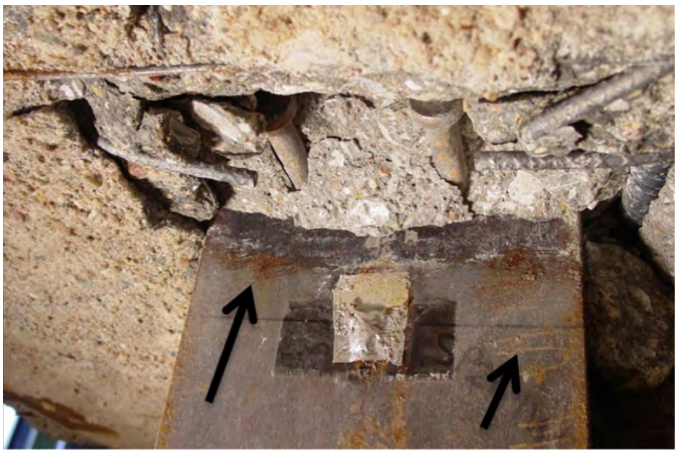

Figure 3.60. Failure of pile-to-slab connection.

Figure 3.61. Yield lines of the web on a small pile.

sustaining any level of damage. Test results indicated that the type of connection used was not capable of completely achieving this objective given the large displacements to which the specimen was subjected. The type of failure observed in the vicinity of the pile-to-slab connections is shown in Figure 3.60.

Inspection of the piles after conclusion of the test revealed formation of yield lines in the webs and flanges of the piles, as shown in Figure 3.61.

Figure 3.62 shows the resulting load–displacement hysteresis curves (positive values represent when the slab was pushed, and negative values represent when the slab was pulled). Figure 3.63 is the skeleton curve, constructed by connecting the apexes of the load–displacement curves at each applied displacement level. Two skeleton curves were constructed. One skeleton curve corresponded to the first cycle at each applied displacement level and another corresponded to the last (fifth) cycle at each applied displacement level.

The skeleton curve indicates that there is no abrupt failure point. Rather, the secant stiffness of the system decreases following a peak value. This behavior is related to gradual failure of the detail used to connect the pile to the slab.

Conclusions and Recommendations

Results of the experimental work, along with extensive numerical and analytical work carried out by Ala (2011) and Ala and Azizinamini (2013a, 2013b) resulted in the following major conclusions:

1. The proposed modification to the existing Australian system has promise for developing a completely jointless system for U.S. practice. Additional work needs to be carried out before the system is put into practice.
2. The type of connection detail used in this study to connect the small piles to the top and bottom slabs needs to be modified. The connection needs to be protected from any damage, and yielding and failure should happen outside the connection. This is similar to the concept used in earthquake design, in which some of the elements of the structure

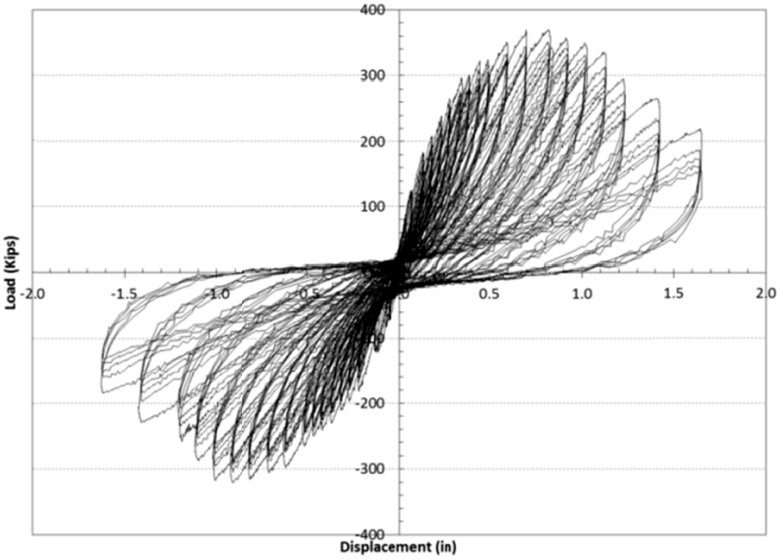

Figure 3.62. Hysteresis load–displacement curves of the test specimen.

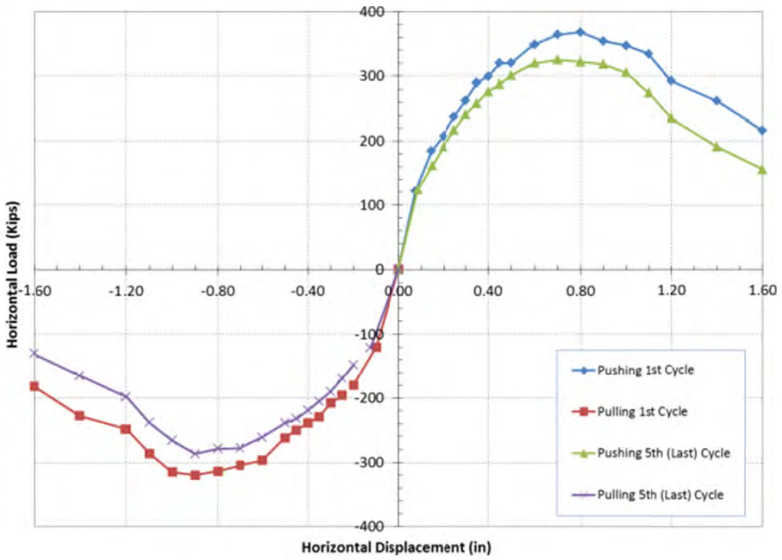

Figure 3.63. Skeleton curve of the hysteresis load–displacement curves.

are "protected" elements and must remain elastic during an entire seismic event.

Tentative Design Provisions

Based on the work carried out, there are two tentative design provisions for the proposed seamless system:

1. The initial design of the system is an iterative process in which the length of the transition and secondary slabs; the shape, size, and spacing of small piles; and the embedment depth of the secondary slab are determined through structural analyses of various system configurations. The initial design will also determine the demand in all components.
2. In the component design, various elements of the system will be designed according to the *LRFD Specifications*. The reduced cracked stiffness of the system in tension may be neglected during the initial design.

Relevant pavement design loadings are the longitudinal strains (thermal effects, creep, and shrinkage) and the out-of-plane effects (traffic, settlement of approach embankments, and rotation transferred from the bridge deck).

Structural Analysis

Structural analysis of the proposed seamless bridge should be carried out as a system analysis in which all bridge components, including the transition zone, are incorporated in the analysis model. Only the effect of uniform temperature change needs to be considered in initial design of the transition system. The calculation of uniform temperature changes should be in accordance with Article 3.12.2 of the *LRFD Specifications* (AASHTO 2010b). The soil–pile interaction can be modeled in the structural analysis by using linear springs. The linear spring stiffness depends on the relative density of the CDF surrounding the small piles and the confinement pressure. Because the CDF is manually compacted, its relative density should be measured during the compaction process, and this compaction should be related to the soil stiffness (Greimann et al. 1987). The connection of the small piles to the slabs can be assumed rigid for analysis.

The structural analyses should take into account the effects of longitudinal stiffness reduction due to development of tensile cracks in the transition slab (temperature reduction with bridge contraction). To do so, an iterative structural analysis of the system in conjunction with cracked section analyses is required. For the first iteration, the tensile forces in the structure can be assumed equal to the compressive forces due to thermal expansion. Cracked section analyses should be conducted for various segments of the transition slab, and the axial stiffness of the slab segments should be modified in each step. The structure is then analyzed using the modified in-plane stiffness to determine the updated in-plane tensile axial forces. This procedure will be repeated until convergence of the axial forces.

Design of Approach Slab and Bridge Deck

1. The resistance against thermal contraction due to the presence of a transition zone will create tensile forces and hence concrete cracking in the bridge deck, approach slab, and transition zone. Additional reinforcement may be required in these areas to control cracking and to achieve desired crack spacing and width.

2. The approach slab axial strength should be adequate to resist compressive thermal stresses to avoid crushing of concrete.
3. The approach slab should be designed for the differential settlement between the bridge abutment and the transition system. Embankment settlement is another important criterion to check for the approach slab. The bridge approach embankments should be designed to achieve a long-term settlement of less than 0.75 in. to minimize the impacts on the motorway pavement (Bridge et al. 2005). To account for the probable geotechnical and construction variations, however, a more conservative approach embankment settlement of 1.5 in. should be assumed for the seamless pavement design (Bridge et al. 2005). Bending analysis should be considered (Bridge et al. 2005).

Design of Transition Slab

1. The transition slab should be designed to avoid concrete crushing in compression and also to achieve a uniform cracking pattern in tension.
2. The transition slab should have adequate punching shear capacity against the design truck heavy wheels and adequate moment transfer capacity between the small piles and the slabs.
3. The thickness of the transition slab is determined from the punching shear requirements, connection to the small piles, and also to some extent the in-plane horizontal stiffness of the system to reduce the movement of the end joint.
4. Reinforcement of the transition slab should be determined from cracked section analysis under tensile in-plane forces.
5. The transition slab should be checked for the maximum bending moments between the rows of small piles.
6. The slab should be designed for two-way (punching shear) and one-way shear.

Design of Secondary Slab (Bottom Layer Slab)

1. The thickness of the secondary slab is governed by punching shear and connection to the small piles (the secondary slab thickness will most likely be equal to the top slab).
2. The secondary slab is designed for the bending moment and one-way shear exerted from the small piles to the slab.
3. The secondary slab should be controlled for the bending moment due to the soil pressure underneath.

Design of Small Piles Connecting Top and Bottom Slabs

1. The required stiffness of the small piles is determined in the initial design phase.
2. The small piles should be designed for the moment, shear, and maximum drift between the two top and bottom slabs.
3. The connection of the pile to the top and bottom slabs should remain elastic for maximum probable longitudinal movement.
4. The design of small piles should consider "overstrength" to prevent failure of connection. In the event that the strength of the pile is larger than the required strength by the designer, the piles should be able to achieve yielding before the failure of the connection.

Connection of Small Piles to Slabs

Figure 3.64 shows the type of connection detail used to connect the piles to the top and bottom slabs. Figure 3.65 shows a portion of the connection that will be embedded in the top and bottom slabs.

The connection should be capable of resisting cyclic loading at maximum probable longitudinal movement of the top slab relative to bottom slab without any damage. The experimental results showed that the detail used needs modifications and is not suitable for the proposed seamless system.

Design of Controlled Density Fill

Design of the CDF consists of selecting the geomaterial type and compaction requirement. The required compaction depends on the stiffness requirement around the small piles and prevention of settlement under the top slab. It is very important to achieve the required compaction around the small piles. Granular material is recommended for ease of

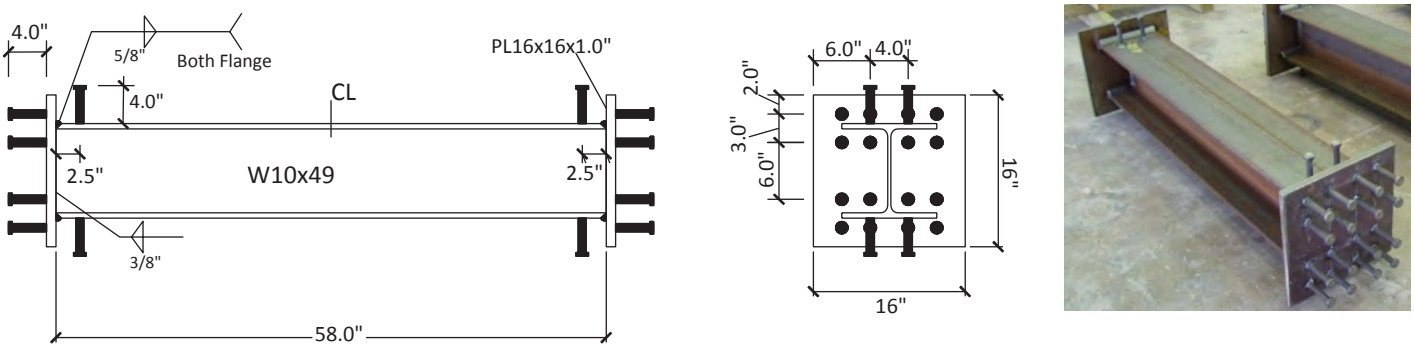

Figure 3.64. Small piles used in the test to connect the upper and lower slabs.

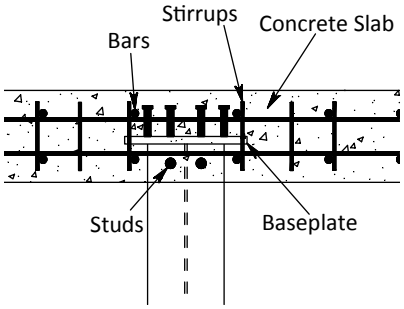

Figure 3.65. Recommended small pile–concrete slab connection.

compaction, low long-term settlement, and reduced potential for gap development around the piles caused by repeated pile movements.

The moisture–density relationship of the soil, maximum and minimum density (relative density) tests, and in-place moisture content and density determinations during placement of the backfill (using a nuclear density gauge) are the recommended soil mechanics tests.

Cracked Section Analysis

The ACI Committee 224 document, *Cracking of Concrete Members in Direct Tension,* provides methods of determining the maximum probable crack width and stiffness reduction for an axially tensioned concrete member (ACI 1997). The maximum probable crack width in a fully cracked member can be determined from Equation 3.1:

$$W_{\max} = 0.10 \times 10^{-3} f_s \sqrt[3]{d_c A} \tag{3.1}$$

where

d_c = distance from the center of the bar to the extreme tension fiber (in.),
f_s = service stress in the reinforcement (ksi), and
A = effective tension area of concrete surrounding the tension reinforcement, and having the same centroid as that reinforcement, divided by the number of bars (in.^{2}).

Once the allowable crack width is determined from Equation 3.1, the service stress–strain in the reinforcement can be determined.

The *LRFD Specifications* define an exposure factor (γ_e) that is 1.00 for a Class 1 exposure condition (crack width of 0.017 in.) and 0.75 for a Class 2 exposure condition. Areas for a Class 2 exposure condition include decks and substructures exposed to water. The crack width is directly proportional to γ_e, which can be adjusted directly to be 0.75 for a Class 2 exposure condition or an approximate crack width of 0.012 in.

The amount of required reinforcing steel (A_s) can be determined from the axial tensile force in the member ($P = f_s \times A_s$, and so $A_s = P/f_s$).

The direct tensile strength of the concrete is f'_t. The stress in the reinforcing bars after the crack occurs is determined from Equation 3.2:

$$f'_{s,cr} = f'_{tl}\left(\frac{1}{\rho} - 1 + n\right) \tag{3.2}$$

The axial load that causes first cracking in the axially tensioned member is given by Equation 3.3:

$$P_{cr} = f'_{s,cr} \times A_s \tag{3.3}$$

The average strain in the tensile member can be calculated from the CEB Model Code, as shown by Equation 3.4:

$$\varepsilon_m = \varepsilon_s \left[1 - k\left(\frac{f_{s,cr}}{f_s}\right)^2\right] \tag{3.4}$$

where $\varepsilon_s = f_s/E_s$, and k = 1.0 for first loading and 0.5 for repeated or sustained loading ($k = 0.5$ for this study).

The effective modulus of elasticity of steel bars is given by Equation 3.5:

$$E_{\text{sm}} = \frac{E_s}{\left[1 - k\left(\frac{f_{c,cr}}{f_s}\right)^2\right]} \tag{3.5}$$

Equation 3.5 is used to increase the stiffness of the reinforcements in the tensile member to compensate for the presence of some concrete after cracking. The effective axial cross-sectional stiffness of the tensile concrete member is $(EA)_{\text{eff}} = E_{\text{sm}}A_s$. The ratio $(EA)_{\text{eff}}/(EA)$ is the section modification factor that should be used in the structural analysis to modify the axial stiffness of the member in tension. Figure 3.66 shows the general flowchart for the cracked section analysis.

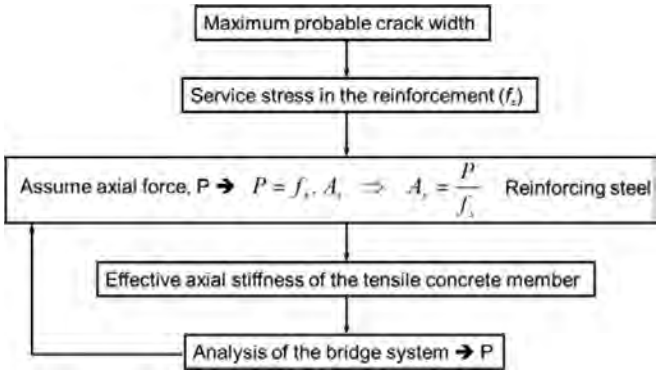

Figure 3.66. Cracked section analysis flowchart.

In conclusion, the combination of experimental, numerical, and analytical work conducted provided information to adapt the seamless bridge system to U.S. practice. Tentative details and design provisions are provided. It is recommended that the following scope of work be carried out to further develop the system:

1. Develop connection details for connecting top and bottom slabs. These connection details should be such that under maximum probable loading, the connection should remain completely elastic without sustaining any damage.
2. Carry out additional laboratory tests to further comprehend the behavior of the system using the new connection details.
3. Refine the tentative design provisions.
4. Conduct a field demonstration project.

Expansion Joints

Although the best option is to eliminate their use, expansion joints may still be needed when the total bridge length exceeds practical limits for jointless bridges. An evaluation of current practice regarding the use of expansion joints was carried out, and recommendations for the best practices were developed and summarized in Chapter 9 of the *Guide*. The following is a brief summary of information provided in the *Guide* for enhancing service life of expansion joints.

Introduction

Bridge elements are subjected to various loads, including traffic and environmental loads, which result in movement of bridge elements. One of the key factors affecting the service life of bridges is how to address thermal expansion and contraction of the bridge elements. This design issue is handled in two distinct ways. One option is to provide expansion joints at designated locations within the superstructure. By doing so, the designer forces all thermal deformation to take place at these discrete locations. The other option is to make the superstructure and deck continuous and assume that the thermal movement will be accommodated by the flexibility of the substructure, such as with the use of integral abutments. In such cases, the joint is usually moved away from the bridge abutment and placed near the end of the approach slab.

The following main issues should be considered when addressing the service life design of various expansion devices:

- Identification of appropriate design methodologies;
- Selection of durable expansion device types considering life-cycle costs;
- Specification of best practices for construction; and
- Development of an effective maintenance plan.

An ideal expansion joint should be able to (Lee 1994)

- Accommodate thermal expansion and contraction;
- Accommodate movement due to traffic-induced loads;
- Provide a smooth ride;
- Prevent the creation of hazards and safety issues;
- Accommodate needs during snow removal;
- Prevent leaking of moisture and other chemicals to elements below the superstructure;
- Have a long service life;
- Be maintenance free or require minimal maintenance; and
- Be cost-effective.

Advantages and disadvantages were identified for several typical expansion device types used in practice. The *Guide* provides a summary of these findings.

Expansion joint devices can be classified into three categories based on the maximum longitudinal movements. The categories and specific devices that were considered within each category are as follows:

- Expansion joints capable of accommodating small longitudinal movements (less than about 3 in.)
  - Compression seal,
  - Poured sealants,
  - Asphaltic plug joint,
  - Sheet seals,
  - Sliding plate joint, and
  - Open joints;
- Expansion joints capable of accommodating medium longitudinal movements (between 3 and 5 in.)
  - Strip seals;
- Expansion joints capable of accommodating large longitudinal movements (in excess of 5 in.)
  - Modular expansion joints, and
  - Finger-plate joints.

Factors and Considerations Influencing Expansion Joint Service Life

Factors that affect the service life of expansion joints were identified and summarized in the form of a fault tree. These summaries are provided in Chapter 9 of the *Guide*. Chapter 1 of the *Guide* includes a description of a fault tree.

Overall Strategies for Enhanced Expansion Joint Service Life

Providing bridge decks with enhanced service life requires a full understanding of the potential deterioration mechanisms. These mechanisms are associated with load-induced conditions, local environmental hazards, production-created

deficiencies, and lack of effective operational procedures. The study concluded that consideration of the following issues can lead to expansion joint devices with enhanced service life:

- Design methodology;
- Expansion joint system selection;
- Life-cycle cost analysis;
- Construction practice specifications;
- Maintenance plan; and
- Retrofit practices for expansion devices.

A detailed discussion of each topic is provided in Chapter 9 of the *Guide*.

Service Life Design Aids for Various Expansion Devices

Two types of tables were developed that can assist in comprehending the service life issues associated with various expansion joint devices and selecting the optimum device. These tables, which are referred to as technology and strategy tables, are briefly described below; additional details are provided in Chapter 9 of the *Guide*.

Technology Tables

Chapter 9 of the *Guide* provides technology tables for various expansion joint devices. These tables summarize service life and durability issues related to expansion joints and aid the design engineer in selecting the proper expansion device. The information could be used in several ways at the design or maintenance level. The purpose of these technology tables is to identify the most common types of service life problems encountered in commonly used expansion joints. This information can subsequently be used to provide possible solutions to service life problems encountered with expansion joints. An example of a technology table is given in Table 3.13.

Strategy Table for Expansion Joint Devices

A strategy table was developed to assist in selecting expansion joint devices. This table lists important parameters related to service life of expansion joint devices. Because of the lack of available quantitative data, qualitative information is provided for most categories in the strategy table, which is shown in Table 3.14.

Joints in Modular Systems: Adjacent Concrete Box Beams

This section summarizes the research topic that evaluated the performance of joints in adjacent box beam bridges, specifically with regard to the transverse connection between box elements. A complete report of this study is given in Appendix C.

Problem Statement

Precast adjacent box beams are commonly used for short- and medium-span bridges (typically 20 to 120 ft), especially on secondary roadways. These bridges consist of multiple precast box beams that are butted against each other to form the bridge deck and superstructure. Adjacent box beams are generally connected using partial- or full-depth grouted shear keys along the sides of each box. Transverse ties are typically used in addition to the grouted shear keys; these ties may vary from a limited number of threaded rods to several posttensioned tendons. In some cases, no additional wearing surface is applied to the structure, but in other cases, a noncomposite topping or a composite structural slab is added.

Bridges constructed using adjacent box beams have been in service for many years and have generally performed well. However, a recurring problem in noncomposite systems with bituminous wearing surfaces is cracking in the grouted joints between adjacent units, resulting in reflective longitudinal cracks in the wearing surface. The development of these cracks over the shear keys allows chloride-laden water to penetrate to the sides and bottom of the beams and cause corrosion of the nonprestressed and prestressed reinforcement. In addition, the load distribution among the beams is adversely affected, meaning the loaded beams are required to carry more load than originally intended. These conditions led to severe beam deterioration and actual midspan fracture and collapse of an exterior beam on a bridge in Pennsylvania.

There is a need to improve the transverse beam-to-beam connections in adjacent box beam systems to avoid these types of problems.

Objectives

The overall objective of this task was to improve the performance of adjacent box beam bridges, specifically with regard to the transverse connection. The specific objectives were to improve the structural capacity of this system in the transverse direction and to prevent longitudinal joint leakage. This was done by developing a detail that has the ability to transfer both moment and shear, instead of only shear, in the transverse direction.

Scope of Work

This study included the following tasks:

- Literature and industry practice review;
- Literature review;
- Posttensioned concept development;
- Testing program;
- Design recommendations; and
- Recommendations for further study.

Table 3.13. Bridge Joints Technology Table

Field Molded (or Field Formed) Joints
Range of Movement: Less than 1 in.
Expected Range of Service Life: 8–9 years

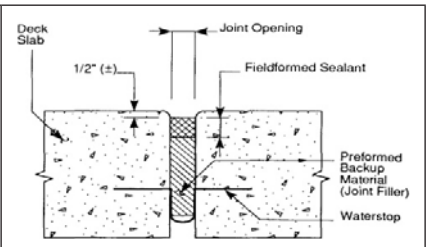

Service Life Problems	Solutions	Advantages	Disadvantages	System Preservation Requirements
Spalling and cracking of adjacent concrete	Deeper notch	Field molded joints are inexpensive and easy to install. They are best suited for single-span bridges with a maximum length of about 100 ft. This detail is an economical solution for simple-span bridges with spans of less than about 100 ft, especially in low-traffic areas where a few hours of interruption to traffic is not a major problem.	It requires maintenance and has a short service life. In most cases, it needs complete replacement every 2 to 3 years.	It requires regular 3-year inspection and replacement in most cases.
	Filling with silicone			
	Beveling edges of concrete			
	Placement of correct silicone thickness			
	Correctly mixing silicone material			
Installation problems	Training installation technicians			
	Providing detailed installation plans by the manufacturer or contractor. Having a representative of the joint supplier onsite during installation.			
Snowplow damage	Not allowing inferior quality of bonding agents			
	Installation slightly below the top of the deck elevation			
Debris accumulation	Inspection and cleaning regularly			
Water leakage	Draining water away from the joint			
	Insulation			
Hot-weather damage	Using high-quality silicone sealer			

Table 3.14. Strategy Table for Expansion Joints

Maximum Longitudinal Movements (in.)	Strategy	Potential Deterioration Mode	Options to Improve Service Life	Life-Cycle Cost		Difficulty Associated with Replacement	Performance Record	Expected Service Life (years)
				Initial	Maintenance			
<1 in.	Field-molded or other equivalent joint types	See technology tables	Provide second layer protection	Low	High	Low	Good	1 to 3
1 to 3 in.	Strip seal joints	See technology tables	Provide second layer protection	Medium	High	High	Very good	3 to 30
	Compression seal joint	See technology tables	Provide second layer protection	Medium	High	High	Very good	3 to 30
>4 in.	Finger-plate joints	See technology tables	See technology tables	High	High	High	Very good	10 to 50
	Modular expansion joints	See technology tables	See technology tables	Very high	Very high	Very high	Good	10 to 50

Results

Literature and Practice Review

A detailed literature review identified and evaluated various design and detailing practices for transverse connections in adjacent box girder bridges. Current practices were identified in Ontario, Canada; Japan; South Korea; and several states in the United States. There have been a variety of shear key details used along with various connection details using posttensioning ties or threaded rods. Most practices in the United States have used partial-depth shear keys, with threaded rod connectors at diaphragm locations.

In Japan, cast-in-place (CIP) concrete is placed in wide, full-depth joints between boxes, and posttensioning is applied through several ducts located at different elevations. All boxes are then covered with an asphalt concrete wearing surface. Longitudinal cracking and concrete deterioration have rarely been reported when this practice is used. In South Korea, the transverse connection between boxes is achieved by the use of a middepth shear key completely filled with CIP concrete, and heavy transverse posttensioning is applied, similar to the Japanese practice.

Research conducted by the West Virginia DOT on several bridges with joint fracture and longitudinal wearing surface cracking revealed that vertical shear failures in the keys were due to inadequate grout installation and inadequate transverse tie force. Consequently, the West Virginia DOT changed its practice to install posttensioned high-strength ties, use pourable epoxy instead of nonshrink grout in shear keys, and sandblast surfaces to be grouted to improve the bonding of shear key material.

In New York, two major changes were adopted in the state DOT's design standards to address longitudinal cracking: shear keys were increased to almost the full depth of the precast boxes, and the number of transverse tendons was increased to three for spans less than 50 ft and 5 ft for longer spans.

The Precast/Prestressed Concrete Institute subcommittee on adjacent member bridges conducted a survey on the current practices in the design and construction of adjacent box girder bridges in the United States and Canada. Most of the transportation agencies reporting had experienced premature reflective cracking in the wearing surfaces on bridges built in the late 1980s and early 1990s. These agencies emphasized the importance of eliminating these cracks, which allow the penetration of water and deicing chemicals leading to the corrosion of reinforcing steel in the sides and bottoms of the concrete boxes. The following preventive actions, among others, were recommended based on lessons learned in the last two decades:

- Use of a CIP deck on top of the adjacent boxes to prevent water leakage and to uniformly distribute the loads on adjacent boxes;
- Use of full-depth shear keys, due to their superior performance over the traditional top flange keys; and
- Use of transverse posttensioning to improve load distribution and minimize differential deflections among adjacent boxes.

Several nonposttensioned alternatives have been proposed to emulate monolithic construction and eliminate the problems associated with posttensioning and shear keys. In these alternatives, a reinforced concrete connection is used along the entire bridge length instead of the posttensioned diaphragms to transfer moment, shear, and torsion.

The Texas DOT developed a unique adjacent member system that eliminates the necessity of either grouting or posttensioning operations to connect adjacent girders. In this system, wide, nearly full-depth shear keys are filled with concrete while placing a reinforced CIP concrete overlay on top. The ordinary slab concrete is allowed to flow into the large shear keys provided by the I-shaped sides of the adjacent box girders.

Similar to the Texas DOT, the state of Illinois also adopted a new connection detail but with a narrower, more conventional shear key. However, they increased the required number of transverse ties to provide better performance of the shear key and assist the beams in working together. A 5-in. CIP concrete overlay was required to help distribute the loads uniformly across all beams and protect the shear keys against cracking.

Previous University of Nebraska–Lincoln Research

Previous research by the University of Nebraska–Lincoln (UNL) investigated the benefits of nonposttensioned systems and developed two new connection details referred to as the wide joint system and the narrow joint system.

The wide joint system has a similar beam and joint shape to the one just described from Texas, but differs in that the UNL concept eliminated the concrete overlay and the diaphragms. Top and bottom transverse reinforcement was used in a wide shear key filled with concrete to connect adjacent boxes instead of the reinforced concrete composite topping. This monolithic joint with top and bottom reinforcement provides a continuous connection that transfers shear and moment between boxes and eliminates the need for intermediate or end diaphragms. The elimination of the CIP topping and diaphragms would significantly speed production and construction operations and would reduce the material, labor, and erection costs. Shear keys used in the wide joint system are wide, full-length and full-depth, and require a slight modification to the AASHTO standard box cross section and consequently the forms.

The narrow joint system has a similar beam and joint shape to the one referred to above from Illinois, but differs in that it eliminated diaphragms and replaced the single middepth transverse tie with top and bottom transverse tie rods every

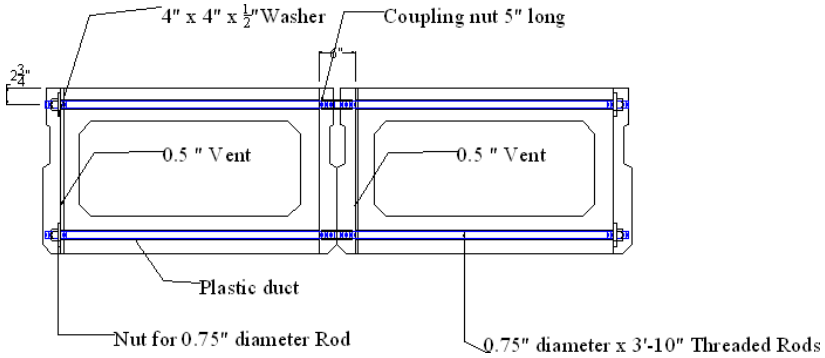

Figure 3.67. UNL narrow joint system with threaded rods.

8 ft to connect each pair of adjacent boxes at the top and bottom flanges (see Figure 3.67). These rods provide continuous connection that transfers shear and moment between adjacent boxes more efficiently than the middepth transverse ties at discrete diaphragm locations. A slight modification is made to the standard box cross section by developing full-length horizontal and full-depth vertical shear keys.

The wide joint and narrow joint specimens were tested using a similar loading scheme of 6.14 kips fatigue loading for 2,000,000 cycles followed by 18.4 kips fatigue loading for 5,000,000 cycles. The two connections had superior performance as there was no cracking or water leakage during testing. The two connections were also tested up to failure under static loading to determine their ultimate flexure and shear capacities. The two systems' capacities were significantly higher than that of current connections.

Posttensioned System Development

A modified version of the UNL narrow joint system was developed to allow for posttensioning with transverse high-strength steel rods. The system continues to eliminate the typical use of diaphragms and a concrete overlay for load distribution, which are details common to most adjacent box girder applications. The system maintains the use of top and bottom reinforcement; however, ducts have been moved inward so that posttensioning extends through the box beam voids (see Figure 3.68). This arrangement simplifies inspection of the posttensioning as it is now unbonded with the box section and shear keys. Construction time is reduced due to the elimination of grouted ducts, and venting is no longer an issue with girder production.

A duct-within-a-duct setup is proposed so that posttensioning can be applied after grouting of the shear key. The interior duct is necessary, as otherwise the duct would close during grouting, and posttensioning could not be threaded between adjacent members. Furthermore, posttensioning should be applied after the shear key is placed for the joints to be placed under initial compression.

To calculate the load effects on the proposed connection, a three-dimensional (3-D) computer model was developed

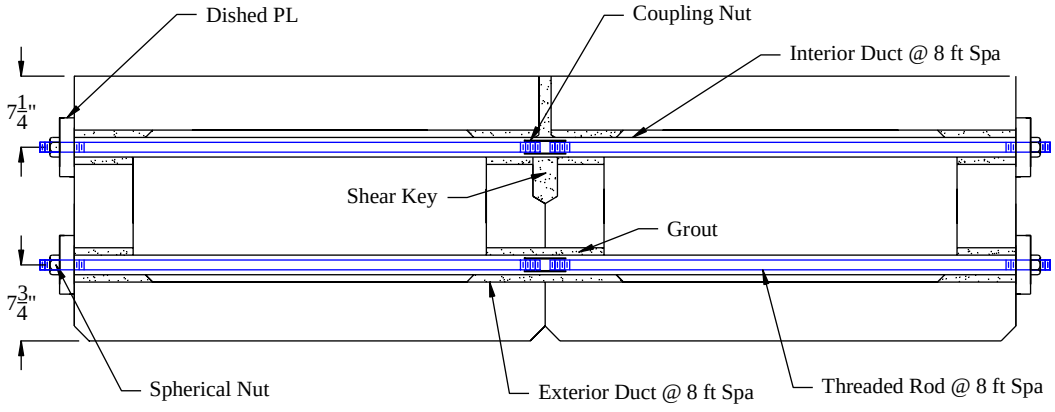

Figure 3.68. Posttensioned system concept.

using SAP2000 to replicate a simple-span adjacent box beam bridge and to conduct a parametric study to determine the effects of box girder depth, span width, and span-to-depth ratio.

The loads applied for analysis included the dead load of concrete curbs and railing and an HL-93 live load with a dynamic load allowance of 0.33. Single- and multiple-lane loadings were applied to determine the most critical loading case for the design of the transverse connection. Dead load due to self-weight and wearing surface was not considered as it is uniformly distributed over the bridge and, therefore, does not generate load effects in the transverse direction. The weight of the concrete curb and railing was assumed to be 0.48 kips/ft applied to the outside box girders. Design charts were developed for the posttensioned system based on the results of the 3-D model analysis. The effects of box girder depth, span width, and span-to-depth ratio were considered.

The effect of the box depth and bridge width on the tension force in the transverse connection for the posttensioned system is shown in Figure 3.69. This figure is developed for zero skew and a span-to-depth ratio of 30. The figure indicates that the tension force increases by increasing the bridge width and decreases by increasing box depth. Also, it can be noticed that the effect of bridge width on the required tension force is higher on narrow bridges (width less than 52 ft) than on wide bridges (width greater than 52 ft). Forces for this chart result from factored loads (1.25 DL [dead load] + 1.75 LL [live load]) and can be divided by the effective prestress of the posttensioning to determine the required area of reinforcement.

Figure 3.70 shows the effect of span-to-depth ratio and box depth on the transverse tension force in the posttensioned connection. This figure was developed for a bridge width of 52 ft and zero skew. The figure indicates that the higher the span-to-depth ratio is, the higher the required transverse tension force will be.

Experimental Program

An experimental program tested the performance of the post-tensioned system under fatigue and ultimate loading. A test specimen was designed using four 48-in.-wide by 27-in.-deep by 8-ft-long box beam elements positioned side by side and connected transversely by grouting and posttensioning. This created an overall specimen 16 ft long by 8 ft wide by 27 in. deep for testing. The length of the specimen consisted of the four box sections connected on each side.

Fatigue was represented by a 5,000,000 cyclic load applied to create tension in the top and bottom transverse ties (tested separately). The performance of the joint was evaluated by data collected from strain gauge, deflection, and leakage monitoring at the critical location of tensile stress along the transverse connection.

Two test frame setups were necessary to develop tension in both the top and bottom elements of the specimen. Top tension was deemed the critical case to test first, because it results in cracking at the top of the member where an actual girder is most susceptible to environmental corrosion. Cracks were monitored by leakage from a dam built around the middle joint, as well as white latex paint to aid with visibility. Beam supports for both cases were placed at stiff locations (i.e., at webs and joints).

To test for top tension, a support beam was placed under the middle joint and at one end of the specimen so that the

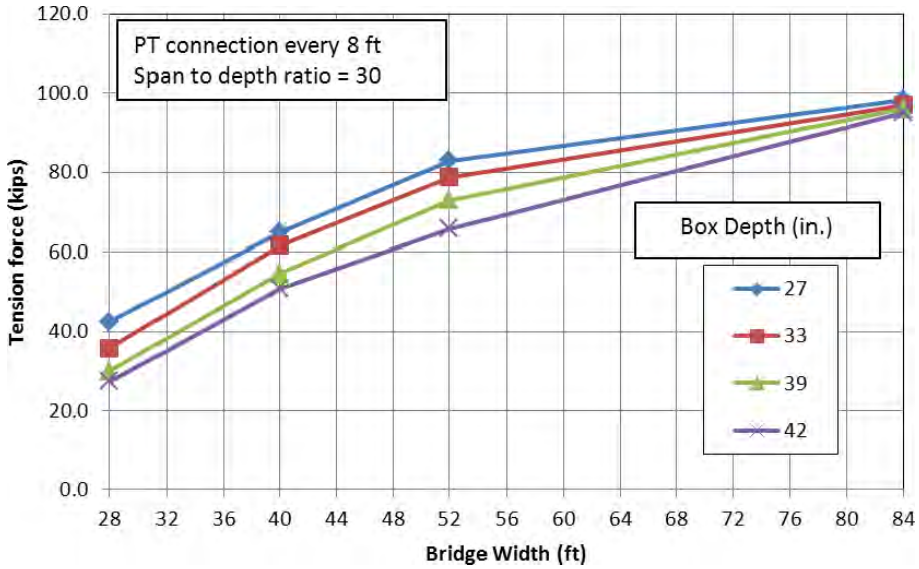

Figure 3.69. Effect of box depth and bridge width on the posttensioned system.

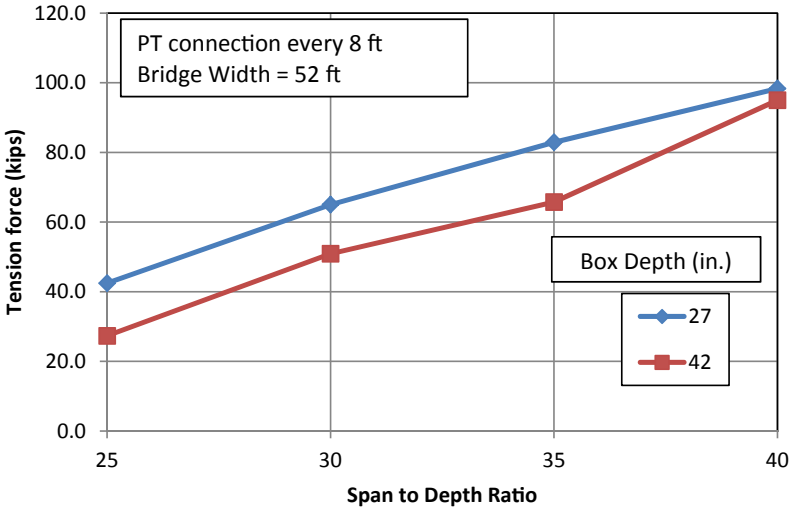

Figure 3.70. Effect of span-to-depth ratio and box depth on the posttensioned system.

opposite end was cantilevered. Thus, a load placed at the cantilevered end would cause tension in the top of the joint directly over the center support.

Testing for bottom tension in the middle joint was done by placing support beams at either end of the specimen with the load applied at the center. A neoprene bearing pad was placed between the specimen and the support beams to provide additional flexibility for the system.

Test Loading

The loads for testing were determined by applying the theory from the previously developed 3-D models of an adjacent box beam bridge system. First, a model was set up to determine the axial force produced by ultimate and fatigue loads in the transverse direction of a prototype bridge with a 64-ft span and thirteen 4-ft-wide by 27-in.-deep adjacent box beams, which totaled 52 feet in width. Bridge loads included an assumed curb and rail load equal to 0.48 kips/ft and 12-ft lanes with standard HL-93 design vehicular and fatigue truck loading. The weight of the structure is uniform and does not affect the transverse direction, thus it was not included in the design analysis. Curb and rail loads were applied to the exterior edge of the exterior box beams. Ultimate loading conditions included single and multiple lanes; fatigue conditions considered a single lane only. Single lanes were placed at the center of the bridge width to create maximum tension in the bottom flange of the box girders and at the edge to create maximum tension in the top flange.

The *LRFD Specifications* include a 33% dynamic load factor for ultimate analysis and a 15% dynamic load factor for fatigue analysis. Long-term effects were accounted for with an infinite life factor of 2 for fatigue. This results in load combinations of 1.25 DL + 1.75 LL for ultimate and 1.25 DL + (0.75)(2) LL for fatigue.

Testing

The top tension test consisted of applying an 18.4-kip load for 5,000,000 cycles at the cantilevered exterior joint of the four-box specimen with supports at the center and opposite edge. Ponded water over the joint was used to monitor joint integrity. Strain gauges were placed next to the load and on either side of the center joint. No joint cracking occurred during the course of the experiment. Supports were then rearranged to both ends of the member, and the load was repositioned to the center joint for tension in the bottom flange. A 17.4-kip load was applied for 5,000,000 cycles, and again no joint cracking occurred.

For ultimate capacity testing, the test setup for bottom tension was used. Ultimate moment capacity was calculated as 280 kip-ft using strain compatibility and was found to be slightly higher during testing. An applied load of 67 kips, in addition to the self-weight of the specimen, reached 300 kip-ft before failure. Cracking did not propagate until reaching a 60-kip total load, and then deflection increased exponentially from 0.1 to 3.31 in. over the next 30 kips applied.

Design Provisions

A method was outlined for determining the required post-tensioning force using Figure 3.70, based on the bridge width and box depth for a given span-to-depth ratio. An example is provided in Appendix C. A construction sequence was also developed for placing adjacent box beams and post-tensioning.

Conclusions and Recommendations

The general objective of this study was to improve the performance of transverse connections currently used in adjacent box girder bridge applications. This was done by developing

a detail capable of transferring moment and shear in the transverse direction. UNL combined the efforts of this research with a previous study at the University of Nebraska–Omaha campus in which intermediate and end diaphragms and a concrete overlay were proven unnecessary for adequate load distribution in the transverse direction of nonposttensioned adjacent box girder connections. The benefits of this system, as well as the modified system that allows for posttensioning, include significantly simplifying box production, improving the rate of construction, easier inspection of voids, and reduced project costs.

It was found that posttensioning also increases the capacity and efficiency of the section because joints are placed under compression and are less likely to experience reflective cracking and leakage.

Based on test results, it can be concluded that a posttensioned transverse connection without diaphragms or concrete overlay can be designed and detailed to have comparable performance to typical connections while being more economical and practical. The tested specimen had excellent performance under both static and cyclic loads.

It is proposed that the transverse, posttensioned connection developed in pursuit of this research be applied in a full-scale application for observation of the joint performance under actual weathering and loading conditions.

Joints in Modular Systems: Closure Pour Details

Problem Statement

The rebar detail used in the closure region between adjacent slabs has been investigated in the past. This study concentrated on the development of an alternative detail, which is discussed in this section. The proposed detail costs less than a headed bar detail, which is commonly used.

Objectives

The work carried out under this topic is a good example of what is meant by proof of concept testing. The main objective of this study was to show that rebar in the closure region of modular bridge systems having a precast girder–slab can be developed by 90° hooks. Limited experimental work was carried out. Results demonstrated the feasibility of the concept; however, additional work will be needed before the detail is used in practice.

Scope of Work

Six specimens containing closure regions and using various details were subjected to both positive and negative moment loading to investigate their behavior and failure modes under ultimate load.

Experimental Program

Figure 3.71 shows a portion of the deck the test specimens were intended to represent. The test specimen modeled an 8-ft-wide and 3.5-ft-long portion of a modular bridge system having a precast slab, as shown in Figure 3.71. Six specimens were constructed to investigate the closure region behavior: two specimens had straight bars without a closure region and were used as control specimens, and the other four specimens contained a closure region between adjacent slabs that was used to analyze different rebar details.

The total width of the closure region for the slabs was 12 in.; the rebar positioning was staggered to avoid constructability issues. The slabs were cast in two stages, the first stage being a 6.5-in. pour of only the outside regions, leaving an open space between them. One month later, the second stage was cast, which included the closure regions and a 2-in. topping over the previously cast regions.

Table 3.15 provides important dimensions and aspects of each specimen.

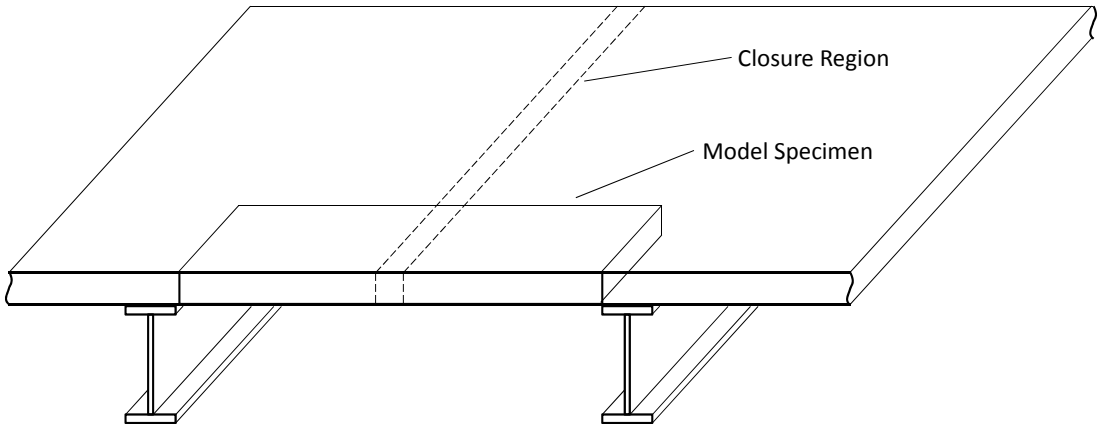

Figure 3.71. Slab section from adjacent slabs.

Table 3.15. Slab Specimen Summary

Specimen	Closure Region (Yes/No)	Rebar Type	Moment Applied	Concrete Cover at Tension Face (in.)	Concrete Cover at Compression Face (in.)
S_N	No	Straight	Negative	3.0	1.5
S_P	No	Straight	Positive	1.5	3.0
HD_N	Yes	Headed	Negative	3.0	1.5
HD_P	Yes	Headed	Positive	1.5	3.0
H_N	Yes	Hooked	Negative	3.0	1.5
H_P	Yes	Hooked	Positive	1.5	3.0

Two slab specimens were built as a control group. These slabs did not have the closure region and used straight rebar as would typically be used in bridge construction.

Two test specimens using a headed bar were formed. The heads at the end of the rebar come in multiple shapes and sizes. Tests performed by the Headed Reinforcement Corporation (HRC) showed that the circular heads provided better connection to the rebar and had a higher ultimate strength than the rectangular heads. Therefore Type 220, No. 4– and No. 5–headed bars were used in the current testing program. Details of the headed bars are given in the HRC200 specification (HRC 2011). Confinement reinforcement was used on both faces of the slab to prevent the vertical punch-out of any of the headed bars in the closure area. Figure 3.72b shows the construction details for the headed bar connection.

The final two specimens were formed using hooked bars. Hooked bars may be obtained from any local steel fabricator,

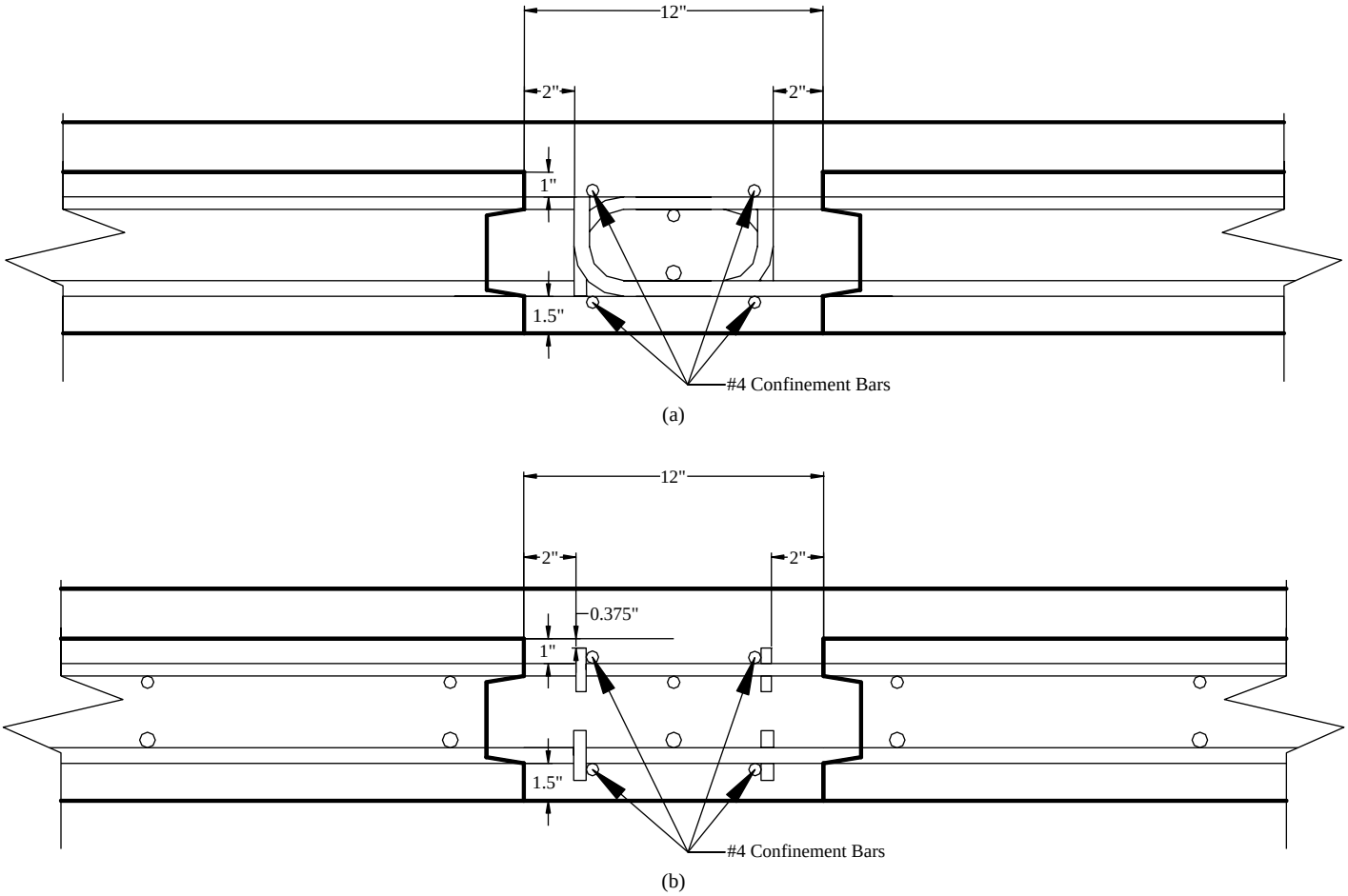

Figure 3.72. (a) Hooked and (b) headed construction details.

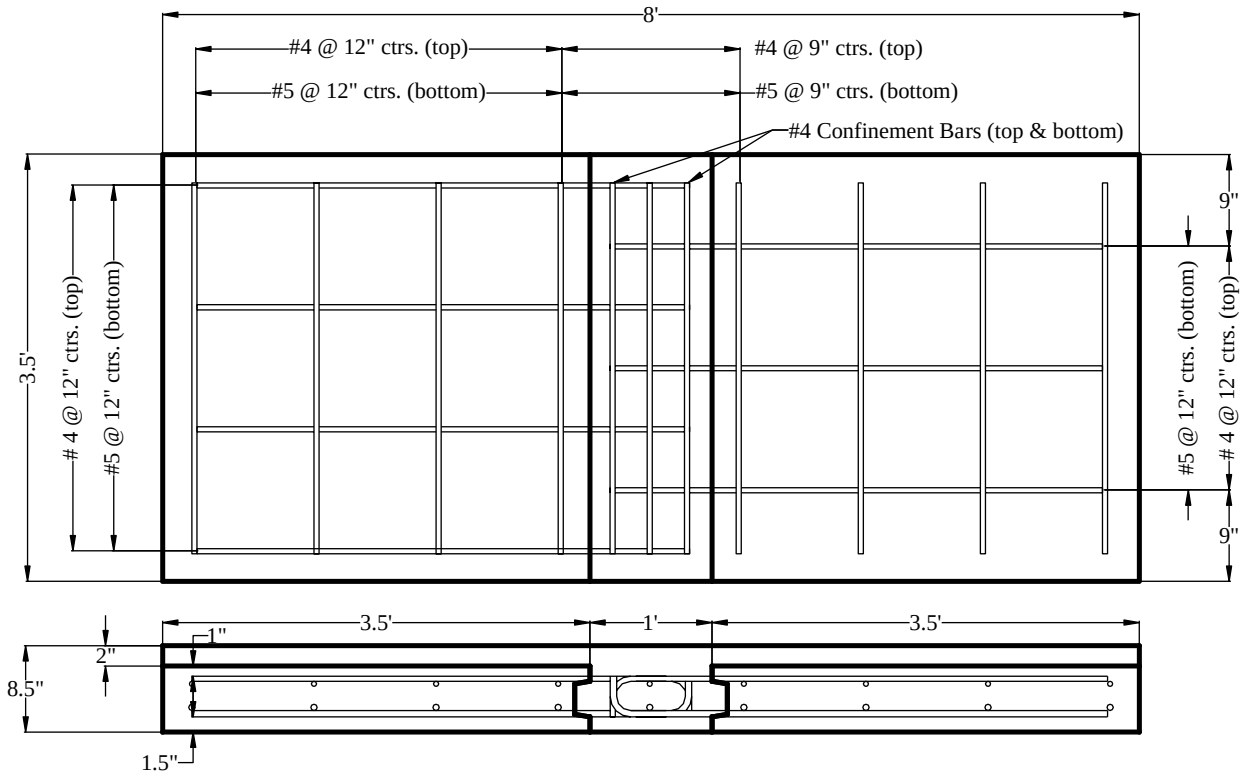

Figure 3.73. Hooked bar construction details.

greatly reducing the time and cost of fabrication and shipment to the work site. The hooked bar also provides greater clearance on both faces compared with the headed end detail. As with the headed rebar, confinement bars were used on both faces of the slab. Figure 3.72a shows the construction details for the hooked bar connection. Additional information and the reinforcement plan for the hooked bar construction can be seen in Figure 3.73. The bend diameter for the hooks was two in.

Photographs of the headed and hooked specimens before casting the closure region are shown in Figure 3.74.

Results

Negative Moment Bending

Deflections were found to be consistent across the width of the slab. However, the end with three bars consistently

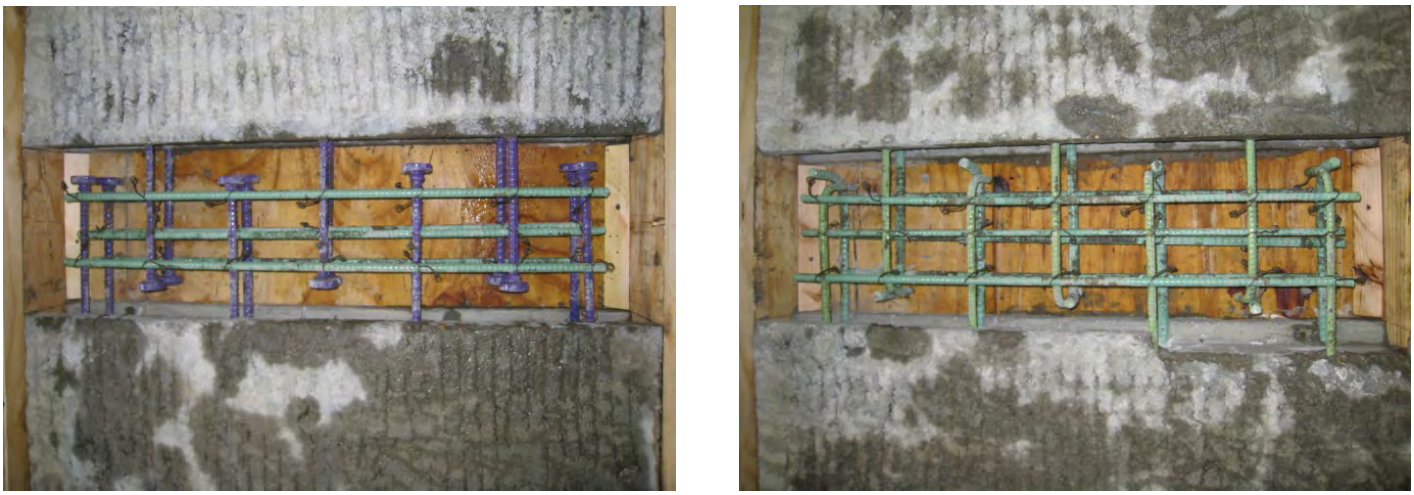

(a) (b)

Figure 3.74. (a) Headed and (b) hooked specimens before closure region casting.

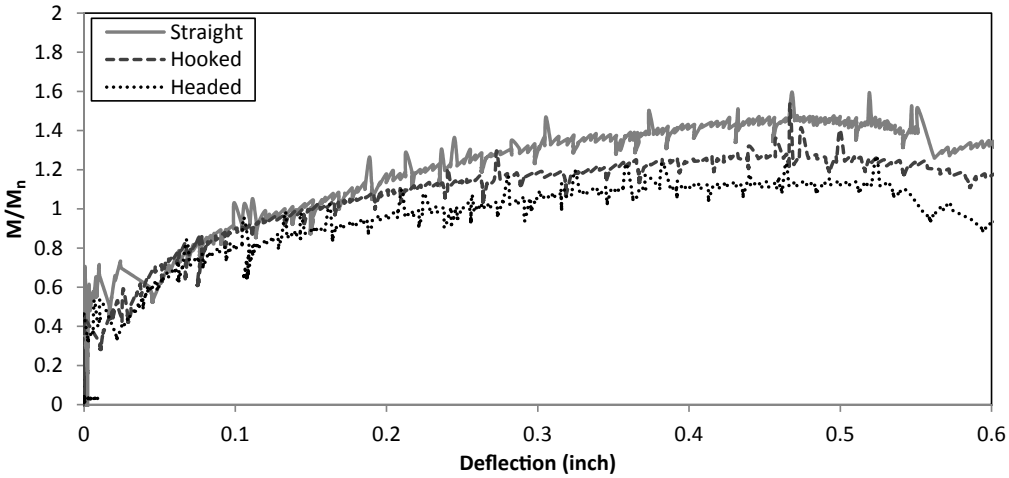

Figure 3.75. Moment versus deflection for the center location (Pot 5) of specimens in negative bending.

experienced slightly higher deflections than the other side with four bars, for both the hooked and headed bar specimens. The moment–deflection relationship at the center location of the specimens for each of the three specimens tested in negative bending is shown in Figure 3.75. The following observations were made from Figure 3.75:

- All the specimens tested in negative bending showed a similar moment–deflection relationship. The small difference in moment–deflection behavior of the different specimens can be partly attributed to differences in material strengths.
- All the specimens show sufficient ductility to give a warning before failure and thereby follow the design philosophy of preventing a brittle mode of failure.
- Hooked rebars, which cost much less and are easier to construct than headed rebars, show behavior similar to headed bars in terms of both strength and ductility.

Positive Moment Bending

The bending behavior of the specimens under positive moment was similar to the bending behavior of the specimens under negative moment. The moment–deflection relationship at the center location of the specimen for each of the three specimens tested in positive bending is shown in Figure 3.76. The following observations were noted from Figure 3.76:

- All the specimens tested in positive bending show a similar moment–deflection relationship. The observed differences

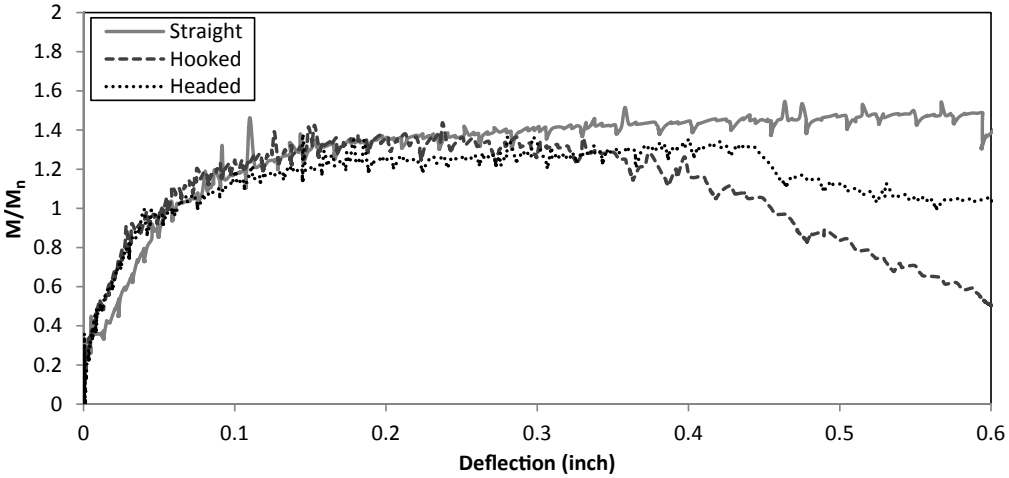

Figure 3.76. Moment versus deflection for the center location (Pot 5) of the specimens in positive bending.

in moment–deflection curves between different specimens for the positive section are smaller than the differences observed for the negative section.
- All the specimens show sufficient ductility to give a warning before failure and thereby follow the design philosophy of preventing a brittle mode of failure.
- The results obtained from hooked rebars, which cost much less and are easier to construct than headed rebars, match well with the results obtained with straight rebar, which indicates the capability of the hooked detail to develop the reinforcement in the closure pour regions.

The ultimate moment capacity M_u of the, along with the ratio M_u/M_n, is shown in Table 3.16. In positive bending, the straight bar specimen and headed bar specimen have the same M_u; however, M_n for the headed bars specimen is higher than the straight bars specimen due to higher f_y reinforcement used in the headed bar specimens. Therefore, M_u/M_n for the headed bar specimen is lower than M_u/M_n of the straight bar specimen. M_u/M_n of the hooked bar specimen is almost the same as the headed bar specimen in positive bending.

For negative bending, the headed bar specimen has the lowest value of M_u and M_u/M_n ratio. The straight bar specimen has the highest value of M_u and M_u/M_n ratio in negative bending. The hooked bar specimen lies in between the two extremes for the case of negative bending (see Table 3.16).

Test results have shown that the longitudinal connection with a hooked bar detail provides adequate flexural capacity and ductility ratio. In addition, a similar cracking pattern was observed in the specimens detailed with hooked bars and headed bars.

Conclusions and Recommendations

Limited experimental work was carried out to evaluate the merits of using a hooked bar detail in the closure pour region versus a headed bar detail. Although the headed bars provide sufficient strength and ductility when subjected to both positive and negative moment, the small cover between the heads of the bars is often a concern to bridge owners because of the potential for development of corrosion. The headed bars are also expensive and not readily available.

The hooked bars were also found to provide adequate strength and ductility for both positive and negative moment. The main advantages of the hooked bar detail are cost and uniform cover over the reinforcement.

Table 3.16. Ultimate Strength of the Specimens

Specimen	Positive Bending			Negative Bending		
	M_u	M_n	M_u/M_n	M_u	M_n	M_u/M_n
Straight	705	478	1.47	398	274	1.45
Headed	705	539	1.31	338	300	1.13
Hooked	642	478	1.34	350	274	1.28

Note: Ultimate strength = kips-in.

High-Performing Sliding Surfaces for Bridge Bearings

This section summarizes the research topic that evaluated the use of high-performing sliding surfaces for bridge bearings that would increase service life through greater wear resistance. A complete report of this study is given in Appendix D. At the time of writing, results of this research have been submitted for publication (Ala et al. 2013a, 2013b).

Problem Statement

Selecting the optimum bearing type depends on the load, movement requirements, and economics. Steel-reinforced elastomeric (SRE) bearings have shown very good performance over the past 40 years due to their low cost and relatively long service life. As a result, SRE bearings are used extensively. However, with certain combinations of load and movement, the capacity of the SRE pad to accommodate the required translation through shear deformation can be exceeded. In these cases, additional movement capacity must be provided by the use of sliding surfaces. All other types of bearings—including cotton duck pads and high-load multirotational pot, disc, and spherical bearings—use sliding surfaces to accommodate expansion requirements.

Currently, polytetrafluorethylene (PTFE) is the material used for sliding surfaces in the United States. PTFE has low frictional characteristics, chemical inertness, and resistance to weathering and water absorption that make it an attractive material for bridge-bearing applications. However, plain PTFE wears under certain service conditions, particularly when subjected to combinations of high contact pressure, high rates of movement, and low temperatures. Fast sliding speeds, especially those associated with traffic movements, have been shown to be much more critical for PTFE wear than slow movements due to temperature. Therefore, wear of the PTFE sliding surface is one of the critical factors affecting the service life of these types of bearings. For improved service life, there is a need to consider other higher-performing sliding materials.

Minimal data exist to develop a life prediction model for sliding surfaces. Designers need to have the capability of predicting the expected service life of sliding surfaces for maintenance and replacement purposes.

Objectives

The main objectives of this study were to determine (1) the feasibility of achieving increased service life of sliding bearings that use PTFE through the use of alternative high-performing sliding materials that have greater wear resistance and (2) whether a life prediction model was feasible for PTFE and other higher-performance sliding surfaces.

Scope of Work

The scope of this research included analytical studies followed by the design, fabrication, and implementation of a limited experimental program to evaluate sliding surfaces used for bridge bearings. The experimental program tested small-scale specimens aimed at comparing the life of sliding materials commonly used in bridge structures against certain alternative high-performance sliding materials. Performance characteristics such as coefficient of friction (COF), rate of wear, and total wear over a specified number of movement cycles were measured and compared.

The study was developed to compare performance and wear of alternative high-performance sliding surfaces with conventional PTFE sliding surfaces over a range of bearing pressures, cycles of movement, and total cumulative travel distances.

Discussions were held with various industry representatives to identify potential materials for consideration. Materials were selected for testing that would be available for bearing manufacturers to use in normal practice.

The following three sliding materials were tested and compared in this study:

1. PTFE (plain, unreinforced) is the sliding material most commonly used in current bridge practice. PTFE was tested in dry and lubricated states and was used as a baseline to compare other materials.
2. MSM (Maurer sliding material) is an example of an innovative sliding material developed as a higher-performing substitute for current PTFE-based material. It is an ultrahigh-molecular-weight polyethylene developed by Maurer Söhne in Germany for use in high-speed rail bridges that experience fast rates of movement at expansion bearings. Recent field applications and experimental testing have shown very satisfactory results in Europe. Because these promising materials are new, no long-term data are available. However, the qualitative service life could be evaluated by conducting cyclic wear testing. MSM was tested in dry and lubricated states for comparison with PTFE.
3. Fluorogold is an example of a reinforced PTFE-based material that was developed by Seismic Energy Products as a higher-performance material for sliding bridge bearings. It is an engineered product composed of virgin PTFE and special glass fiber reinforcing agents that improve wear. Again, the qualitative service life could be evaluated by conducting cyclic wear testing. Fluorogold was tested in only the dry state.

The study also evaluated the feasibility of developing life prediction models for sliding materials based on the results of this testing and previous research.

Analytical studies were performed to evaluate the magnitude of horizontal movement due to girder–end rotation at expansion bearings under cyclic truck load. These studies would assist in determining realistic movement testing speeds in which to evaluate the various sliding surface materials. Bearing movement due to truck load is low-amplitude, high-cycle movement with fast movement speed, but movement due to temperature load is high-amplitude, low-cycle movement with low movement speed.

Another objective was to evaluate the feasibility of developing life prediction models for sliding materials that could be used for service life design. Design provisions were further developed for calculating the required thickness of the sliding surface based on the available literature, theoretical studies, and the results of the experimental program.

Experimental Program

A proof of concept test program was conducted. Sliding material specimen sizes (3-in. diameter), initial testing speed (25 in./min), and initial contact pressure (3,000 psi) were established to be consistent with tests performed and reported in NCHRP Report 432 (Stanton et al. 1999).

The overall program was conducted in four major phases:

1. Phase 1 developed an analysis of a prototype bridge that computed and evaluated bridge movements and movement speed at expansion bearings due to truck loads.
2. Phase 2 developed the concept of an experimental program that was aimed at constructing a system capable of performing wear tests on multiple sliding materials to simulate various travel speeds and contact pressures. Test specimens were also designed as part of this phase.
3. Phase 3 constructed the test apparatus.
4. Phase 4 conducted the experimental testing.

A 3-in.-diameter specimen size was selected for all tests in this experimental program to be consistent with previous PTFE testing performed in Europe (Campbell and Kong 1987) and with testing reported in NCHRP Report 432 (Stanton et al. 1999). Previous MSM studies were performed on samples with diameters of 3.0 and 6.1 in., with most tests performed on 3.0-in.-diameter samples. Previous studies have also shown that the size of the sliding surface specimen has minimal effect on its behavior, including the COF.

The test setup for the sliding surface wear tests used an MTS cyclic actuator, which was vertically installed in a large steel frame. A specially designed sliding material test fixture was installed below and connected to the actuator.

The test fixture included a center moving plate (attached to the MTS actuator) with stainless steel surfaces attached to each side. This moving plate was sandwiched between two stationary material test specimens mounted on steel backing plates. Two horizontal hydraulic jacks applied horizontal pressure, perpendicular to the surface of the sliding specimens, to create the required contact pressure.

In all tests, the cyclic displacement was applied on a sine wave with a stroke length of 1 in. In other words, the center plate with stainless steel surfaces was moved upward from its initial central position 1 in., it was then moved back down for 2 in. (past the initial central position by 1 in.), and then back up 1 in. to the original position. The total movement per complete cycle was 4 in.

Plain PTFE specimens were tested first to establish a baseline for comparison of MSM and Fluorogold results. This was followed by MSM (dimpled), Fluorogold (plain), and dimpled PTFE. MSM specimens and the dimpled set of PTFE specimens were first tested for a prescribed number of cycles in a lubricated condition. Testing was then stopped, the specimens cleaned, and the testing resumed in the unlubricated condition. All tests were conducted at room temperature.

Sliding speed was chosen to simulate the fast sliding speed associated with truck passage, which is low amplitude and high frequency, and results in a very large accumulative movement. However, the sliding of a bearing due to daily thermal movements is high amplitude, low frequency, and has considerably less accumulated movement.

An initial sliding speed of 25 in./min was chosen for this study to be consistent with the maximum sliding speed for PTFE wear tests reported by Stanton et al. (1999) in NCHRP Report 432. The cycle frequency was initially set to 0.1 Hz (25 in./min) for all tests and was maintained for initial PTFE testing until the entire thickness was worn down. However, because of time limitations, this frequency was increased to 0.2 Hz (50 in./min) after about 116,000 cycles for the MSM and Fluorogold specimens.

An initial contact pressure of 3,000 psi was chosen to be compatible with previous wear rate tests reported in NCHRP Report 432 (Stanton et al. 1999).

Results

Performance Tests

This research confirmed that high-performance sliding materials could be used effectively to increase the service life of bearings that use sliding surfaces by providing substantially improved wear resistance over long-term accumulated movement, particularly when subjected to high movement speeds and high contact pressures. However, these materials also exhibited higher COFs than plain PTFE at the contact pressures tested, which needs to be considered in the overall selection of a sliding surface.

Figure 3.77 shows a plot of thickness reduction versus accumulated travel distance for PTFE, MSM, and Fluorogold for various combinations of contact pressure and sliding speed.

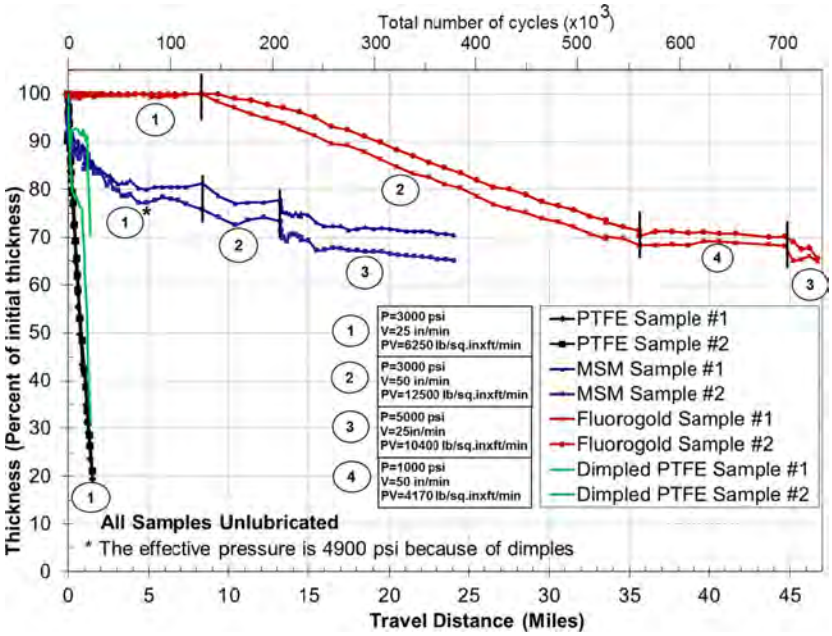

Figure 3.77. Thickness reduction for sliding surfaces versus travel distance and numbers of cycles.

"PV" in the figure refers to the PV factor, a useful parameter for examining the wear rate that is obtained by multiplying pressure and velocity.

The following observations were made concerning the performance of the MSM, Fluorogold, and PTFE samples:

1. Tests confirmed that both MSM and Fluorogold can provide considerably greater wear resistance than conventional plain PTFE and can be used to increase service life when sliding surfaces are subject to high movement speed and high contact pressure.
2. Plain PTFE was shown to wear at a very high consistent rate under the initial combination of high sliding speed and contact pressure, resulting in 80% thickness loss within less than 2 mi of accumulated sliding length.
3. Fluorogold exhibited the best wear resistance of all materials tested, with no material thickness loss over about 8 mi of accumulated sliding length within the initial high values of pressure and velocity, but it started to show some wear at a much higher travel speed (50 in./min).
4. Plain PTFE and Fluorogold (a PTFE-based material) both exhibited rather constant rates of wear that varied for different combinations of pressure and velocity. The wear rate for Fluorogold was very close to zero in the initial PV zone, but exhibited a constant wear rate (albeit very low) in higher PV zones. Plain PTFE exhibited consistent wear behavior, and showed very low wear in a relatively low PV zone (about a third of the initial PV). This indicated that a correlation may exist between wear rate and PV factor for PTFE-based materials.
5. MSM exhibited some initial thickness reduction of about 10% (described in item No. 6), but showed only about 10% additional loss over 13 mi (20.9 km) of accumulated travel.
6. MSM exhibited different behavior with respect to thickness reduction than plain PTFE or Fluorogold. MSM samples did not exhibit constant wear rates within PV zones; instead, they appeared to exhibit initial rapid thickness reduction at the beginning of each zone, after which the rates tended to slow down or stabilize as the tests proceeded. The initial thickness reduction was attributed to compressive deformation and creep and was not necessarily due to wear. This behavior made determining consistent wear rates for MSM difficult. Because of inconsistent wear rates, it was concluded that the PV factor may not be a suitable wear characteristic for MSM, as it is for PTFE-based materials.
7. The results of the SHRP 2 study, combined with the results reported in NCHRP Report 432, indicate the potential of service life prediction based on the PV factor and further confirm the potential of the PV limit transition between zones of low wear and severe wear. It was concluded that the PV factor could be used in a service life design method for PTFE-based sliding materials based on wear over an accumulated length of travel.
8. Fluorogold exhibited a COF about 2% higher than plain PTFE at the initial contact pressure of 3,000 psi. Unlubricated MSM, however, had a COF that was considerably higher. The COF of MSM was found to reduce considerably with increased contact pressure. At 5,000-psi contact pressure, MSM COF was comparable to Fluorogold COF at 3,000 psi. Lubricated MSM had a relatively low COF that was comparable with lubricated PTFE.

Based on the limited proof of concept testing, Fluorogold (a glass-reinforced PTFE sliding material) exhibited the best overall high performance with a combination of high wear resistance and relatively low unlubricated COF.

Life Prediction Results

The results of this study, combined with the findings in NCHRP Report 432, indicated the potential of service life prediction based on the PV factor for PTFE-based sliding materials and further confirmed the potential of the PV limit transition between zones of low wear and severe wear. It was concluded that the PV factor could be used in a service life design method based on wear over an accumulated length of travel.

Figure 3.78 shows the wear rate versus PV data for plain PTFE tests performed in this study combined with data from

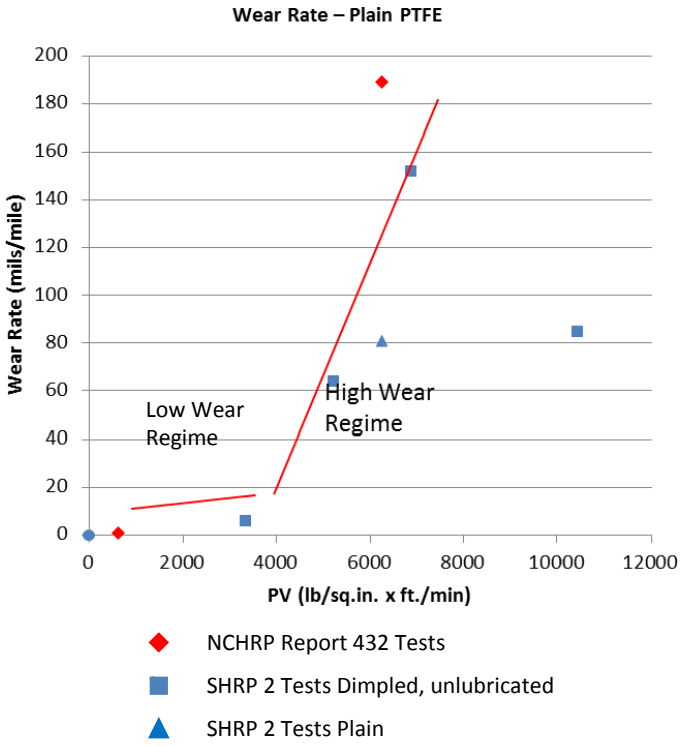

Figure 3.78. Variation of wear rate with PV for plain PTFE.

the NCHRP Report 432 tests. From this plot, there appears to be a PV limit beyond which the wear rate increases significantly. It also appears that a service life design curve for wear rate is possible, which would be a function of PV as shown in the figure. It is recognized that the results shown are from very limited test data, and further testing would be required to establish more reliable curves and a true PV limit.

Similar to the plain PTFE test results, the Fluorogold (glass-reinforced PTFE) test results also indicated the potential of using the PV factor as a means of predicting service life. Like plain PTFE, the Fluorogold had a PV limit differentiating zones of higher wear and very low wear, albeit the wear rates are significantly lower than those of plain PTFE. As with plain PTFE, further testing is needed to establish a more reliable curve and to establish the real PV limit.

MSM exhibited different behavior with respect to thickness reduction than plain PTFE or Fluorogold. MSM samples did not exhibit constant wear rates within PV zones, and it was concluded that the PV factor may not be a suitable wear characteristic for MSM as it is with PTFE-based materials.

Sliding Surface Design Procedure for Service Life

A proposed procedure was developed for design of sliding surfaces for service life. The procedure first determines demand requirements, which are based on bridge loads, traffic, and temperature data. Supply requirements are then determined based on selected material properties for the proposed sliding surface. The method uses a PV deterioration model based on test results as described above and illustrated in Figure 3.78.

For a sliding surface material being considered, the service life is determined for a trial thickness using a PV model; this service life is compared with the design service life of the bridge system. If the service life of the sliding surface is less than the design service life of the bridge system, there are three options:

1. Consider required replacement schedule.
2. Consider increased thickness of the sliding surface material, or increased area of sliding surface, which reduces contact pressure and reduces wear rate.
3. Consider a higher-performing sliding material with greater wear resistance.

Depending on the options chosen, various demand and supply steps will be repeated with new parameter values to arrive at a final solution.

Conclusions and Recommendations

This research program, as part of SHRP 2 Project R19A, confirmed the feasibility of achieving increased service life of sliding bearings that are subject to high sliding speeds through the use of alternative high-performing materials that have greater wear resistance than conventional plain PTFE.

Only proof of concept testing was performed in this study. To establish more reliable wear rates for the materials sampled, additional testing with various contact pressures and velocity combinations is required. Such testing would allow the development of a more statistically reliable model of PV versus wear rate for various types of PTFE-based sliding materials for actual service life design. Test data developed in this study, combined with those reported in NCHRP Report 432, are adequate for confirming a trend, but they provide a limited basis for developing reliable design curves.

The effects of temperature were not considered in this study, but were evaluated in the NCHRP Report 432 study. Further testing is required to properly evaluate temperature as part of the wear rate model for service life design along with pressure and velocity.

Field testing is needed to determine actual bridge movements and movement speeds at sliding expansion bearings for different types of girders (steel and concrete) under truck load and thermal load. There are little current data to substantiate these load responses, and the results of analytical studies need to be validated against actual conditions.

Corrosion-Resistant Reinforced Concrete Structures

This section summarizes the research topic that evaluated the feasibility of increasing the corrosion threshold of conventional steel by electrochemically treating concrete containing conventional steel (black bars). A complete report of this study is given in Appendix E.

Problem Statement

According to Wipf (2006), over the last decades, the principle techniques for corrosion prevention in bridge decks have included increased concrete cover depth to minimize the intrusion of chlorides from salts or ocean spray to the level of reinforcement and the application of epoxy coating over the steel reinforcement to protect the steel from chlorides and corrosion. However, increasing concrete cover depth increases both dead load and construction costs and does not eliminate the occurrence of cracks, which facilitate the intrusion of chlorides. In addition, cracks appear wider at the surface with increased cover depth. Epoxy coatings limit the exposure of the steel to chlorides, oxygen, and moisture and add minimally to bridge construction costs. However, holes and breaks in the epoxy coating at cracked locations, in combination with high chloride concentrations, can result in corrosion of the steel reinforcement, which affects the overall performance of the bridge. Moreover, epoxy coatings in aging

bridge decks may become brittle and eventually delaminate from the steel reinforcement.

Dense (low-permeability) concretes, corrosion inhibitors, and both nonmetallic and steel-alloy corrosion-resistant reinforcement are among the most common techniques being considered as alternative measures for mitigating corrosion in reinforced concrete structures (Wipf 2006).

This research topic evaluated the means of achieving corrosion resistance in reinforced concrete with conventional reinforcing steel. The chloride threshold of conventional steel reinforcement would be increased by pretreating the concrete electrochemically through the chloride extraction method. The chloride threshold is the minimum concentration of chloride in the concrete immediately surrounding the steel to initiate corrosion. For comparison, stainless steel (316LN) and titanium bars were used, which are known to have high corrosion resistance. This research builds on work completed to date, including that sponsored by FHWA (Hartt et al. 2006, 2009).

Objectives

The main objective was to determine the corrosion resistance of electrochemically treated concrete with black bar compared with both the black bar and with corrosion-resistant material. Corrosion-resistant materials used for comparison included commercially available stainless steel rebar (316LN) and titanium bar. The corrosion resistance of treated and untreated concrete samples was compared with the performance of conventional black reinforcing steel, which would provide the low level of protection, and to corrosion-resistant reinforcement, which would provide the upper level of protection.

Scope of Work

To increase the threshold level (thus, the corrosion resistance) in reinforced concrete structures containing conventional reinforcing steel, electrochemical treatment was applied. Reinforced concrete specimens with different levels of pretreatment were prepared and tested to determine their critical chloride (corrosion initiation) threshold. Reinforced concrete structures that can tolerate a higher level of chlorides before corrosion initiates will provide longer service lives. The electrochemical treatment was applied at low and high levels of pretreatment to increase the threshold level of black bars (mild steel).

Tasks carried out to achieve the objectives of this study were as follows:

- Summarize the literature of different steel reinforcement.
- Obtain material and equipment to be used during the testing stage.
- Fabricate specimens containing the selected reinforcement (mild steel [black bar], stainless steel, or titanium).
- Conduct the electrochemical treatment on the test specimens containing mild reinforcement.
- Apply cycles of wetting and drying. The wet stage had chloride solution ponded over the specimens.
- Monitor the samples by measuring the macrocell current and half-cell potential. Analyze the results and provide new recommendations.
- Prepare the final report and recommendations.

Experimental Program

Reinforced concrete specimens were prepared in the laboratory and subjected to an accelerated testing regime under controlled conditions. The corrosion resistance of each combination within the test matrix was compared with each of the other combinations. All specimens were prepared and tested in triplicate to provide statistically significant results.

The test matrix included conventional reinforcing steel (black bar), black bar with two levels of electrochemical treatment, stainless steel, and titanium bar.

The specimen preparation and testing procedure considered to test the different matrices followed ASTM G109, Standard Test Method for Determining the Effects of Chemical Admixtures on the Corrosion of Embedded Steel Reinforcement in Concrete Exposed to Chloride Environments (ASTM G109 2007a).

Five variables were evaluated by placing different bars in conventional concrete:

- Black bar in untreated concrete (control);
- Black bar in concrete subjected to low electrochemical treatment;
- Black bar in concrete subjected to high electrochemical treatment;
- Stainless steel (316LN) in untreated concrete (control); and
- Titanium steel in untreated concrete (control).

Three specimens of each variable were prepared for a total of 15 prepared specimens.

The concrete samples were prepared in compliance with ASTM G109. The length of the wet–dry cycle was modified to optimize, and thereby accelerate, the corrosion of the reinforcement.

Testing was conducted as follows:

1. Each sample was placed on two nonelectrically conducting supports. The first reading was taken 1 month after the specimens were cast.
2. The specimens were ponded with a salt solution (approximately 400 mL at a depth of 1.5 in.) for 4 days. A loose-fitting

plastic cover was used to minimize evaporation. After 4 days, the salt solution was vacuumed off, and the specimens were allowed to dry for 10 days. The cycle was repeated until the termination of the test program.

3. The voltage across a resistor connected between the top and bottom bars was measured with a voltmeter, and the corrosion potential was measured by a half-cell system with a silver–silver chloride electrode. Measurements were taken at three times during each cycle: before ponding with the salt solution, after removal of the solution, and in the middle of the dry cycle.
4. The test was to be terminated when the integrated macrocell current was equal to or greater than 150 C, which is equivalent to a macrocell current of 10 μA, as specified by ASTM G109.

Results

The concrete had a compressive strength of 4,830 psi, which is an average of three cylinders. Due to time constraints, the testing was terminated after 26 cycles. Table 3.17 lists the labels given to each specimen.

Figure 3.79 shows the half-cell potential readings for all specimens varying with time.

For steel reinforcement, a potential value more positive than –200 mV indicates there is a greater than 90% probability that no corrosion is occurring. This condition was observed in all but three specimens (one each from the groups of no, low, and high treatment). For these three specimens, the potential value was between –200 and –300 mV, which indicates that corrosion activity is uncertain.

Table 3.17. Sample Summary

Label	Type of Reinforcement	Type of Treatment
BB_1	Black bar	None
BB_2	Black bar	None
BB_3	Black bar	None
ECL_1	Black bar	Low level of electrochemical treatment
ECL_2	Black bar	Low level of electrochemical treatment
ECL_3	Black bar	Low level of electrochemical treatment
ECH_1	Black bar	High level of electrochemical treatment
ECH_2	Black bar	High level of electrochemical treatment
ECH_3	Black bar	High level of electrochemical treatment
SS_1	Stainless steel 316LN	None
SS_2	Stainless steel 316LN	None
SS_3	Stainless steel 316LN	None
Ti_1	Titanium	None
Ti_2	Titanium	None
Ti_3	Titanium	None

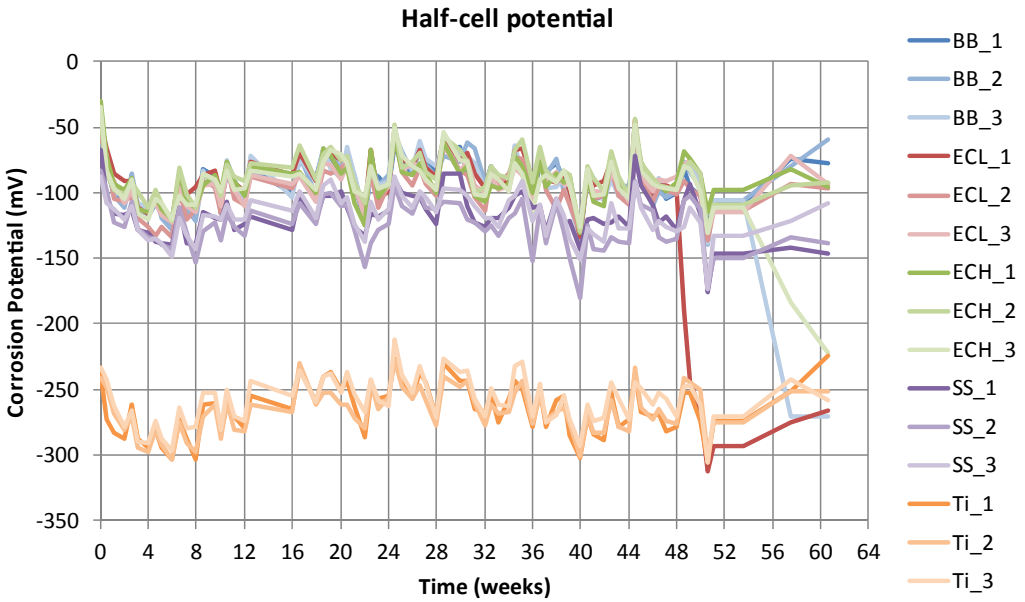

Figure 3.79. Half-cell potential for all 15 specimens.

The integrated macrocell charge is calculated using Equation 3.6:

$$TC_j = TC_{j-1} + \left[\left(t_j - t_{j-1}\right) \times \left(i_j + i_{j-1}\right)/2\right] \quad (3.6)$$

where

TC = total corrosion (C);
t_j = time (s) at which measurement of the macrocell is carried out; and
i_j = macrocell current (amperes) at time t_j.

The total integrated charge was calculated using the current measurements and Equation 3.6. If the charge was greater than 150 C, then the test was terminated (ASTM G109). The results, plotted in Figure 3.80, show the variation of total charge with time. All values are below 150 C.

The macrocell data indicate that one specimen each from the three specimen groups containing black bars (plain, low treatment level, and high treatment level) showed an increase in current. This is consistent with the half-cell potential data, which indicated uncertain corrosion activity in the same three specimens.

These three specimens were selected to remove the rebar for visual inspection along with two control specimens (one each containing stainless steel and titanium): BB_3, ECL_1, ECH_3, SS_1, and Ti_1. BB_3 showed approximately a 0.75-in. length of corrosion product; ECL_1 showed approximately a 1-in. length of corrosion product; and ECH_3 showed approximately 0.25-in. length of corrosion product. SS_1 and Ti_1 did not show any signs of corrosion.

Conclusions and Recommendations

During the time period available for this project, one of the black bar specimens and one of the electrochemically treated black bar specimens from each of the low and high treatment levels showed an increase in current or potential values indicative of uncertain corrosion activity. The top bars of these specimens and two additional specimens, one each containing stainless steel and titanium reinforcements, were removed for visual observation.

The stainless steel and titanium bars did not exhibit corrosion within the available time period.

To discern differences between black bars and electrochemically treated black bars, a longer test period is needed.

Initial observations indicate that electrochemically treated black bars may not provide the protection expected of stainless steel or titanium; however, whether they provide benefits over the black bars without treatment cannot be concluded from this study due to time constraints. To draw firm conclusions, additional research and extended testing periods are needed.

New Galvanic Systems to Achieve Long-Term Corrosion Protection

The study evaluated different promising concepts associated with new galvanic systems to delay the onset of corrosion and reduce the rate of corrosion of the reinforcing steel. A complete report of this study is given in Appendix F.

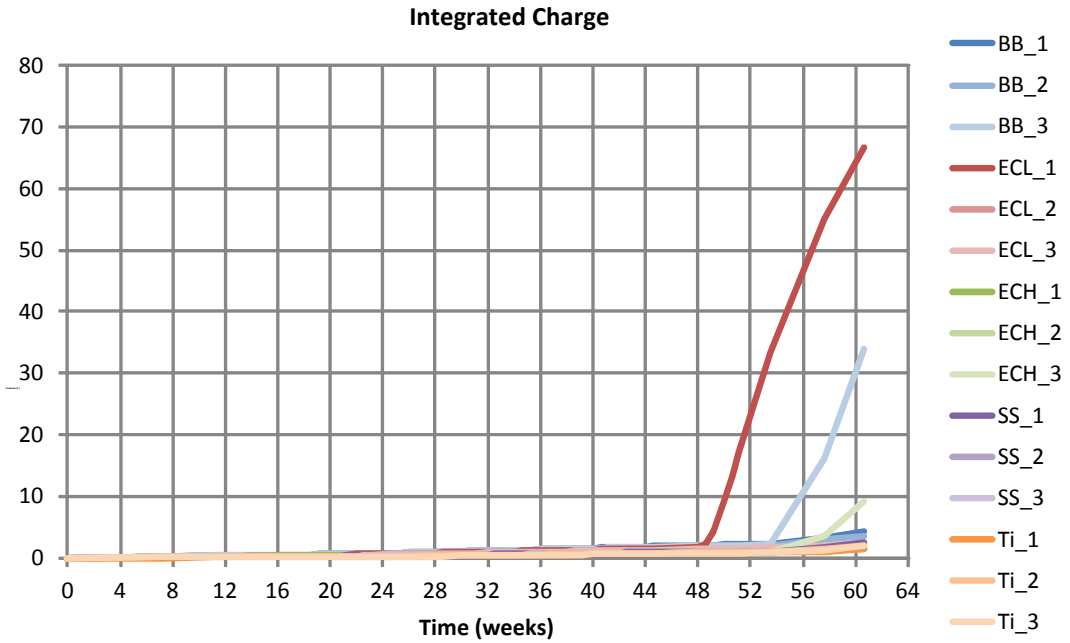

Figure 3.80. Integrated macrocell charge for all 15 samples.

Problem Statement

Cathodic protection has been used in marine and underground structures, storage tanks, and pipelines to protect steel from corrosion (Virmani and Clemeña 1998). Cathodic protection was not used in steel reinforced concrete structures until 1973, when it was applied to a bridge deck (Stratfall 1974). There are two main types of cathodic protection: impressed current cathodic protection and sacrificial galvanic protection. Galvanic systems can delay the onset of corrosion and reduce the rate of corrosion of the reinforcing steel in reinforced structures. Further, the degree of protection achieved and the extension in the service life of the reinforced concrete bridge elements can be extended by improving the performance of galvanic corrosion-protection systems.

Concrete patch repairs are very common in reinforced concrete structures. Often these concrete structures are chloride contaminated beyond the location of the patch repairs, leading to accelerated corrosion around the patch. This phenomenon is referred to as ring anode corrosion or the halo effect. Ring anode corrosion can be eliminated by including galvanic anodes within the repair. The galvanic anode corrodes instead of the reinforcing steel. This type of application now has a 10-year successful history (Sergi et al. 2008). The knowledge gained from this application has led to the development of higher-output galvanic anodes. Initial testing of such anodes has shown improved performance and an ability to globally protect the reinforcing steel.

Historically, galvanic anodes provided a level of current output per unit that was sometimes too low to achieve the desired level of protection. The development of improved anode units that can produce a higher level of current or increasing the driving voltage between the anode and steel reinforcement would improve the performance and allow galvanic anodes to meet the full range of corrosion protection levels that may be desired. The advantages of these types of galvanic systems over impressed current cathodic protection are the self-regulating current output of the system and the much-reduced requirement of monitoring and maintenance.

Recent initial work has enabled increased performance of galvanic anodes by modification of the surface area of the metal by design and by an increase in the driving voltage of the anode unit. It is also possible to increase the current density output by using high-voltage anodes.

Objective

The objective was to evaluate different promising concepts associated with the new galvanic systems in order to delay the onset of corrosion and to reduce the rate of corrosion of the reinforcing steel. The galvanic systems evaluated had an ordinary anode and one with a larger anode surface (four times the amount of zinc than ordinary anodes) and two levels of high-voltage anode.

Scope of Work

Small-scale laboratory testing was conducted to evaluate the potential of using galvanic anodes to extend the service life of reinforced-concrete structures and the level of protection provided by different anode systems (higher metal surface, higher voltage output). Data collection included the measurement of the current, current density, potentials, and polarization versus time.

The following tasks were carried out to achieve the objectives of this topic:

- Summarize the literature of cathodic protection, including the galvanic systems.
- Obtain material and equipment to be used during the testing stage.
- Fabricate samples using different galvanic systems.
- Set up an automated monitoring system to collect the long-term data.
- Analyze the collected data and destructively analyze the anodes and steel bars.
- Prepare the final report and provide recommendations based on the results.

Appendix F provides more detailed information about each task.

Experimental Program

The ability of embedded galvanic anodes to provide sufficient output to protect cathodically the reinforcing steel from further corrosion was determined using small concrete slab samples. The levels of protection of different anodes with varying output were studied.

The specimens measured 18 × 18 in. and were 8 in. thick to simulate a portion of a bridge deck. The test matrix included conventional reinforcing steel and galvanic anodes with different surface areas or voltage outputs.

The concrete slabs were cast in two layers. The bottom layer had uncontaminated concrete, and the top layer had concrete contaminated with salt.

Five variables were evaluated:

- Black bar embedded in concrete (without anode, control);
- Black bar embedded in concrete with ordinary anode (OA);
- Black bar embedded in concrete, with a larger anode having a surface area four times the ordinary (OA4);
- Black bar embedded in concrete with high-voltage anode (under development) at Level 1 (provides higher applied voltage than a standard galvanic anode) (HVAL); and

- Black bar embedded in concrete with high-voltage anode (under development) at Level 2 (higher voltage than Level 1) (HVAH).

Three specimens for each variable were prepared. The testing procedures for the determination of the corrosion activity involved the following:

1. Measuring half-cell potentials (ASTM C876 2009) at nine locations on the specimen.
2. Measuring the current flowing from the anode to each pair of rebars (measured hourly), including a total of four pairs, two on top and two at the bottom of the specimen, while at the same time measuring the corrosion potential by using embedded electrodes.
3. Measuring the current flowing during depolarization (when the anode was disconnected). The corrosion potential was measured by both the embedded electrodes and the half-cell system. A second data logger with quick-reading capability (10 reads/s) was used during the procedure to capture the exact moment when the anode was turned off and on.

The following steps were performed:

1. Seven days after casting, before connecting the reinforcement to the anode for the first time, the corrosion potential was measured to establish the baseline level of corrosion potential of the steel using a half-cell system with a silver–silver chloride electrode. The tip of the reference electrode was positioned on a small wet pad to stabilize the readings. The same procedure was repeated three times during each wet–dry cycle. The corrosion potential was measured before ponding with the water, after removal of the water, and at the middle of the dry cycle.
2. Immediately after the first potential reading, the first anode was connected to the steel. The current delivered by the anode was measured, and then the anode immediately disconnected. The second anode was then connected to the steel and the current was measured. If both anodes were active (i.e., produced currents on the order of milliamperes), one of them was chosen and permanently connected to the steel. The other anode remained redundant until the end of the experiment. If one anode appeared faulty (e.g., the electrical connection was problematic), the spare anode would be used instead.
3. The specimens were ponded with water (no salt) for 4 days. Approximately 2 L of water (around 10-mm height) were added to the reservoir. At the end of the wet period, water was removed by vacuum.
4. A data logger was used to take readings every hour. The automated acquisition system recorded the total current measurements.
5. For depolarization measurements, approximately every 10 weeks a map of the potential across the surface of the specimen was obtained while the anode and steel bars were connected. The anode was then disconnected (using the switch).
6. Four hours later, a new potential map was obtained. The difference between the instant-off potential and the 4-hour depolarization potential was the value of interest; its use is described in Appendix F.
7. Twenty-four hours after disconnection, another potential map was determined. The difference between the instant-off potential and this 24-hour depolarization potential was the value of interest. After the conclusion of the depolarization test, the anode was reconnected to all steel bars. The anode was kept connected to the reinforcement until the next depolarization test.

Results

The following data were collected from each specimen: the half-cell potential system; the current flowing from the anodes to each pair of rebars and the corrosion potential at the location of two embedded electrodes in the each specimen; and the current flowing during the instant-off and -on procedure from the anodes to each pair of rebars and the corrosion potential at the location of two embedded electrodes.

The first half-cell potential measurement was taken on Day 0. After establishing the base line readings, all samples were subjected to cycles of 4 days' wet and 10 days' dry periods. Aside from the half-cell readings taken at the end of each dry cycle, two extra sets of readings were conducted to better evaluate and observe the specimens during the wet–dry cycles.

Each specimen was identified using the labels given in Table 3.18. Five variables were tested, and three specimens for each variable were made and tested (15 distinct specimens) to provide statistical significance.

Two anodes were installed in each specimen, but only one was used in the tests. The output voltage of each anode was measured separately. The anode with the highest potential reading measured was selected and connected permanently to the rebars throughout the experiment. Figure 3.81 shows the half-cell potential readings for all specimens. This plot represents the average values of corrosion potential measured at nine distinct points on each slab. The measurement was conducted three times during each wet–dry cycle.

Initially, all specimens had similar corrosion-potential values. The control specimens (BB), with no anode, had the lowest corrosion-potential values, which remained steady throughout the experiment. All specimens with anodes had their corrosion potential shift in the negative direction after the anode was connected to the rebars.

The OA, OA4, and HVAL specimens showed steady potential readings. Two HVAH specimens produced variable results, which may be due to variation in production of the prototypes. The highest negative corrosion potentials were provided by the

Table 3.18. Sample Labels

Label	Type of Anode
BB_1	None
BB_2	None
BB_3	None
OA_1	Ordinary anode
OA_2	Ordinary anode
OA_3	Ordinary anode
OA4_1	Anode with four times the surface area of the ordinary anode
OA4_2	Anode with four times the surface area of the ordinary anode
OA4_3	Anode with four times the surface area of the ordinary anode
HVAL_1	High-voltage anode—low level
HVAL_2	High-voltage anode—low level
HVAL_3	High-voltage anode—low level
HVAH_1	High-voltage anode—high level
HVAH_2	High-voltage anode—high level
HVAH_3	High-voltage anode—high level

HVAH specimens, followed by the HVAL and OA4 specimens, then by OA, and finally by the BB specimens. Higher negative-corrosion potentials indicate that more corrosion protection is being provided.

The electrical current flowing from the anode to the four pairs of bars over a period of 56 weeks was measured. In addition, corrosion potential data were collected at the two locations of the embedded reference electrodes. A very good agreement was found between those of embedded values and the surface-potential values.

The corrosion rate was estimated through a depolarization testing procedure. Four depolarization measurements were conducted at approximately 10-week intervals. The tests consisted of collecting a series of readings during the temporary disconnection of the anodes, at 4 and 24 h after disconnection, and finally during the anode reconnection (turn on). The procedure started with the initial reading taken before the anodes were disconnected; an intermediate reading was conducted 4 h after the anodes were disconnected (4 h off). Finally, 24 h after disconnection and before reconnection (turn on) of the anodes, a final reading was taken (24 h off).

The data collected during this procedure were used to estimate the corrosion rate using the Butler–Volmer equation. During the fourth depolarization period of 24 h, it was observed that the corrosion potential of the control specimens did not change; however, all the specimens with anodes showed a large shift in potential after the disconnection of the anodes. The largest change was observed for the HVAH specimens, followed by the HVAL and OA4 specimens, and finally by the OA specimens. The potential of the reinforcing steel 4 h after disconnection averaged –112 mV for all specimens. The corrosion potential of the reinforcing steel 24 h after disconnection averaged –66 mV.

Figure 3.82 shows normalized values of the corrosion potential during the fourth depolarization period.

Table 3.19 shows the corrosion rate estimation.

Even though the concrete used in the specimens had a high level of salt per unit volume of concrete, the results indicated no corrosion activity.

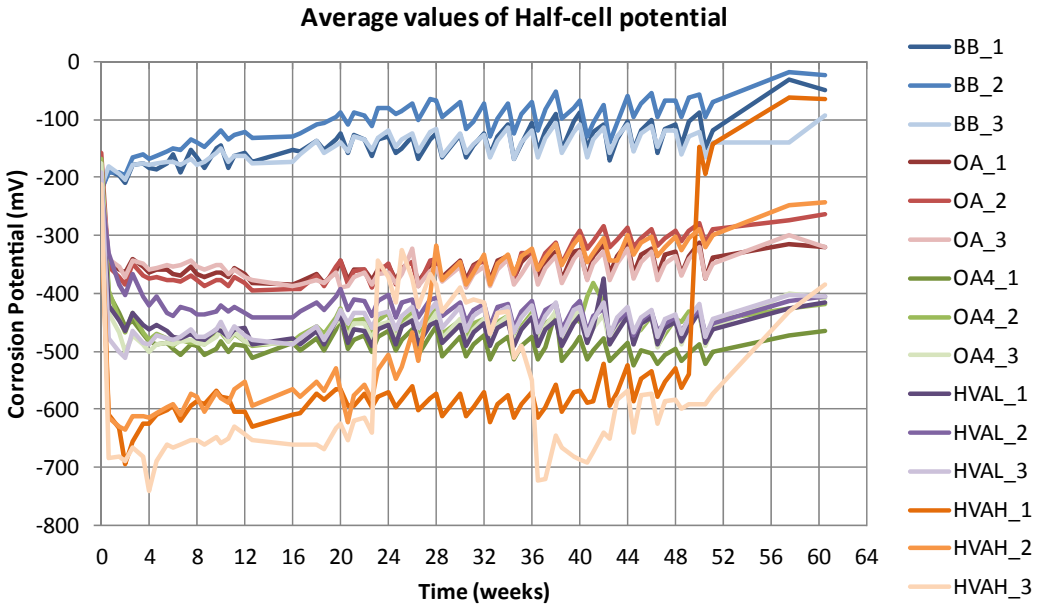

Figure 3.81. Half-cell potential for all 15 samples.

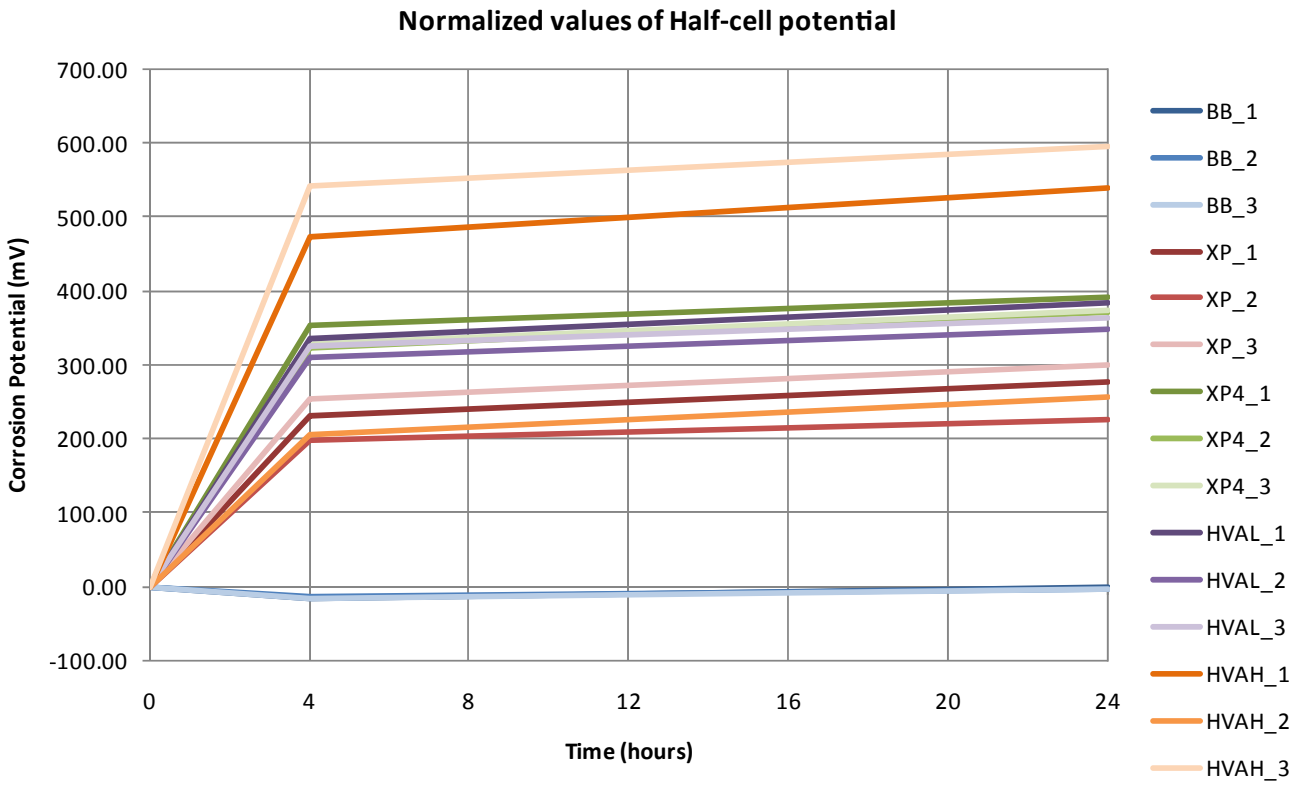

Figure 3.82. Normalized values of half-cell potential during the fourth depolarization.

Table 3.19. Corrosion Rate Estimation

Label	i_{appl} (mA/m²)	ΔE (mV)	β_c (mV)	β_a (mV)	i_{corr} (mA/m²)	Corrosion Rate (μA/cm²)	Rating
OA_1	331.32	277.00	120	60	1.64	0.16	Negligible
OA_2	161.54	227.00	120	60	2.08	0.21	Negligible
OA_3	293.71	300.00	120	60	0.93	0.09	Negligible
OA4_1	728.08	392.00	120	60	0.40	0.04	Negligible
OA4_2	528.61	371.89	120	60	0.42	0.04	Negligible
OA4_3	512.58	373.33	120	60	0.40	0.04	Negligible
HVAL_1	526.21	384.56	120	60	0.33	0.03	Negligible
HVAL_2	450.59	348.00	120	60	0.57	0.06	Negligible
HVAL_3	480.73	364.11	120	60	0.45	0.04	Negligible
HVAH_1	1201.89	540.22	120	60	0.04	0.00	Negligible
HVAH_2	186.49	255.78	120	60	1.39	0.14	Negligible
HVAH_3	2597.31	594.33	120	60	0.03	0.00	Negligible

Note: i_{corr} = corrosion rate; i_{appl} = applied electrical current; ΔE = observed corrosion potential; β_c = cathodic Tafel's slope; and β_a = anodic Tafel's slope.

Conclusions and Recommendations

The test results indicated that there was no corrosion in any of the specimens in the given time period. The testing further indicated that specimens with high-level, high-voltage anodes (HVAH) provided increased corrosion protection, which is indicated by higher current and the generation of more negative potential values than the low-level, high-voltage anodes (HVAL). Anodes having four times the surface area (OA4) provided more current and corrosion protection than OA anodes. HVAL anodes exhibited similar corrosion protection as the OA4 anodes. Both high-voltage anodes and OA4 anodes provided better corrosion protection than OA anodes.

Due to time constraints, the tests were terminated without observing corrosion in some of the specimens. Further research with an extended time frame is recommended.

Self-Stressing Deck Systems

This section summarizes the research topic that evaluated a system for imparting longitudinal prestress force over the interior support of a continuous structure using imposed support settlement. Additional information may be found in the doctoral dissertation by Marcelo Ferreira da Silva (da Silva 2011). At the time of writing, papers detailing the results of the research have been submitted for publication (Silva et al. 2013; Yakel and Azizinamini 2013).

Problem Statement

Bridges often use continuity over the interior supports to reduce force effects within the spans. As a result, negative bending moment is produced over the interior supports. In structures built with composite construction, this moment produces tensile stresses in the concrete deck and compressive stress in the bottom flanges of the steel girders. The tensile stress in the deck often leads to cracking, which allows intrusion of moisture and road salt, causing corrosion of the reinforcement and supporting girders. Continued maintenance is required to forestall the deterioration; however, eventual replacement of the deck is typically required.

One accepted method of countering the negative effects due to tensile deck stress is to reduce or eliminate the tensile stress through precompression of the deck. The system being presented uses the self-weight of the structure to induce a compressive force in the deck. The compressive force is developed by first raising the interior supports above their final elevation while the deck is cast (CIP construction) or the panels are placed (precast construction). Once the concrete has cured, the supports are lowered to their final elevation. Continuity of the steel member and composite action with the deck produce a compressive stress in the concrete slab that is balanced by tensile stresses in the bottom of the steel member.

As a result of the compression in the slab, cracking over the interior support is reduced, which then increases durability. In addition, the magnitude of the compression force in the bottom flange is reduced, which can lead to section size reduction and possibly splice elimination, making the overall bridge design more efficient and cheaper than conventional design.

The characteristics described apply to any system that precompresses the deck over the interior support, such as longitudinal posttensioning using steel strands. However, one of the biggest advantages of the self-stressing system is that precompression of the deck is accomplished without the use of costly and time-consuming posttensioning techniques, thus reducing the cost and time for bridge construction. Because prestressing strands are not used, potential corrosion of strands and associated loss of prestressing force are eliminated.

Although the concept of using the continuity of a bridge to prestress the bridge deck is simple, the technique has never been extensively researched or used in practice. Laboratory testing on a CIP self-stressing system is reported by Yakel et al. (2007). The research reported here is largely a continuation of that effort. Nagai et al. (2000) report on a field application similar to the self-stressing method, which they refer to as the piano method. Both of these sources emphasize the need for time-dependent analysis to predict the creep and shrinkage effect in the induced compressive force. A Highways for LIFE program bridge constructed by the Oregon DOT effectively used self-stressing, although it was used to address an uplift issue at the abutments and not to improve the performance of the deck (Ardani et al. 2010). Finally, the Inverset system uses a deck that is cast on the ground while a steel girder is held in place above. On righting the system, gravity induces a compression within the slab (Fort Miller Company, Inc. 1998).

Objective

The objective of the research reported in this section was to develop guidelines of the self-stressing method system for use on multispan continuous structures with composite CIP or precast bridge decks. Consequently, the research focused on the development of guidelines for use of the self-stressing deck system in practice. The self-stressing system can be a cheaper alternative to posttensioning for imparting a longitudinal compressive stress in the bridge deck and can minimize the size, if not completely eliminate the extent, of cracking of the concrete bridge deck. Although steel girders are used throughout the discussion, the concept could be adapted for concrete girders, as well.

Scope of Work

The work carried out under this project was an extension of the CIP experimentation that had been conducted previously. To this end, a small-scale test specimen similar to the original was

tested; the main difference was that the deck was composed of precast panels rather than CIP. Additionally, the system had two steel girders, rather than one, to provide stability while the precast panels were placed. Finally, the magnitude of the initial prestressing force imparted on the structure was greater than in the CIP testing.

A design procedure and guide was developed to assist in the use of the system. A design based on the proposed procedure was then compared with a structure to be constructed using conventional methods.

Experimental Program

A small-scale test specimen was built and tested to investigate the parameters that affect the performance of the self-stressing system when used in conjunction with a precast deck. The test specimen was composed of two W12 × 22 steel girders placed over three supports 15 ft apart. Ten 3-ft long, full-depth (6-in.) concrete precast panels were placed on top of the girders. The panels were 5 ft wide, and the girders were spaced 3 ft apart, resulting in a 1-ft overhang to each side. Shear studs welded to the top of the girder projected through block-outs in the precast deck panels. Figure 3.83 shows a 3-D sketch of the test specimen.

The test specimen was built in the structural laboratory and generally represents a quarter-scale model of a prototype structure.

The first step was to lift the intermediate support to a predetermined height. Two hydraulic jacks, shown in Figure 3.84a, were placed under the central beam to lift the girder 1 in. Steel washers were used as shim plates (Figure 3.84b) to keep the support lifted while the deck was constructed. The completed precast panels to be used in the construction of the specimen are shown in Figure 3.85. As the precast panels were placed

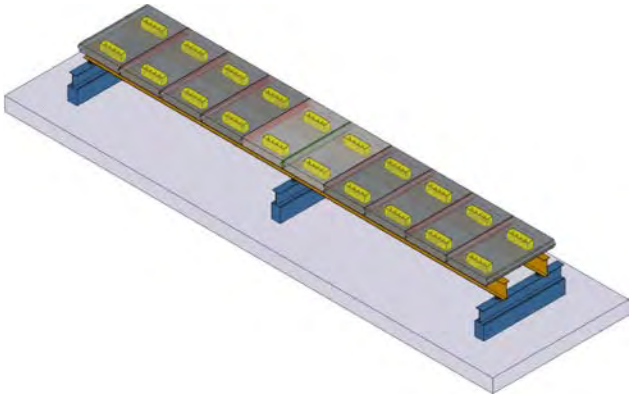

Figure 3.83. 3-D view of self-stressing system specimen.

over the girder (Figure 3.86a), the panel-to-panel connections were accomplished using high-strength epoxy spread over the match-cast shear key (Figure 3.86b).

Once all panels were set in place, the shear pocket block-outs and the center panel-to-panel connection were filled with nonshrink grout. After allowing the grout to harden, the shim plates were removed. Lowering the interior support created compressive force (self-stressing) in the specimen.

The amount of prestressing achieved was directly proportional to the amount of displacement initially introduced during the construction. Figure 3.87 shows the compressive stress measured at the top surface of the concrete deck compared with the predicted values. The maximum compressive stress located at the interior support was 2.30 ksi, or approximately 30% of the concrete compressive strength. Good agreement between the measured and calculated values was observed.

Within the deck, the time-dependent analysis predicted a reduction in the precompression force of 30%, meaning the

(a) (b)

Figure 3.84. (a) Pancake jacks used to shim the system and (b) central support shimmed 1.0 in.

(a)

(b)

Figure 3.85. (a) Precast concrete deck panels organized in sequence and (b) match-cast detail.

maximum compressive stress over the support would be reduced from 2.3 ksi to 1.6 ksi. Recall that the target value of precompression to achieve the desired beneficial effects was 0.25 ksi, so the loss was acceptable and was expected. The changes in these values demonstrate the need to compensate for losses when determining the amount of precompression to apply. The "estimated" line in Figure 3.87 reduced stresses at the top surface of the precast deck obtained from the time-dependent analysis. Note that only the initial values of stress from testing are reported, as the long-term changes in stress resulting from creep cannot be directly measured.

It was observed after 63 days that the monitored strains within the system were no longer changing, so the decision was made to stop the monitoring and begin the ultimate load test. The ultimate load test was conducted to determine what effect the self-stressing method, as implemented with precast panels, would have on the maximum capacity of the system. The test would also provide in-depth information and better understanding of the critical sections of the bridge, such as at midspan (maximum positive moment) and at the interior support (maximum negative moment).

The ultimate loading was conducted to determine the failure mode that may govern the design of a self-stressing method. The loading was applied to the specimen by two spreader beams located at the midpoint of each span. The beams were connected to four hydraulic rams (two per beam)

(a)

(b)

Figure 3.86. (a) Placing precast concrete panels and (b) high-strength epoxy spread over the match-cast shear key.

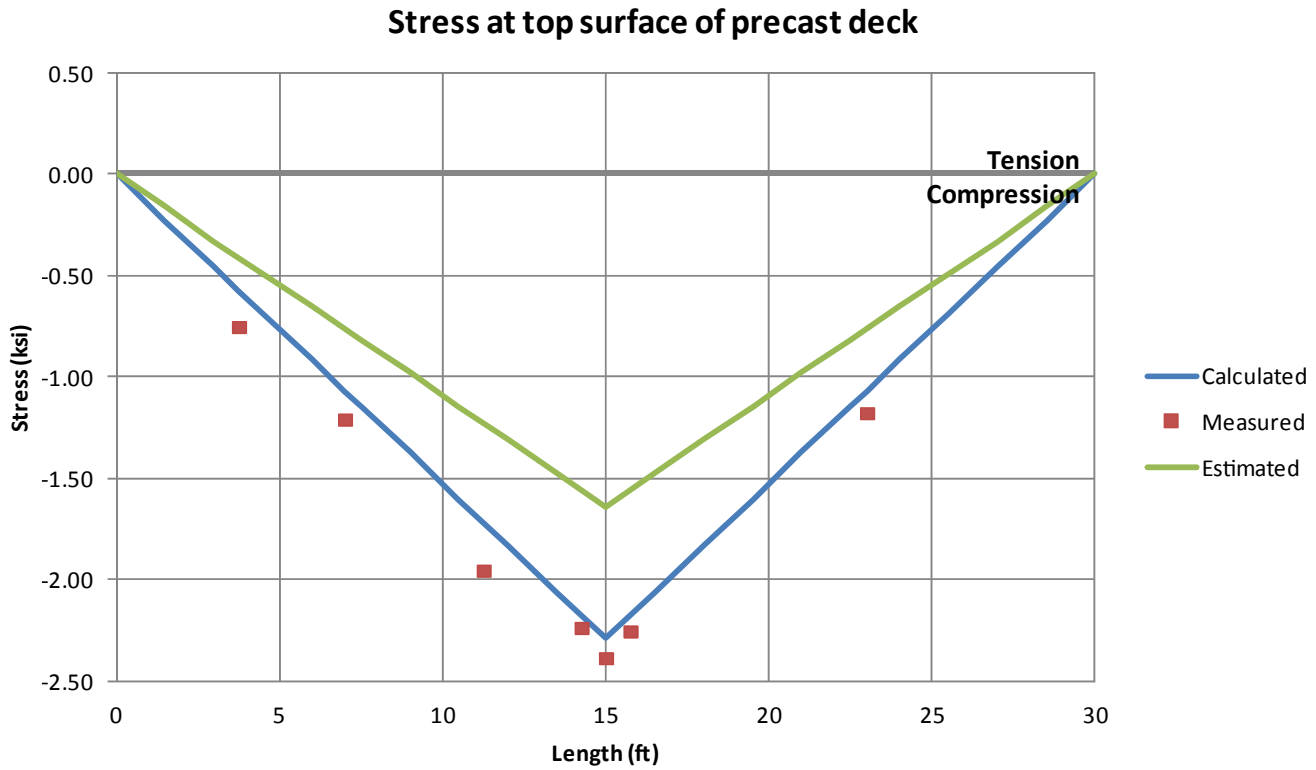

Figure 3.87. Stress at top surface of precast deck panels after shim removal.

through high-strength rods, as shown in Figure 3.88. Elastomeric pads were place under the spreader beams to transfer the load to the deck.

During the test, the data acquisition system was used to record all strains in both the concrete and steel, deflections, and hydraulic pressure in the rams (applied load). Figure 3.89 shows the ultimate load test setup in the structural laboratory. The analysis of the recorded data and observed mode of failure are discussed in the following section.

Results

Load Required to Induce Cracking

To illustrate the benefit of the precompressed deck, Figure 3.90 shows an estimation of cracking moment. Figure 3.90, b and c, show the stress analysis for conventional construction with no deck precompression and for the self-stressing test specimen, respectively. The required moment (force "P") to crack the deck at the interior support was three times greater. In these calculations, a 40% precompression loss was assumed to account for the time-dependent effects. Thus, a final compressive stress of 1.38 ksi (2.3 ksi × 60%) was assumed.

Self-Stressing Ultimate Strength Test Results

Loading was applied as small increments of displacement, pausing for data acquisition and inspection. Figure 3.91 shows the load–displacement curve obtained for the self-stressing test specimen. The initial response of the system was linear up to a level of applied displacement of 0.3 in., corresponding to a load of 110 kips; this point is labeled as 1 in Figure 3.91.

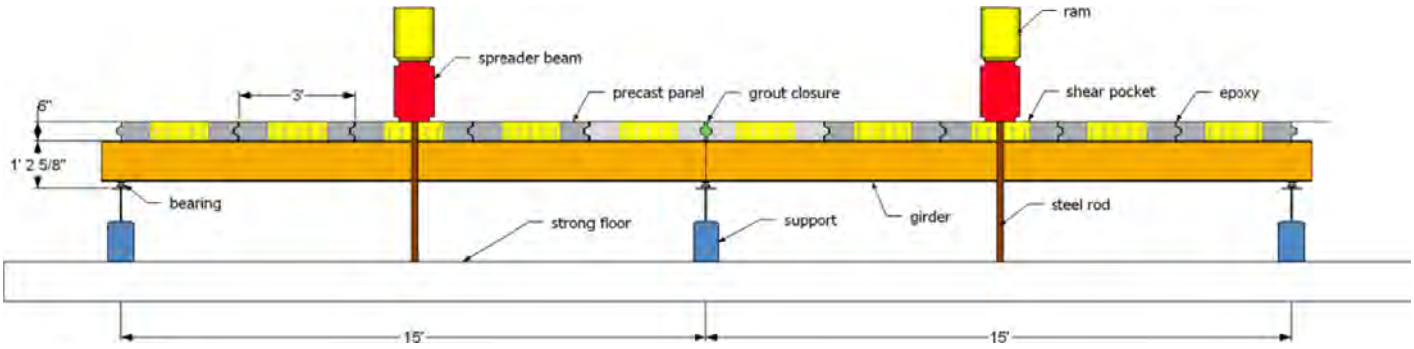

Figure 3.88. Sketch of the ultimate load test setup (side view).

Figure 3.89. Ultimate load test setup.

Beyond this point, the load displacement began to display a nonlinear response. Strain data indicated that this change in response corresponded with the onset of yielding in the bottom flange.

At an applied displacement level of 1.5 in., the load was removed to allow adjustment of a support when a sliding element was nearing the end of the available travel. The specimen showed residual deformation (0.75 in.) after unloading. Although the girder had undergone some degree of plastic deformation, the slope of the load–displacement curve during the reloading stage (Box 2) was nearly equal to that at the start of the test.

The specimen reached a maximum loading capacity of 230 kips (Box 3), which is over twice the load observed at the linear elastic limit of 110 kips. The bridge displayed good ductility at this maximum load value with a vertical displacement of 2.3 in., which is approximately seven times the deflection at the elastic limit. The drop in load from the maximum value corresponded to development of localized crushing of the concrete near the west loading point. It is important to note that beyond this point, the specimen sustained a reduced level of load while subjected to a very large value of deflection (Box 4).

The maximum predicted ultimate capacity based on strain compatibly method was 217 kips, which compares well with the observed experimental maximum load of 230 kips.

Cast-in-Place Ultimate Strength Test Results

For comparison, the results obtained from the CIP specimen are shown in Figure 3.92. The load–deflection response of the system was nearly linear until a deflection of approximately 0.25 in., which corresponded to an applied load of 55 kips. The unloading of the system seen in Figure 3.92 at about 60 kips was done to correct the loading frame. After correction, the loading was resumed. At 72 kips, yielding of the web occurred near the pier. This corresponded to a deflection of 1.1 in. at midspan. It can also be seen in Figure 3.92 that the specimen exhibited a sufficient amount of ductility.

There were very few notable events observed before the ultimate load was reached. At a load of 65 kips the transverse crack pattern was first observed. The load ceased to increase

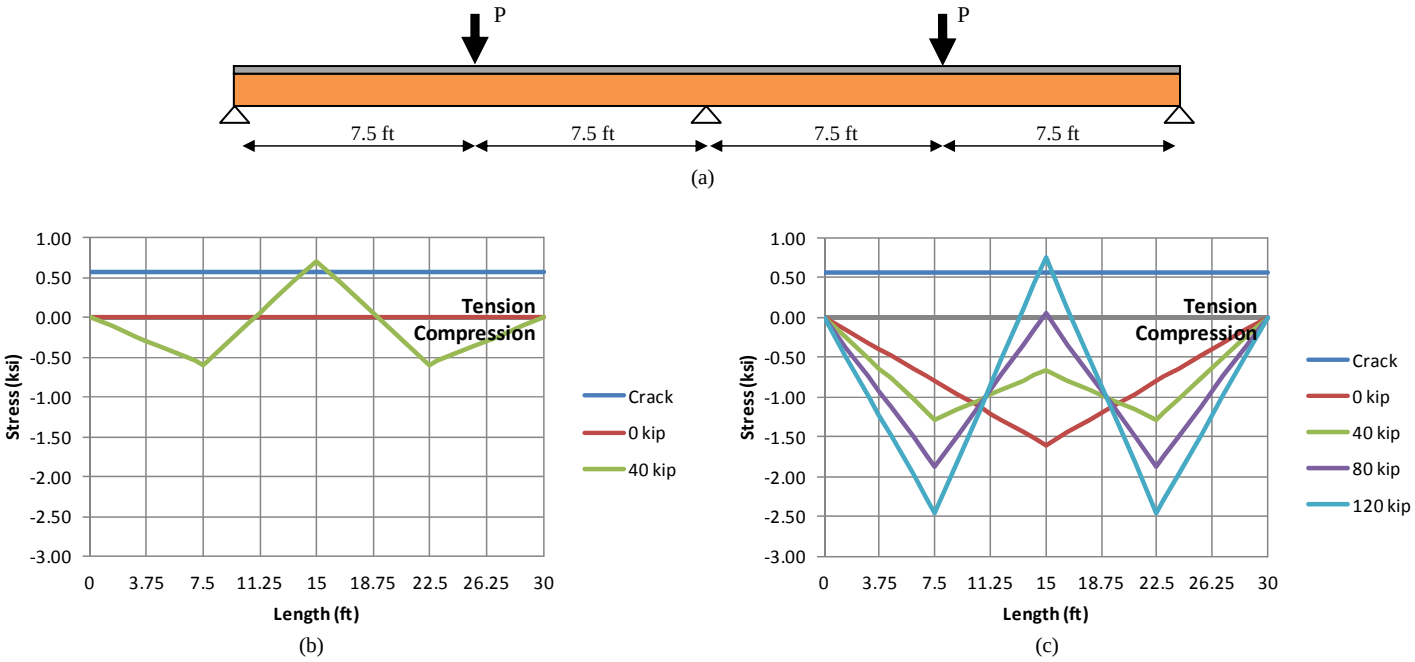

Figure 3.90. (a) Schematic of required moment (force P) to crack the deck and stress analysis between (b) conventional construction and (c) self-stressing construction.

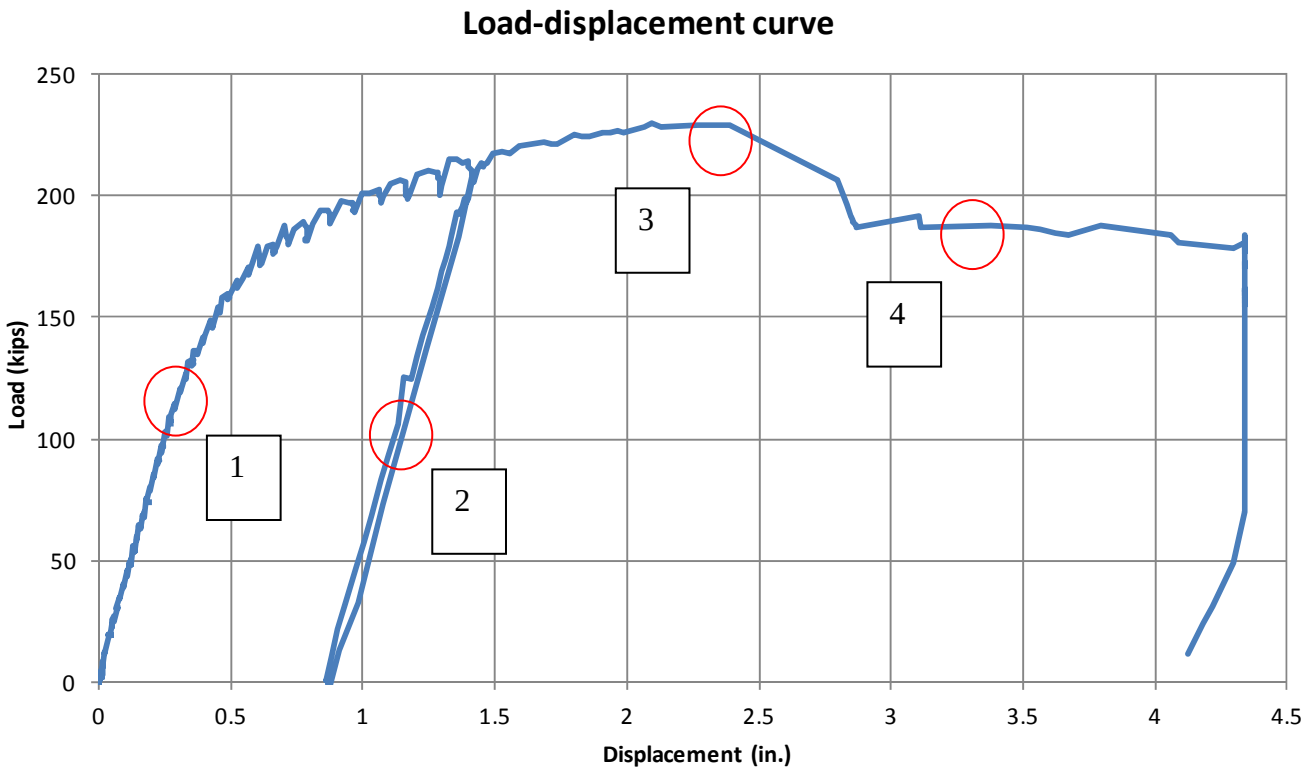

Figure 3.91. Load–displacement curve for ultimate load testing.

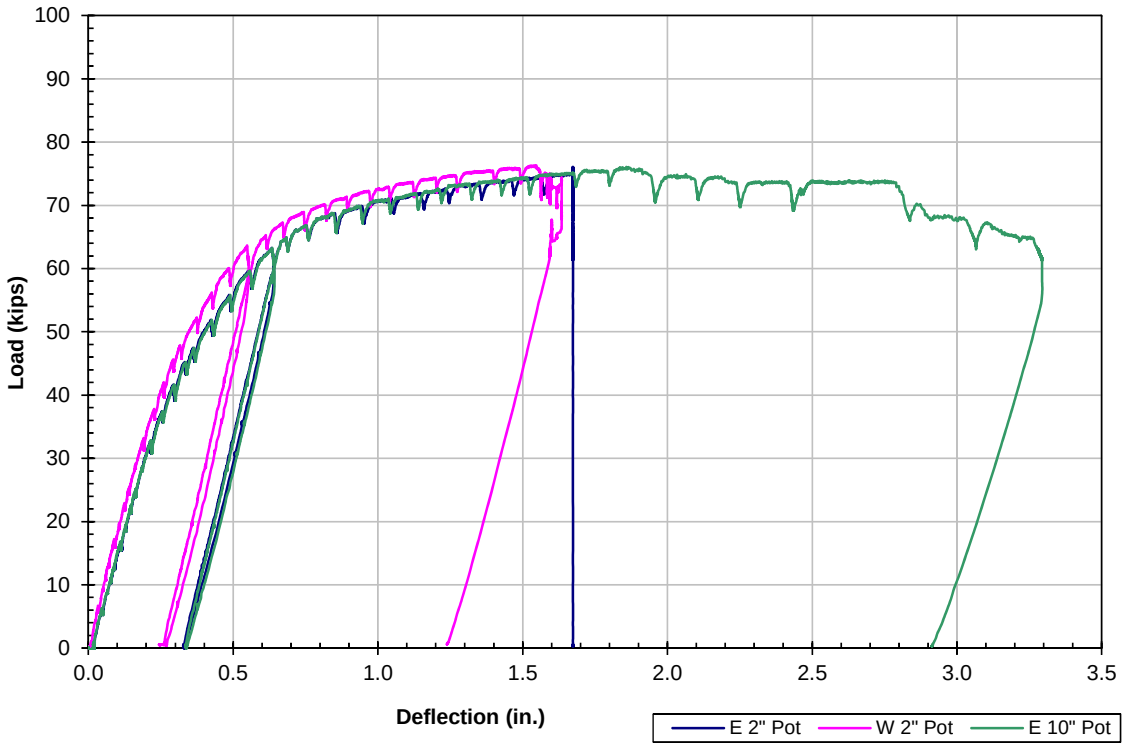

Figure 3.92. Load–deflection curve during the ultimate load test.

after reaching 75 kips, at which point the vertical deflection at the middle of the east span was 1.65 in. The deflection continued to increase with no increase in load until crushing was observed at the top of the deck. Beyond this point, the specimen was able to absorb additional deflection, but at a reduced level of loading. The maximum deflection at the end of the test was approximately 3.25 in. at midspan. The observed ultimate load was slightly lower than the predicted failure load of 81 kips. This difference can likely be attributed to the fact that design calculations were made assuming the yield strength for the beam of 50 ksi. The material testing showed that the actual yield strength of the beam was slightly lower at 47.6 ksi.

Failure Modes

Although the bridge was constructed using an innovative method, the observed modes of failure were similar to those of a two-span continuous composite steel–concrete bridge constructed using conventional details, as listed below:

- Cracking in the vicinity of interior support;
- Yielding of girder bottom flange (large deformation);
- Combination of web and bottom flange buckling; and
- Concrete crushing.

Figure 3.93 shows the only tensile crack located at the closure region. Because steel reinforcement was not contained in this region, the crack width is much greater than if reinforcement were used to distribute the cracks. This is certainly a feature of the behavior that needs to be addressed. One solution would be to have two closure regions within the spans, such as at points of inflection, rather than a single closure over the interior support. The panel positioning would then be adjusted such that there would be no joint directly over the support.

Figure 3.93. Crack at the closure region due to tensile force over the interior support.

Figure 3.94. Large deformation due to yielding of bottom flange at midspan.

Figure 3.94 shows the final deformed shape of the bridge after the ultimate load testing. It is clearly visible that the bridge had undergone large deformations due to yielding of the girder bottom flange.

Conclusions and Recommendations

The self-stressing method was used to construct a prototype bridge using the precast concrete panel system, and the proof of concept was successfully conducted and validated. The testing was deemed a success because the cracking was satisfactorily delayed. Because the bottom flange stress at the interior support region was completely eliminated, a single girder cross section could be used throughout the bridge length.

The self-stressing method applied to precast concrete decks is proposed as an alternative to the conventional posttensioned concrete deck system used for preventing transverse deck cracking. If a CIP deck is considered, the self-stressing method can reduce or eliminate shrinkage cracks, which is often an issue even before the bridge is opened to traffic.

Both analytical and numerical solutions have shown good agreement with the experimental results. Thus, both methods can be used to design a bridge using the self-stressing method. Time-dependent analysis should be carried out to determine the amount of precompression loss and additional stress induced in the girder due to the time-dependent effect.

Guidelines were developed to facilitate the dissemination of the method, and a design example is provided to aid bridge engineers considering the self-stressing method. The design example illustrates advantages of the self-stressing method over

the conventional method, such as the reduction of compressive stress at the girder bottom flange (mitigating buckling) and the development of compressive stress in the deck (reducing cracking).

Delayed Composite Systems

Problem Statement

The majority of bridge decks for beam–slab bridges are constructed using field-cast concrete. Although accelerated construction and rapid renewal is one of the foci of SHRP 2, addressing the durability of this commonly used bridge deck construction method is extremely important.

CIP bridge deck systems are known to exhibit transverse cracking before bridges are opened to traffic. This cracking is partly attributed to restraining forces that are provided by shear studs preventing fresh concrete from shrinking. Closure of these cracks through the introduction of compression from posttensioning should greatly enhance the durability of these bridge decks. This compression can be maximized by using the delayed composite system. One of the main features of the delayed composite system is that it isolates the shear studs over the steel beams and prevents development of the composite action until the bridge deck is precompressed through posttensioning.

The proposed research builds on previous pilot studies of delayed composite action for precast full-depth deck systems for steel superstructures (Azizinamini and Yakel 2006) and concrete superstructures (Fallaha et al. 2004). The previously developed systems propose openings in the top of the deck that must be filled with a nonshrinking grout or concrete. This leaves a joint exposed to the deck surface that is not precompressed by the posttensioning. From a durability perspective, this exposed joint could be a potential risk. The proposed research addresses increased durability through the minimization or elimination of surface joints in the deck. The proposed systems would provide delayed composite action by incorporating a continuous void with a completed CIP concrete deck over it with small grout tubes penetrating the deck surface.

Objectives

The main objective of this research was to determine the viability of the delayed composite system for CIP systems. CIP bridge deck concrete is subjected to early shrinkage and to shortening caused by a drop in temperature in the hydration cycle and cold weather. These two effects combine to create demand for deck concrete shortening. When concrete sets, it is anchored to the supporting girders through immediate composite action, with studs for steel girders and shear bars for concrete girders. The interaction restrains free shortening of the deck and creates tensile stresses beyond the tensile capacity of the young, weak concrete. This causes cracking in the first few days of deck life. Allowing the deck to slide relative to the girders with very little frictional effect would allow for shrinkage and temperature shortening to take place freely in the deck before it is "locked in" with the girders. It is important to have a system that will allow for low friction before composite action takes effect. Thus, this project focused on methods to achieve delayed composite action as effectively as possible.

The fundamental concept is to provide open channels over the girders where shear connectors (studs or reinforcing bars) are located. These channels isolate the shear connectors while fresh concrete is placed and is allowed to hydrate, undergoing volume changes due to temperature drop in the hydration cycle and shrinkage. The next step in the process is to posttension the deck. The amount of posttensioning needed to eliminate crack-inducing tension in the deck is considerably reduced by two effects: (1) the deck is free to slide relative to the girders through means of low friction bearing, and (2) the deck is posttensioned before development of the composite action; thus the entire posttensioning force is taken up by the deck, not the deck–girder system. Also, the much stiffer girders do not share in a prestressing force they do not need or that can possibly harm them. The final step is to develop the composite action through grouting of the channels.

Scope of Work

The scope of work for the research was proposed in four tasks as follows:

1. Research the components of the encapsulated channel concept to determine the best configuration to isolate the shear studs, minimize friction restraint between the girder top flange and the deck form supports, provide space for the posttensioning, and allow for complete grouting. Select the more promising components of the CIP alternative for further investigation in the remaining tasks.
2. Develop sufficient design and detailing for the encapsulated channel concept selected in Task 1 for further investigation. (The design concentrated on the design of the frictionless contact interface between the girder top flange and the deck form supports and on complete grouting of the channel.)
3. Perform laboratory testing of details developed in Tasks 1 and 2 using a small-scale laboratory test to prove the feasibility of the concept. (The dimensions and geometry of the small-scale laboratory test specimen were to be finalized after conducting Tasks 1 and 2.)
4. Develop the scope of future research to develop detailing and design guidelines based on the results of Tasks 1, 2, and 3.

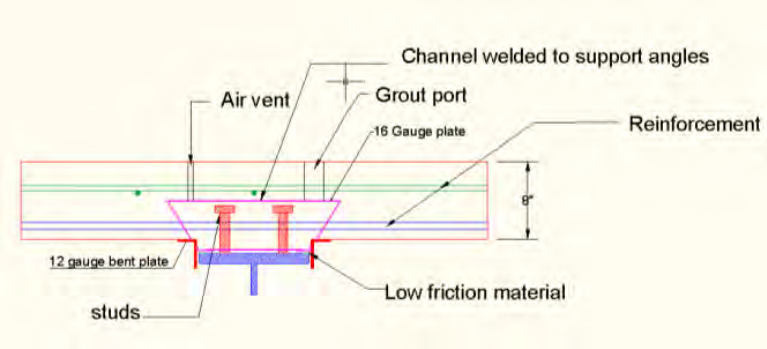

Figure 3.95. Proposed delayed composite system for interior beams.

Results

A bridge deck system was developed for delayed composite action over interior girders. The purpose of the system is to allow the concrete deck to move relative to the girder, which will prevent creep and shrinkage cracks shortly after the deck is poured. This is done by isolating the top flange of the steel girder with an enclosed apparatus that rests on a low friction bearing, allowing for movement relative to the steel girder. The channel is filled with grout after initial creep and shrinkage have occurred. Figure 3.95 shows the proposed system for interior beams.

The support angles were made from bent 12-gauge steel sheet. The channel top plate, bent plate for bearing, and lateral support strips consisted of 16-gauge steel sheet. The top plate was bent and had holes drilled for reinforcement and grout and air holes for pouring of the concrete.

Various plastics were researched as possible low-friction materials to be used between the supporting straps of the channel and the top flange of the girder. The results of the investigation identified the three most promising options as high-density polyethylene sheet, ultrahigh-molecular-weight sheet, and PTFE sheet. Test specimens were prepared as shown in Figure 3.96.

During the preparation of the test specimens it was noticed that the bent angle plate at the base of the void would rotate and bind against the sides of the top flange, increasing the friction. Greater clearance between the bent angle plate and the side of the top flange is proposed to reduce this binding friction.

The concept introduced here is applicable to interior girders only. An alternate system for delayed composite action over exterior girders has not been developed and is currently considered not viable.

Conclusions and Recommendations

The delayed composite action system for CIP systems is determined not to be viable at this time. Further research is not recommended.

Membranes for Bridge Decks

As part of the research study, a manual devoted to waterproofing was developed. The objective was to include this manual as an appendix to the *Guide*. However, it was determined that additional work was necessary before publishing the waterproofing manual. Following is a brief summary of the information in the manual.

Problem Statement

The major contributors to concrete deck deterioration are salt, water, and direct contact from traffic. One solution to these harmful factors is to protect the concrete surface by separating it from these elements with a waterproofing membrane. This solution has been addressed in both European and Canadian bridge codes. One of the most comprehensive European specifications is the guidelines on waterproofing membranes included in the handbook on bridge decks published by the

Figure 3.96. Test specimen for interior girders.

Norwegian Public Roads Administration (2009). The use of membranes in Europe is an accepted practice, but only a limited use exists in the United States. European practice does not have the level of service life issues that exists in the United States. The major difference between U.S. and European practices is that the membranes used in Europe are of a much higher quality and have higher initial costs.

Only a very limited amount of coordinated research and analysis into the waterproofing of bridge decks has been conducted in the United States. The recently published *NCHRP Synthesis of Highway Practice 425: Waterproofing Membranes for Concrete Bridge Decks* (Russell 2012) is an update of NCHRP Synthesis 220 (Manning 1995) with the same title as NCHRP Synthesis 425. The survey and literature review for NCHRP Synthesis 425 reported that most Canadian provinces and many European countries require the use of waterproofing membranes on all new bridge decks. In contrast, only 60% of U.S. state agencies reported the use of waterproofing membranes.

Bridge decks are subject to traffic wear and chloride penetration due to winter deicing salt. Concrete decks will typically develop transverse and longitudinal cracks even before they are opened to traffic. These decks are horizontal elements and, as a result, salt-laden water can easily intrude to the level of the reinforcement. In many cases, it takes only a few months before the chloride threshold at the level of the reinforcement is exceeded at these crack locations, resulting in initiation of corrosion when unprotected reinforcement is used. Asphalt overlays alone can protect concrete decks against wear; however, they do not waterproof the deck. Use of a waterproofing system is, therefore, needed to protect the concrete bridge deck from intrusion of these harmful chlorides when asphalt overlays are used.

There are several principle classes of waterproofing for bridge decks. The level of traffic (wear) and climate (chlorides) in which the bridge is located are among the two major factors dictating the type of waterproofing system that should be selected. The following systems can be considered:

- Asphalt overlay directly applied to concrete deck is subject to leakage, and therefore provides resistance against wear from traffic only.
- Low-viscosity epoxy, silane, or siloxane sealers can seal the cracks, but they provide a limited lifespan for protection against chloride ingress and corrosion.
- Concrete-based overlays provide a layer of material over the bridge deck with low permeability that can provide resistance to chloride intrusion. However, these overlays are prone to cracking and delamination. Research studies are being carried out to examine the feasibility of using a very thin layer of ultrahigh-performance concrete as overlay (Harris et al. 2011).
- Membrane systems combined with an asphalt overlay provide resistance against wear and chloride intrusion.

A good-quality membrane together with an asphalt overlay can be very effective in providing resistance to both wear and chloride intrusion. The life of the overlay system and membrane will be much less than 100 years; however, this system has many advantages:

- The asphalt overlay can be milled and resurfaced as needed without replacement of the membrane, depending on the wear life of the asphalt.
- The replacement or repair of the membrane may be a relatively simple task.
- Concrete protected by a membrane can provide a very long service life.
- If designed and installed correctly, the membrane can protect the concrete deck for a long period.

The European experience indicates that the service life of a well-designed and correctly installed membrane can be more than 30 years and may extend to 60 years with a special system (NCHRP 1996).

In the United States, the expected service life of waterproofing membranes is generally 16 to 20 years when installed on new bridge decks and anywhere between 6 and 20 years when installed on existing bridge decks (Russell 2012).

The level of traffic and climate are not the only factors that should be used for selecting waterproofing. A particular construction type may result in the development of weak areas within a concrete deck. In phase-constructed bridges, construction joints or closure pours (or both) between phases can result in the development of longitudinal and transverse cracking. Use of a membrane system in the closure pour region could be an effective approach for eliminating many corrosion problems reported in conjunction with phase-constructed and modular system bridges.

Objective

The objective of this topic was to develop the best strategies for waterproofing concrete deck systems with membranes for various conditions and to develop a methodology for predicting the service life of different systems.

Scope of Work

The scope of the work to achieve the objective of this topic included collecting the available information with respect to use of membrane systems in the United States and Europe and developing the first edition of a best practices manual for waterproofing concrete deck systems.

Results

A draft version of the best practices manual for membrane use in U.S. practice was developed in cooperation with industry. However, the research team felt that additional work needs to be carried out before publishing the work. Following is a summary of some of the findings.

Concrete bridge decks are structurally compromised, and their longevity reduced, by exposure to liquid water, chloride, and carbon dioxide ingress. Their vulnerability is increased in more northern regions where deicing salts are used in winter, and the concrete becomes more susceptible to cracking from thermal cycling.

The cost of maintenance of a bridge deck over time can be significantly reduced if a greater initial investment is made by the use of a higher standard of membrane at the time of construction or rehabilitation.

Many U.S. state agencies do not use any waterproofing on their bridges.

To provide optimum performance, the waterproofing system must be compatible with the surface quality of the substrate and with the asphalt paving.

The NCHRP Synthesis 425 survey revealed several types of defects observed with waterproofing membranes, predominantly a lack of adhesion between the membrane and the concrete deck, a lack of adhesion between the membrane and the asphalt surface, and moisture penetrating through the membrane. All types of defects were more prominent with membranes applied to existing bridge decks than with membranes applied to new bridge decks. Most manufacturers recommend a primer on the concrete deck and a tack coat on the waterproofing membrane to improve the adhesion between the layers.

Development and Brief Content of *Design Guide for Bridges for Service Life*

The results and essence of the entire research effort were incorporated into a single document for service life design of bridges, the *Design Guide for Bridges for Service Life* (the *Guide*).

This section of the final report provides a summary of the philosophy, content, and general framework used in the *Guide*. The *Guide* is a stand-alone document and the project's main product. Close collaboration was maintained with the AASHTO T-9 bridge subcommittee while developing the *Guide*.

Introduction

The design for service life should be approached in a systematic manner and must be transparent to the owner. It must provide the owner with a clear picture of the costs required to keep the bridge functional during the entire target service life of the bridge, with a clear roadmap for timely interventions and any other actions needed.

The traditional approaches for enhancing the service life of bridges used in various codes, such as the *AASHTO LRFD Specifications, Eurocode,* or *British Standards,* are mainly in an indirect form, specifying use of certain details such as cover thickness, crack width, and concrete compressive strength. Although such information is useful, it is not adequate to design for service life in a systematic manner.

The design for service life for bridges should be approached in a systematic manner and not as a series of isolated tasks, each addressing the service life of a particular portion of the bridge. The bridge maintenance program, retrofit or replacement options, and an overall management plan should all be part of this systematic service life design approach.

It was concluded that the major missing element for designing bridges for service life was the absence of a framework that would allow the problem to be approached in a systematic manner and provide a complete solution in a format that could ensure long-lasting bridges. Individual solutions for given details that have historically reduced service life of bridges, a maintenance plan, a retrofit plan or replacement plan, and bridge management and life-cycle cost analysis are components of this systematic framework, but they are not the framework itself. The framework steps should begin during the design stage and should provide the owner with complete information for ensuring the serviceability of the bridge for a specified target service life. It is important that the resulting systematic plan be transparent and identify the challenges for the period of specified service life at the design stage. It should also eliminate surprises for the owner for the period of specified service life.

Guide Approach to Design for Service Life

A major aspect of assessing the merits of any feasible alternative bridge system for a given job is addressing the service life design considerations. A general framework for a systematic approach to design for service life requires the following main elements:

- Identifying a feasible bridge system;
- For each feasible bridge system, identifying the element, component, and subsystems that should be considered for service life design;
- Identifying the factors that can affect the service life of different elements, components, and subsystems;
- Identifying various strategies that could mitigate adverse effect(s) of factors capable of reducing service life;
- Selecting the optimum strategies considering interaction among various strategies;

- Predicting the service life of various bridge elements, components, or subsystems; and
- Using life-cycle cost analysis to develop maintenance, retrofit, or replacement plans for bridge elements, components, and subsystems, such that the bridge as a system can provide the desired service life.

The *Guide* uses the above approach and, when appropriate, communicates the information using flowcharts to ensure the transparency of the process. Figure 3.97 shows an example of a flowchart used in the *Guide* that can facilitate the service life design process.

The factors affecting the service life of particular elements, components, or subsystems of a bridge can be identified using a fault tree, which provides a systematic method of identifying factors in various categories and successive subcategories. The *Guide* uses fault tree analysis to identify the factors that can affect the service life of a particular bridge.

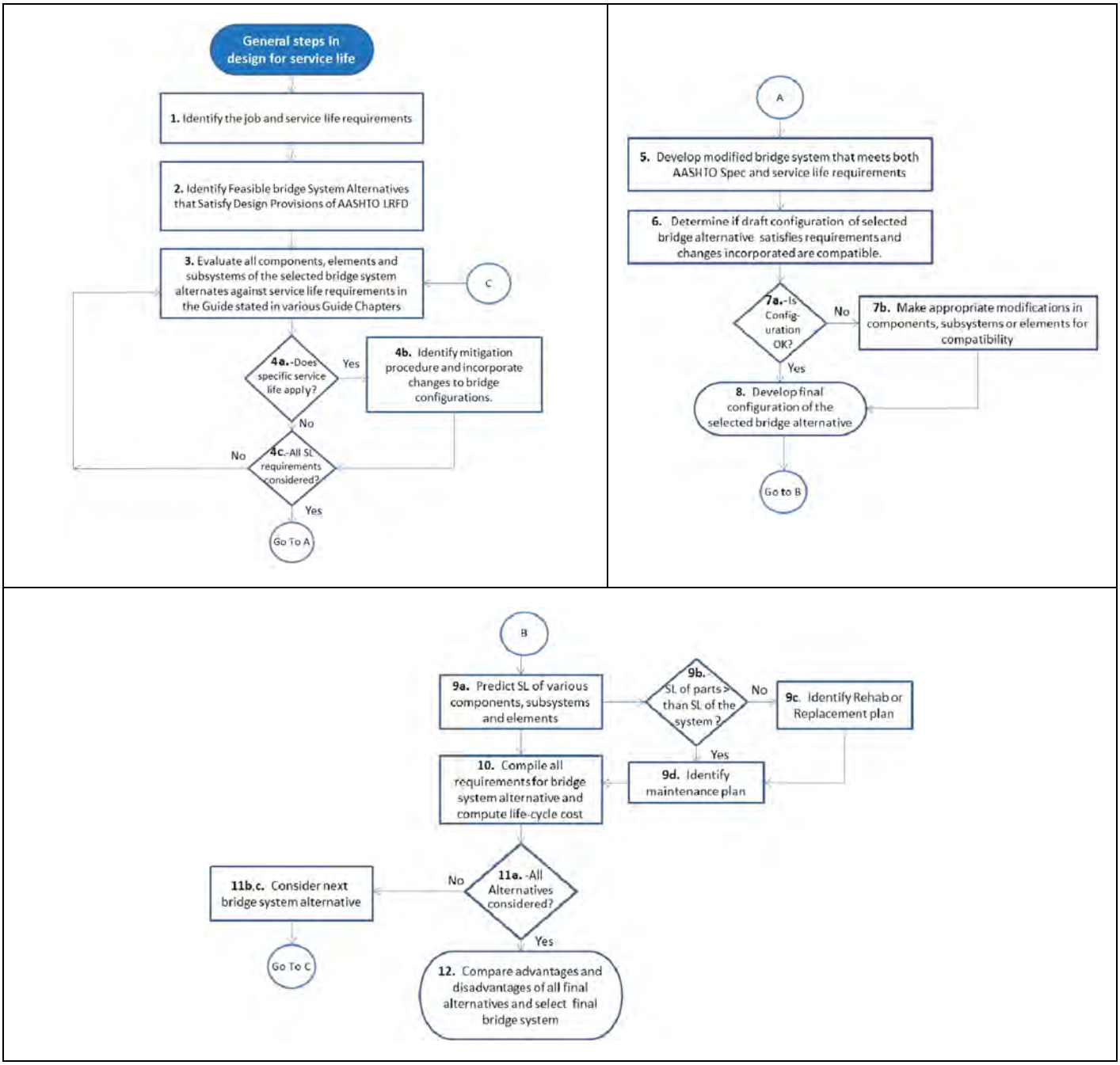

Figure 3.97. Example of flowcharts that can be used in service life design processes.

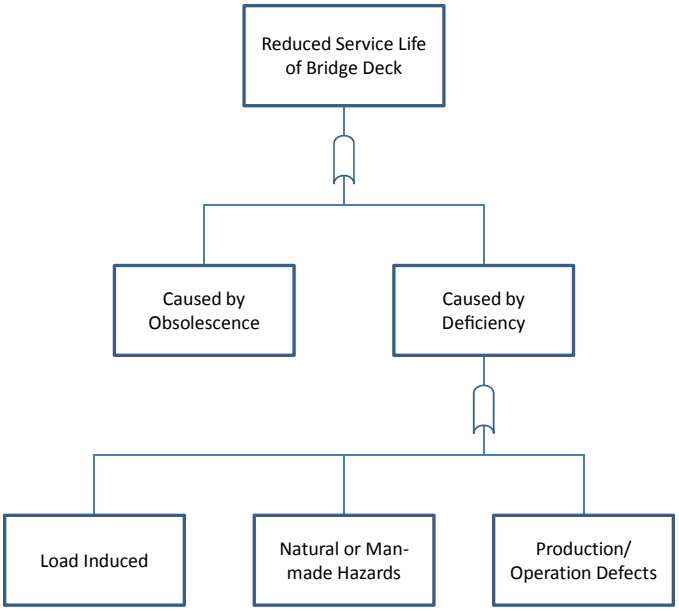

Figure 3.98. Starting point for fault tree.

Figure 3.98 and Figure 3.99 show portions of a fault tree used in the *Guide* to assist in the design of bridge decks for service life.

In Figures 3.98 and 3.99, the factors inside the circles are the most basic factors capable of reducing the service life. For these basic factors, an array of strategies capable of mitigating adverse service life effects should be identified, and the optimum strategy selected. Based on the results of the study, the *Guide* provides strategies capable of mitigating various factors that can reduce the service life of bridges. As an example, Table 3.20 shows some of the strategies and their advantages and disadvantages, listed in the *Guide*, for some of the basic factors identified in Figure 3.99.

Constructing the fault tree and identifying feasible and cost-effective strategies and solutions for a particular service life issue are dependent on many factors that vary from location to location and state to state, and also depend on local practices and preferences. Consequently, the end result of the service life design process does not necessarily need to be the development of a unique solution.

Identifying possible solutions and strategies to mitigate factors affecting service life could be based on data collected by local DOTs or agencies responsible for the bridge. The life-cycle cost analysis should be included in the strategy selection process and should include design, maintenance, inspection, retrofit, replacement, and user cost to be complete.

It is important that the entire service life design process be communicated and shared with the owner, especially with respect to the life-cycle cost analysis portion of the process. The entire process should be transparent.

In identifying the array of strategies to mitigate factors capable of adversely affecting service life, it should be noted that there are different ways of achieving enhanced service life of existing and new bridges. Enhancement of service life can be accomplished by using improved, more durable materials and systems during original construction that will require minimal maintenance or by improving techniques and optimizing the

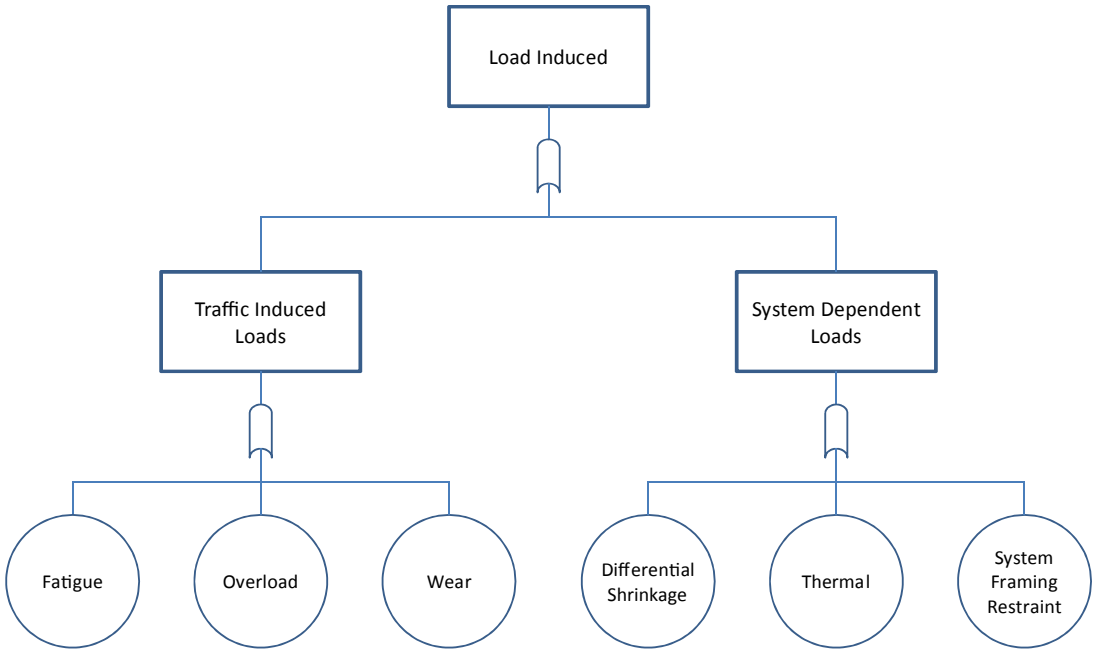

Figure 3.99. Continuation of fault tree for load-induced factor shown in Figure 3.98.

Table 3.20. Possible Mitigating Strategies for Various Service Life Issues for Traffic-Induced Loads

Service Life Issue	Mitigating Strategy	Advantages	Disadvantages
Fatigue	Design per AASHTO *LRFD Bridge Design Specifications*	Minimizes possibility of reinforcement failure	May increase area of steel
Overload	Increase deck thickness	Minimizes cracking	Adds weight to bridge structure, increases cost
Overload	Minimize bar spacing for given amount of steel	Improves crack control	Does not add to strength. Higher labor. More prone to corrosion and difficult to construct
Wear and Abrasion	Implement concrete mix design strategies	Identified in Chapter 4, Materials	Identified in Chapter 4, Materials
Wear and Abrasion	Implement membranes and overlays	Protects surface from direct contact with tires	Requires periodic rehabilitation every 5 to 10 years

timing of interventions such as preventive maintenance actions. Interventions can be planned and carried out based on an assessment of individual bridge conditions and needs or based on a program of preventive maintenance actions. By acknowledging that service life can be extended by either using more durable, deterioration-resistant materials or by planned intervention, a cost comparison can be made to determine the most cost-effective approach for various environmental exposure levels and various levels of available maintenance and preservation actions.

Guide Approach for Predicting Service Life of Bridge Elements, Components, or Subsystems

An important step in the design for service life specified in the *Guide* is the ability to predict the service life of various bridge elements, components, or subsystems. If deterioration models are available, they can be used to predict service life. Other approaches could include the use of data collected over the years by local agencies capable of developing deterioration models, expert opinion, or use of strategies that could avoid deterioration (avoidance of deterioration method) altogether.

Summary of *Guide* Steps for Design for Service

Bridge elements, components, and subsystems deteriorate at different rates and have different service lives. The service life of a bridge system is governed by the service life of its critical elements, components, and subsystems. The service life of a bridge system is reached when the service life of critical bridge elements, components, or subsystems is reached, including the ability to repair or replace them economically, or because of other considerations.

The *Guide* provides very detailed instruction on steps that are needed in the design for service life process. The following is a brief summary of these steps.

Step 1. Identify the project requirements, particularly those that will influence the service life.

Step 2. Identify feasible bridge systems capable of meeting the project demand.

Step 3. Select each feasible bridge system one at a time and carry out Steps 4 through 10.

Step 4. Identify the factors that influence the service life of bridge elements, components, and subsystems, such as traffic and environmental factors.

Step 5. Identify modes of failures and consequences (e.g., the corrosion of reinforcement, causing corrosion-induced cracking and loss of strength).

Step 6. Identify suitable approaches for mitigating the failure modes or assessing the risk of damage (e.g., through life-cycle cost analysis) of the use of higher-performing materials for sliding surfaces in bearings or the use of material prone to deterioration at lower initial cost.

Step 7. Modify the bridge element, component, or subsystem under consideration by using the selected strategy, and ensure the compatibility between different strategies used for various bridge elements, components, or subsystems.

Step 8. Estimate the service life of the bridge element, component, or subsystem using available data.

Step 9. Compare the service life of the bridge element, component, or subsystem to the service life of the bridge system and develop appropriate maintenance, retrofit, and replacement plans.

Step 10. Develop the design, fabrication, construction, operation, maintenance, replacement, and management plans for achieving the specified design life for the bridge system.

Step 11. Conduct life-cycle cost analysis for each feasible bridge system meeting strength and service life requirements, and select the optimum bridge system.

Step 12. When specified by the owner or for unique bridges, document the entire design for service life processes in a document called an Owner's Manual. Conduct an independent review of the document and provide it to bridge owner at the time of opening the bridge to traffic.

Owner's Manual for Service Life Design

The *Guide* suggests providing an Owner's Manual for unique bridges or when required by the owner that summarizes the entire design for service life process and recommendations. The purpose of the manual is to equip owners with the complete knowledge necessary to keep the bridge operational for the specified service life period. The Owner's Manual should be provided to the bridge owner at the time of opening the bridge to traffic.

The entire design for service life must be well documented and must include assumptions, limitations, and other information of which the owner should be aware. The *Guide* suggests that the Owner's Manual include complete information with respect to "hot spots" for more detailed or frequent inspections, as well as maintenance, retrofit, or replacement information for various bridge features. The manual should also include a complete management plan with respect to service life that provides information on timely maintenance actions and identifies the replacement parts and methodologies for replacement with information on the level of interruption, if any, to traffic. For unique bridges the *Guide* suggests that a bridge instrumentation and monitoring plan be developed and be correlated with the bridge service life management plan. Additional information in the Owner's Manual should include the material properties in critical bridge elements, components, or subsystems as used during construction versus the assumed values during the design process. This information will be important for rating bridges.

For unique bridges the *Guide* suggests that the designer exercise good engineering judgment for incorporating detail and the extent of information to be included in the owner's manual. The bridge Owner's Manual may be considered as an equivalent of a design calculation document, customarily provided to the bridge owner, except that it contains much more detailed information. The *Guide* also suggests that an independent review of the Owner's Manual be carried out before submitting it to the Owner.

CHAPTER 4

Summary, Conclusion, and Recommendations

The main objective of SHRP 2 Project R19A, Bridges for Service Life Beyond 100 Years: Innovative Systems, Subsystems and Components, was to develop the methodology and means to design bridges for service life. The term "100 years" in the original project title represents a vision in which enhanced service life of bridges is achieved. In the early stages of the research, it was not clear what form the ultimate product or result of the project would be. To gather information regarding the state of knowledge for service life, the research team searched both published and unpublished data in the United States and abroad. This extensive search indicated that currently there is no comprehensive document that can be used to design bridges for service life in a manner similar to design for strength, which is provided by the *LRFD Specifications*.

During this search one point became evident. In some cases, designers, or even specifications, were referring to design of concrete for durability and service life as design of bridges for service life. It is very important to recognize that a bridge as a system contains many parts that are not concrete, and although design of concrete portions for service life is important, it is not by itself equivalent to design of overall bridges for service life.

Review of the state of knowledge also indicated that a general framework or systematic approach that could be used as a basis for designing bridges for service life is lacking.

Consequently, the following important questions were raised:

1. What are the service life issues?
2. What are the knowledge gaps with respect to service life?
3. What framework should be used to design bridges for service life?
4. How should the design for service life be communicated to end users?

An extensive amount of work was carried out to identify and comprehend the issues that have historically resulted in reduced service life for bridges. A summary of this work is provided in Chapters 2 and 3.

In evaluating the knowledge gaps, the study identified a significant number of issues that needed additional research to develop practical solutions. Considering the project limitations, the original request for proposal asked for only proof of concept testing to evaluate possibilities. In this case, proof of concept refers to a process in which a solution to a given problem is identified; limited testing is conducted to examine the feasibility of the concept; and if appropriate, further research is recommended for others to complete the development of the concept. Following this approach, the project prioritized a number of needed research topics into three categories. Topics in Categories 1 and 2 were addressed within this project; no work was carried out on Category 3 topics. Chapter 3 provides a summary of Category 1 and 2 topics, and Appendix A describes Category 3 topics.

One of the major study observations was that although eliminating movable or expansion joints was recognized by many to be the most effective approach to enhance bridge service life, there was no corresponding scientific approach to design jointless bridges.

At this point in the project, the research team was faced with two important questions (Questions 3 and 4 listed above): How should design for service life be approached? and How should the information about service life design be communicated to the end users? The team ultimately concluded that development of the *Design Guide for Bridges for Service Life* was the answer. The *Guide* is now available through TRB (http://www.trb.org/Design/Blurbs/168760.aspx).

The main objective of the *Guide* is to provide information about, and define procedures for, systematically designing both new and existing bridges for service life and durability. The *Guide*'s initial approach to designing for service life is to provide a body of knowledge relating to bridge durability under different exposure conditions and constraints and to establish an array of options capable of enhancing service life

relative to those conditions. However, the philosophy used in the *Guide* could also be used to establish a plan for designing a specific bridge for service life by customizing certain steps within the framework.

In general application, the *Guide* is not intended to dictate a unique solution for any specific service life problem or identify the "best and only" solution, unless it is used to establish a plan for the service life design of a specific bridge. The *Guide* does not include discussions on the application of the framework for the service life design of specific bridges. Further work is needed to elaborate on the steps for customizing the *Guide* for specific bridges, especially for signature and long-span bridges.

The *Guide* recognizes that not all bridges can or need to have 100 years of service life. Therefore, maintenance, rehabilitation, and replacement are part of the service life design process.

Included in the *Guide* are 11 chapters, each devoted to particular bridge elements, components, subsystems, or systems. Collectively, these chapters provide a basis for approaching service life design in a logical and systematic manner.

The vision to develop the *Guide* was born from the need to have a single reference for integrating the many related activities that are necessary to keep a bridge in service for a specified period of time. Closer examination of the *Guide* reveals this vision of an integrated approach, in which the design of a bridge is viewed in a holistic manner. The current concept of design, for the most part, refers to checking supply and demand with respect to strength on an individual element basis. In contrast, design of a bridge should be viewed as a process in which a structure, on a total-system basis, is created to last a specified period of time. For a bridge to last and provide its intended function for a specified period of time, it is necessary to consider more than just strength parameters.

There is a need for future development of the *Guide.* However, further development should be undertaken only after having a comprehensive blueprint for its final state, as the evolution of the *Guide* will be incremental. Each incremental development should be a step in turning the *Guide* into a document that can provide comprehensive procedures to design, construct, and keep bridges in service for specified periods of time. Further development of the *Guide* should not be approached as simply updating chapters and incorporating missing data. Instead, integrating the various activities necessary to keep a bridge functional for a specified period of time should be the objective. Future development of the *Guide* should focus on seamlessly connecting the activities of design, fabrication, construction, inspection, maintenance, and retrofit. Currently, several independent documents govern design, fabrication, construction, and management of bridges, and each of these steps has its own governing specifications. The roadmap for future development of the *Guide* should be constructed such that the divisions and boundaries between each of these stages are eliminated, and the entire process of keeping a bridge in service for a specified period of time is seamlessly connected and transparent to the owner.

The *Guide* also contains significant amounts of information that may not be needed or relevant for certain agencies. For instance, in rural areas or smaller municipalities where there are many short-span bridges, customized and reduced versions of the *Guide* may better serve the local bridge community. For longer-span or more complex bridges, higher expectations with respect to service life and more corresponding information will be required.

The main elements missing from the first edition of the *Guide* are detailed examples and tools capable of demonstrating how to apply and navigate through the massive amount of information provided. The development of these tools and examples should not take place in a vacuum and should be done in cooperation with the bridge community.

This final report and the *Guide* also include several innovative ideas, details, and design procedures. These new ideas are mainly placed in the appendices, signifying that these ideas have not yet been used in practice and that their use should be approached with caution.

References

AASHTO. 1996. *AASHTO Standard Specifications for Highway Bridges,* 16th ed. American Association of State Highway and Transportation Officials, Washington, D.C.

AASHTO. 2004. *AASHTO LRFD Bridge Design Specifications,* 3rd ed. American Association of State Highway and Transportation Officials, Washington, D.C.

AASHTO. 2010a. *AASHTO LRFD Bridge Construction Specifications,* 3rd ed. American Association of State Highway and Transportation Officials, Washington, D.C.

AASHTO. 2010b. *AASHTO LRFD Bridge Design Specifications,* 5th ed. American Association of State Highway and Transportation Officials, Washington, D.C.

Abendroth, R. E., L. F. Greimann, and P. E. Ebner. 1989. Abutment Pile Design for Jointless Bridges. *Journal of Structural Engineering,* Vol. 115, No. 11, pp. 2914–2929.

ACI. 1997. *Cracking of Concrete Members in Direct Tension.* ACI 224.2R-92. Committee 224, American Concrete Institute, Farmington Hills, Mich.

ACI 224R. 2001. *Control of Cracking in Concrete Structures.* ACI 224R-01. American Concrete Institute, Farmington Hills, Mich.

ACI 365. 2000. *Service-Life Prediction.* ACI 365R-00. American Concrete Institute Committee 365, ACI, Farmington Hills, Mich.

ACI 546. 2006. *Guide for the Selection of Materials for the Repair of Concrete.* ACI 546.3R-06. American Concrete Institute Committee 546, ACI, Farmington Hills, Mich.

Ala, N. 2011. *Seamless Bridge System for the U.S. Practice.* PhD dissertation. University of Nebraska–Lincoln.

Ala, N., and A. Azizinamini. 2013a. Analytical Study and Design Provisions for Seamless Bridge System for the U.S. Practice. Submitted for publication to *Journal of Bridge Engineering.*

Ala, N., and A. Azizinamini. 2013b. Experimental Study of New Seamless Bridge System. Submitted for publication to *Journal of Bridge Engineering.*

Ala, N., E. Power, and A. Azizinamini. 2013a. Experimental Evaluation of High Performance Sliding Surfaces. Submitted for publication to *Journal of Bridge Engineering.*

Ala, N., E. Power, and A. Azizinamini. 2013b. Predicting Service Life of Sliding Surfaces in Bridge Bearing Devices. Submitted for publication to *Journal of Bridge Engineering.*

Alampalli, S., G. Schongar, and H. Greenberg. 2004. In-Service Performance of an FRP Superstructure. FHWA/NY/SR-94/141. New York State Department of Transportation.

Ardani, A., J. Mallela, and G. Hoffman, G. 2010. Oregon Demonstration Project: Alternate Project Delivery and Accelerated Bridge Construction on OR 38, Drain to Elkton. Washington, D.C.: Federal Highway Administration.

Arminox. 1999. *Pier in Progreso, Mexico: Inspection Report. Evaluation of the Stainless Steel Reinforcement.* http://www.arminox.com/Files/Filer/Arminox%20doks/Arminox_Progreso_Inspec_Report_web.pdf. Accessed Nov. 19, 2013.

Arockiasamy, M., N. Butrieng, and M. Sivakumar. 2004. State-of-the-Art of Integral Abutment Bridges: Design and Practice. *Journal of Bridge Engineering,* Vol. 9, No. 5, pp. 497–506.

Arockiasamy, M., and M. Sivakumar. 2005. Effects of Restraint Moments in Integral Abutment Bridges. *Integral Abutment and Jointless Bridges: The 2005 FHWA Conference,* Baltimore, Md., pp. 185–198.

Astaneh-Asl, A., B. Bolt, K. M. McMullin, R. R. Donikian, D. Modjtahedi, and S. Cho. 1994. *Seismic Performance of Steel Bridges During the 1994 Northridge Earthquake.* Report UCB/CE-STEEL-94-01. Department of Civil and Environmental Engineering, University of California, Berkeley.

ASTM B348. 2011a. Standard Specification for Titanium and Titanium Alloy Bars and Billets. ASTM International, West Conshohocken, Pa.

ASTM A955. 2011b. Standard Specification for Deformed and Plain Stainless-Steel Bars for Concrete Reinforcement. ASTM International, West Conshohocken, Pa.

ASTM A1010-01. 2001. Standard Specification for Higher-Strength Martensitic Stainless Steel Plate, Sheet, and Strip. ASTM International, West Conshohocken, Pa.

ASTM C192. 2007a. Standard Practice for Making and Curing Concrete Test Specimens in the Laboratory. ASTM International, West Conshohocken, Pa.

ASTM C192. 2007b. Standard Practice for Making and Curing Concrete Test Specimens in the Laboratory, ASTM International, West Conshohocken, Pa.

ASTM C876. 2009. Standard Test Method for Corrosion Potentials of Uncoated Reinforcing Steel in Concrete. ASTM International, West Conshohocken, Pa.

ASTM C881. 2010. Specification for Epoxy-Resin-Base Bonding Systems for Concrete. ASTM International, West Conshohocken, Pa.

ASTM G109. 2007a. Standard Test Method for Determining the Effects of Chemical Admixtures on the Corrosion of Embedded Steel Reinforcement in Concrete Exposed to Chloride Environments. ASTM International, West Conshohocken, Pa.

ASTM G109. 2007b. Standard Test Method for Determining Effects of Chemical Admixtures on Corrosion of Embedded Steel Reinforcement in Concrete Exposed to Chloride Environments. ASTM International, West Conshohocken, Pa.

Azizinamini, A. 2008. *Proc., 2008 Accelerated Bridge Construction: Highway for Life Conference.* Federal Highway Administration, Baltimore, Md.

Azizinamini, A. 2013. Overview of the Simple for Dead–Continuous for Live Bridge System. Submitted for publication to *Engineering Journal.*

Azizinamini, A., and S. K. Ghosh. 1997. Steel-Reinforced Concrete Structures in 1995 Hyogoken-Nanbu Earthquake. *Journal of Structural Engineering,* Vol. 123, No. 8, pp. 986–992.

Azizinamini, A., and A. J. Yakel. 2005. Innovative Steel Bridge System for Short Span Bridges to Accelerate Construction. *Proc., 2005 FHWA Accelerated Bridge Construction Conference: Path to Future,* San Diego, Calif.

Azizinamini, A., and A. Yakel. 2006. Delayed Development of Composite Action in Steel Girder Bridges. *Journal of Bridge Structures,* Vol. 2, No. 3, pp. 119–132.

Azizinamini, A., and J. Gull. 2012a. *Improved Inspection Techniques for Steel Prestressing/Post-Tensioning Strand.* Final report. BDK80 977-13, Vol. I. Florida Department of Transportation, Tallahassee.

Azizinamini, A., and J. Gull. 2012b. *Florida Department of Transportation Protocol for Condition Assessment of Steel Strands in Post-Tensioned Segmental Concrete Bridges.* Final report. BDK80 977-13, Vol. II. Florida Department of Transportation, Tallahassee.

Azizinamini, A., N. J. Lampe, and A. J. Yakel. 2003. *Toward Development of a Steel Bridge System: Simple for Dead Load and Continuous for Live Load.* Final report. Nebraska Department of Roads and National Bridge Research Organization, Lincoln.

Azizinamini, A., A. J. Yakel, and S. Javidi Niroumand. 2008. Use of Steel Bridge System with Continuity for Live Load Only in Conjunction with Conventional and Accelerated Bridge Construction Methodologies. *Proc., 2008 Accelerated Bridge Construction: Highway for Life Construction,* Federal Highway Administration, Baltimore, Md., pp. 107–114.

Azizinamini, A., A. J. Yakel, and J. P. Swendroski. 2003. *Development of a Design Guide for Phase Construction of Steel Girder Bridges.* NDOR Project No. SPR-PL-1 (038) P530. National Bridge Research Organization, Department of Civil Engineering, University of Nebraska–Lincoln.

Badie, S. S., M. K. Tadros, and K. E. Pedersen. 2001. Re-Examination of I-Girder/Pier Connection in Jointless Bridges. *PCI Journal,* March–April, pp. 62–74.

Bakht, B., L. G. Jaeger, and M. S. Cheung. 1983. Transverse Shear in Multi-Beam Bridges. *Journal of Structural Engineering,* Vol. 109, No. 4, 1983, pp. 936–949.

Bard, A. and L. Faulkner. 2001. *Electrochemical Methods: Fundamentals and Applications,* 2nd ed. John Wiley and Sons, Inc., New York.

Barnhart, R. A. 1982. FHWA Position on Cathodic Protection. Memorandum. Federal Highway Administration.

Bennett, J., T. J. Schue, K. C. Clear, D. L. Lankard, W. H. Hartt, and W. J. Swiat. 1993. *Electrochemical Chloride Removal and Protection of Concrete Bridge Components: Laboratory Studies.* SHRP-S-65. Strategic Highway Research Program, National Research Council, Washington, D.C.

Bentz, D. P., M. A. Peltz, K. A. Snyder, and J. M. Davis. 2009. VERDICT: Viscosity Enhancers Reducing Diffusion in Concrete Technology. *Concrete International,* Vol. 31, No. 1, pp. 31–36.

Bentz, D. P., and W. J. Weiss. 2011. *NISTIR 7765: Internal Curing: A 2010 State-of-the-Art Review.* National Institute of Standards and Technology, Gaithersburg, Md.

Birgisson, B. 2006. Nanomodification of Cement Paste to Improve Bulk Properties of Concrete. National Science Foundation Workshop on Nanomodification of Cementitious Materials, University of Florida, Gainesville, Aug. 8–11.

Brena, S. F., C. Bonczar, S. Civjan, J. T. DeJong, and D. S. Crovo. 2007. Evaluation of Seasonal and Yearly Behavior of an Integral Abutment Bridge. *Journal of Bridge Engineering,* Vol. 12, No. 3, pp. 296–305.

Bridge, R., S. Griffiths, and G. Bowmaker. 2005. The Concept of a Seamless Concrete Pavement and Bridge Deck. In *Australian Structural Engineering Conference 2005* (M. G. Stewart and B. Dockrill, eds.), Sydney, N.S.W., Australia, pp. 289–298.

Bruneau, M., J. W. Wilson, and R. Tremblay. 1996. Performance of Steel Bridge During the 1995 Hyogoken-Nanbu (Kobe, Japan) Earthquake. *Canadian Journal of Civil Engineering,* Vol. 23, No. 23, pp. 678–713.

BSI. 2012. *Cathodic Protection of Steel in Concrete.* BS EN ISO 12696:2012. British Standards Institution. February.

Burke, M. P., Jr. 1990. Integral Bridges. In *Transportation Research Record 1275,* TRB, National Research Council, Washington, D.C., pp. 53–61.

Burke, M. P., Jr. 1996. An Introduction to the Design and Construction of Integral Bridges. Workshop on Integral Bridges, Federal Highway Administration, West Virginia Department of Transportation and West Virginia University, Nov. 13–15.

Burke, M. P., Jr. 2009. *Integral and Semi-Integral Bridges.* Wiley-Blackwell.

Caltrans. 2008. Seismic Design Criteria, Version 1.4. August.

Campbell, T. I., and W. L. Kong. 1987. *TFE Sliding Surfaces in Bridge Bearings.* Report No. ME-87-06. Ministry of Transportation and Communications, Research and Development, Report No. ME-87-06, Downsview, Ontario, Canada.

Caner, A. 1996. *Analysis and Design of Jointless Bridge Decks Supported by Simple-Span Girders.* PhD dissertation. North Carolina State University, Raleigh.

Caner, A., and P. Zia. 1998. Behavior and Design of Link Slabs for Jointless Bridge Decks. *PCI Journal,* Vol. 43, pp. 68–80.

CEB-FIP. 1993. *CEB-FIP Model Code 1990.* Redwood Books, Trowbridge, Wiltshire, United Kingdom.

Chang, L. M., and Y. J. Lee. 2001. *Evaluation and Policy for Bridge Deck Expansion Joints.* FHWA/IN/JTRP-2000/1. Joint Transportation Research Program, Indiana Department of Transportation and Purdue University, West Lafayette.

Chang, L. M., and Y. J. Lee. 2002. Evaluation of Performance of Bridge Deck Expansion Joints. *Journal of Performance of Constructed Facility,* Vol. 16, No. 1, pp. 3–9.

Chen, R., and J. A. Yura. 1995. *Wax Build-Up on the Surfaces of Natural Rubber Bridge Bearings.* Research Report 1304-4. Center for Transportation Research, University of Texas, Austin.

Chong, K. P., and E. J. Garboczi. 2002. Smart and Designer Structural Material Systems. *International Journal of Progress in Structural Engineering and Materials,* Vol. 4, No. 4, pp. 417–430.

Chung, R. (ed.). 1996. The January 17, 1995 Hyogoken-Nanbu (Kobe, Japan) Earthquake Performance of Structures, Lifelines, and Fire Protection Systems. *NIST Special Publication 901.* Building and Fire Research Laboratory, National Institute of Standards and Technology, Gaithersburg, Md.

Civjan, S. A., C. Bonczar, S. F. Brena, J. DeJong, and D. Crovo. 2007. Integral Abutment Bridge Behavior: Parametric Analysis of a Massachusetts Bridge. *Journal of Bridge Engineering,* Vol. 12, No. 1, pp. 64–71.

Clemeña, G. G. 2003. *Investigation of the Resistance of Several New Metallic Reinforcing Bars to Chloride-Induced Corrosion in Concrete.* VTRC 04-R7. Virginia Transportation Research Council, Charlottesville, December.

Clemeña, G., and D. R. Jackson. 1997. Pilot Applications of Electrochemical Chloride Extraction on Concrete Bridge Decks in Virginia.

In *Transportation Research Record 1597,* TRB, National Research Council, Washington, D.C., pp. 70–76.

Clifton, J. R. 1991. *Predicting Remaining Service Life of Concrete.* NISTIR 4712. National Institute of Standards and Technology, Gaithersburg, Md.

Clifton, J. R., and L. I. Knab. 1989. *Service Life of Concrete.* NISTIR 89-4086. U.S. Department of Commerce.

Connal, J. 2003. Integral Abutment Bridges: Australian and US Practice. Seminar on Design and Construction of Integral Bridges, PWD Malaysia, 12th International Conference of the Road Engineering Association of Malaysia (REAM), Kuala Lumpur, Malaysia. July.

da Silva, M. Ferreira. 2011. Development of Self-Stressing System for Bridge Application with Emphasis on Precast Panel Deck System. PhD dissertation. University of Nebraska–Lincoln.

Davidson, E., D. W. White, and L. Kahn. 2012. *Evaluation of Performance and Maximum Length of Continuous Decks in Bridges, Part 2.* Final report. Office of Materials and Research, Georgia Department of Transportation, Atlanta, August.

de Ibarra, Y. S., J. J. Gaitero, E. Erkizia, and I. Campillo. 2006. Atomic Force Microscopy and Nanoindentation of Cement Pastes with Nanotube Dispersions. *Physica Status Solidi A,* Vol. 203, No. 6, pp. 1076–81.

Dexter, R. J., W. J. Wright, and J. W. Fisher. 2004. Fatigue and Fracture of Steel Girders. *Journal of Bridge Engineering,* Vol. 9, No. 3, pp. 278–286.

Donachie, M. J. 2000. *Titanium: A Technical Guide.* ASM International, Materials Park, Ohio.

Doust, S. E. 2011. *Extending Integral Concepts to Curved Bridge Systems.* PhD dissertation. University of Nebraska–Lincoln.

Doust, S. E., and A. Azizinamini. 2011a. End Displacements in Curved Steel I-Girder Integral Abutment Bridges. Submitted for publication to *Journal of Bridge Engineering.*

Doust, S. E., and A. Azizinamini. 2011b. Optimum Pile Orientation in Straight and Curved Steel I-Girder Integral Abutment Bridges. Submitted for publication to *Journal of Bridge Engineering.*

DuPont de Nemours Co. *Design of Neoprene Bridge Bearing Pads.* Wilmington, D.C., 1959.

Durham, R. A., and M. O. Durham. 2005. Cathodic Protection: Consequences and Standards from Using CP Systems to Prevent Corrosion. *Industry Applications Magazine,* IEEE, Vol. 11, No. 1, pp. 41–47.

Eggert, H., J. Grote, and W. Kauschke. *Lager im Bauwesen.* 1981. *Bearings in Civil Engineering.* Wilhelm Ernst and Sohn, Berlin (English translation).

Elremaily, A., and A. Azizinamini. 2001a. Design Provisions for Connections Between Steel Beams and Concrete Filled Tube Columns. *Journal of Constructional Steel Research,* Vol. 57, No. 9, pp. 971–995.

Elremaily, A., and A. Azizinamini. 2001b. Experimental Behavior of Steel Beam to CFT Column Connections. *Journal of Constructional Steel Research,* Vol. 57, No. 10, pp. 1099–1119.

El-Safty, A. K. 1994. *Behavior of Jointless Bridge Decks.* PhD dissertation. North Carolina State University, Raleigh.

El-Safty, A., and A. M. Okeil. 2008. Extending the Service Life of Bridges Using Continuous Decks. *PCI Journal,* Vol. 53, No. 6, pp. 96–111.

ELTECH Research Corporation. 1993. *Cathodic Protection of Reinforced Concrete Bridge Elements: A State-of-the-Art Report.* SHRP-S-337. Strategic Highway Research Program, Washington, D.C.

Fallaha, S., C. Sun, M. Lafferty, and M. Tadros. 2004. High-Performance Precast Concrete NUDECK Panel System for Nebraska's Skyline Bridge. *PCI Journal,* September–October, pp. 40–50.

Farimani, M. R., S. N. Javidi, D. T. Kowalski, and A. Azizinamini. 2013. Numerical Analysis and Design Provision Development of Simple for Dead–Continuous for Live Bridge System. Submitted for publication to *Engineering Journal.*

Fennema, J. L., J. A. Laman, and D. G. Linzel. 2004. Predicted and Measured Response of an Integral Abutment Bridge. *Journal of Bridge Engineering,* Vol. 10, No. 6, pp. 666–677.

FHWA. 1989. Technical Advisory T5140.22: Uncoated Weathering Steel in Structures. Federal Highway Administration. http://www.fhwa.dot.gov/bridge/t514022.cfm. Accessed Nov. 23, 2013.

Fincher, H. E. 1983. *Evaluation of Rubber Expansion Joints for Bridges.* Report No. FHWA/IN/RTC-83/1. Federal Highway Administration, pp. 15–16.

Fisher, J., D. Hall, R. McCabe, K. Price, C. Seim, and S. Woods. 2006. Steel Bridges in the United States: Past, Present, and Future. In *Transportation Research Circular Number E-C104: 50 Years of Interstate Structures: Past, Present, and Future.* Transportation Research Board of the National Academies, Washington, D.C.

Fisher, J. W. 1984. *Fatigue and Fracture of Steel Bridges:* Case Studies. Wiley Interscience, New York.

Fisher, J. W. 1997. The Evolution of Fatigue-Resistant Steel Bridges. 1997 Distinguished Lectureship. Presented at 76th Annual Meeting of the Transportation Research Board, Washington, D.C.

Fisher, J. W., E. Statnikov, and L. Tehini, L. 2002. Fatigue Strength Improvement of Bridge Girders by Ultrasonic Impact Treatment (UIT). *Welding in the World,* Vol. 46, No. 9/10, pp 16–22.

Fisher, J. W., P. A. Albrecht, B. T. Yen, D. J. Klingerman, and B. M. McNamee. 1974. *NCHRP Report 147: Fatigue Strength of Steel Beams with Transverse Stiffeners and Attachments.* HRB, National Research Council, Washington, D.C.

Fisher, J. W., B. M. Barthelemy, D. R. Mertz, and J. A. Edinger. 1980. *NCHRP Report 227: Fatigue Behavior of Full-Scale Welded Bridge Attachments.* TRB, National Research Council, Washington, D.C.

Fisher, J. W., K. H. Frank, M. A. Hirt, and B. M. McNamee. 1970. *NCHRP Report 102: Effect of the Fatigue Strength of Steel Beams.* HRB, National Research Council, Washington D.C.

Fisher, J. W., A. Nussbaumer, P. B. Keating, and B. T. Yen. 1993. *NCHRP Report 354: Resistance of Welded Details Under Variable Amplitude Long-Life Fatigue Loading.* TRB, National Research Council, Washington, D.C.

Fisher, J. W., B. Yen, D. Wang, and J. Mann. 1987. *NCHRP Report 302: Fatigue and Fracture Evaluation for Rating of Riveted Bridges.* TRB, National Research Council, Washington, D.C.

Fort Miller Company, Inc. 1998. *Inverset Bridge System—Design Installation and Technical Manual.* Schuylerville, NY: Product literature, 2nd Ed.

Freyermuth, C. L. 1969. Design of Continuous Highway Bridges with Precast, Prestressed Concrete Girders. *PCI Journal,* April, pp. 14–39.

Froes, F. H., M. N. Gungor, and M. A. Iman. 2007. Cost-Affordable Titanium: The Component Fabrication Perspective. *Journal of Materials,* Vol. 59, No. 6, pp. 28–31.

Fuller, S. K., and S. R. Petersen. 1995. *NIST Handbook 135: Life-Cycle Costing Manual.* U.S. Department of Commerce.

Fyfe, E., P. Milligan, and S. Watson. 2006. A Discussion of Failure Modes on High Load Bridge Bearings Which Have Resulted in the Current Design Methods, Philosophy, and Guidelines for Disc Bearings. *6th World Congress on Joints, Bearings and Seismic Systems for Concrete Structures,* Halifax, Nova Scotia, Canada.

Gastal, F. P. S. L. 1986. *Instantaneous and Time-Dependent Response and Strength of Jointless Bridge Beams.* PhD dissertation. North Carolina State University, Raleigh.

Glass, G. K., and B. Reddy. 2002. The Influence of the Steel Concrete Interface on the Risk of Chloride-Induced Corrosion. In *COST 521: Corrosion of Steel in Reinforced Concrete Structures: Final Reports of Single Projects* (R. Weydert, ed.), Luxembourg University of Applied Sciences, Luxembourg, pp. 227–232.

Gong, L., D. Darwin, J. Browning, and C. E. Locke. 2006. *Evaluation of Multiple Corrosion Protection Systems and Stainless Steel Clad Reinforcement for Reinforced Concrete.* SM Report Number 82. University of Kansas Center for Research, Inc., Lawrence, January.

Gong, L., D. Darwin, J. P. Browning, and C. E. Locke. 2002. *Evaluation of Mechanical and Corrosion Properties of MMFX Reinforcing Steel for Concrete.* SM Report No. 70. University of Kansas, Lawrence, December.

Greimann, L. F., R. E. Abendroth, D. E. Johnson, and P. B. Ebner. 1987. Pile design and tests for integral abutment bridges. Final Report, HR-273, and Addendum. Iowa Department of Transportation and College of Engineering, Iowa State University, Ames.

Griffiths, S., G. Bowmaker, C. Bryce, and R. Q. Bridge. 2005. Design and Construction of Seamless Pavement on Westlink M7, Sydney, Australia. *Proc., 8th International Conference on Concrete Pavements,* International Society for Concrete Pavements, Colorado Springs, Colo., pp. 21–38.

Gull, J. H., A. J. Yakel, and A. Azizinamini. 2013. Experimental Investigation of Longitudinal Closure Pour Detail for Prefabricated Slabs Used in Modular Construction. Submitted for publication to *Journal of Bridge Engineering.*

Hakenjos, V., K. Richter, A. Gerber, and J. Wiedemyer. 1985. Studies of Movements of Bridge Structures As a Result of Temperature and Traffic Load, Taking a Steel Bridge As an Example. *Stahlbau,* Vol. 54, No. 2, pp. 55–59 (in German).

Hanna, K., G. Morcous, and M. Tadros. 2009. Transverse Post-Tensioning Design and Detailing of Precast, Prestressed Concrete Adjacent-Box-Girder Bridges. *PCI Journal,* Fall 2009, pp. 64–78.

Hanna, K. E., G. Morcous, and M. K. Tadros. 2007. Transverse Design and Detailing of Adjacent Box Beam Bridges. PCI National Bridge Conference, Phoenix, Ariz., October.

Hanna, K., G. Morcous, and M. Tadros. Forthcoming. Design, Detailing, and Testing of Non-Post-Tensioned Transverse Connections in Adjacent Box Girder Bridges. *PCI Journal.*

Hansen, J., K. Hanna, and M. K. Tadros. 2012. Simplified Transverse Post-Tensioning Construction and Maintenance of Adjacent Box Girders. *PCI Journal,* Spring 2012, pp. 64–79.

Hanson, N. W., D. M. Schultz, J. J. Roller, A. Azizinamini, and H. T. Tang. 1987. Testing of Large-Scale Concrete Containment Structural Elements. *Nuclear Engineering and Design,* Vol. 100, No. 2, pp. 129–149.

Harris, D. K., J. Sarkar, and T. M. Ahlborn. 2011. Characterization of Interface Bond of Ultra-High-Performance Concrete Bridge Deck Overlays. In *Transportation Research Record: Journal of the Transportation Research Board, No. 2240,* Transportation Research Board of the National Academies, Washington, D.C., pp. 40–49.

Hartt, W. H., R. G. Powers, D. K. Lysogorski, M. Paredes, F. P. Marino, and R. Simmons. 2009. *Corrosion Resistant Alloys for Reinforced Concrete.* FHWA-HRT-09-020. Federal Highway Administration.

Hartt, W. H., R. G. Powers, D. K. Lysogorski, M. Paredes, and Y. P. Virmani. 2006. *Job Site Evaluation of Corrosion-Resistant Alloys for Use As Reinforcement in Concrete.* FHWA-HRT-060-078. Federal Highway Administration, McLean, Va.

Haugeto, W., and A. Ranasinghe. 2008. Link Slab Continuity Detail on Long-Span Bridges. *Proc., International Bridge Conference,* Pittsburgh, Pa.

He, X., and X. Shi. 2008. Chloride Permeability and Microstructure of Portland Cement Mortars Incorporating Nanomaterials. *TRR 2070 Transportation Research Board,* pp. 13–21.

Headed Reinforcement Corporation (HRC). 2011. *HRC200 Series.* http://www2.hrc-usa.com/downloads/products/HRC200/HRC200-SPEC.pdf. Accessed 2012.

Heffron, R. 2007. Innovative Techniques for Extending the Service Life of Deteriorating Concrete Piers and Wharves. *PORTS 2007: 30 Years of Sharing Ideas: 1977–2007, Proc., 11th Triennial International Conference on Ports,* San Diego, Calif., March 25–28.

Heymsfield, E., J. McDonald, and R. R. Avent. 2001. Neoprene Bearing Pad Slippage at Louisiana Bridges. *Journal of Bridge Engineering,* 30–36.

Hookham, C. J. 1990. Rehabilitation of Great Lakes Steel's Number One Dock. In *Paul Klieger Symposium on Performance of Concrete,* SP-122 (D. Whiting, ed.), American Concrete Institute, Farmington Hills, Mich., pp. 385–399.

Huckelbridge, A. A., H. El-Esnawi, and F. Moses. 1995. Shear Key Performance in Multi-Beam Box Girder Bridges. *Journal of Performance of Constructed Facilities,* Vol. 9, No. 4, pp. 271–285.

Iowa DOT CTRE Project 02-103. Report.

Jacobsen, F. K., and R. K. Taylor. 1971. *TFE Expansion Bearings for Highway Bridges.* Report No. RDR-31. Illinois State Division of Highways, Springfield.

Jung, Y. S., D. G. Zollinger, and S. D. Tayabji. 2007. *Best Practices of Concrete Pavement Transition Design and Construction. Report No. FHWA/TX-07/0-5320-1.* Texas Department of Transportation, Austin.

Kahl, S. 2005. Box-Beam Concerns Found Under the Bridge. *C&T Research Record No. 102.* Construction and Technology Division, Michigan Department of Transportation, Lansing.

Keating, P., and J. W. Fisher. 1986. *NCHRP Report 286: Evaluation of Fatigue Tests and Design Criteria on Welded Details.* TRB, National Research Council, Washington, D.C.

Kepler, J. L., D. Darwin, and C. E. Locke. 2000. *Evaluation of Corrosion Protection Methods for Reinforced Concrete Highway Structures.* SM Report No. 58. University of Kansas Center for Research, Lawrence.

Kim, Y. Y., G. Fischer, and V. C. Li. 2004. Performance of Bridge Deck Link Slabs Designed with Ductile Engineered Cementitious Composite. *ACI Structural Journal,* Vol. 101, No. 6, pp. 792–801.

Lebek, D. E. 1985. *Bridge Bearings, Draft 1.* Technical Committee on Road Bridges, Permanent International Association of Road Congresses, Paris.

Lee, D. J. 1994. *Bridge Bearing and Expansion Joints,* 2nd ed. E. & F. N. Spon, London, pp. 52–53.

Lehman, D. E., C. W. Roeder, R. Larson, and K. Curtin. 2003. *Cotton Duck Bearing Pads: Engineering Evaluation and Design Recommendations.* Report No. WA-RD 569.1. Washington State Department of Transportation, Olympia.

Lepech, M., and V. C. Li. 2005. Design and Field Demonstration of ECC Link Slabs for Jointless Bridge Decks. *Proc., 3rd International Conference on Construction Materials: Performance, Innovations and Structural Implications,* Vancouver, British Columbia, Canada, Aug. 22–24.

Lepech, M. D., and V. Li. 2009a. Application of ECC for Bridge Deck Link Slabs. *Materials and Structures,* Vol. 42, No. 9, pp. 1185–1195.

Lepech, M. D., and V. Li. 2009b. *Design and Field Demonstration of ECC Link Slabs for Jointless Bridge Decks.* George G. Brown Laboratory, University of Michigan, Ann Arbor.

Li, H., H. Xiao, J. Yuan, and J. Ou. 2004. Microstructure of Cement Mortar with Nanoparticles. *Composites Part B: Engineering,* Vol. 35, No. 2, pp. 185–189.

Li, V. C. 2003. On Engineered Cementitious Composites (ECC): A Review of the Material and Its Applications. *Journal of Advanced Concrete Technology,* Vol. 1, No. 3, pp. 215–230.

Manning, D. G., and A. K. C. Ip. 1994. Rehabilitating Corrosion-Damaged Bridges Through the Electrochemical Migration of Chloride Ions. *Concrete Bridges in Aggressive Environments,* SP 151, American Concrete Institute, Detroit, Mich., pp. 221–244.

Manning, D. M. 1995. *NCHRP 220: Synthesis of Highway Practice: Waterproofing Membranes for Concrete Bridge Decks.* TRB, National Research Council, Washington, D.C.

Maurer Söhne. 2003. Maurer MSM® Sliding Bearings. August. http://www.maurer-soehne.com/files/bauwerkschutzsysteme/pdf/en/productinfo/MAURER_MSM_sliding_bearings.pdf. Accessed Nov. 20, 2013.

McCullough, C. 1930. Cost Economies in Concrete Bridges. *Highway Research Board Proceedings,* National Research Council, Washington, D.C.

McDonald, D. B., D. W. Pfeifer, and M. R. Sherman. 1998. *Corrosion Evaluation of Epoxy-Coated, Metallic-Clad, and Solid Metallic Reinforcing Bars in Concrete.* No. FHWA-RD-98-153. Federal Highway Administration.

McDonald, J., E. Heymsfield, E., and R. R. Avent. 2000. Slippage of Neoprene Bridge Bearings. *Journal of Bridge Engineering,* 216–223.

McDonald, D. B., M. R. Sherman, D. W. Pfeifer, and Y. P. Virmani. 1995. Stainless Steel Reinforcing As Corrosion Protection. *Concrete International,* Vol. 17, No. 5, pp. 65–70.

Metals Handbook. 1998. ASM International, Materials Park, Ohio.

Michigan DOT. 2005. Bridge Decks Going Jointless: Cementitious Composites Improve Durability of Link Slabs. In *Research Record No. 100: Construction and Technology,* Michigan Department of Transportation, Lansing.

Michigan DOT. 2006. Engineered Cementitious Composite May Replace Bridge Deck Joints. *Research Spotlight,* Office of Research and Best Practices, Michigan Department of Transportation, Lansing.

Miller, R. A., R. Castrodale, A. Mirmiran, and M. Hastak. 2004. *NCHRP Report 519: Connection of Simple-Span Precast Concrete Girders for Continuity.* Transportation Research Board of the National Academies, Washington, D.C.

Modjeski and Masters, Inc. 2008. *Birmingham Bridge Forensic Inspection.* Final report summary. Pennsylvania Department of Transportation, Engineering District 11, Bridgeville.

Mogawer, W. S., and A. J. Austerman. 2004. *Evaluation of Asphaltic Expansion Joints.* New England Transportation Consortium, Storrs, Conn.

Mokha, A. S., M. C. Constantinou, and A. M. Reinhorn. 1990. Teflon Bearings in Base Isolation, I: Testing. *Journal of Structural Engineering,* Vol. 116, No. 2, pp. 438–454.

Mothe, R. N. 2006. *Partial Continuity in Prestressed Concrete Girder Bridges with Jointless Decks.* MS thesis. Louisiana State University, Baton Rouge.

Muller-Rochholz, J. F. W., M. Fienrich, and M. Breitbach. 1986. Measurement of Horizontal Bridge Movements Due to Temperature, Wind, and Traffic Loadings. *Joint Sealing and Bearing Systems for Concrete Structures,* ACI Publication SP94, Vol. 1, 1986, pp. 409–418.

NACE Standard RP0290-2000. 2000. Impressed Current Cathodic Protection of Reinforcing Steel in Atmospherically Exposed Concrete Structures. National Association of Corrosion Engineers International, Houston, Tex.

Nagai, M., Y. Okui, T. Ohta, H. Nakamura, M. Inomoto, K. Nishio, et al. 2000. Time Dependent Stress Variation of a Composite Two-I-Girder Bridge—Chidorinosawagawa Bridges. In *Bridge Management 4.* London: Thomas Telford.

NBI. 2013. Bridges and Structures: National Bridge Inventory (NBI). Federal Highway Administration. http://www.fhwa.dot.gov/bridge/nbi.cfm. Accessed Dec. 15, 2013.

NCHRP. 1996. *NCHRP Report 381: Report on the 1995 Scanning Review of European Bridge Structures.* TRB, National Research Council, Washington, D.C.

NCHRP. 2004. *NCHRP Synthesis 333: Concrete Bridge Desk Performance: A Synthesis of Highway Practice.* Transportation Research Board of the National Academies, Washington, D.C.

Norwegian Public Roads Administration. 2009. General Specifications 2, Standard Specification Texts for Bridges and Quays, Principal specification 8. In *Handbook 026E,* Oslo, Norway. March (translation of November 2007 ed.).

NSBA. 2005. *Steel Bridge Design Handbook.* National Steel Bridge Alliance and Federal Highway Administration. http://www.aisc.org/contentNSBA.aspx?id=20244.

Nürnberger, U. 1996. *Stainless Steel in Concrete: State of the Art Report.* European Federation of Corrosion Publication No. 18. EFC Working Party on Corrosion of Reinforcement in Concrete, European Federation of Corrosion.

NYSDOT. 2008. Continuity Retrofit. In *Bridge Design Manual,* New York State Department of Transportation, Albany, pp. 20–26.

Oesterle, R. G., J. D. Glikin, and S. C. Larson. 1989. *NCHRP Report 322: Design of Precast Prestressed Bridge Girders Made Continuous.* TRB, National Research Council, Washington, D.C.

Oesterle, R. G., and H. R. Lotfi. 2005. Transverse Movement in Skewed Integral Abutment Bridges. *Proc., FHWA Conference on Integral Abutment and Jointless Bridges,* Baltimore, Md.

Oesterle, R. G., A. B. Mehrabi, H. Tabatabai, A. Scanlon, and C. A. Ligozio. 2004. Continuity Considerations in Prestressed Concrete Jointless Bridges. *Proc., 2004 Structures Congress: Building on the Past: Securing the Future,* American Society of Civil Engineers, Nashville, Tenn., pp. 227–234.

Oesterle, R. G., and J. S. Volz. 2005. Effective Temperature and Longitudinal Movement in Integral Abutment Bridges. *Proc., FHWA Conference on Integral Abutment and Jointless Bridges,* Baltimore, Md.

Ozyildirim, C. 1998. Permeability Specifications for High-Performance Concrete Decks. In *Transportation Research Record 1610,* TRB, National Research Council, Washington, D.C., pp. 1–5.

Ozyildirim, C. 1999. HPC Bridge Decks in Virginia. *ACI Concrete International,* Vol. 21, No. 2, pp. 59–60.

Patty, J., F. Seible, and C. Uang. 2002. *Seismic Response of Integral Bridge Connections.* Final report. Caltrans, Sacramento.

PCI. 2003. *Precast Prestressed Concrete Bridge Design Manual,* 2nd ed., Precast/Prestressed Concrete Institute, Chicago, Ill.

PCI Bridges Committee. 2011. The State of the Practice of Precast/Prestressed Adjacent Box Beam Bridges. Chicago, Ill.

Pemmaraju Venkata, H. P., G. Tsiatas, and K. W. Lee. 2006. The Buried Joint Approach for Expansion Joint Retrofit: A Case Study. Presented at 85th Annual Meeting of the Transportation Research Board, Washington, D.C.

Polder, R. B. 1998. Cathodic Protection of Reinforced Concrete Structures in The Netherlands: Experience and Developments. *HERON,* Vol. 43, No. 1, pp. 3–14.

Pritchard, B. (ed.). 1994. *Continuous and Integral Bridges.* E. & F. N. Spon, London.

Purvis, R. 2003. *NCHRP Synthesis 319: Bridge Deck Joint Performance.* Transportation Research Board of the National Academies, Washington, D.C.

Qian, S., M. D. Lepech, Y. Y. Kim, and V. C. Li. 2009. Introduction of Transition Zone Design for Bridge Deck Link Slabs Using Ductile Concrete. *ACI Structural Journal,* Vol. 106, No. 1, pp. 96–105.

Qing, Y., Z. Zenan, K. Deyu, and C. Rongshen. 2007. Influence of Nano-SiO_2 Addition on Properties of Hardened Cement Paste As Compared with Silica Fume. *Construction and Building Materials,* Vol. 21, No. 3, pp. 539–545.

Ratner, M., and D. Ratner. 2003. *Nanotechnology: A Gentle Introduction to the Next Big Idea.* Pearson Education, London.

Roeder, C. W., and J. F. Stanton. 1991. State-of-the-Art Elastomeric Bridge Bearing Design. *ACI Journal,* Vol. 88, pp. 31–41.

Roeder, C. W., J. F. Stanton, and A. W. Taylor. 1987. *NCHRP Report 298: Performance of Elastomeric Bearings.* TRB, National Research Council, Washington, D.C.

Roeder, C. W., J. F. Stanton, and T. Feller. 1989. *NCHRP Report 325: Low Temperature Behavior and Acceptance Criteria for Elastomeric Bearings.* TRB, National Research Council, Washington, D.C.

Russell, H. G. 2012. *NCHRP Synthesis of Highway Practice 425: Waterproofing Membranes for Concrete Bridge Decks.* Transportation Research Board of the National Academies, Washington, D.C.

Salas, R. M., A. L. Kotys, J. S. West, A. J. Schokker, J. E. Breen, and M. E. Kreger. 2003. *Long-Term Post-Tensioned Beam Exposure Test Specimens Final Evaluation.* Research Report 1405-7. Center for Transportation Research, Bureau of Engineering Research, University of Texas, Austin.

Scully, J. R., and M. F. Hurley. 2007. *Investigation of the Corrosion Propagation Characteristics of New Metallic Reinforcing Bars.* Final Report VTRC 07-CR9. Virginia Transportation Research Council, Charlottesville.

Seismic Energy Products. 2010. Fluorogold® Slide Bearings. Seismic Energy Products, Athens, Tex. http://www.registrocdt.cl/registrocdt/uploads/FICHAS/TECNOAV/Aislantes%20S%C3%ADsmicos/fluorogold.pdf. Accessed Nov. 20, 2013.

Sergi, G., and C. L. Page. 1994. *The Effects of Cathodic Protection on Alkali–Silica Reaction in Reinforced Concrete: Stage 2.* TRL Contractor Report 62. Department of Transport, United Kingdom.

Sergi, G., D. Simpson, and J. Potter. 2008. Long-Term Performance and Versatility of Zinc Sacrificial Anodes for Control of Reinforcement Corrosion. *EUROCORR 2008: European Corrosion Congress,* Edinburgh, Scotland.

Sharp, S. R., G. G. Clemeña, Y. P. Virmani, G. E. Stoner, and R. G. Kelly. 2002. *Electrochemical Chloride Extraction: Influence of Concrete Surface on Treatment.* FHWA-RD-02-107 and VTRC 02-R. Virginia Center for Transportation Innovation and Research, Charlottesville.

Sherafati, A. 2011. *Expanding the Length of Jointless Bridges by Providing Rotational Capacity over the Pile Head.* PhD dissertation. University of Nebraska–Lincoln.

Sherafati, A., and A. Azizinamini. 2013. Flexible Pile-Cap Connection in Jointless Bridges, Part II: Theory and Design. Submitted for publication to *Journal of Bridge Engineering.*

Sherafati, A., M. Sotudeh Chafi, and A. Azizinamini. 2012. Buckling of Piles in Cohesive Soil Supporting Jointless Bridges. *Bridge Structures: Assessment, Design and Construction,* Vol. 8, No. 1, pp. 15–24.

Sherafati, A., A. J. Yakel, and A. Azizinamini. 2013. Flexible Pile-Cap Connection in Jointless Bridges, Part I: Experiment. Submitted for publication to *Journal of Bridge Engineering.*

Sherman, M. R., R. L. Carrasquillo, and D. W. Fowler. 1993. *Field Evaluation of Bridge Corrosion Protection Measures.* Texas Department of Transportation, Austin.

Shinozuka, M. (ed.), D. Ballantyne, R. Borcherdt, I. Buckle, T. O'Rourke, and A. Schiff. 1995. *The Hanshin–Awaji Earthquake of January 17, 1995: Performance of Lifelines.* Technical Report NCEER-95-0015. National Center for Earthquake Engineering Research, Buffalo, N.Y.

Siegwart, M., J. F. Lyness, B. J. McFarland, and G. Doyle. 2005. The Effect of Electrochemical Chloride Extraction on Pre-Stressed Concrete. *Construction and Building Materials,* Vol. 19, No. 8, pp. 585–594.

Silva, M. F., A. J. Yakel, and A. Azizinamini. 2013. Self-Stressing System for Bridge Application with Emphasis on Precast Panel Deck System. Submitted for publication to *Journal of Bridge Engineering.*

Smith, F. N., and M. Tullmin. 1999. Using Stainless Steels As Long-Lasting Rebar Material. *Materials Performance,* Vol. 38, No. 5, pp. 72–76.

Snedeker, K. 2009. *Evaluation of Performance and Maximum Length of Continuous Decks in Simple-Span Bridges.* MS thesis. Georgia Institute of Technology, Atlanta.

Snedeker, K., D. W. White, and L. Kahn. 2011. *Evaluation of Performance and Maximum Length of Continuous Decks in Bridges, Part 1.* Final report, Project No. 09-07. Office of Materials and Research, Georgia Department of Transportation, Atlanta.

Soderqvist, M.-K., and E. Vesikari. 2003. LIFECON: Generic Technical Handbook for a Predictive Life Cycle Management System of Concrete Structures (LMS). Report funded by the European Community under the Competitive and Sustainable Growth Programme.

Stanton, J. F., and C. W. Roeder. 1982. *NCHRP Report 248: Elastomeric Bearings Design, Construction, and Materials.* NCHRP Report 248. TRB, National Research Council, Washington, D.C.

Stanton, J. F., C. W. Roeder, and T. I. Campbell. 1999. Appendix C, Friction and Wear of PTFE Sliding Surfaces. In *NCHRP Report 432: High-Load Multi-Rotational Bridge Bearings,* TRB, National Research Council, Washington, D.C.

Stanton, J. F., C. W. Roeder, P. Mackenzie-Helnwein, C. White, C. Kuester, and B. Craig. 2008. *NCHRP Report 596: Rotation Limits for Elastomeric Bearings.* Transportation Research Board of the National Academies, Washington, D.C.

Stratfall, R. F. 1974. Experimental Cathodic Protection of a Bridge Deck. In *Transportation Research Record 500,* TRB, National Research Council, Washington, D.C., pp. 1–15.

Telang, N. M., and A. M. Mehrabi. 2003. Cracked Girders. *Public Roads,* Vol. 67, No. 3.

TIMET. 1999. *Corrosion Resistance of Titanium.* Titanium Metals Corporation, Denver, Colo. http://www.parrinst.com/wp-content/uploads/downloads/2011/07/Parr_Titanium-Corrosion-Info.pdf. Accessed Nov. 20, 2013.

TRB. 2006. *Transportation Research Circular E-C107: Control of Cracking in Concrete: State of the Art.* Transportation Research Board of the National Academies, Washington, D.C.

Ulku, E., U. Attanayake, and H. Aktan. 2009a. *Retrofit Design Details for Deck Joint Elimination over Abutments.* Presented at 88th Annual Meeting of the Transportation Research Board, Washington, D.C.

Ulku, E., U. Attanayake, and H. Aktan. 2009b. Jointless Bridge Deck with Link Slabs: Design for Durability. In *Transportation Research Record: Journal of the Transportation Research Board, No. 2131,* Transportation Research Board of the National Academies, Washington, D.C., pp. 68–78.

Vector Corrosion Technologies. 2013. [System Selector Chart] http://www.vector-corrosion.com/wordpress/wp-content/uploads/2009/07/DOC_0003.PDF. Accessed Jan. 29, 2014.

Velivasakis, E. E., S. K. Henriksen, and D. W. Whitmore. 1997. Halting Corrosion by Chloride Extraction and Realkalization. *Concrete International,* Vol. 19, No. 12, pp. 39–45.

Virmani, Y. P., and G. G. Clemeña. 1998. *Corrosion Protection: Concrete Bridges.* Report No. FHWA-RD-98-088. Federal Highway Administration.

Wallbank, E. J. 1989. *The Performance of Concrete in Bridges: A Survey of 200 Highway Bridges.* Department of Transport, HMSO, London.

Wassef, W. G., D. Davis, S. Sritharan, J. R. Vander Werff, R. E. Abendroth, J. Redmond, and L. F. Greimann. 2004. *NCHRP Report 527: Integral Steel Box-Beam Pier Caps.* Transportation Research Board, Washington, D.C.

Wasserman, E. P. 1987. Jointless Bridge Decks. *Engineering Journal,* 3rd Quarter, pp. 93–100.

Williamson, G., R. E. Weyers, M. C. Brown, and M. M. Sprikel. 2007. *Bridge Deck Service Life Prediction and Cost.* VTRC 08-CR4. Virginia Transportation Research Council, Charlottesville.

Wing, K. M., and M. J. Kowalsky. 2005. Behavior, Analysis and Design of an Instrumented Link Slab Bridge. *Journal of Bridge Engineering,* Vol. 10, No. 3, pp. 331–344.

Wipf, T. J. 2006. Evaluation of Corrosion Resistance of Different Steel Reinforcement Types.

Wright, W. J., H. Tjiang, J. Hartmann, and P. Albrecht. 2000. Fracture Resistance of Modern Bridge Steels. *Proc., ASCE Structures Congress,* Philadelphia, Pa.

Yakel, A. J., and A. Azizinamini. 2013. Testing of Self-Stressing System for Bridge Application. Submitted for publication to *Journal of Bridge Engineering.*

Yakel, A., M. Farimani, N. Mossahebi, and A. Azizinamini, 2007. Three Innovative Concepts for Short Span Steel Bridges. *Final Report for Nebraska Department of Roads, National Bridge Research Organization (NaBRO),* Department of Civil Engineering, University of Nebraska–Lincoln.

Yuen, L. H. 2005. *Performance of Concrete Bridge Deck Joints.* MS thesis. Brigham Young University, Provo, Utah.

Yura, J., A. Kumar, A. Yakut, C. Topkaya, E. Becker, and J. Collingwood. 2001. *NCHRP Report 449: Elastomeric Bridge Bearings: Recommended Test Methods.* TRB, National Research Council, Washington D.C.

Zia, P., A. Caner, and A. K. El-Safty. 1995. *Jointless Bridge Decks.* Report No. FHWA/NC/95-006. Center for Transportation Engineering Studies, North Carolina State University, Raleigh.

APPENDIX A

Brief Description of Category 3 Research Topics

As a result of the activities within Phase 1, several concepts were identified that merit research by others. This appendix summarizes the topics classified as Category 3 research topics and provides brief introductory comments for some of them. During the development of the Phase 1 report, limited research was conducted on some of these topics; however, these investigations are not documented.

Concrete Durability: Using Smart Materials and Nanotechnology to Enhance the Service Life of Concrete Elements

This section provides two innovative approaches to improving concrete durability through the use of nanotechnologies: the use of self-healing systems for closing cracks and the use of nanoparticles for reducing the permeability of existing concrete.

Background

Nanotechnology is a branch of engineering that deals with the design and manufacture of extremely small electronic circuits and mechanical devices built at the molecular level of matter and the use of very small particles to improve the properties of materials (Chong and Garboczi 2002; Ratner and Ratner 2003). Nano indicates one billionth of a unit of measure. Nanotechnology can be used successfully in a variety of construction materials, including concrete. Nanoparticulate additives are now widely used as fillers in protective paints, coatings, and clean-up systems for buildings.

Cement hydration products are porous with a pore-size distribution that ranges from nanometers to millimeters. The pores are a pathway for water and other aggressive solutions to penetrate into concrete, causing cracking and deterioration. Thus, a better understanding of cement hydrates at the nanoscale would provide information for reducing and minimizing the pores. The addition of nanoparticles such as nanosilica and nanoclays to concrete can reduce the occurrence and size of pores that can improve concrete strength and durability through physical and chemical interactions. The microstructure of the binder is expected to be uniform without apparent lime crystals or large pores.

Nanomaterials for use in concrete include nanosilica (nano-SiO_2), nanoclays, nanotubes, nanocomposites, and nanotitanium dioxide (nano-TiO_2). Nanotubes are very thin sheets (one atom thick) that are rolled into a cylinder (de Ibarra 2006). Carbon nanotubes have the potential to enhance strength, effectively hinder crack propagation in cement composites, and act as nucleating agents. Reinforcing concrete with nanofibers may produce tougher concretes by interrupting crack formation as soon as it is initiated.

A very small amount of nano-SiO_2 reduces cement permeability and makes cement paste denser than the control paste (He and Shi 2008). Nanosilica is more effective than silica fume in increasing the strength of mortar (Li et al. 2004). Also, the strength of the interfacial transition zone is increased, and there are more pozzolanic reactions in nanosilica cement paste than in silica fume cement paste (Qing et al. 2007). The addition of polymer-modified nanoclay is also able to increase compressive strength in cement paste (Birgisson 2006).

Past attempts to improve concrete life have focused on producing denser, less porous concretes; unfortunately, these formulations have a greater tendency to crack. Another approach to improve the permeability of concrete has been to reduce diffusion in concrete by using viscosity-enhancing admixtures (Bentz et al. 2009). Larger molecules, such as cellulose ether and xanthum gum, increased viscosity but did not reduce diffusion rates. Smaller molecules, less than 100 nm (nanometers), slowed ion diffusion.

Smart materials in the simplest case would detect and warn of problems. In a more advanced form, they could not only detect but correct problems. One idea is the application of

electrorheological fluids for vibration control of structures. According to Chong and Garboczi (2002), "Electrorheological fluids stiffen very rapidly in an electric field, changing their elastic and damping properties. [. . .] An important research challenge in smart structures and materials is to achieve optimal performance of the total system rather than just in the individual components. Among the topics requiring study are materials with energy-absorbing and variable damping properties, as well as materials having a stiffness that varies with changes in stress, temperature, or acceleration. [. . .] There is [also] the associated problem of simply being able to detect (predict) when repair is needed and when it has been satisfactorily accomplished."

Self-Healing Systems: Using Nanotechnologies for Closing Cracks

One approach for incorporating smart materials is to use conventional concrete and add nanomaterials to fresh concrete that could detect cracks and start the self-healing process by filling those cracks. The concept of self-healing concrete was inspired by biological systems in which damage triggers an automatic healing response. The new self-healing concrete uses the same idea, in which the addition of self-healing properties would be activated when cracking occurs. Based on recent investigation, certain microcapsules can be added to the concrete mixture to change the behavior of concrete after cracking. The new technology consists of three components:

- A composite material, in this case concrete;
- A microencapsulated healing agent; and
- A catalyst.

When cracks form in such concrete, the crack will tear the microcapsule and thus release the healing agent (see Figure A.1). The agent then flows into the crack through capillary action and the pressure from osmosis. The agent will then come into contact with the catalyst, which will initiate the polymerization process. This whole process results in the formation of insoluble crystals that will fill the crack up to a width of 400 μm (microns). The polymerization process also bonds the crack closed. The specifications of self-healing concrete are as follows:

- Quantity: 100 to 200 capsules per cubic inch;
- Capsule size: ~100 μm; and
- Regained strength: as much as 75% of the original strength.

One approach for achieving self-healing concrete is to embed hollow fibers (which act as microcapsules) in the repair matrix before it is subjected to damage. When cracking occurs in the concrete, all fibers in the crack path are broken, and the repair materials are released from inside the hollow fibers, infiltrating the matrix. The repair material penetrates and rebonds the crack. Consequently, this mechanism occurs when needed, repairing the concrete automatically without manual intervention. Neither fibers nor the released material sacrifices strength for durability. Figure A.2 shows the self-repairing mechanism.

Because the healing component of this newly developed concrete is not released during the mixing of the fresh concrete, the fresh concrete properties remain unchanged. Fibers with high aspect ratios can improve the ductile behavior of concrete and also increase strength and stiffness. Generally speaking, fibers can improve concrete behavior. When self-healing concrete is activated, the repaired region is more ductile and stronger in tension than the original concrete. Using self-healing concrete will address many of the issues associated with multiple failure modes.

Fibers can be used to increase reinforcing bars' resistance to corrosion. The fibers are coated with a substance that may be dissolved in salt water. These fibers are filled with an anti-corrosion chemical component. When the fibers come in contact with salt water, the coating substance is released and attaches to the rebar, delaying or even preventing further corrosion.

Purpose and Scope

Smart materials and nanomaterials have the potential to enhance the properties of concrete and provide long-lasting service with minimal maintenance. This study could explore available smart materials and nanomaterials that can be used in concrete. The potential candidates should be evaluated for their effectiveness in enhancing the properties of concrete and sealing the cracks or performing self-healing.

Suggested Research Methodology for Others

This section provides a guideline for others to continue research in this field. It is recommended this research be carried out in two phases. In the first phase, literature will be surveyed to determine smart materials and nanomaterials that can be used in concrete for improving the paste and the interfacial transition zone, and materials with potential for improvement will be selected.

In the second phase, the potential smart materials and nanomaterials will be added to concrete mixtures prepared in the laboratory. The concretes will be tested for strength, permeability, and shrinkage to determine improvements against controls without smart materials and nanomaterials. Concrete samples will be evaluated under a microscope to

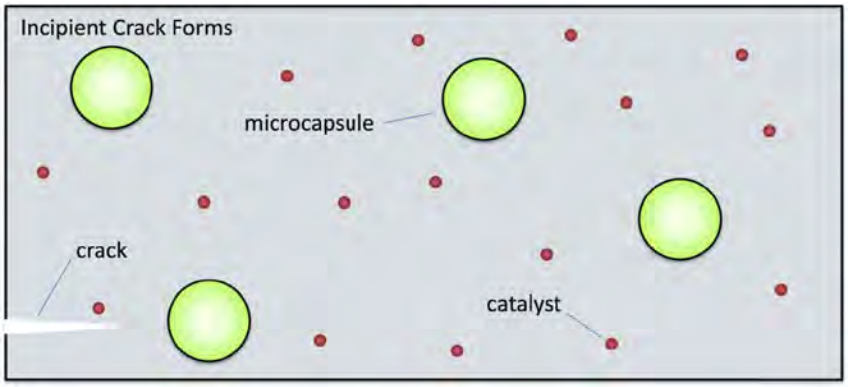

(a)

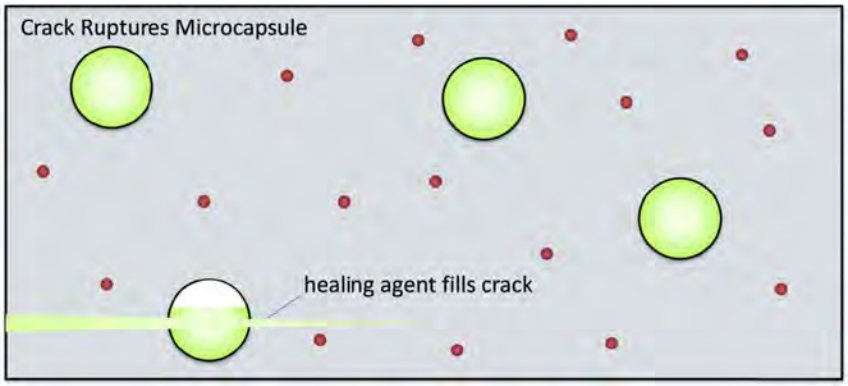

(b)

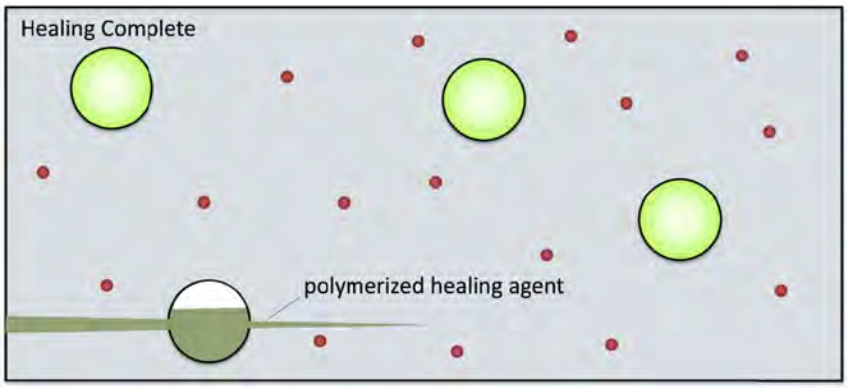

(c)

Figure A.1. Self-healing concrete process: (a) incipient crack forms (lower left); (b) crack ruptures microcapsule, releasing healing agent; and (c) polymerized healing agent fills crack.

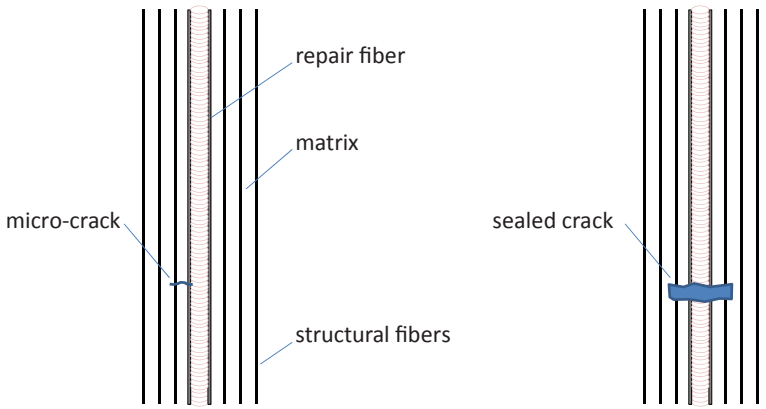

Figure A.2. Self-repairing mechanism.

determine improvements in the microstructure that can lead to enhancements.

Using Nanoparticles to Reduce the Permeability of Existing Concrete

The second part of the study would involve the use of charged nanoparticles to reduce concrete permeability. Treatment of concrete using charged nanoparticles has the potential to improve the concrete properties of existing structures. If successful, this technique could be used to extend the service life of existing structures or to eliminate the need to replace certain structures with new structures.

Charged nanoparticles can be moved into open pores and moved through the pore structure of the cover concrete toward the surface of the steel, decreasing the porosity and forming a much less permeable concrete cover, thus restricting further migration of chlorides to the steel. The improved permeability of the concrete will improve the structure's resistance to corrosion and can be used to extend the service life of existing reinforced concrete structures.

Use of this technique on concrete bridge decks could eliminate the need to apply overlays, in many situations reducing dead load, maintaining load rating, and maintaining clearances on overhead structures.

Purpose and Scope

Charged nanoparticles could be evaluated on chloride-contaminated and, possibly, new reinforced concrete elements. Treatment with charged nanoparticles would enhance the properties of the concrete cover up to the steel interface by reducing porosity and defect size, which act as initiation sites for the corrosion of the steel. The scope of the research would be to identify the correct type and size of nanoparticles that would allow their penetration into the concrete pore structure and to evaluate the increased corrosion resistance provided to the steel.

Suggested Research Methodology for Others

The purpose of this section is to provide a guideline for others to continue research in this field. It is recommended this research be carried out in the laboratory using samples of reinforced concrete elements subjected to chloride contamination. Chloride-contaminated samples would be subjected to treatment using charged nanomaterials. The ability to improve concrete properties would be determined by testing samples cored from the elements for strength and permeability. The improvements in corrosion resistance will be determined by exposing the treated and untreated reinforced concrete samples to high levels of chloride solution and measuring chloride profiles and corrosion activity. If corrosion is initiated after a sample has been treated, the level of chloride at the steel depth would be determined and compared with threshold levels for untreated concrete elements.

Development of Innovative Hybrid Orthotropic Deck System for Short-Span Bridges

Several concepts have been identified that are related to steel bridge systems. One concept that was studied by the principal investigator of the R19A project is related to an innovative orthotropic deck system for short-span steel bridges. According to John Fisher of Lehigh University (phone communication, May 2008), an orthotropic deck system is the only deck system that has a chance of providing 100-plus years of service life. However, the available systems are suited for long-span bridges and are prone to fatigue and delamination of membranes that are used for the riding surface. Both of these problems are related to the flexibility of the top steel plates used in orthotropic deck systems. The use of a steel-only option is to produce a lightweight deck system for long-span bridges. For long-span bridges, a steel orthotropic deck system provides a lightweight alternative. However, for short-span bridges, some increase in deck weight is tolerable. The innovative orthotropic deck system described in the following paragraphs takes advantage of steel and concrete to develop a system that should have well over 100 years of service life.

The high cost of orthotropic decks, which is primarily due to fabrication, prohibits their use for short- and medium-span bridges. They become an affordable option for long-span bridges because of their light weight. However, with modifications, the concept of an orthotropic bridge deck may be well suited for short- to medium-span bridges.

The proposed concept is to develop a system in which the deck consists of top and bottom steel plates with a series of vertical plates. Such a system could also act as the top flange of girders and presents various options for accelerated bridge construction. Once the system is transported to the field, the hollow spaces between the top and bottom plates could be filled with concrete. The proposed system is shown in Figure A.3. Advances in welding technology make this system possible by allowing welding of the steel elements from the "blind" side or outer surface.

General Description of Proposed Hybrid Orthotropic Deck System

The proposed hybrid orthotropic deck system consists of a top and bottom plate with a cavity. The cavity is divided into smaller cells by using vertical ribs. These smaller cavities are filled with self-consolidating concrete. The total thickness of the deck is about 4 in. (for 10-ft spacing between girders),

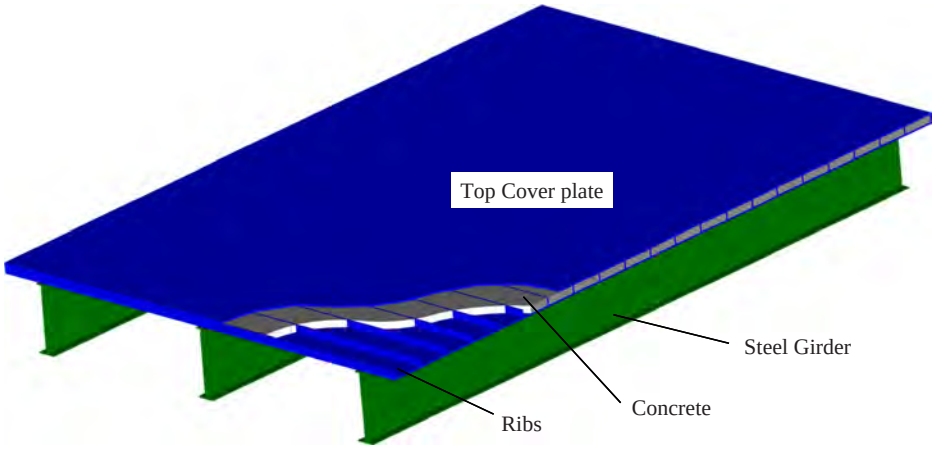

Figure A.3. Proposed hybrid orthotropic deck system.

and the thicknesses of the top and bottom plates are less than 0.25 in. The system offers the following advantages:

- There is a significant increase of the load-resistance capacity of the deck.
- The concrete sandwiched between the top and bottom plates is protected from wear and weathering elements and could last 100-plus years without any maintenance or special design provision.
- The concrete between the top and bottom plates stiffens the deck system to a point that could eliminate fatigue cracking in the deck components.
- The system lends itself to modular construction and could significantly decrease on-site construction activities. The system could be used for both new and existing bridges.
- The concrete between the top and bottom plates stiffens the system and can therefore eliminate the delamination of wearing surfaces seen in purely steel orthotropic deck systems.
- The addition of concrete prevents the orthotropic deck components from buckling, which makes it possible to decrease the thickness of the steel plates.
- The concrete inside the cells could be added after the deck is attached to girders, thereby reducing the weight of pieces that have to be transported.
- The deck system is so stiff that it could eliminate the need for cross frames in the positive bending regions of steel bridges and, therefore, eliminate a detail that is a source of many fatigue-related issues with steel bridges.
- The weight of the system is about 30% lower than an all-concrete option.

The disadvantages of the proposed system include a potentially higher initial cost and the addition of weight (as compared with a purely steel orthotropic deck system). In addition, inspecting a large portion of this deck system for fatigue cracking that is due to the presence of the concrete would be impossible. However, past research indicates that presence of the concrete can effectively prevent crack propagation (Hanson et al. 1987).

Preliminary Study

A preliminary finite element study was performed using the general-purpose finite element program ABAQUS to investigate the general behavior of the system. Figures A.4 through A.6 show the dimensions of the structure modeled. In conventional orthotropic bridge decks, the ribs are parallel to girder direction, as shown in Figure A.4. However, in this preliminary study, the possibility of a transverse orthotropic deck was also considered, in which the direction of the ribs is perpendicular to the girder direction, as shown in Figure A.5.

A parametric study was performed to investigate bridge behavior with different orthotropic deck geometries. The

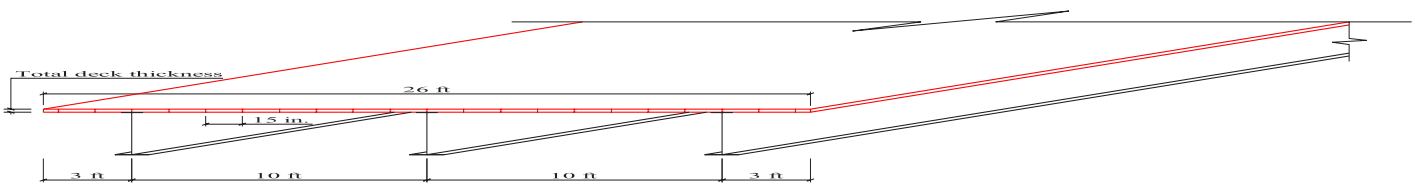

Figure A.4. Longitudinal ribs.

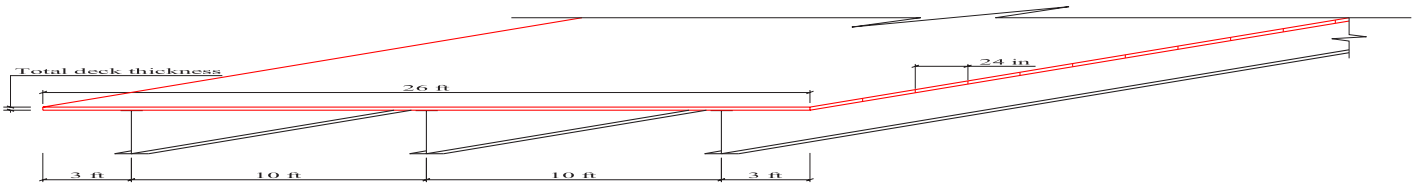

Figure A.5. Transverse ribs.

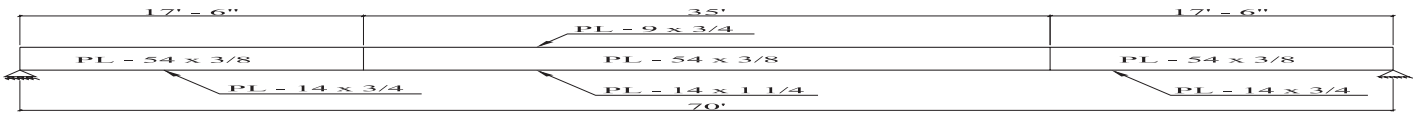

Figure A.6. Supporting girders.

geometric specifications that can be changed in the orthotropic deck are total deck thickness, thickness of the plates (top, bottom, and ribs), and spacing between the ribs. The rib orientation can be either longitudinal or transverse. The spacing of the rib plates greatly affects the cost of the deck because welding of these plates comprises a majority of the fabrication cost. Table A.1 presents the deck dimensions that were modeled.

Figure A.7 shows a typical model structure with a longitudinal orthotropic deck.

To investigate the behavior of the structure, five analyses were performed on each combination of parameters:

1. Analysis of the steel part of the structure only (orthotropic deck and steel girders without concrete) under its self-weight.
2. Buckling analysis of the steel part of the structure only (orthotropic deck and steel girders without concrete). This analysis helps to find the potential buckling modes of the structure when no concrete exists.
3. Analysis of the structure under the weight of wet concrete filled in the orthotropic deck hollow spaces.
4. Buckling analysis of the structure with hollow spaces of the orthotropic deck filled with hardened concrete. The buckling modes that resulted from this analysis will also be used in the ultimate load analysis of the structure as the implied imperfections.
5. Ultimate load analysis of the structure. This analysis resulted in the load–deflection curves of the structure. Two major loading conditions were considered: two HS-20 trucks side by side and one HS-20 truck on the bridge such that one wheel line was centered between two adjacent girders.

Table A.1. Dimensions of Hybrid Orthotropic Deck Bridge Modeled

Deck Direction	Total Deck Thickness (in.)	Deck Plate Thickness (in.)
Longitudinal	4.0	0.250
		0.125
	3.0	0.250
		0.125
Transverse	4.0	0.250
		0.125
	3.0	0.250
		0.125

Dead Load Results

Table A.2 summarizes the maximum deflections and maximum von Mises stresses in the orthotropic deck and girders due to the weight of steel and wet concrete. The maximum stresses occurred midway between the two adjacent girders. The deflection of the deck and girder were measured relative to the undeformed shape of the structure.

Ultimate Loading of Structure with Hardened Concrete

The buckling mode shape of the structure resulting from a buckling analysis of the whole structure with hardened concrete was incorporated into the ultimate loading of the structure as an imperfection.

A concrete damage plasticity model was included in the concrete model of the structure to address the concrete crushing effect in the analysis (CEB-FIP 1993).

Two Trucks Side by Side

Figure A.8 shows an example of the von Mises stresses in the bridge at the ultimate load with two HS-20 trucks side by side.

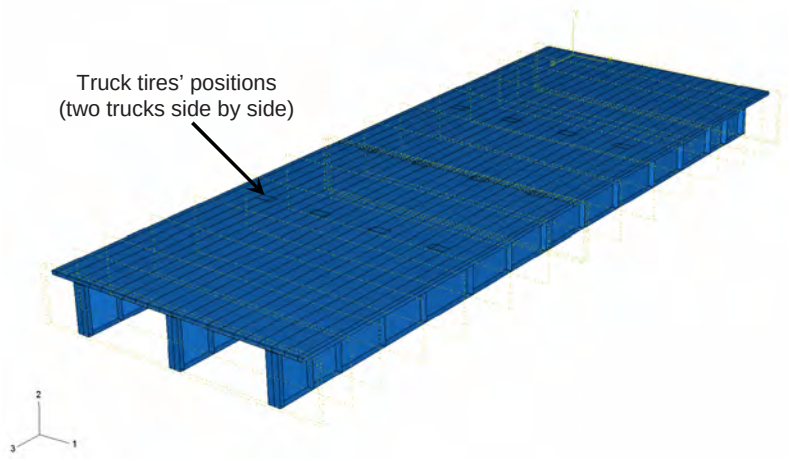

Figure A.7. Structure modeled with ABAQUS with a longitudinal orthotropic deck.

Table A.2. Modeled Structure's Responses Under Construction

				Maximum Deflection		Maximum von Mises Stress	
Deck Direction	**Total Deck Thickness (in.)**	**Deck Plate Thickness (in.)**	**Construction Stage**	**Orthotropic Deck (in.)**	**Girder (in.)**	**Orthotropic Deck (psi)**	**Girder (psi)**
Longitudinal	4.0	0.250	Steel self-weight	0.18	0.15	1,250	2,204
			Wet concrete and steel weight	0.42	0.34	3,485	5,015
		0.125	Steel self-weight	0.24	0.13	2,151	1,626
			Wet concrete and steel weight	0.9	0.33	9,836	4,318
	3.0	0.250	Steel self-weight	0.18	0.15	1,609	2,223
			Wet concrete and steel weight	0.37	0.3	3,872	4,343
		0.125	Steel self-weight	0.25	0.13	2,422	1,657
			Wet concrete and steel weight	0.81	0.31	9,420	3,894
Transverse	4.0	0.250	Steel self-weight	0.16	0.16	1,860	2,200
			Wet concrete and steel weight	0.37	0.37	4,420	5,034
		0.125	Steel self-weight	0.16	0.15	2,111	1,752
			Wet concrete and steel weight	0.43	0.43	5,898	4,897
	3.0	0.250	Steel self-weight	0.16	0.16	2,233	2,218
			Wet concrete and steel weight	0.32	0.32	4,457	4,374
		0.125	Steel self-weight	0.15	0.15	2,907	1,728
			Wet concrete and steel weight	0.36	0.35	6,554	4,084

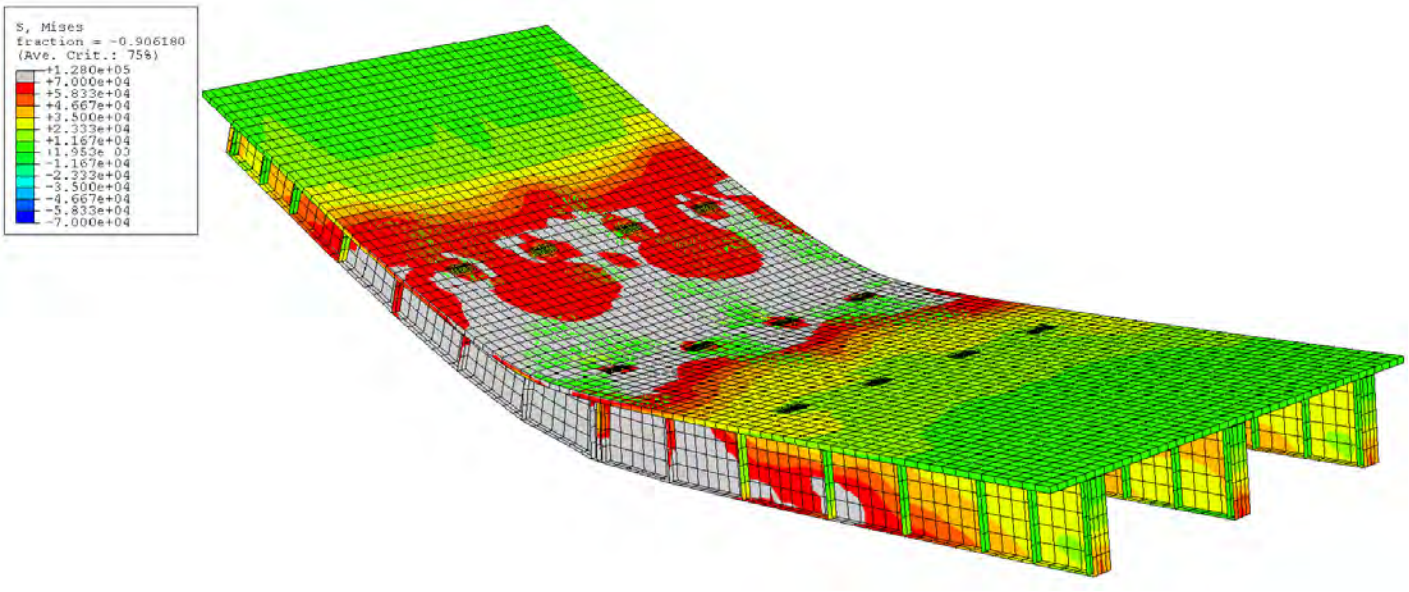

Figure A.8. Von Mises stresses in the bridge; gray represents yielded regions.

Figure A.9 shows an example of the deflections in the bridge due to the ultimate loading of the structure with two HS-20 trucks side by side. This is the final stage of the loading.

One Truck with One Side on the Middle of the Girders' Spacing

Figure A.10 shows an example of von Mises stresses in the bridge at the ultimate load with one truck on the bridge.

Figure A.11 shows an example of the deflections in the bridge due to the ultimate loading of the structure with one truck on the bridge. This is the final stage of the loading.

Load–Deflection Results

The following two subsections describe the results obtained from the ultimate loading of the structure. This discussion provides an understanding of how changes in the dimensions

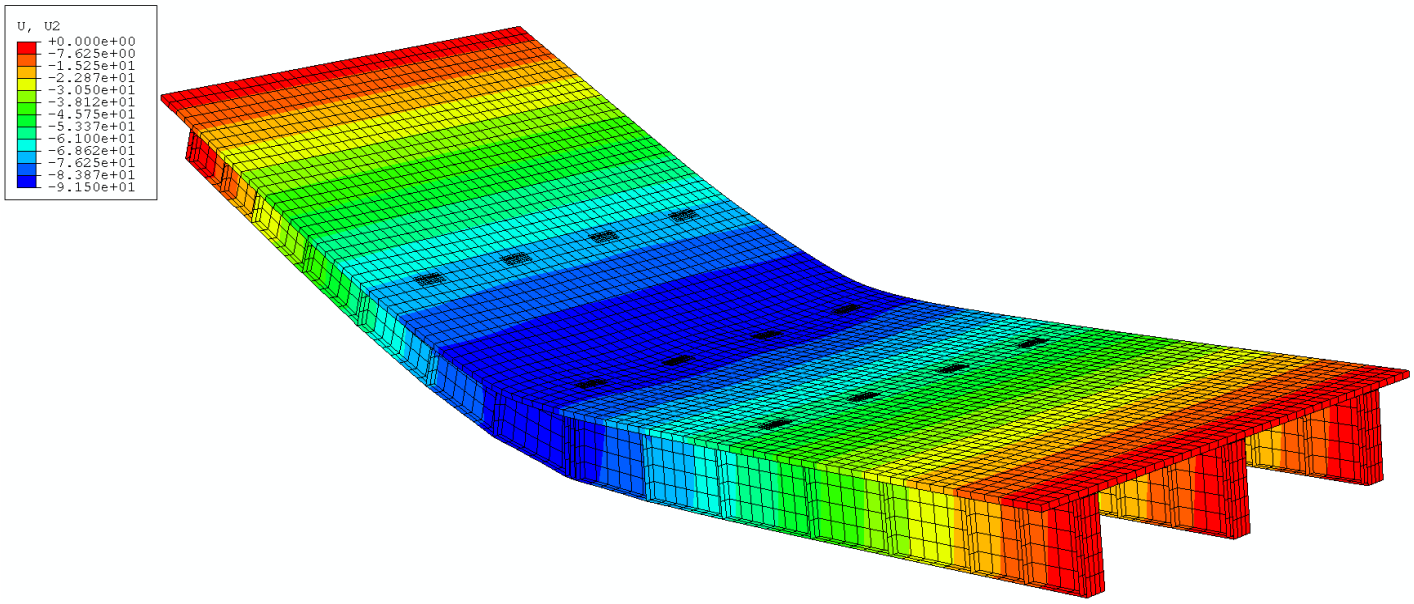

Figure A.9. An example of the deflections in the bridge at the ultimate load.

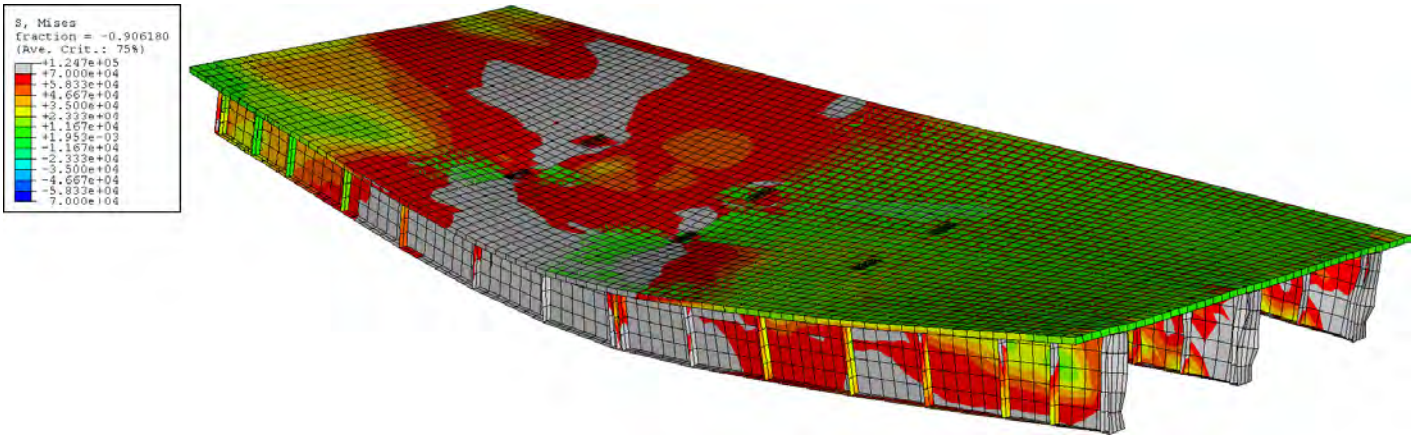

Figure A.10. Von Mises stresses in the bridge; gray represents yielded regions.

of the structure affect load resistance and the ultimate ductility of the structure.

Two Trucks Side by Side

Figure A.12 shows the load–deflection curve of the structure associated with the ultimate load analysis of the structure using two trucks on the bridge side by side. The deflection is associated with girder deflection at midspan.

Figure A.13 shows the load–deflection curve of the structure associated with the ultimate load analysis of the structure in terms of the number of bridge weights that can be applied to the bridge.

As these curves show, decreasing the thickness of the orthotropic deck plates will reduce the ultimate load capacity. However, the system still has significant reserve capacity.

Figure A.13 may also be used to find the most efficient dimensions for the structure if it is assumed that the most efficient structure is the one that carries larger loads compared with its self-weight.

One Truck with One Side on the Middle of Girders Spacing

Figure A.14 shows the load–deflection curve associated with the response of the orthotropic deck.

Conclusions from Finite Element Study

The following are the conclusions of the preliminary finite element analysis performed on a hybrid orthotropic deck system:

- Buckling in the deck of the completed structure is unlikely. Adequately stiffened girders prevent the buckling failure mode from governing.

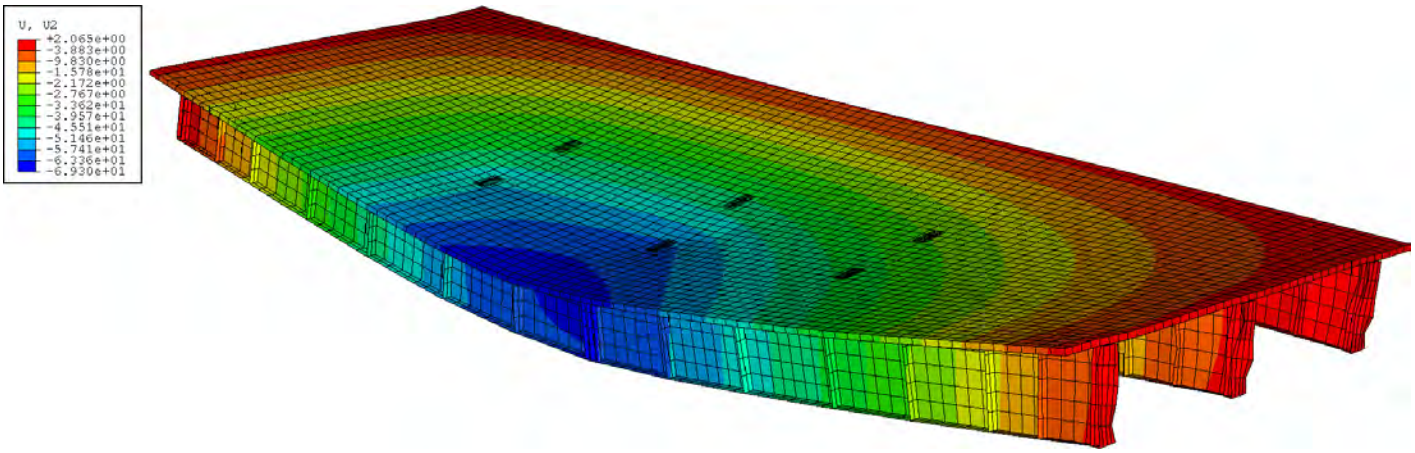

Figure A.11. An example of the deflections in the bridge at the ultimate load.

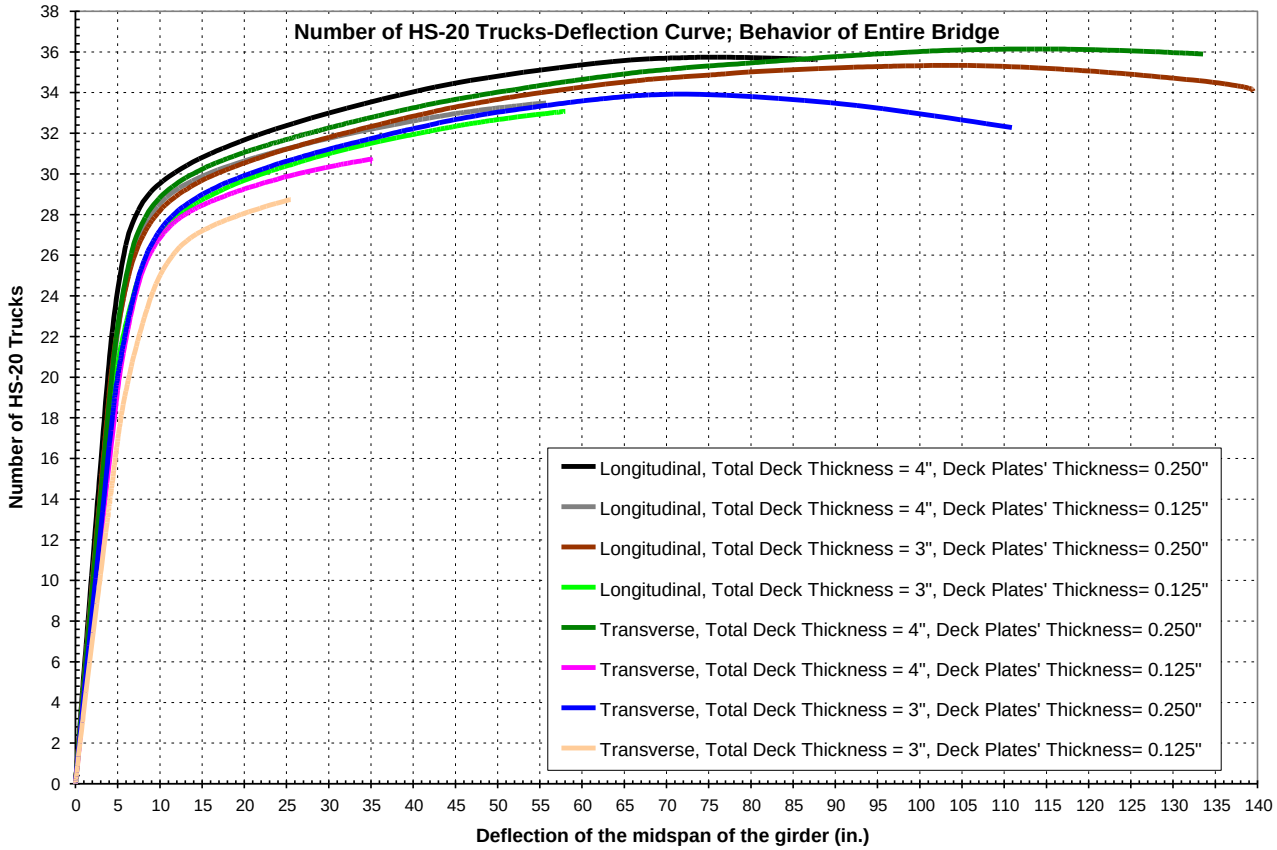

Figure A.12. Load–deflection curves of the structure associated with two trucks side by side.

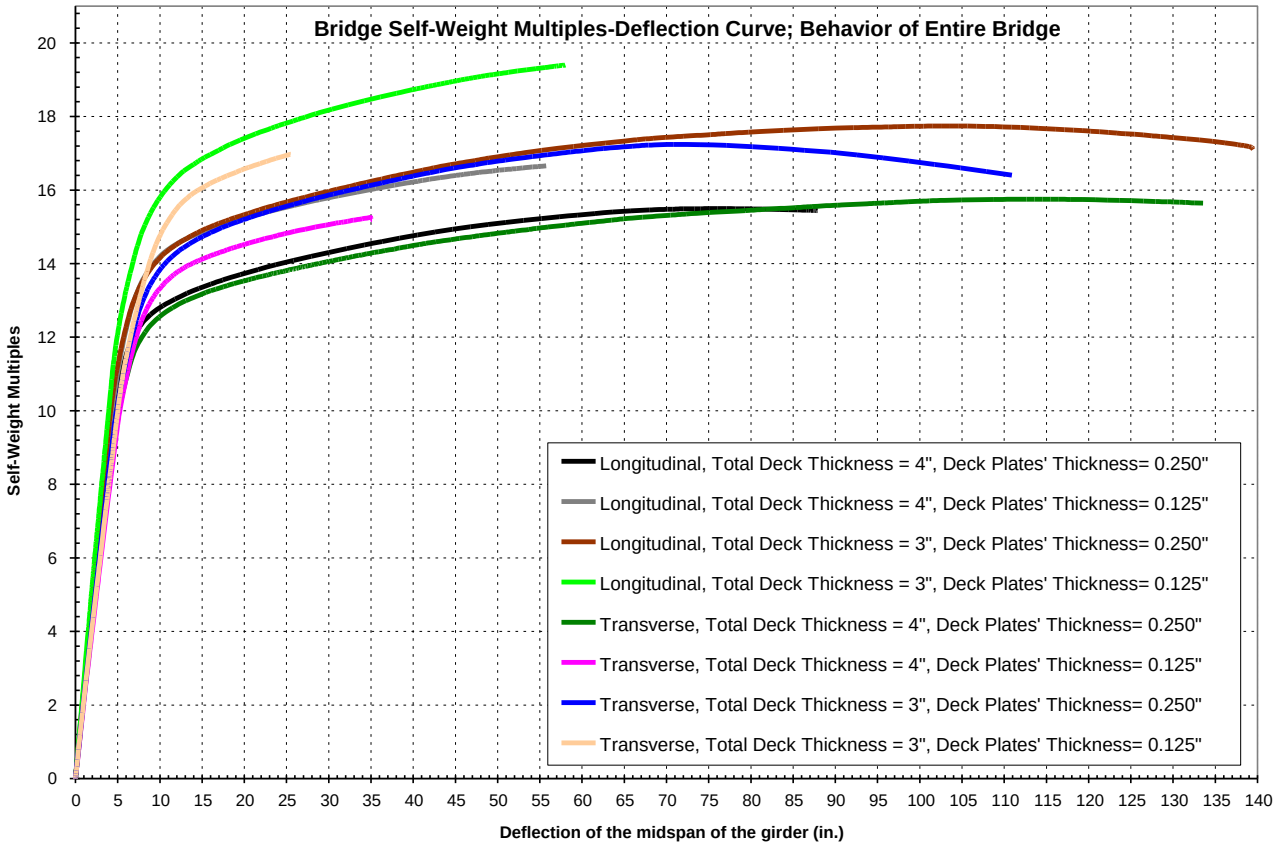

Figure A.13. Load–deflection curves in terms of bridge weight using two trucks side by side.

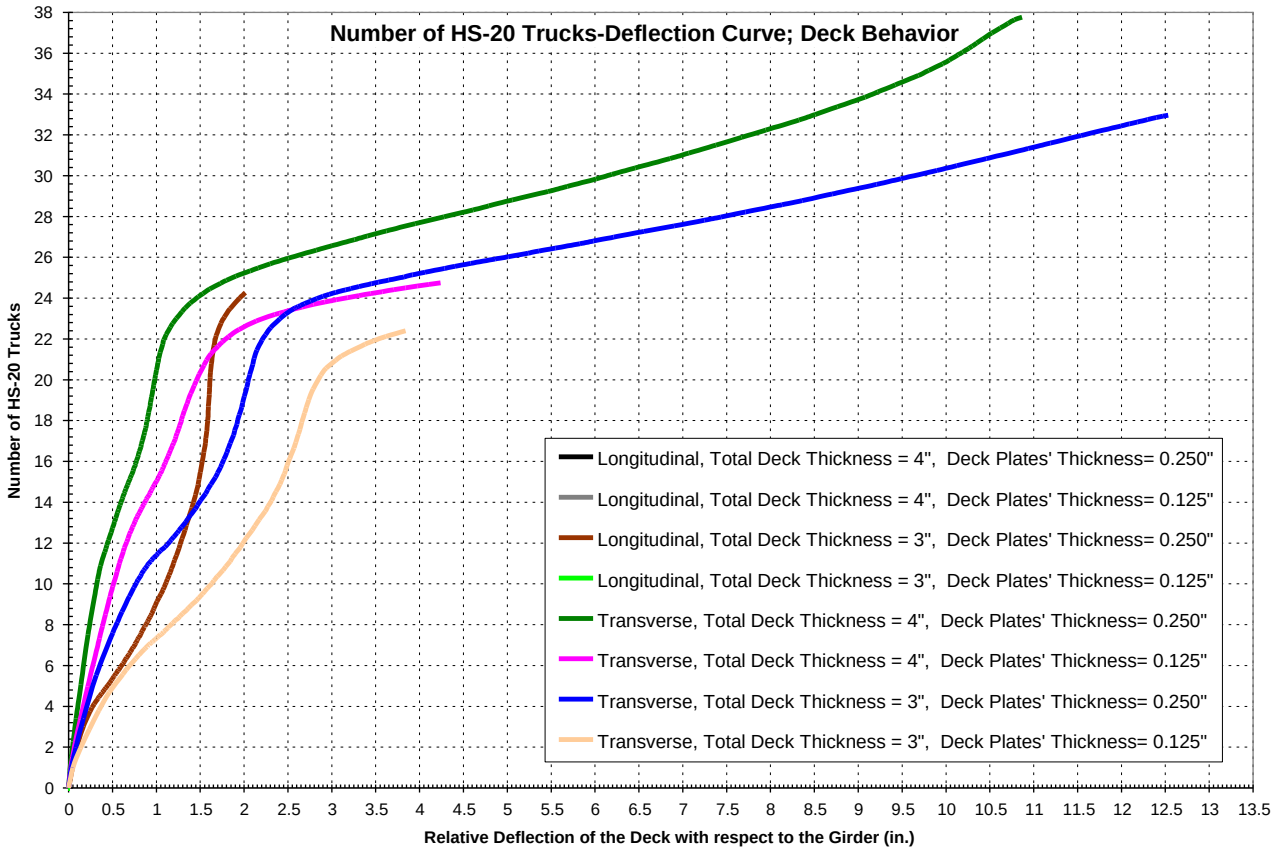

Figure A.14. Load–deflection curves in terms of bridge weight using one truck with one side on the middle of girders spacing.

- An efficient spacing between the ribs of an orthotropic deck can be obtained from cost analysis.
- Increasing the orthotropic deck plate thickness will increase the ultimate ductility of the bridge and, to a lesser extent, the ultimate load-carrying capacity of the bridge.

Possible Research Plan for Others

The issues needing investigation are listed below:

Welding process—So-called blind welding technology using laser welding is one available technology that can be used to weld steel plates from the "blind" side.

Optimal orthotropic deck dimensions—The behavior, efficiency, constructibility, and economy of the proposed hybrid orthotropic deck system depend on a number of factors, including its dimensions. The thickness of the deck plates, the thickness of the deck, and the distance between the ribs are some of the dimensions to be investigated.

Economical bridge span—The proposed hybrid orthotropic deck system would not be economical for all span lengths. This range can be a subject of research.

Connection to supporting girders—There is a need to develop details that could be used to attach prefabricated sections to each other and to steel girders.

Corrosion protection of the orthotropic steel plates—Corrosion protection philosophy needs to be developed for exposed steel. Use of A1010 steel is an alternative. A1010 steel costs about twice as much as regular steel; however, it has excellent corrosion properties.

The following steps are suggested for investigating the merits of the system:

Step 1. Conduct a preliminary cost analysis and finite element study to determine the most efficient configuration of the orthotropic deck system.

Step 2. Determine the best available welding technology through discussion with industry.

Step 3. Perform laboratory testing of a small-scale, one-girder hybrid orthotropic deck system under fatigue and then ultimate loading. The test specimen should include the riding surface, and membrane delamination from the riding surface should be evaluated.

Step 4. Develop detailed design, fabrication, and construction guidelines.

Development of Seismic Details for Simple for Dead and Continuous for Live Load Steel Bridge System

Recently a new steel bridge system, referred to as simple for dead load and continuous for live load, has gained popularity in nonseismic areas of the country. Research conducted over the past 10 years (Azizinamini 2013) has resulted in the development of complete design and detailing provisions for this new system for nonseismic applications. As there are no bolts or expansion joints in this system, it should have a long service life. This system is also best suited for accelerating the construction process. It is ideal for building individual spans off site, transporting them to the final location, and then joining the spans over the middle piers to create continuity for live load. Another version of the system that uses adjacent beam technology can significantly reduce the on-site construction activities.

Background

To date no research studies have been conducted to extend the applicability of this system to seismic regions. The main objective of this proposed concept as a research area is to use the available research data (for nonseismic application) and conduct mainly numerical work to develop details and design provisions for extending the application of the simple for dead and continuous for live steel bridge system to highly seismic areas. The focus of the study should be on using this system in conjunction with accelerated bridge construction philosophy. This work should provide highly seismic areas with an excellent steel bridge system alternative that does not have expansion joints and potentially produces long service life while meeting seismic design requirements.

Brief Overview of Seismic Design Requirements

Steel bridges are about 40% lighter than concrete alternatives and, at first glance, are expected to provide better performance in a major earthquake. However, observations from a past earthquake demonstrate that the use of wrong details or systems could result in steel bridges sustaining major damage (Astaneh-Asl et al. 1994). In the 1995 Hyogoken-Nanbu earthquake in Kobe, Japan (Bruneau et al. 1996; Chung 1996; Shinozuka et al. 1995; Azizinamini and Ghosh 1997), steel bridges suffered damage to superstructure elements (inadequate cross-frame detailing leading to lateral bending of the girder webs near girder ends) resulting in major retrofit activities and closing of major highways, such as the Hanshin Expressway, for more than a year. The Kobe experience demonstrated that even minor damage to steel bridges in seismic events can result in types of damage that could be very difficult to repair. Among the lessons to be learned is that critical elements of the bridge that are difficult to inspect and repair must be protected from any level of damage and remain elastic during the entire seismic excitation.

Seismic input is largely unknown; therefore, the design philosophy for buildings and bridges is to work on behavior of the structure under known conditions. Specifically, the design objective is to predefine the damage locations and design them accordingly by providing adequate levels of ductility. In the case of bridges, the preferred damage locations are at the ends of pier columns (formation of plastic hinges). In the direction of traffic, it is preferred to put columns in double curvature, as shown in Figure A.15. This arrangement allows larger portions of the pier column (two plastic hinges versus one for single curvature) to participate in energy dissipation.

In the transverse direction, pier columns are usually designed to act in single curvature, as shown in Figure A.16.

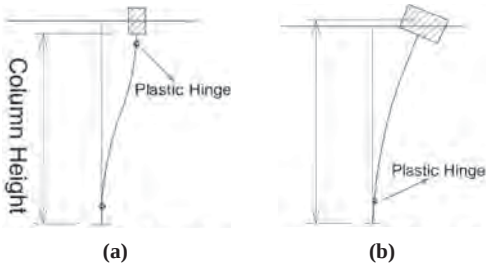

Figure A.16. Deflected shape of pier column in (a) longitudinal and (b) transverse directions.

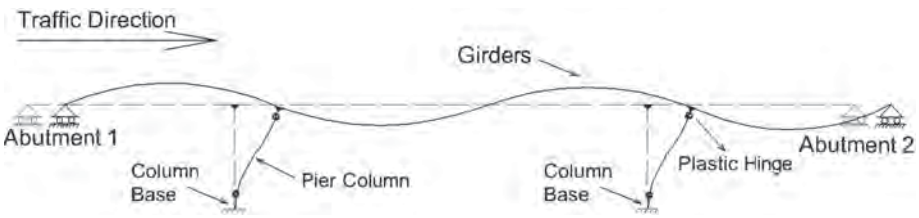

Figure A.15. Deflected shape of a three-span bridge under the longitudinal (along traffic) direction.

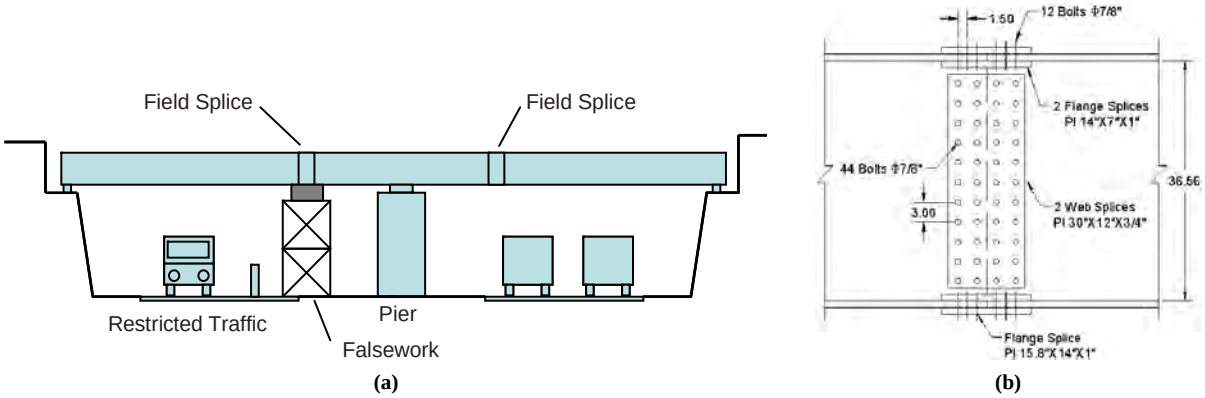

Figure A.17. (a) Conventional two-span continuous bridge girder and (b) typical splice detail.

Under longitudinal excitation, plastic hinges are located near the top and bottom of the columns; under transverse excitation, the plastic hinge is located near the bottom of the pier column.

Seismic design of steel bridges is still a developing subject. One of the most comprehensive design provisions for design of bridges for seismic events is given by Caltrans Seismic Design Criteria (Caltrans 2008).

The main design requirement in the seismic design of bridges is to keep the superstructure elements, called protected elements, completely elastic during an entire seismic event. The inelasticity is then forced to take place at predefined locations within the substructure. The predefined damage locations are the weak links or fuses that control the level of forces to be transmitted to superstructure elements. This design approach, which is referred to as the capacity design approach, is used for designing bridges in seismic regions.

In the capacity design approach, protected elements are designed for the largest possible force effects they might experience, considering overstrength that may exist because of higher actual material strength than that specified in design. The capacities of the bridge elements in the desired damage location (plastic hinge locations) are controlled through design. The plastic hinge regions are also detailed so that they can provide the desired capacities while deforming in an inelastic manner during a seismic event (ductility through adequate detailing).

Brief Description of Simple for Dead and Continuous for Live Load Steel Bridge System

Continuous steel bridges are usually constructed so that the system provides continuity for noncomposite dead loads in addition to superimposed dead load and live loads. Figure A.17 shows a conventional two-span continuous steel bridge girder. For a large number of bridges, the construction sequence consists of first placing a middle segment over the interior support and then connecting the two end pieces by using a bolted or welded field splice.

In the simple for dead load and continuous for live load system, the girders are spliced over the pier. Girders are placed spanning directly from abutment to pier within each span. The individual spans are simply supported when the deck is cast. Once the deck is in place, reinforcing steel cast into the deck provides continuity of the tensile forces for live load and superimposed dead loads (the weight of barrier and future wearing surfaces) only. The compressive component is transferred through direct bearing of the bottom flanges. An example of this detail is shown in Figure A.18.

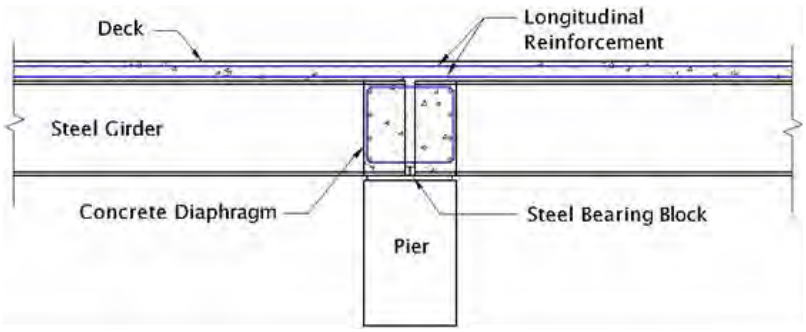

Figure A.18. Simple for dead and continuous for live detail.

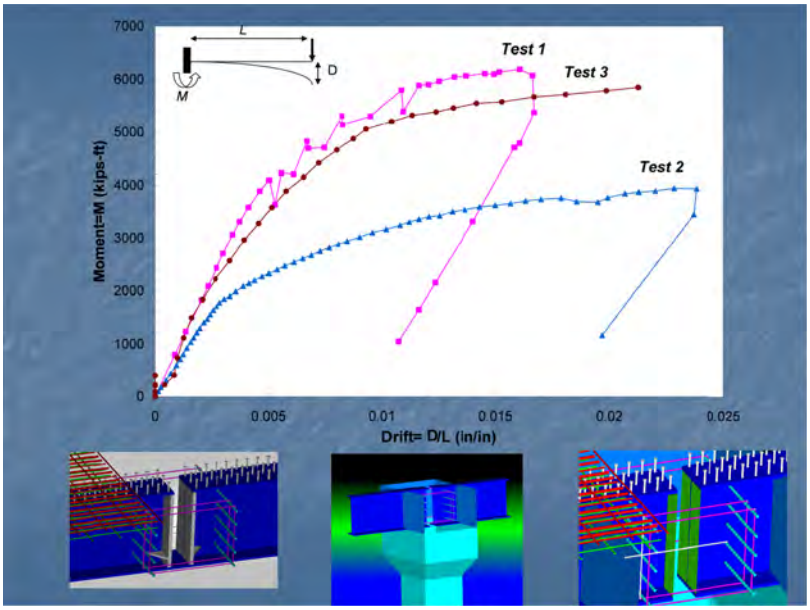

Figure A.19. Comparing performances of various details for connecting girder ends over the pier in nonseismic regions.

The main challenge is to use the correct detail over the pier to connect the girder ends. Bottom flanges of steel embedded in the concrete diaphragm transmit large stresses to the concrete and, if not detailed correctly, can crush the concrete. Figure A.19 shows the results of tests on three details that could be used to connect girder ends over the pier in nonseismic regions.

The main lesson learned is that the bottom flanges of the steel girders embedded in the concrete diaphragm should be connected somehow. This arrangement will allow the transfer of compressive force (generated by live loads) from one girder to another girder without passing through the concrete diaphragm. The three test specimens shown in Figure A.19 were identical, except the details used at the ends of the girders, embedded in the concrete diaphragm. In one specimen, labeled Test 2 in Figure A.19, the ends of the girders did not incorporate any detail and were simply embedded in the concrete diaphragm. As noted, the capacity of that specimen was significantly less than the other two specimens, in which the ends of the girders incorporated details that allowed a smooth path for transferring the compressive force from one girder to another.

In nonseismic applications, the forces to be transmitted from the bottom flange of one girder to another girder in the concrete diaphragm are predominantly compressive, and the detail to be used is not required to handle tension force. Figure A.20 shows a detail that is suitable for nonseismic application and has been used in several bridges in service. However, in seismic application, the types of details shown in Figure A.20 will not work. In seismic areas, the detail at the ends of the girder in the concrete diaphragm region needs to be able to resist cyclic loading, which will involve both tension and compression. In nonseismic application it only needs to resist compressive-type force. Further, in seismic applications the entire concrete diaphragm region, including the girders ends and details, needs to remain completely elastic (protected elements) during the entire seismic event. An additional requirement is that the predefined damage areas (plastic hinge locations) must be forced to be at some distance away from the concrete diaphragm region, allowing repair and inspection after a major seismic event.

Figure A.20. Detail used in nonseismic regions.

Simple for Dead and Continuous for Live Load System Using Adjacent Beam Technology

The adjacent box concept uses prefabricated units consisting of an individual steel box girder topped by a portion of deck slab, as shown in Figure A.21. These units are prefabricated and then shipped to the job site. The portion of the deck shown in Figure A.21 is cast at the fabrication shop or temporary staging location. Once on site, the individual units are set in place on the supports adjacent to one another, as shown in Figure A.22. A longitudinal deck closure strip between the individual units is then cast to join them. At the same time, the turndown over the interior support is cast. The interior turndown connects the spans and provides continuity between them for subsequent loading (live load).

The individual units (steel box and pretop deck) are relatively lightweight, typically less than 100 tons for spans of 140 ft. Once the pretop girders are placed side by side, they are then connected through casting closure pour regions.

Figure A.23 shows the closure region detail. One option is to use headed bars, as shown in Figure A.24, in the closure pour regions.

Figure A.25 shows a rendering of the closure splice region over the interior support. The hooked bar ends from each span anchor the longitudinal reinforcement into the turndown and provide continuity over the support. A similar detail is shown in Figure A.26.

Objective

The objective of the study must be to develop recommendations for extending the application of the simple for dead and continuous for live load steel bridge system to highly seismic areas.

Figure A.21. Single (interior) box girder and deck unit.

Figure A.22. Three adjacent box girder units.

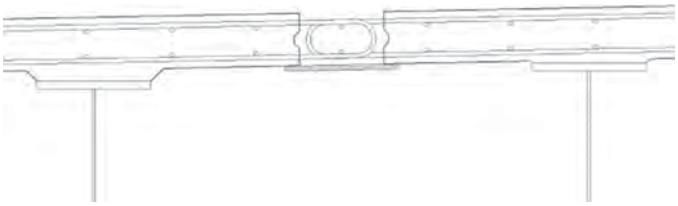

Figure A.23. Closure region detail.

Suggested Scope of Work

An extensive amount of research data for the proposed system in nonseismic regions exists. However, there are specific requirements for seismic applications that need to be addressed. For seismic applications, the detail over the pier should have the following characteristics:

1. It should be adequate for cyclic loading (designed for tension and compression).
2. The plastic hinge locations should be at some distance away from the girder ends and column ends near bearings.
3. Design should follow a capacity design philosophy, allowing different performance levels as desired by the owner.

To achieve these objectives, the following five tasks should be carried out:

Task 1. Develop preliminary ideas on types of details that could be used to join the girder ends over the pier.

During a seismic event, the column moment becomes a torsional force for the concrete diaphragm, as shown in Figure A.27.

The concrete diaphragm will be the protected element and must remain elastic. Therefore, the concrete diaphragm

Figure A.24. Headed bar detail.

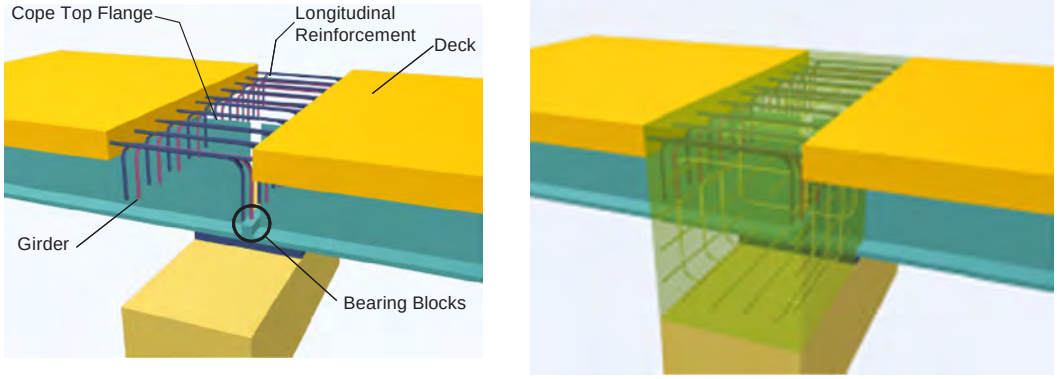

Figure A.25. Interior support continuity detail.

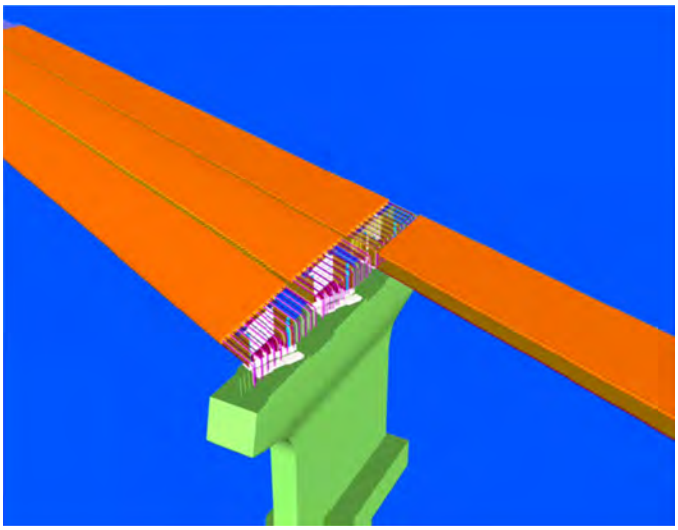

Figure A.26. Interior support detail showing multiple girders.

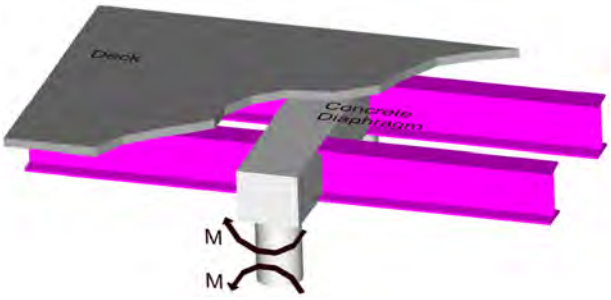

Figure A.27. Transfer column moment to concrete diaphragm.

must be designed for maximum credible torsion and remain elastic. Several approaches can be used to ensure that the concrete diaphragm remains elastic under maximum credible torsion. Posttensioning the concrete diaphragm is one possibility (Patty et al. 2002). Further, the plastic hinge at the column end must form at some distance away from the column ends. The detail to be selected will be such that it will create a frame action between superstructure and substructure (integral pier cap). The integral pier cap detail is the preferred choice in some parts of the United States, such as the West Coast, because of aesthetics considerations.

Task 2. Modify the existing detailed nonlinear finite element models used in a previous research study (Farimani et al. 2013) on applicable nonseismic details to determine the force transfer mechanisms of the details identified under Task 1.

Figure A.28 shows an example of models used in previous research studies.

Task 3. Conduct small-scale tests to verify specific aspects of the detail selected under Task 1. This test can also be used as a means to calibrate the analysis model in Task 2.

Task 4. Based on the results of Tasks 1, 2, and 3, develop preliminary design provisions using a capacity design approach.

Task 5. Develop a plan of action for research studies by others to develop test-verified details suitable for seismic regions.

List and Description of Other Category 3 Research Concepts

Table A.3 lists other concepts for Category 3 research areas that have been identified and are proposed for research by others.

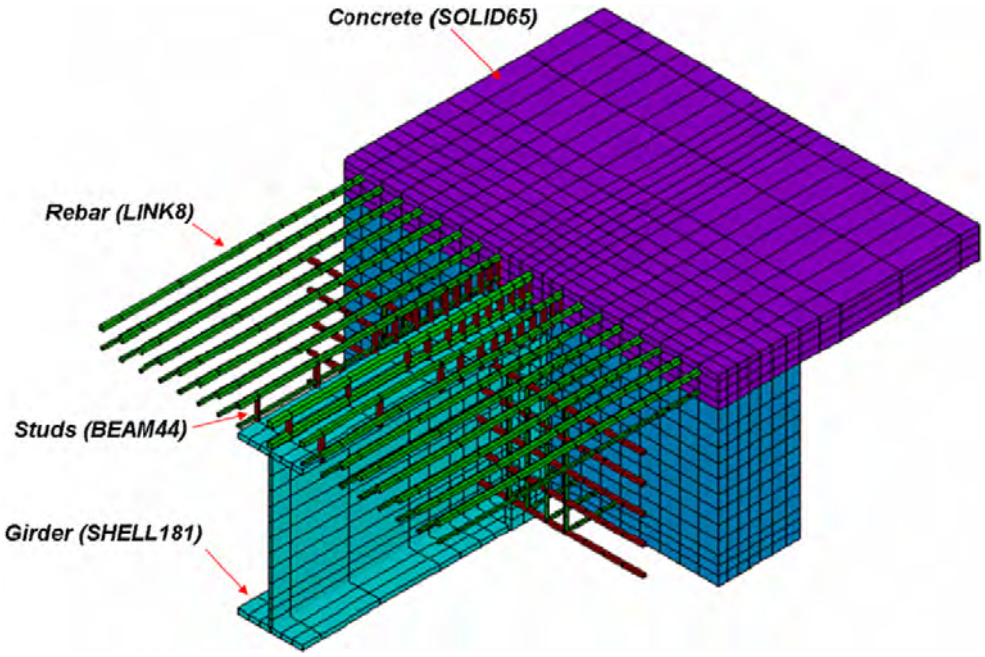

Figure A.28. Typical finite element models used to investigate force transfer mechanism for nonseismic details.

Table A.3. Additional List of Category 3 Research Items

Research Area	Topic
Concrete durability	Develop tension limits and mix designs defining low-cracking concrete.
	Investigate use of nanomaterials to improve the paste and the interface between the aggregate and the paste, leading to reduced permeability.
	Determine lightweight concrete benefits.
	Investigate fatigue in concrete (predicting microcrushing of deck concrete).
	Investigate use of inorganic nanomaterials and electric field for filling cracks, even when they are very tight.
	Investigate using smart materials to respond to distress in concrete. For example, if cracks occur, the smart material would close the crack; if the pH decreases, the smart material would increase the pH.
Bridge deck	Develop systems for protecting the underside of the bridge deck from seawater intrusion, which may include innovative means and methods of forming for the deck.
Substructure	Investigate high-performance concrete applications in splash zones needed to reduce concrete permeability and enhance chemical resistance to salt water.
	Investigate jacketing systems for piles and shafts.
	Consider incorporating with new construction to protect critical parts before damage and chloride intrusion can occur.
	Investigate pile splicing systems for improvements in long-term durability.
	Develop substructure components using innovative (composite) construction materials that have strong resistance to saltwater environments.
Bearings	Develop life prediction model using fatigue testing for steel-reinforced elastomeric bearings.
	Develop life prediction model using fatigue testing for cotton duck pads.
	Develop life prediction model using fatigue testing for high-load multirotational disc bearings.
	Develop life prediction model using fatigue testing for high-load multirotational pot bearings.
	Determine the proper orientation of guided bearings for curved and skewed bridges by analytical study.
Joints	Develop rapid replaceable expansion joint assembly.

(continued on next page)

Table A.3. Additional List of Category 3 Research Items (continued)

Research Area	Topic
Fatigue and fracture	Develop guide for fatigue retrofitting.
	Investigate potential cracking problem with galvanized steel members.
	Develop toughness standards for tubular and hollow-section members.
	Develop criteria that tie inspection frequency of fracture critical members to level of damage accumulation, that is, to average daily truck traffic.
	Investigate the feasibility of using a coating system for crack detection.
	Investigate the use of real-time instrumentation and monitoring for crack detection and monitoring.
Corrosion protection	Develop a best practices manual.
Steel bridge systems	None for Category 1
Concrete bridge systems	Develop nonposttensioned systems that will ensure transverse continuity and nonleaking joints for adjacent member bridges.
	Add threaded-rod continuity to create full continuity for deck weight and to eliminate potential creep restraint cracking at the piers (Nebraska; Alberta, Canada; Illinois; Florida).
	Add posttensioning to keep superstructure sections under compression that are prone to cracking.

APPENDIX B

Converting Existing Simple-Span Steel Bridges to Continuous

Problem Statement

A large number of steel bridges have been constructed as a series of simple spans with deck expansion joints at each pier. This was a popular system concept because it was easy to design and construct. Leaking deck joints, however, have become a leading cause of deterioration and subsequent reduced service life for all types of bridges. Figure B.1 shows a typical example of a steel bridge simple-span system with a leaking deck joint over a pier. New bridge systems that eliminate deck joints as much as possible have now become the norm. Converting existing simple-span systems to continuous and eliminating deck joints have also been used as ways to extend the service life of existing bridges.

Converting existing bridges to continuous has often been done as part of overall bridge rehabilitation when decks were being replaced. However, types of details and levels of achieved continuity have varied considerably. Some state departments of transportation (DOTs) have developed specific guidelines for splicing girders over piers, and others have addressed this on a case-by-case design basis. As a result, many variations exist in the industry.

Figure B.1. Steel simple-span girders with deck joint over pier.

There is a need to provide more uniform and consistent guidelines regarding design criteria, details, and performance that will result in cost-effective service life extension.

Objectives

The objectives of the study presented in this appendix were to review current state DOT criteria and details for converting existing simple-span steel bridges to continuous and to develop recommendations for consistent cost-effective approaches.

Scope of Work

The scope of work for this study included

- Collecting, reviewing, and summarizing the state of current practice from various states;
- Developing recommended criteria for continuity retrofit that include guidelines for analysis, along with considering system behavior; and
- Developing recommended details.

Results

Review of Current Practice

A brief survey of national HDR, Inc., offices was conducted to identify current state DOT practice and experience, if any, for converting existing simple-span steel bridges to continuous. Reference was made to three possible approaches:

- Converting girders to fully continuous for dead load and live load;
- Converting to continuous for live load only; and

- Converting by using a continuous slab over the joint and not connecting the girders (link slab).

Specific questions focused on the respondent's local industry experience concerning steel girder continuity retrofit, such as

- What experience have you or your state had in developing design, procedures, and details for converting existing simple-span steel bridges to continuous?
- What standards, if any, does your state DOT have, either in a design manual or standard design drawings, for doing this?

It was found that a number of states have performed such conversions, primarily during deck replacement rehabilitations, but few have specific design procedures or standard details. Some states have guidelines for new design, but not for retrofit of existing; however, these details for new design could also be adapted for continuity retrofit.

The following subsections summarize various practices around the country.

New York Experience

The New York State DOT (NYSDOT) provides a good summary of criteria for continuity retrofit in the NYSDOT *Bridge Design Manual,* which discusses feasibility, general design considerations, and design guidelines (NYSDOT 2008). The manual addresses full continuity versus continuous for live load and discusses advantages and disadvantages. Figure B.2 shows typical details from the NYSDOT manual.

Fully continuous retrofits are advantageous because the combined girder behaves like a conventional continuous girder, and a single bearing can be used. Continuity is provided for deck dead load and live load, with simple-span behavior for steel girder dead load. However, this concept requires more complex splice details for the web and flanges and may require long flange cover plates to accommodate the larger negative moment, which can make the retrofit costly.

For continuous for live load retrofits, only the girder flanges are spliced, and two lines of bearings from the existing simple-span configuration are retained. The top flange detail uses a

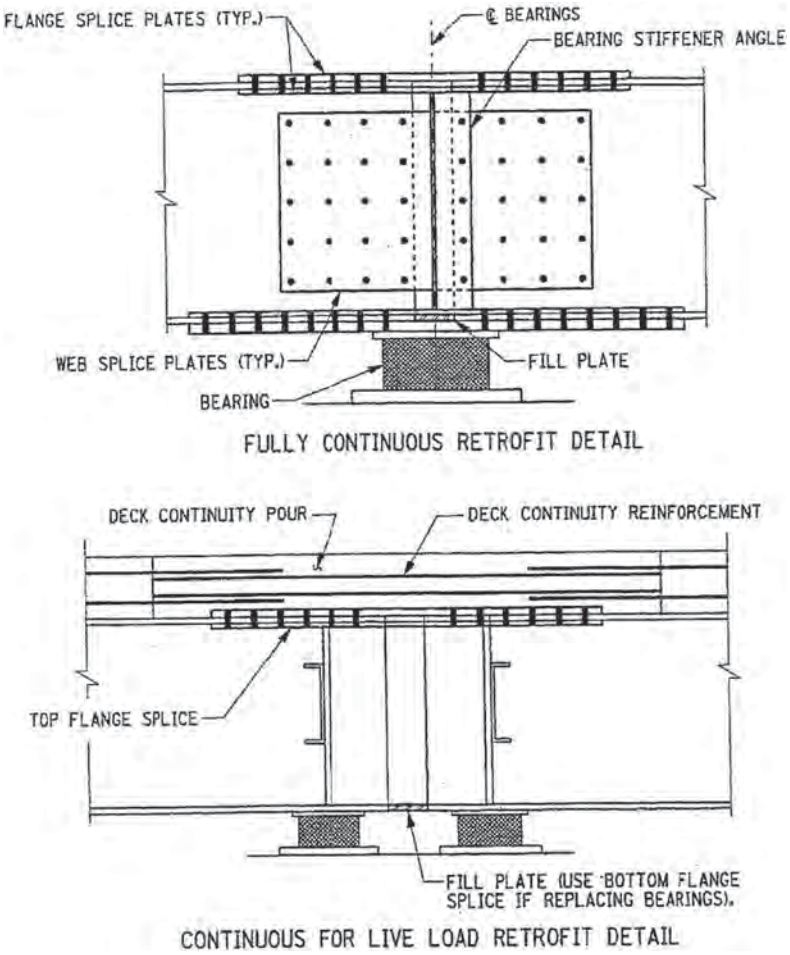

Figure B.2. Typical details for converting simple-span beams to continuous from the NYSDOT* Bridge Design Manual *(2008).

conventional splice, but the bottom flange connection can be made using a compression block fitted and welded between the ends of the girders. This live load retrofit method also adapts well if the existing deck is not fully replaced, but only a short section over the pier.

New York State Thruway Authority Experience

From about 1988 to 1992, the New York State Thruway Authority (NYSTA) routinely converted many bridges to continuous for live load by simply joining the bottom flanges and making the deck continuous over the joint. This practice was halted because of concerns of properly analyzing the resulting semirigid connection. Many of these bridges are still in service, usually with a crack over the joint, but are otherwise performing well. These were simple details with little cost.

Around 1995, NYSTA developed a standard for the design and detailing of a fully continuous retrofit splice. After implementing on a few retrofits, primarily on grade separation structures, it became clear that they were not cost-effective, and the NYSTA stopped doing them. The cost of cleaning and painting the old steel, combined with the extensive field work required to remove the end diaphragms, field drill numerous bolt holes, rework the pedestals, and so on, started to approach the cost of new steel. This was also found on a retrofit in Pennsylvania reported later.

Tennessee Experience

The Tennessee DOT has experience with new design for bridges that have girders constructed as simple spans that are then converted to continuous. Over several years they developed and experimented with different concepts.

The first was a detail for simple span for noncomposite dead loads and continuous for composite dead loads and live loads. Continuity over interior supports was achieved by a cast-in-place concrete diaphragm (see Figure B.3).

The Tennessee DOT then thought that more overall economy could be realized by a concept that made the beams also continuous for the dead load of the wet concrete slab. This modification was achieved by a splice detail, as shown in Figure B.4. The bottom flange was connected by a welded cover plate and wedge kicker plates, and the top flange was spliced with a single-shear bolted cover plate. The top and bottom cover plates were extended to accommodate the additional negative moment bending stress due to continuity. This detail was also combined with a concrete diaphragm over the piers.

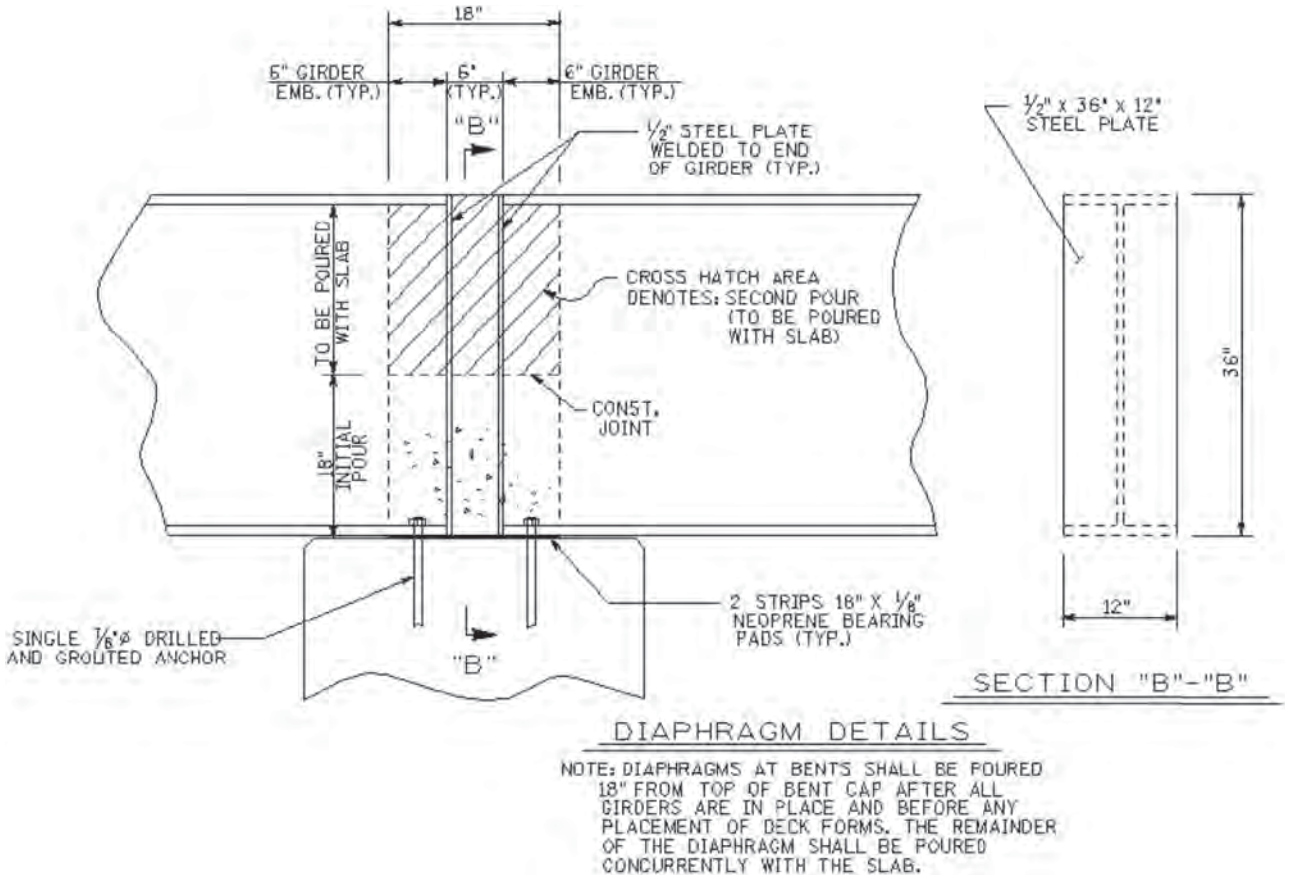

Figure B.3. Tennessee continuity diaphragm detail.

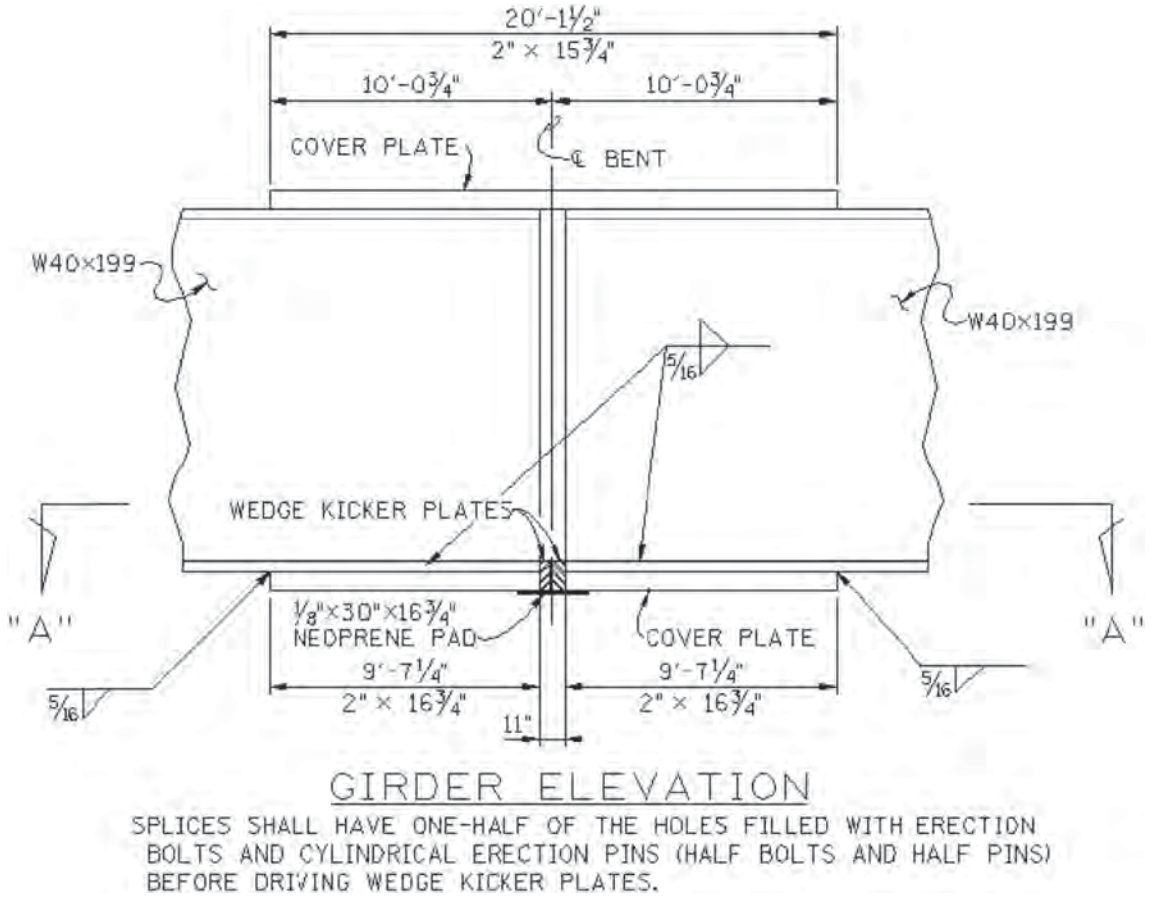

Figure B.4. Tennessee splice detail.

New Mexico Experience

The New Mexico DOT developed a girder connection using a splice plate for the top flange and placed the connection bolts outside the poured concrete diaphragm at the piers (Figure B.5). Bolts placed heads-up and nuts-exposed-down permitted tightening after pouring of the deck and pier diaphragms.

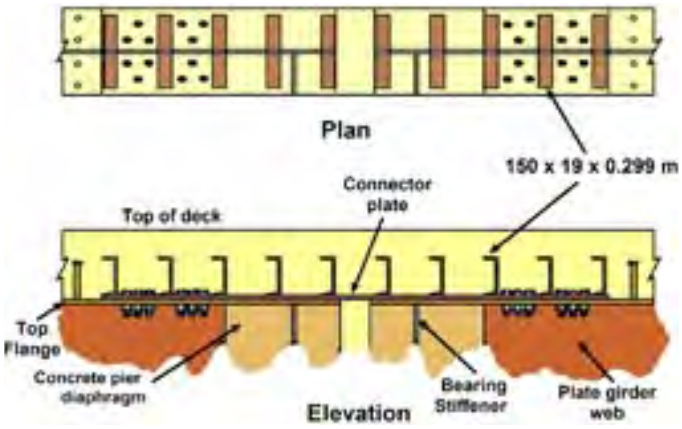

Figure B.5. New Mexico top flange connection plate detail.

After deck pours, the bolt heads were locked into the concrete deck. Bolts were then tightened by turning nuts from below. Final tightening came after all concrete had been poured for the deck and pier and abutment diaphragms, before opening for traffic.

The design required adding reinforcing bars to normal longitudinal deck reinforcement over the piers. The additional reinforcement achieved the required negative moment capacity for the bridge's continuous live-load function. Under live loads the continuity connection plate would be lightly stressed. It was considered that the continuity plate connection would also add redundancy in the event that future deck deterioration reduced the effectiveness of the deck reinforcement for negative moment capacity.

Pennsylvania Experience

In Pennsylvania, the simple-span approaches to the Fort Pitt Bridge in Pittsburgh were all converted to continuous. A series of spans in the 72- to 83-ft span-length range were retrofitted by adding top and bottom flange splices and web splices to achieve continuity for the deck dead load and live load (see Figure B.6). In a shorter span unit with a series of

(a) (b)

Source: HDR, Inc.

Figure B.6. Simple-span girders made continuous in Pittsburgh, Pennsylvania: (a) rolled I-beams and (b) riveted plate girders.

five 54-ft spans, alternate plans were prepared for stringer rehabilitation with continuity splices versus full stringer replacement. For this unit, all contractors bid full stringer replacement. It was determined these short spans had a high number of continuity splices with respect to total steel weight, making stringer replacement more economical.

West Virginia Experience

In West Virginia, a continuity detail was used for new construction on a two-span continuous overpass bridge. Figure B.7 shows the splice, which was designed for live load continuity. The top flange connection used a bolted splice, and the bottom flange connection used bearing plates and wedges for compression. The top flange splice and bottom flange continuity plates were not installed until after the deck was placed in positive moment regions.

Two Other Continuity Concepts: Elimination of Top Flange Splice and Link Slab

Figure B.8 shows an economical and functional live load continuity detail that has been used for spans up to about 150 ft. It uses bottom flange bearing plates and wedges for compression, but relies on a concrete diaphragm and top concrete slab for top flange continuity without a top flange splice. Eliminating the top flange splice creates a simpler construction sequencing.

Another way of providing continuity and thereby eliminating joints over piers is the link slab concept, in which the

Figure B.7. West Virginia live load continuity detail.

Figure B.8. Continuity without top flange splice.

girders are not directly spliced; rather, the deck is made continuous over the open gap between girder ends. See the link slab section in the main report for more detail.

Design Considerations

There are many benefits of converting simple spans to continuous, including reducing the potential for continued deterioration due to leaking joints, increasing resistance to seismic displacements, and slightly improving the load-carrying capacity of the superstructure.

The design for continuity retrofit needs to consider the system behavior of continuous girders as opposed to original simple-span behavior. For multispan continuous systems, larger movements may be realized at abutments or at interior piers if original fixed conditions are converted to full expansion conditions. Also, increased vulnerability to fatigue may result due to portions of the retrofitted beams being subjected to stress reversals and higher stress ranges than the original simple-span construction. The end regions of retrofitted girders originally designed for small simple-span positive moments are subjected to larger magnitude negative moments. Although the deck joints over the piers are eliminated, the retrofitted deck in this area is subjected to tension under service loads, and crack control measures must be considered. Continuity can also increase seismic loads on individual piers depending on retrofitted bearing fixity configurations. Deck replacement projects provide excellent opportunities to include girder retrofit because girders will be readily accessible and future costs of maintaining the joints will be eliminated (NYSDOT 2008).

Conclusions and Recommendations

There are several viable continuity retrofit options:

- All continuity retrofit options require a system evaluation for both girder stress and movement at bearings.
- A continuous for live load retrofit splice is typically more cost-effective than a full continuity retrofit splice. A splice detail that uses bottom flange butt plates and eliminates the top flange splice by using connection diaphragm and deck is recommended over details with a top flange splice.
- A link slab detail without stringer splice details is most economical if accompanying deck cracking is acceptable.
- Continuity splice details need to match existing as-built conditions.
- Full stringer replacement can be most economical for short spans accompanied with deck replacement, cleaning, and painting.

APPENDIX C

Joints in Modular Systems of Adjacent Box Girders

This appendix presents details of the experimental testing performed on a precast adjacent box beam system with transverse posttensioning. Additional information describing the development of the system can be found in the following PCI journal articles: Simplified Transverse Post-Tensioning Construction and Maintenance of Adjacent Box Girders (Hansen et al. 2012) and Transverse Post-Tensioning Design and Detailing of Precast, Prestressed Concrete Adjacent-Box-Girder Bridges (Hanna et al. 2009). A source of general information is the PCI Bridges Committee publication titled The State of the Practice of Precast/Prestressed Adjacent Box Beam Bridges (PCI 2011).

Background and Problem Statement

Precast adjacent box beam bridges are one of the prevalent box girder systems for short- and medium-span bridges (typically 20 to 127 ft), especially on secondary roadways. These bridges consist of multiple precast box beams that are butted against each other to form the bridge deck and superstructure. The system also has applicability to accelerated bridge construction for rapid delivery. Adjacent box beams are generally connected using partial- or full-depth grouted shear keys along the sides of each box. Transverse ties are usually used in addition to the grouted shear keys; these may vary from a limited number of threaded rods to several posttensioned tendons. In some cases, no topping is applied to the structure, but in other cases a noncomposite topping or a composite structural slab is added.

Bridges constructed using box beams have been in service for many years and have generally performed well. However, a recurring problem is cracking in the grouted joints between adjacent units (see Figure C.1), which results in reflective cracks in the wearing surface and deterioration and cracking on the bottoms of beams (see Figure C.2 through Figure C.6). The development of these longitudinal cracks over the shear keys jeopardizes the durability and structural behavior of adjacent box girder bridges (Kahl 2005; Huckelbridge et al. 1995). In most cases, the cracking leads to leakage, which allows chloride-laden water to penetrate the sides and bottom of the beams and cause corrosion of the nonprestressed and prestressed reinforcement. In addition, the load distribution among the beams is adversely affected, so that the loaded beams are required to carry more load than originally intended (Huckelbridge et al. 1995).

Objectives of the Research

The general objective of this research topic is to improve the performance of adjacent box beam bridges, specifically with regard to the transverse connection. The overall objectives are (1) to achieve the structural capacity of this system in the transverse direction and (2) to prevent longitudinal joint leakage. These objectives are accomplished by developing a detail that has the ability to transfer moment and shear in the transverse direction.

Previous Research

Previous research by the University of Nebraska–Lincoln (UNL) investigated the benefits of nonposttensioned systems and developed two new connection details that are both efficient and economically practical. Advantages of these systems include

- Improved production;
- Easier inspection of voids;
- Better drainage of moisture;
- Lighter weight for handling and shipping; and
- Continuous rather than discrete (quarter-point) connections.

Below is a brief description of the two systems; additional information can be found in (Hanna et al. 2011).

Figure C.1. Crack developed in joint between adjacent box beams.

Wide Joint System

The wide joint system developed by UNL does not use a topping or diaphragms. Top and bottom transverse reinforcement is used in a wide shear key filled with concrete to connect adjacent boxes instead of the reinforced concrete composite topping. This monolithic joint with top and bottom reinforcement provides continuous connection that transfers shear and moment between boxes and eliminates the need for intermediate or end diaphragms. The elimination of topping and diaphragms will significantly speed the production and construction operations and reduce the material, labor, and

Figure C.2. Crack developed in adjacent box beam bridges.

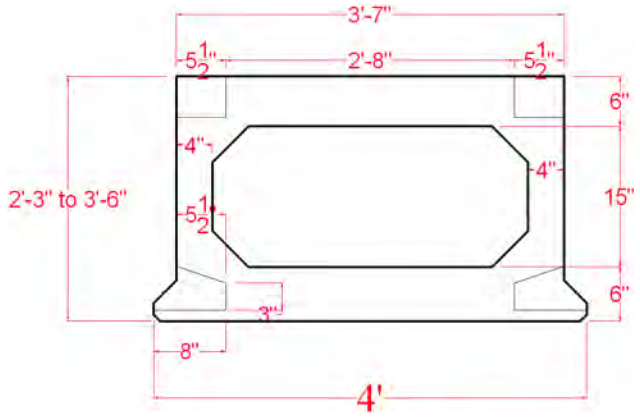

Figure C.3. Wide joint system box dimensions.

erection costs. Shear keys used in the wide joint system are wide full-length and full-depth shear keys that require a slight modification to the AASHTO standard box cross section and consequently the forms. Figure C.3 shows a modified 33-in.-deep and 48-in.-wide AASHTO PCI box section as an example. Modifications include (1) a 5-in.-wide shear key (2.5 in. at each box side); (2) two block-outs every 4 ft at the top flange, which are 4 in. deep, 5.5 in. long, and 5.5 in. wide; and (3) two block-outs every 4 ft at the bottom flange, which are 8 in. long and 4 in. wide. Two reinforced concrete connections are used at the block-out locations (every 4 ft) in the top and bottom flanges to connect adjacent boxes. Reinforcing steel bars extending from the top and bottom flanges of each box are lap spliced using short bars confined by 3-in.-diameter, 1-in.-pitch, 0.125-in.-thick spirals, as shown in Figure C.4. This confinement reinforcement is necessary to provide adequate development length for such short lap splices. It is also recommended that the top surface of the box and the shear keys have 0.5 in. of extra thickness to be grinded to provide a roughened surface for skid resistance and shear transfer. The use of self-consolidating concrete to fill the wide shear key is also recommended to eliminate the need for grouting, which is a costly and time-consuming operation.

Narrow Joint System

The narrow joint system developed by UNL does not use diaphragms and incorporates top and bottom transverse ties rather than a single middepth transverse found in other details. Grade 75 threaded rods are used every 8 ft to connect each pair of adjacent boxes at the top and bottom flanges. These rods provide continuous connection that transfers shear and moment between adjacent boxes more efficiently than the middepth transverse ties at discrete diaphragm locations. A slight modification is made to the standard box cross section by developing full-length horizontal and full-depth vertical shear keys, as shown in Figure C.5. The boxes are

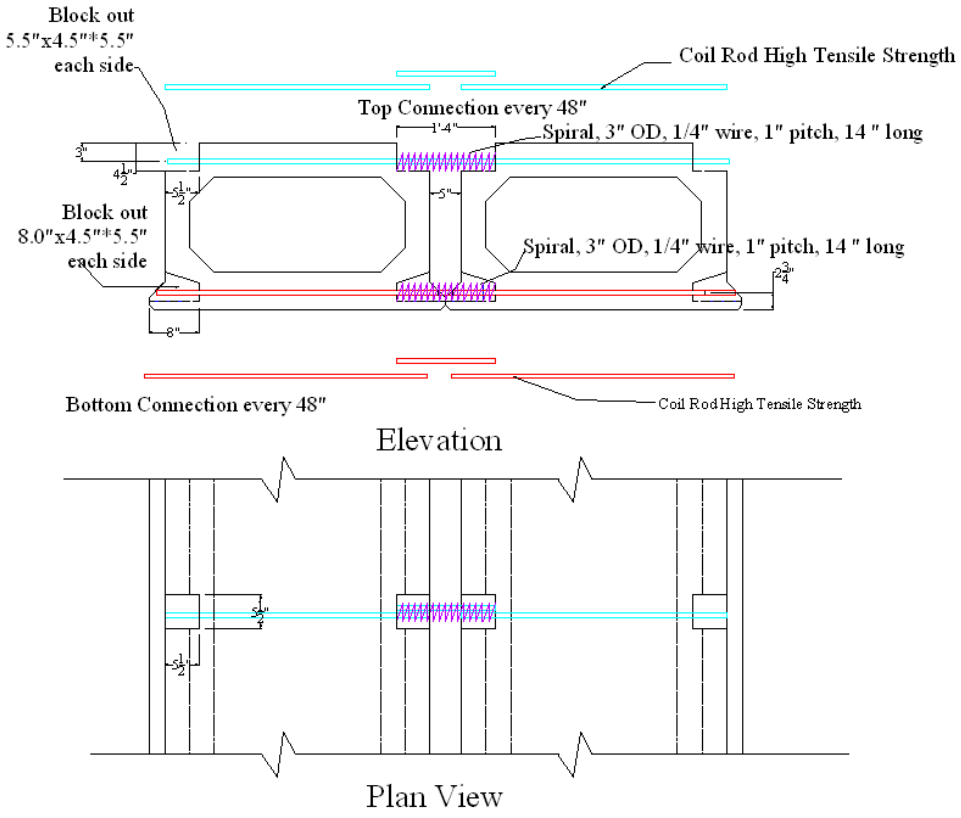

Figure C.4. Wide joint connection details.

fabricated with a plastic duct at the top and bottom flanges to create openings for the threaded rods, as shown in Figure C.6. The bottom duct is inserted between the two layers of prestressing strands, and the top plastic duct is located 3 in. from the top surface to provide adequate concrete cover. Vertical vents are provided at one side of each box to allow the air to escape while the ducts are grouted.

Posttensioned System Development

A modified version of the narrow joint system has been developed by UNL to allow for posttensioning of the transverse high-strength steel rods. Details of the development of the system including literature review, numerical studies, and recommended design provisions can be found in Hansen et al. 2012 and Hanna et al. 2009.

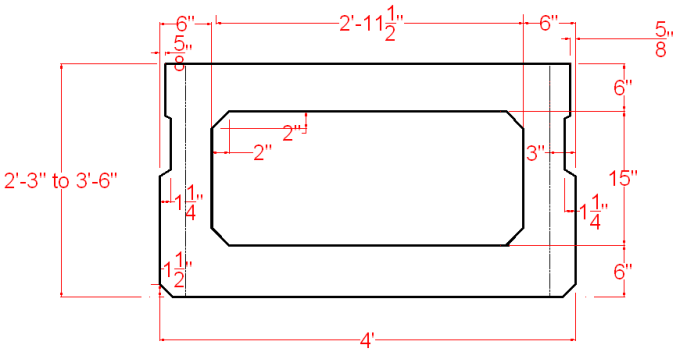

Figure C.5. Narrow joint system box dimensions.

The system continues to eliminate the typical use of diaphragms and a concrete topping for load distribution, a detail common to most adjacent box girder applications. The system maintains the use of top and bottom reinforcement; however, ducts have been moved inward so that posttensioning extends between girder voids. This arrangement simplifies inspection of the posttensioning as it is now unbonded with the box section and shear keys. Construction time is reduced due to the elimination of grouted ducts, and venting is no longer an issue of girder production.

A duct-within-a-duct setup is being proposed so that posttensioning can be applied after grouting of the shear key. The interior duct is necessary; without it, the duct would close during grouting, and posttensioning could not be threaded between adjacent members. Posttensioning should be applied after the shear key is placed for the joints to be placed under initial compression. Figure C.7 is a diagram of the proposed modifications to the current AASHTO PCI box section.

The exterior ducts have a diameter of 3.5 in. to provide enough space for an interior duct, high-strength steel rods, and couplers. This duct can be formed by plastic tubing cut

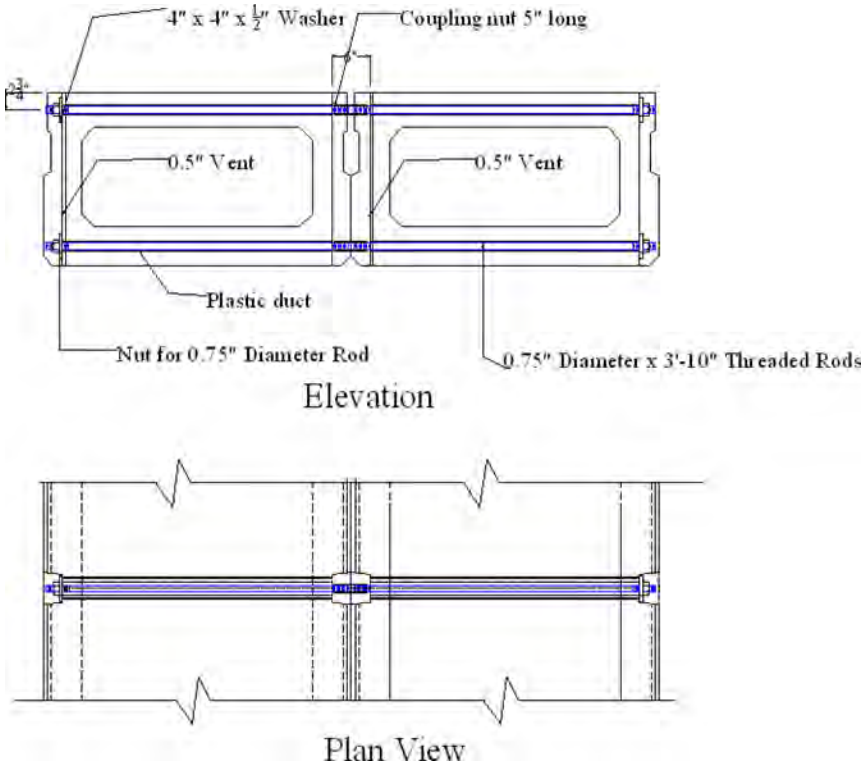

Figure C.6. Narrow joint connection details.

to the appropriate dimensions. Reinforcement should be provided for confinement about these locations. The diameter opening of 3.5 in. is used to provide a moment arm of 12 in. and still keep the duct flush with the top and bottom flanges. Shear keys extend the full horizontal length at the top of the girders and the full vertical depth every 8 ft along the member. Figure C.8 shows how the end girders must be made flat at the exterior face of the bridge in order to provide an even surface for bearing of the posttensioning materials. The high-strength steel rods should be cut at even-length increments of 4 ft in order for couplers to be placed at the joint between adjacent members. This is done for ease of construction. It is also recommended that an 8-ft length be used so that members can be placed two at a time, thereby reducing problems with construction tolerance.

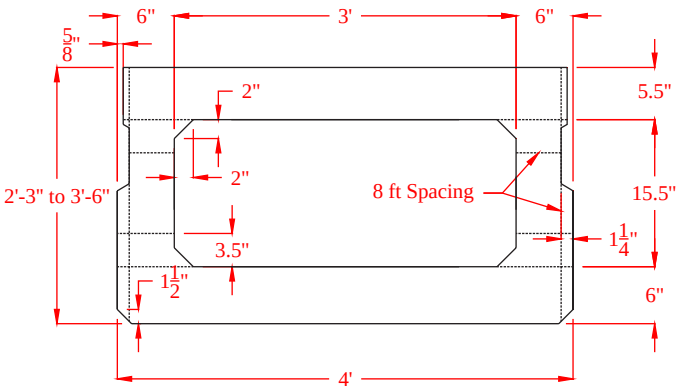

Figure C.7. Posttensioned system box dimensions.

Experimental Program

Introduction

An experimental program was developed to test the performance of the posttensioned system. A test specimen was designed using four 48-in.-wide × 27-in.-deep × 8-ft-long box beam elements that were positioned side by side and connected transversely by grouting and posttensioning. This created an overall specimen 16 ft long × 8 ft wide × 27 in. deep for testing. The length of the specimen consisted of the four box sections connected on each side.

The effectiveness of the developed system was analyzed based on its joint performance under fatigue and ultimate loading. Fatigue can be represented by a 5,000,000-cycle load applied to create tension in the top and bottom transverse ties of the 16-ft × 8-ft × 27-in. specimen, which was used to represent a 52-ft × 64-ft × 27-in. prototype bridge. The performance of the joint was evaluated by data collected from strain gauge, deflection, and leakage monitoring at critical locations of tensile stress along the transverse connections.

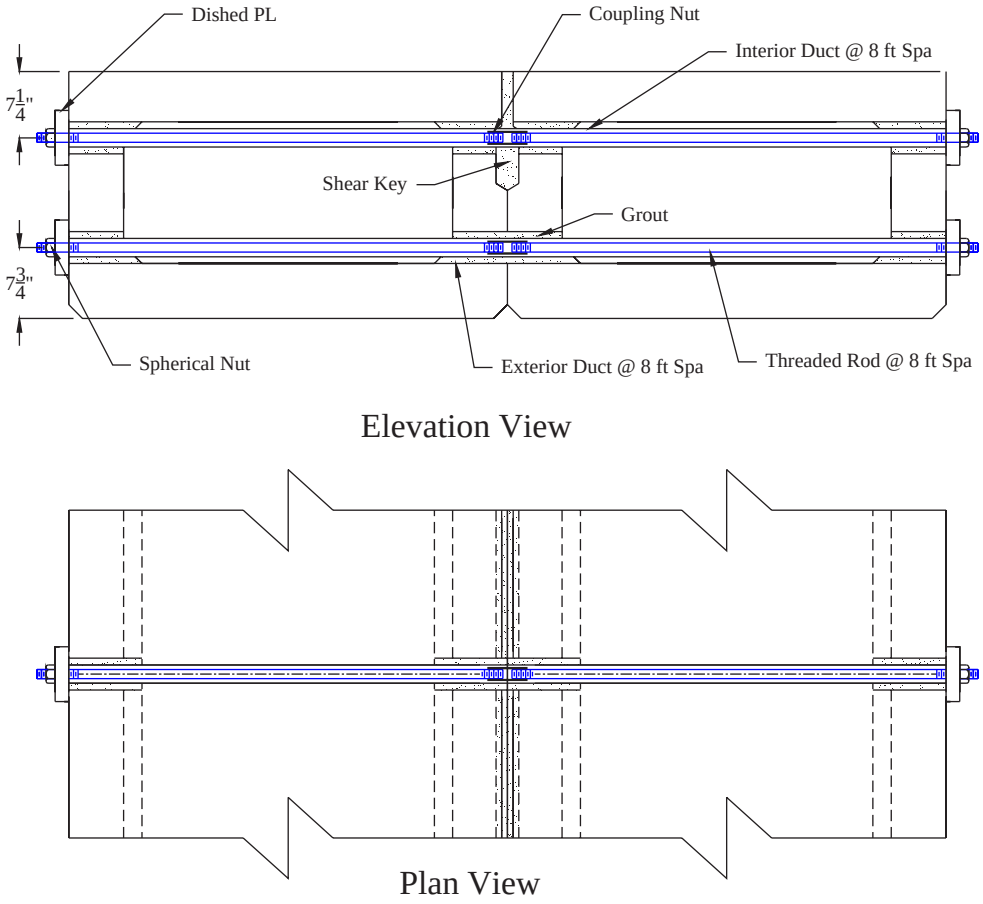

Figure C.8. Posttensioned connection details.

Construction Overview

Construction of the 16 ft × 8 ft × 27 in. specimen mentioned in the system analysis began by tying together the reinforcement and building the interior and exterior wooden forms.

Tying the bottom cage reinforcement began by laying out No. 4 U bars at an 11-in. spacing and then overlaying the rebar with No. 4 straight longitudinal bars. Markings on the steel were used to achieve the desired clear cover and spacing. A top bar served to stabilize the structure and keep the bars positioned at a 90° angle from the floor. This bar was removed when joining the top and bottom cages because it interfered with the top reinforcement and transverse duct. No. 3 C bars were attached 3 in. up on the legs of the No. 4 U bars for ease of construction. In the final step, the second layer of the bottom No. 4 longitudinal reinforcement was tied to the No. 3 C bars after having been placed before the No. 3 C bars had been tied. Figure C.9 shows a complete view of the bottom cage reinforcement. A crane was used to move the cages from the workstation to a safe location for storage.

After completion of the bottom cage reinforcement, the top cage reinforcement was tied. Straight No. 5 longitudinal bars were attached to No. 4 A1 bars at 9-in. spacing, and additional No. 4 straight longitudinal bars were used on the legs of the reinforcement to provide an attachment for the No. 3 D bars at 12-in. spacing. Chairs held up the No. 4 A1 bars during casting so that enough clear cover existed between the interior box form and the No. 3 D bars. Figure C.10 shows a complete view of the top cage reinforcement.

Figure C.9. Bottom cage reinforcement.

Figure C.10. Top cage reinforcement.

Figure C.11. Box girder without side forms.

Once reinforcement preparations were complete, exterior supports for the interior form were built to connect the top and bottom cages. Interior forms had been constructed before this part of the experimental setup was executed. Supports were made by cutting end boards and screwing them to wooden 2 × 4s for extra bearing against the ground. These 2 × 4s were meant to provide the support for the interior forms and top reinforcement until the specimen was cast and could handle the loads. Lines were sketched to ensure screws became fully embedded into the interior form. All sides toward the interior of the form were covered with oil before construction began. A saw was used to cut the end boards so that posttensioning could be viewed from within the girder voids. Eventually this form was lifted and placed over the bottom reinforcement. The stabilizing bar at the top of the bottom reinforcement was removed to complete the section by lowering the top reinforcement cage. One-inch individual chairs were used to hold up the top and bottom reinforcement and provide enough clear cover for the bars. The No. 3 D bars of the top reinforcement had to be supported by ties to prevent the bars from bowing in the middle and reducing the clear cover to the interior form.

Foam tubes were added to create the 3.5-in. ducts for the transverse posttensioning located at the middle of each girder (Figure C.11). The tubes were cut at an angle to fit the interior box chamfer. Three-eighths-inch-diameter, 7-in.-long lag screws held the tubes in place until after the concrete was cast and had strengthened enough for pullout. These screws had to be embedded at least 4.5 in. to avoid interfering with the side forms.

Additional reinforcement was added at the center of each girder to prevent cracking about this duct. The reinforcement includes No. 4 longitudinal bars above and below each foam tube and running the full length of the girder, as well as No. 4 bars cut to fit vertically along either side of the tube. The easiest way to place this steel was to drill holes in the end sections of the exterior form and remove the tubing for the bottom duct. A wood block was used to prevent concrete from flowing out of the holes. The tubing was then reattached to the structure.

Lifting points consisting of 4-in. steel hoops were attached as necessary handles for rearranging individual girders after the concrete was cast and had hardened enough to withstand the transverse posttensioning. These hoops were positioned close to the end zones of each girder. Because stronger lifting points were required to lift all four girders as a single specimen, two bent No. 6 bars were added as supports located near the inside face of each exterior girder. These bars were placed over the top of wood planks spanning the width of the girder's exterior side forms. The main function of this board was to keep the sides from bowing when concrete was placed, as well as to hold down the interior form, which experienced uplift pressure during casting. Wood was also placed along the top and bottom edges of the side forms to help with bowing. Side forms were simplified by eliminating the chamfer originally detailed at the bottom edges. Corners where the side forms intersect with the end boards were connected by L-shaped brackets and liquid nail. Screws fixed the form sides into the concrete bed and were covered with duct tape as a precaution against concrete spillage, which would hinder form removal. Additional braces against bowing were located at the middle of each girder.

Ready Mix Concrete Co. delivered concrete for casting at 9:00 a.m. on September 13, 2010. The order was for 8-ksi concrete with a 10-in. slump. Admixture was used to increase the flowability to greater than a 22-in. spread. Concrete was poured along one side of the forms until it flowed under the interior form and could be seen from the opposite opening. Problems with flowability of the first two specimens resulted in the need to cut holes in the girders so that the concrete could be spread by vibration. Leftover concrete was used for strength specimens that gave a 28-day compressive strength

Figure C.12. Box girder immediately after casting.

Figure C.14. Specimen after grouting shear keys.

of 12 ksi, which is much higher than the expected 8 ksi ordered. Burlap sacks were used to provide moisture as the specimen cured. Removal of the forms began after 1 day. All girders appeared fully developed. Pictures representing the girders immediately after casting and form removal can be viewed in Figure C.12 and Figure C.13, respectively.

An unforeseen issue with bearing on the end girders required a second form setup to grout the exterior shear keys. This process was similar to the initial side form setup. Issues occurred during casting because the grout leaked heavily from the form. In addition, not enough bracing was provided, and as a result the end girders look bowed. Grout was intended to have at least 8-ksi strength and reach a 28-day strength of 10 ksi. Achieving this strength is important because the girders are not meant to fail as a result of crushed bearings. It should be noted that with time the grout at the bearing location experienced excessive cracking; however, the actual specimen had only a few cracks due to shrinkage. Cracking at the bearings was most likely due to an inadequate ability to provide moisture during curing, as the majority of the section was encased by the form setup.

Figure C.13. Box girder without interior and exterior forms.

The final step in forming the specimen was to position the box girders adjacent to each other so that preparation could begin for pouring the interior shear keys. A continuous polyvinyl chloride pipe was inserted into the duct to keep the hole open for posttensioning. Posttensioning was tightened to 5 kips before grouting. This was done as a way to get the boxes as close together as possible before grout was poured. Posttensioning materials included a 1.5- × 6- × 6-in. dished plate, spherical nuts, couplers, and 8-ft–1-in.-diameter threaded rods with 150 ksi ultimate strength. This material was manufactured by Williams Form.

Grout used for the shear key was a semifluid, nonshrink mix that did not contain corrosive chemicals that could pose a risk to the posttensioning. The grout was the same as used at the bearing locations and specified with the same design strength as the girders (8 ksi). Similar to the bearing grout, the joint grout reached a 2-day strength of 10 ksi.

Once the joint grout reached 8 ksi, the posttensioning was jacked to 0.7 × fpu × Aps (amperes), or 90 kips, according to AASHTO specifications. Jacking started at the top and was done in cycles of 30 kips plus the load already applied to the bar not undergoing additional stress.

Figure C.14 and Figure C.15 represent the shear key grouting and posttensioning process, respectively.

Test Setup

Instrumentation

The final stage before proceeding with the experiment was to set up the actual test frame. Both top and bottom tension were tested for the specimen, meaning two test frame setups were necessary. Top tension was deemed the critical case to test first as it results in cracking at the top of the member

Figure C.15. Jacking the specimen to AASHTO specifications.

Figure C.16. Initial specimen lifting.

where an actual girder is most susceptible to environmental corrosion. Cracks were monitored by leakage from a dam built around the middle joint, as well as white latex paint to aid with visibility.

Beam supports for both cases were placed at stiff locations, at webs and joints. For top tension, the beams were placed at the middle joint and edge of the specimen so that a load could be applied at the center of the connection between the two cantilevered girders. Bottom tension was created by placing the supports at either end of the specimen with the load applied at the center. A neoprene bearing pad was placed between the specimen and the beams to provide additional flexibility for the system.

The specimen was able to handle its own weight as it was lifted to the initial top tension test frame setup. No visible damage took place. After placement, a beam had to be set on top of the specimen to prevent it from lifting off its support under loading. This beam was placed as close to the end as lab conditions would allow. No visible damage took place when the specimen finished the top tension test and was lifted again in order to rearrange the supports for the bottom tension setup.

An actuator was used to apply 5,000,000 cycles of loading to a 15- × 15-in. bearing plate on the specimen. Five strain gauges were placed to monitor changes in strain near the load and middle joint. Pictures of the test frame setups are shown in Figures C.16 through C.18.

After fatigue testing, the specimen was moved to concrete blocks so that it could be tested for ultimate capacity. Bearing was provided by 4- × 8-in. planks at each end of the specimen. The specimen did not crack during lifting and placement. A loading cell was placed directly over the center joint to produce tension once more in the bottom flange (see Figure C.19). A deflection gauge was placed beneath the specimen to take measurements along with the five strain gauges at the joint.

Figure C.17. Actuator at exterior joint for top tension setup.

Figure C.18. Actuator at interior joint for bottom tension setup.

Figure C.19. Actuator at interior joint for ultimate capacity test.

Loading

The loads for testing were determined by using the theory of the previously developed 3-D models of the adjacent box girder system. The first model was used to determine the axial force produced by ultimate and fatigue loads in the transverse direction of a 52-ft × 64-ft × 27-in. bridge (Figure C.20). Bridge loads included an assumed curb and rail load equal to 0.48 kips/ft and 12-ft lanes with standard HL-93 design vehicular and fatigue truck loading. Because the weight of the structure is uniform and does not affect the transverse direction, it was not included in the design analysis. Curb and rail loads were applied to the exterior edge of the exterior box girders. Ultimate loading conditions included single and multiple lanes; fatigue conditions considered a single lane only. Single lanes were placed at the center of the bridge width to create maximum tension in the bottom flange of the box girders and at the edge to create maximum tension in the top flange.

LRFD specifications include a 33% dynamic load factor for ultimate analysis and a 15% dynamic load factor for fatigue analysis. Long-term effects are accounted for with an infinite life factor of 2 for fatigue. This translates to load and resistance factor design load combinations of 1.25 D + 1.75 L for ultimate and 1.25 D + (0.75)(2) L for fatigue.

Ultimate axial and fatigue demands were 80.288 and 15.318 kips, respectively. The ultimate demand is comparable to the estimated effective posttensioning force of 82 kips required by the previously developed design charts. The 82 kips is based on a span-to-depth ratio of 30, and the SAP2000 model represents a span-to-depth ratio of 28.4 (i.e., 64 ft/27 in. = 28.4). The posttensioning system for the experiment is a threaded rod, with a yield strength of 120 ksi. AASHTO estimates the effective force per duct after losses to be 0.80 × fpu × Aps = 0.80 × 120 ksi × 0.85 in.^{2} = 81.6 kips. This is enough to handle the anticipated loads.

The second model developed was used to determine the loads required to reach fatigue and ultimate capacity of the experimental 16-ft × 8-ft × 27-in. system. Modeling differed from the large-span bridge in several ways. The supports were along the transverse direction, thus making the dead weight of the structure act in the transverse direction. Bottom tension was created by a simple-span setup with load at the center connection between middle girders. Top tension resulted from a simple span with cantilever setup in which the load was applied at the connection of the two cantilevered end girders (see Figure C.21). Supports were assumed at 7 in. from the edge of each exterior girder for bottom tension and 7 in. from the end with supports at the connection between the two middle girders for top tension. An additional support was placed at the center of the top flange near the end support to represent the actual lab conditions.

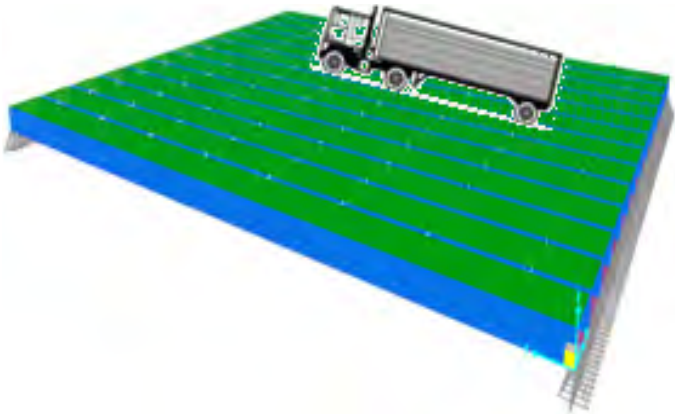

Figure C.20. 52-ft × 64-ft × 27-in. adjacent box girder SAP2000 3-D model.

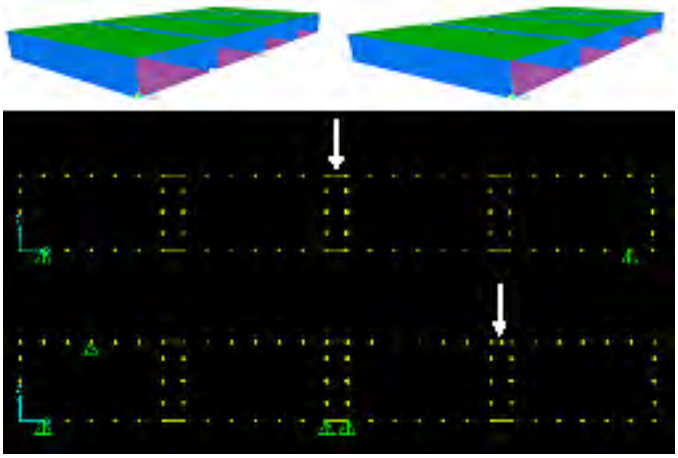

Figure C.21. Model for top and bottom tension setups of 16-ft × 8-ft × 27-in. specimen.

Analysis showed that the axial forces due to dead weight for the bottom and top tension setups were 4.9 and 21.4 kips, respectively. A load equal to 17.4 kips brings the axial force to fatigue conditions for the bottom tension setup; however, the fatigue load is already surpassed by the top tension setup. Fatigue for this condition will instead be represented by a fatigue truck wheel load equal to 18.4 kips, which creates a tension in the top flange equal to 51.6 kips. This value is acceptable because it is less than the ultimate axial force.

Ultimate capacity of the 16-ft × 8-ft × 27-in. specimen was determined by strain compatibility and found to be 280 kips/ft. A single-point load causing positive moment on a simply supported beam is equal to four times the moment divided by the span length (i.e., $M = PL/4$). Span length, assuming a 4-in. bearing on both sides, was 15 ft 4 in. This relationship indicates that a total load of 73.0 kips will induce failure. Part of this load was due to the weight of the box (approximately 1.5 kips per linear foot). The corresponding moment due to weight would be 48.5 kips/ft. The actual load to cause failure would produce 231.5 kips/ft of moment. Solving for the load gives a 60-kip applied force to break the joint between adjacent boxes.

Loads were not factored when solving for the resultant forces of the experimental setup because the analysis is meant to determine the loads required to reach the design conditions. A summary of results is provided in Table C.1.

Test Results

The box girder experienced a deflection of 0.10 to 0.12 in. during the top tension fatigue test. No cracking occurred in the joint; however, cracking was noticed in the top flanges of the box girder. The cracks were due to shrinkage and occurred before loading. Testing continued because the focus of the test was on the joint and not the flange. The dam began to leak over the joint near the end of the test. This formed a water stain that made the specimen joint appear failed when it was not.

Strain gauge data suggested that the stress on the box girder was the same before and after top tension loading. Two of the gauges had overlapping initial and final strains. These occurred under the load and on the northwest side of the joint. The strain gauge on the southeast side of the joint initially read nearly half the average value of the other strain gauges (36 με). At the end of the test, however, this strain gauge had increased to the 36-με average. The northeast strain gauge also doubled, suggesting that the load was being unevenly distributed to the east. The last strain gauge broke, and accurate data were unobtainable from the specimen.

As mentioned earlier, leakage was noticed along the flange of the box girder. This leakage occurred mostly at a crack on the northeast side and parallel to the joint. Smaller leaks were due to cracks located northwest and southwest of the joint. These cracks occurred where the top boards for bracing had been placed during the initial casting of the individual girder specimens (perpendicular to the joint). As the measurement on the west side did not show any strain loss, it is reasonable to conclude that parallel cracking caused the strain loss on the east side. It can also be inferred that the crack caused some strain loss in the specimen that otherwise would not have occurred. Strain gauge data are shown in Figure C.22. Figure C.23 and Figure C.24 show interior and exterior views, respectively, of the northeast crack and leakage.

The box girder experienced a deflection of 0.08 to 0.11 in. during the bottom tension fatigue test. No cracking occurred in the joint, and leakage decreased because the top flange was under compression.

Again, strain gauge results suggested zero loss of strain. Two of the gauges had overlapping initial and final strains. These occurred under the load and on the southeast side of the joint. The strain gauge on the northwest side of the joint lost approximately 5 με, and the strain gauge on the northeast side increased by approximately 5 με. The southwest strain gauge appeared to overlap, but the initial readings showed a loss of strain when the load was constant. This is probably because the strain gauge should have been replaced after the top tension test. The adhesive for the strain gauges did not hold up well after being submerged in water a second time.

Table C.1 Results of (a) Full-Scale, (b) Fatigue, and (c) Capacity Analyses

(a)

52 ft × 64 ft × 27 in.	Fatigue	Ultimate
Maximum axial force	15.3 kips	80.3 kips

(b)

16 ft × 8 ft × 27 in.	Axial Force Due to Weight	Applied Load	Total Axial Force
Top tension	21.4 kips	18.4 kips	51.6 kips
Bottom tension	4.9 kips	15.3 kips	15.3 kips

(c)

16 ft × 8 ft × 27 in.	Weight	Applied	Capacity
Moment	44.1 kips/ft	235.9 kips/ft	280.0 kips/ft
Load	23.0 kips	61.5 kips	84.5 kips

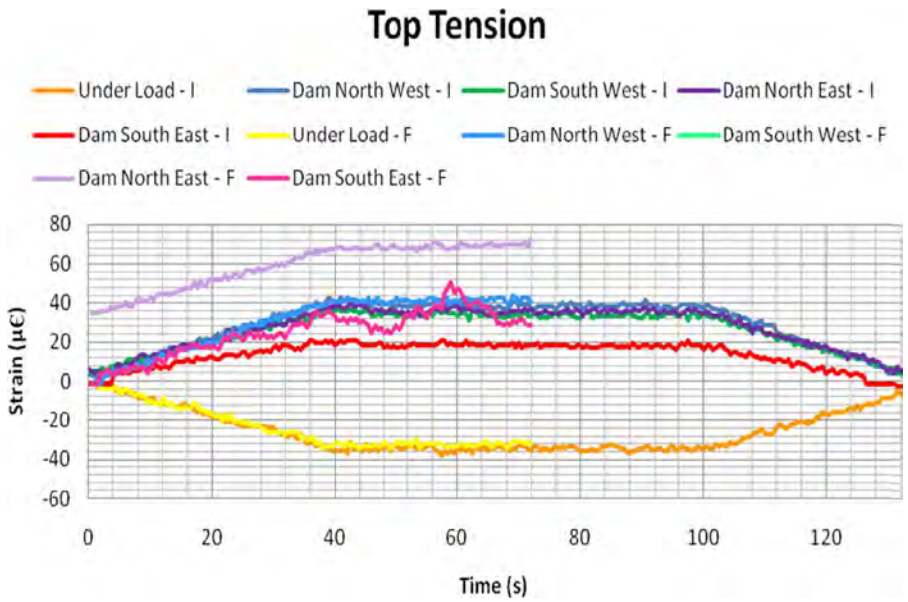

Figure C.22. Initial and final strains on specimen (top tension).

Both north strain gauges and the southwest strain gauge had to be replaced before obtaining their final readings. Once more, results suggested that the parallel crack caused the changes in strain. It makes sense that the northeast gauge would experience a greater strain because it was on the compression side of the crack, while the northwest gauge would lose strain as a result of the increasing tension on the other side of the crack. Strain gauge data are shown in Figure C.25.

The ultimate load taken by the specimen was 67 kips applied and 90 kips total. This was greater than the expected 61.5 kips applied and 84.5 kips total loading from hand calculations. The joint cracked evenly across the bottom and extended up to where the web indents and forms the shear key that runs the entire length of the specimen (see Figure C.26). Deflection stayed evenly below 0.1 in. for approximately 60 kips before increasing exponentially to 3.31 in. between 40 and 67 kips (see Figure C.27).

Conclusions and Future Work

Conclusions

The general objective of this research topic was to improve the performance of the transverse connections currently used in adjacent box girder bridge applications. This was done by developing a detail capable of transferring moment and shear in the transverse direction. Benefits of the modified system, which allows for posttensioning, include significantly simplifying box

Figure C.23. Interior view of cracking at flange along northeast side of joint.

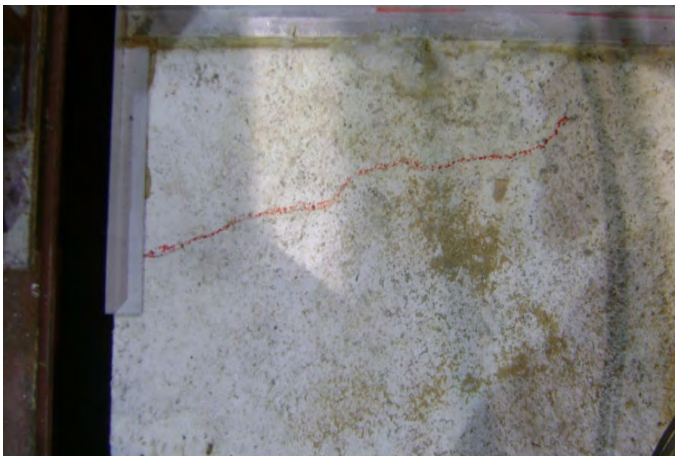

Figure C.24. Exterior view of cracking at flange along northeast side of joint.

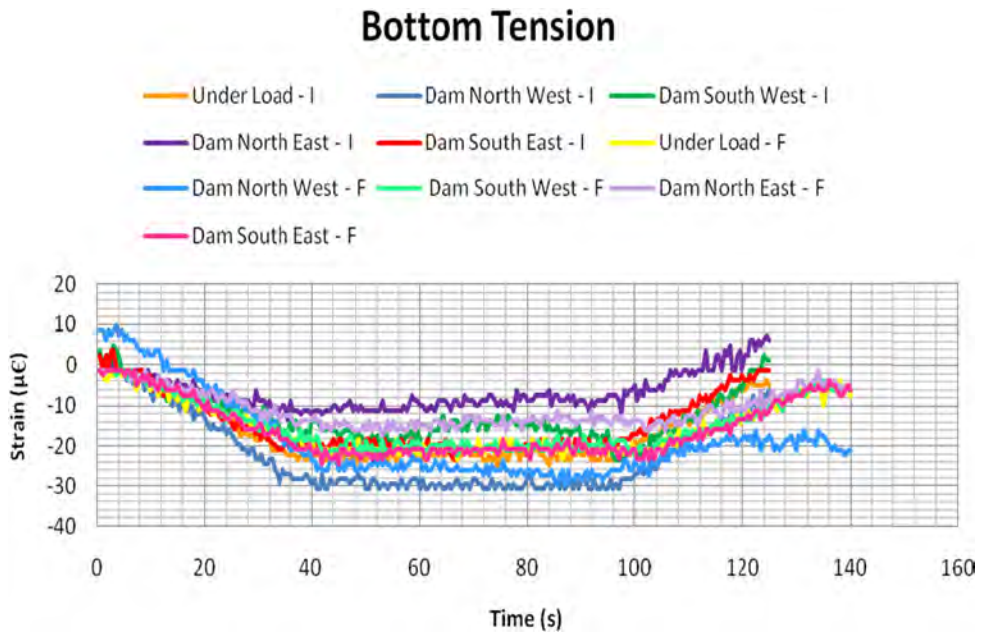

Figure C.25. Initial and final strains on specimen (bottom tension).

production, improving the rate of construction, allowing easier inspection of voids, and reducing projects costs. It was found that posttensioning also increases the capacity and efficiency of the section because joints are placed under compression and are less likely to experience reflective cracking and leakage.

The experimental program under this research topic consisted of applying an 18.4-kip load for 5,000,000 cycles at an exterior joint of the four-box specimen with supports at the center and opposite edge. This produced tension at the more critical top flange, where the system is vulnerable to environmental chemicals and corrosives. Cracking was monitored by a dam over the joint and five strain gauges placed next to the load and on either side of the center joint. No cracking or strain loss occurred during the course of the experiment. Supports were then rearranged to both ends of the member, and the load was repositioned to the center joint for tension in the bottom flange. A 17.4-kip load was applied for 5,000,000 cycles, and again no cracking or strain loss occurred.

Figure C.26. Side (bottom left) and underside (bottom right) cracking.

Ultimate capacity was calculated as 280 kips/ft using strain compatibility and found to be slightly higher during testing. An applied load of 67 kips, in addition to the self-weight of the specimen, reached 300 kips/ft before failure. Cracking did not propagate until after reaching a 60-kip total load, and then deflection increased exponentially from 0.1 to 3.31 in. over the next 30 kips applied.

Based on the test results, it can be concluded that a post-tensioned transverse connection without diaphragms or a concrete overlay can be designed and detailed to have comparable performance to typical connections while being more economical and practical. The tested specimen had excellent performance under both static and cyclic loads.

Future Work

It is proposed that the transverse, posttensioned connection developed in pursuit of this research be applied in a full-scale application for observation of the joint performance under actual weathering and loading conditions.

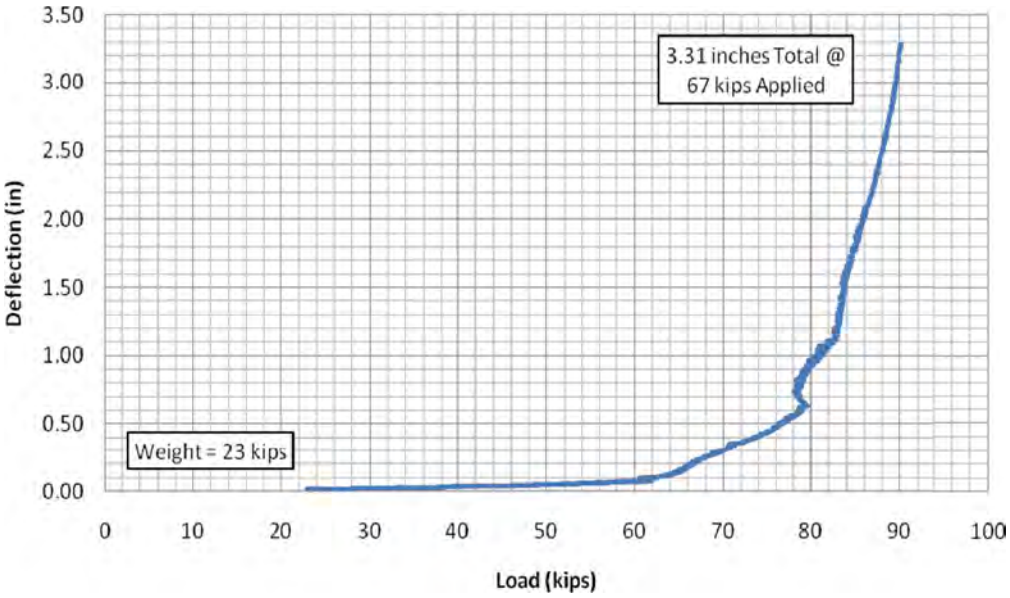

Figure C.27. Total load versus deflection of specimen.

APPENDIX D

Wear of Sliding Surfaces in Bridge Bearings

Bearings are an important bridge element that must be considered when evaluating potential ways to extend overall bridge service life. Bridge superstructures experience translational movements and rotations caused by traffic loading, thermal effects, creep and shrinkage, wind and seismic forces, initial construction tolerances, and other sources. Bridge bearings are designed and built to accommodate these movements and rotations while supporting required gravity loads, transmitting those loads to the substructure, and providing the necessary restraint to the structure.

Background and Problem Statement

Newer types of bridge bearings using elastomeric materials have improved durability expectations. Steel-reinforced elastomeric bearings have shown very good performance over the past 40 years due to their low cost and relatively long service life. However, with certain combinations of load and movement, the capacity of elastomeric pads to accommodate the required translation through shear deformation of the elastomer can be exceeded. In these cases, there is a need to provide additional movement capacity by means of sliding surfaces. Further, other types of bearings—including cotton duck pads and high-load multirotational pot, disc, and spherical bearings—use sliding surfaces to accommodate expansion requirements. Currently, polytetrafluorethylene (PTFE) is the material typically used for sliding surfaces. However, the service life of plain PTFE can be shortened due to eventual wear and deterioration of the surface, particularly when subjected to high pressures, fast sliding speeds, or cold temperatures. There are minimal data to determine a life prediction model for sliding surfaces using PTFE.

Research Objectives

The main objective of this research was to determine the feasibility of achieving increased service life with bearings that use sliding surfaces for movement through the use of alternative high-performing materials in lieu of conventional plain PTFE. The study compared performance and wear of alternative high-performance sliding surfaces with plain PTFE over a range of bearing pressures, sliding speeds, cycles of movement, and total cumulative travel distances.

The scope of this research was to conduct a proof of concept experimental program on small-scale sliding surface specimens. Performance characteristics such as coefficient of friction (COF), rate of wear, and total wear over a specified number of movement cycles were measured and compared.

Two alternative materials were tested along with plain PTFE. The first was a relatively new German product, Maurer sliding material (MSM), which was shown by testing in Europe to have improved wear resistance over plain PTFE. The second was a glass-filled PTFE, Fluorogold, which was also described as providing significantly greater wear resistance than plain PTFE.

Analytical studies were performed to evaluate the magnitude of horizontal movement due to girder end rotation at expansion bearings under cyclic truck load. These studies assisted in determining realistic movement testing speeds with which to evaluate the various sliding surface materials. Bearing movement due to truck load is low-amplitude, high-cycle movement with fast movement speed, but movement due to temperature load is high-amplitude, low-cycle movement with low movement speed.

Another objective was to evaluate the feasibility of developing life prediction models for sliding materials that could be used for service life design. Design provisions were further developed for calculating the required thickness of the sliding surface based on the available literature, theoretical studies, and the results of the experimental program.

Summary of Available Data

Previous research reported in NCHRP Report 432 (Stanton et al. 1999) and earlier by Campbell and Kong (1987)

demonstrated the properties and wear behavior of PTFE. Key results of these studies are summarized in later sections, which are "Other PTFE Research" and "Phase Two Conceptual Design of the Experiment." This previously reported behavior was used as a starting point for the research reported here.

Stanton et al. (1999) reported that low temperatures, fast sliding speeds, high contact pressures, rough mating surfaces, and contamination of the sliding interface all contribute to an increased wear rate of PTFE. However, fast sliding speed was shown to be a dominant parameter. Movement due to temperature change is low-cycle, high-amplitude movement, with a slow movement rate, and produces the least amount of wear. But movement due to truck load and associated dynamic effects is high-cycle, low-amplitude movement and has a much faster sliding speed. Wear rates associated with high sliding speeds have been shown to be significantly greater than wear rates at lower sliding speeds. Unfortunately, there are little actual field data to confirm the amount of movement and movement rates at expansion bearings due to truck load, and theoretical analysis is the only currently available way of estimating this behavior.

Alternative high-performing sliding materials with potentially greater resistance to wear when subjected to high movement speeds were investigated as part of this research and were identified for experimental study. Current data relating to the behavior of these materials were available in some cases from the manufacturers, and when relevant, were used as a basis for this study. Descriptions and data for the two high-performance sliding materials studied, MSM and Fluorogold, are summarized in the following subsections.

Maurer Sliding Material

MSM was primarily developed to accommodate fast bridge movements caused by high-speed trains. In contrast to conventional bridges, which experience slower movement due to live load, a bridge for high-speed trains will undergo fairly fast loading. The German Transrapid magnetic train guideway required the bearing material to move at sliding speeds up to 15 mm/s (35 in./min) and provide 80 years of service life. To meet these needs, Maurer developed a new sliding material that exceeded the performance requirements. Based on manufacturer data, material such as MSM could be considered a high-performing alternative sliding surface to PTFE.

Table D.1. Parameters in Long-Term Sliding Tests by Maurer

Parameter Tested	PTFE	MSM
Contact pressure	30 N/mm² (4,350 lb/in.²)	60 N/mm² (8,700 lb/in.²)
Average sliding velocity	2 mm/s (5 in./min)	15 mm/s (35 in./min)
Total accumulated sliding distance	20,000 m (12 mi)	50,000 m (31 mi)

The manufacturer has conducted tests in Europe comparing MSM with PTFE in accordance with provisions of EN1337-2 (Dansk Standard), which specifies the sliding elements for structural bearings.

Long-term sliding tests were carried out on dimpled and lubricated MSM and PTFE specimens. The test parameters for both MSM and PTFE are summarized in Table D.1. In these tests, MSM was subjected to higher pressures and movement velocities than PTFE.

Figure D.1 shows test results comparing COF with total sliding path and various temperatures. The study showed that MSM could accommodate a much longer total sliding movement than PTFE and had considerably greater performance at lower temperatures.

Figure D.2 and Figure D.3 show the surface conditions of sliding material and stainless steel mating surface for MSM

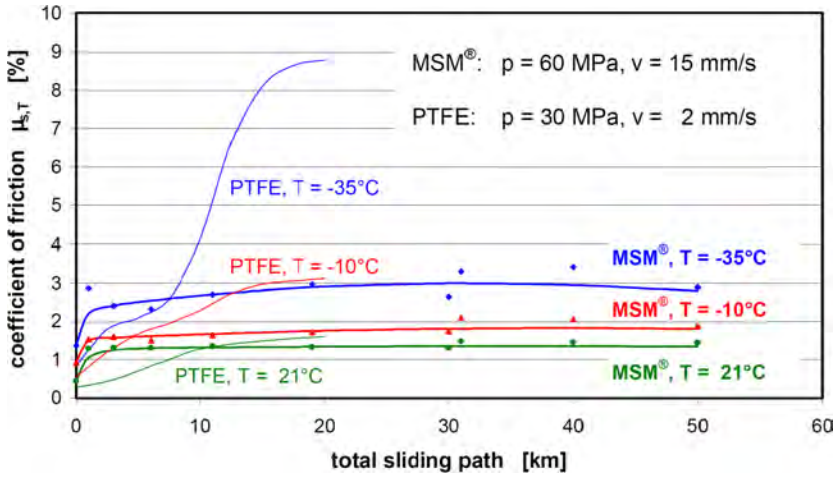

Figure D.1. Long-term test of MSM compared with PTFE.

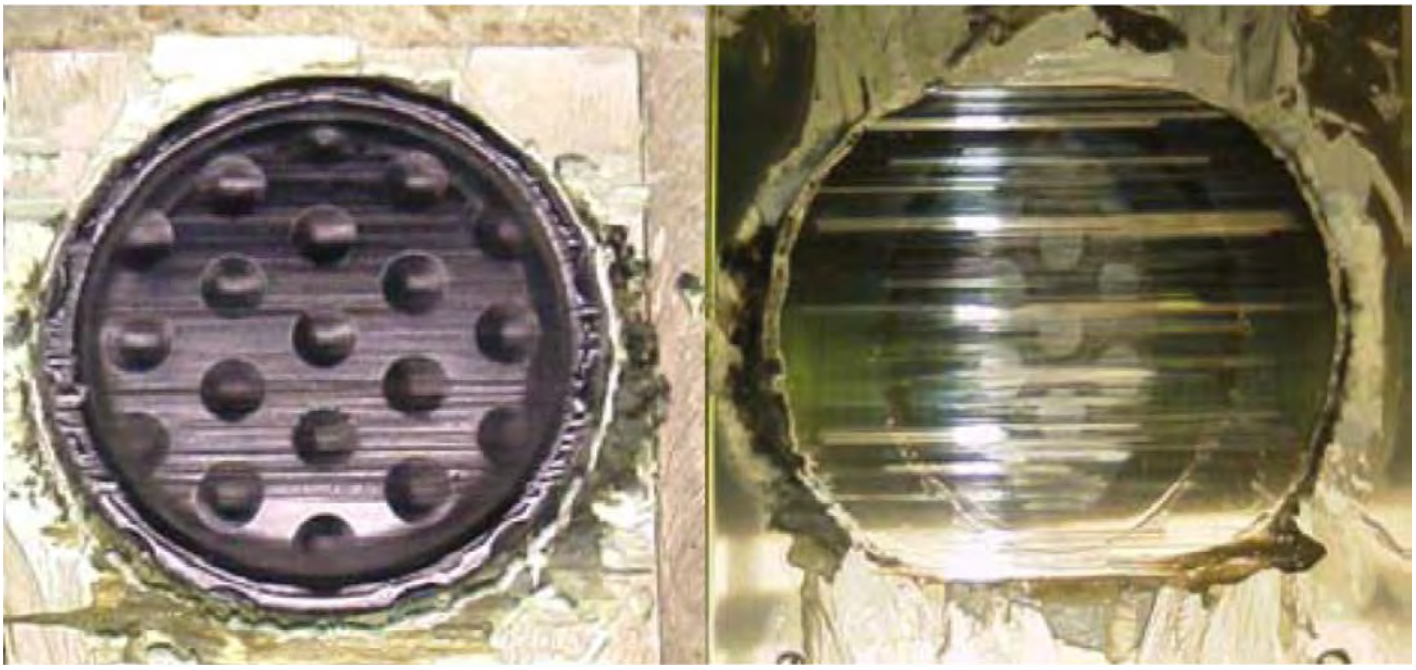

Figure D.2. Shape of MSM after sliding path of more than 50,000 m (31 mi).

and PTFE, respectively, after testing. The PTFE photo represents a total accumulated sliding length of 10,000 m (6 mi), and that of MSM represents more than 50,000 m (31 mi).

In these tests, the MSM surface was only slightly abraded, but the PTFE showed considerable wear and shredding of material.

MSM also demonstrated high compression strength and could accommodate double the stress of PTFE. This ability could reduce the dimensions of the bearing, if feasible. Tests also showed that MSM experienced very limited abrasion, which extends its life to more than 50,000 m even at high stresses and high loading rates. From these tests on lubricated samples, it appeared that MSM could provide an excellent alternative for many bearing types that use sliding surfaces.

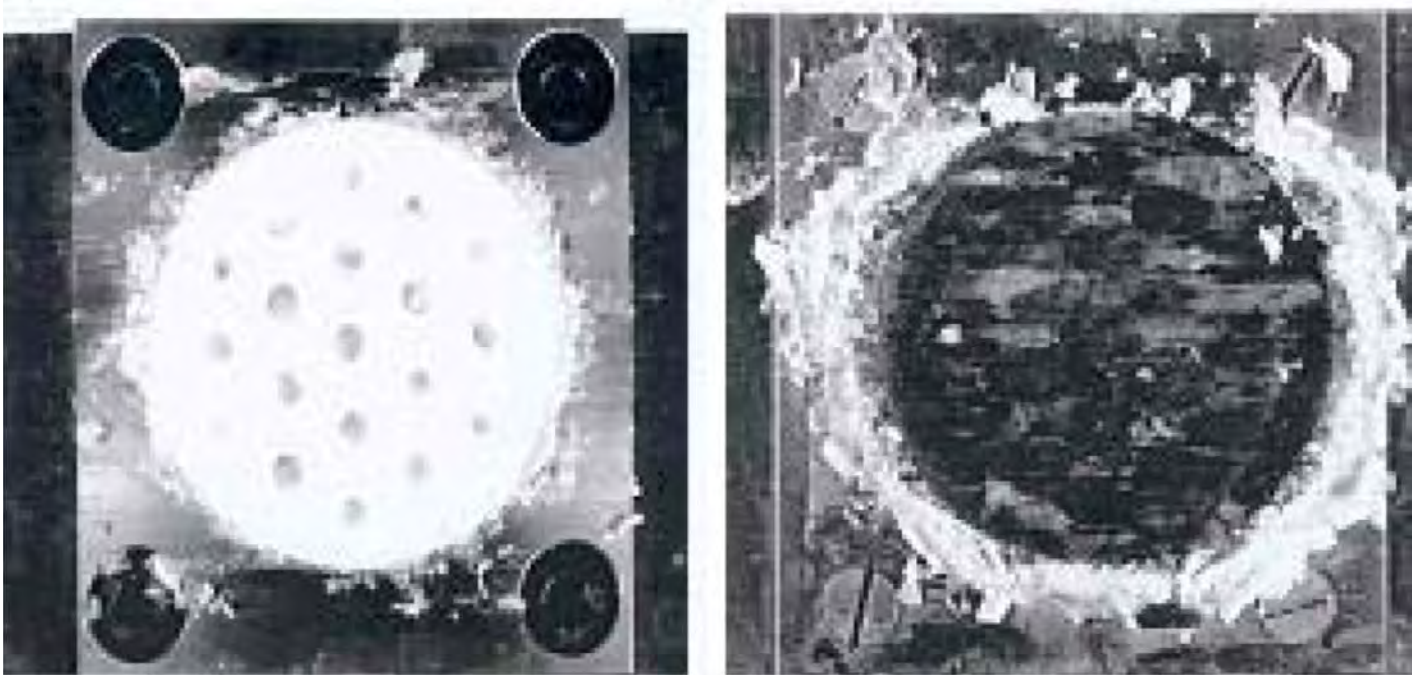

Figure D.3. Shape of PTFE after sliding path of 10,000 m (6 mi).

Further testing on unlubricated samples, however, will indicate whether this product could be a true sliding surface alternative for conventional-type bridges in U.S. practice, which typically use unlubricated, plain PTFE. There is concern whether such lubrication would remain throughout the service life of the structure under field conditions.

Fluorogold

Another high-performing sliding surface, Fluorogold, was identified for comparative testing with plain PTFE and MSM. Fluorogold is a proprietary glass-filled, reinforced PTFE with enhanced characteristics. Fluorogold sliding bearing systems are engineered products of Seismic Energy Products, Athens, Texas.

Based on manufacturer's information, "Fluorogold is comprised of virgin PTFE and special reinforcing agents. This blend yields a structural material that offers significantly higher mechanical properties than plain PTFE. Compressive creep is virtually eliminated, wear is substantially reduced, and initial deformation is decreased; however, the low friction and chemical inertness of PTFE are retained. This structural bearing surface is bonded to a back-up steel plate with a high-temperature homogenous epoxy system that is cured under precise heat and pressure in hydraulic presses. All Fluorogold bearings are factory bonded using strictly controlled, semiautomated procedures developed to eliminate poor quality field-made bonds. The maximum design pressure of Fluorogold slide bearings, without elastomeric backing, is 2,000 psi. For neoprene-backed bearings, the maximum recommended pressure is 800 psi, and for the cotton duck–reinforced elastomer, it is 1,500 psi."

The decision was made to incorporate Fluorogold into the testing program as a high-performance PTFE-based material to compare with MSM and plain PTFE.

Other PTFE Research

NCHRP Report 432, Appendix C: Friction and Wear of PTFE Surfaces

In Appendix C of NCHRP Report 432, Stanton et al. (1999) describe research conducted on the friction and wear of five types of PTFE-based sliding surfaces:

- Flat, unfilled, unlubricated (plain) PTFE;
- Dimpled, lubricated PTFE;
- Woven PTFE;
- 25% Glass-filled PTFE; and
- 15% Glass-filled PTFE.

The testing program considered temperature, contact pressure, and sliding speed and compared COF and wear over the range of variables. The research program tested small-scale specimens (3-in. diameter). Wear was found to be primarily dependent on sliding speed, although the pressure was typically constant in the wear portion of the study.

Plain PTFE was shown to have the lowest wear resistance. Lubricated PTFE had the greatest wear resistance, but it was questionable as to how long the lubrication would last in actual field conditions. Woven and glass-filled PTFE materials were shown to have significantly increased wear resistance compared with plain PTFE, but they exhibited a higher COF.

Certain initial test parameters used in the NCHRP study, such as specimen size, contact pressure, and movement speed, were duplicated in this study to compare results, which are discussed in this appendix.

PTFE Sliding Surfaces in Bridge Bearings

Research performed on wear of PTFE sliding surfaces by Campbell and Kong (1987) indicated that the combination of pressure times velocity (PV) could be used as a base parameter to predict the corresponding rate of wear. Their research indicated that there was a PV threshold below which there would be a low-wear regime and above which there would be a high-wear regime. This concept was evaluated as part of the study reported here.

Research Program

Scope of Study

This research topic included analytical studies followed by design, fabrication, and implementation of a limited experimental program to evaluate sliding surfaces used for bridge bearings. The experimental program included proof of concept testing aimed at comparing the life of sliding materials commonly used in bridge structures with certain alternative high-performance sliding materials. Specific material parameters such as wear rate and COF were studied. The following three sliding materials were tested and compared in this study:

1. PTFE, the base material most commonly used in current bridge practice, was tested in plain and lubricated states.
2. MSM, developed by Maurer Söhne in Germany, is an alternative material for bridge sliding bearings. MSM, which was developed for use in high-speed rail bridges, was tested in plain and lubricated states.
3. Fluorogold, developed by Seismic Energy Products (Athens, Texas), is an engineered product comprising virgin PTFE and special glass fiber–reinforcing agents. This material was tested only in a plain state.

The research program was conducted in four major phases:

1. Phase 1 developed an analysis of a prototype bridge that computed and evaluated bridge movements and movement speed at expansion bearings due to truck loads.
2. Phase 2 developed the concept of an experimental program that was aimed at constructing a system capable of

performing wear tests on multiple sliding materials to simulate various travel speeds and contact pressures. Test specimens were also designed as part of this phase.
3. Phase 3 constructed the test set up in the University of Nebraska–Lincoln structures laboratory.
4. Phase 4 conducted the experimental testing.

Phase 1: Determination of Bridge Movements

Finite element (FE) analysis and theoretical methods were used to calculate the movements that a sliding bearing might experience during its service life.

Prototype Bridge Structure

An FE model was developed to compute the simple-span bridge horizontal movement at an expansion bearing due to passage of a truck. Because the bridge movements depend on the bridge geometry and vary case by case, analyses were carried out on a 200-ft simple-span prototype steel bridge with four girders, as shown in Figure D.4.

The FE package ABAQUS was used to develop a model of the prototype bridge. Reduced-integration shell elements were used to model the girders and the deck. Figure D.5 shows the schematic of the model developed.

The passage of AASHTO HL-93 trucks was considered in evaluating the bridge horizontal movements at the expansion bearings. Figure D.5 shows the bridge with one truck located at the midspan of the bridge. Figure D.6, a, b, and c shows the vertical displacement contours due to the self-weight of the bridge and one, two, and three trucks, respectively, located side by side at midspan. One end of the girders was restrained with a pinned boundary condition (fixed end) and was free to move with a roller boundary condition (expansion end) at the other end.

Table D.2 summarizes the movements and rotations at the roller bearings of the external girder (which experience the greatest deformations).

A More General Case: Traffic-Related Movement

Three major factors contribute to the traffic-related horizontal movements at bridge bearings:

1. Rotation of the girder ends.
2. Horizontal movement at the expansion bearing transferred from the other fixed end of the girder. In other words, if one end of the girder is pinned and restrained against horizontal movement, its theoretical movement due to girder end rotation movement is transferred to the expansion end of the girder.
3. Dynamic effects, which include the following effects:
   a. A dynamic impact factor, which can be taken as 1.33 (AASHTO 2010b); and
   b. Vibration of the bridge after the truck is passed (dynamic decay).

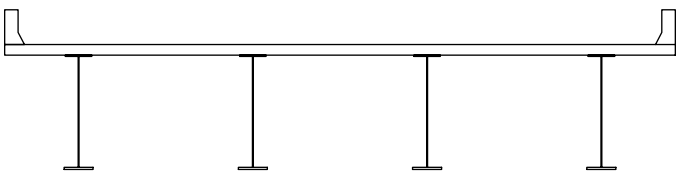

Figure D.4. Schematic of 200-ft simple-span prototype bridge.

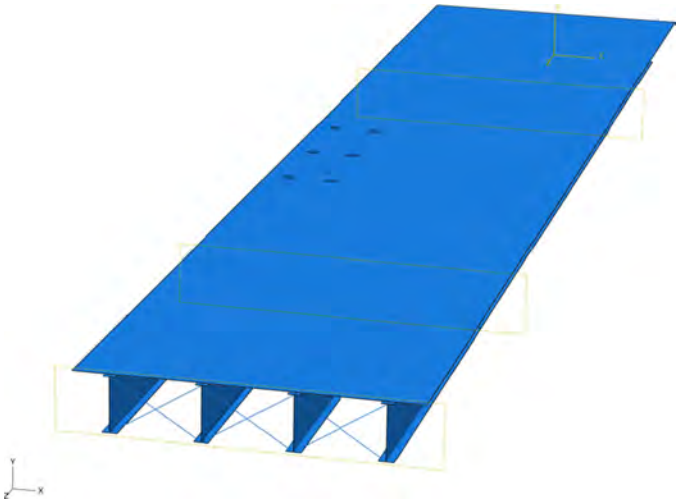

Figure D.5. ABAQUS FE model of prototype bridge.

Figure D.7 shows a general simply supported beam with a concentrated load at midspan and the bridge girder cross section under bending moment in which θD_1 is the horizontal movement of the bearing.

Equations D.1 and D.2 can be written for the above simply supported beam as follows:

$$\Delta = \frac{Pl^3}{48EI} \tag{D.1}$$

$$\theta = \frac{Pl^2}{16EI} \qquad \theta = \frac{3\Delta}{l} \tag{D.2}$$

Although the *AASHTO LRFD Bridge Design Specifications* (*LRFD Specifications*) (AASHTO 2010b) allow greater values, the maximum allowable live load deflection used by many states is span/800 for a bridge under vehicular loads. Therefore, for a worst-case scenario of a concentrated load at midspan of the bridge, the maximum probable rotation at the support can be determined as follows:

$$\theta = \frac{3 \times \frac{l}{800}}{l} = \frac{3}{800}\text{rad.} = 0.00375 \text{ rad.}$$

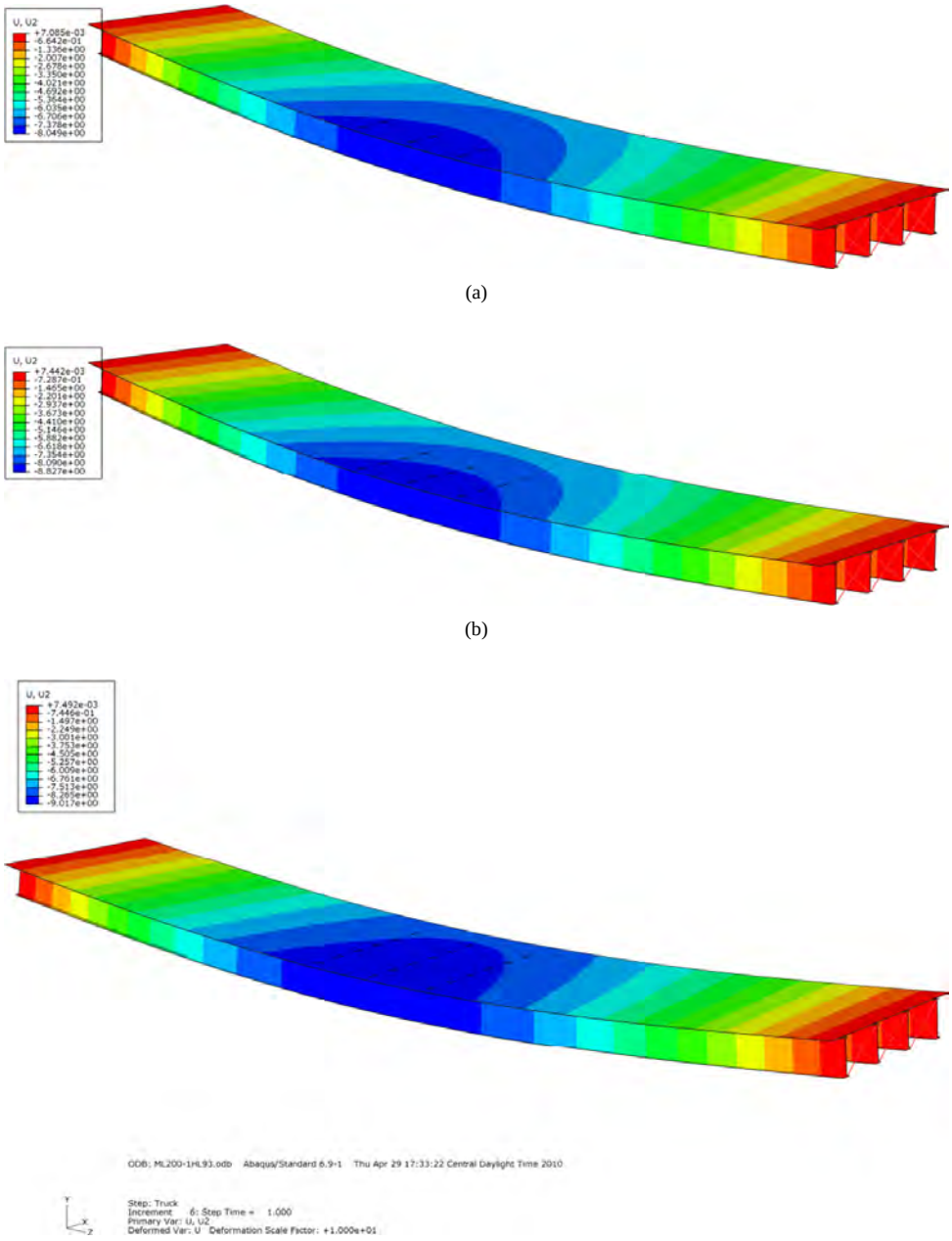

Figure D.6. Vertical displacement contours due to self-weight of bridge and (a) one, (b) two, and (c) three trucks located side by side.

It should be noted that both ends of the beam will experience the rotation θ, and the girder bottom flanges will tend to move outward horizontally. With one end pinned and restrained from horizontal movement, the opposite end will be forced to move a total of $2\theta D_1$.

For a range of spans and girder depths, the movement can be calculated as follows:

- For D_1 equal to 30 in., the maximum probable horizontal movement will be $0.00375 \times 30 \times 2 = 0.225$ in.
- For D_1 equal to 70 in. (which is the case for the 200-ft span under consideration), the maximum probable horizontal movement will be $0.00375 \times 70 \times 2 = 0.525$ in.

For structures with the above range of variables designed in accordance with the *LRFD Specifications*, the maximum probable horizontal movement at the expansion bearing due to the passage of a truck (with one end fixed) would be between 0.225 and 0.525 in. for D_1 ranging from 30 to 70 in. This range represents the maximum probable bearing

Table D.2. Movements of Prototype Bridge

Load	Bearing Type	Midspan Deflection (in.)	Horizontal Deformation at Bearing (in.)	Rotational Deformation at Bearing (Rad.)
Weight of girder plus deck	Roller	6.62	1.18	0.0148
1 HL-93 Truck	Roller	1.28	0.15	0.0025
2 HL-93 Trucks	Roller	2.04	0.26	0.0040
3 HL-93 Trucks	Roller	2.31	0.33	0.0043

horizontal movement for a simple-span bridge, because most bridges are designed to have lower midspan deflections due to live loads (L/800 is the upper limit).

Comparison of Approximate Results Against FE Study

The horizontal movement due to one truck passage determined from the FE study on the prototype bridge was 0.146 in., which is less than the above-mentioned range of horizontal movement determined from approximate methods.

The lower amount determined from the FE study is considered to be due to the presence of the other girders in the model, which increased the stiffness of the whole system.

Effects of Vibration

When a truck travels over a bridge, and after it has completely crossed over, the bridge continues to vibrate with progressively reducing amplitude because of damping. The principles of structural dynamics were used to determine the dynamic effects of a truck passage on the prototype bridge.

Structures dissipate energy, mainly through friction, during vibration. The progressively reduced amplitude of vibration is caused by the presence of damping forces that dissipate the input energy. Damping is a function of the structure, and its value has been determined from dynamic evaluation of various types of structures.

In most actual physical systems it is very difficult to find the exact expression for the damping force; a viscous damping model is widely chosen for its ease in mathematical treatment. In this model, the damping force is expressed as the viscous damping coefficient (C) multiplied by the velocity of the movement. In a critically damped system, the amplitude converges to zero as fast as possible without oscillating. The damping ratio is defined as the ratio of the damping coefficient in the system's differential equation to the critical damping coefficient.

The structure damping ratio is typically 2% to 10%, depending on the type of construction (bolted steel ~6%, reinforced concrete ~5%, and welded steel ~2%).

Generally, damping would be ignored for nontransient events (such as wind loading or crowd loading), but it would be important for transient events (e.g., impulse loads).

After the passage of a truck over the bridge, the bridge will vibrate until the structure's damping dissipates the amplitude of the motion, as described in Figure D.8.

Assuming 7% damping, the dynamic decay can be determined from Equation D.3:

$$\delta = \ln \frac{\text{Peak@cycle1}}{\text{Peak@cycle2}} = \frac{2\pi\xi}{\sqrt{1-\xi^2}} = 0.441 \qquad \text{(D.3)}$$

Having the dynamic decay determined according to Equation D.3, the number of cycles (N) to transition from an

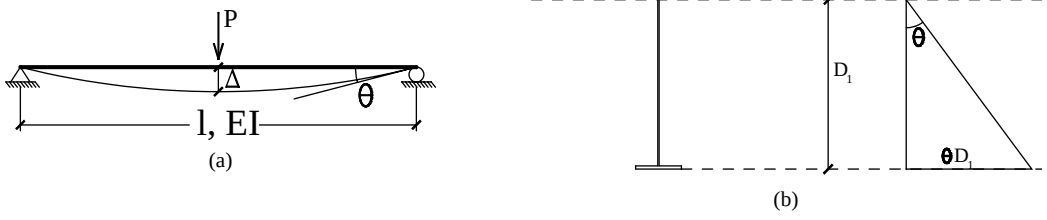

Figure D.7. (a) A simply supported girder with a concentrated force at midspan and (b) bridge girder section under bending moment.

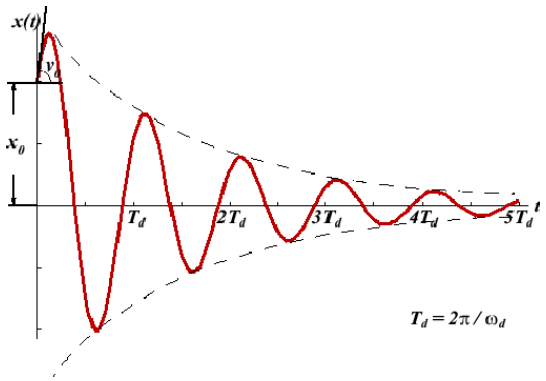

Figure D.8. Decay of free vibration for a single degree of freedom system with damping.

amplitude of x_i to an amplitude of x_{i+k} can be calculated from Equation D.4:

$$N = \frac{1}{\delta}\ln\frac{x_i}{x_{i+k}} \tag{D.4}$$

The number of cycles required to reduce the free vibration amplitude to 10% of the first cycle's amplitude can be determined from Equation D.5:

$$N_{10\%} = \frac{1}{\delta}\ln\frac{10}{1} = \frac{\sqrt{1-\xi^2}}{2\pi\xi}\ln 10 = 0.366\frac{\sqrt{1-\xi^2}}{\xi} \cong \frac{0.366}{\xi} \tag{D.5}$$

For example, for $\xi = 7\% \Rightarrow N_{10\%} = 5$ cycles.

Figure D.9 shows the number of cycles required to reduce the free vibration amplitude by 90% and 95% (decay) for various damping ratios. As this figure shows, for a 7% damping ratio, five cycles will be enough to reduce the first cycle's amplitude to 10% for a free vibration.

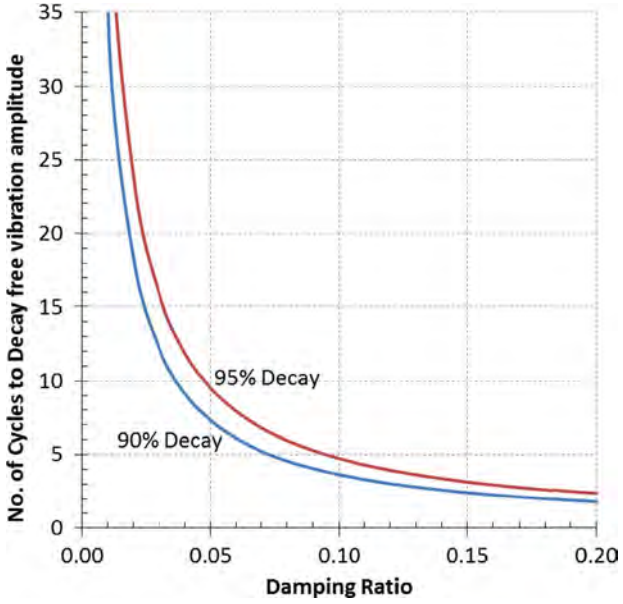

Figure D.9. Number of cycles required to reduce the free vibration amplitude by 90% and 95% (decay) for various damping ratios.

To calculate the total travel distance from the first cycle to 90% reduced amplitude, Equations D.6 and D.7 can be used:

$$\delta = \ln\frac{\text{Peak@cycle1}}{\text{Peak@cycle2}} \Rightarrow e^{\delta} = \frac{\text{Peak@cycle1}}{\text{Peak@cycle2}}$$

$$\Rightarrow e^{-\delta} = \frac{\text{Peak@cycle2}}{\text{Peak@cycle1}} \tag{D.6}$$

$$\text{Total travel} = 2x_1 + 2x_1e^{-0.5\delta} + 2x_1e^{-\delta} + 2x_1e^{-1.5\delta} + 2x_1e^{-2\delta} + \cdots$$

$$= 2x_1\left(1 + e^{-0.5\delta} + e^{-\delta} + e^{-1.5\delta} + e^{-2\delta} + \cdots\right) \tag{D.7}$$

Two main elements contribute to the cumulative total travel distance caused by each passage of a truck on a simply supported bridge (the discussions presented and equations developed are for simply supported bridges and could conservatively be used for continuous bridges):

1. The deflection and rebound of the bridge (forced movement) during passage of a truck causes the bridge bearings to experience horizontal movements. The following items could be considered in calculating the total horizontal movement of the bearings during passage of a truck:
   a. For a simply supported girder, once a truck reaches the bridge midspan, the girder deflection is at a maximum, as is the horizontal movement at the bearings due to end rotation. As the truck moves toward the end of the span, the girder rebounds to its original position; consequently, the bearings rebound to their original position. Therefore, the total horizontal movement of the bearings during passage of one truck is equal to two times the horizontal movement resulting from girder maximum displacement.
   b. If one end is fixed against translation, then movement due to girder end rotation is transferred to the expansion end. If both ends of the span have expansion bearings, each end experiences horizontal movement due to girder rotation, and there is no movement transfer. In the case of the three-dimensional (3-D) FE model for the prototype bridge, the fixed and expansion ends of the bridge are represented in the bridge model, and the resulting movement at the expansion end reflects the movement transfer from the fixed end.
   c. Trucks are moving objects, and therefore a dynamic impact factor needs to be considered. In this study an impact factor of 1.33, as recommended by the *LRFD Specifications,* was used.

2. After the truck clears the span, the bridge bounces back to its original position, and then continues upward to a deflection slightly less than the initial downward deflection caused by the truck during its passage. The bridge will continue to vibrate up and down until the structure's damping dissipates the amplitude of the motion, as shown in Figure D.8.

The term $2x_1$ in Equation D.7 is the amplitude of movement (x_1 is the maximum initial horizontal movement at the expansion bearing). Note that the amplitude of the movement is two times the initial maximum horizontal movement.

Equation D.7 includes all the above-mentioned effects except the 1.33 impact factor. This equation can be plotted as shown in Figure D.10. As this figure shows, for a 7% damping ratio (on the horizontal axis), the total travel distance at the expansion bearing will be 10.1 times the maximum initial horizontal movement. This factor is 7.4 for a 10% damping ratio.

Therefore, every time a truck passes the bridge, the total movement, including the movement due to vibration, will be approximately 10.1 times the first deformation due to the truck passage for a 7% damping ratio and about 7.4 times for a 10% damping ratio.

For the prototype bridge, the maximum initial horizontal movement (one direction) due to truck passage was calculated from the FE analysis as 0.146 in. A dynamic impact factor of 1.33 should also be applied to this movement to account for the fact that the truck is a moving object. Note that the prototype bridge FE model was a 3-D model with one end of the girders pinned (restrained against horizontal movements) and the other end of the girders free to expand. The horizontal movement of 0.146 in. was directly extracted from the 3-D model at the actual location of the expansion bearings under the bottom flange of the girder, and it already accounts for the horizontal movement transfer from the fixed end. Thus, the multiplier 2, for the transferred horizontal movement from the fixed end of the girder, does not apply to this case; therefore, the total cumulative horizontal movement due to one truck passage is as follows:

$$\text{Cumulative movement} = 0.146 \times 1.33 \times 7.4 = 1.44 \text{ in.}$$

The 7.4 factor shown in the above equation accounts for free vibration of the bridge and is obtained from Figure D.10, assuming a 10% damping ratio.

According to National Bridge Inventory (NBI 2013) data, the average daily truck traffic (ADTT) of most bridges ranges from 50 to over 5,000. For an ADTT of 1,000, the total horizontal movement of the expansion bearing, in miles, over a 100-year service life could be estimated as follows:

$$(1{,}000 \times 365 \times 100 \text{ years}) \times 1.44/12/5{,}280 \approx 800 \text{ mi}$$

Table D.3 summarizes the results for similar calculations considering ADTTs ranging from 1,000 to 5,000, with vibration included. For comparison, the table also summarizes the total cumulative movement without vibration, considering only one full cycle of movement (i.e., initial deflection and rebound to the original position after truck passage).

It is concluded that total cumulative horizontal movement at an expansion bearing due to truck load can be very significant, especially when movement due to free vibration is also considered.

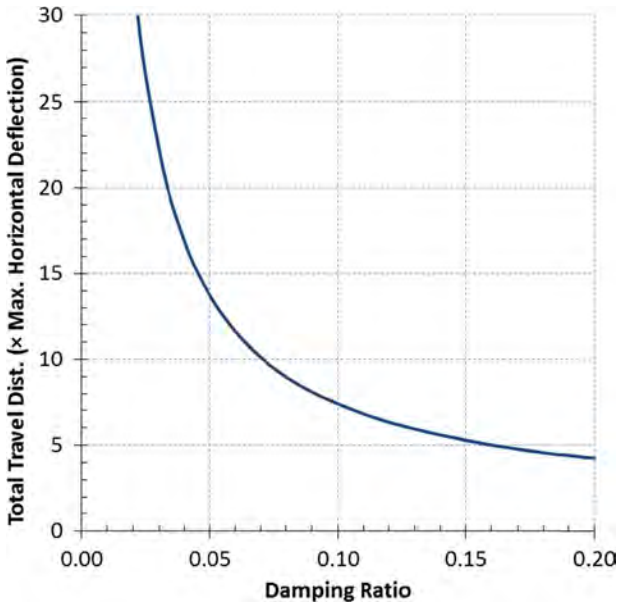

Figure D.10. Graph to determine total travel distance (to determine total travel distance of the sliding bearing, the maximum initial horizontal movement is multiplied by the number read from this plot).

Table D.3. Approximate Cumulative Movement over 100 Years Due to Truck Load

ADTT	Approximate Total Cumulative Travel (mi)	
	With Vibration (10% damping ratio)	Without Vibration (one cycle)
1,000	800	200
2,000	1,700	450
3,000	2,500	700
4,000	3,300	900
5,000	4,100	1,100

Bearing Movements Due to Temperature Variations

Temperature fluctuations, including daily and seasonal temperature changes, also contribute to total horizontal movement of expansion bearings. The accumulated movement of the prototype bridge bearings with 100-plus years of service life due to daily and annual temperature variations was evaluated.

Daily Temperature Variation

Assuming 40°F average daily temperature change, the accumulated bearing movement can be determined as follows:

$$\Delta L_{\text{Daily}} = 2 \times \alpha . L . \Delta T = 2 \times 7 \times 10^{-6} \times (200 \times 12) \times 40 = 1.34 \text{ in.}$$

For 100 years of service life, the total daily accumulated bearing movement is given by the following equation:

$$\Delta L_{\text{Total, daily}} = 365 \times 100 \times 1.34 = 48{,}910 \text{ in.} = 4{,}076 \text{ ft}$$

Annual Temperature Variation

If an average annual temperature variation of 110°F is assumed, the annual end movement due to this thermal load can be determined as follows:

$$\Delta L_{\text{Annual}} = 2 \times \alpha . L . \Delta T = 2 \times 7 \times 10^{-6} \times (200 \times 12) \times 110 = 3.70 \text{ in.}$$

For 100 years of service life, the total annual movement is given by

$$\Delta L_{\text{Total, annual}} = 100 \times 3.70 = 370 \text{ in.} = 30.8 \text{ ft.}$$

Total Accumulative Bridge Movement Due to Thermal Loads

Finally, the total horizontal movement at the expansion bearing for the prototype bridge over 100 years of service life due to both daily and annual temperature variation is given as follows:

$$\Delta L_{\text{Total}} = \Delta L_{\text{Total, annual}} + \Delta L_{\text{Total, daily}} = 4{,}076 + 308 = 4{,}107 \text{ ft}$$

Speed of Bearing Movement for Truck Load

The speed of travel for the sliding bearing can be determined from the general formula given by Equation D.8:

$$\text{Average travel speed} = \frac{\text{Distance traveled}}{\text{Travel time}} \tag{D.8}$$

As previously discussed, high-speed movement causes the majority of sliding-material damage. Bridge deflection during the passage of a truck, and subsequent free bridge vibration, results in different sliding speeds.

Sliding Speed During Truck Passage

The time for a truck to pass the bridge can be calculated as shown by Equation D.9:

$$t = \frac{\text{Bridge span}}{\text{Truck speed}} \tag{D.9}$$

The slip rate of the bearing can be determined as shown by Equation D.10:

$$\text{Slip rate} = \frac{1.33a \times \theta \times D_1 \times 2}{t} \tag{D.10}$$

where

a = 2, if entire horizontal movement due to girder rotation at both ends is taken at one end of the girder (as for a simple-span girder with one end fixed and one end expansion). Otherwise, use 1;
θ = rotation of the girder end due to truck passage (Rad);
D_1 = depth of neutral axis measured from the bottom flange (in.); and
1.33 = dynamic impact factor due to truck passage.

The following discussion outlines the steps in calculating the slip rate or velocity of horizontal movement at the expansion bearing during passage of trucks for the prototype bridge.

If it is assumed that the truck passes the bridge's 200-ft span with a speed of about 50 mph, then time in seconds for the truck to cross the bridge would be as follows:

$$t = \frac{x}{t} = \frac{200 \text{ ft}}{50 \text{ mph} \times 5{,}280 \text{ ft/mi}} \times 3{,}600 \text{ s/h} = 2.73 \text{ s}$$

The horizontal movement at the expansion bearing for the prototype bridge from FE results was 0.146 in.; therefore, in the slip rate equation above (Equation D.10), $\theta D_1 = 0.146$ in., and $a = 1$.

From the equation for t above, it would take the truck 2.73 s to cross the bridge. During this period the horizontal movement will be twice the 0.146-in. deflection (bridge moving down and then returning to its original undeflected position). Therefore, the slip rate or velocity of horizontal movement during passage of one truck, considering the impact factor, will be as follows:

$$\text{Slip rate of the bearing} = \frac{\text{Bearing movement}}{t} = \frac{0.146 \text{ in.} \times 2 \times 1.33}{2.73 \text{ s}} = 0.142 \text{ in./s}$$

If the bearing movement from the more general case approximate analysis is used, the slip rate would be as follows:

$$\text{Slip rate of the bearing} = \frac{\text{Bearing movement}}{t} = \frac{0.525 \text{ in.} \times 2 \times 1.33}{2.73 \text{ s}} = 0.51 \text{ in./s}$$

Table D.4. Sliding-Surface Slip Rate for Various Speed Limits During Truck Passage

Truck Speed (mph)	Slip Rate (in./min)	
	From FE Analysis	From Approximate Analysis
40	6.8	18.4
50	8.5	23.0
60	10.3	27.8

Table D.4 shows the same calculations for other truck speeds, with unit conversion to inches per minute, for movements representing FE analysis and the approximate analysis.

Sliding Speed Due to Bridge Free Vibration After Truck Passage

Once a truck has crossed the bridge, the bridge continues to vibrate freely until the vibration is damped out. The average sliding speed of horizontal movement after truck passage is equal to the cumulative movement after truck passage divided by the time required for that cumulative movement to occur. This sliding speed due to free vibration is independent of the initial truck speed and depends rather on the dynamic characteristics of the bridge (stiffness, mass, and damping).

The distance traveled due to free vibration after truck passage can be computed by Equation D.11:

$$\text{Distance traveled during free vibration} = 1.33 \times a \times \theta \times D_1 \times (f - 2) \quad \text{(D.11)}$$

where

- a = 2, if entire horizontal movement due to girder rotation at both ends is taken at one end of the girder (as for a simple-span girder with one end fixed and one end expansion). Otherwise, use 1;
- θ = rotation of the girder end due to truck passage (Rad);
- D_1 = depth of neutral axis measured from the bottom flange (in.);
- 1.33 = dynamic impact factor due to truck passage; and
- f = factor used for calculating total distance traveled taken from Figure D.10 (this value is 13.7, 10.1, and 7.4 for damping ratios of 5%, 7%, and 10%, respectively).

The term $(a \times \theta \times D_1)$ in Equation D.11 is the initial maximum movement at the expansion bearing, which from the FE analysis of the prototype bridge was 0.146 in.

Figure D.11 shows the total horizontal movement with time and how the cycles of movement dissipate over time after the truck leaves the span.

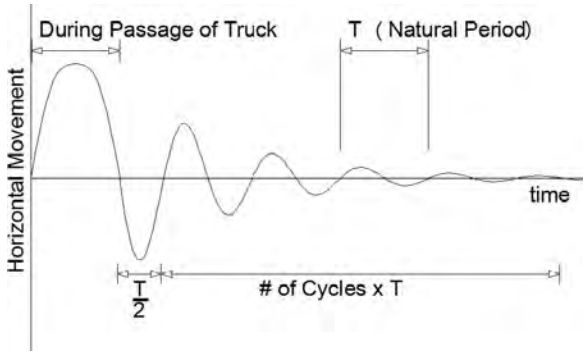

Figure D.11. Cycles of horizontal movement with time.

The total time t for the free vibration after truck passage can be determined from Equation D.12:

$$t = \frac{T}{2} + \frac{0.366}{\xi} \times T \quad \text{(D.12)}$$

where T is the free vibration period of the bridge, which is discussed in the next section on natural frequency, and ξ is the damping ratio.

The term $0.366/\xi$, which is from Equation D.5, is the number of cycles required to reduce the free vibration amplitude to 10% of the first cycle amplitude.

For the prototype bridge, the horizontal movement of 0.146 in. was directly extracted from the 3-D model at the actual location of the roller bearings under the bottom flange of the girder. Therefore, the multiplier 2, for the transferred horizontal movement from the other end of the girder, does not apply to this case.

From Equation D.11, the distance traveled due to free vibration after truck passage with a 10% damping ratio can be calculated as follows:

$$\text{Distance traveled during free vibration} = 1.33 \times 0.146 \times (7.4 - 2) = 1.05 \text{ in.}$$

Time t for this amount of travel can be computed from Equation D.12, and with a 10% damping ratio is given by

$$t = \frac{1.26}{2} + \frac{0.366}{0.10} \times 1.26 = 5.2 \text{ s}$$

Therefore, the speed of movement is

$$\text{Speed} = \frac{1.05}{\frac{5.2}{60}} = 12.1 \text{ in./min}$$

This is the average speed of bearing movement during the free vibration phase that occurs after passage of a truck. It is

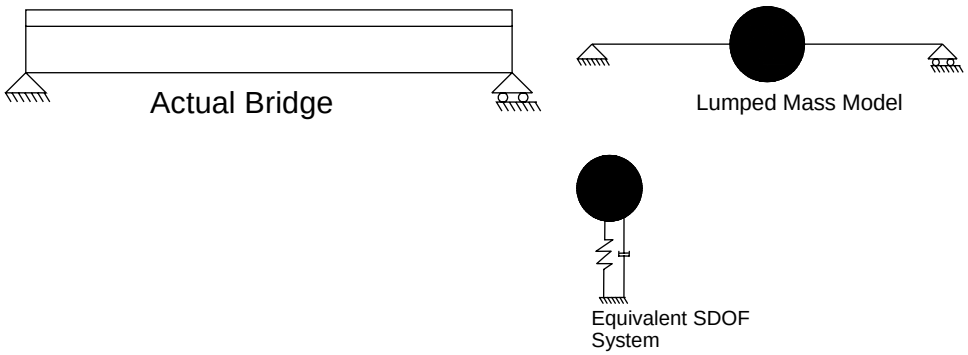

Figure D.12. Modeling of bridge girder using the single degree of freedom (SDOF) system to determine the natural frequency of the structure.

based on the initial movement from the FE analysis and assumes a 10% damping ratio.

Natural Frequency of the Bridge Structure

The natural frequency of the bridge can be determined by considering the structure as a single degree of freedom (SDOF) system, as shown in Figure D.12.

The first step is to determine the stiffness of the equivalent SDOF system. Table D.2 shows that the external girder's midspan deflection under the weight of an HL-93 truck is 1.28 in. HL-93 truck weight is 72,000 lb. Therefore, the midspan stiffness of the girder can be determined as follows:

$$K = \frac{\text{Load}}{\text{Deflection}} = \frac{72{,}000}{1.28} = 56{,}250 \text{ lb/in.}$$

Now the total mass of the bridge (M) can be determined as follows (bridge span is 200 ft, and bridge width is 42 ft):

$$\text{Area of each girder} = 20 \times 1 + 84 \times 0.625 + 22 \times 1.57$$

$$= 107.04 \text{ in.}^2$$

$$w = \left(\frac{8}{12} \times 150 \times 200 \times 42\right) + \left(4 \times \frac{107.04}{12^2} \times 200 \times 486\right)$$

$$= 1{,}129{,}008 \text{ lb}$$

$$M = \frac{w}{g} = \frac{1{,}129{,}008}{386.4} = 2{,}921.86 \text{ lb } \frac{s^2}{\text{in.}}$$

Therefore, the bridge period can be determined from the following equation:

$$T_n = 2\pi\sqrt{\frac{K_{LM}^e M}{K_e}}$$

where K_{LM}^e is load–mass factor for elastic range (0.78 for this case). This factor is used because the entire bridge mass has been concentrated at the midspan of the bridge, and the midspan stiffness of the bridge is used (the uniform distributed bridge mass has been concentrated as a lump mass).

$$T = 2 \times \pi\sqrt{\frac{0.78 \times 2{,}921.86}{56{,}250}} = 1.26 \text{ s}$$

Phase 2: Conceptual Design of the Experiment

Test Parameters

NCHRP Report 432 (Stanton et al. 1999) describes the following parameters to be significant in the wear of PTFE surfaces:

- Contact pressure;
- Temperature;
- Lubrication;
- Type of PTFE;
- Sliding speed (speed of travel);
- Travel distance; and
- The type of backing material to the sliding surface (neoprene, fabric, steel pads).

The literature review revealed that the COF of PTFE decreases when the contact pressure (or the compressive stress on the mating surfaces) increases. The effects of this parameter on MSM material were also studied in this project.

Although temperature has been proven to affect the wear behavior of PTFE, this parameter was not studied in this project because of the limited scope, which was proof of concept testing only.

Lubrication has been shown to modify PTFE performance. Stanton et al. (1999) reported that "dimpled lubricated PTFE is the most resistant PTFE to wear." However, plain unlubricated PTFE was compared with the other materials in this study because this is the material used most often in practice.

Lubrication is not used much in normal U.S. practice because of the uncertainty of how long it will last.

The sliding speed is an important factor in the behavior of PTFE material. There exists a sliding speed beyond which the level of friction in PTFE appears to remain constant. However, there is a large discrepancy between the values of this speed among different researchers. The lowest speed has been identified by Mokha et al. (1990) to be around 240 to 480 in./min. The calculated sliding speed for the prototype bridge ranges from approximately 8 to 13 in./min. Therefore, as can be seen for the prototype bridge, the sliding speed is far below the lowest speed range suggested by Mokha et al. (1990), so COF in real-life bridges will vary.

Experimental Approach

Two approaches were considered for the type of movement to be investigated in the experimental program: (1) simulating temperature-induced bridge movements, which are low-frequency, high-amplitude movements; and (2) simulating horizontal movements due to truck passage, which are high-frequency, low-amplitude movements.

Truck passage, as discussed in previous sections, causes significantly higher movement speeds and cumulative total movements for the expansion bearing sliding surface throughout the life of the structure, although its movement amplitude is smaller than the amplitude of temperature-induced movement. Further, the contact pressure during a truck passage is higher than the contact pressure during thermal movements, which increases wear.

Considering all this information, it was concluded that selecting the second testing strategy will result in simulating a more severe condition for a sliding surface.

Mating Surfaces

The *LRFD Specifications* require the use of stainless steel for flat mating surfaces. This stainless steel should be Type 304, conforming to ASTM A167/A264, and have a surface finish of 0.20 μm RMS or better.

The *LRFD Specifications* further state that "ASTM A240M, Type 304, stainless steel, with a surface finish of 4.0×10^{-4} mm (0.40 μm) RMS or better, is appropriate, but the surface measurements are inherently inexact, and hence it is not a specified alternative."

For this study, ASTM A240M was used to be comparable with previous research testing.

Contact Pressure

The *LRFD Specifications* state the values in Figure D.13 as the range of contact pressures for PTFE.

The contact pressures in the long-term sliding test carried out by Maurer on MSM sliding bearings were 4.35 ksi for dimpled PTFE and 8.70 ksi for MSM.

Campbell and Kong (1987) suggest allowable contact pressures of 4.35 ksi under dead load and 6.525 ksi under total load for PTFE in bearings in the United States.

In the experimental program reported in NCHRP Report 432, contact pressures of 500 to 6,000 psi were used (Stanton et al. 1999). For their wear rate experiments, a contact pressure of 3,000 psi was used, which was considered an upper bound.

For this study, an initial contact pressure of 3,000 psi was chosen to be compatible with previous wear tests.

Temperature

All tests were carried out at room temperature. To maintain room temperature, a fan was installed to cool the samples during the experiment when heat due to friction was observed or experienced.

Lubrication

Lubrication has been shown to enhance PTFE performance. NCHRP Report 432 (Stanton et al. 1999) notes that dimpled

Material	Average Contact Stress (ksi)		Edge Contact Stress (ksi)	
	Permanent Loads	All Loads	Permanent Loads	All Loads
Unconfined PTFE: Unfilled Sheets	1.5	2.5	2.0	3.0
Filled Sheets with Maximum Filler Content	3.0	4.5	3.5	5.5
Confined Sheet PTFE	3.0	4.5	3.5	5.5
Woven PTFE Fiber over a Metallic Substrate	3.0	4.5	3.5	5.5
Reinforced Woven PTFE over a Metallic Substrate	4.0	5.5	4.5	7.0

Source: AASHTO 2010b.

Figure D.13. **LRFD Specifications *maximum contact stress for PTFE at service limit state (ksi).***

lubricated PTFE is the PTFE most resistant to wear. However, it is uncertain that sliding material lubrication in a bridge bearing will stay in place over the life of the bridge. Because unlubricated, plain PTFE is most commonly used in practice, it was chosen as the base PTFE sliding material to be compared against MSM and filled PTFE (Fluorogold) in wear tests. Lubricated PTFE and MSM samples were used, however, to evaluate and compare COF in the lubricated condition.

Type of PTFE

Flat, unlubricated, unfilled (plain) PTFE exhibits much higher wear than dimpled lubricated, woven, or glass-filled PTFE (Stanton et al. 1999), but because it is the most commonly used sliding material in U.S. practice, it was used as the base material for establishing wear rates and for comparison. Plain PTFE was also tested in previous research, so the results from this study could be compared against previous results for establishing baseline wear rates.

Previous studies have shown that plain PTFE will experience significant wear at low cumulative movements when subjected to high sliding speeds; however, much higher cumulative movements were expected for Fluorogold and MSM. Failure of PTFE is based on the level of wear, which occurs within relatively low travel distances. The travel distance to wear out MSM and Fluorogold has not yet been established; however, it was expected that preliminary wear rates would be developed in this study.

Sliding Speed (Speed of Travel)

Two types of slip rates (sliding speeds) can be considered for the sliding surfaces of bridge bearings. The sliding of a bearing due to the passage of a truck is of a low-amplitude, high-frequency nature, but it results in a very large accumulative movement. The sliding of a bearing due to daily thermal movements is of a high-amplitude, low-frequency nature.

As previously discussed, the sliding rate for a simple-span bridge with a 200-ft span and the passage of a truck with a speed of 50 mph is about 0.107 in./s, or about 6.42 in./min. This value for a speed of 70 mph would be 8.99 in./min.

The speeds used in the long-term sliding test carried out by Maurer on MSM sliding bearings were 0.0787 in./s (4.72 in./min) for dimpled PTFE and 0.59055 in./s (35.43 in./min) for MSM (MSM material was developed to be used in high-speed railroad bridge bearings).

Based on the report by Campbell and Kong (1987), little information is available for sliding speeds of bearings in real service. In their document they reported thermal movement rates up to 0.000024 in./s (0.0014 in./min) (reinforced concrete bridge) and 0.000157 in./s (0.0094 in./min) (unsurfaced steel box) for a 200-ft-span bridge. These values are negligible compared with live load movement speeds as high as 0.787 in./s (47 in./min) for a steel railway bridge and 2.756 in./s (165 in./min) for a steel–concrete composite bridge. Therefore, in their report, Campbell and Kong recommended performing laboratory tests using maximum speeds of 2.756 in./s (165 in./min).

The maximum sliding speed for the PTFE wear tests carried out for NCHRP Report 432 (Stanton et al. 1999) was 25 in./min. To be consistent with that study, an initial sliding speed of 25 in./min was adopted for this study.

The actuators in the structures laboratory of the University of Nebraska–Lincoln have a maximum capacity to apply slip rates of about 60 in./min (for the prescribed travel amplitude).

Travel Distance

Based on the results of the FE and theoretical studies carried out in the previous sections of this appendix, the average accumulated travel distance at an expansion bearing due to truck load for a common simple-span steel stringer-type bridge, within the parameters studied and in 100 years of service life, would range between 300 to 1,500 mi depending on the AADT, bridge length, bridge stiffness, and so forth. These values would be different for concrete structures.

The travel distances used in the long-term sliding test carried out by Maurer on MSM sliding bearings were approximately 13 mi for dimpled and lubricated PTFE and 31 mi for dimpled and lubricated MSM.

Traffic-induced movements range from 476 ft (0.09 mi) to 16,404 ft (3.1 mi) per year (Lebek 1985; Muller-Rochholz et al. 1986; Hakenjos et al. 1985); therefore, for a 100-year service life, the accumulated movement distance discussed in these reports could range from 9 to 313 mi.

Extended long-term field measurements and monitoring are necessary to verify the actual amount of bearing movement due to truck load.

Types of Backing Material for PTFE

Various types of backing materials for sliding surfaces can be used, such as neoprene or fabric pads or steel plates. However, for wear testing, where no rotation is permitted, the simplest method is to use steel plates and chemically bonding and recessing the PTFE. This method was used in this study to be compatible with previous tests by other researchers.

Size of Sliding Surface Specimens

Discs having a diameter of 3 in. have commonly been used in PTFE testing in Europe and can be an accepted standard (Campbell and Kong 1987). This specimen size was also used in the studies for NCHRP Report 432. The previous MSM

studies were performed on samples with diameters of 3.0 and 6.1 in., with most tests performed on 3.0-in.-diameter samples. Previous studies have also shown that the size of the sliding surface specimen has a minimal effect on its behavior, including its COF.

A 3-in.-diameter specimen size was selected for all tests in this experimental program.

Thickness of Sample, Backing Plate, and Mating Surface

A minimum thickness is required for the PTFE sheets to accommodate wear and ensure a uniform bearing. According to the *LRFD Specifications,* at least 0.0625-in. thickness is required for all PTFE sheets after compression. This value is at least 0.1875 in. for recessed PTFE sheets when the maximum dimension of the PTFE is equal to or less than 24.0 in.

For stainless steel mating surfaces, the *LRFD Specifications* also recommend at least 16-gauge thickness when the maximum dimension of the surface is less than or equal to 12 in. This thickness ensures no buckling or wrinkling. The *LRFD Specifications* also require that the mating surface for flat sliding surfaces be attached to a backing plate by welding in such a way that it remains flat and in full contact with its backing plate throughout its service life.

The restrictions on the attachment of the mating surface are primarily intended to ensure that the surface is flat and retains uniform contact with the PTFE at all times without adversely affecting the friction of the surface or gouging or cutting the PTFE.

In the studies for NCHRP Report 432, 0.25-in. thickness was used for dimpled PTFE, and 0.125-in. thickness was used for plain PTFE. A 0.06-in.-thick stainless steel plate, highly polished to a No. 8 mirror finish, was used as the mating surface.

The most common thickness used for Fluorogold is 0.094 (3⁄32) in.; it is supplied from the factory already bonded to a backer plate. A thickness of 0.125 (1⁄8) in. is also available.

The thickness of MSM varies between 5 and 8 mm (0.1969 and 0.3150 in.). Normally, an 8-mm (0.3150-in.) thickness is used.

Plan of Tests

Because of the more intense wear condition resulting from traffic loads, tests were carried out at high movement speeds to simulate conditions due to truck passage.

The significant parameters affecting the wear of sliding surfaces were selected based on previously undertaken research, most common industry practices, code requirements, and limitations of the available equipment.

The stroke length was 1 in. That is, the stainless steel plate moved upward from its central position 1 in., and then it moved back down for 2 in. (i.e., it passed the initial central position by 1 in.), and then back up to the original position. The total movement per complete cycle was 4 in.

The flat mating surface was 0.06-in.-thick Type 304 stainless steel with a finish of 0.20 μm RMS.

Steel plates were used as the backing plate material for all the experiments. The sliding surfaces were mechanically recessed in or chemically bonded to (or both) the backing material to ensure that no failure would occur in the sliding surface backing-material plane.

The standard size of a 3-in. diameter was selected for all specimens.

The thickness of all plain PTFE specimens was 0.25 in. The thickness of the MSM specimens was 0.315 in. (8 mm). A thickness of 0.094 (3⁄32) in. was used for the Fluorogold specimens.

Table D.5 and Table D.6 summarize the testing program parameters.

Attachment of PTFE to Backing Plate

Typically, PTFE is recessed one-half of its thickness into the backing plate to prevent creep. In some cases, it is also chemically bonded. When bonded, PTFE sheets are typically etched on one side to increase bonding capability.

Table D.5 identifies the type of attachment between the sliding material specimens and the backing plates for this study. PTFE and MSM specimens were recessed and bonded. Fluorogold specimens were only chemically bonded as typically provided by the manufacturer.

The sliding surface specimens were oriented such that the direction of texture on the etched side was perpendicular to the direction of sliding.

The stainless steel mating surfaces were aligned such that the direction of sliding was perpendicular to the direction of polishing (to the extent practicable).

Design of Test Fixture

The test setup used for the sliding surface wear tests is shown in Figure D.14. In this test setup, an MTS cyclic actuator was vertically installed in a large steel frame. The bearing test fixture was installed below and connected to the actuator.

The sliding surface test fixture consisted of four main components:

1. A moving steel plate with a stainless steel plate mounted on both sides (sliding platform);
2. Two stationary sliding surface specimens connected to backing plates;
3. Two horizontal hydraulic jacks that applied contact pressure; and
4. An MTS actuator that provided vertical cyclic movement.

Table D.5. Experimental Program: Test Specimen Parameters

	Type of Specimen	Total No. of Samples	Sample Diameter (in.)	Sample Thickness	Mating Surface	Backing Material to Sliding Surface and Stainless Steel Surfaces	Connection to the Backing Plate
1	Flat unlubricated, unfilled PTFE (plain PTFE)	2	3	¼ in.	Stainless steel Type 304, 0.06-in. thickness, highly polished to No. 8 mirror finish	Steel plate	⅛ in. Recessed and bonded
2	Dimpled unlubricated, unfilled PTFE	2	3	¼ in.	Stainless steel Type 304, 0.06-in. thickness, highly polished to No. 8 mirror finish	Steel plate	⅛ in. Recessed and bonded
3	Dimpled unlubricated MSM	2	3	8 mm (5⁄16 in.)	Stainless steel Type 304, 0.06-in. thickness, highly polished to No. 8 mirror finish	Steel plate	5 mm Recessed and bonded
4	Unlubricated Fluorogold	2	3	3⁄32 in.	Stainless Steel Type 304, 0.06-in. thickness, highly polished to No. 8 mirror finish	Steel plate	Bonded

Table D.6. Experimental Program: Test Parameters

	Type of Specimen	Displacement per Cycle (Amplitude) (in.)	Contact Pressure (psi)	Slip Rate (in./min)	Cycling Frequency (Hz)	PV (lb/in.^{2} × ft/min)
1	Flat unlubricated, unfilled PTFE (plain PTFE)	2	3,000	25	0.10	6,250
2	Dimpled unlubricated, unfilled PTFE	2	3,000	25	0.10	6,250
			1,000			2,080
			1,500			3,120
			2,000			4,160
3	Dimpled unlubricated MSM	2	3,000 (4,900 effective)	25	0.10	6,250
				50	0.20	12,500
			5,000	25	0.10	10,410
4	Unlubricated Fluorogold	2	3,000	25	0.10	6,250
				50	0.20	12,500
			1,000	50	0.20	4,160
			5,000	25	0.10	10,410

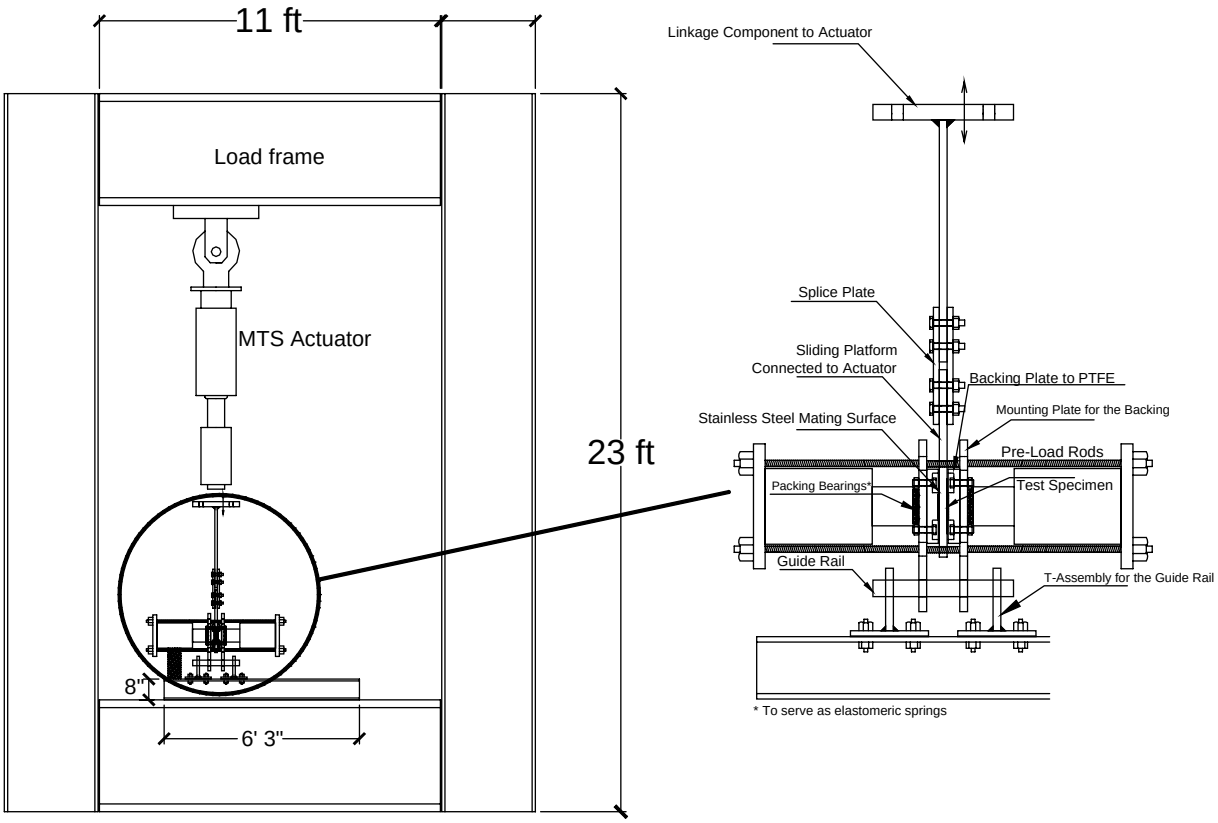

Figure D.14. Sketch of loading frame and test fixture for wear tests in University of Nebraska–Lincoln structures lab.

The sliding platform was sandwiched between the two stationary sliding surface specimens mounted on steel backing plates. The two horizontal hydraulic jacks applied horizontal pressure perpendicular to the surface of the sliding specimens to create the required contact pressure.

Each backing plate was mounted on another larger plate (a mounting plate for the backing plate) that held the backing plate and specimen stationary.

A reaction plate was placed on the outside of each hydraulic jack, and four Dywidag rods ran from the four corners of the west reaction plate through both specimen mounting plates and then to the east reaction plate. This arrangement resulted in an equal force on both backing plates. This entire system was supported on a bottom railing system. To run the test, the sliding platform, which was connected to the cyclic MTS actuator using T plates, moved upward and downward by the MTS cyclic actuator (see Figure D.15).

The bottom rail consisted of two 2-in.-diameter stainless steel rods machined to slip fit the holes on two T assemblies. A camshaft bearing was press-fitted into the hole on each T assembly. The same type of hole was also prepared on the bottom of the two mounting plates through which the stainless steel rod ran. Thus, the 2-in.-diameter stainless steel rods almost perfectly fit in the holes and at the same time, the plates slid easily on the rods (see Figure D.16 and Figure D.17).

A neoprene pad was placed between the horizontal actuators' piston and the mounting plate for the sliding surface. This pad, which is called a packing bearing, worked as a spring and retained the pressure exerted from the actuators to the plates in case the plates moved slightly, or in case the actuators leaked slightly and lost some pressure.

Phase 3: Construction of Test Apparatus

The frame in which the test fixture and the MTS actuators were installed was assembled on the laboratory strong floor (see Figure D.18). Two MTS actuators were installed with the potential of being able to run two test setups simultaneously; however, it was ultimately decided to use only one. Both the MTS actuators were mounted (posttensioned) on the top girder while the frame was lying on the strong floor. The MTS actuators were restrained against out-of-plane swiveling. Two precast concrete columns were leveled and then posttensioned to the strong floor. The entire frame was lifted afterward and tied to the columns (see Figure D.19). The frame was also posttensioned to the strong floor.

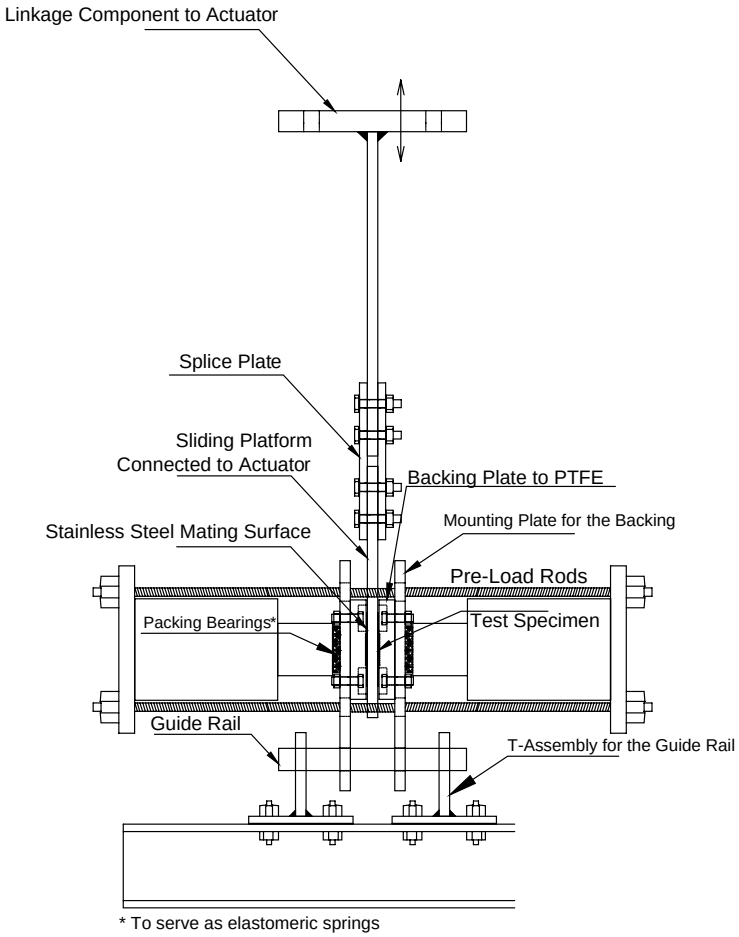

Figure D.15. Sketch of test fixture.

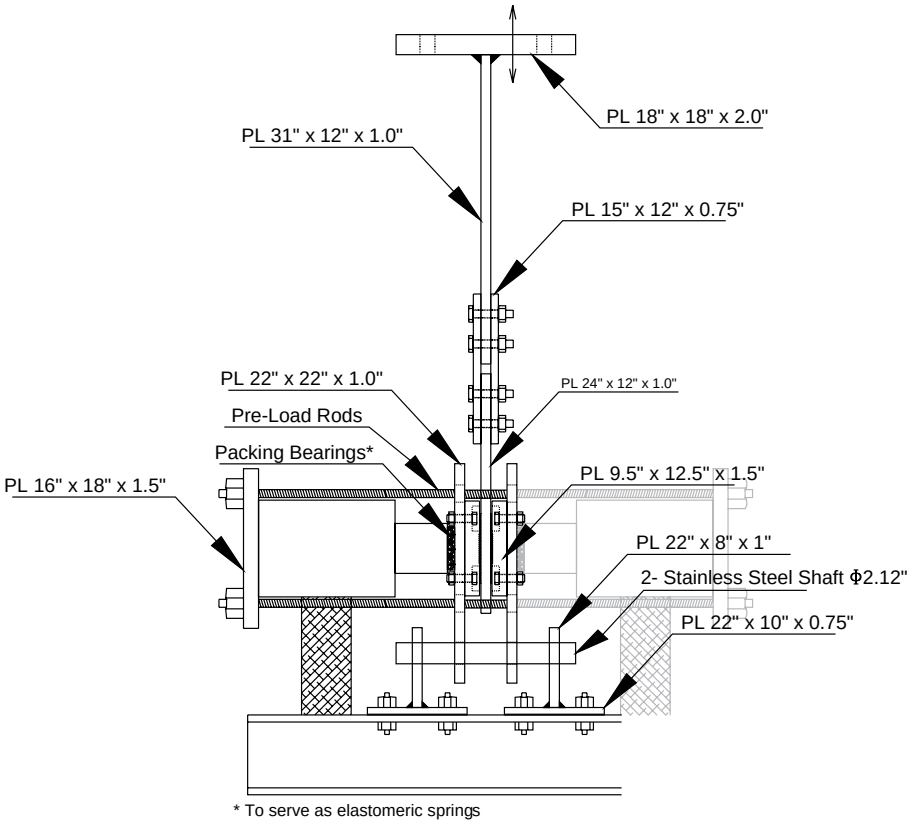

Figure D.16. Dimensions of components in test fixture.

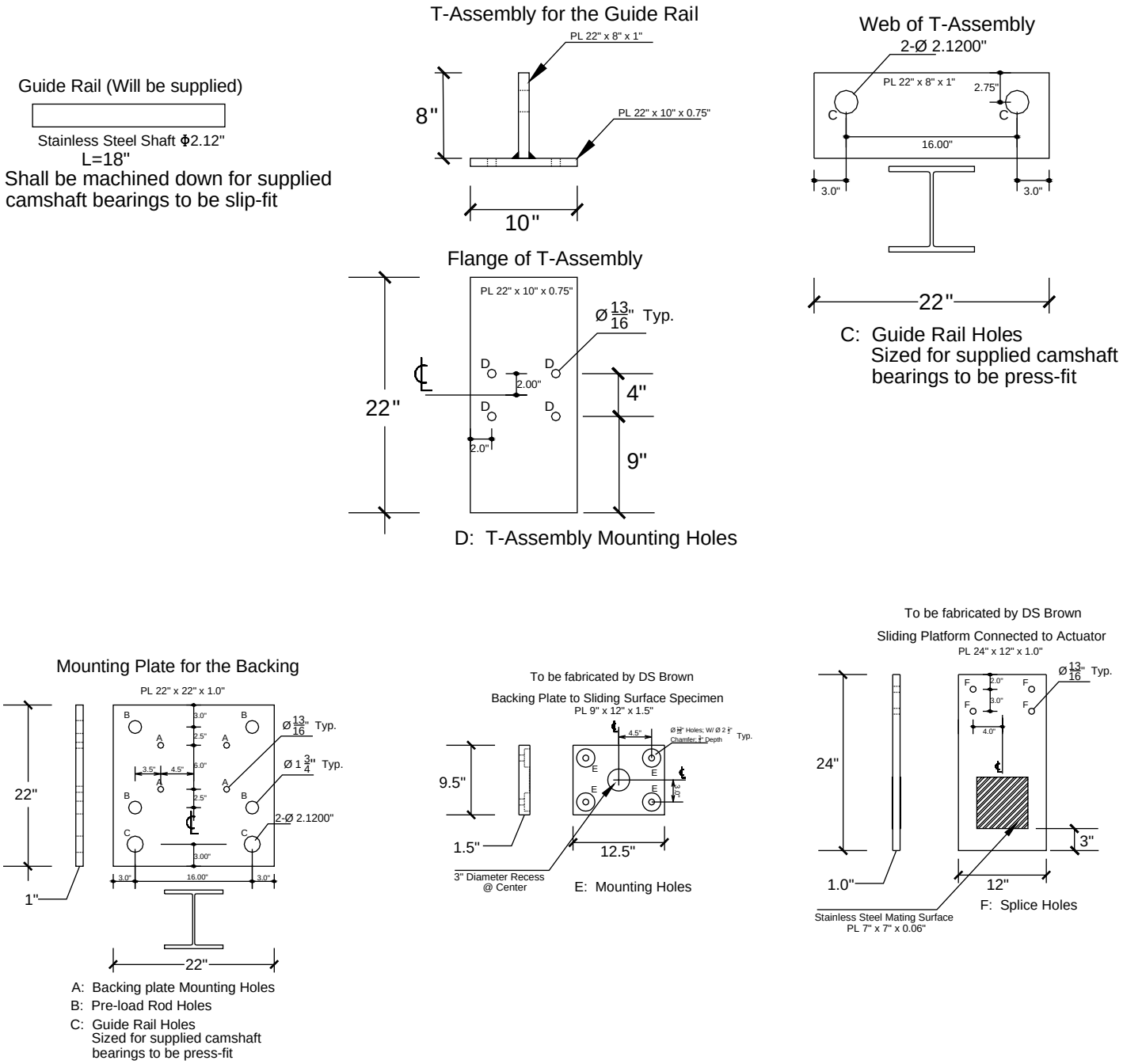

Figure D.17. Sketches of components of test fixture.

The bearing test fixture was then assembled on the bottom element of the frame (see Figure D.20).

Figure D.21 and Figure D.22 show the assembled test fixture.

Phase 4: Testing

Plain PTFE specimens were tested first to establish a baseline against which to compare MSM and Fluorogold results. This was followed by MSM (dimpled), Fluorogold (plain), and dimpled PTFE. MSM and the second set of PTFE specimens were first tested for a prescribed number of cycles in a lubricated condition. Testing was then stopped, the specimens were cleaned, and the testing resumed in the unlubricated condition. All tests were conducted at room temperature.

In all tests, the cyclic displacement was applied on a sine wave with a stroke length of 1 in. (total cycle length of 4 in.) at an initial sliding speed of 25 in./min (0.41667 in./s). The

Figure D.18. Test frame and MTS actuators being assembled on the strong floor.

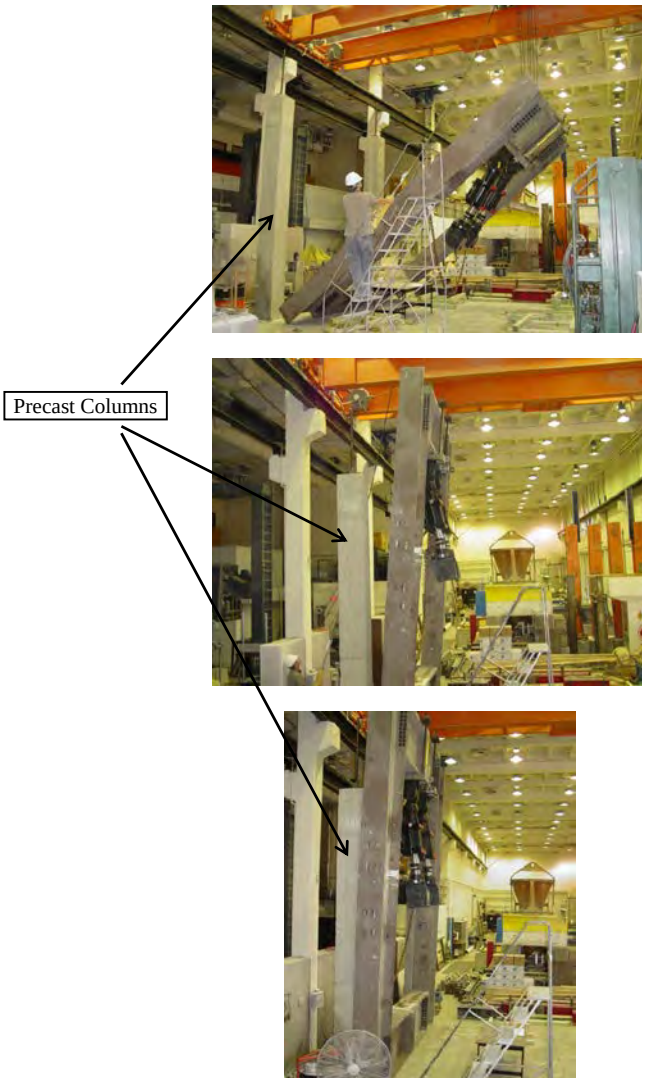

Figure D.19. Lifting operation of test frame with MTS actuators.

Figure D.20. Assembly of test fixture on bottom element of frame.

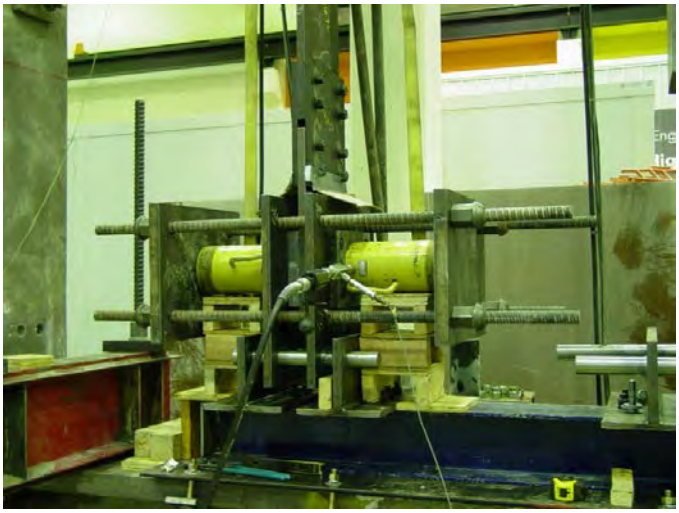

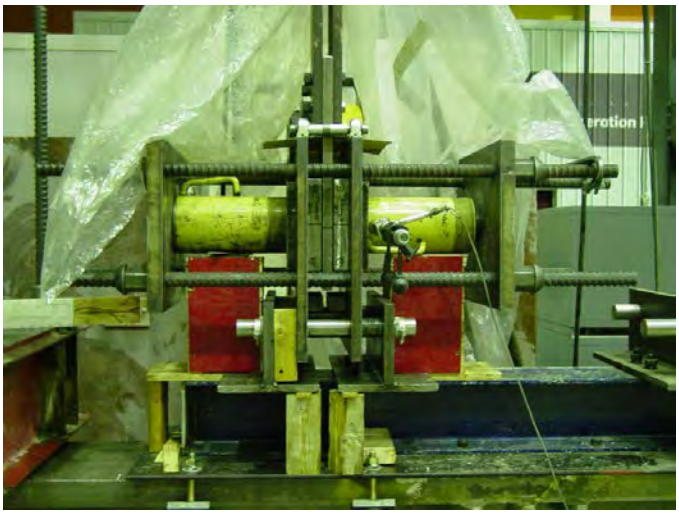

Figure D.21. Completed test fixture.

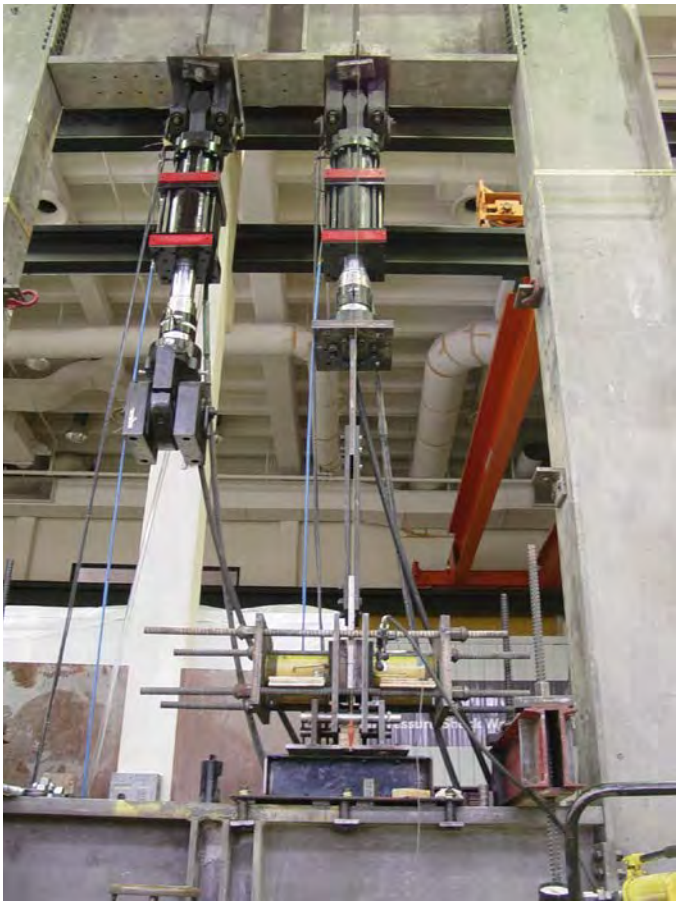

Figure D.22. Completed test fixture in test frame.

cycle frequency was initially set to 0.1 Hz (25 in./min) for all tests. This frequency was maintained for PTFE until the entire thickness was worn down. However, because of the time limitation, the frequency was increased for MSM and Fluorogold specimens to 0.2 Hz (50 in./min) after about 116,000 cycles.

The sliding surface samples were cycled under the prescribed pressure and cycle rate for various numbers of cycles, and the thickness change after various cyclic intervals was measured using a feeler gauge. The cycling intervals were 50, 100, 200, 250, 500, 1,000, 2,000, 4,000, and 8,000 at the rate of 0.1 Hz, and 16,000, which was applied at the rate of 0.2 Hz. The pressure on the samples was constantly recorded, monitored, and reset to the prescribed pressure if needed.

The spacing between the stainless steel backing plates and the sliding-material backing plates was measured at four corners, and the averages were used to determine the change in sliding material thickness.

The tests were terminated when there was close to steel-on-steel contact for the plain PTFE samples (i.e., when the entire thickness of the testing samples was nearly worn away). However, achieving this level of erosion required a much longer cyclic testing time for the high-performance sliding surfaces, and the tests had to be terminated well before the thicknesses of the samples were worn out.

The following is the step-by-step sequence of the experiment for each sliding material test:

1. The two sliding material specimens, which were attached to steel backing plates, were connected to the mounting plates (see Figures D.15, D.16, and D.17), and the bolts were torqued.
2. The steel plate with the stainless steel mating sheets on each side was attached to the MTS actuator using splice plates, and the bolts were torqued.
3. The MTS actuator was moved vertically until the centerline of the stainless steel mating sheet was located on the centerline of the backing plates to the sliding material specimens.

4. The mounting plates for the sliding material specimens were pushed toward each other until the samples touched the stainless steel mating sheet.
5. The packing bearings (neoprene pads) were placed.
6. The horizontal jacks were placed on a wooden support bench on both sides of the fixture.
7. The Dywidag rods were placed through the holes, and the reaction plates were placed behind the jacks on the rods. The nuts were turned on the Dywidag rods but were not tightened.
8. The fixture was leveled and adjusted using the nuts on the Dywidag rods. The nuts were slightly tightened to prevent the system from moving.
9. The thicknesses of the samples were measured using a feeler gauge to measure the spaces between the backing plate to the sliding surface and the backing plate to the stainless steel. These measurements were carried out on four corners of each plate (eight measurements total).
10. The jacks were loaded until the required pressure on the sliding material was reached. This pressure was set by measuring the force in the jacks. For example, if 3,000-psi pressure was required on the sliding surfaces, the jacks were loaded to 21,000 lbs of force (knowing the samples are 3 in. in diameter, their area is about 7 in.^{2}).
11. The thicknesses of the samples were measured again.
12. The MTS machine was set to the desired numbers of cycles (with the wave type and amplitude also set), and cycling was started. The MTS system continuously recorded the force required to cycle the actuators (10 measurements per second).
13. During the cycles, the force in the horizontal jacks was monitored and reset to the desired value if there was a drop in the force.
14. After the MTS actuator was stopped, the thicknesses were measured again.
15. Steps 10 to 14 were repeated.
16. After the test on a sliding material was finished, the force in the horizontal jacks was released, the steel backing plates with the test specimens were spread apart, and the backing plate with the stainless steel mating sheets was removed. Finally, the backing plates with the sliding material specimens were removed. The process returned to Step 1 for the next sliding material to be tested.

Test Results

COF, the amount of accumulated wear, and the wear rate were evaluated and compared in the experimental program.

Coefficient of Friction

COF is an important parameter for a sliding surface because it controls the level of restraint at the bearing and the amount of force transferred between the bridge superstructure and substructure. It can also affect the wear rate of the sliding surface material.

Process for Measuring Coefficient of Friction

COF was determined by measuring the force needed to move the center sliding plate with the stainless steel mating surfaces in between the stationary material test specimens. This force, which was recorded by the MTS machine during the tests, would typically include the following three components:

1. The net force needed to move the center steel plate with the stainless steel mating surfaces against the two stationary material specimens (friction force);
2. The inertial force needed to keep the motion going; and
3. The weight of the attachments to the actuator.

The measured force was set equal to zero at the beginning of the tests so the forces measured by the MTS machine were only the friction forces plus the inertial forces. Once the inertial force is known, the friction force can be determined by subtracting the inertial forces from the total measured forces.

For the sine displacement shape and for a stroke length of 1 in. at a 25-in./min pace, it can be shown that the maximum inertial force is about 0.43 times the mass that the MTS machine is moving, which is negligible compared with the actual forces that the machine is experiencing. Therefore, the inertial force was neglected, and the measured force from the actuator was the actual friction force.

The cross-sectional area of each test specimen was 7.07 in.^{2}. With a surface pressure of 3,000 psi, this results in 21.2-kip force. COF can now be determined as follows:

$$\text{Friction force} = \mu \times N$$

where μ is COF, and N is equal to 21.2 kips.

For the actual calculations, the real values of the perpendicular force that were recorded during the tests, and had minor variations, were used.

Measured Results

Figure D.23 shows the variation in calculated COF for the three sliding surface materials (PTFE, Fluorogold, and MSM) against the number of cycles and accumulated travel distance for the baseline test parameters (P = 3,000 psi; V = 25 in./min). Static and dynamic COF values were experienced for all three materials. As shown in Figure D.23, the COF values experienced an initial spike (static value) that gradually decreased to a more stable value as the cycles increased (dynamic value). The spikes occurred when cyclic testing restarted after thickness measurements were taken.

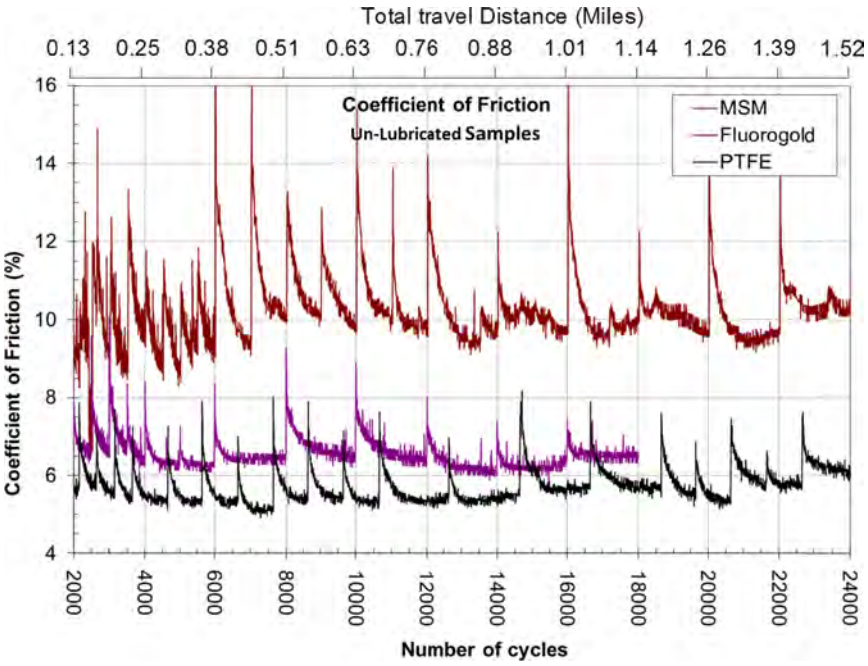

Figure D.23. Variation of COF for sliding surfaces versus the total numbers of cycles and total travel distance (P = 3,000 psi; V = 25 in./min).

Figure D.24 and Figure D.25, respectively, show the maximum (static) and minimum (dynamic) values of COF for all three test materials for the baseline test parameters (P = 3,000 psi; V = 25 in./min). In each figure, the lowest curves represent plain PTFE, the middle curves represent Fluorogold, and the highest curves represent MSM. The static values were taken from the first cycle of each cyclic testing interval, and the dynamic values were taken from the last cycles of each cyclic testing interval.

As expected, plain PTFE exhibited the lowest values, with static values ranging from about 7% to 8% and dynamic values ranging from about 5% to 6%. (The results from the second

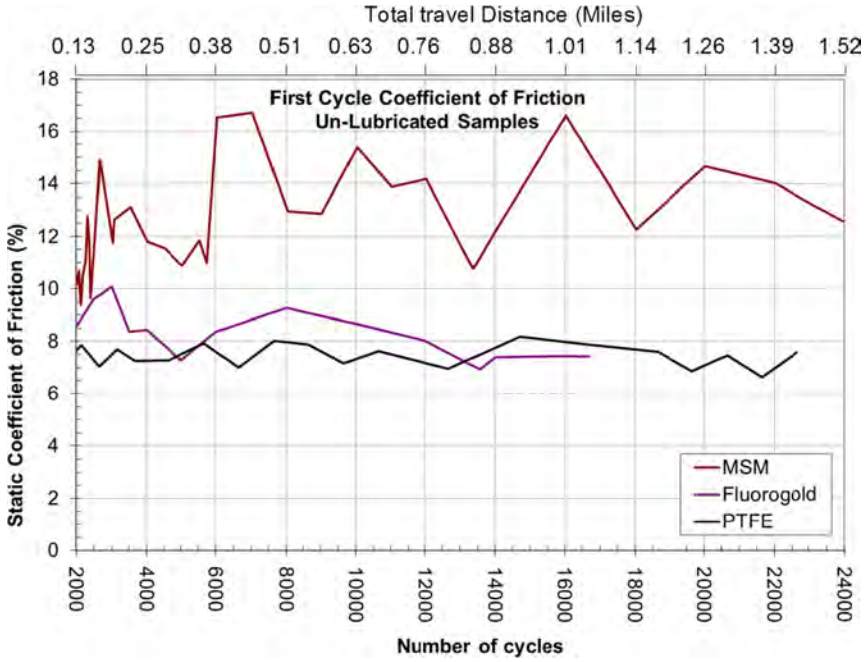

Figure D.24. Variation of static COF for sliding surfaces versus number of cycles (P = 3,000 psi; V = 25 in./min).

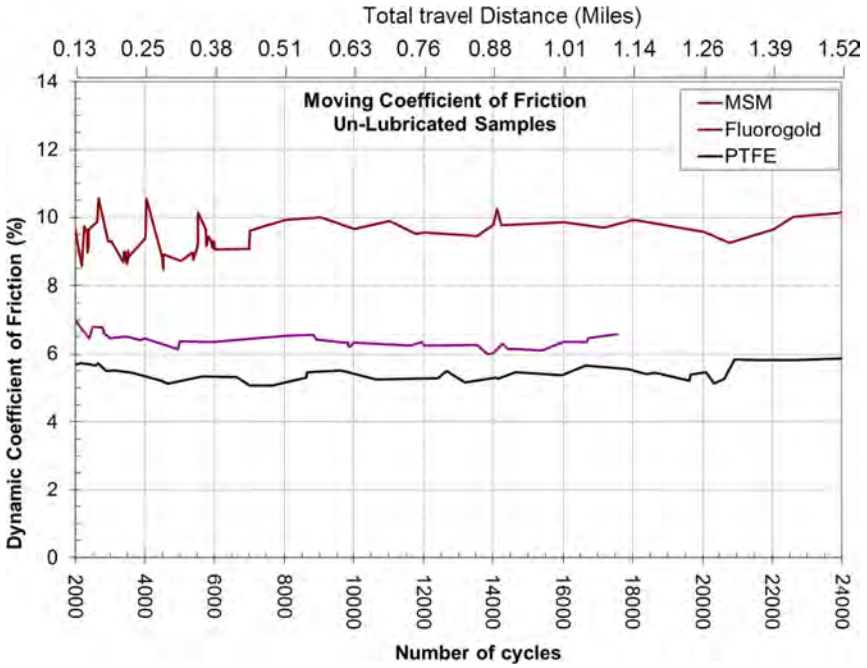

Figure D.25. Variation of dynamic COF for sliding surfaces versus number of cycles (P = 3,000 psi; V = 25 in./min).

set of PTFE specimens, which are not shown in Figures D.23 through D.25, showed lower COF values, of about 3% to 3.5% at this pressure and speed [see Figure D.28].) Fluorogold showed relatively good performance and had static values somewhat comparable with the first PTFE specimen tests, with values typically ranging from about 7% to 9%, and had dynamic values in the 6% to 7% range. These tests showed that Fluorogold had a COF only slightly higher than that of plain PTFE. Unlubricated MSM, however, exhibited much higher COFs, with wide fluctuation in static values ranging from 10% to 17%. Dynamic values were also high but more stable, ranging from about 9% to 10%. Overall, the values found for MSM in this study were nearly twice the values found for plain PTFE at the initial pressures (3,000 psi) and testing speed. (It should be noted that the literature for MSM indicates that COF is lower for higher contact pressures, and it has greater performance than plain PTFE in low temperatures.) MSM tested in this study at a higher contact pressure (5,000 psi) exhibited a lower COF. See the section titled "Effect of Contact Pressure Variation."

Test results for COF in this study were somewhat comparable with values reported in NCHRP Report 432, Appendix C. At 3,000-psi pressure, 25-in./min sliding speed, and room temperature, NCHRP Report 432 showed plain PTFE to have an initial spike of about 11%, which dropped to about 4.5% to 5% with subsequent cycles, but then gradually increased to about 8% with a greater number of cycles. Glass-filled samples had initial spikes up to the 14% range, but subsequent values dropped to the 5% to 7% range; these values were comparable with the ones obtained in this study. The NCHRP Report 432 tests showed that higher sliding speeds (i.e., going from 2.5 to 25 in./min) had somewhat higher COFs, given the same contact pressure and temperature (3,000 psi at room temperature).

Figure D.26 shows the *LRFD Specifications* recommended values for COF. Fluorogold test results were comparable with glass-filled recommended values, but plain PTFE tests in this study showed higher values. However, results from this study were comparable with NCHRP Report 432 results when considering sliding speeds of 25 in./min.

	Pressure (ksi)	Coefficient of Friction			
		0.5	1.0	2.0	>3.0
Type PTFE	Temperature (°F)				
Dimpled Lubricated	68	0.04	0.030	0.025	0.020
	−13	0.06	0.045	0.040	0.030
	−49	0.10	0.075	0.060	0.050
Unfilled or Dimpled Unlubricated	68	0.08	0.070	0.050	0.030
	−13	0.20	0.180	0.130	0.100
	−49	0.20	0.180	0.130	0.100
Filled	68	0.24	0.170	0.090	0.060
	−13	0.44	0.320	0.250	0.200
	−49	0.65	0.550	0.450	0.350
Woven	68	0.08	0.070	0.060	0.045
	−13	0.20	0.180	0.130	0.100
	−49	0.20	0.180	0.130	0.100

Source: AASHTO (2010b).

Figure D.26. AASHTO-recommended design COFs based on 0.2-μm-finish mating surface.

Lubricated Specimen Results

The MSM specimens and the second set of PTFE specimens, which were both dimpled, were initially tested using silicone grease lubrication that was shipped together with the test specimens from the manufacturer. The samples were cycled for 50- and 150-cycle intervals. The baseline test parameters (P = 3,000 psi; V = 25 in./min) were also used for these tests. This was done to determine the lubricated COF of the MSM sliding surfaces, which would correspond to the way this material was tested previously by Maurer and the way this material has typically been used in practice. As shown in Figure D.27, the lubricated COFs for the MSM and PTFE materials were significantly lower than the unlubricated cases (see Figure D.23).

The COF of each material seemed to behave oppositely from one another in the early cycles, with PTFE having a low value at the start that rose sharply before stabilizing to a more consistent value. MSM started with a high value and dropped sharply before stabilizing to a more consistent value. Ultimately, the lubricated PTFE COF was comparable for MSM and PTFE, with PTFE having only slightly lower values than MSM. Results of lubricated PTFE tests from this study were comparable to

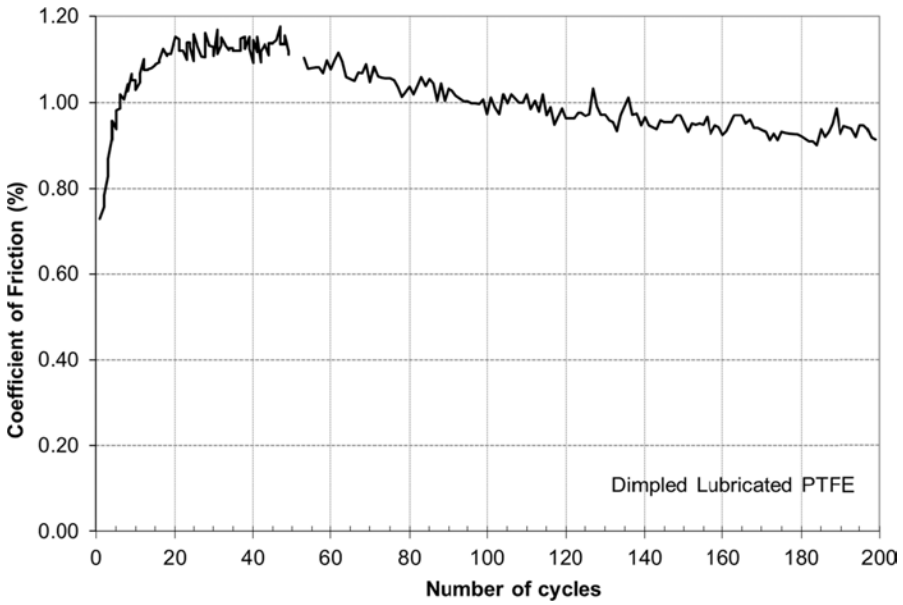

(a)

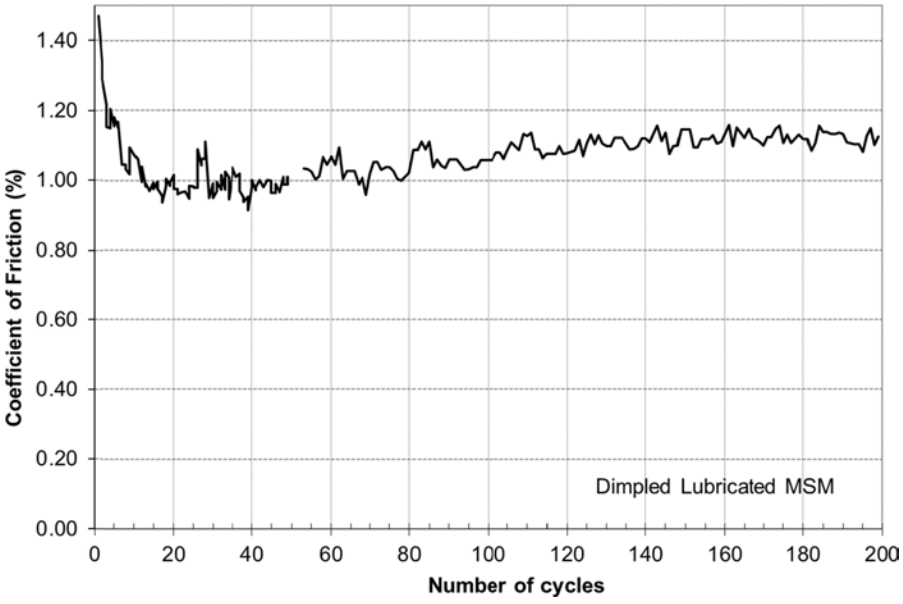

(b)

Figure D.27. Coefficients of friction for dimpled, lubricated (a) PTFE and (b) MSM sliding surfaces (P = 3,000 psi; V = 25 in./min).

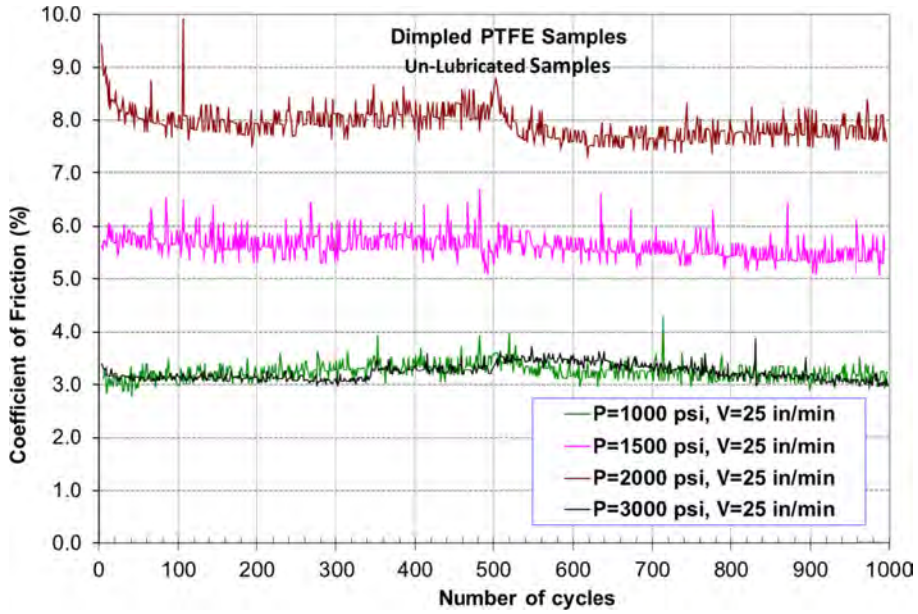

Figure D.28. Comparison of COFs of dimpled PTFE samples for various contact pressures (V = 25 in./min).

results in NCHRP Report 432, which reported COFs of about 1% for lubricated PTFE at this pressure and sliding speed.

Effect of Contact Pressure Variation

In the second set of PTFE samples (dimpled, unlubricated), the contact pressure was changed at various intervals, and COFs were recorded. Figure D.28 shows the comparison of COFs of these samples for various contact pressures (V = 25 in./min). The sequence of applied pressures was 3,000, 1,000, 1,500, and 2,000 psi.

As shown in Figure D.28, there was little difference in COF when the pressure was reduced from the initial 3,000-psi pressure to 1,000-psi pressure. The coefficient increased, however, with progressive increases in pressure from 1,000 to 1,500 psi and ultimately to 2,000 psi. Previous research showed that higher pressures resulted in lower COFs. The results shown in Figure D.28, however, show a somewhat opposite effect. This may have been due to continued use of the same samples with varying pressures at various stages of testing, instead of using new samples for each new pressure test. In this research, the condition of the sliding surfaces was likely very different at the start of each new phase because of continuing wear and degradation of the material surface. Previous research has also shown that at a 25-in./min speed, COF will increase with increasing cycles because of material surface wear. Therefore, it is likely that the behavior shown in Figure D.28 was influenced by continuing surface wear of the sliding material.

Figure D.29 and Figure D.30 show COFs at a contact pressure of 5,000 psi for unlubricated MSM and Fluorogold samples, respectively. At this higher pressure, MSM experienced a significant reduction in dynamic COF from about 9% to 10% to about 7% to 7.5%. This reduction is consistent with manufacturer data that indicates this trend and recommends use of this material at higher pressures. Fluorogold experienced an increase in COF from about 6.5% to 9% at this higher pressure. It should be noted, however, that Fluorogold literature recommends limiting the contact pressure to 2,500 psi, which results in a lower COF.

Thickness Reduction

The average thicknesses of the specimens were measured using a caliper at three locations on the periphery of each specimen before mounting it in the test fixture. The average thickness change for the specimens was also determined at various stages of the cyclic testing using a feeler gauge at four corners between the sliding-surface backing plates and the stainless steel backing plate. The feeler-gauge measurements were carried out at various cycling intervals, which were more frequent at the beginning of the tests and less frequent toward the end.

Figure D.31 shows the percentage thickness reductions of the various samples with respect to the travel distance and number of cycles. The circled numbers depicted on the graph and designated in the text as PV1 through PV4 represent the various combinations of pressure and testing velocity (PV zones) that were evaluated.

In Figure D.31, the bottom lines (black and green) are for PTFE, the middle lines (blue) are for MSM, and the top lines (red) are for Fluorogold. The two lines shown for MSM and

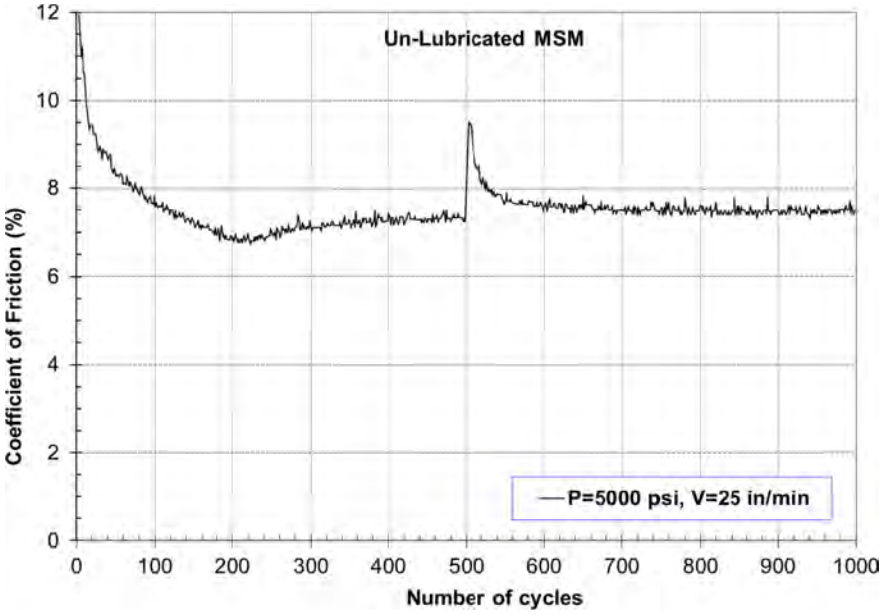

Figure D.29. COF of MSM samples at high pressure of 5,000 psi (V = 25 in./min).

Fluorogold represent the values for the two simultaneously tested specimens. Initially (PV1), all materials were tested at a 25.0-in./min travel speed and 3,000-psi contact pressure.

As expected, the plain PTFE specimens exhibited severe wear at this initial PV combination, and were substantially worn with 80% reduction after about 1.5 mi of accumulated travel. The rate of wear was initially higher, but became more constant after about half the travel length.

The unlubricated MSM specimens performed significantly better than PTFE, but they had about a 10% initial thickness reduction at the start of testing, possibly due to material compression. Thereafter, the specimens exhibited another 10% thickness reduction within the first 3 mi of accumulated travel. The material then became somewhat stabilized with little or no additional thickness reduction throughout the remainder of the PV zone, which was carried out to about 8 mi of accumulated

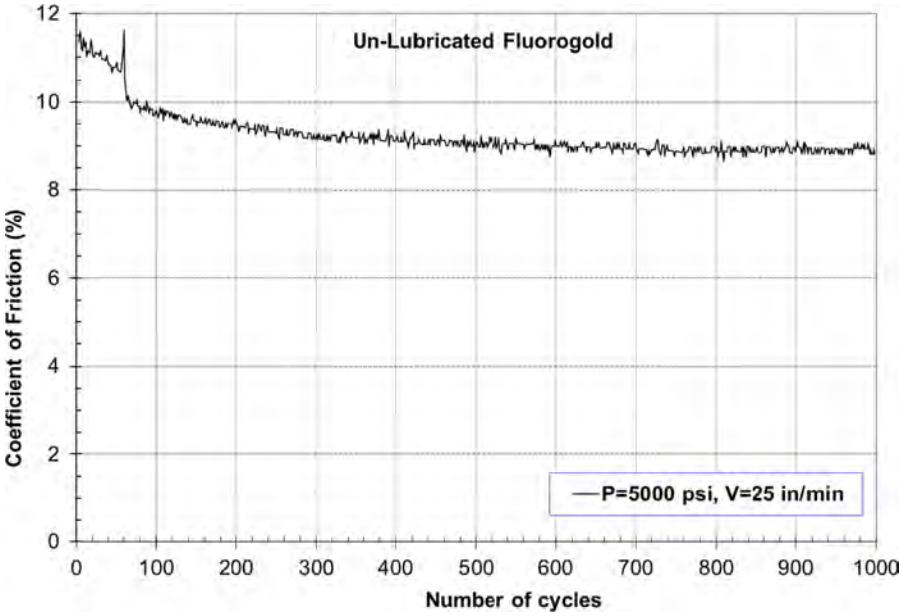

Figure D.30. COF of Fluorogold samples at high pressure of 5,000 psi (V = 25 in./min).

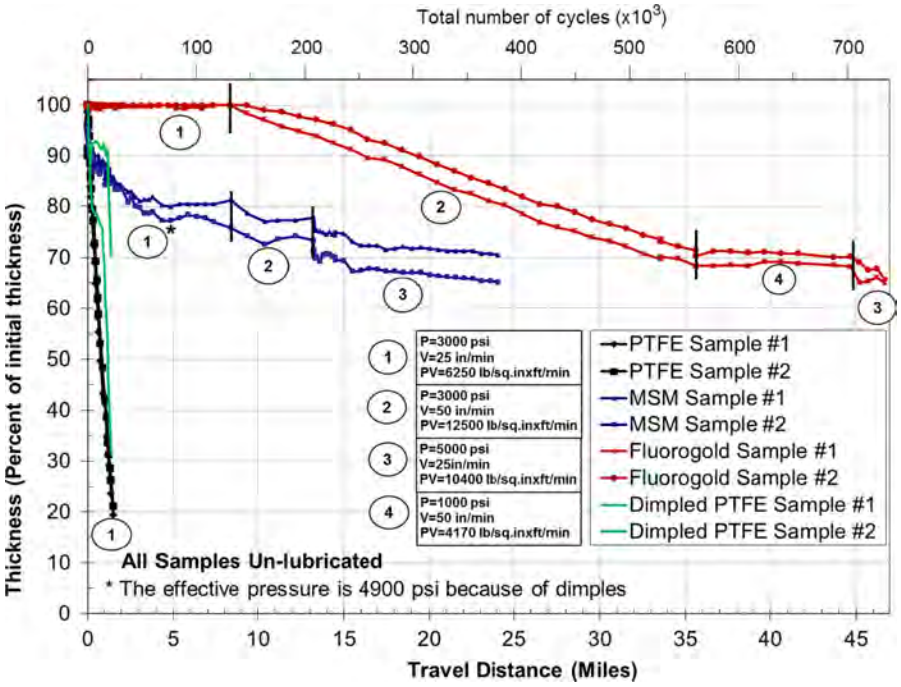

Figure D.31. Thickness reductions for sliding surfaces versus travel distance and numbers of cycles.

travel. In PV2, the travel speed was increased to 50 in./min to accelerate testing. Some additional thickness reduction was observed in this PV zone, but the material again stabilized with no additional loss after about 2 mi of travel. In PV3 the pressure was increased to 5,000 psi and the speed was reduced to the original 25 in./min. The material experienced some immediate compression under the added pressure and then exhibited about 5% of additional uniform wear until the test was stopped after about 11 mi of additional travel. The overall MSM test was carried out to about 24 mi of accumulated travel, and the overall average thickness reduction due to combined compression and wear at the end of testing was about 32%. About one-half the thickness reduction may have been due to material compression.

The Fluorogold specimens performed exceptionally well, with no measured thickness loss within the first zone of testing (about 8 mi of travel). In PV2, the travel velocity was increased to 50 in./min, and the material showed a consistent rate of wear that resulted in about 30% thickness reduction over about 28 mi of travel. In PV4, the pressure was reduced to 1,000 psi with the same 50-in./min velocity, and no additional thickness reduction was observed. Finally, in PV3, with 5,000-psi pressure and 25-in./min velocity, the material again started to show wear, with about 3% loss over about an additional 2 mi of travel before the testing was terminated. The material ultimately had about 34% reduction in thickness at the end of testing, which covered about 47 mi of accumulated travel.

Figure D.32 shows the percentage thickness reductions for the two separate PTFE tests on a larger horizontal-axis scale. Again, the circled numbers represent various PV zones. The first PTFE test was conducted at a constant pressure and velocity, PV1, which was similar to the initial PV for the MSM and Fluorogold tests, and resulted in significant consistent wear. In the second PTFE test, the pressure and velocity were modified to evaluate wear under various conditions, and the two specimens exhibited some inconsistent behavior. In PV2 with only 1,000-psi pressure, both specimens exhibited only minor wear. In PV3 with 1,500 psi, one of the specimens showed no wear, but the other exhibited very heavy wear. In PV4 with 2,000 psi and 50-in./min speed, both specimens again showed consistent heavy wear.

The following conclusions can be derived from the test results shown in Figure D.31 and Figure D.32:

- The wear behavior of plain PTFE and Fluorogold (a reinforced PTFE) is similar in that both materials experience very consistent rates of wear depending on the combination of contact pressure and velocity (PV). Fluorogold exhibited significantly greater wear resistance than plain PTFE, but under certain PV levels, both materials exhibited very consistent, albeit different, wear rates. However, MSM, which is a completely different type of material, behaved differently. It had significantly greater wear resistance than plain PTFE, but it also exhibited a certain amount of compressibility, which in some cases resulted in nonuniform thickness loss or wear. A faster thickness reduction was observed at the beginning of the cycles in each test zone.

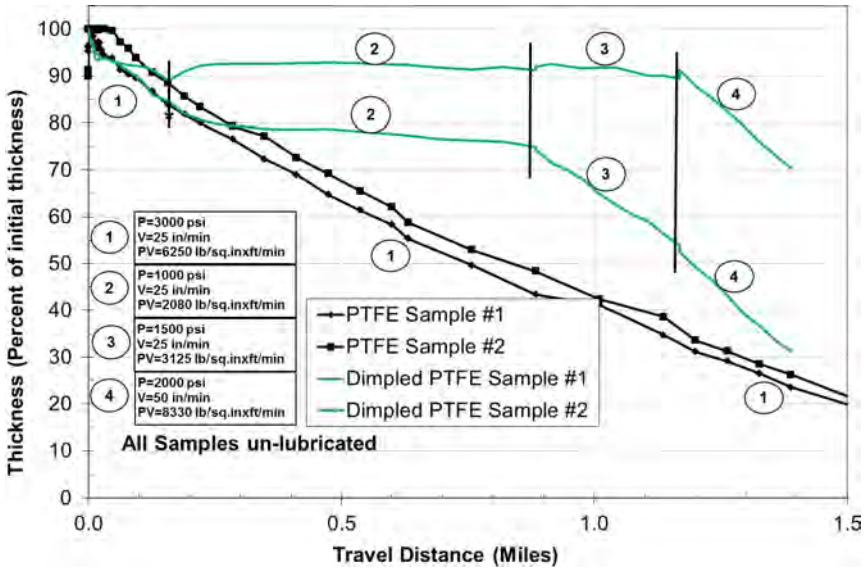

Figure D.32. PTFE thickness reduction versus travel distance.

- For PTFE and Fluorogold, there were combinations of contact pressure and velocity in which the wear rate was virtually zero. This behavior was not observed for the MSM material, possibly because of material compressibility. Even though there may have been no real material wear, thickness reduction was still observed.
- Regardless of material wear behavior, the study showed that high-performance sliding materials (Fluorogold and MSM) demonstrated significantly lower wear rates than plain PTFE, which is the most used material in the United States.
- The thickness–travel distance curves for PTFE-based materials (plain PTFE and Fluorogold) were almost linear for all samples at all levels of contact pressure and velocity, whereas the MSM curves were not linear.
- Fluorogold did not experience creep. The tests showed that Fluorogold has a slight increase in COF, but it does not have creep and has very good wear characteristics.

To establish more reliable wear rates for the samples used, additional testing with various contact pressures and velocity combinations are required. For each combination, a new sliding sample should be used. In addition, the numbers of data points (total cumulative travel distance) should be adequate to represent the real behavior of the material being tested. In the current study, the experiment on Fluorogold was terminated after only a few cycles in PV Zone 3 (see Figure D.31); as a result, material wear characteristics may not be totally representative for that PV combination.

Figure D.33 shows the stainless steel mating surface and the sliding surface specimens before and after cyclic testing. The PTFE showed considerable wear and loss of thickness in the form of flaking and shedding of the material. The MSM specimens showed signs of rough surface abrasion, but the dimples were still somewhat evident. The Fluorogold specimens showed some surface abrasion, but they did not exhibit the type of material deterioration and shredding that was found with plain PTFE.

Wear Rate

Measured Wear Rates

Previous research has shown a wide range in wear rates for PTFE sliding surfaces depending on material type, lubrication, sliding speed, contact pressure, and temperature (Stanton et al. 1999). In this study, at the initial high pressure and fast sliding speed, plain PTFE was shown to have a very high wear rate that was consistent with previous studies. High-performance sliding materials such as MSM and Fluorogold showed significantly lower rates of wear. Wear rates for the various materials tested in this study were developed from the measured thickness reductions that occurred over the accumulated lengths of travel by determining the slopes of the thickness reduction curves, as shown in Figure D.31. A moving-window averaging technique was used to determine the wear rate based on the thickness changes for various stages of the experiment.

Plain PTFE and Fluorogold (filled PTFE) exhibited rather constant rates of wear that varied for different combinations of pressure and velocity. The wear rate for Fluorogold was very close to zero in the initial PV zone, but exhibited a constant wear rate in PV zones with higher sliding speeds or higher pressures.

The wear rate for MSM samples exhibited a different trend than that of PTFE. MSM samples did not exhibit constant wear rates within PV zones, but appeared to lose thickness more rapidly at the beginning of each zone. The rates tended to slow or stabilize as the tests proceeded. Based on discussions

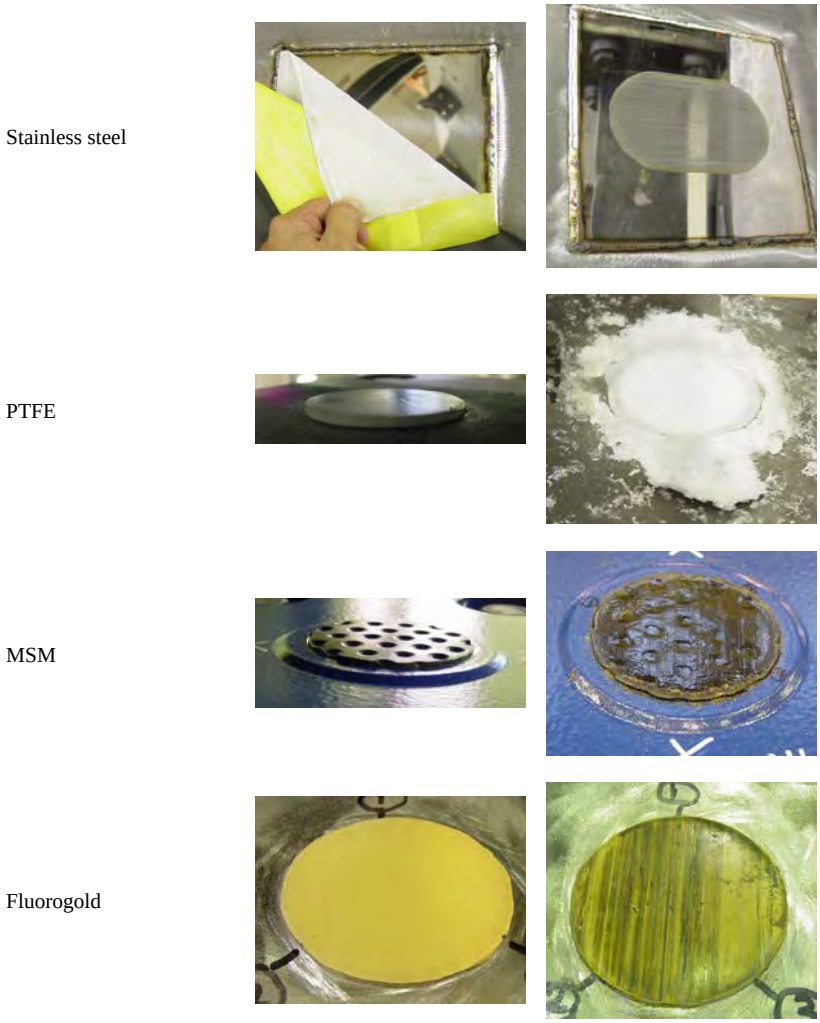

Figure D.33. Stainless steel mating surface and sliding surface specimens (left) before and (right) after testing.

with MSM manufacturer representatives, it was concluded that MSM experiences some thickness reduction from compression and creep while not necessarily losing thickness due to wear. Because of this, it is difficult to determine consistent wear rates for MSM, and PV may not be a suitable wear characteristic, as it is for PTFE-based materials.

Table D.7 summarizes the wear rate values that were determined in this study for all samples under various contact pressures and travel speeds.

Table D.8 shows wear results from NCHRP Report 432 (Stanton et al. 1999) for various PTFE-based sliding materials based on constant pressure, but with variable sliding speed, temperature, and lubrication. Each of these factors was shown to have considerable effect on wear rate. These earlier results confirmed the significant increase in wear due to high sliding speeds and low temperatures, and also confirmed that braided and glass-filled PTFE materials showed greater wear resistance.

Wear Rate for Predicting Service Life

Campbell and Kong (1987) studied the relationship between contact pressure (P) and sliding speed or velocity (V) on the wear of PTFE sliding surfaces. Figure D.34 shows curves developed from tests for sliding speed, pressure, and PV. From this, they developed a general mathematical model for predicting the wear of plain PTFE sliding surfaces as a function of the PV factor, as shown in Equation D.13:

$$h = KPVt \tag{D.13}$$

where

h = reduction in thickness (in.);
K = wear factor (in.^{3}-min/lb-ft-h);
P = contact pressure (psi);
V = sliding velocity (ft/min); and
t = total time under load (h).

Their research also indicated that two distinct values exist for the wear factors: one that is associated with mild wear regimes

Table D.7. Calculated Average Wear Rates Based on Slope of Thickness Reduction Graphs

	Sample Effective Area ($in.^2$)	P ($lb/in.^2$)	P Effective ($lb/in.^2$)	V (in./min)	PV ($lb/in.^2$ ft/min)	PV Effective ($lb/in.^2$ ft/min)	Wear Rate Sample 1 (mil/mi)	Wear Rate Sample 2 (mil/mi)	Average Wear Rate (mil/mi)
Unlubricated PTFE	7.07	3,000	3,000	25	6,250	6,250	81.21	80.32	80.78
Dimpled unlubricated PTFE	4.19	1,000	1,600	25	2,083	3,333	9.89	2.98	6.43
		1,500	2,500		3,125	5,208	110.35	18.48	64.42
		2,000	3,300		4,167	6,875	152.32	151.05	151.68
		3,000	5,000		6,250	10,417	121.18	49.18	85.18
MSM	4.19	3,000	5,000	25	6,250	10,417	0.88	1.17	1.01
		5,000	8,400		10,417	17,500	0.75	0.68	0.71
		3,000	5,000	50	12,500	20,833	0.6	0.32	0.48
Fluorogold	7.07	3,000	3,000	25	6,250	6,250	0.06	0.03	0.04
		5,000	5,000		10,417	10,417	0.89	1.68	1.29
		3,000	3,000	50	12,500	12,500	0.95	0.92	0.94
		1,000	1,000	50	4,167	4,167	0.01	0.12	0.07

Table D.8. PTFE Wear Rates with Constant 3,000-psi Pressure

Material	Lubrication	V (in./min)	T (°F)	PV ($lb/in.^2$ ft/min)	Wear Rate (mil/mi)
Unfilled PTFE	Dimpled lubricated	2.5	68	625	0.3
		25	68	6,250	0.5
	Flat unlubricated	2.5	68	625	0.7
		25	68	6,250	189
		2.5	–13	625	10
		25	–13	6,250	259
Woven PTFE	Flat unlubricated	2.5	68	625	0.3
		25	68	6,250	17
		2.5	–13	625	27
		25	–13	6,250	24
15% Glass filled	Flat unlubricated	2.5	68	625	–1
		25	68	6,250	–0.5
		2.5	–13	625	no result
		25	–13	6,250	6
25% Glass filled	Flat unlubricated	2.5	68	625	–0.3
		25	68	6,250	2
		2.5	–13	625	4
		25	–13	6,250	46

Source: Stanton et al. (1999).

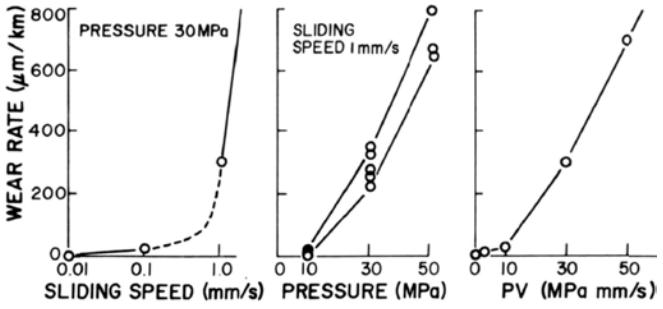

Source: Campbell and Kong (1987).

Figure D.34. Variation of wear rate with (a) sliding speed, (b) pressure, and (c) PV.

(low K), and one associated with severe wear regimes (high K). There was an abrupt transition between the two regimes at a so-called PV limit.

The results of the SHRP 2 study combined with the results in NCHRP Report 432 also indicated the potential of service life prediction based on the PV factor and further confirmed the potential of the PV limit transition between zones of low wear and severe wear.

Figure D.35 shows the wear rate versus PV data for plain PTFE tests performed in this study combined with NCHRP Report 432 tests. From this plot, there appears to be a PV limit beyond which the wear rate increases significantly. There further appears to be the potential for a service life design curve for wear rate, which would be a function of PV as shown on the figure. It is recognized that the results shown are from very limited test data and that further testing would be required to establish more reliable curves and a true PV limit.

As with plain PTFE, the Fluorogold (glass-reinforced PTFE) test results also indicated the potential of the PV factor as a means of predicting service life. Figure D.36 shows test results for wear rate versus PV factor over the range of PV zones tested. Test results from NCHRP Report 432 for glass-filled samples are also plotted. Similar behavior to plain PTFE is shown in that there appear to be a PV limit differentiating zones of higher wear and very low wear, albeit the wear rates are significantly lower than plain PTFE. As with plain PTFE, further testing is needed to establish a more reliable curve and the real PV limit.

Proposed Wear Rate Methodology

In addition to the PV factor, two other factors can contribute to predicting overall wear rate for a PTFE-based sliding material: temperature and lubrication.

Considering all these factors, Equation D.14 can be considered as a general equation for estimating the wear rate for a sliding surface as a function of material type and other contributing parameters:

$$\text{wear rate} = \text{base wear rate} \times CT \times CL \qquad \text{(D.14)}$$

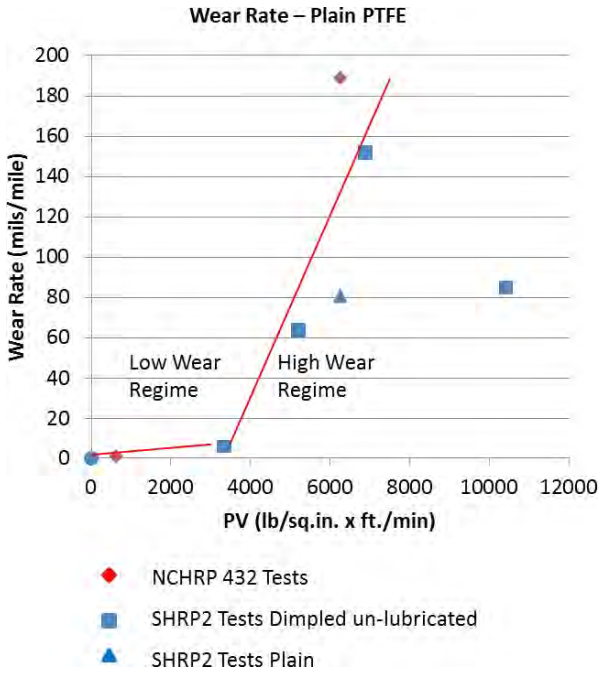

Figure D.35. Variation of wear rate with PV for plain PTFE.

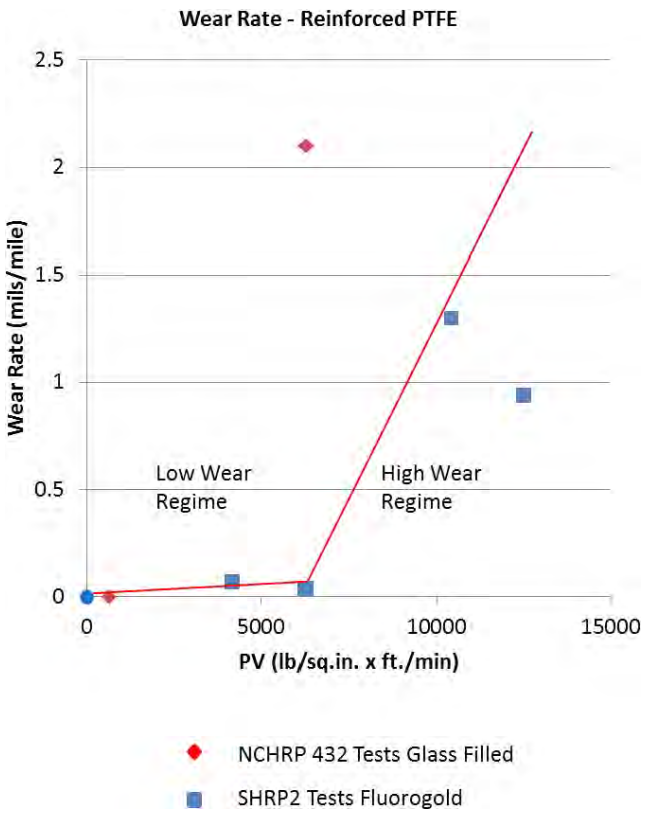

Figure D.36. Variation of wear rate with PV for Fluorogold sliding material.

where

wear rate = total thickness reduction (mil) per mile of travel distance;
base wear rate = defined as a function of material type, contact pressure, and velocity from PV curves based on experimental tests for plain PTFE, glass-filled PTFE, or braided PTFE;
CT = modification factor for the effects of low temperature (function of material type);
CL = modification factors for the effects of lubrication (function of material type);
P = contact pressure acting vertical to the sliding surface; and
V = travel speed of the sliding bearing.

The base wear rate defined in this procedure is the wear rate determined from tests conducted at various combinations of speed and contact pressure at room temperature, without lubrication. The effects of low temperature and lubrication can be included by the factors *CT* and *CL,* respectively, which are added to the equation for the sake of being complete. In low-temperature regions, *CT* would be greater than one, which results in greater wear. With lubrication, *CL* would be considerably less than one, which results in less wear. These factors are also a function of material type and must be determined from tests. At this time, there are insufficient data to develop these factors accurately for final service life design, but estimates can be drawn from Table D.8.

The travel speed of the sliding bearing can be determined from the methods described in the subsection "Speed of Bearing Movement for Truck Load."

Once the wear rate is known, the total amount of wear can be determined over the design life of the bearing from the expected cumulative amount of bearing travel as described in "Phase 1: Determination of Bridge Movements."

Sliding Surface Design Procedure for Service Life

The following steps summarize the proposed procedure for design of sliding surfaces for service life. The procedure involves first determining demand requirements, which are based on bridge loads, traffic, and temperature data. Supply requirements are then determined based on selected material properties for the proposed sliding surface.

The first major part of the proposed procedure for design of sliding surfaces, determining demand requirements, involves three steps:

Step D1. Calculate pressure (P; an unfactored average contact stress measured in pounds per square inch) on trial sliding surface due to all loads and due to permanent loads, based on the *LRFD Specifications* design criteria. Maximum allowable contact stress will vary based on the type of sliding surface material.

Step D2. Calculate sliding movement velocity (V; measured in inches per minute) of the sliding surface for vertical truck load, vibration, and thermal movement.

Step D3. Calculate total accumulated movement per year (M) computed for truck passage and vibration based on ADTT and computed for thermal movement based on daily and yearly thermal variations.

The second major part of the proposed procedure, determining supply requirements, involves three main steps:

Step S1. Calculate PV factors and determine base wear rates from PV curves for the sliding material under consideration (Figure D.35 for plain PTFE). Determine wear rate as a function of base wear rate by using Equation D.14, with factors for temperature zone effect (*CT*) and use of lubrication (*CL*). At this time, there are insufficient data to develop these factors accurately for final service life design. Until further tests are conducted, these factors are assumed to be equal to one.

Step S2. Determine wear in mils due to 1 year of accumulated sliding movement based on truck passage and vibration and for thermal movement, as follows:

wear (mils/year) = [wear rate (mils/mi) × accumulated sliding movement (mi)].

Step S3. Considering the standard thicknesses available for the sliding material under consideration, determine the service life of the sliding surface material for a trial thickness and compare it with the design service life of the bridge system. If the service life of the sliding surface is less than the design service life of the bridge system, there are three options:

a. Consider the required replacement schedule;
b. Consider increased thickness of the sliding surface material, or increased area of the sliding surface, which reduces contact pressure and reduces wear rate; or
c. Consider higher-performing sliding material with greater wear resistance.

Depending on the options chosen, various demand and supply steps will be repeated with new parameter values to arrive at a final solution.

Summary and Conclusions

Many bearing types currently use PTFE as a sliding material to accommodate horizontal bridge movements. Previous research investigating the behavior of sliding materials for bearings has shown that plain PTFE can experience considerable wear, particularly when subjected to high rates of horizontal movement. This type of movement, which is due mostly to girder end rotations associated with cyclic truck loads, is low-amplitude, high-cycle movement with fast movement speed.

Movement due to thermal load, however, is high-amplitude, low-cycle movement with slow movement speed, and is less likely to cause wear. Fast sliding speed combined with high contact pressure and low temperatures all contribute to PTFE wear. Currently there are minimal data to confirm actual bearing movements due to truck load or test data to determine a life prediction model for sliding surfaces that use PTFE.

This research program, as part of SHRP 2 Project R19A, studied the feasibility of achieving increased service life of sliding bearings that are subject to high sliding speeds through the use of alternative high-performing materials that have greater wear resistance than conventional plain PTFE. Two potential high-performance sliding materials were studied: (1) MSM, an ultrahigh-molecular-weight polyethylene developed in Germany; and (2) Fluorogold, a special glass fiber–reinforced PTFE. Plain PTFE was also studied to use as a benchmark for high-performance material comparison.

The research program conducted both analytical studies and testing. The analytical studies first investigated potential bearing movements and movement speeds due to truck load and thermal load. A proof of concept testing program studied relative performance characteristics between plain PTFE, MSM, and Fluorogold, specifically with regard to COF and wear under similar conditions. The test program evaluated material wear associated with combined high movement speed and high contact pressure because it would serve as an upper bound on the main parameters affecting wear.

Analytical Study

The analytical studies determined potential bearing movement speeds under truck loading and thermal loading and evaluated potential accumulated sliding movement over a bearing design life. For simplicity, the analytical studies considered a 200-ft simple-span, multisteel girder prototype bridge with one end fixed and one end expanded. Girder deflections and end bearing movements were computed using both a 3-D FE model and an approximate single line-girder analysis with a maximum girder deflection of L/800. The study included a dynamic analysis that investigated the potential bearing movement due to free vibration and damping of the span after passage of a truck, which greatly increases the total accumulated movement.

The following conclusions were determined from the analytical studies:

1. The FE analysis calculated the horizontal one-direction sliding for a single truck load at the expansion bearing to be about 0.15 in. Considering LL + I, this amount was 0.20 in., which resulted in a cycle of 0.40 in. per truck passage considering rebound to the original position after truck passage.
2. The approximate method, which considered a single line girder and assumed a maximum girder deflection of L/800 under truck LL + I, determined the maximum one-direction horizontal movement to be approximately 0.50 in., with a total cycle of about 1.0 in. per truck passage. This value was considered an upper bound.
3. The considerably lower value obtained from the FE analysis was attributed to the presence of the other girders in the bridge system, which increased the bending stiffness of the external girder.
4. The dynamic analysis showed that the total movement, which includes the amount of movement due to truck passage and following free vibration, would be approximately 7.4 times the maximum one direction of movement due to truck passage for a 10% damping ratio.
5. Considering the FE analysis, with a maximum LL + I one-direction movement of 0.15 in., the accumulated total expansion end movement due to truck load with vibration (10% damping ratio) over a 100-year service life with an ADTT of 1,000 would be approximately 800 mi.
6. Without considering additional movement due to free vibration, FE analysis showed that the accumulated total expansion end movement due to truck load for only a single cycle of movement per each truck passage would be approximately 200 mi over the same service life and truck volume as Number 5 above.
7. For the prototype bridge, the total accumulated movement due to daily and annual thermal variation was only about 0.8 mi over a 100-year service life.
8. Computed bearing sliding speeds for the initial full cycle of movement were based on the time for a truck to pass the bridge, which varies depending on truck speed. For the prototype bridge with movements computed from FE analysis, the expansion bearing slip rates were computed to be about 7 in./min for a 40 mph truck speed and about 10 in./min for a 60 mph truck speed. Using movements computed from the approximate analysis, the corresponding slip rates were about 18 and 28 in./min for 40 and 60 mph truck speeds, respectively. (These slip rates were considered to be high-end limits.) Little field data are available to confirm slip rates for actual sliding bearings in service.
9. The sliding speed due to free vibration is independent of the initial truck speed and depends rather on the dynamic characteristics of the bridge (stiffness, mass, and damping). For the prototype bridge, the computed bearing sliding speed during the period of free vibration was 12.1 in./min.

Test Program

A proof of concept test program was conducted at the University of Nebraska–Lincoln structures laboratory. Sliding

material specimen sizes (3-in. diameter), initial testing speed (25 in./min), and initial contact pressure (3,000 psi) were established to be consistent with tests reported in NCHRP Report 432.

The test setup used for the sliding surface wear tests used an MTS cyclic actuator that was vertically installed in a large steel frame. A specially designed sliding material test fixture was installed below and connected to the actuator.

The test fixture included a center moving plate (attached to the MTS actuator) with stainless steel surfaces attached to each side. This moving plate was sandwiched between two stationary material test specimens mounted on steel backing plates. Two horizontal hydraulic jacks applied horizontal pressure perpendicular to the surface of the sliding specimens to create the required contact pressure.

In all tests, the cyclic displacement was applied on a sine wave with a stroke length of 1 in. In other words, the center plate with stainless steel surfaces was moved upward from its initial central position 1 in. It was then moved back down for 2 in. (past the initial central position by 1 in.), and then back up 1 in. to the original position. The total movement per complete cycle was 4 in.

Plain PTFE specimens were tested first to establish a baseline with which to compare the MSM and Fluorogold results. This was followed by MSM (dimpled), Fluorogold (plain), and dimpled PTFE. MSM specimens and the dimpled set of PTFE specimens were first tested for a prescribed number of cycles in a lubricated condition. Testing was then stopped, the specimens were cleaned, and testing was resumed in the unlubricated condition. All tests were conducted at room temperature.

The cycle frequency was initially set to 0.1 Hz (25 in./min) for all tests and was maintained for initial PTFE testing until the entire thickness was worn down. However, because of time limitations, this frequency was increased to 0.2 Hz (50 in./min) after about 116,000 cycles for the MSM and Fluorogold specimens.

Based on the results of this limited experimental investigation, the following conclusions were drawn:

1. Tests confirmed that both MSM and Fluorogold can provide considerably greater wear resistance than conventional plain PTFE and can be used to increase service life when sliding surfaces are subject to high movement speed and high contact pressure.
2. Plain PTFE was shown to wear at a very high consistent rate under the initial combination of high sliding speed and contact pressure, resulting in 80% thickness loss within less than 2 mi of accumulated sliding length.
3. Fluorogold exhibited the best wear resistance of all materials tested, with no material thickness loss over about 8 mi of accumulated sliding length within the initial high values of pressure and velocity. It started to show some wear at a much higher travel speed (50 in./min).
4. Plain PTFE and Fluorogold (a PTFE-based material) both exhibited rather constant rates of wear that varied for different combinations of pressure and velocity. The wear rate for Fluorogold was very close to zero in the initial PV zone, which exhibited a constant wear rate (albeit very low) in higher PV zones. Plain PTFE exhibited consistent wear behavior and showed very low wear in a relatively low PV zone (about one third of the initial PV). This finding indicated that a correlation occurred between wear rate and PV factor for PTFE-based materials.
5. MSM exhibited some initial thickness reduction of about 10% (described in the next item), but showed only about 10% additional loss over 13 mi (20.9 km) of accumulated travel.
6. MSM exhibited different behavior with respect to thickness reduction than plain PTFE or Fluorogold. MSM samples did not exhibit constant wear rates within PV zones, but appeared to exhibit initial rapid thickness reduction at the beginning of each zone. The wear rates tended to slow or stabilize as the tests proceeded. The initial thickness reduction was attributed to compressive deformation and creep, and was not necessarily due to wear. This behavior made determining consistent wear rates for MSM difficult. Because of inconsistent wear rates, it was concluded that the PV factor may not be a suitable wear characteristic for MSM, as it is with PTFE-based materials.
7. The results of the SHRP 2 study combined with NCHRP Report 432 results indicated the potential of service life prediction based on the PV factor and further confirmed the potential of the PV limit transition between zones of low wear and severe wear. It was concluded that the PV factor could be used in a service life design method for PTFE-based sliding materials based on wear over an accumulated length of travel.
8. Fluorogold exhibited a COF of about 2% higher than plain PTFE at the initial contact pressure of 3,000 psi. Unlubricated MSM, however, had a COF that was considerably higher. The COF of MSM was found to reduce considerably with increased contact pressure. At 5,000-psi contact pressure, the MSM COF was comparable with the Fluorogold COF at 3,000 psi. Lubricated MSM had a relatively low COF that was comparable with lubricated PTFE.
9. Based on the limited proof of concept testing, Fluorogold (a glass-reinforced PTFE sliding material) exhibited the best overall high performance with a combination of high wear resistance and relatively low unlubricated COF.

Recommendations for Future Work

Only proof of concept testing was performed in this study. To establish more reliable wear rates for the materials sampled, additional testing with various contact pressures and velocity combinations is required. From this, a more statistically reliable model of PV versus wear rate for various types of PTFE-based sliding materials could be developed for actual service life design. Test data developed in this study combined with those reported in NCHRP Report 432 are adequate for confirming a trend, but they provide a limited basis for developing reliable design curves.

The effects of temperature were not considered in this study, but they were evaluated in the NCHRP Report 432 study. Further testing is required to properly evaluate temperature as part of the wear rate model for service life design along with pressure and velocity.

Field testing is needed to determine actual bridge movements and movement speeds at sliding expansion bearings for different types of girders (steel and concrete) under truck load and thermal load. There are little current data to substantiate these movements and movement speeds, and the results of analytical studies need to be validated against actual conditions.

APPENDIX E

Improving the Corrosion Resistance of Conventional Reinforcement

Background

Delaying the onset of corrosion is one of the most important factors determining the service life of a reinforced concrete structure. Corrosion-resistant structures can be achieved by preventing salt from penetrating to the level of the reinforcing steel, by using corrosion-resistant reinforcement, or by using both of these techniques simultaneously. Research has shown that the corrosion resistance of various types of reinforcing bars is dependent on the type of bar and the handling and treatment of the bars before and after concrete placement. Studies have shown that electrochemical treatment may increase corrosion resistance by up to 10 times (Glass and Reddy 2002).

Problem Statement

Over the past decades, the principal techniques for corrosion prevention in bridge decks have included increased concrete cover to slow the intrusion of chlorides from salts or ocean spray to the level of reinforcement and the application of epoxy coating over the steel reinforcement to protect the steel from chlorides and corrosion. However, increased concrete cover depth increases both dead load and construction costs, and it does not eliminate the occurrence of cracks, which facilitate the intrusion of chlorides. Epoxy coating limits the exposure of the steel to chlorides, oxygen, and moisture and adds nominally to bridge construction costs. However, holes and breaks in the epoxy coating, in combination with high chloride concentrations, can result in corrosion of the steel reinforcement. Moreover, epoxy coating in aging bridge decks may become brittle and eventually delaminate from the steel reinforcement.

Dense (low-permeability) concretes, corrosion inhibitors, and both nonmetallic and steel-alloy corrosion-resistant reinforcement are among the most common techniques being considered as alternative measures for mitigating corrosion in reinforced concrete structures.

This research topic evaluated means of achieving corrosion resistance in concrete reinforced with conventional reinforcing steel by pretreating the concrete electrochemically. For comparison, stainless steel (316LN) and titanium bars were used that are known to have high corrosion resistance. This research was built on work completed to date, including work sponsored by the Federal Highway Administration (FHWA) (Hartt et al. 2006, 2009).

Description of the Concept

Reinforced concrete structures that can tolerate a higher level of chlorides before corrosion initiates will provide longer service lives. If the critical chloride threshold of conventional steel can be increased to a level close to or equal to stainless steel (316LN), service lives greater than 100 years may be achievable with conventional cover depth and low-permeability concretes.

Corrosion-Resistant Reinforcement

Titanium would extend time-to-corrosion cracking by about 130 times compared with black bars (Gong et al. 2006). However, its initial cost in today's market is five times that of stainless steel.

Stainless steel contains a minimum of 12% chromium, which creates an invisible film that helps resist oxidation. The chloride threshold is at least 10 times greater than carbon steel (Gong et al. 2006). A 65-plus-year-old bridge in the Gulf of Mexico with 304 stainless steel reinforcement is showing that it is possible to achieve 100 years of service life (Arminox 1999).

Electrochemical Treatment

Electrochemical treatments involve the application of a direct current for a period of time sufficient to change the environment around the reinforcing steel. The two most common electrochemical treatments used on reinforced concrete

structures are electrochemical chloride extraction (ECE) and realkalization. Electrochemical treatments can be used to migrate ions such as chlorides out of concrete, as in the case of ECE. Realkalization and other electrochemical treatments can also be used to increase the pH of concrete. The purpose of these electrochemical treatments is to create a passive, noncorroding environment around the reinforcing steel.

Objectives of the Research

The main objective of this research was to determine the corrosion resistance of electrochemically treated concrete with black bar and compare it with the resistance of untreated concrete with black bar and corrosion-resistant material. Corrosion-resistant materials used for comparison included commercially available stainless steel rebar (316LN) and titanium bar. The corrosion resistance of treated and untreated concrete samples was compared with the performance of conventional black reinforcing steel and corrosion-resistant reinforcement.

Research Approach

Introduction

To increase the chloride threshold level (thus, the corrosion resistance) in reinforced concrete structures with conventional reinforcing steel, electrochemical treatment was applied in both low and high levels.

Organization and Conduct of the Research

Reinforced concrete specimens with different levels of pretreatment were prepared and tested to determine their critical chloride (corrosion initiation) threshold. The electrochemical treatment was applied at low and high levels of pretreatment to increase the threshold level of black bars (mild steel).

The following list of tasks describes how the research team accomplished the project objectives:

Task 1. Summarize the literature on studies of different steel reinforcement.
Task 2. Obtain material and equipment to be used during the testing stage.
Task 3. Fabricate specimens with the selected reinforcement (mild steel [black bar], stainless steel, or titanium).
Task 4. Conduct the electrochemical treatment on a selected number of test specimens with mild reinforcement.
Task 5. Apply cycles of wetting and drying periods. The wet stage had chloride solution ponded over the specimens.
Task 6. Monitor the samples by measuring the macrocell current and half-cell potential. Analyze the results and provide new recommendations.
Task 7. Prepare the final report and recommendations.

Analysis of Available Data

A literature survey on different corrosion-resistant reinforcements and electrochemical treatments was conducted. A summary of the literature on titanium reinforcing bars, stainless steel reinforcement, and electrochemical treatments is included here.

Titanium Reinforcing Bars

Titanium is a corrosion-resistant material that could potentially be used in transportation structures as a primary reinforcement to extend service life with minimal maintenance; however, the cost of titanium is currently as much as five times that of stainless steel. Froes et al. (2007) report that 1 lb of carbon steel ingot and 1 lb of titanium cost $0.15 and $9.07, respectively.

- Titanium is lighter than stainless steel, has similar strengths, and has lower coefficients of thermal expansion and elastic modulus. Its properties are as follows (Donachie 2000; *Metals Handbook* 1998).
- The relative density is 4.51.
- The coefficient of linear expansion is 5.0 in. $\times 10^{-6}$ in. per in./°F.
- The tensile strength of elemental titanium is 35 ksi, but it can be as high as 180 ksi with titanium alloys.
- The modulus of elasticity is 17×10^6 psi.

Titanium (ASTM B348 2011a) metal's corrosion resistance is due to a stable, protective, strongly adherent oxide film (TIMET 1999). This film forms instantly when a fresh surface is exposed to air or moisture. The oxide layer increases in thickness with time, reaching 250 Å in 4 years. The film growth is accelerated under strongly oxidizing conditions, such as heating in air, anodic polarization in an electrolyte, or exposure to oxidizing agents. The composition of this film varies from TiO_2 at the surface to Ti_2O_3 to TiO at the metal interface. The oxide film on titanium is very stable and is attacked by only a few substances, most notably hydrofluoric acid. Titanium is capable of healing this film almost instantly in any environment in which a trace of moisture or oxygen is present. Anhydrous conditions in the absence of a source of oxygen should be avoided because the protective film may not be regenerated if damaged. Titanium has excellent resistance to corrosion by neutral chloride solutions, even at relatively high temperatures. Titanium and its alloys may be affected in aqueous chloride environments by crevice corrosion.

Stainless Steel Reinforcement

The term stainless steel refers to a group of corrosion-resistant steels that contain a minimum of 12% chromium (Scully and Hurley 2007). The chromium creates an invisible surface film

that helps stainless steel resist oxidation. Other metals can be added to increase corrosion resistance.

Various grades of stainless steels have been developed for use as reinforcement in concrete to resist chloride environments. Stainless steel reinforcements are available as solid bars or stainless steel–clad bars. Stainless steel offers many advantages:

- Chloride threshold values for stainless steel have been reported to be at least 10 times greater than for carbon steel (Clemeña 2003; Gong et al. 2006).
- Stainless steel has inherent corrosion resistance and does not require the aid of other corrosion protection methods, such as cathodic protection or corrosion inhibitors.
- Stainless steel has good strength and ductility, and many of the commonly used grades also exhibit good weldability.
- Solid stainless steel bars can withstand shipping, handling, and bending without the danger of damage to the coating.
- Exposed ends are not a problem in solid stainless steel bars and do not have to be repaired as they do in stainless steel–clad bars (Smith and Tullmin 1999).

Solid stainless steel is used in Europe rather than stainless steel–clad carbon steel because the process of fusing the two types of metal together is not considered cost-effective. Another advantage of solid stainless steel bars is that they can be shipped, handled, and bent without fear of damage to the coating. In addition, the ends do not have to be coated after cutting (NCHRP 2004).

Stainless steel is often used in areas where sufficient cover cannot be obtained or at construction joints and critical gaps between columns and decks. Because of the cost of stainless steel, estimated to be four to six times more than black bar, many engineers do not expect it to become a standard for all reinforcement (Nürnberger 1996). Gong et al. (2002) compared the costs of different types of reinforcement in a thick deck. They reported an initial cost of deck area for stainless steel was approximately 1.4 times more expensive than conventional reinforcement. However, based on total costs over 75 years, the stainless steel reinforcement was more economical.

The types of stainless steel reinforcement that have been most commonly used are types 304, 316, and 316LN. All three types are austenitic stainless steel (Smith and Tullmin 1999). The FHWA report *Corrosion Evaluation of Epoxy-Coated, Metallic-Clad, and Solid Metallic Reinforcing Bars in Concrete* (McDonald et al. 1998) looked at two types of solid stainless steel in concrete exposure specimens, Types 304 and 316 (ASTM A955 2011b).

The results show that the lowest corrosion rates for Type 304 bars were obtained when the stainless steel was used in both mats. Cracks in the concrete did not appear to affect the performance of the bars. Half the bars from specimens that contained black steel in the bottom mat exhibited moderate to high corrosion currents and had red rust on them. When the stainless steel bars were used in both mats, the specimens did not exhibit any signs of chloride-induced corrosion, even when the slabs were precracked (McDonald et al. 1998).

McDonald et al. (1998) reported that all specimens containing Type 316 solid stainless steel showed good corrosion performance. There was no distinguishable difference between precracked and uncracked slabs or between slabs with a black steel cathode or a stainless steel cathode. Measured corrosion for all conditions was about 800 times lower than that of the black steel specimens. During visual inspection of the slabs, only one of the bars exhibited corrosion, and it was considered to be minor.

Both types of stainless steel, Types 304 and 316, were able to tolerate chloride levels much higher than the threshold level of black steel before the initiation of corrosion, especially when both mats were stainless steel. The threshold for Type 304 stainless steel with a stainless steel cathode was 7 to 18 kg/m^3 (which is 12 to 30 lb/yd^3). For Type 316 stainless steel in both mats, the chloride concentration threshold ranged from 12 to 20 kg/m^3 (which is 20 to 33 lb/yd^3). Even when the stainless steel bars were coupled to black steel cathodes, the chloride concentration for the initiation of corrosion was still about twice that of black steel for Type 304 and 15 times the threshold of black steel for Type 316. The results from the study indicated that Type 316 stainless steel bars may be better than Type 304 bars for use in concrete because they are less susceptible to galvanic effects if they are coupled to carbon steel bars (McDonald et al. 1998).

Stainless steel and stainless steel–clad reinforcement have been used in a number of structures in the past 25 years, but none of these structures is old enough that corrosion damage would be expected, even if no protection measures had been used. So far, stainless steel reinforcement is performing satisfactorily. For example, in 1984, Type 304 stainless steel reinforcing bars were installed in part of a bridge deck north of Detroit, Michigan. The rest of the bridge was built using epoxy-coated steel. The deck was inspected and cores were removed in 1993 by Michigan Department of Transportation officials. No delaminations or corrosion-induced cracks were present on the deck. Two of the cores had longitudinal cracks (from temperature and shrinkage) that intersected the reinforcing steel, but no evidence of corrosion was found, except for minor staining on one bar at the crack location. The chloride ion concentrations had approached the corrosion threshold for black steel, but had not exceeded it significantly (McDonald et al. 1998).

The actual costs of three bridge projects that were constructed in Illinois in 1994 with black or epoxy-coated steel (or both) were compared with what the costs would have been, according to industry experts, had stainless steel or titanium reinforcement been used. The use of epoxy-coated reinforcement had very little effect on the overall price of the projects, but stainless steel would have increased the

total cost by 5.5% to 15.6%. Titanium would have increased the total bridge cost by 35% to 90% (McDonald et al. 1995).

Results from both field and laboratory studies of stainless steel as a corrosion-resistant reinforcement have been promising. Stainless steel exhibits excellent corrosion resistance in severe corrosion environments. No corrosion-induced damage was reported in any of the studies reviewed for this report. A 1994 report indicated that stainless steel should extend the time-to-corrosion in reinforced concrete structures by 65 to 130 times compared with black steel. When long-term durability is important, the extra cost of using stainless steel appears to be justified by the expected service life extension provided (McDonald et al. 1995).

An outstanding example of a stainless steel–reinforced bridge is the Progreso Pier in the Gulf of Mexico. The bridge is a 2.2-km-long concrete pier leading out into the Gulf of Mexico, built in the 1940s and still operating today. The structure used the equivalent of 304 steel to reinforce the arches of the pier. Despite the harsh environment, combined with relatively high porosity and some casting defects in the concrete, no significant corrosion problems have been observed (Arminox 1999). The chloride levels at the surface of the reinforcement were more than 20 times the traditionally assumed corrosion threshold level. Based on the condition and aging of the pier, and the limited number of investigations carried out, it appears that a 100-year service life is possible with stainless steel.

Electrochemical Treatment

Electrochemical treatments can be applied to concrete structures containing reinforcement to remove chlorides from the concrete (ECE) or to increase the pH of carbonated concrete (realkalization). Electrochemical treatments involve the application of current to cause changes in the chemistry of the concrete. The steel, which acts like a cathode, is connected to the negative pole of a direct current power source. The anode, which is typically either steel or a titanium mesh, is temporarily placed on the concrete surface and is connected to the positive pole of the power source. An electrolyte is placed on the concrete and allows the current to flow. Due to the applied electric field, negatively charged ions, like chlorides, migrate from the rebar toward the surface and out of the concrete. At the same time, the passage of current through the system generates hydroxyl ions (OH^-) at the steel–concrete interface, increasing the pH of the concrete.

Studies indicate that electrochemical treatments can successfully remove substantial amounts of chloride from contaminated concrete and lead to an increase in the pH of the concrete and repassivation of corroding reinforcing steel (Kepler et al. 2000). Studies have indicated that adverse side effects can be avoided as long as current densities are kept below 5 A/m^2 of concrete surface (Bennett et al. 1993). Studies have demonstrated that a current density of less than 1 A/m^2 of concrete surface is sufficient for treatment (Clemeña and Jackson 1997; Manning and Ip 1994). The first electrochemical treatment (ECE) application to a bridge in North America was completed in 1989. The treated sections remain passive (noncorroding). No additional corrosion damage has occurred to date.

Electrochemical treatments have been used to provide corrosion protection for structures suffering from chloride contamination, as well as carbonation. Research indicates that electrochemical treatments can be applied to new structures to increase long-term corrosion resistance by increasing the chloride corrosion threshold value potentially to the point that concrete completely saturated in salt water will not corrode. The increased tolerance to chlorides is believed to be primarily due to the increased alkalinity at the vicinity of the steel (Glass and Reddy 2002). The migration of alkali ions to the steel–concrete interface induces the precipitation of alkaline compounds that can block existing defects and large pores. It is known that corrosion on the surface of the steel reinforcement in the presence of chlorides initiates at such defects and pores, so their reduction in size below a certain critical size substantially increases resistance to corrosion. The subject research is exploring such a possibility.

Conclusions and Findings

A survey of existing literature indicated that proper stainless steel (e.g., 304 and 316LN) and titanium are expected to provide satisfactory corrosion resistance and extend the service life of structures.

The literature survey also indicated that electrochemical treatment of black bars in reinforced concrete may provide improved corrosion resistance and extend the service life of reinforced concrete structures.

Experimental Program

Testing Facility

All specimens were prepared at the University of Nebraska–Lincoln at the civil engineering laboratory.

Specimen Preparation

Reinforced concrete specimens were prepared in the laboratory and subjected to an accelerated testing regime under controlled conditions. The corrosion resistance of each combination within the test matrix was compared. All specimens were prepared and tested in triplicate to provide statistically significant results.

The test matrix included conventional reinforcing steel (black bar), black bar with two levels of electrochemical treatment, stainless steel bar, and titanium bar.

Test Setup

The specimen preparation and testing procedure considered to test the different matrices followed ASTM G109 (ASTM G109 2007a). Figure E.1 shows a three-dimensional view of a test specimen.

Five variables were evaluated; different bars were placed in conventional concrete:

- Black bars in untreated concrete (control);
- Black bars in concrete subjected to low electrochemical treatment;
- Black bars in concrete subjected to high electrochemical treatment;
- Stainless steel (316LN) in untreated concrete; and
- Titanium bars in untreated concrete.

Three specimens of each variable were prepared (15 specimens total). Figure E.2 shows the measurements of the specimens.

Materials

The list of materials used is described and illustrated below.

- Concrete was supplied by Concrete Industries Inc., a Lincoln, Nebraska, ready-mix concrete company, which provided the concrete on August 8, 2010.
- Steel reinforcement was as follows (see Figure E.3):
  - 27 Mild steel rebars (black bars), Grade 60, 0.5-in. diameter (No. 4) and 14 in. long;
  - Nine stainless steel rebars, Type 316LN, 0.5-in. diameter (No. 4) and 14 in. long; and
  - Nine titanium rods, Grade 2, 0.5-in. diameter and 14 in. long.
- Stainless steel screws and nuts
  - 45 Stainless steel screws (one per bar) with a diameter smaller than the bar diameter (coarse thread <0.2 in.), 1 to 1.5 in. long; and
  - 90 Stainless steel nuts (two per bar) to fit the screws;
- Two-part waterproof epoxy that met the resistance requirements by ASTM C881 for a Type IV, Grade 2, Class E specification epoxy (ASTM C881 2010);
- Heat-shrink tube with internal adhesive (see Figure E.4).
- Electroplater tape (not needed if heat-shrink tube is used).
- Neoprene tubing (not needed if heat-shrink tube is used) with 0.125-in. wall thickness and same inner diameter as the diameter of the bar.
- Sodium chloride.
- Salt solution prepared by dissolving three parts of sodium chloride in 97 parts of water by mass.
- Epoxy sealer for application to the concrete specimen after manufacture. Type III, Grade 1, Class C epoxy sealer was used in accordance with ASTM specifications (ASTM C881 2010).
- Plastic dams measuring 3 in. wide and 6 in. long with a minimum height of 3 in. and a wall thickness ±0.125 in. for placement on the test specimen.
- Silicone caulk for sealing the outside of the plastic dam to the top of the concrete.
- Reference electrode, such as saturated calomel or silver–silver chloride electrode for measuring the corrosion potential.
- Hexane to wash the sandblasted reinforcements.
- Multimeter to measure the macrocell voltage between electrode and rebars.

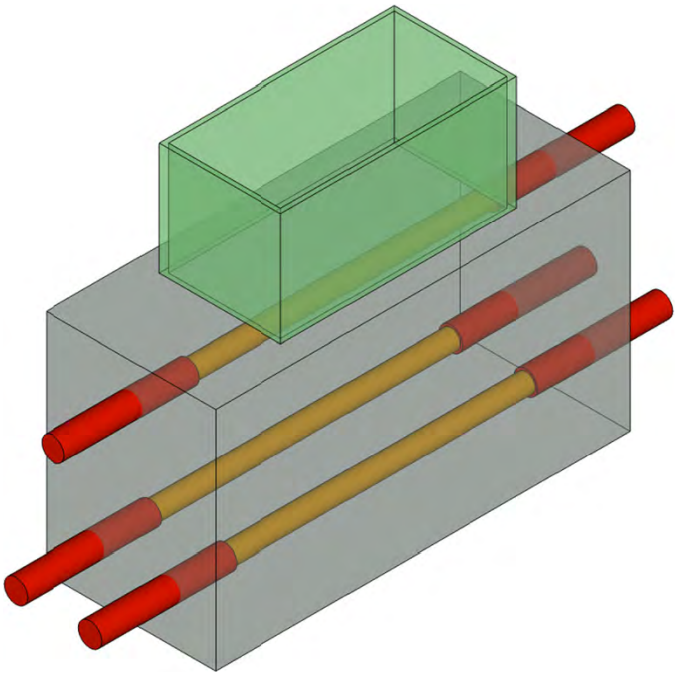

Figure E.1. Three-dimensional view of test specimen.

Casting of Specimen

The concrete samples were prepared in compliance with ASTM G109 (2007a). The samples were prepared according to the following instructions:

1. The rebars were cleaned by sandblasting to near white metal, after which they were soaked in hexane and air dried. Figure E.5 shows sample bars before and after sandblasting.
2. One end of each bar was drilled and tapped with a stainless steel screw and two nuts. At both ends of each rebar a 2-in.-long piece of heat-shrink tubing was placed so that 8 in. of bar remained bare. The rebar lengths protruding from the form were coated with two-part epoxy. Figure E.6 shows the application of heat-shrink tubing and the epoxy coating.

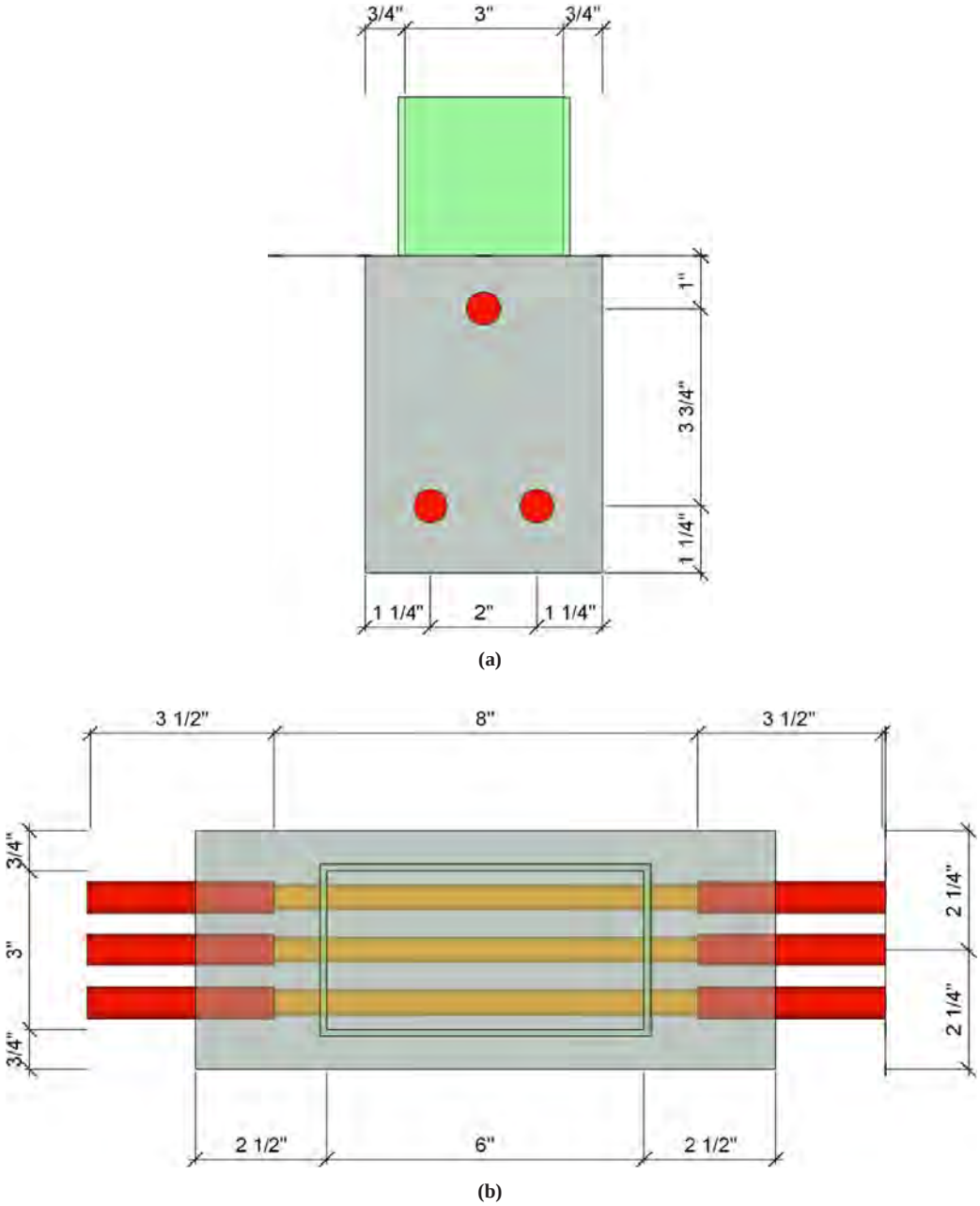

Figure E.2. (a) Front and (b) top views showing dimensions of specimens for corrosion-resistance testing. Green area in front view is a dam.

Figure E.3. Steel reinforcement: (a) black bars, (b) stainless steel rebars, and (c) titanium rods.

Figure E.4. Heat-shrink tube.

3. Wooden forms measuring 11 × 6 × 4.5 in. were fabricated (see Figure E.7a). To facilitate form removal, oil was used on the form surface.
4. The rebar was placed so that approximately 2 in. of it projected from the form. This 2-in. section was taped to isolate it from the environment, leaving 8 in. of the rebar inside the concrete exposed to chlorides. The clear cover of concrete was 0.75 in. for the top rebar. Figure E.8 shows samples ready for concrete placement.
5. The concrete used was made in accordance with ASTM specifications (ASTM C192 2007b). A local ready-mix company delivered the concrete to the structural laboratory at the University of Nebraska–Lincoln. The concrete had a water–cement ratio equal to 0.5, a cement content of 600 lb/yd^3, air content of 5%, and minimum slump of 2 in. After placement and consolidation, the top surface

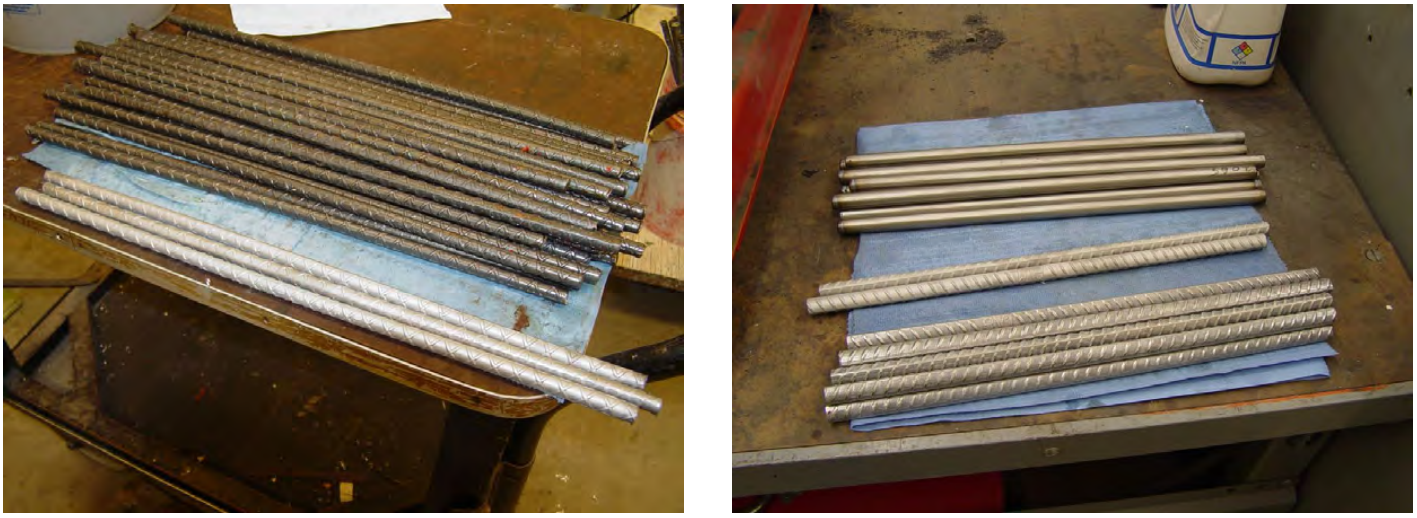

(a) (b)

Figure E.5. Samples of (a) black bar and (b) stainless steel and titanium rebars before and after sandblasting.

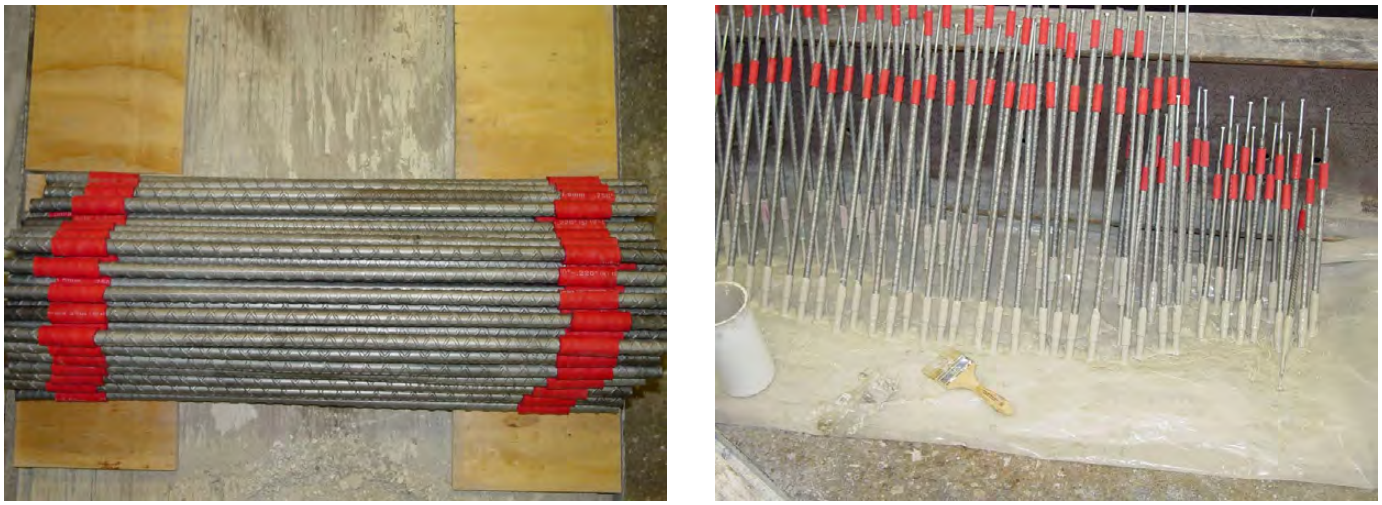

(a) (b)

Figure E.6. (a) Application of heat-shrink tubing and (b) rebars after receiving epoxy coating.

(a)

(b)

Figure E.7. (a) Wooden forms before and (b) after application of oil.

was finished with a wood float. Figure E.9 shows samples before and after concrete pour.

6. A plastic sheet was used to prevent moisture loss (see Figure E.10a); the forms were removed 4 days after casting.
7. After the forms were removed, electrochemical treatments were conducted on selected specimens. In the low-level ECE treatment, each specimen received a current of 8.1 mA for a period of 28 h. For the high-level electrochemical treatment, each specimen received a current of 16.2 mA for a period of 28 h (see Figure E.11).
8. To prevent the electrochemical solution from becoming too acidic, lime (calcium hydroxide) was added. A titanium mesh was placed at the bottom of the plastic dam and later connected to the positive pole of the power supply. The rebars were connected to the negative pole. Multimeters were used to measure the amount of current flowing to each sample. Figure E.12 shows the three principal stages of ECE treatment.
9. The specimens were cured for 28 days at ambient temperature. At the conclusion of the curing period, the top (wood-floated) surface was wire brushed. The specimens were allowed to dry for 2 weeks before the four vertical sides were coated with an epoxy sealer.
10. The plastic dam was placed and sealed with silicone caulk. Finally, an epoxy sealer was applied to the region outside the dam (top surface only). The top rebar was connected

(a)

(b)

Figure E.8. Samples ready for concrete placement: (a) three samples with one variable and (b) all 15 samples.

(a)

(b)

Figure E.9. (a) Concrete being placed into forms and (b) samples after wood-float finishing.

(a)

(b)

Figure E.10. (a) Samples covered by plastic to retain moisture and (b) sample removal from the wooden form.

(a)

(b)

Figure E.11. Electrochemical treatment readings at (a) low and (b) high levels.

(a)

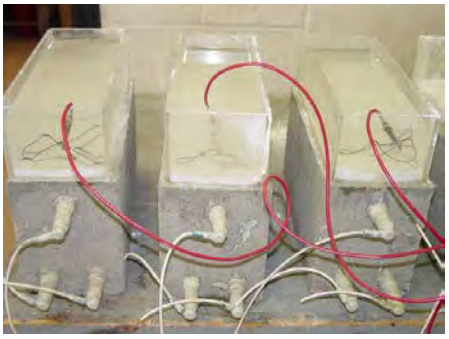

(b)

(c)

Figure E.12. Three principal stages of ECE: (a) before, (b) during, and (c) after electrochemical treatment.

to the two bottom bars through a wire and one 100-Ω resistor. Figure E.13 shows the specimens prepared for the wet–dry cycle.

Testing Procedure

After discussion and literature review, the team decided to slightly change the length of the wet–dry cycle specified in ASTM G109 (ASTM 2007a). The short cycle selected was intended to optimize and therefore accelerate the corrosion of the rebars.

The testing was conducted as follows:

1. Each sample was placed on two nonelectrically conducting supports. The first reading was taken 1 month after the specimens were cast.
2. The specimens were ponded with a salt solution (approximately 400 mL at a depth of 1.5 in.) for 4 days. A loose-fitting plastic cover was used to minimize evaporation. After 4 days, the salt solution was vacuumed off (see Figure E.14), and the specimens were allowed to dry for 10 days. The cycle was repeated until the termination of the test program.
3. The voltage across the resistor between the top and bottom bars was measured by a voltmeter, and the corrosion potential was measured by a half-cell system (see Figure E.15) with a silver–silver chloride electrode. Measurements were taken before ponding with the salt solution, after removal of the solution, and in the middle of the dry cycle.
4. The test was to be terminated when the integrated macrocell current was equal to or greater than 150 C, which is equivalent to a macrocell current of 10 μA as specified by ASTM G109 (ASTM G109 2007a).

Test Results

The concrete had a compressive strength of 4,830 psi, which was an average of three cylinders. Due to time constraints, the testing was terminated after 26 cycles. Table E.1 shows

Figure E.13. Specimens ready to start the wet–dry cycle.

Figure E.14. The salt solution was removed by vacuuming after the wet period was finished.

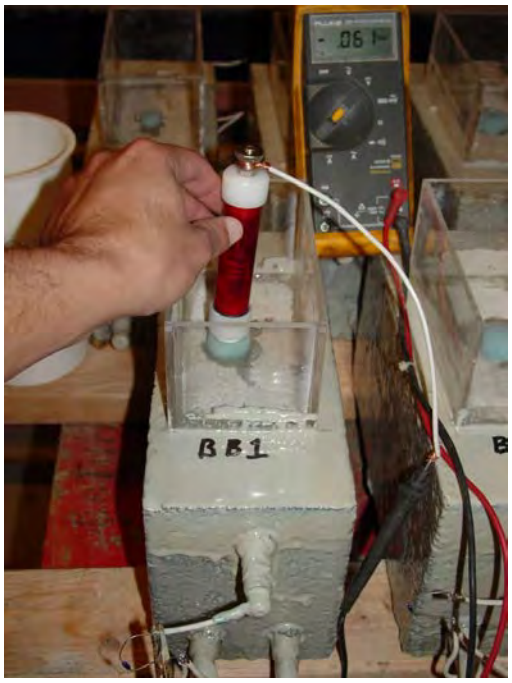

Figure E.15. Measuring the half-cell potential.

Table E.1. Samples Summary

Label	Type of Reinforcement	Type of Treatment
BB_1	Black bar	None
BB_2	Black bar	None
BB_3	Black bar	None
ECL_1	Black bar	Low level of electrochemical treatment
ECL_2	Black bar	Low level of electrochemical treatment
ECL_3	Black bar	Low level of electrochemical treatment
ECH_1	Black bar	High level of electrochemical treatment
ECH_2	Black bar	High level of electrochemical treatment
ECH_3	Black bar	High level of electrochemical treatment
SS_1	Stainless steel 316LN	None
SS_2	Stainless steel 316LN	None
SS_3	Stainless steel 316LN	None
Ti_1	Titanium	None
Ti_2	Titanium	None
Ti_3	Titanium	None

the summary of labels given to each specimen. Five variables were considered for testing, and three identical specimens for each variable were made to provide statistical significance.

The initial reading was taken on September 23, 2010 (Day 0). The samples were then subjected to successive cycles of 4 days wet and 10 days dry. At the end of each dry cycle, corrosion potential and current across resistor readings were taken for each specimen. Although not required by ASTM G109 (ASTM G109 2007a), additional readings were conducted at the end of each wet cycle and at the middle of each dry cycle.

Half-Cell Potential Data

Figure E.16 shows the half-cell potential readings for all specimens varying with time.

The potential values were more positive than –0.20 V, indicating that there was a greater than 90% probability that no reinforcing steel corrosion was occurring, except with three

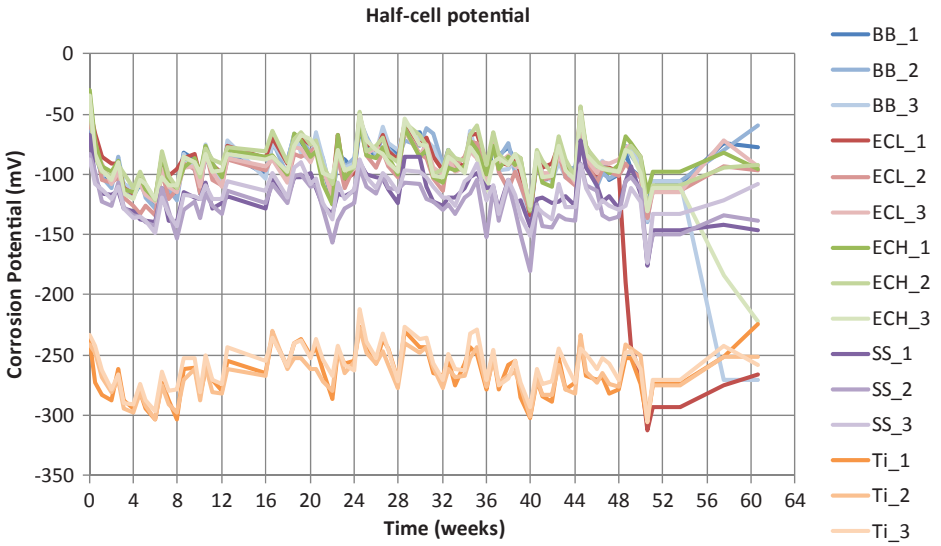

Figure E.16. Half-cell potential for all 15 specimens.

specimens that exceeded the –0.20-V limit. The three specimens were from three groups with black bars with values between –0.20 and –0.30 V, indicating that corrosion activity was uncertain.

Current Data

The integrated macrocell charge is calculated based on Equation E.1:

$$TC_j = TC_{j-1} + [(t_j - t_{j-1}) \times (i_j + i_{j-1})/2] \quad \text{(E.1)}$$

where

TC = total corrosion (C);
t_j = time (s) at which measurement of the macrocell is carried out; and
i_j = macrocell current (A) at time t_j.

Table E.2 shows the electrical current measured across the 100-Ω resistor installed between the top and bottom rebars. As expected, the negative values shown in Table E.2 indicate that the top rebar is the anode and bottom rebar is the cathode.

The total integrated charge, which is used to determine the end of testing, can be calculated using the current measurements and Equation E.1. If the charge is greater than 150 C, the test is terminated (ASTM G109 2007a). The results were plotted in Figure E.17, which shows the variation of total charge with time. All values are below 150 C.

The current data indicated one specimen in three groups (black bar and both electrochemical treatments with black bars) showed an increase in current. This finding is similar to the potential data showing uncertain corrosion activity in the same three specimens.

These specimens were selected for removal of the rebar for visual inspection along with control specimens with stainless steel and titanium (BB3, ECL1, ECH3, SS1, and Ti1), as shown in Figure E.18.

BB3 showed an approximately 0.75-in. length of corrosion product (see Figure E.19b). The final integrated charge was 35 C, and the lowest corrosion potential was –270 mV. The maximum macrocell current measured was 11.4 μA.

ECL1 showed an approximately 1-in. length of corrosion product (see Figure E.20b). The final integrated charge was 70 C, and the lowest corrosion potential was –300 mV. The maximum macrocell current measured was 11.8 μA.

ECH3 showed an approximately 0.25-in. length of corrosion product (see Figure E.21b). The final integrated charge was 10 C, and the lowest corrosion potential was –220 mV. The maximum macrocell current measured was 3.8 μA.

As shown in Figure E.22, SS1 did not show any signs of corrosion. The final integrated charge was around 1 C, and the lowest corrosion potential was –150 mV. The maximum macrocell current measured was nearly 0.2 μA.

As shown in Figure E.23, Ti1 did not show any signs of corrosion. The final integrated charge was around 1 C, and lowest corrosion potential was –250 mV. The maximum macrocell current measured was 0.035 μA.

Conclusions

During the time available for this project, only one specimen from a set of three with black bars and electrochemically treated black bars showed an increase in current or potential values indicative of uncertain corrosion activity. The top bars in these specimens and in additional specimens with stainless steel and titanium reinforcements were removed for visual observation.

The stainless steel and titanium bars did not exhibit corrosion within the available time period.

To discern differences between black bars and electrochemically treated black bars, a longer test period is needed.

Thus, initial observations indicate that electrochemically treated black bars may not provide the protection expected of stainless steel or titanium; however, whether they provide benefits over black bars without treatment cannot be concluded from this study due to time constraints. To draw firm conclusions, additional research and extended testing periods are needed.

Table E.2. Measured Electrical Current

Time	BB1	BB2	BB3	ECL1	ECL2	ECL3	ECH1	ECH2	ECH3	SS1	SS2	SS3	Ti1	Ti2	Ti3
Day	μA	μA	μA	μA	μA	μA	μA	μA	μA	μA	μA	μA	μA	μA	μA
0	0	0	0	0	0	0	0	0	0	0	0	0	0	0	0
50	–0.07	–0.06	–0.065	–0.06	–0.02	–0.055	–0.05	–0.025	–0.05	–0.035	–0.02	–0.025	–0.01	–0.015	–0.02
302	–0.095	–0.09	–0.1	–0.08	–0.07	–0.075	–0.045	–0.04	–0.04	–0.04	–0.045	–0.045	–0.04	–0.045	–0.04
308	–0.13	–0.09	–0.09	–0.08	–0.055	–0.07	–0.04	–0.045	–0.035	–0.02	–0.02	–0.04	–0.04	–0.03	–0.035
312	–0.12	–0.08	–0.08	–0.07	–0.07	–0.065	–0.04	–0.04	–0.035	–0.05	–0.065	–0.045	–0.04	–0.04	–0.035
336	–0.055	–0.05	–0.04	–0.055	–0.035	–0.045	–0.025	–0.02	–0.02	–0.015	–0.015	–0.02	–0.025	–0.035	–0.03
340	–0.05	–0.05	–0.04	–3.6	–0.035	–0.04	–0.03	–0.025	–0.025	–0.015	–0.01	–0.02	–0.03	–0.03	–0.03
344	–0.06	–0.05	–0.055	–8.7	–0.045	–0.05	–0.035	–0.025	–0.02	–0.045	–0.025	–0.025	–0.04	–0.04	–0.03
350	–0.06	–0.06	–0.06	–10.6	–0.04	–0.05	–0.02	–0.035	–0.02	–0.02	–0.015	–0.02	–0.025	–0.035	–0.03
354	–0.06	–0.05	–0.055	–11.5	–0.06	–0.05	–0.025	–0.02	–0.03	–0.025	–0.02	–0.02	–0.025	–0.06	–0.03
358	–0.1	–0.1	–0.08	–11.8	–0.06	–0.065	–0.03	–0.035	–0.03	–0.03	–0.03	–0.02	–0.03	–0.07	–0.025
375	–0.1	–0.1	–0.08	–10.3	–0.06	–0.065	–0.03	–0.035	–0.03	–0.03	–0.03	–0.02	–0.03	–0.07	–0.025
403	–0.6	–0.6	–11.4	–7.5	–0.3	–0.2	–0.2	–0.2	–2.2	–0.6	–0.1	–0.1	–0.1	–0.2	–0.3
424	–0.8	–0.1	–8.3	–5.4	–0.3	–0.3	–0.3	–0.2	–3.8	–0.18	–0.28	–0.34	–0.35	–0.37	–0.4

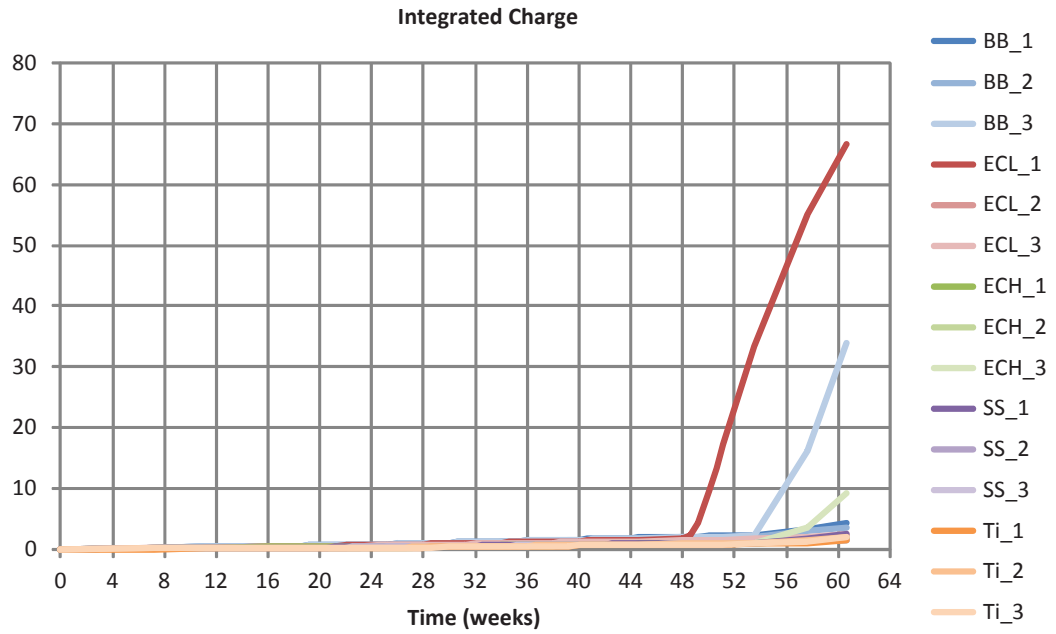

Figure E.17. Integrated macrocell charge for all 15 specimens.

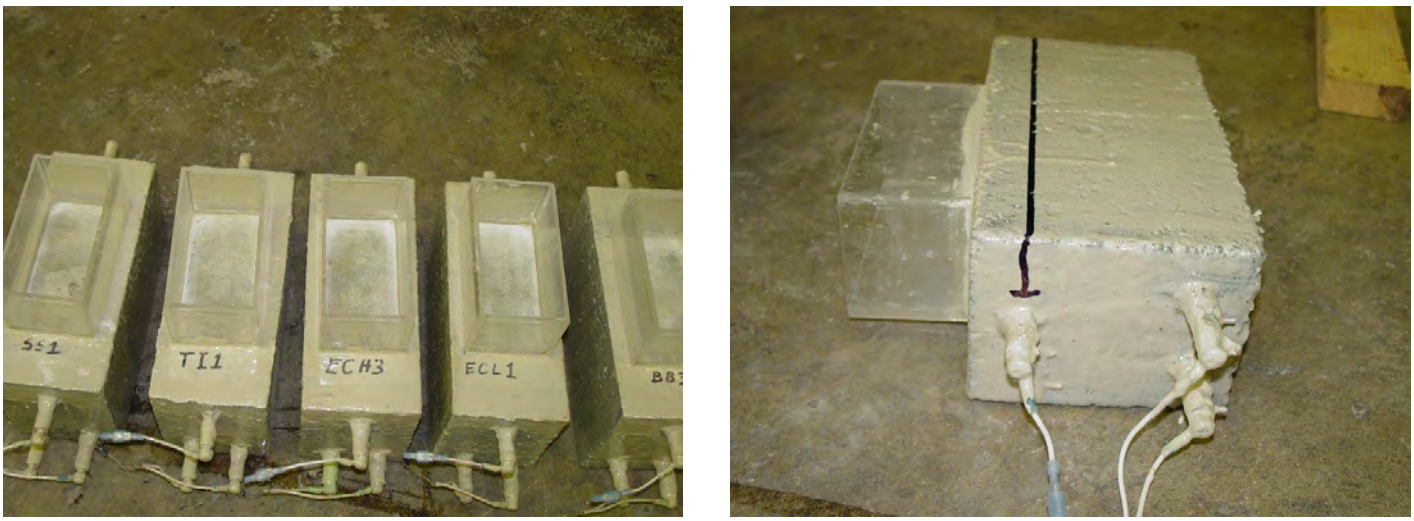

(a) (b)

Figure E.18. (a) Specimens selected for rebar removal and (b) guide line for saw cut.

(a) (b)

Figure E.19. BB3 specimen: (a) overall view and (b) close-up of rebar.

(a)

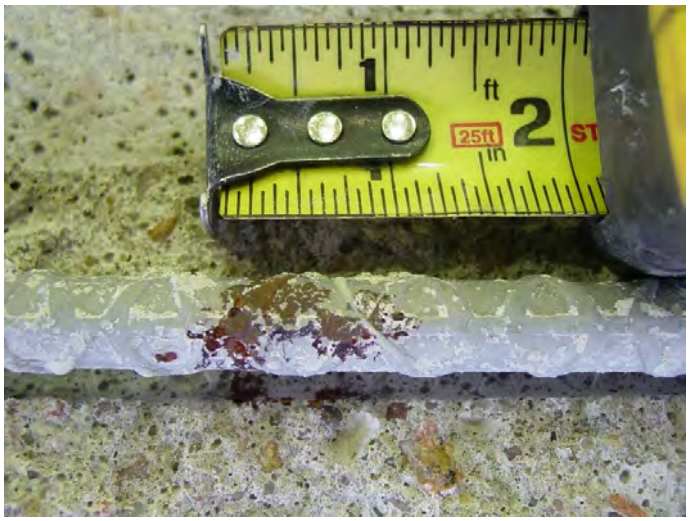

(b)

Figure E.20. ECL1 specimen: (a) overall view and (b) close-up of rebar.

(a)

(b)

Figure E.21. ECH3 specimen: (a) overall view and (b) close-up of rebar.

(a)

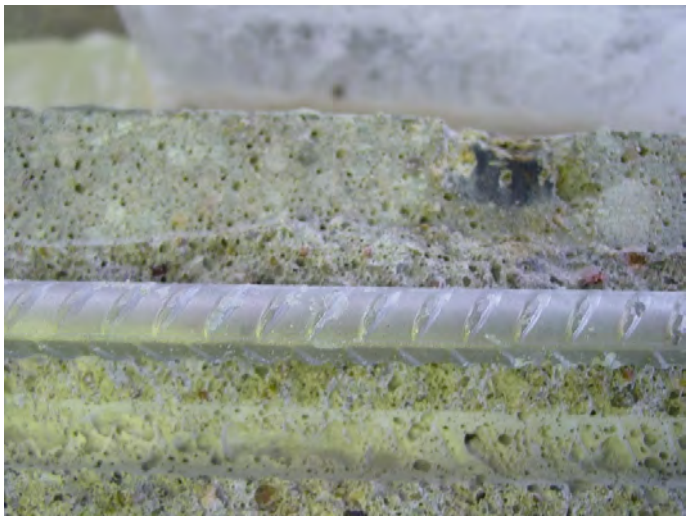

(b)

Figure E.22. SS1 specimen: (a) overall view and (b) close-up of rebar.

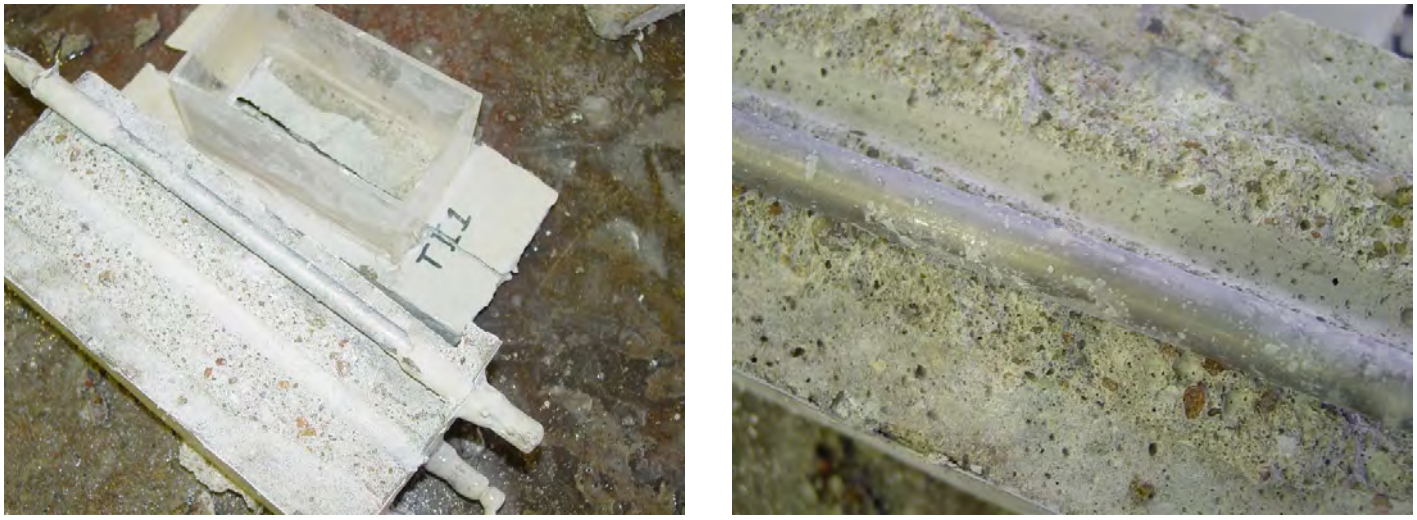

(a) (b)

Figure E.23. Ti1 specimen: (a) overall view and (b) close-up of rebar.

APPENDIX F

New Galvanic Systems to Achieve Long-Term Cathodic Protection

Background

Cathodic protection has been used in several areas, including marine and underground structures, storage tanks, and pipelines to protect steel from corrosion (Virmani and Clemeña 1998). Cathodic protection was not used in steel-reinforced concrete structures until applied to a bridge deck in 1973 (Stratfall 1974). The two main types of cathodic protection are impressed current cathodic protection (ICCP) and sacrificial galvanic protection. Most systems installed to date have been of the ICCP type. ICCP requires a power source and an anode material that enables the required current to flow between the installed generally inert anode and the steel cathode. Although ICCP systems are theoretically very good, many systems across the United States have failed and are no longer in service. In numerous cases, failure was due to a lack of dedicated maintenance and monitoring of the electrical systems and components or because the systems had been damaged by normal structure maintenance operations.

In the galvanic system, the anode sacrifices itself and provides protection for the reinforcement. Galvanic systems do not require the same level of maintenance and monitoring as ICCP systems. They are practical, easy to install, and can be used in both new construction and repair; however, they have a limited life span.

Concrete patch repairs are very common in reinforced concrete structures. Often these concrete structures are chloride contaminated beyond the location of patch repairs, leading to accelerated corrosion around the patch. This phenomenon is referred to as ring anode corrosion, or the halo effect.

Ring anode corrosion can be eliminated by including galvanic anodes within the repair. The galvanic anode corrodes instead of the reinforcing steel. This type of application now has a 10-year successful history (Sergi et al. 2008). The knowledge gained from this application has led to the development of higher-output galvanic anodes. Initial testing of such anodes has shown improved performance and an ability to globally protect the reinforcing steel.

Known galvanic cathodic protection systems use activated anodic metals such as zinc. Activation of the metal can be achieved by exposure to chlorides when the anode is in contact with seawater (e.g., zinc jackets around reinforced concrete columns in seawater) or by embedment in a highly alkaline mortar. In the latter case, anodes are discrete "point" anodes, or units embedded in the concrete in proximity to the steel reinforcement.

Depending on the service requirements, corrosion protection can be divided into three distinct levels: corrosion prevention, corrosion control, and cathodic protection (Vector Corrosion Technologies 2013):

- *Corrosion prevention*—Corrosion prevention is used to prevent corrosion from initiating in contaminated concrete. If concrete repair projects are completed in accordance with industry guidelines (International Concrete Repair Institute), the replacement of damaged concrete will address the areas with the highest level of corrosion activity. However, after the repairs are complete, new corrosion sites are likely to form in the remaining contaminated concrete. Research in the area of corrosion prevention indicates that a low applied current density (in the order of 0.4 mA/m^2 of steel surface area) is effective in preventing the initiation of corrosion in concrete with significant chloride concentrations. The required current will decrease over time as chemical reactions increase the alkalinity and decrease the concentration of chloride ions around the reinforcing steel.
- *Corrosion control*—Corrosion control systems are used when corrosion has initiated but has not yet progressed to the point of causing concrete damage. The use of corrosion control systems will provide a significant reduction in the corrosion rate and an increased service life of the

rehabilitated structure. In many cases, this level of protection can be provided with low incremental cost, as the protection can be targeted at specific areas of contamination or corrosion activity. The current requirements for corrosion control are higher than for corrosion prevention, generally in the range of 1 to 7 mA/m^2. Similar to corrosion prevention, the current density required to provide corrosion control decreases over time as the beneficial effects of chemical reactions build up the alkalinity and decrease chloride concentrations around the reinforcing steel.

- *Cathodic protection*—Cathodic protection provides the highest level of protection and is intended to address ongoing corrosion activity. Cathodic protection should be selected when the highest level of protection is necessary and the cost is economically justified. Current industry standards for cathodic protection are based on 100-mV depolarization acceptance criteria. This level of protection generally requires an initial operating current between 5 and 20 mA/m^2. Current may be provided by galvanic anodes or by an impressed current power supply.

Historically, galvanic anodes provided a level of current output per unit that was sometimes too low to achieve the desired level of protection. The development of improved anode units that can produce a higher level of current by increasing the driving voltage between the anode and steel reinforcement has improved performance and allowed galvanic anodes to meet the full range of desirable corrosion protection levels. The advantages of these types of galvanic systems over ICCP are the self-regulating current output of the system and the much-reduced requirement of monitoring and maintenance.

Some recent initial work has enabled increased performance of galvanic anodes by modifying the surface area of the metal by design and increasing the driving voltage of the anode unit. Figure F.1 shows the increase in cumulative charge with time of anodes with increasing metal surface area.

It is also possible to increase the current density output by using high-voltage anodes, as shown in Figure F.2.

Problem Statement

Galvanic systems can delay the onset of corrosion and reduce the rate of corrosion of the reinforcing steel in reinforced structures. Furthermore, the degree of protection achieved and the extension in the service life of the reinforced concrete bridge elements can be extended by improving the performance of galvanic systems.

Description of the Concept

Galvanic systems make use of a sacrificial metal, such as zinc, which is naturally anodic when coupled to steel and corrodes preferentially to the steel cathode, giving up electrons to protect the steel (Virmani and Clemeña 1998).

Objectives of the Research

The objective of this research was to evaluate different promising concepts associated with the new galvanic systems in order to delay the onset of corrosion and to reduce the rate of corrosion of the reinforcing steel. The galvanic systems evaluated had an ordinary anode, an anode with a larger surface (four times more zinc than ordinary anodes), and two levels of high-voltage anode.

Before the initiation of the laboratory evaluation of the anodes, a comprehensive literature survey was conducted.

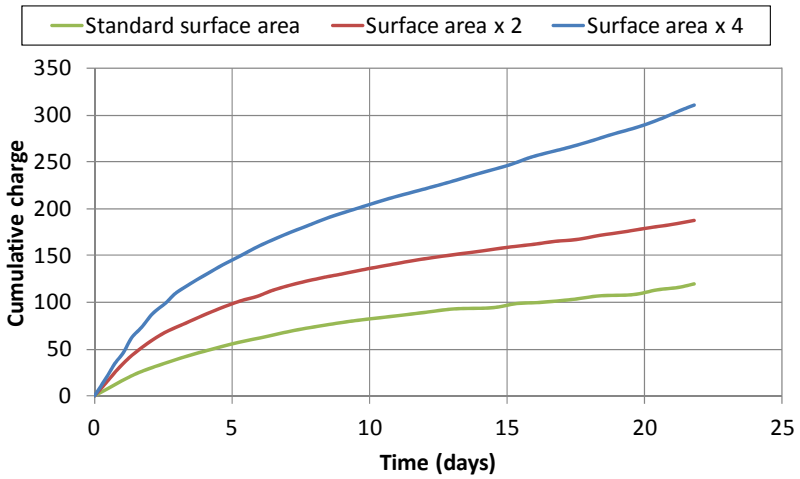

Figure F.1. Cumulative charge with time of anodes with different metal surface areas.

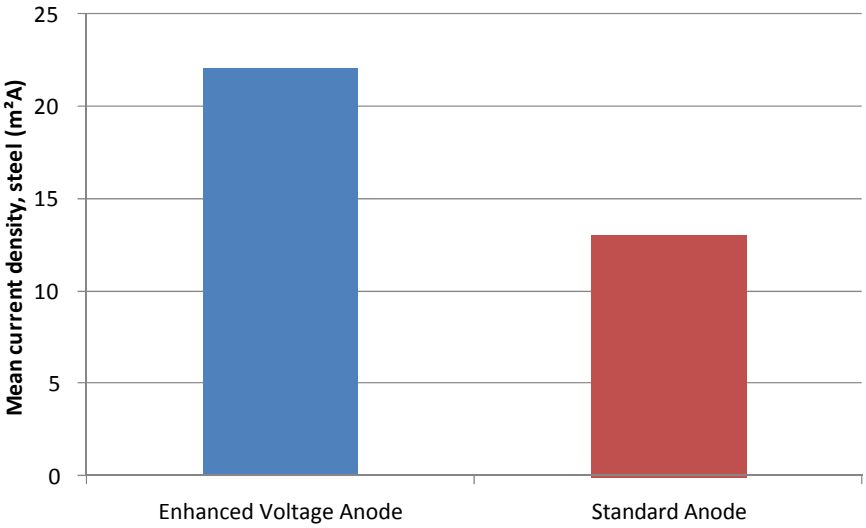

Figure F.2. Mean current density over 2 months for anodes with enhanced voltage output.

Research Approach

Introduction

Cathodic protection is used to extend the service life of reinforced concrete structures, generally existing structures, which are chloride contaminated and are exhibiting corrosion.

The intent of this research was not to test specific products, but rather to evaluate the ability of galvanic anodes in general to provide corrosion prevention or cathodic protection. Because available galvanic anodes offer limited protection, the ability to improve the level of protection of anodes with more surface area or with higher voltage output was investigated. Currently, proprietary systems exist for more surface area and for high-voltage output; these systems were evaluated to determine the extent of protection in highly chloride-contaminated concrete. Anode-embedding mortar and its effects on current output were not addressed in this research, but should be pursued in future studies.

Organization and Conduct of the Research

Small-scale laboratory testing was conducted to evaluate the potential of using galvanic anodes to extend the service life of reinforced concrete structures and the level of protection provided by different anode systems (increased metal surface, higher-voltage output). Data collection included the measurement of the current, current density, potentials, and polarization versus time.

The following tasks were accomplished to meet the research objectives:

Task 1. Summarize the literature of cathodic protection, including galvanic systems.

Task 2. Obtain material and equipment to be used during the testing stage.

Task 3. Fabricate samples using different galvanic systems.

Task 4. Set up automated monitoring system to collect long-term data.

Task 5. Analyze the collected data and destructively analyze anodes and steel bars.

Task 6. Prepare the final report and provide recommendations based on the results.

Analysis of Available Data

A Federal Highway Administration (FHWA) report states, "The only rehabilitation technique that has proven to stop corrosion in salt-contaminated bridge decks regardless of the chloride content of the concrete is cathodic protection" (R. A. Barnhart, memorandum, FHWA Position on Cathodic Protection, 1982). An advantage of using cathodic protection as a repair method for reinforced concrete bridges is that only spalls and delaminated concrete need to be repaired. Chloride-contaminated concrete that is still sound can remain in place because the cathodic protection system will reduce the concentration of chloride ions adjacent to the protected reinforcing bars, preventing further corrosion. This can significantly reduce repair costs (Polder 1998).

There are three basics components to a cathodic corrosion protection system (Durham and Durham 2005):

- An anode that supplies current in a corrosion circuit;
- A cathode that receives current in a corrosion circuit; and
- An electrolyte that is a nonmetallic medium, with some moisture content, which supports the flow of ionic current.

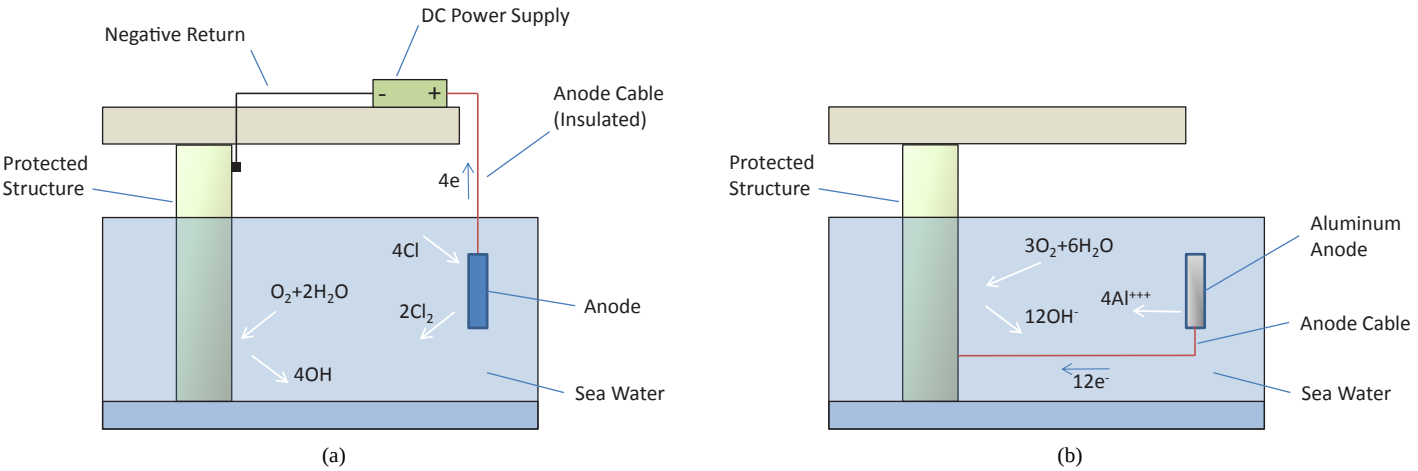

Figure F.3. Scheme of cathodic protection systems: (a) impressed current and (b) sacrificial anode.

The current for cathodic protection can be supplied to a bridge deck by one of two methods: (1) an external power source (impressed current) or (2) an anode that is made from a material that is more active and corrodes preferentially to the reinforcing steel (sacrificial anode). Refer to Figure F.3 for schematics of these two cathodic protection systems.

Both impressed current and sacrificial galvanic systems have been used successfully on bridges in the United States. Each method has specific characteristics that make it more effective than the other in a given situation. Table F.1 lists some of the general characteristics of each method. Impressed current systems are used most often on bridge decks. Some impressed current anodes can also be used on bridge substructure members. The use of galvanic anodes has historically been limited to substructure members (Kepler et al. 2000); however, deck applications have become much more common in recent years.

Table F.2 lists some estimated current density requirements for cathodic protection in various material and environmental conditions (Kepler et al. 2000).

The following conclusions are based on a review of studies reporting the performance of various cathodic protection systems (Kepler et al. 2000):

- Cathodic protection can effectively stop corrosion in contaminated reinforced concrete structures and reduce the concentration of chloride ions at the steel surface of protected reinforcement.
- The most common impressed-current anode in use for cathodic protection of reinforced concrete bridge decks is the titanium mesh anode, used in conjunction with a concrete overlay.
- Zinc mesh pile jacket anodes show promise as sacrificial anodes for the splash zone of bridge piles in a marine environment. Zinc–hydrogel anodes can provide protection for substructure members in marine or inland environments, as long as water can be kept out of the system. Activated zinc anode strips can be embedded in concrete jackets and overlays to provide distributed corrosion protection.
- Cathodic protection can be applied effectively and safely to prestressed concrete bridge members. However, if the resistivity of the concrete is not uniform, it may be difficult to obtain sufficient protection at locations where resistivity is high without generating hydrogen in areas of low resistance. Cathodic protection is not recommended for prestressed concrete structures with very diverse resistivity, which is often caused by large variations in moisture content.
- When applying cathodic protection to prestressed concrete, the voltage should be kept low enough that the potential required for hydrogen generation at the surface of the prestressing steel is not reached.

Table F.1. Comparison of Characteristics of Cathodic Protection

Impressed Current	Sacrificial Anode
External power required	Requires no external power
Driving voltage can be varied	Fixed driving voltage
Current can be varied	Limited current
Can be designed for almost any current requirement	Usually used where current requirements are small
Can be used in any level of resistivity	Usually used in low-resistivity electrolytes

Table F.2. Practical Cathodic Protection Current Density Requirements for Varying Environments

Environment Surrounding Steel Reinforcement	Current Density (mA per m² of reinforcement)
Alkaline, no corrosion occurring, low oxygen resupply[a]	0.1
Alkaline, no corrosion occurring, exposed structure[a]	1–3
Alkaline, chloride present, dry, good-quality concrete, high cover, light corrosion observed on reinforcement	3–7
Chloride present, wet, poor-quality concrete, medium-low cover, widespread pitting and general corrosion on steel	8–20
High chloride levels, wet fluctuating environment, high oxygen level, hot, severe corrosion on steel, low cover	30–50

[a] This is typical of a corrosion prevention (cathodic prevention) application as described in BS EN ISO 12696:2012, *Cathodic Protection of Steel in Concrete* (BSI 2012). The current requirement for cathodic prevention (corrosion prevention) in the standard is stated as 0.2–2 mA/m².

Impressed current systems can be costly and may require significant maintenance and monitoring. Galvanic systems may be easier to use; however, they provide a limited service life and level of corrosion protection. In repairs, sacrificial galvanic anodes are considered for localized corrosion protection because they are simple and easy to apply.

Experimental Program

Testing Facility

All test specimens were prepared at the University of Nebraska–Lincoln in the civil engineering laboratory.

Construction Overview

The ability of embedded galvanic anodes to provide sufficient output to cathodically protect the reinforcing steel from further corrosion was determined using slabs. Different anodes with varying output and levels of protection were studied.

The specimens measured 18- × 18-in. and were 8 in. thick to simulate a portion of a bridge deck. The test matrix included conventional reinforcing steel and galvanic anodes with different surface areas or voltage outputs.

Test Setup

The concrete slabs were cast in two layers. The bottom layer had uncontaminated concrete, and the top layer had concrete contaminated with salt. Figure F.4 shows the galvanic system test specimen.

Five variables were evaluated:

- Black bar embedded in concrete without anode as a control specimen (BB);
- Black bar embedded in concrete with ordinary anode (OA);
- Black bar embedded in concrete with a larger anode having a surface area four times the ordinary (OA4);
- Black bar embedded in concrete with a high-voltage anode (under development) at Level 1; this provided higher applied voltage than a standard galvanic anode (HVAL); and
- Black bar embedded in concrete with a high-voltage anode (under development) at Level 2; this provided a higher voltage than Level 1 (HVAH).

Three specimens of each variable were prepared. The dimensions of the specimens are given in Figure F.5. The thickness of the slab was 8 in.

Material

The following materials were used to evaluate the new galvanic systems:

- Concrete
  - Concrete (1 yd³) with proportions given in the specimen preparation below was delivered by the local ready-mixed concrete plant.

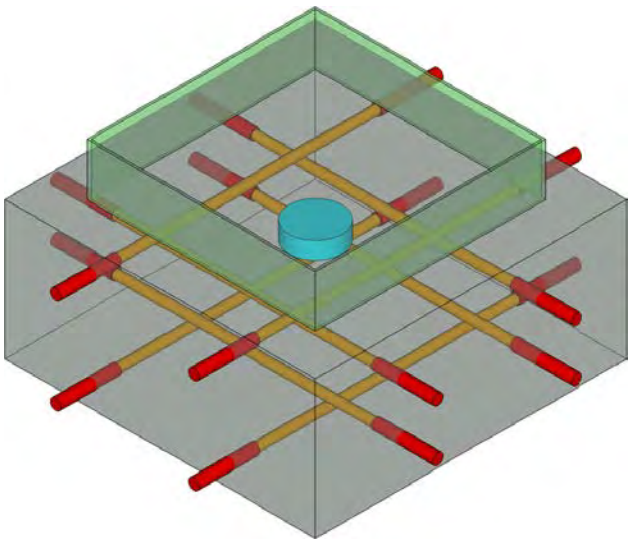

Figure F.4. Three-dimensional view of new galvanic system test specimen.

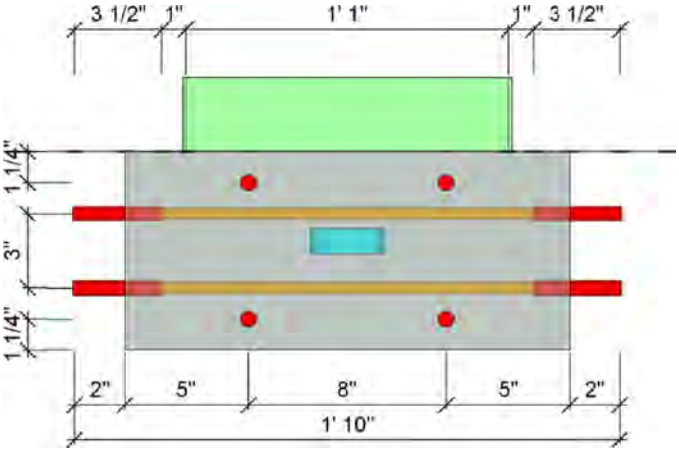

(a)

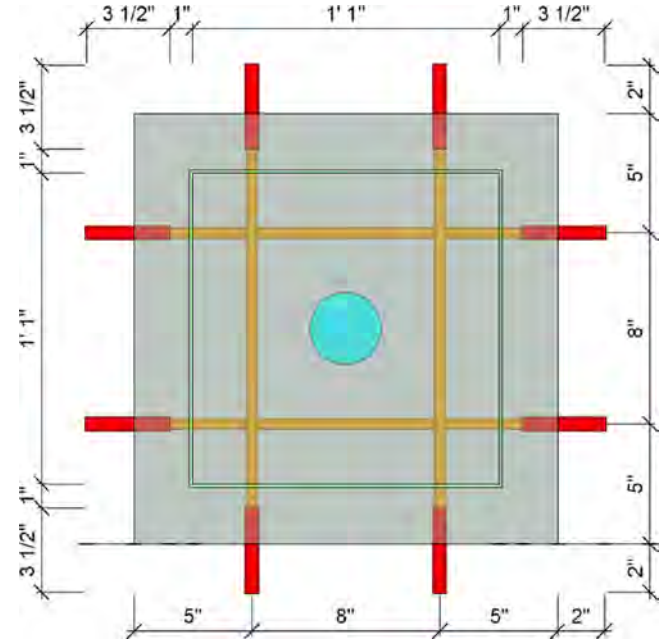

(b)

Figure F.5. Dimensions of test specimen: (a) side view and (b) top view; dam on top is shown in light green.

  - Half of the volume (0.5 yd^3) was used to cast the bottom 4-in. layer. After approximately 5 days of curing, the remaining 4-in. upper layer was cast using concrete with a 10-lb/yd^3 admixed chloride.
- Steel reinforcement consisted of 120 mild steel rebars (eight black bars per specimen), Grade 60, 0.5 in. in diameter (No. 4), and 22 in. long (see Figure F.6).
- Stainless steel screws and nuts
  - 120 Stainless steel screws (one per bar) with a diameter smaller than the bar diameter (coarse thread <0.2 in.), 1 to 1.5 in. long; and
  - 240 Stainless steel nuts (two per bar) to fit the screws.

Figure F.6. Mild steel reinforcement with a length of 22 in.

- Two-part waterproof epoxy; this epoxy met the chemical resistance requirement by ASTM C881 for a Type IV, Grade 3, Class E specification epoxy (ASTM C881 2010).
- Heat-shrink tube with internal adhesive (see Figure F.7).
- Sodium chloride.
- Epoxy sealer to cover the sides and top surface outside the dam. Type III, Grade 1, Class C epoxy sealer was used in accordance with ASTM specifications (ASTM C881 2010).
- Plastic dams measuring 13 in. wide and 13 in. long with a minimum height of 3 in. and a wall thickness of ±⅛ in. for placement on the test specimen.
- Silicone caulk for sealing the outside of the plastic dam on top of the concrete.

Figure F.7. Heat-shrink tube.

(a)

(b)

(c)

(d)

Figure F.8. Four types of anode were used: (a) ordinary anodes (OA), (b) anodes with four times more zinc than an ordinary anode (OA4), and high-voltage anodes with (c) low output (HVAL) and (d) high output (HVAH).

- Six sacrificial anodes of each type (i.e., ordinary anodes, anodes with a larger surface [four times more zinc than ordinary anodes], and two levels of high-voltage anode) for a total of 24 (see Figure F.8). Anodes were connected to the junction box by wire.
- Reference electrodes
  - Surface electrodes (e.g., silver–silver chloride electrodes); and
  - 30 Embeddable reference electrodes (see Figure F.9), such as silver–silver chloride electrodes, for measuring the corrosion potential and for long-term monitoring.
- Multimeter.
- Automated data acquisition system to record all the voltage and current outputs.

Figure F.9. Embeddable reference electrode.

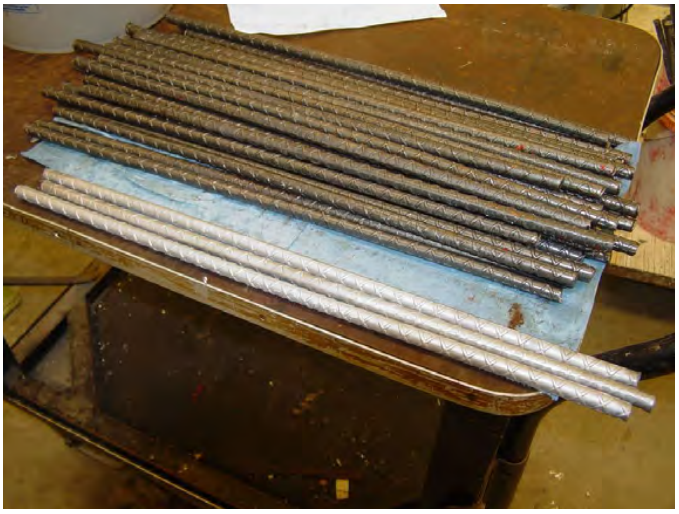

Figure F.10. Mild reinforcement before and after sandblasting.

Specimen Preparation

The concrete slabs were prepared similar to the ones described in ASTM G109 (ASTM G109 2007a). The rebars were cleaned by sandblasting to a near white metal finish, soaked in hexane, and air dried as shown in Figure F.10.

One end of each bar was drilled and tapped with a stainless steel screw and two nuts. At both ends of each rebar a 2-in. piece of heat-shrink tubing was placed so that 13 in. of bar were kept bare inside the slab. The rebar lengths protruding from the form were coated with two-part epoxy. Figure F.11 shows the application of heat-shrink tubing and epoxy coating.

Wooden forms measuring 18 × 18 × 8 in. were fabricated and brushed with oil as shown in Figure F.12 for easy form removal.

The rebar was placed so that approximately 2 in. projected from the form, as shown in Figure F.13. The minimum concrete cover over bars was 1 in.

The concrete was made in accordance with ASTM C192 (ASTM C192 2007b) and had a water–cement ratio equal to 0.5, a cement content of 600 lb/yd^3, an air content of 5%, and a minimum slump of 2 in. The first 4-in. layer was cast with conventional concrete (no salt admixed). A plastic sheet was used to keep the moisture in the concrete until the placement of the upper second layer, as shown in Figure F.14b.

Before placing the second layer, two anodes were placed close to each other in the center of the mold on top of the bottom layer. In addition, two embeddable reference electrodes were fixed at two locations, as shown in Figure F.15.

The top 4 in. of concrete was placed with concrete admixed with chloride (10 lb/yd^3). Concrete was consolidated by rodding and finished by a wood float, as shown in Figure F.16.

Wet burlap and plastic sheet were used for curing. Forms were removed 4 days after casting, although the burlap and plastic sheet were kept until 28 days.

After 28 days of curing, the plastic dam was placed on top, as shown in Figure F.17. All four vertical sides and the top surface outside the plastic dam were sealed with an epoxy sealer. Wires were attached to the junction box.

Testing Procedure

The testing procedure for the determination of corrosion activity involved measuring

1. Half-cell potentials (ASTM C876 2009) at nine locations on the specimen;
2. Current flowing from the anode to each pair (a total of four pairs, two on top and two at the bottom of the specimen) of rebars hourly; at the same time, the corrosion potential was measured by the embedded electrodes; and

(a) (b)

Figure F.11. (a) Application of heat-shrink tubing and (b) rebars after epoxy coating of ends.

(a)

(b)

Figure F.12. (a) Wooden forms before and (b) after application of oil.

(a)

(b)

Figure F.13. (a) Forms ready for placement of concrete and (b) specimen close-up (*bottom layer*).

(a)

(b)

Figure F.14. (a) Specimens after placement of bottom layer and (b) plastic sheet to prevent moisture loss.

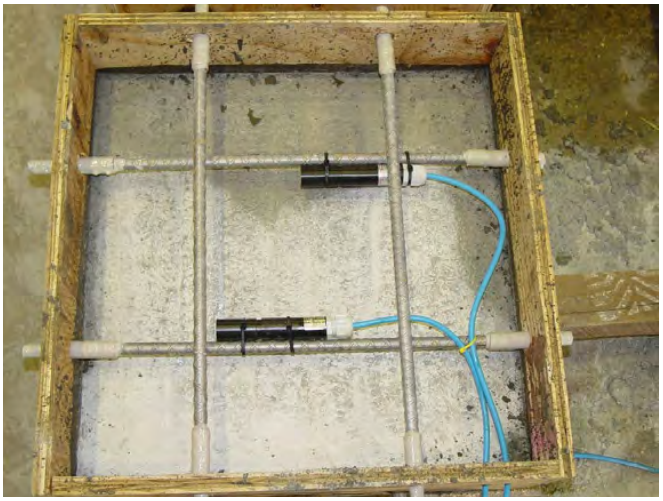

(a)

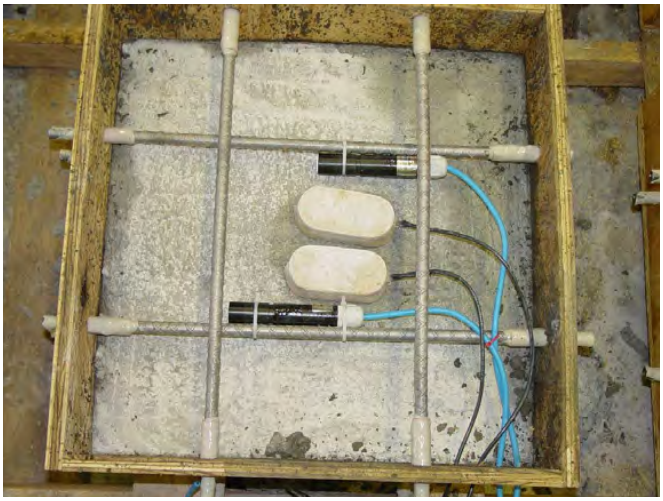

(b)

Figure F.15. Installation of (a) embeddable electrode and (b) OA4 anode.

(a)

(b)

Figure F.16. (a) Casting of the second layer of concrete and (b) specimens after wood-float finishing.

Figure F.17. Specimens ready to start the wet–dry cycle.

3. Current flowing during depolarization when the anode was disconnected; at the same time, the corrosion potential were measured by both the embedded electrodes and the half-cell system. A second data logger with quick reading capability (10 reads per second) was used during the procedure to capture the exact moment when the anode was turned off and on.

The following steps were used in the testing procedure:

Step 1. Seven days after casting, before connecting the anode to the rebars for the first time, the corrosion potential was measured to establish the baseline level of corrosion potential of the steel. A half-cell system with a silver–silver chloride electrode was used to measure the corrosion potential. The tip of the reference electrode was positioned on a small wet pad to stabilize the readings,

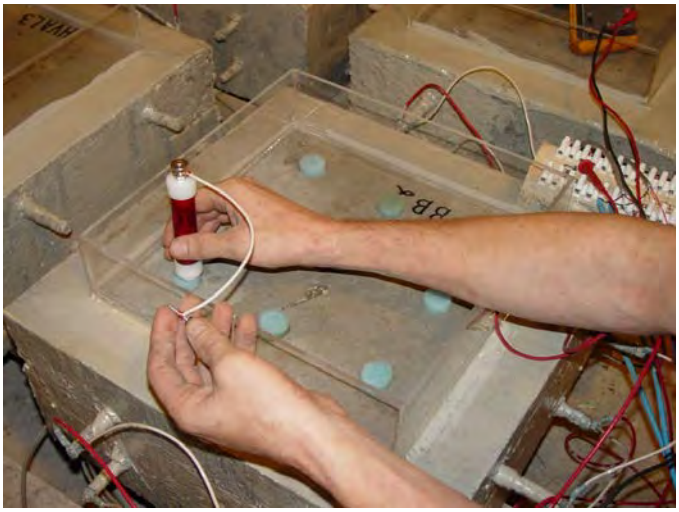

Figure F.18. Measuring the half-cell potential.

Figure F.19. Vacuuming off the water at the end of the wet period.

as shown in Figure F.18. The same procedure was repeated three times during each wet–dry cycle. The corrosion potential was measured before ponding with the water, after removal of the water, and at the middle of the dry cycle.

Step 2. Immediately after the first potential map, the first anode was connected to the steel. The current delivered by the anode was measured, after which the anode was immediately disconnected. The second anode was then connected to the steel, and the current was measured. If both anodes were active (i.e., produced currents of the order of milliamperes), one of them was chosen and permanently connected to the steel. The other anode remained redundant until the end of the experiment. If one anode appeared faulty (e.g., the electrical connection was problematic), the spare anode would be used.

Step 3. The specimens were ponded with water (no salt) for 4 days. Approximately 2 L water (around 10-mm height) were added to the reservoir. At the end of the wet period, water was removed by vacuum, as shown in Figure F.19.

Step 4. The data logger (see Figure F.20) was used to take readings every hour. The automated acquisition system recorded the total current measurements.

Step 5. For the depolarization measurements at approximately every 10 weeks, a potential map was determined while the anode and steel bars were connected. The anode was then disconnected (using the switch).

Step 6. Four hours later, a new potential map was determined. The difference between the instant-off potential and the 4-h depolarization potential were used to determine the parameter $Depol_4$.

Step 7. Twenty-four hours after disconnection, another potential map was determined. The difference between the instant-off potential and this 24-hour depolarization potential was used to determine the parameter $Depol_{24}$.

After the conclusion of the depolarization test, the anode was reconnected to all steel bars. The anode was kept connected to all the rebars via the junction box until the next depolarization test.

The test specimens are shown in Figure F.21.

Test Results

This section summarizes the data collected from

- The half-cell potential system;
- The current flowing from the anodes to each pair of rebars and the corrosion potential at the location of two embedded electrodes in each specimen; and

Figure F.20. Laptop and data logger system used to collect the data.

Figure F.21. Test specimens.

- The current flowing during the instant-off and -on procedure from the anodes to each pair of rebars and the corrosion potential at the location of two embedded electrodes.

The experimental program started with the first half-cell potential measurement taken on September 23, 2010 (Day 0). After establishing the baseline readings, all samples were subjected to cycles of 4 days wet and 10 days dry. In addition to the half-cell readings taken at the end of each dry cycle, two extra sets of readings were taken to better evaluate and observe the specimens during the wet–dry cycles.

Each specimen was identified using the labels given in Table F.3. Five variables were tested; three specimens for each variable were made (for a total of 15 specimens) to provide statistical significance.

Although two anodes were installed in each specimen, only one was used in the tests. The output voltage of each anode was measured separately. The anode with the higher potential reading measured was selected and was connected permanently with the rebars throughout the experiment. Table F.4 shows the potential reading from each anode measured by a multimeter. The shaded values refer to the chosen anodes.

Half-Cell Potential Data

Figure F.22 shows the half-cell potential readings for all specimens. This plot represents the average values of corrosion potential measured at nine distinct points on each slab. The measurement was conducted three times during each wet–dry cycle.

Initially all specimens had similar corrosion potential values. The control specimens (BB), with no anode, had the lowest negative corrosion potential values; these values were steady throughout the experiment. All specimens with anodes had their corrosion potential shift in the negative direction after the anode was connected to the rebars.

The OA, OA4, and HVAL specimens had steady potential readings. Two HVAH specimens produced variable results that may have been due to variation in the production of the prototypes. The highest negative corrosion potentials were provided by the HVAH specimens, followed by the HVAL and OA4 specimens, then by OA, and finally by the BB specimens. Higher negative corrosion potentials indicate that more corrosion protection was being provided.

Table F.3. Sample Labels

Label	Type of Anode
BB_1	None
BB_2	None
BB_3	None
OA_1	Ordinary anode
OA_2	Ordinary anode
OA_3	Ordinary anode
OA4_1	Anode with four times the surface area of the ordinary anode
OA4_2	Anode with four times the surface area of the ordinary anode
OA4_3	Anode with four times the surface area of the ordinary anode
HVAL_1	High-voltage anode: low level
HVAL_2	High-voltage anode: low level
HVAL_3	High-voltage anode: low level
HVAH_1	High-voltage anode: high level
HVAH_2	High-voltage anode: high level
HVAH_3	High-voltage anode: high level

Current Flow and Corrosion Potential

Data were collected hourly by the data-logger system. Seven outputs were collected for each specimen. Table F.5 shows the

Table F.4. Initial Voltage Output

Label	Anode 1	Anode 2
OA_1	0.925 V	0.927 V
OA_2	0.971 V	0.961 V
OA_3	0.927 V	0.923 V
OA4_1	0.852 V	0.832 V
OA4_2	0.845 V	0.853 V
OA4_3	0.888 V	0.894 V
HVAL_1	1.864 V	0.837 V
HVAL_2	0.815 V	0.778 V
HVAL_3	1.714 V	1.463 V
HVAH_1	2.245 v	1.817 V
HVAH_2	3.270 v	2.555 V
HVAH_3	3.320 v	1.767 V

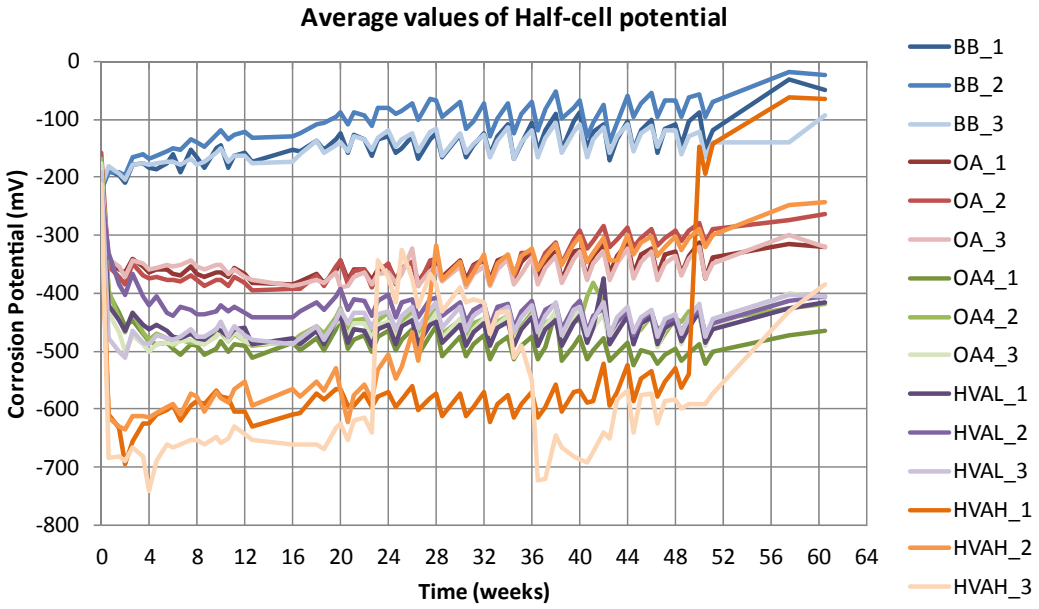

Figure F.22. Half-cell potential for all 15 specimens.

labels used to identify each one of these outputs, and Figure F.23 shows the location of each monitored element on the sample. Two data analyses were conducted. The first series of data presented the electrical current flowing from the anode to all four pairs of rebars. The second data series presented the corrosion potential measured by the embedded electrodes at two locations.

Electrical Current Data Analysis

This subsection presents the measurement of electrical current flowing from the anode to the four pairs of rebars. The data logger recorded the voltage (electrical potential) hourly across the resistors. The electrical current was calculated by dividing the voltage by the resistance; that is, $i = V/R$, where i is the current in milliamperes, V is the voltage in millivolts, and R is a 10-ohm resistor.

Figure F.24 through Figure F.27 show the data collected over 56 weeks. The plots show the variation of electrical current in milliamperes with time in weeks.

For the control specimens (BB), since no anode was installed, there is no current plot. Figure F.24 shows the results for the OA specimens. The ordinary anodes contained the least amount of zinc among all anodes tested. The initial current provided by this anode was 0.5 to 0.7 mA. The final current value decreased to a range of 0.1 to 0.3 mA.

Figure F.25 shows the results for OA4 specimens. The OA4 anode had four times the surface area as the ordinary anode. The initial current provide by this anode was 1.0 to 1.4 mA. The final current value decreased to a range of 0.4 to 0.6 mA.

Figure F.26 shows the results for HVAL specimens. The high-voltage anode (HVAL) contained the same amount of zinc as the ordinary anode, but the voltage of the anode was enhanced. The initial current provided by this anode was 0.6 to 1.4 mA. The final current value decreased to around 0.4 mA. The current results were very similar to the OA4 anode results.

Table F.5. Description of Identifying Labels

Label	Description
TopL	Two longitudinal rebars at top layer
TopT	Two transverse rebars at top layer
BotT	Two transverse rebars at bottom layer
BotL	Two longitudinal rebars at bottom layer
Anode	Anode
EMid	Embedded electrode at middle of reinforcement
ECor	Embedded electrode at corner of reinforcement

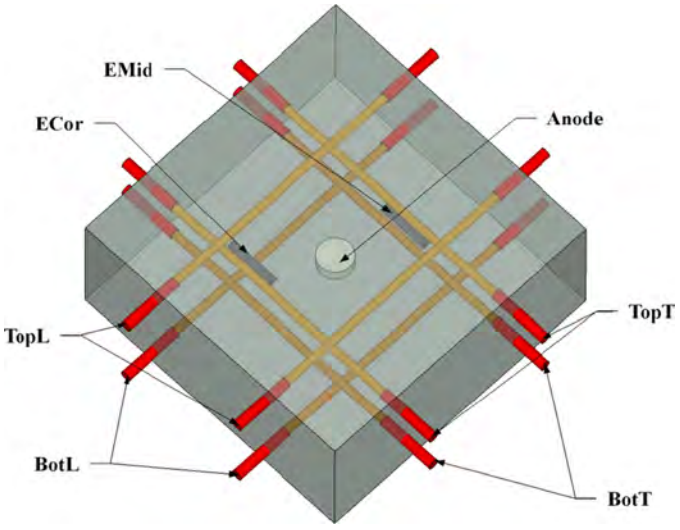

Figure F.23. Identification of monitored elements.

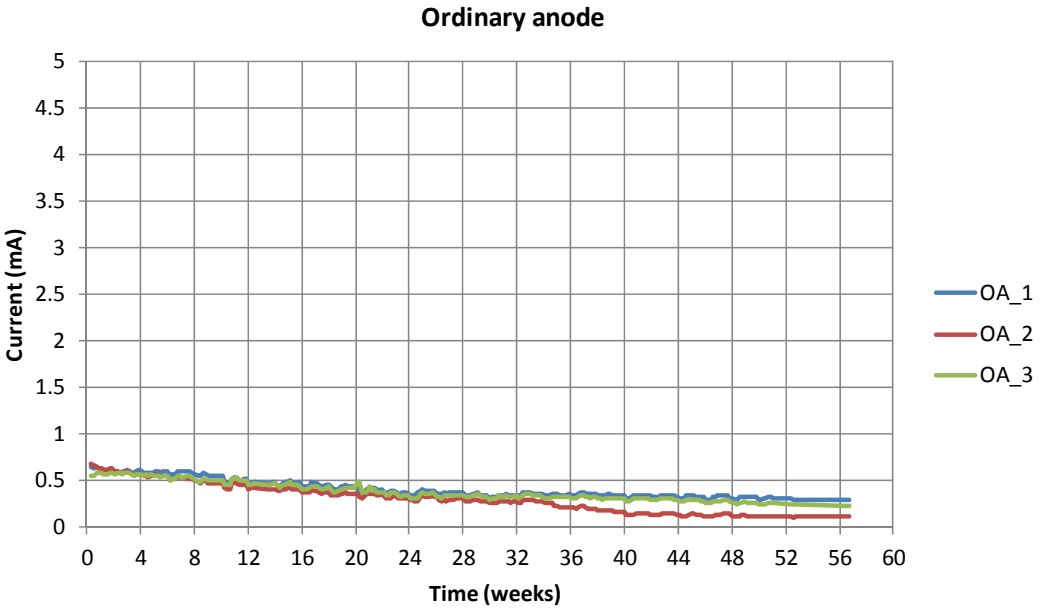

Figure F.24. Electrical current variation for specimens with OA anodes.

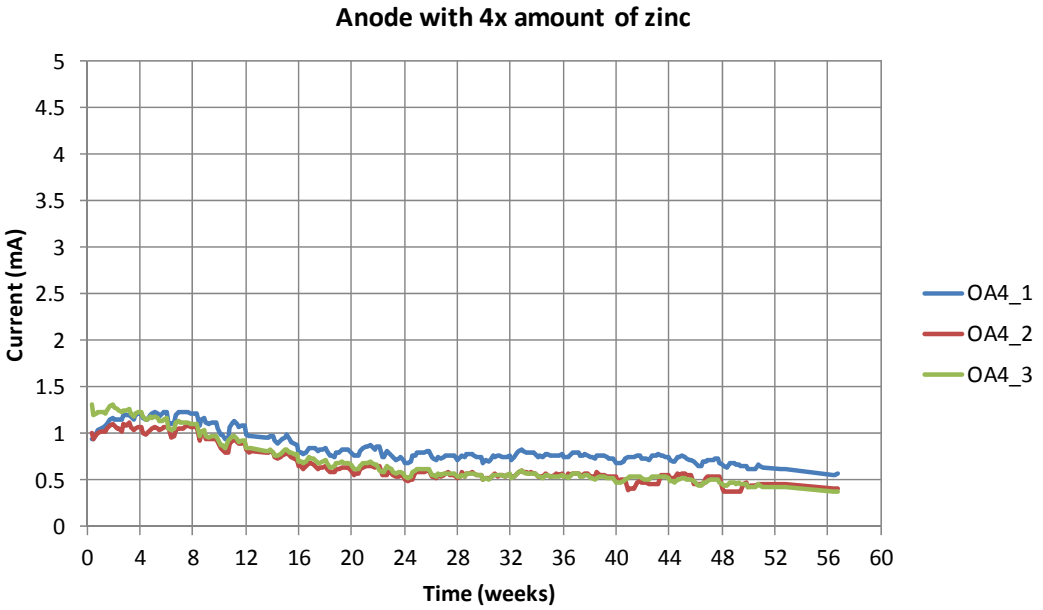

Figure F.25. Electrical current variation for specimens with OA4 anodes.

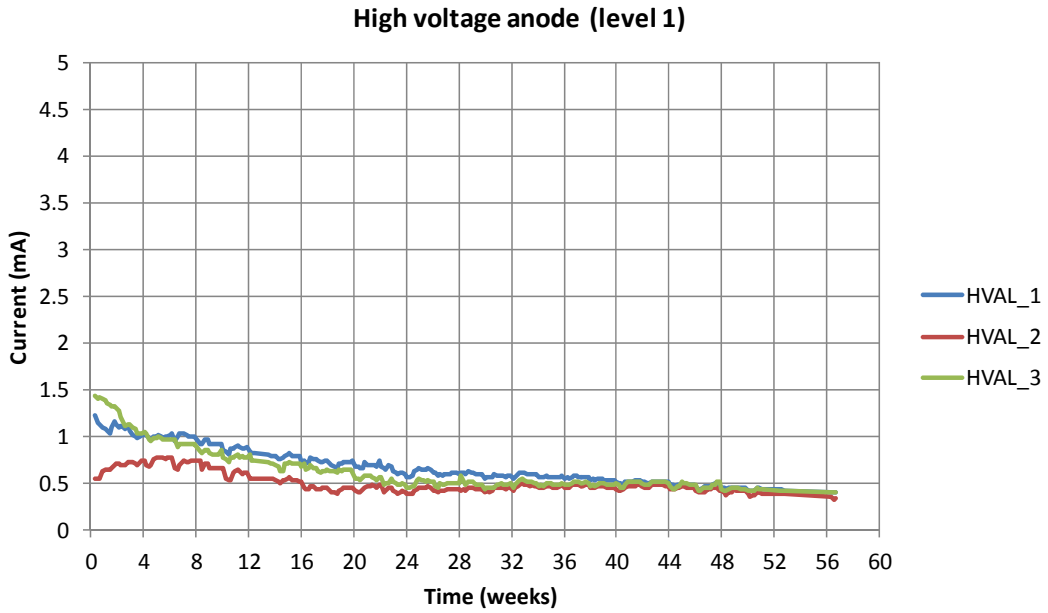

Figure F.26. Electrical current variation for specimens with HVAL anodes.

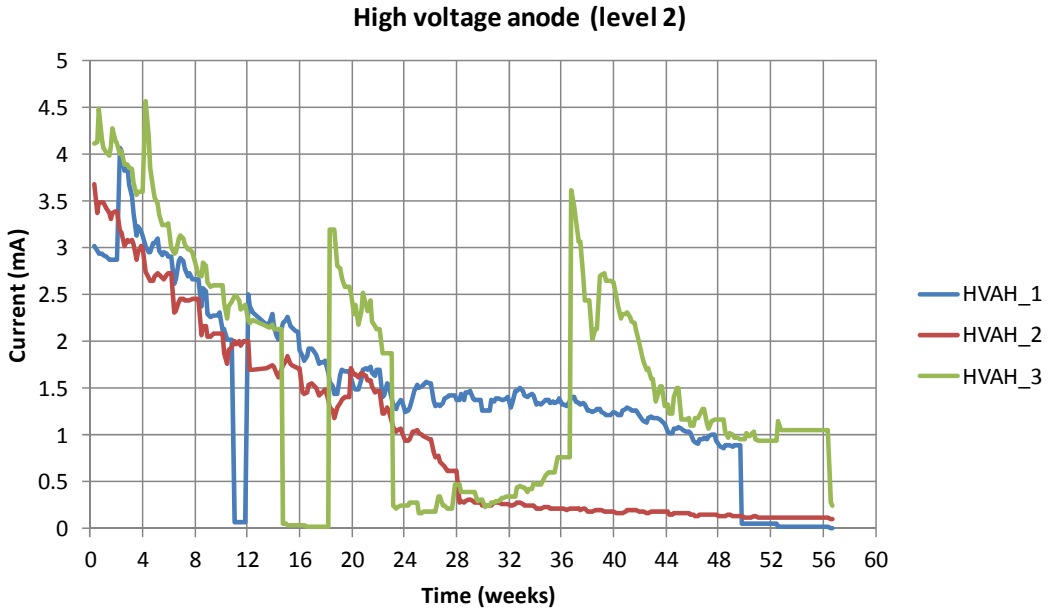

Figure F.27. Electrical current variation for specimens with HVAH anodes.

Figure F.27 shows the results for HVAH specimens. The high-voltage anode (HVAH) contained the same amount of zinc as the ordinary anode, but the voltage of the anode was increased to be greater than the HVAL anodes. The initial current provided by this anode was 3.0 to 4.2 mA. The final current decreased to a range of 0.2 to 0.3 mA. During the early stage of the testing, a sudden drop in the current occurred for both HVAH_1 and HVAH_3. The spare anode was connected, and the testing continued.

Corrosion Potential Data

This subsection presents the corrosion potential data collected at the two locations of the embedded reference electrodes identified in Table F.5. The data logger recorded the potential of the reinforcing steel relative to the embedded reference electrodes on an hourly basis. Although all embedded electrodes were tested individually during the installation, some of them exhibited abrupt changes of corrosion potential measurements during the test. It was believed that these unexpected changes were caused by malfunctioning electrodes that could not be detected during the preliminary tests. Regardless of the malfunctioning of some embedded electrodes, the results clearly indicated the difference in behavior of various anode types.

Figure F.28 through Figure F.32 show the data collected over 56 weeks. The plots show the variation in corrosion potential (in millivolts) with time (days) for all 15 specimens. The data from the malfunctioning embedded electrodes were removed from the plot.

Figure F.28 shows the results for BB specimens. No anode was installed in the specimens, and consequently no great variation of corrosion potential was observed. The electrical potential measured by the embedded electrodes was around −250 mV, which decreased to values of −100 mV at the end of testing. Very good agreement was found between the embedded electrode values and the surface potential values.

Figure F.29 shows the results for the OA specimens. The electrical potential measured by the embedded electrodes ranged from −400 to −300 mV; these values decreased to around −300 to −150 mV at the end of testing. The average values of the corrosion potential measured at the top surface of each test specimen showed good agreement with the potential values from the embedded electrodes.

Figure F.30 shows the results for OA4 specimens. The electrical potential measured by the embedded electrodes was around −500 mV, which decreased to a range of −350 to −500 mV at the end of testing. Again, good agreement was observed between the average corrosion potential measured at the top surface of each test specimen and that obtained from the embedded electrodes.

Figure F.31 shows the results for HVAL specimens. The electrical potential measured by the embedded electrodes was around −450 mV; this value was largely maintained at the end of testing. The potential values measured at the top surface of each test specimen showed similar behavior.

Figure F.32 shows the results for specimens with the HVAH anodes. Unlike the other anodes, the HVAH specimens showed greater variation of the corrosion potential measurements. The electrical potential measured by the embedded electrodes ranged from −650 to −800 mV, which decreased to a range of −100 to −400 mV at the end of testing. Aside from the larger variability of the measurements, the potential measured at the surface of all three specimens followed the same trend and magnitudes of the values measured inside the concrete.

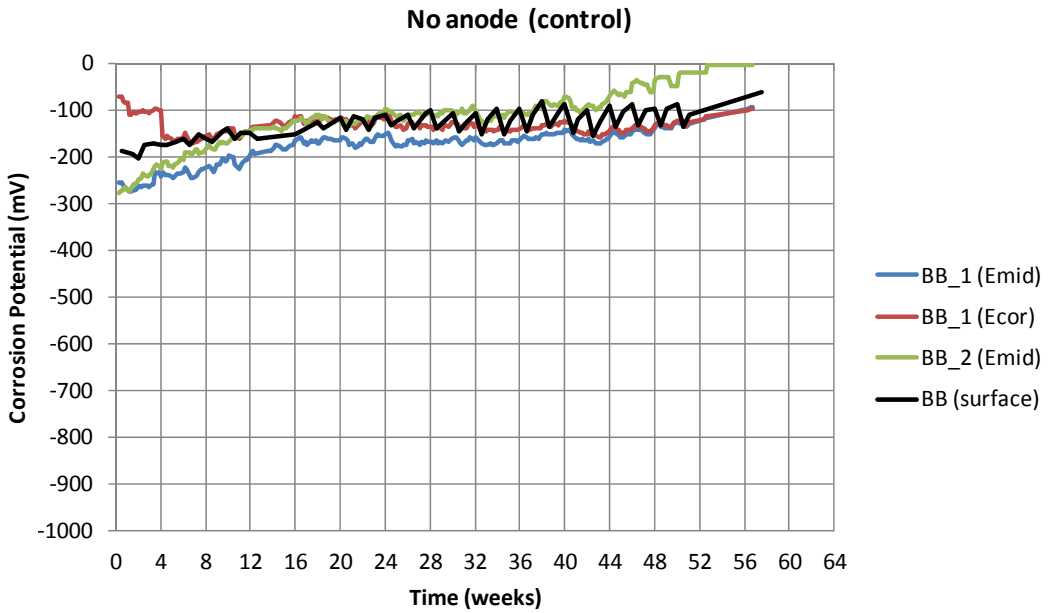

Figure F.28. Corrosion potential data for control specimens (BB).

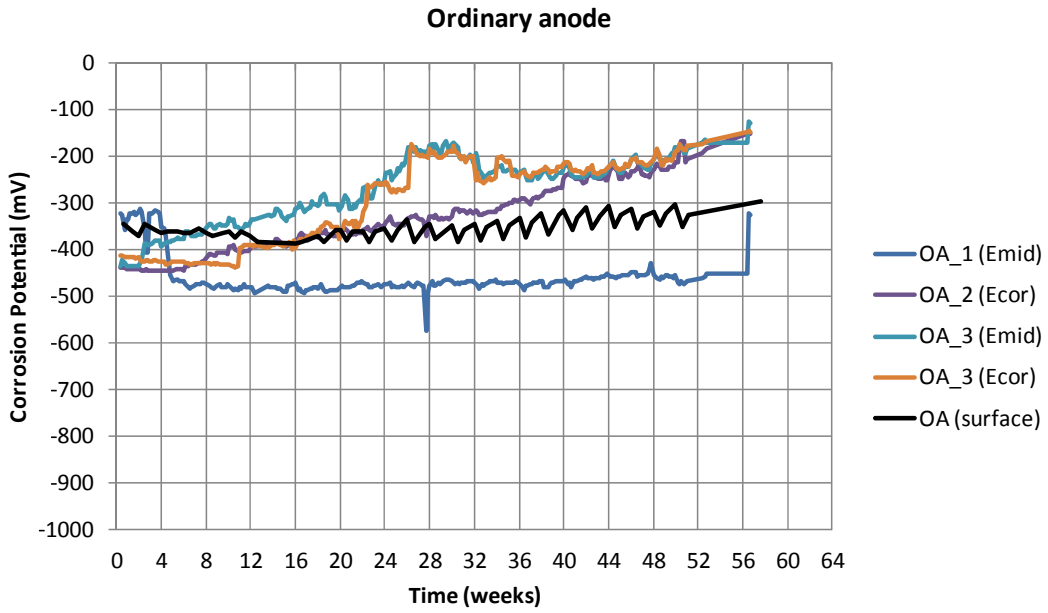

Figure F.29. Corrosion potential data for specimens with OA anodes.

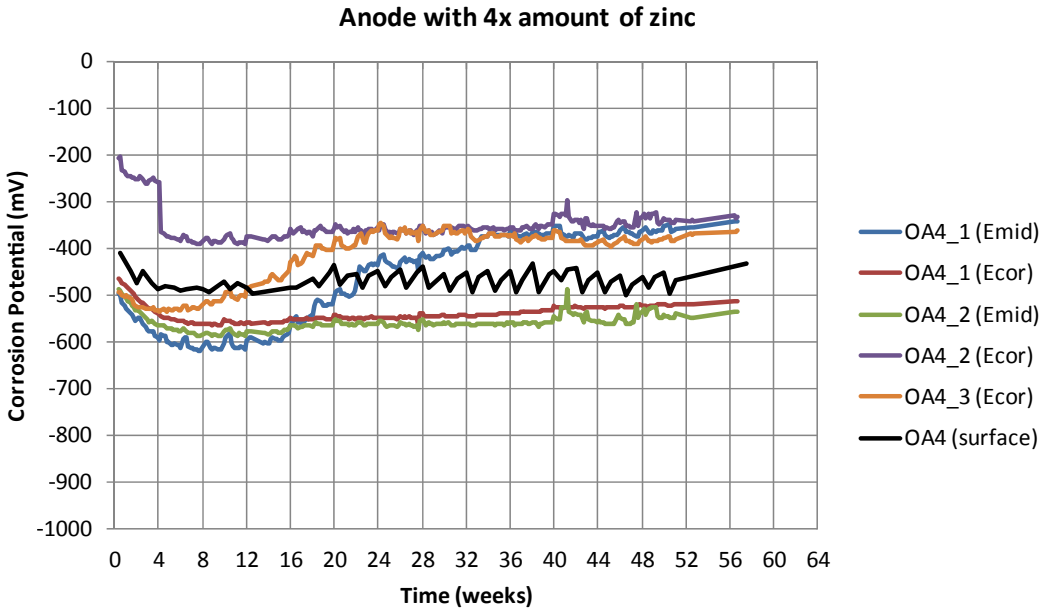

Figure F.30. Corrosion potential data for specimens with OA4 anodes.

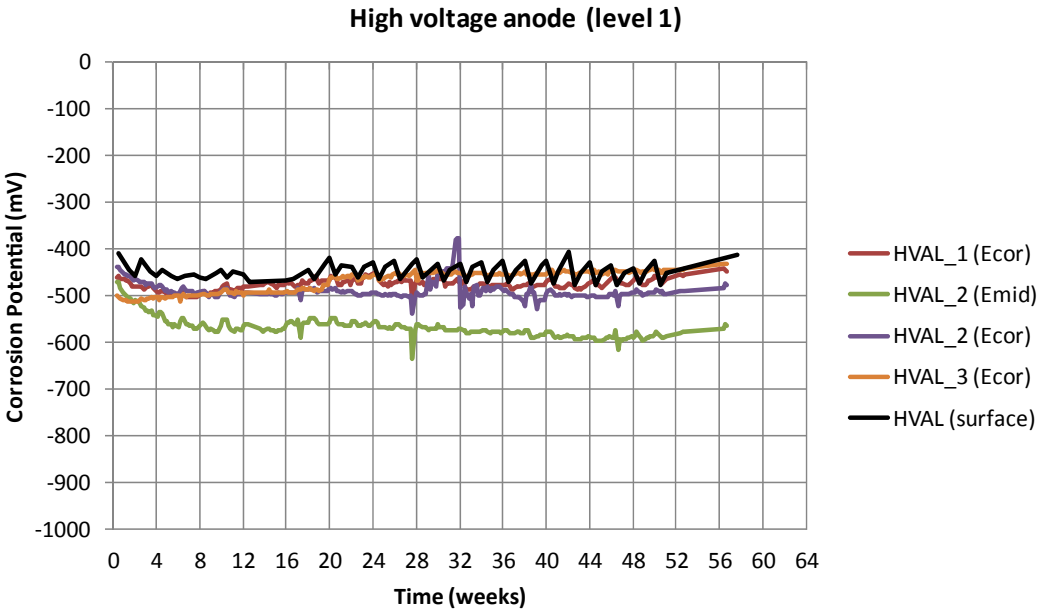

Figure F.31. Corrosion potential varying with time for specimens with HVAL anodes.

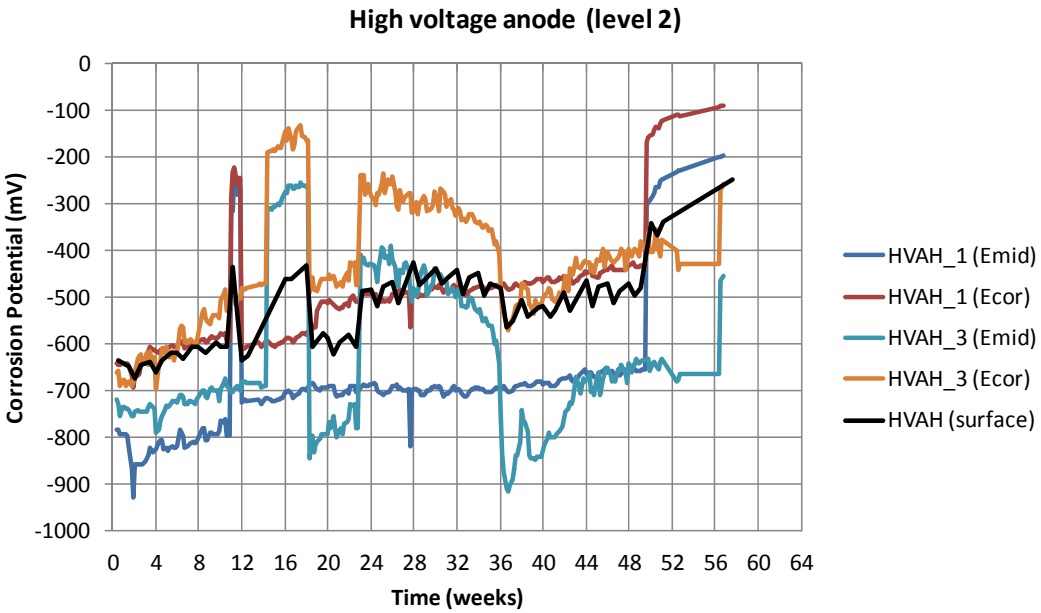

Figure F.32. Corrosion potential data for specimens with HVAH anodes.

Depolarization Testing

Corrosion rates were estimated through a depolarization testing procedure. Four depolarization measurements were conducted at approximately 10-week intervals. The tests consisted of collecting a series of readings during the temporary disconnection of the anodes, 4 and 24 h after disconnection, and finally during the anode reconnection (turn-on). The procedure started with the initial reading taken before the anodes were disconnected, and an intermediate reading was conducted 4 h after the anodes were disconnected (4 h off). Finally, 24 h after disconnection and before reconnection (turn-on) of the anodes, a final reading was taken (24 h off).

The data collected during this procedure were used to estimate the corrosion rate by using the Butler–Volmer equation (see Equation F.1), which describes one of the most fundamental relationships in electrochemistry (Bard and Faulkner 2001). The equation describes how the electrical current on an electrode depends on the electrode potential, considering that both a cathodic and an anodic reaction occur on the same electrode. In other words, the equation can be used to estimate the corrosion rate of steel reinforcement in concrete.

The data collected during the 24-h depolarization test period was used to estimate the corrosion current of the reinforcing steel in each of the test specimens with anodes using a solution to the Butler–Volmer equation.

$$i_{corr} = \frac{i_{appl}}{\exp\left(\frac{2.3\Delta E}{\beta_c}\right) - \exp\left(\frac{-2.3\Delta E}{\beta_a}\right)} \quad \text{(F.1)}$$

where

i_{corr} = corrosion rate (mA/m^2);
i_{appl} = applied electrical current (mA/m^2);
ΔE = observed corrosion potential (mV);
β_c = cathodic Tafel's slope (assumed 120 mV); and
β_a = anodic Tafel's slope (assumed 60 mV).

Table F.6 shows typical corrosion rate values and their respective level of relevance.

Table F.6. Typical Corrosion Rate Values

Measurement	Corrosion Rate
<0.5 μA/cm^2	Negligible
0.5–5 μA/cm^2	Slow
5–15 μA/cm^2	Moderate
>15 μA/cm^2	High

Table F.7. Variation of Corrosion Potential During First Depolarization Period

	Time of Measurement		
Sample Label	0 Hour (mV)	4 Hours (mV)	24 Hours (mV)
BB_1	–149.8	–153.4	–149.9
BB_2	–127.3	–125.9	–123.0
BB_3	–157.8	–148.1	–162.3
OA_1	–364.1	–116.3	–122.0
OA_2	–377.6	–108.9	–88.9
OA_3	–351.7	–87.9	–69.9
OA4_1	–496.6	–110.0	–81.9
OA4_2	–465.8	–106.0	–83.2
OA4_3	–474.6	–83.9	–62.2
HVAL_1	–463.0	–111.8	–85.4
HVAL_2	–431.1	–106.4	–90.4
HVAL_3	–463.2	–94.1	–65.1
HVAH_1	–568.8	–82.1	–44.4
HVAH_2	–570.2	–92.6	–91.0
HVAH_3	–648.1	–131.2	–127.4

First Depolarization

Table F.7 shows the corrosion potential measurements during a 24-h depolarization period. The presented values were calculated by taking the average over all nine surface points of each specimen.

During the 24-h depolarization period, it was observed that control specimens did not exhibit changes to the corrosion potential; however, all the specimens with anodes showed a large shift in potential after the disconnection of the anode. The largest change was observed for the HVAH specimens, followed by HVAL and OA4 specimens, and finally by the OA specimens. In the specimens with anodes, the corrosion potential of the reinforcing steel 4 h after disconnection averaged −103 mV. The corrosion potentials decreased further to around −84 mV after 24 h.

Figure F.33 shows the normalized values of corrosion potentials during the first depolarization period.

Table F.8 shows the corrosion rate estimation.

Although the concrete used in the specimens had a high level of salt per unit volume of concrete, the results indicated little or no corrosion.

Second Depolarization

Table F.9 shows the variation of corrosion potentials during the second 24-h depolarization test period. The values presented are the average of all nine surface corrosion potential measurements taken on each sample.

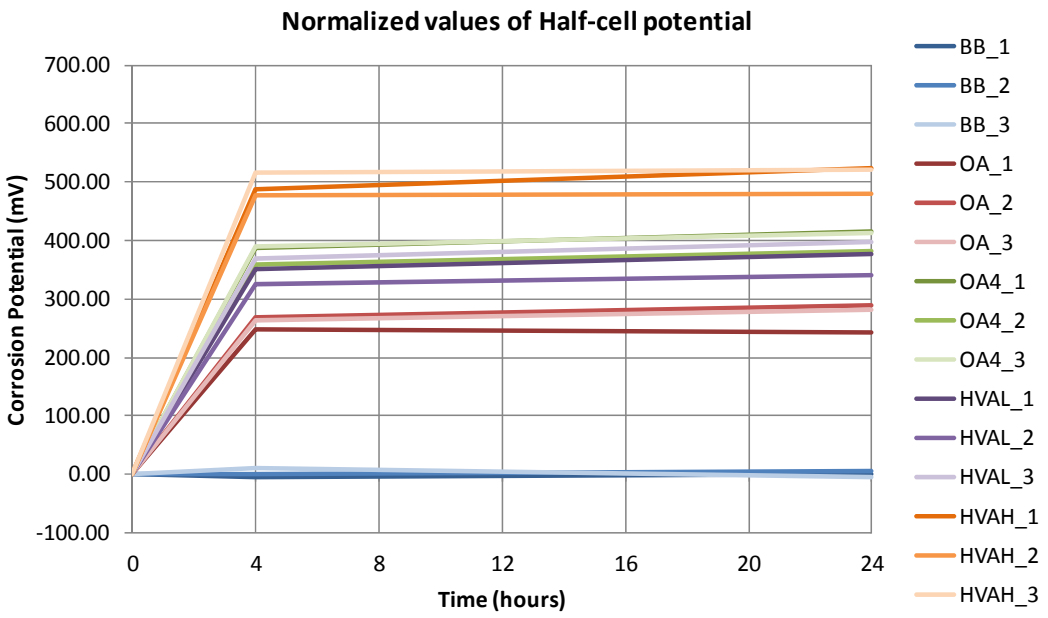

Figure F.33. Normalized values of half-cell potential during first depolarization.

Table F.8. Corrosion Rate Estimation

Label	i_{appl} (mA/m²)	ΔE (mV)	β_c (mV)	β_a (mV)	i_{corr} (mA/m²)	Corrosion Rate (µA/cm²)	Rating
OA_1	538.02	242.11	120	60	5.19	0.52	Slow
OA_2	460.28	288.67	120	60	1.82	0.18	Negligible
OA_3	487.00	281.78	120	60	2.20	0.22	Negligible
OA4_1	1110.67	414.67	120	60	0.39	0.04	Negligible
OA4_2	941.92	382.56	120	60	0.62	0.06	Negligible
OA4_3	968.46	412.33	120	60	0.36	0.04	Negligible
HVAL_1	907.29	377.56	120	60	0.65	0.07	Negligible
HVAL_2	670.29	340.67	120	60	0.98	0.10	Negligible
HVAL_3	804.60	398.11	120	60	0.39	0.04	Negligible
HVAH_1	2279.74	524.33	120	60	0.10	0.01	Negligible
HVAH_2	2072.82	479.22	120	60	0.21	0.02	Negligible
HVAH_3	2605.68	520.67	120	60	0.12	0.01	Negligible

Table F.9. Variation of Corrosion Potential During Second Depolarization Period

Sample	Time of Measurement		
	0 Hour (mV)	4 Hours (mV)	24 Hours (mV)
BB_1	–134.9	–132.4	–111.9
BB_2	–94.9	–91.0	–77.0
BB_3	–144.4	–136.2	–122.7
OA_1	–362.1	–99.7	–63.3
OA_2	–354.2	–85.0	–55.6
OA_3	–365.1	–82.9	–40.6
OA4_1	–463.2	–95.4	–53.8
OA4_2	–440.6	–95.0	–54.3
OA4_3	–452.0	–92.8	–46.4
HVAL_1	–447.4	–104.4	–54.6
HVAL_2	–404.7	–87.7	–54.7
HVAL_3	–445.6	–79.0	–45.8
HVAH_1	–565.6	–88.1	–9.8
HVAH_2	–529.3	–72.6	–21.4
HVAH_3	–631.9	–98.2	–27.1

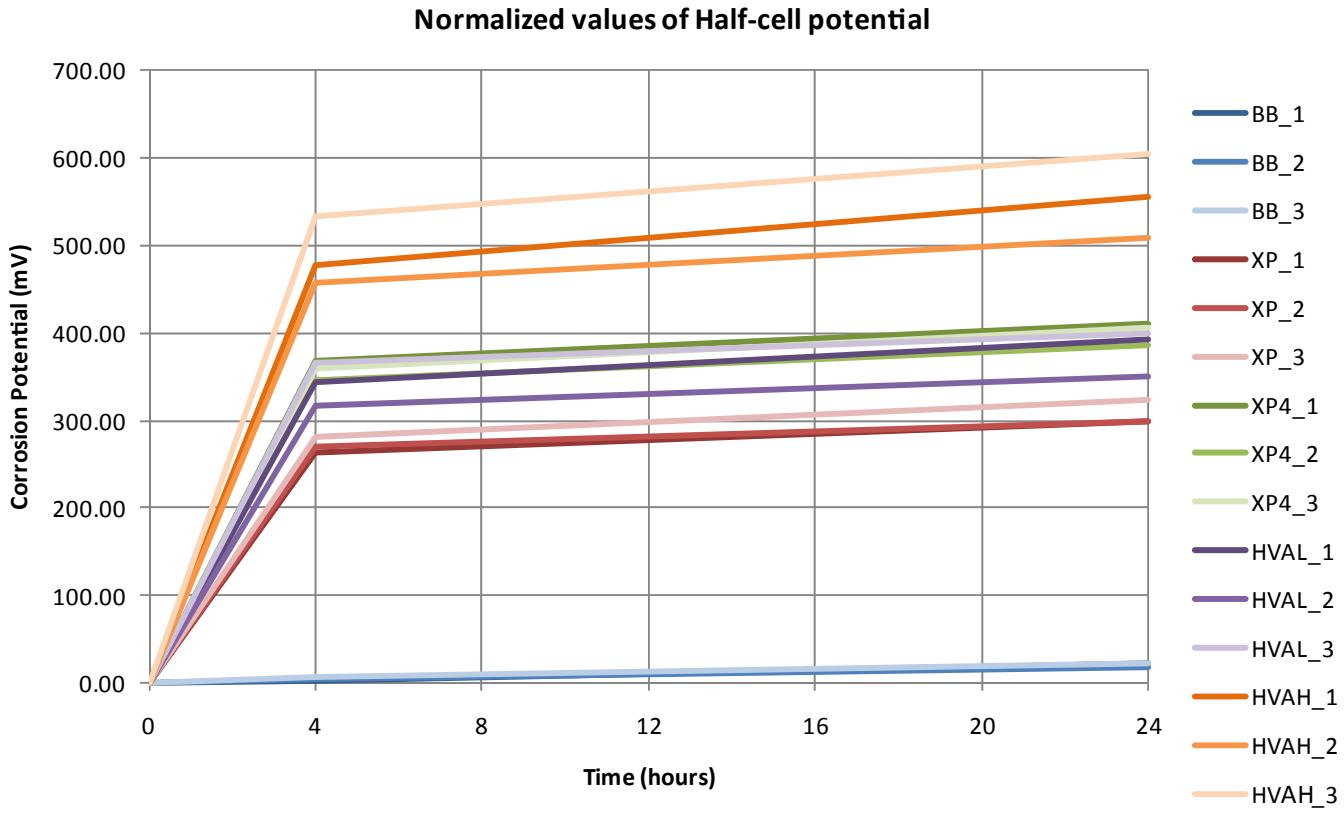

Figure F.34. Normalized values of half-cell potential during second depolarization.

During the second depolarization period of 24 h, it was observed that the corrosion potential of the control specimens did not change; however, all the specimens with anodes showed a large shift in potential after the disconnection of the anodes. The largest change was observed for the HVAH specimens, followed by HVAL and OA4 specimens, and finally by the OA specimens. Despite the different initial corrosion potential of each sample, the potential of the reinforcing steel 4 h after disconnection was around −90 mV for all specimens with anodes. The corrosion potential of the reinforcing steel 24 h after disconnection averaged −44 mV.

Figure F.34 shows normalized values of the corrosion potential during the second depolarization period.

Table F.10 shows the corrosion rate estimation.

Table F.10. Corrosion Rate Estimation

Label	i_{appl} (mA/m²)	ΔE (mV)	β_c (mV)	β_a (mV)	i_{corr} (mA/m²)	Corrosion Rate (μA/cm²)	Rating
OA_1	432.66	298.78	120	60	1.41	0.14	Negligible
OA_2	350.86	298.67	120	60	1.15	0.11	Negligible
OA_3	402.85	324.56	120	60	0.80	0.08	Negligible
OA4_1	814.88	409.44	120	60	0.32	0.03	Negligible
OA4_2	630.26	386.22	120	60	0.38	0.04	Negligible
OA4_3	682.24	405.56	120	60	0.29	0.03	Negligible
HVAL_1	714.72	392.89	120	60	0.38	0.04	Negligible
HVAL_2	441.83	350.00	120	60	0.54	0.05	Negligible
HVAL_3	634.69	399.78	120	60	0.30	0.03	Negligible
HVAH_1	1662.79	555.78	120	60	0.04	0.00	Negligible
HVAH_2	1393.41	507.89	120	60	0.08	0.01	Negligible
HVAH_3	2467.85	604.78	120	60	0.02	0.00	Negligible

Even though the concrete used in the specimens had a high level of salt per unit volume of concrete, the results indicated no corrosion activity.

Third Depolarization

Table F.11 shows the variation of corrosion potential during the third 24-h depolarization period. The values presented were calculated by taking the average of all nine surface corrosion potential measurements for each sample.

During the third 24-h depolarization period, it was observed that the corrosion potentials of the control specimens did not change; however, all the specimens with anodes showed a large shift in potential after the disconnection of the anodes. The largest change was observed for the HVAH specimens, followed by HVAL and OA4 specimens, and finally by the OA specimens. Despite the different initial corrosion potential of each sample, the potential of the reinforcing steel 4 h after disconnection was around −95 mV for all specimens with anodes. The corrosion potential of the reinforcing steel 24 h after disconnection averaged −52 mV.

Figure F.35 shows normalized values of the corrosion potential during the third depolarization period.

Table F.12 shows the corrosion rate estimation.

Even though the concrete used in the specimens had a high level of salt per unit volume of concrete, the results indicated no corrosion activity.

Table F.11. Variation of Corrosion Potential During Third Depolarization Period

Sample	Time of Measurement		
	0 Hour (mV)	4 Hours (mV)	24 Hours (mV)
BB_1	−134.1	−137.6	−127.4
BB_2	−64.1	−68.4	−65.7
BB_3	−122.7	−127.7	−126.2
OA_1	−350.0	−92.1	−54.0
OA_2	−342.8	−92.4	−52.4
OA_3	−361.3	−85.6	−42.6
OA4_1	−473.0	−110.7	−67.6
OA4_2	−439.3	−101.1	−59.1
OA4_3	−448.6	−95.1	−58.9
HVAL_1	−454.1	−104.7	−54.2
HVAL_2	−411.6	−95.6	−59.3
HVAL_3	−428.3	−92.1	−56.7
HVAH_1	−581.4	−87.1	−24.7
HVAH_2	−402.9	−86.8	−33.3
HVAH_3	−367.8	−100.1	−59.7

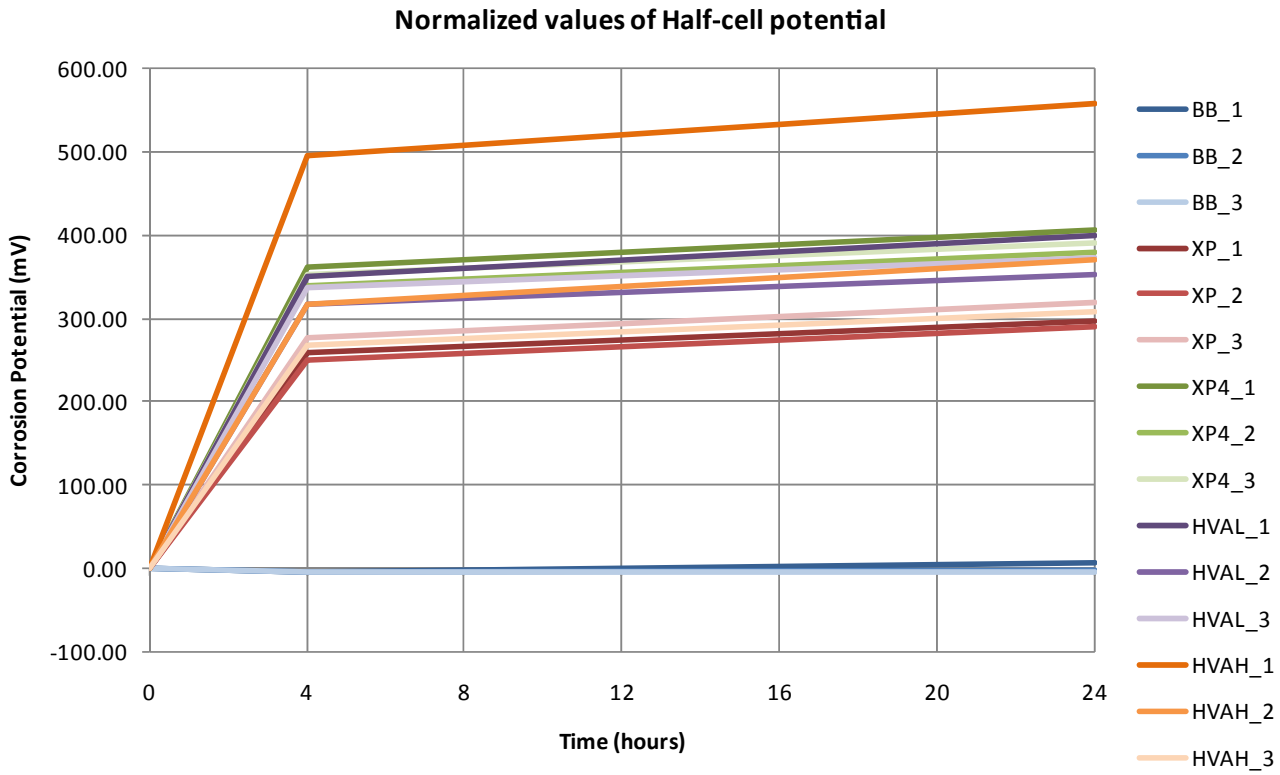

Figure F.35. Normalized values of half-cell potential during third depolarization.

Table F.12. Corrosion Rate Estimation

Label	i_{appl} (mA/m²)	ΔE (mV)	β_c (mV)	β_a (mV)	i_{corr} (mA/m²)	Corrosion Rate (μA/cm²)	Rating
OA_1	365.78	296.00	120	60	1.26	0.13	Negligible
OA_2	282.76	290.33	120	60	1.08	0.11	Negligible
OA_3	330.75	318.78	120	60	0.73	0.07	Negligible
OA4_1	757.58	405.44	120	60	0.32	0.03	Negligible
OA4_2	555.11	380.22	120	60	0.38	0.04	Negligible
OA4_3	570.26	389.67	120	60	0.33	0.03	Negligible
HVAL_1	602.47	399.89	120	60	0.28	0.03	Negligible
HVAL_2	433.49	352.22	120	60	0.51	0.05	Negligible
HVAL_3	496.30	371.67	120	60	0.40	0.04	Negligible
HVAH_1	1403.08	556.78	120	60	0.03	0.00	Negligible
HVAH_2	519.70	369.56	120	60	0.44	0.04	Negligible
HVAH_3	241.89	308.11	120	60	0.66	0.07	Negligible

Fourth Depolarization

Table F.13 shows the variation of corrosion potential during the fourth 24-h depolarization period. The values presented were calculated by taking the average of all nine surface corrosion potential measurements for each sample.

During the fourth 24-h depolarization period, it was observed that the corrosion potential of the control specimens did not change; however, all of the specimens with anodes showed a large shift in potential after the disconnection of the anodes. The largest change was observed for the HVAH specimens, followed by HVAL and OA4 specimens, and finally by the OA specimens. The potential of the reinforcing steel 4 h after disconnection averaged –112 mV for all specimens. The corrosion potential of the reinforcing steel 24 h after disconnection averaged –66 mV.

Figure F.36 shows normalized values of the corrosion potential during the fourth depolarization period.

Table F.14 shows the corrosion rate estimation.

Even though the concrete used in the specimens had a high level of salt per unit volume of concrete, the results indicated no corrosion activity.

Table F.13. Variation of Corrosion Potential During Fourth Depolarization Period

Sample	Time of Measurement		
	0 Hour (mV)	4 Hours (mV)	24 Hours (mV)
BB_1	–102.4	–118.6	–104.3
BB_2	–79.7	–93.6	–83.1
BB_3	–121.4	–138.4	–123.4
OA_1	–328.2	–96.6	–51.2
OA_2	–307.7	–108.6	–80.7
OA_3	–340.0	–86.7	–40.0
OA4_1	–489.7	–137.6	–97.7
OA4_2	–442.0	–120.3	–70.1
OA4_3	–440.8	–112.4	–67.4
HVAL_1	–452.1	–116.4	–67.6
HVAL_2	–424.3	–115.4	–76.3
HVAL_3	–427.4	–101.8	–63.3
HVAH_1	–569.7	–97.1	–29.4
HVAH_2	–315.7	–109.1	–59.9
HVAH_3	–681.8	–140.2	–87.4

Conclusions

The test results indicated that there was no corrosion in any of the specimens in the given time period. The testing further indicated that specimens with high-level, high-voltage anodes (HVAH) provided increased corrosion protection by having higher current and generating more negative potential values than the low-level, high-voltage anodes (HVAL). Anodes with four times the surface area (OA4) provided more current and corrosion protection than ordinary (OA) anodes. HVAL anodes exhibited current and potential values similar to the OA4 anodes. Both high-voltage anodes and OA4 anodes provided higher current and generated more negative potential values, indicating better corrosion protection than OA anodes.

Recommendation

Due to time constraints, the tests were terminated without observing corrosion in the specimens. Further research with an extended time frame is recommended.

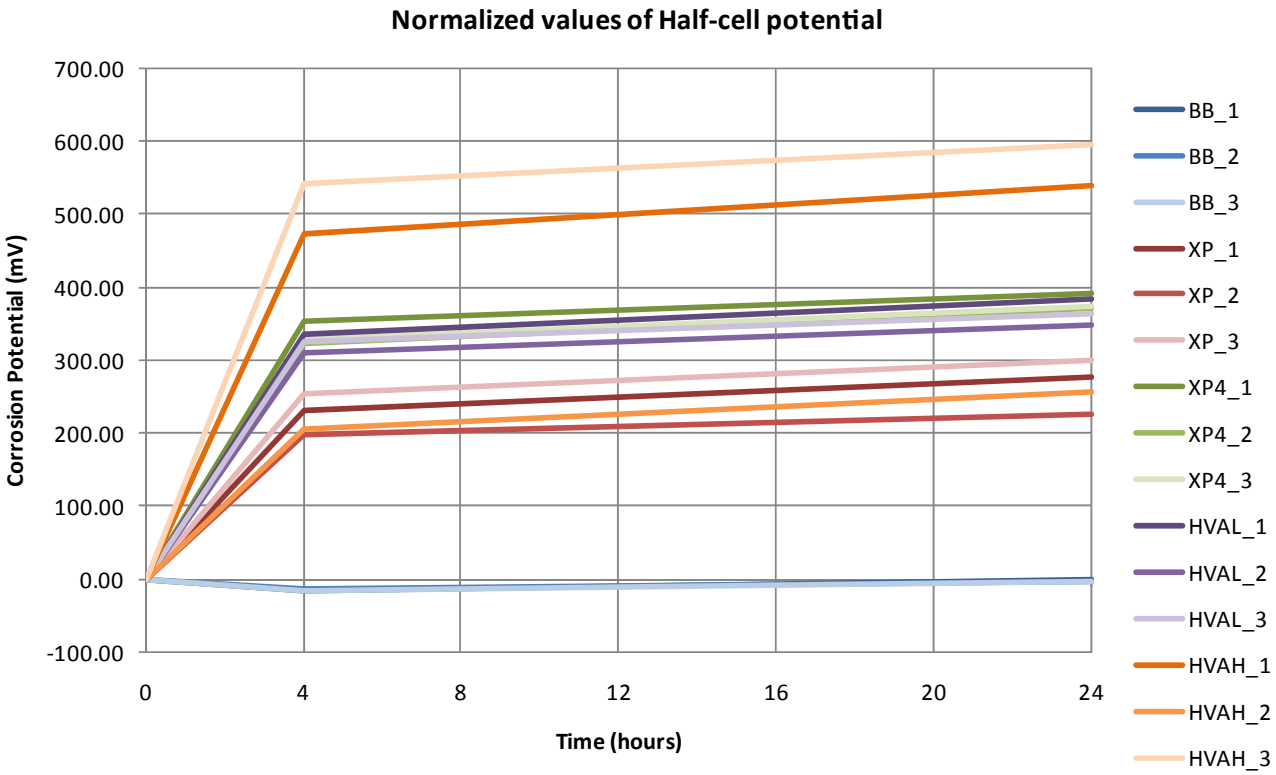

Figure F.36. Normalized values of half-cell potential during fourth depolarization.

Table F.14. Corrosion Rate Estimation

Label	i_{appl} (mA/m²)	ΔE (mV)	β_c (mV)	β_a (mV)	i_{corr} (mA/m²)	Corrosion Rate (µA/cm²)	Rating
OA_1	331.32	277.00	120	60	1.64	0.16	Negligible
OA_2	161.54	227.00	120	60	2.08	0.21	Negligible
OA_3	293.71	300.00	120	60	0.93	0.09	Negligible
OA4_1	728.08	392.00	120	60	0.40	0.04	Negligible
OA4_2	528.61	371.89	120	60	0.42	0.04	Negligible
OA4_3	512.58	373.33	120	60	0.40	0.04	Negligible
HVAL_1	526.21	384.56	120	60	0.33	0.03	Negligible
HVAL_2	450.59	348.00	120	60	0.57	0.06	Negligible
HVAL_3	480.73	364.11	120	60	0.45	0.04	Negligible
HVAH_1	1201.89	540.22	120	60	0.04	0.00	Negligible
HVAH_2	186.49	255.78	120	60	1.39	0.14	Negligible
HVAH_3	2597.31	594.33	120	60	0.03	0.00	Negligible

TRB OVERSIGHT COMMITTEE FOR THE STRATEGIC HIGHWAY RESEARCH PROGRAM 2*

CHAIR: **Kirk T. Steudle,** *Director, Michigan Department of Transportation*

MEMBERS

H. Norman Abramson, *Executive Vice President (retired), Southwest Research Institute*
Alan C. Clark, *MPO Director, Houston–Galveston Area Council*
Frank L. Danchetz, *Vice President, ARCADIS-US, Inc.*
Malcolm Dougherty, *Director, California Department of Transportation*
Stanley Gee, *Executive Deputy Commissioner, New York State Department of Transportation*
Mary L. Klein, *President and CEO, NatureServe*
Michael P. Lewis, *Director, Rhode Island Department of Transportation*
John R. Njord, *Executive Director (retired), Utah Department of Transportation*
Charles F. Potts, *Chief Executive Officer, Heritage Construction and Materials*
Ananth K. Prasad, *Secretary, Florida Department of Transportation*
Gerald M. Ross, *Chief Engineer (retired), Georgia Department of Transportation*
George E. Schoener, *Executive Director, I-95 Corridor Coalition*
Kumares C. Sinha, *Olson Distinguished Professor of Civil Engineering, Purdue University*
Paul Trombino III, *Director, Iowa Department of Transportation*

EX OFFICIO MEMBERS

Victor M. Mendez, *Administrator, Federal Highway Administration*
David L. Strickland, *Administrator, National Highway Transportation Safety Administration*
Frederick "Bud" Wright, *Executive Director, American Association of State Highway and Transportation Officials*

LIAISONS

Ken Jacoby, *Communications and Outreach Team Director, Office of Corporate Research, Technology, and Innovation Management, Federal Highway Administration*
Tony Kane, *Director, Engineering and Technical Services, American Association of State Highway and Transportation Officials*
Jeffrey F. Paniati, *Executive Director, Federal Highway Administration*
John Pearson, *Program Director, Council of Deputy Ministers Responsible for Transportation and Highway Safety, Canada*
Michael F. Trentacoste, *Associate Administrator, Research, Development, and Technology, Federal Highway Administration*

*Membership as of November 2013.

RENEWAL TECHNICAL COORDINATING COMMITTEE*

CHAIR: **Daniel D'Angelo,** *Recovery Acting Manager, Director and Deputy Chief Engineer, Office of Design, New York State Department of Transportation*

MEMBERS

Rachel Arulraj, *Director of Virtual Design & Construction, Parsons Brinckerhoff*
Michael E. Ayers, *Consultant, Technology Services, American Concrete Pavement Association*
Thomas E. Baker, *State Materials Engineer, Washington State Department of Transportation*
John E. Breen, *Al-Rashid Chair in Civil Engineering Emeritus, University of Texas at Austin*
Steven D. DeWitt, *Chief Engineer (retired), North Carolina Turnpike Authority*
Tom W. Donovan, *Senior Right of Way Agent (retired), California Department of Transportation*
Alan D. Fisher, *Manager, Construction Structures Group, Cianbro Corporation*
Michael Hemmingsen, *Davison Transportation Service Center Manager (retired), Michigan Department of Transportation*
Bruce Johnson, *State Bridge Engineer, Oregon Department of Transportation, Bridge Engineering Section*
Leonnie Kavanagh, *PhD Candidate, Seasonal Lecturer, Civil Engineering Department, University of Manitoba*
Cathy Nelson, *Technical Services Manager/Chief Engineer (retired), Oregon Department of Transportation*
John J. Robinson, Jr., *Assistant Chief Counsel, Pennsylvania Department of Transportation, Governor's Office of General Counsel*
Ted M. Scott II, *Director, Engineering, American Trucking Associations, Inc.*
Gary D. Taylor, *Professional Engineer*
Gary C. Whited, *Program Manager, Construction and Materials Support Center, University of Wisconsin–Madison*

AASHTO LIAISON

James T. McDonnell, *Program Director for Engineering, American Association of State Highway and Transportation Officials*

FHWA LIAISONS

Steve Gaj, *Leader, System Management and Monitoring Team, Office of Asset Management, Federal Highway Administration*
Cheryl Allen Richter, *Assistant Director, Pavement Research and Development, Office of Infrastructure Research and Development, Federal Highway Administration*
J. B. "Butch" Wlaschin, *Director, Office of Asset Management, Federal Highway Administration*

CANADA LIAISON

Lance Vigfusson, *Assistant Deputy Minister of Engineering & Operations, Manitoba Infrastructure and Transportation*

*Membership as of November 2013.

Related SHRP 2 Research

Geotechnical Solutions for Soil Improvement, Rapid Embankment Construction, and Stabilization of the Pavement Working Platform (R02)

Innovative Bridge Designs for Rapid Renewal (R04)

Nondestructive Testing to Identify Concrete Bridge Deck Deterioration (R06A)

Mapping Voids, Debonding, Delaminations, Moisture, and Other Defects Behind or Within Tunnel Linings (R06G)

Performance Specifications for Rapid Highway Renewal (R07)

Process of Managing Risk on Rapid Renewal Projects (R09)

Project Management Strategies for Complex Projects (R10)

Bridges for Service Life Beyond 100 Years: Service Limit State Design (R19B)